Design of new β-sheet breakers and artificial proteases against protein aggregation

Dissertation

Submitted to attain the academic degree of

Doctor of natural sciences

Dr. rer. nat.

presented by

Vanesa Redondo Garrosa

Faculty of Chemistry

University of Duisburg-Essen

Essen, 2021

DOI: 10.17185/duepublico/74682
URN: urn:nbn:de:hbz:465-20220714-105638-2

Design neuer β-Faltblattbrecher und künstlichen Proteasen gegen Proteinaggregation

Dissertation

zur Erlangung des akademischen Grades eines

Doktors der Naturwissenschaften

Dr. rer. nat.

vorgelegt von

Vanesa Redondo Garrosa

Fakultät für Chemie

Universität Duisburg-Essen

Essen, 2021

The present work was carried out in the period from July 2017 to July 2021 in the working group of Prof. Dr. Thomas Schrader at the Institute of Organic Chemistry at the University of Duisburg-Essen, Essen.

First examiner: Prof. Dr. Thomas Schrader

Second examiner: Prof. Dr. Michael Ehrmann

Chair of the examination board: Prof. Dr. Alexander Probst

The **oral defense** was on 06.08.2021

Die vorliegende Arbeit wurde im Zeitraum von Juli 2017 bis Juli 2021 im Arbeitskreis von Prof. Dr. Thomas Schrader am Institut für Organische Chemie der Universität Duisburg-Essen, Standort Essen, durchgeführt.

Referent: Prof. Dr. Thomas Schrader

Korreferent: Prof. Dr. Michael Ehrmann

Prüfungsvorsitzender: Prof. Dr. Alexander Probst

Tag der Disputation: 06.08.2021

Affidavit

I hereby certify that I have written the present thesis entitled

"Design of new β-sheet breakers and artificial proteases against protein aggregation"

myself and that I have not used any auxiliary means or sources other than those indicated. Furthermore, I hereby declare that I have not submitted this dissertation in this or any other form to any other university.

Essen, June 2021. _____

Vanesa Redondo Garrosa

Die Eidesstattliche Erklärung

Hiermit bestätige ich, dass ich die vorliegende Arbeit mit dem Titel

„Design neuer β-Faltblattbrecher und künstlichen Proteasen gegen Proteinaggregation“

selbst verfasst und keine, außer den angegebenen, Hilfsmitteln und Quellen benutzt habe. Des Weiteren erkläre ich hiermit, dass ich diese Dissertation in dieser oder anderer Form noch bei keiner anderen Universität eingereicht habe.

Essen, Juni 2021. _____

Vanesa Redondo Garrosa

"Una vez conoces a alguien, nunca lo olvidas realmente"

El viaje de Chihiro. Sen to Chihiro no Kamikakushi

List of abbreviations

aa	Amino acid
Aβ	Amyloid-β
ACH	Amyloid Cascade Hypothesis
AChEIs	Acetylcholinesterase inhibitors
ACN	Acetonitrile
AcOH	Acetic acid
AD	Alzheimer's disease
ADDLS	Aβ-Derived Diffusible Ligands
AFM	Atomic Force Microscopy
AL	Amyloid light-chain amyloidosis
Ala, A	Alanine
APP	Amyloid Precursor Protein
4-AMP	4-aminomethylpiperidine
Arg, R	Arginine
Asn, N	Asparagine
Asp, D	Aspartic acid, aspartate
AuNPs	Gold Nanopartciles
BACE1	β-secretase 1
BBB	Blood–Brain Barrier
Boc	di-*tert*-butyl dicarbonate
Cbz	Benzyl chloroformate
CD	Circular Dichroism
$CDCl_3$	Deuterated chloroform
CFS	Cerebrospinal fluid
$CHCl_3$	Chloroform

CJD	Creutzfeldt-Jacob disease
Cryo-EM	Cryogenic electronic emission
CTF	C-Terminal Fragment
Cy	Cyclohexane
Cyclen	1,4,7,10-tetraazacyclododecane
Cys, C	Cysteine
DAD	donor-aceptor-donor
DCM	Dichloromethane
DDA	donor-donor-aceptor
DIPEA	*N,N*-Diisopropylethylamine
DMF	Dimethylformamide
DMSO	Dimethyl sulfoxide
DNA	Deoxyribonucleic Acid
ECM	Extracelular matix
EtOAc	Ethyl acetate
FA	Formic acid
FDA	United States Food and Drug Administration
Fmoc	Fluorenylmethoxycarbonyl
GABA	γ-aminobutyric acid
Gbn	γ-globulin
Glu, E	Glutamic acid
Gln, Q	Glutamine
Gly, G	Glycine
HCTU	O-(1H-6-Chlorobenzotriazole-1-yl)-1,1,3,3-tetramethyluronium hexafluorophosphate
Hepes	4-(2-hydroxyethyl)-1-piperazineethanesulfonic acid

HFIP	Hexafluoro-isopropanol
h-IAPP	Human islet amyloid polypeptide
His, H	Histidine
HRMS	High-resolution mass spectrometry
HPLC	High-performance liquid chromatography
HTRA1	High-temperature requirement A1(Serine protease)
Ile, I	Isoleucine
IR	Infrared Absorption Spectroscopy
kDa	Kilo Dalton
LC	Light chain protein
Leu, L	Leucine
Lys, K	Lysine
MALDI-TOF	Matrix-Assisted Laser Desorption/Ionization- Time-Of-Flight
Me	Methyl
MeOD	Deuterated methanol
MeOH	Methanol
Met, M	Methionine
MD	Molecular Dynamics
MHz	Mega Hertz
µm	Micrometer
µL	Microliter
mL	Mililiter
MMPs	Matrix metalloproteinases
Mp	Melting point
MS	Mass spectrometry
NDGA	NorDihydroGuaiaretic Acid

NFTs	NeuroFibrillary Tangles
nm	nanometer
NMDA	N-methyl-D-aspartate
NMR	Neclear Magnetic Resonance
NTA	NitriloTricetic Acid
PAGE	Polyacrylamide gel electrophoresis
PBS	Phosphate-buffered saline
PCD	poly-(choloromethylstyrene-*co*-divinylbenzene)
PD	Parkinson Disease
PET	Positron Emission Tomography
Phe,F	Phenylalanine
PIB	Pittsburg Compound B
PMB	*para*-Methyl benzoic
PPA	Polyphosphoric acid
ppm	parts per million
Pro,P	Proline
PSEN1/2	Presenilin ½
PyCloP	Chlorotripyrrolidinophosphonium hexafluorophosphate
R_f	Retention factor
SAI-VL	SAI protein variable
scFv	single-chain variable Fragment
SDS	Sodium dodecyl sulfate
Ser, S	Serine
SET	Single-Electron Transfer
SGSM	Selective γ-Secretase Modulators
S_NAr	Nucleophilic Aromatic Substitution

S_N2	Bimolecular Nucleophilic Substitution
SS-NMR	Solid State Nuclear Magnetic Resonance
SPPS	Solid Phase Peptide Synthesis
STAB	Sodium triacetoxyhydroborate
τ	Tau
TEG	Triethylene glycol
TFA	Trifluoroacetic acid
THF	Tetrahydrofuran
TLC	Thin layer chromatography
TIPS	Triisopropyl silane
Thr, T	Threonine
ThT	Thioflavin T
TRINADES	TRIfunctional NAnoparticle DESign
Trimer	3-(3-(3-nitro-1H-pyrazole-5-carboxamido)-1H-pyrazole-5-carboxamido)-1H-pyrazole-5-carboxylate
Trp, W	Tryptophan
Trt	Trityl group
Tyr, T	Tyrosine
UV	Ultraviolet
Val,V	Valine
WHO	World Health Organization

Summary

Alois Alzheimer described the symptoms of a neurodegenerative disease that was later named after him, Alzheimer's disease (AD), for the first time in 1907. Although several approaches have been developed to fight one of the most common neurodegenerative diseases nowadays, a successful pharmacological treatment that slows or stops the damage and destruction of neurons has not yet been found, and only palliative therapies are used.

Going through this thesis, Chapter 1 will first provide an introduction to AD and the proteins involved in this dreadful neurodegenerative disease, as well as all the processes in which they are involved. Consequently, some guidelines for both patient and family to face the disease are provided. In the latter part of this chapter, different therapies to fight against the substantial damage of the neurons are commented. A route through immunotherapy, the intervention of the APP process, and methods of modulation of Aβ aggregation and degradation will provide the necessary theoretical background to understand the aim of this thesis. The most relevant therapeutic approaches to modulate Aβ are deeply explained in this final section, such as aminopyrazoles and artificial metalloproteases.

In the first section of the Chapter 3, an approach to interrupt processes involved in ACH, where Aβ is cleaved from APP and leads to Aβ aggregation, is described. New metalloproteases were designed, synthesized and evaluated with different techniques such as ThT fluorescence or CD spectroscopy. A pioneer MS method (proteomics) was used to analyze the peptide cleavage from the original full length of Aβ induced by the metalloproteases.

New β-sheet breakers against protein aggregation are commented in the second part of the Chapter 3. The synthesis of the compounds is detailed in this section as well as their evaluation with several techniques to prove the ability to prevent LC and Aβ aggregation. Extraordinary images of an aminopyrazole derivative altering SAI-VL aggregation were taken using the AFM technique.

In the outlook section, new challenges are discussed, and future possibilities for improving molecules capable of slowing down protein aggregation emerge.

At the end of this dissertation, all the synthetic procedures towards the target molecules as well as experimental conditions for the biophysical assays are thoroughly detailed.

Zusammenfassung

Alois Alzheimer beschrieb 1907 erstmals die Symptome einer neurodegenerativen Erkrankung, die später nach ihm als Alzheimer-Krankheit (AD) benannt wurde. Obwohl mehrere Ansätze zur Bekämpfung dieser, mit einer der häufigsten neurodegenerativen Erkrankungen unserer Zeit entwickelt wurden, konnte eine erfolgreiche pharmakologische Behandlung, die die Schädigung und Zerstörung von Neuronen verlangsamt oder stoppt, noch nicht gefunden werden. Nur palliative Therapien kommen hierfür derzeit zum Einsatz.

Im Verlauf dieser Arbeit wird in Kapitel eins zunächst eine Einführung zur Alzheimer-Krankheit und die an dieser schrecklichen neurodegenerativen Erkrankung beteiligten Proteine gegeben sowie alle Prozesse, an denen diese beteiligt sind. Anschließend werden einige Richtlinien für Patienten und deren Familien zum Umgang mit der Krankheit gegeben. Im letzten Teil dieses Kapitels sind verschiedene Therapien zur Bekämpfung der erheblichen Schädigung der Neuronen beschrieben. Dabei bilden die Immuntherapie, der Eingriff in den APP-Prozess und die Methoden zur Modulation der Aggregation und des Abbaus von Aβ den notwendigen theoretischen Hintergrund zum Verständnis des Ziels dieser Arbeit. Die wichtigsten therapeutischen Ansätze zur Modulation von Aβ werden im letzten Abschnitt ausführlich erläutert wie unter anderem Aminopyrazole und künstliche Metalloproteasen.

Im ersten Abschnitt des dritten Kapitels wird ein Ansatz zur Unterbrechung der an ACH beteiligten Prozesse, der Aβ-Abspaltung von APP mit folgender Aβ-Aggregation, beschrieben. Neue künstliche Metalloproteasen wurden entworfen, synthetisiert und mit verschiedenen Techniken wie ThT-Fluoreszenz oder CD-Spektroskopie untersucht. Eine bahnbrechende MS-Methode (Proteomics) wurde verwendet, wobei induziert durch Metallproteasen, die Spaltung des Volllängen-Aβ-Proteins analysiert wurde.

Neue β-Sheet-Brecher gegen Proteinaggregation werden im zweiten Teil des dritten Kapitels behandelt. Die Synthese der Verbindungen ist in diesem Abschnitt detailliert beschrieben, ebenso wie die verschiedenen Techniken, die deren Fähigkeit LC und Aβ-Aggregation zu verhindern, nachweisen. Außergewöhnliche Bilder eines Aminopyrazol-Derivats, das die SAI-VL-Aggregation verändert, wurden mit der AFM-Technik aufgenommen.

Im Ausblick werden kommende Herausforderungen diskutiert und Möglichkeiten zur zukünftigen Verbesserung von Molekülen zur Verlangsamung der Proteinaggregation aufgezeigt.

Am Ende dieser Dissertation sind alle synthetischen Verfahren zur Darstellung der Zielmoleküle sowie die experimentellen Bedingungen der biophysikalischen Assays ausführlich beschrieben.

Table of Contents

1. Introduction

1.1 Alzheimer's disease (AD)

1.1.1 Overview

Dementia is a term for several diseases that are mostly progressive and unremitting, affecting memory, cognitive abilities and behavior, and significantly interferes with a person's ability to maintain daily activities.[1] Alzheimer's disease (AD) is the most prevalent form of dementia with 50 million people affected worldwide. This means there is a recent case of AD every 3 seconds and scientists estimate that in 2050 this community will rise to 152 million.[2] In 2017 the World Health Organization (WHO) published a remarkable report called *Global action plan on the public health response to dementia 2017-2025*, guiding the WHO Member States to formulate this response through a multiphase, stepwise approach. According to this report, improvements in the population with dementia health responses have the potential to reduce the number of cases by 10-20%. For that reason, a new global dementia action plan was proposed to improve the needs of people with dementia and also their carers and families.[3]

An important factor in AD is, as is well known, age. Only 5% of the cases are genetically inherited and have an early onset and 95 % of patients suffer from sporadic outbreaks and have a later onset (> 80 years).[4] Even though the diagnosis is only possible after the patient's death, some symptoms are that are typical for the disease. These are categorized into 3 phases. In the first phase, the patient's short-term memory is restricted, and a loss of recent events or names is usual. This stems from the loss of around 25% of the hippocampus. After around two to four years, the damage to the limbic system worsens and the short-term memory is almost entirely lost and the patient has difficulties communicating. The patient also has trouble with orientation and concentration (the long-term memory is affected) and a personality change may be observed. This intermediate phase lasts for two to ten years and is followed by the third and final stage. Now 90% of the hippocampus is destroyed and the attack spreads to the cerebral cortex, leading to the loss of long-term memory; the patient totally loses any capacity to communicate or work. After one to three years, the patient dies.[5]

---

[1] Towards a dementia plan: a WHO guide, *World Health Organization*, **2018**.

[2] C. Patterson, World Alzheimer Report 2018: The state of the art of dementia research: New frontiers, *Alzheimer's disease Int*ernational, **2018**.

[3] Global action plan on the public health response to dementia 2017-2025, *World Health Organization*, **2017**.

[4] Avramopoulos D., *Genome Medicine*, **2009**, *1*(34).

[5] Pallas, M.; Camis, A.*, Current Pharmaceutical Design*, **2006**, *12*(33), 4389-4408.

However, AD can be diagnosed with more than 95% accuracy in living patients by combining techniques such as a complete evaluation of the cognitive function by neuropsychological and physical tests or taking a careful history from patients and their families.[6]

1.1.2 History and pathology of AD

Since Alois Alzheimer (1864-1915) published his well-known article in 1907[7,8] describing the symptoms of an unknown disease, our knowledge of this disease, named Alzheimer's disease by his mentor in 1910, is continuously growing. Nowadays, AD is one of the most common neurodegenerative diseases and scientific people around the world are joining forces across disciplines and collecting essential facts to discover more about this disease.[9]

Alzheimer was the first person to describe extracellular amyloid deposits (plaques) and intracellular neurofibrillary tangles (NFTs) in the brain slices of his patient (Figure 1).

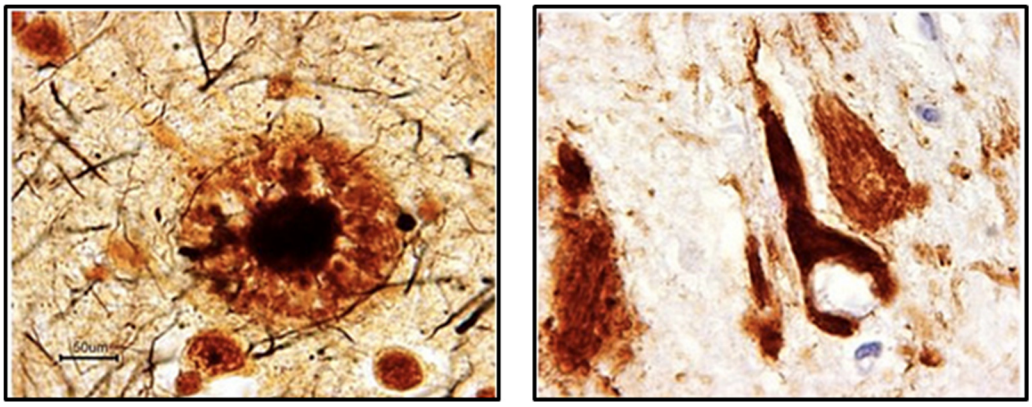

Figure 1. Stained amyloid deposits (right) and neurofibrillary tangles (left) in brain slices of a dementia patient.[10]

The extracellular plaques are small spherical structures around 10 to 160 nm in diameter consisting of amyloid-β (Aβ) peptide fragments. These peptide fragments are mainly comprised of 40 or 42 amino acid residues in length. The secondary structure is formed with a β-sheet in which parallel strands of amino acids are associated with each other due to hydrogen bonds. Recent studies show that deposits can be identified using Congo red, Thioflavin-S, or antibodies directed to these peptide fragments.

The NFTs are composed of intraneuronal aggregates of hyperphosphorylated and misfolded tau (τ), gives stability to microtubules. This protein aggregates inside neurons and their

[6] Mucke, L. Alzheimer's disease. *Nature*, **2009**, *461*, 895–897.
[7] Stelzmann, R.A.; Norman Schnitzlein; H. and Reed Murtagh, F., *Clinical Anatomy*, **1995**, *8*, 429-431.
[8] Alzheimer, A; *Zeitschrift für die gesamte Neurologie und Psychiatrie*, **1911**, *1*, 356-385.
[9] Bondi, M.W.; Edmonds, E.C.; Salmon, D.P., *Journal of the International Neuropsychological Society*, **2017**, *23*,818-831.
[10] taken from: http://dementiasos.files.wordpress.com/2011/12/dem-plaque-tangle.jpg, (Accessed March 27, **2020**).

processes, and microtubules tend to depolymerize, leading to neuronal dysfunction that correlates with the severity of the cognitive decline. NFTs like amyloid plaques can be identified using hematoxylineosin, silver staining, or an antibody against the microtubule-associated protein tau.[11,12]

1.1.3 The amyloid precursor protein (APP)

As mentioned above, most scientists agreed that there are two key proteins in the brain involved in dementia. One of them is Aβ which reaches abnormal levels in the brain of someone with Alzheimer's and forms plaques that collect between neurons and disrupt cell function. On the other hand, tau (τ) also reaches abnormal levels forming neurofibrillary tangles that block the neuron's transport system.[2] What scientists don't know is precisely how these proteins relate to each other or what causes them to build to such damaging levels. However, for 20 years, the amyloid cascade hypothesis (ACH) of AD has focused on the Aβ peptide formed from the amyloid precursor protein (APP) as the center of neurodegeneration.

The ACH is based on a neuron-centric characterization of the origin and development of the disease. The APP has a vital role in AD due to the sequential proteolytic cleavages that result in the generation of Aβ peptides. So, mutations in the APP gene will induce a cascade of events leading to neuronal cell death. The APP is partially responsible for cell growth and the brain's development as a transmembrane protein, but its concrete function in those processes is still unknown. It has three essential Isoforms: APP_{695}, APP_{751}, and APP_{770}. The only one capable of producing Aβ is APP_{695} which is also the most common one.[13] Its transmembrane function derives from a short intracellular and a long extracellular part. APP can be proteolytically cut at three points with the α-, β- and γ-secretase. These processes are generally divided into amyloidogenic and nonamyloidogenic ways (Figure 2).[14]

[11] Wippold, F.J.; Cairns, N.; Vo, K.; Holtzman, D.M.; Morris, J.C., *American Journal of Neuroradiology*, **2007**.
[12] Mot, R.T.; Hulette, M.C., *Neuroimaging Clinics*, **2005**, *15*(4), 755 – 765.
[13] Nalivaeva N.; Turner A., *FEBS letters*, **2013**, *587*(13), 2046-2054.
[14] Zheng H.; Koo E.H., *Molecular Neurodegeneration*, **2011**, *6*(27).

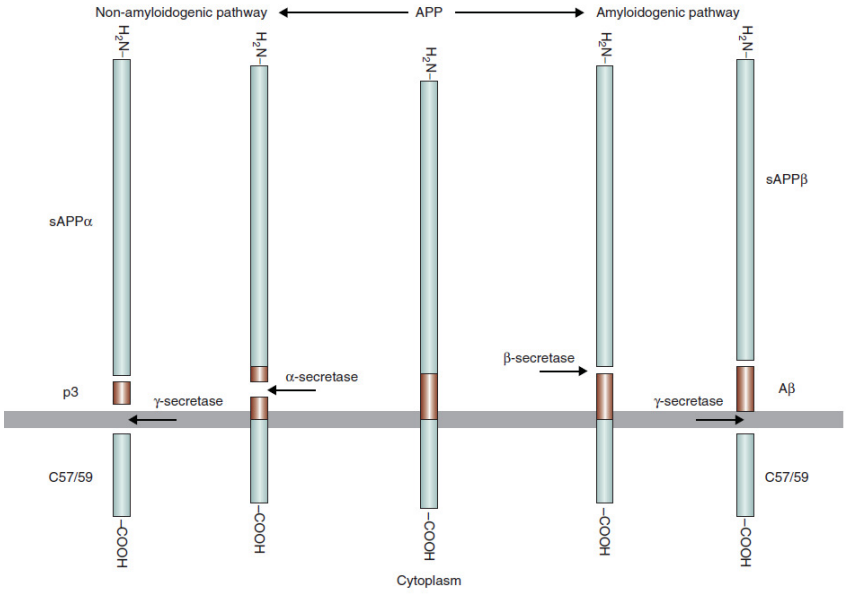

Figure 2. Nonamyloidogenic and amyloidogenic pathways of the proteolytic cleavage of the APP. [4]

The nonamyloidogenic way starts with the α-secretase, which cleaves APP into APPsα and α-CTF. While APPsα leaves the membrane, α-CTF remains inside it and is cut into a short oligopeptide p3 via γ-secretase.[15] Similarly, the amyloidogenic way starts by cleaving APP into APPsβ (N-Terminal fragment) and β-CTF (C-Terminal Fragment) with the β-secretase (BACE1). This γ-secretase cleaves β-CTF again to produce Aβ. Depending on the position of the γ-secretase cuts, there are isoforms of Aβ with 38 to 43 amino acids. The most prevalent isoforms are $A\beta_{40}$ and $A\beta_{42}$. Even though $A\beta_{40}$ makes up 90 to 95% of the Aβ isoforms in the brain, $A\beta_{42}$ is more prone to aggregate due to the higher non-polarity which stems from the two additional amino acids (Figure 3).[16]

5 10 15 20 25 30 35 40

D A E F R H D S G Y E V H H Q K L V F F A E D V G S N K G A I I G L M V G G V V I A

Figure 3. Amino acid (aa) sequence of Aβ (1-42): aa (1-27) hydrophilic region and aa (28-42) hydrophobic region. The cationic aa are shown in blue, anionic in red and the hydrophobic region underlined.[17]

In 2006, a connection between tau protein and APP was investigated by E. Mandelkow and E.M. Mandelkow, giving a potential pathway to link them.[18] Nowadays, this field is intensely investigated *in vitro* and *in vivo* leading to an important hypothesis where Aβ is

[15] Wolfe M.S, *Journal of Medicinal Chemistry*, **2001**, *44*(13), 2039-2060.
[16] a) Chiang P.K.; Lam M.A.; Luo Y.; *Current Molecular Medicine*, **2008**, *6*, 580-584. b) Teplow D.B., *Amyloid: The Journal of Protein Folding Disorders*, **1998**, *5*, 121-142. c) Ahmed M.; Davis J.; Aucoin D. *et al.*, *Nature Structural and Molecular Biology*, **2010**, *17*, 561-567.
[17] a) Ritcher L.; Munter L. Ness J. *et al.*, *Proc. Natl. Acad.Sci. U.S.A,* **2010**, *107*(33), 14597-14602. b) Serpell L.C., *Biochimica et biophysica acta*, **2009**, *1502*, 16-30.
[18] Goldsbury C.; Mocanu M.; Thies E. *et al.*, *Traffic*, **2006**, *7*(7), 873-888.

precisely required as an initial trigger and tau reciprocally intensifies Aβ deposition.[19] As mentioned before, even with all the information in hand, we still don't know how entirely Aβ and tau proteins link, and furthermore, the mechanisms behind these potential physiological aspects of APP are still unproven.

1.1.4 The amyloid cascade hypothesis (ACH)

Since its discovery in 1984 by George Glenner, Aβ was thought the cause of AD due to toxic species such as plaques and fibrils of Aβ. However, Hardy and Higgins uncovered the first mutation in the APP gene. They postulated in 1992, *"Our hypothesis is that deposition of amyloid β protein (AβP), the main component of the plaques, is the causative agent of Alzheimer's pathology and that the neurofibrillary tangles, cell loss, vascular damage, and dementia follow as a direct result of this deposition."*[20] These words were the beginning of a *cascade* of ideas to build the amyloid cascade hypothesis (ACH). In 1996, Schneuner and co-workers identified two mutations in the genes that encode the γ-secretase proteins presenilin 1/2 (PSEN1/2), which affect the position where γ-secretase cuts APP.[21] In 1999, McLean *et al*. demonstrated that not only but also correlates with higher markers of disease severity which means that soluble Aβ oligomers are the main causative factor in AD.[22] Some years ago, in 2010, Cizas *et al*. determined the most toxic oligomers of $A\beta_{42}$ (small oligomers) in neuronal cells and appealed to scientists to investigate in depth the original ACH and acknowledge soluble Aβ oligomers as toxic species responsible for the development of AD pathology.[23]

As previously mentioned, monomeric Aβ might have a physiological function and is supposed to play a role in neurological pathways. As it is well-known, $A\beta_{42}$ is more prone to aggregation than $A\beta_{40}$ and in many studies, it has been considered responsible for plaque formation. A large number of studies reflect that changes in the conformational structure of the soluble $A\beta_{42}$ monomers from the helical to the abnormal β-sheet conformation form dimers or trimers that aggregate into large oligomers and subsequently on to protofibrils, fibrils, and further on plaques. The conversion between these phases is dynamic and reversible.[24] The aggregation process is shown in figure 4.

[19] a) Moore et al., *Cell Reports*, **2015**, *11*, 689-696. b) Peters F.; Salihoglu H.; Pratsch K. et al., *The EMBO journal*, **2019**, *38*(23).
[20] Hardy J.A.; Higgins G.A., *Science*, **1992**, 256(5054), 184-185.
[21] Scheuner D.; Eckman C.; Jensen M. *et al*., *Nature Medicine*, **1996**, *2*, 864-870.
[22] McLean C.A.; Robert A.; Cherny *et al*., *Annals of Neurology*, **1999**, *46*(6), 860-866.
[23] Cizas P.; Budvytyte R.; Morkuniene R. *et al*., *Arch Biochem Biophys*, **2010,** *496*, 84-92.
[24] DaSilva K.A.; Shaw J.E.; McLaurin J., *Experimental Neurology*, **2010**, *223*, 311-321.

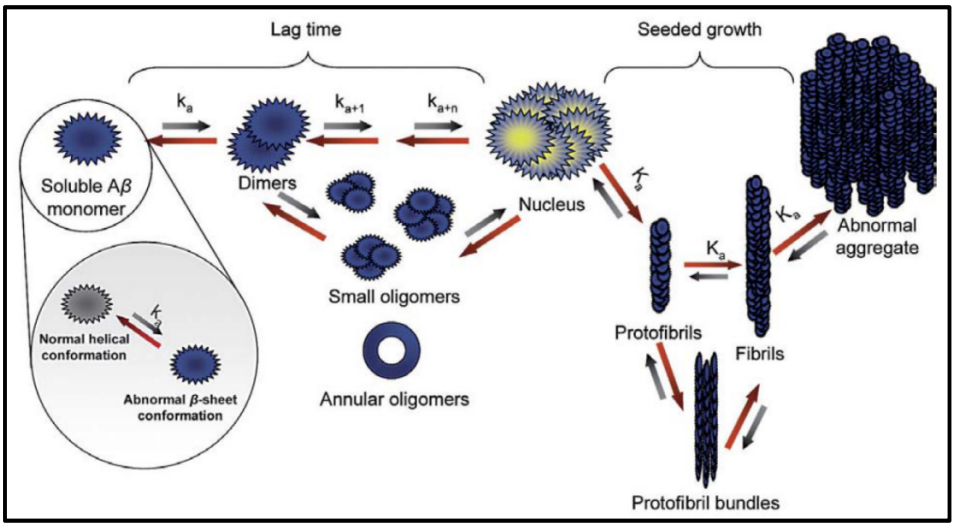

Figure 4. Schematic overview of Aβ aggregation.[25]

The Aβ oligomers are present in many shapes and sizes, such as Aβ-derived diffusible ligands (ADDLs) or annular oligomers. It is important to emphasize that monomers of Aβ are not toxic, but oligomers are, leading to neuronal cell death. The most neurotoxic species are the annular oligomers.[26] Details of Aβ species can be found below in Table 1. Additional SS-NMR technique determined fibrils of Aβ. Aβ (1-42) is consisting of parallel-stacked hairpin-like structures of peptides. Residues 18-42 form a β-strand-turn-β-strand hairpin motif which again consists of two intermolecular and parallel β-sheets (β1 and β2) formed by residues 18-26 and 31-42. This arrangement is stabilized by a salt bridge between D23 and K28 (Figure 5).[27, 28]

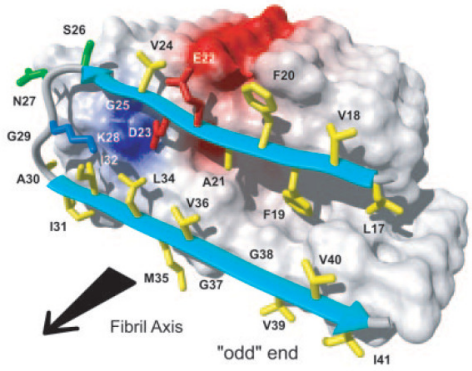

Figure 5. 3D structure of Aβ (1-42) fibril. B-sheets regions in blue arrows, secondary structure in gray, hydrophobic aa in yellow, polar aa in green, negative charged aa in red, and positive charged aa in dark blue. The aa sequence is from K17 to I41.[28]

[25] Finder V.H.; Glockshuber R., *Neurodegenerative Diseases*, **2007**, *4*, 13-27.
[26] Teplow D.B. *et al.*, *The Journal of Biological Chemistry*, **1999**, *274*(36), 25945-259952.
[27] Streltsov V. *et al.*, *The Journal of Neuroscience*, **2011**, *31*, 1419-1426.
[28] Lühr T.; Ritter C.; Adrian M. *et al.*, *Proc. Natl. Acad.Sci. U.S.A*, **2005**, *102*, 17342-17347.

Table 1. Ovierview of Aβ species.[25]

Aβ species	Characteristics
Monomers	Soluble amphipathic molecule, generated from APP; potential α-helical, random coil or β-sheet conformation
Dimers	Intracellular localization *in vivo*, in human brain extracts and *in vitro*; hydrophobic core; diameter of about 35 nm
Trimers	Observed *in vivo* in mouse models; potential key role as a subunit of toxic oligomers
Small oligomers	Observed *in vivo* in AD patients as well as in mouse models and *in vitro*; heteromorphous; comprising of 3-50 monomers; mostly transient and unstable, but toxic
Annular oligomers	Observed in cell culture and *in vitro* experiments; potential role as membrane-disrupting pore or ion channels
ADDLS	Observed in murine and human brain extracts as wells as i*n vitro*; nonfibrillar; neurotoxic; 17-42 kDa; trimers to 24mers
Protofibrils	Observed *in vitro*; short; flexible, rod-like structure; maximum size 8 x 200 nm; binding Congo red and Thioflavin T; precursor of mature fibrils; toxic
Fibrils	Observed in AD patients as wells as in mouse models and *in vitro*; bond Congo red and Thioflavin T; stable, filamentous Aβ aggregates composed of repeating Aβ units perpendicular to the fiber axis
Plaques	Observed *in vivo* in AD patients as well as in mouse models; large extracellular Aβ deposits; predominantly composed of fibrils; not toxic; surrounded by dystrophic dendrites, axons, activated microglia and reactive astrocytes

The ACH is the most substantive model of the pathogenesis of AD, but several studies *in vivo* led to a revision of ACH. The ACH involves an imbalance between Aβ production and Aβ deposition in the brain.[29] These deposits imply neuronal cell damage and as a consequence hyperphosphorylation of tau occurs, leading to neuronal cell death. So in recent years, a modification of ACH was proposed where the accumulation of Aβ is more important than extracellular deposits. In figure 6 shows a comparison between the classical ACH and the modified ACH.[30]

[29] Armstrong R.A., *Folia Neuropathologica*, **2014**, *52*, 211-225.
[30] Wirths O.; Multhaup G.; Bayer T.A., *Journal of Neurochemistry*, **2004**, *91*, 513-520.

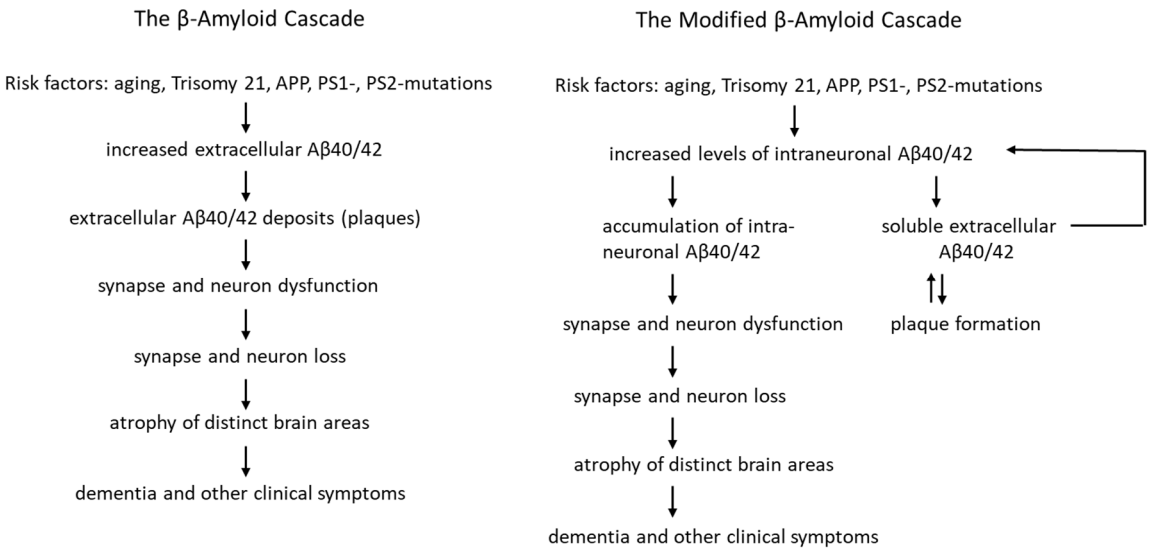

Figure 6. Comparison between classical and modified amyloid cascade hypothesis.[30]

1.1.5 The role of Tau

As mention before, tau is the other protein involved in AD. It is not only presented in AD but also other neurodegenerative diseases (tauopathies) such as Pick's disease.[31] However, a complete connection between Aβ and tau has not yet been established.[2]

Tau is predisposed to be phosphorylated, which leads to destabilize the microtubules, and consequently, a misfolding and aggregation of the protein occurs. Changes in subcellular levels emerge, and these alterations could induce pathological effects.[32] The aggregation of Tau causes oligomer formation, subsequently NFTs and, in the end, neuronal death. Lamentably, a precise mechanism by which tau reaches abnormal levels in the brain is not yet understood.[33] In multiple studies, some peptide motifs of tau such as VQIINK[280] or VQIVYK[311] were identified by NMR techniques or Cryo-EM[34] (cryogenic electron microscopy), which likely mediate intermolecular interaction between tau molecules to form oligomers associated with aggregation.[35]

1.2 Diagnosis of AD

Nowadays, thanks to the intensive investigation of the different forms of expressing dementia, we are able to determine approximately which disease a person is suffering. Some diseases, such as Parkinson's disease (PD) or Creutzfeldt-Jacob disease (CJD), share common characteristics and symptoms with AD, hampering the precise diagnosis. At the

[31] Wolfe M., *Scientifica*, **2012**,*4.*
[32] Avila J. *et al.*, *Physiol. Rew.*, **2004**, *84*, 361-384.
[33] Gendron T., Petrucelli L., *Mol. Neurodegeneration*, **2009**, *3*(13).
[34] Zhang W. *et al.*, *Nature*, **2020**, 283-287.
[35] Peterson D. *et al.*, *Biochemistry*, **2008**, *47*, 7393-7404.

moment, the full comprehensive and accurate diagnosis is only possible *post mortem* by the detection of Aβ deposits in the brain. On the other hand, there are multiple diagnostic methods that can be used to identify potential diseases.[36]

First and foremost, when you suspect Alzheimer's, your own, or someone close, arrange a visit with a doctor and explain what happens and the difficulties that you identify. Thereby, they will be able to evaluate the information and decide if there are enough reasons to deepen into the exploration. The following phase is an exhaustive evaluation and exploration by a neurologist. An elaborated neuropsychological examination is carried out to clarify the characteristics and scope of the cognitive, the attitude, and its possible impact on daily life.[37] Besides, a complex neuroimaging test, such as Positron Emission Tomography (PET), is required to detect and quantify amyloid plaques which are the main feature of AD. Over the past decade, PET with carbon-11-labeled Pittsburg Compound B (PIB), which is an analog of thioflavin T (ThT) and binds Aβ deposits with high sensitivity and specificity, emerged to detect these amyloid plaques even in tracer concentrations. PIB-PET has a limit to use of 10 min due to the half-life of ^{11}C, so not long ago another amyloid labelled with fluorine 18, 110-minute half-life, came out to replace PIB-PET.[38] Less commonly, a genetic test is carried out if there is a background of AD in the family.

In March 2020, a multidisciplinary group published results where they used a newly developed Aβ analog ($A\beta^{pH}$) to detect, for the first time, phagocytic uptake of Aβ into glial cell lysosomes IN REAL TIME. This pioneering tool can be used to answer questions associated with Aβ mechanisms and develop new therapeutic strategies to promote Aβ clearance.[39]

1.3 Therapy of AD

Until now, there is not a pharmacologic treatment for AD that slows or stops the damage and destruction of neurons. Only palliative treatments are approved by the U.S. Food and Drug Administration (FDA), which relieve the AD symptoms. The FDA has authorized five drugs for the treatment: rivastigmine, galantamine, donepezil, memantine, and memantine combined with donepezil.[40] These drugs are mostly antidepressants and antipsychotics. The first three drugs are acetylcholinesterase inhibitors (AChEIs) which show benefit on cognitive symptoms as well as memory and concentration, and an N-methyl-D-aspartate

[36] Alzheimer's Association, *Azlheimer's & Dementia*, **2011**, *7*, 208-244.
[37] Com es diagnostic l'Alzheimer?, *Fundació Pasqual Maragall*, **2017**.
[38] Laforce R.; Rabinovici G.D, *Alzheimer's Research & Therapy*, **2011**, *3*(31).
[39] Prakash P.; Hethava K.P.; Korte N.; Izquierdo P. *et al.*, *Biorxiv*, **2020**.
[40] Alzheimer's Association, *Alzheimers Dement.*, **2020**.

(NMDA) receptor antagonist memantine which blocks specific receptors in the brain under abnormal conditions that can damage neurons.[41]

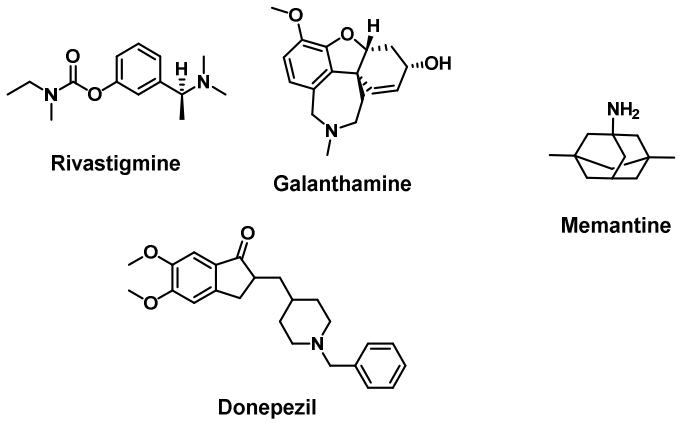

Figure 7. Structure of the five approved drugs by the FDA. Acetylcholinesterase inhibitors (AChEIs) (left) and N-methyl-D-aspartate (NMDA) receptor antagonist (right).[40]

Acetylcholinesterase (AChE) is an important enzyme involved in the cholinergic nervous system, which decomposes acetylcholine (ACh) to acetate and choline (Figure 8). Inhibition of AChE leads to enhanced activity of ACh receptors and, as a result, improved long-term potentiation. The AChEIs were approved for the treatment of mild and moderate stages of AD.[42] Even though there exist diverse side-effects as well as insomnia, nausea, diarrhoea, and occasionally in high doses, i.e., of donepezil breathing problems and bradycardia.[43]

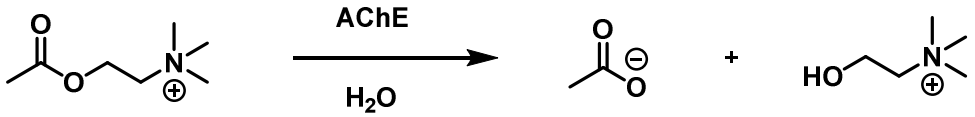

Figure 8. Catalysis of acetylcholinesterase (AChE). [42]

Glutamate is a neurotransmitter involved in the regulation of neuronal growth, learning, and memory. Under normal circumstances, the glutamate cycle controls the glutamate that is accessible for receptors. Under abnormal conditions, the glutamate is accumulated, leading to a persistent decrease of activation of NMDA receptors, leading to neuronal toxicity. Beyond that, memantine is an uncompetitive NMDA receptor antagonist that blocks the continuous activation of NMDA receptors and protect neurons from apoptosis due to the glutamate-mediated excitotoxicity .[43]

[41] Apostolova L.G., *Continuum*, **2016**, *22*, 419-434.
[42] Sharma K., *Molecular Medicine Reports*, **2019**, *20*, 1479-1487.
[43] Blennow K.; de Leon M.J; Zetterberg H., *The Lancet*, **2006**, *368*(9533), 387-403.

1.3.1 Immunotherapy

Since Schenk *et al.* reported in 1999[44] an active immunization with human $A\beta_{42}$ that attenuates Aβ deposition, several works have been developed using passive immunization, obtaining similar results. These results were the beginning to start clinical trials with the vaccine AN1792, composed of $A\beta_{42}$.[45] However, this anti- Aβ vaccine failed in the final stages (phase II) of the clinical assays because 6% of the treated patients developed meningoencephalitis. For this reason, the second generation of active vaccines was developed and, at the moment, are tested.[46]

As noted, immunization against Aβ can be achieved in two different pathways (Figure 9). Active immunization will full-length Aβ or parts of it that leads to polyclonal antibody response and it generates anti- Aβ antibodies recognizing multiple epitopes on the protein. The second way is passive immunization consisting of the directed administration of already selected antibodies against Aβ to the patient. These bind to Aβ molecules and targets them for clearance. Both active and passive immunization have disadvantages and are under investigation. In the case of active vaccination with AN1792, as described above the side-effect emerged in 6% of treated patients and it was suggested due to a T-cell response against the mid- terminal and C-terminal part of the peptide. But on the other hand, only a doctor's visits are necessary what does not happen in the passive vaccination, requiring monthly meetings.[47]

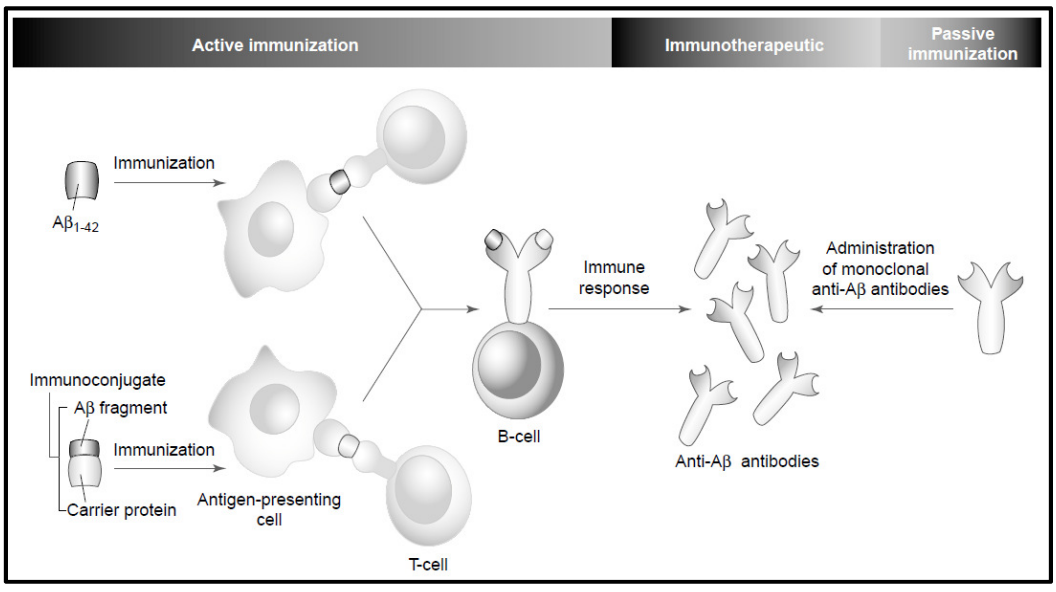

Figure 9. Pathways of immunization against Aβ.[48]

[44] Schenk D.; Barbour R.; Dunn W. *et al.*, *Nature*, **1999**, *400*, 173-177.
[45] Vellas B.; Black R.; Rhal L.J. *et al.*, *Current Alzheimer Research*, **2009**, *6*, 144-151.
[46] Marciani D.J, *Research*, **2019**.
[47] Lemere C.A., *Molecular Neurodegeneration*, **2013**, *8*(36).
[48] Schenk D.; Hagen M.; Seubert P., *Current Opinion in Immunology*, **2004**, *16*, 599-606.

1.3.2 Intervention of APP processing

Another approach to fight AD is modulating the APP process, which could reduce the activity of the amyloidogenic APP cleavage pathway and Aβ cannot be generated. This modulation can be achieved by inhibiting or modulating β-secretase or γ- secretase activity.[49]

The β-secretase enzyme is involved not only in the first stages of APP but also expresses in other tissues such as the pancreas. For example, a β-secretase inhibitor called Verubecestat or MK8931 (designed by Merck) was tested in clinical phase III in 2016, but in February 2018, the trial was terminated by a committee since this drug failed to show significant benefits. In February 2019, a paper was published with the clinical assay results, reporting side-effects and concluding the trial. Even though several compounds show only partially inhibitory activity and fail in clinical trials, they give us a clue for further investigations.[50]

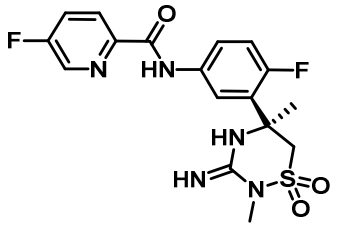

Figure 10. Structure of Verubecestat from Merck (β-secretase inhibitor).[51]

In the case of γ-secretase, most drugs failed because the enzyme is involved in the proteolysis of many intramembranous signalling proteins. The enzyme interferes with Notch protein, which is responsible for the regulating of cell proliferation, differentiation, and growth and induces severe side effects such as gastrointestinal disorders or increasing risk of skin cancer.[43] For example, Semagacestat (LY-450139), from Eli Lilly, was designed to reduce the levels of Aβ in plasma and the cerebrospinal fluid (CFS). The clinical results showed to an inability to retard AD and adverse effects such as weight loss, increased risk for skin cancer, and risk of infection related to Notch signalling activity. The trial was also terminated in phase III.[52] Another promising drug Avagacestat, designed by Bristol-Myers Squibb, was discarded too due to a lack of efficacy and adverse side-effects.[53]

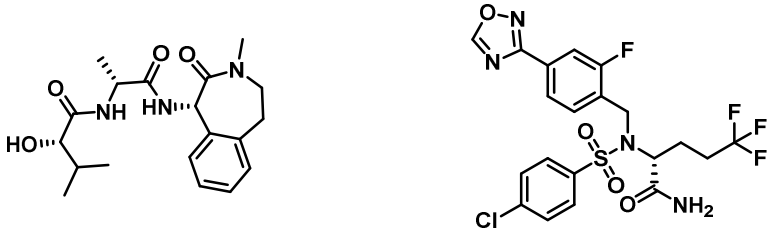

Figure 11. Structure of Semegacestat (left) and Avagacestat (right) (γ-secretase inhibitors).

[49] Folch J.; Petro D. *et al.*, *Neural Plasticity*, **2016**, Article ID 8501693.
[50] Egan M.F. *et al., Alzheimer's Research & Therapy*, **2019**, *11*, 68.
[51] Kennedy M.E *et al.*, *Science Translational Medicine*, **2016**, *8*(363).
[52] Doody R.S *et al.*, *The New England Journal of Medicine*, **2013**, *369*(4).
[53] Coric V.; Salloway S.; van Dyck C.H. *et al.*, *JAMA Neurology*, **2015**, *72*, 1324-1333.

For this reason, selective γ- secretase modulators (SGSM) were designed to prevent the side-effects associated with the enzyme inhibition. The purpose of these modulators is to block the APP process without interfering in the Notch pathway. Some examples of these drugs are ibuprofen or R-flurbiprofen but these compounds did not show efficacy for AD.[49] As mentioned before, negative results in clinical trials lead to improve and refine these drugs.

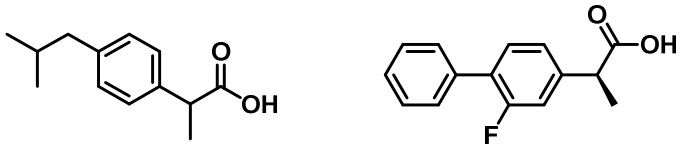

Figure 12. Structure of Ibuprofen (left) and Tarenflurbil (R-flurbiprofen, right) (γ-secretase modulators).

1.3.3 Modulation of Aβ aggregation and degradation

Another therapeutic approach is the modulation of Aβ aggregation or degradation into non-toxic or inactive species.

1.3.3.1 Peptides

Peptides, compared with antibodies, have some limitations such as low oral bioavailability (injection is required) or short half-life (rapid degradation). However, drugs that require injection for administration have become more accepted, and pharmaceuticals support the idea of studying peptides as drug candidates. Besides, the small size of peptides gives the ability to penetrate into tissues better than antibodies and due to the short half-life, they do not accumulate in tissues. Peptides offer greater efficacy, selectivity and specificity than small organic molecules. For these reasons, peptides are becoming increasingly active as drugs against a considerable number of diseases.[54]

In 1996, Tjernberg and co-workers found a short amino acid sequence KLVFF (Figure 13), related with the hydrophobic region of Aβ (16-20) (Figure 3), that inhibited the polymerization of Aβ. The challenge of Tjernberg was to identify the most important regions of Aβ involved in polymerization, and based on this, synthesize a small peptide ligand to bind the whole sequence of Aβ and inhibit the polymerization.[55]

[54] Vlieghe P. *et al.*, *Drug Discovery Today*, **2010**, *15*(1/2), 40-56.
[55] Tjernberg L.O. *et al.*, *The Journal of Biological Chemistry*, **1996**, *271*(15), 8545-8548.

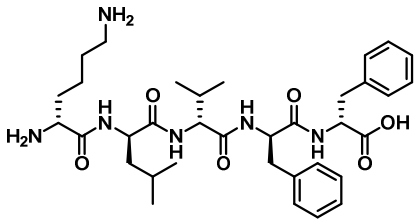

Figure 13. Structure of KLVFF, a small peptide designed by Tjernberg in 1996 that inhibits Aβ polymerization.[55]

In accordance with this small fragment (KLVFF), Gordon *et al.* developed several N-methyl amino acids (figure 14), designed to inhibit Aβ fibrillogenesis and disassemble fibrils due to the high solubility of the modification in the chain of the small peptide.[56]

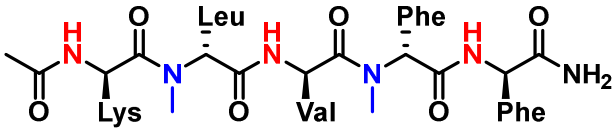

Figure 14. N-methylation of the peptide KLVFF in β-strand conformation. The modification of the peptide presents two sides; one (red) that is able to form hydrogen bonds through the amide hydrogens and the second side (blue) in which the capacity of forming hydrogen bond is reduced due to methylation.[56]

Later on, Soto *et al.* synthesized another pentapeptide LVFFA (Figure 15), based on Tjernberg studies, specific for Aβ, inhibit Aβ aggregation powerfully and reduces Aβ cell toxicity.[57] This peptide served as a template for different peptide modifications such as LPFFD (Figure 15) peptide, which showed a significant reduction of Aβ plaques in AD model mice.[58]

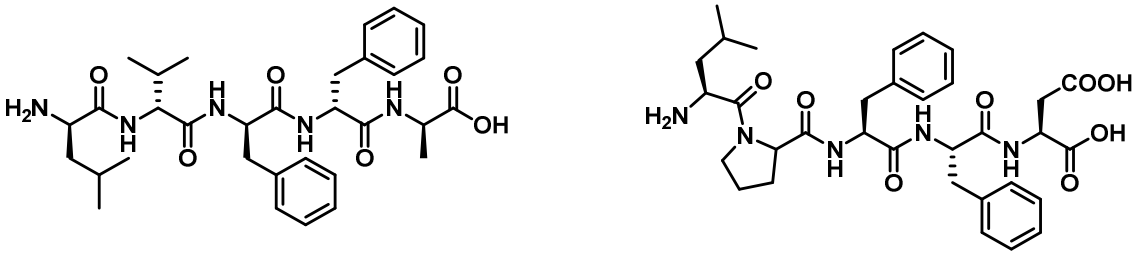

Figure 15. Structure of pentapeptides LVFFA (left) and LPFFD (right), synthesized by Soto *et al.*[58]

Two D-enantiomeric peptides, D1 and D3 (Figure 16), were identified by a new technique called mirror-image phage display selection. D1-peptide is a 12-mer (QSHYRHISPAQV)

[56] Gordon D.J. *et al.*, *The Journal of Peptide Research*, **2002**, *60*, 37-55.
[57] Estrada L.D; Lasagna C.; Soto C., *Pharmacological Mechanisms in Alzheimer's Therapeutics*, **2007**, *15*, 238-254.
[58] Soto C. *et al.*, *Nature Medicine*, **1998**, *4*(7), 822-826.

that reduces Aβ cell toxicity and amyloid deposits but it is not suitable as an aggregation inhibitor but rather as one molecular prober for *in vivo* imaging amyloid plaques.[59]

Further on, D3-peptide was identified with promising results being more efficient than D1. D3 is also a 12-mer peptide (RPRTRLHTHRNR) that modulates Aβ aggregation and reduces Aβ cell toxicity. *In vivo* studies showed that D3 significantly reduced plaques and inflammatory processes in the brain of transgenic AD mice.[60,61]

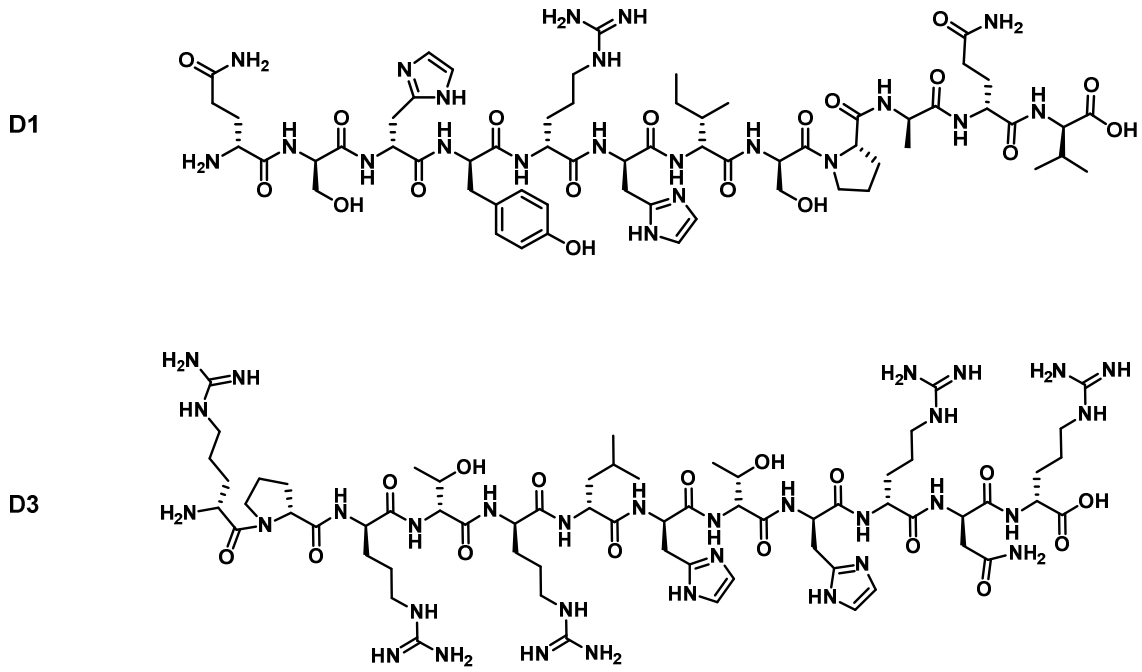

Figure 16. Structure of D1 (top) and D3 (bottom) peptides.[59,60,61]

In principle, the phage display selection uses a bacteriophage coat protein to connect to a peptide. With the concept of the technique, libraries of random amino acid sequences are feasible to develop. Schumacher and co-workers developed a new technique based on phage display, named mirror-image phage display, to obtain D-amino acids.[62] It's known that D-amino acids are protease-resistant by comparison with L-amino acids. Also, D-form shows lower immunogenicity, even though immunogenicity levels depend on administration dose and frequency. In the case of the mirror-image phage display technique, L-peptides supported on the surface of a phage bind to a D-target molecule (previously mirrored from L-target). The complex formed is again mirrored, obtaining D-peptides and the original L-

[59] a) Wiesehan K. *et al.*, *ChemBioChem*, **2003**, *4*, 748-753. b) Van Groen T. *et al.*, *ChemMedChem*, **2009**, *4*, 276-282. c) Funke A.S. *et al.*, *PLoS ONE*, **2012**, *7*(7).

[60] Liu.H. *et al.*, *Rejuvenation Research*, **2010**, *13*(2-3), 210-213.

[61] Funke S.A. *et al.*, *ACS Chemical Neuroscience*, **2010**, *1*, 1639-1648.

[62] Schumacher N.M. *et al.*, *Science*, **1996**, *271*, 1854-1857.

target molecule. In figure 17, the basic principles of these two techniques are schematically presented.[63]

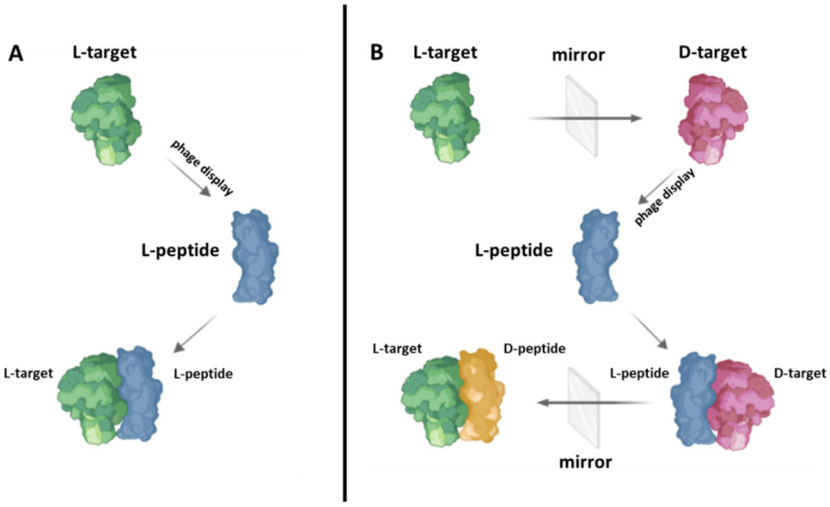

Figure 17. Scheme of phage display (A) and mirror-image phage display (B).[58]

In 2010, Müller-Schiffmann *et al.* developed a hybrid compound between D3-peptide and a β-sheet breaking aminopyrazole. This combination of different classes of drugs links covalently to each other to produce superior synergistic effects and lead to novel properties.[64]

1.3.3.2 Small aromatic molecules

In 2010, Ladiwala *et al.* evaluated different small aromatic molecules and classified them into three classes by their interactions with $A\beta_{42}$ soluble oligomers (Figure 18).[65]

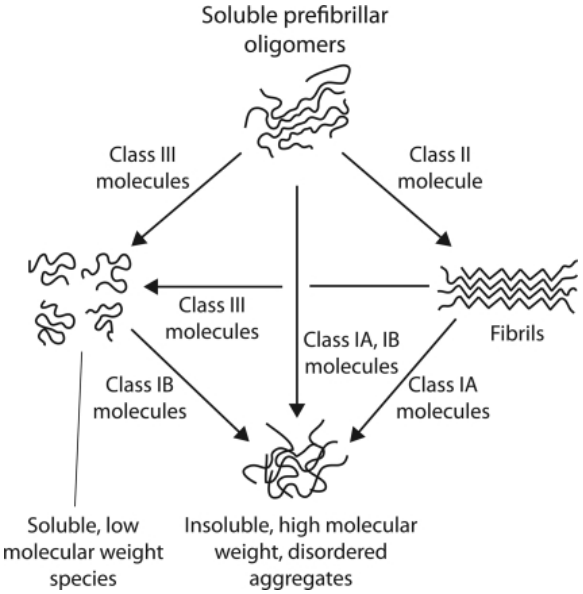

Figure 18. Overview of different pathways to remodel Aβ soluble oligomers with small aromatic molecules.[65]

[63] Wiesehan K.; Willbold D., *ChemBioChem*, **2003**, *4*, 811-815.
[64] *Muller-Schiffmann A. et al., Angewandte International Edition,* **2010,** *49,* 8743-8746.
[65] Ladiwala *et al.*, *The Journal of Biological Chemistry*, **2011**, *286*(5), 3209-3218.

The aromatic compound related to class I converts soluble oligomers into large (non-toxic conformers). In this group, they referred to molecules such as myricetin, nordihydroguaiaretic acid (NDGA) and riluzole (Figure 19).[54] It has been demonstrated that polyphenols like NDGA bind specifically to free Aβ and inhibit the polymerization of Aβ disaggregating Aβ fibrils.[66] In the case of myricetin, a natural product, it was shown that this polyphenol also binds the fibrillary Aβ and is also considered a tau aggregation inhibitor.[67,68] Riluzole significantly reduced Aβ oligomers, although the this approved FDA drug's action mechanism has not been completely determined and described.[69]

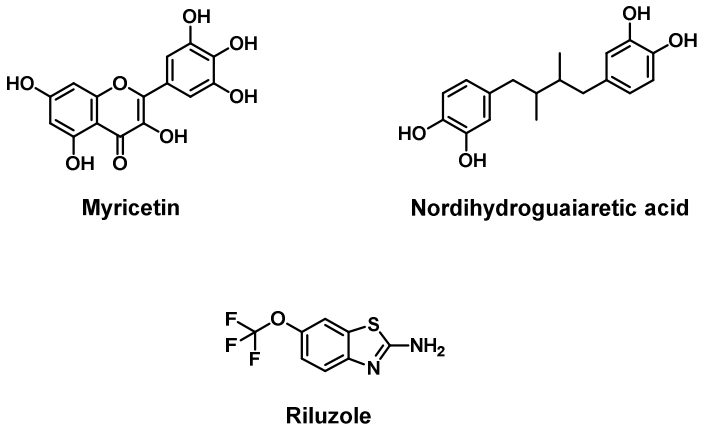

Figure 19. Structure of class I aromatic small molecules, myricetin, NDGA and riluzole.

In class II, it was categorized methylene blue (Figure 20) as an aromatic molecule that transforms soluble oligomers into fibrils in a rapid form.[54] It is well-known that Aβ fibrils are more toxic than Aβ monomers but it was demonstrated that methylene blue rapidly remodels Aβ oligomers into β-sheet-rich fibrils, which are inactive against disaggregated and fibrillary Aβ. Compared with tau protein, methylene blue has been shown in clinical trials that slow dementia progression.[70]

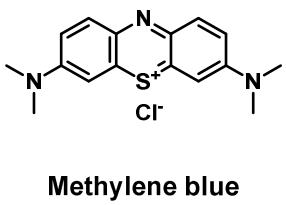

Figure 20. Structure of class II aromatic small molecule, methylene blue.

[66] Ono K. *et al., Journal of Neurochemistry*, **2003**, *87*, 172-181.
[67] DeToma A.S; Choi J.; Braymer J.; Lim M.H, *ChemBioChem*, **2011**, *12*(8), 1198-1201.
[68] Blair L.J. *et al.*, *Alzheimer's research & Therapy*, **2013**, *5*(41).
[69] Mokhtari Z. *et al.*, *Neurophysiology*, **2019**, *51*(4), 266-271.
[70] Cisek K.; Cooper G.L.; Huseby C.J.; Kuret J., *Current Alzheimer Research*, **2014**, *11*, 918-927.

Tannic acid or piceid (Figure 21) are categorized in class III, which remodel soluble oligomers into low molecular weight (non-toxic species).[54,71] Part of the current thesis is based on class III well-known molecules, aminopyrazoles. In the following section, the process of obtaining a potent molecule that disassembles preformed Aβ fibrils is explained in detail.

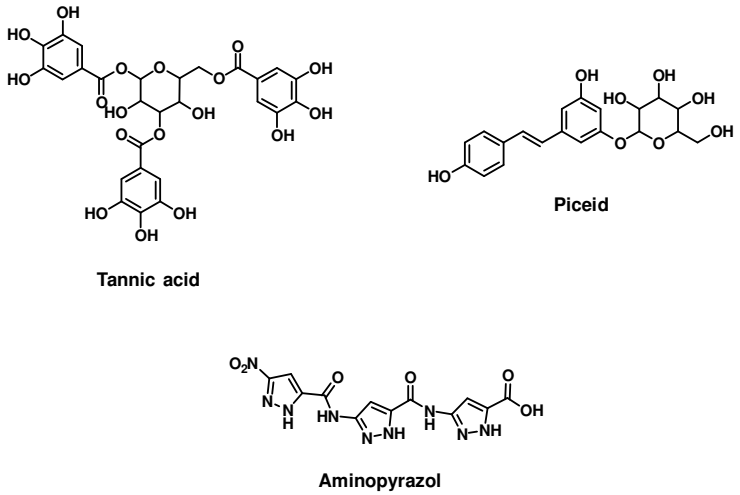

Figure 21. Structure of class III aromatic small molecules, tannic acid, piceid and a trimeric unit of aminopyrazole.

1.3.3.3 Aminopyrazoles: a prospective study

Kirsten and Schrader designed for the first time, in 1996, an aromatic system that selectively binds the backbone of a misfolded dipeptide with a cross-β-sheet conformation and stabilizes the system via hydrogen bonding.[72]

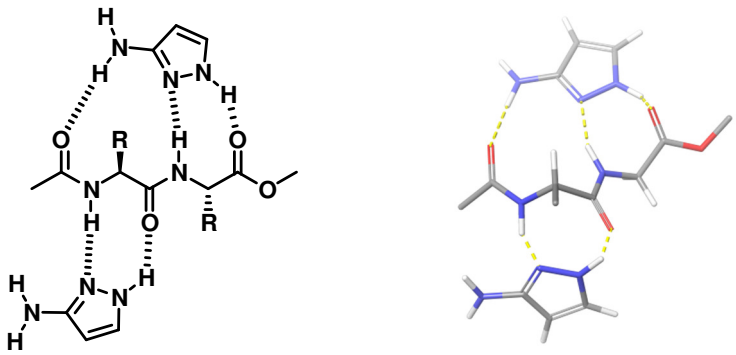

Figure 22. Stabilization of the backbone of a dipeptide, according to Kirsten and Schrader. One molecule of aminopyrazole forms three hydrogen bonds with the dipeptide and another molecule of aminopyrazole interacts simultaneously with the dipeptide forming two hydrogen bonds.[73]

[71] Ono K. *et al.*, *BBA*, **2004**, *1690*, 193-202.
[72] Kirsten C.; Schrader T., *Chemical Communication*, **1996**, 2089-2090.
[73] Kirsten C.; Schrader T., *Journal of the American Society*, **1997**, *119*(50), 12061-12068.

It should be noted that aminopyrazoles are in a tautomeric equilibrium between a DAD arrangement, the predominant, which has the favorable sequence for peptide complexation and a DDA tautomer not complementary to a peptide strand.[74]

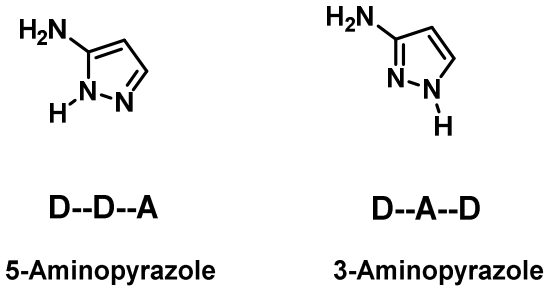

Figure 23. Tautomers of the monomeric aminopyrazole with their respective hydrogen bond patterns.[74]

Rzepecki *et al*. optimized the concept using the monomeric unit 3-aminopyrazole-5-carboxylic acid as a building block and forming oligomeric aminopyrazole units, which bind more strongly to β-sheet structures due to a large number of hydrogen bonds.[74] Dimers, trimer and tetramers were synthesized and tested. It was found that oligomers showed poor solubility, so further modifications attaching proteinogenic amino acids were carried out to increase these hybrid compounds' solubility. Trimer compound **1** was identified as the most effective inhibitor of $A\beta_{40}$ and *in vitro* experiments showed that this ligand prevents and disaggregates Aβ oligomers.[75]

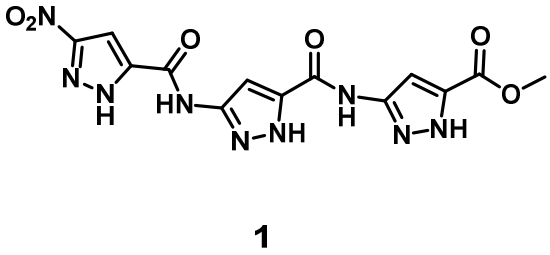

1

Figure 24. Structure of the trimer **1**.[75]

Hochdörffer synthesized many compounds functionalizing the trimer ligand in the C-terminus with various peptide residues and with linkers as GABA or TEG to increase water solubility and lipophilicity. Trimer-KKKKKG **2** was found as a potent inhibitor of the aggregation of $A\beta_{42}$, and at the same time, Trimer-K **3** showed the most efficient suppression of Aβ fibril formation.[76]

[74]Rzepecki P., "Neue ß-Faltblattliganden zur Hemmung der Aggregation des Amyloid-ß-Peptids", Marburg, **2004**.
[75] Rzepecki P. *et al.*, *The Journal of Biological Chemistry*, **2004**, *279*(46), 47497-47505.
[76]Hochdörffer K., "Oligomere Aminopyrazole gegen die pathologische Aggregation des Alzheimer-Peptids", Essen, **2009.**

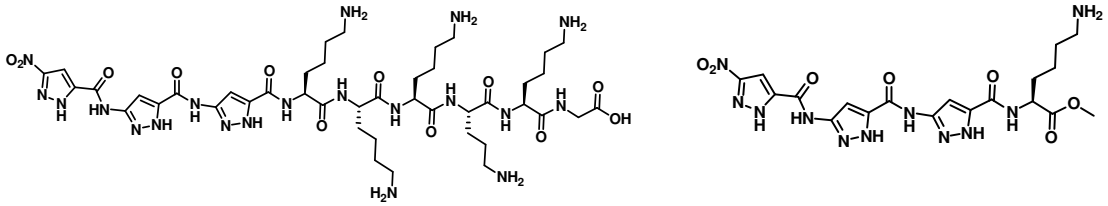

Figure 25. Structures of Trimer-KKKKKG **2** and Trimer-K **3**.[76]

Based on these promising results, März-Berberich synthesized a hybrid compound between aminopyrazoles and the well-known D-peptides (D1- and D3-peptides), which has been discussed in the section 1.3.3.1. Thanks to solid phase synthesis, it was feasible to attach the peptide, previously synthesized by solid-phase peptide synthesis (SPPS), to the trimer.[77]

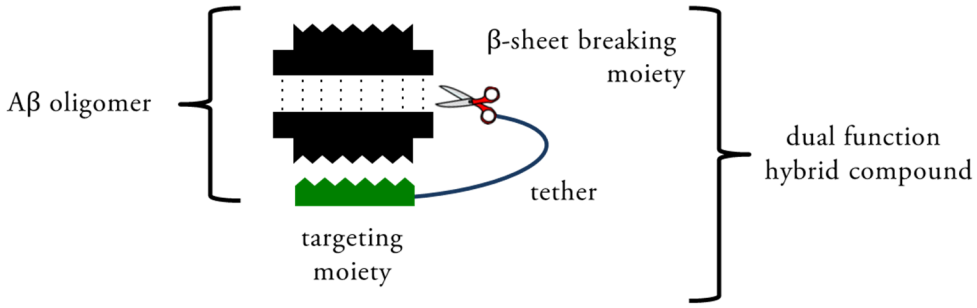

Figure 26. Schematic representation of bifunctional hybrid compounds.[64]

A large number of hybrid compounds were synthesized and biophysically tested, thanks to Korth and workers, finding a potential hybrid compound, Trimer-TEG-D3 **4**, that showed strong inhibition of Aβ oligomerization. MD simulations showed that the spacer TEG (blue) is required for an optimal cooperative effect between Aβ moiety and the β-sheet-breaker because this linker has an adequate spacer length. It was also found that the glutamate bridge (orange) is spatially closed to the basic amino acid residues of D3 peptide (green) while the trimeric unit (red) interacts with F19 and F20 (gray). These elements are crucial and can destabilize Aβ peptide due to the synergistic cooperation between them.[64]

[77] März-Berberich J., "Aminopyrazol-Hybridverbindungen gegen Aggregation und Neurotoxizität des Alzheimer-Peptids", Essen, **2010**.

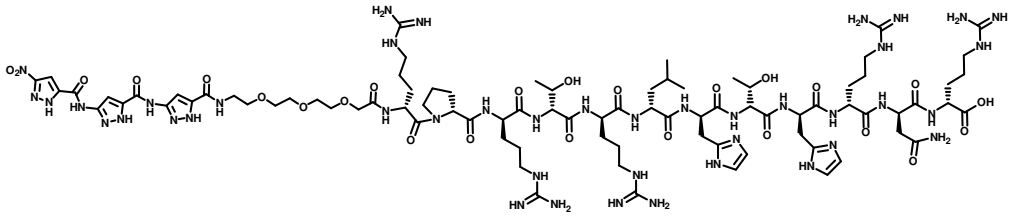

4

Trimer-TEG-D3

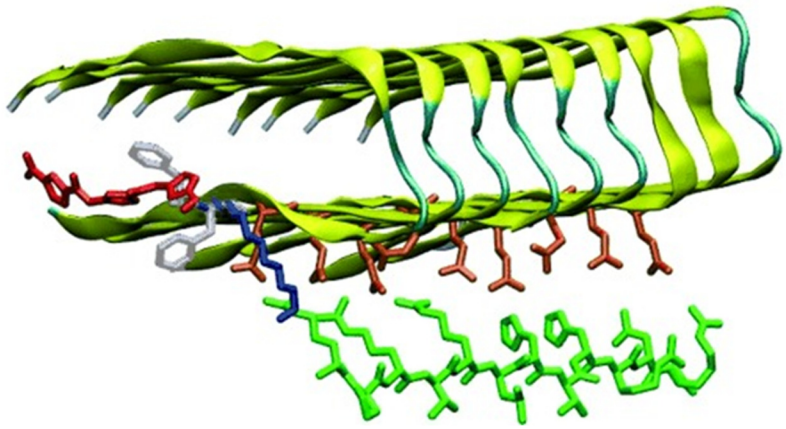

Figure 27. Structure of Trimer-TEG-D3 hybrid compound (top). MD simulations of Trimer-TEG-D3 (bottom). Aβ ligand model in yellow, glutamates residues in orange, phenylalanines 19 and 20 in gray, trimer in red, TEG spacer in blue and D3 peptide in green.[64]

Besides, trimer derivatives were synthesized and their activity against Aβ was measured. Trimer-TEG-KKKKKG **6**, Trimer-TEG-LPFFD **7** and Trimer-TEG-K-OMe **5** were the most efficient inhibitors of Aβ and were able to reduce the toxicity of $A\beta_{42}$ in cell cultures.[77]

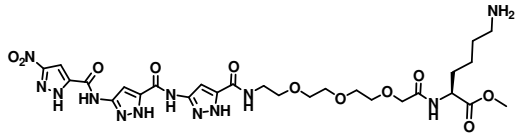

Trimer-TEG-K-OMe

5

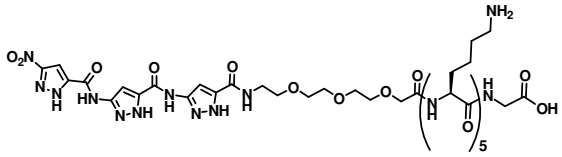

Trimer-TEG-KKKKKG

6

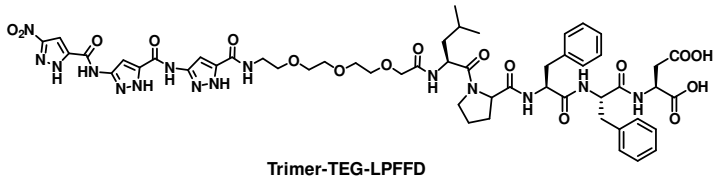

Trimer-TEG-LPFFD

7

Figure 28. Structures of the new trimer derivatives synthesized by März-Berberich.[77]

Furthermore, März-Berberich's approach was to connect aminopyrazoles derivatives with antibodies using passive immunization. The starting point of this method is the non-

covalent linkage of two active substances via metal complexation.[77] The aminopyrazole derivative **9** was designed to link an IC16 antibody or its scFv which specifically recognizes Aβ (1-16) sequence and the antibody fragment region 1-8.[78]

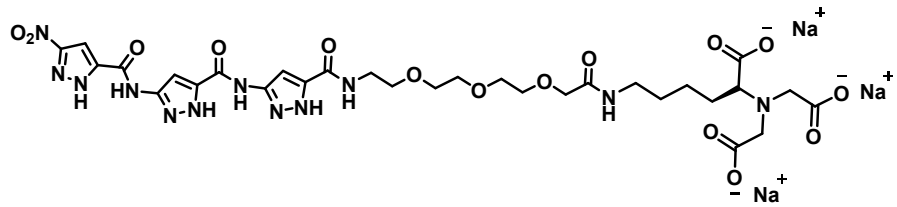

8

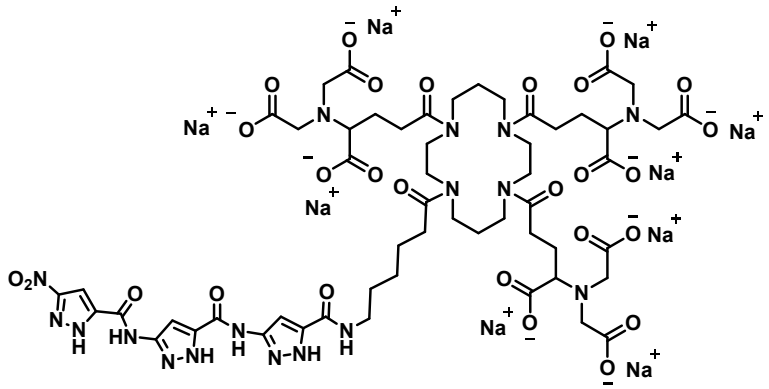

9

Figure 29. Structure of Trimer-mono-NTA **8** synthesized by März-Berberich and Trimer-tris(NTA)-cyclam **9** by Hellmert.[79]

The epitope contains a hexahistidine C-terminal region that could be complexed via Ni^{2+} complexation with a nitrilotriacetic acid unit (NTA). The aminopyrazole derivative was not able to link strongly to the antibody and the complex didn't show stability. To increase the stability, Hellmert equipped the aminopyrazole derivative with more NTA units attached in a cyclam unit. In biological experiments, the trimer-cyclam tris (Ni II-NTA)-IC16-scFv complex was stable (confirmed via PAGE) and showed a strong increase in affinity towards $Aβ_{42}$.[80]

[78] Müller-Schiffmann A. *et al.*, *Brain*, **2016**, *139*(2), 509-525.
[79] Hellmert M., "Hochentwickelte Aminopyrazol-Hybride gegen pathologische Prozesse der Alzheimer-Krankheit", Essen, **2014**.
[80] Hellmert M. *et al.*, *Organic & Biomolecular Chemistry*, **2015**, *13*, 2974-2979.

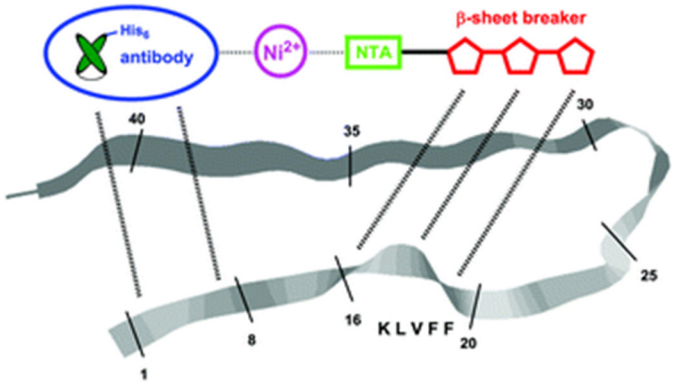

Figure 30. Schematic representation of trimer-cyclam tris (Ni II-NTA)-IC16-scFv complex.[78]

An additional attempt by Hellmert was to design and link artificial proteases with an aminopyrazole. By linking the recognition unit (trimer) to an artificial protease the Aβ peptide fragments could be hydrolytically cleaved into smaller peptides, preventing the toxic effect of Aβ aggregation. This is the starting point of our well-known topic of designing and synthesizing artificial proteases combined with aminopyrazoles derivatives on the surface of a nanoparticle. The system could enhance a synergistic binding to Aβ and proteolytic cleavage of the protein. However, due to the poor solubility of the complex in aqueous media, its efficiency could not be experimentally proven.[79]

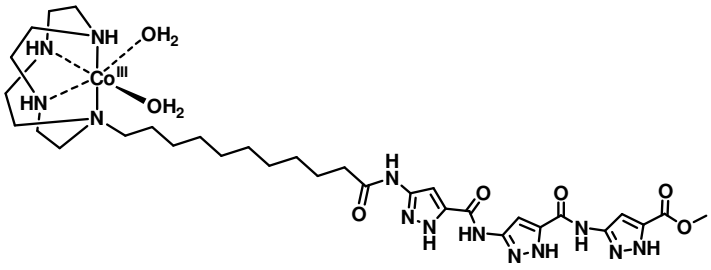

10

Figure 31. Structure of the trimer-cyclen hybrid as an artificial protease according to Hellmert.[79]

Following the work of preventing Aβ fibrillogenesis, Streich and Akkari designed, synthesized and tested two different ligand species, D3 derivatives and aminopyrazole ligands (Figure 32). These two ligand types interacted in different ways with Aβ and inhibited it in different pathways. D3 is a β-selector which specifically recognizes Aβ while the aminopyrazole unit is a β-sheet breaker that interacts and breaks the Aβ. Thanks to the the University Duisburg-Essen's technical chemistry department led by Prof. Barcikowski, two types of ligands were immobilized on the surface of a small, monodisperse gold nanoparticle to probe the inhibitory effect against Aβ aggregation.[81]

[81] Streich C.; Akkari L., *ACS Nano*, **2016**, *10*, 7582-7597.

D3-Cys (D3_5+)	RPRTRLHTHRNRC
D3-$(Lys)_3$-Cys (D3_8+)	RPRTRLHTHRNRKKKC
D3-$(Lys)_5$-Cys (D3_10+)	RPRTRLHTHRNRKKKKKC
Trimer-$(Lys)_5$-Cys (Trimer_5+)	Trimer-KKKKKC
Trimer-$(Lys)_8$-Cys (Trimer_8+)	Trimer-KKKKKKKKC

Figure 32. Schematic representation of the different ligands synthesized and tested by Streich and Akkari.

The gold nanoparticles (AuNPs) were generated by the top-down process, where a slicing of bulk material ends with a self-assembling nanoscale object.[82] The AuNPs were prepared in aqueous solution by laser ablation focused on the material, evaporated, re-condensed to form NPs and subsequently size-classified using centrifugation.[83]

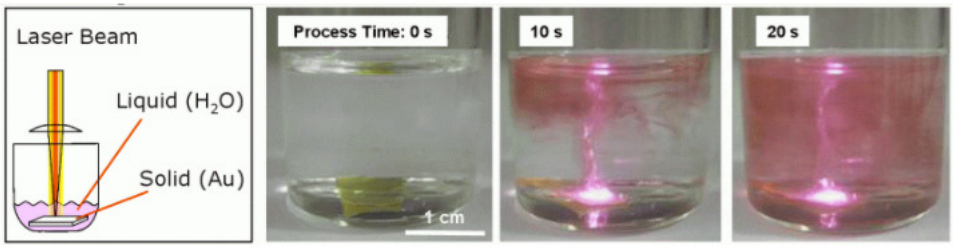

Figure 33. Synthesis of AuNPs for medical application by laser ablation in aqueous medium.[84]

Monofunctional and bifunctional conjugates were obtained by immobilizing the two ligand types in different ratios on the gold nanoparticle surface. New bifunctional conjugate (D3_5+ and Trimer_5+ combined) showed a strong interaction with Aβ. This immobilization of the ligands on nanoparticles led to a considerably inhibitory effect demonstrated in the several biophysical assays.[85]

[82] Hu X. *et al.*, *Front.Bioeng. Biotechnol.*, **2020**, *8*, 990.
[83] Barcikowski S. *et al.*, *Appl. Phys. A.*, **2007**, *87*(1), 47-55.
[84] taken from: https://www.uni-due.de/barcikowski/forschen.htm, (Accessed March 17, **2021**)
[85] Akkari L.,"Neuartige peptidische Ligandenkonjugate zur Hemmung der pathologischen Aggregation von Amyloid-beta bei Morbus Alzheimer", Essen, **2017**.

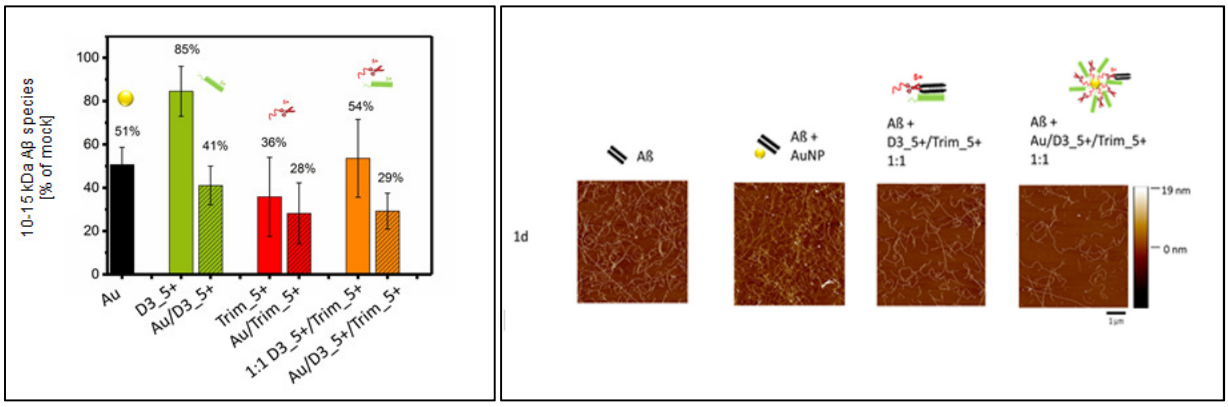

Figure 34. Left image: Cell culture experiment of D3_5+ and Trimer_5+ (1:1 mixture) for 10-15 KDa Aβ species (c(AuNP)= 50 µg/mL, c(Ligand$_{monofunc.}$)= 10 µM, c(Ligand$_{bifunc.}$)= 5 µM). Right image: AFM images of Aβ fibrils after one day of incubation with D3_5+ and Trimer_5+ (1:1 mixture) and the corresponding bifunctional conjugate (209 lig / NP) (c (AuNP) = 125 µg / mL, c (Ligand) = 12.5 µM, c (Aβ) = 50 µM).[85]

1.3.3.4 Natural and artificial metalloproteases

Natural metalloproteases or metallopeptidases are proteases composed of a diverse group of endo- and exo-peptidases. The current MEROPS database classifies metallopeptidases into 54 families, and these ones grouped into 15 clans based on metal ion binding motifs and similarities in 3-D structure. They are important in many aspects of biology, ranging from cell proliferation, differentiation and remodeling of the extracellular matrix (ECM) to vascularization and cell migration (Table 2).

Mechanisms of metalloprotease action underlying these events include the proteolytic cleavage of growth factors so that they can become available to cells not in direct physical contact, degradation of the ECM so that founder cells can move across tissues into nearby stroma, and regulated receptor cleavage to terminate migratory signaling. [86,87]

[86] Nagase H., *Current Protocols in Protein Sciencie*, **2001**, *21.4.1-21.4.13*.
[87] Chang C., Werb Z., *Trends Cell Biol.*, **2001**, 11(11).

Table 2. Some of the biological functions of metallopeptidases.[86]

Biological processes	Enzyme [family]
Antibiotic resistance	
β-Lactamase activity	Membrane dipeptidase [M19]
Vancomycin resistance	VanX D-Ala-D-Ala-dipeptidase (vancomycin-resistant *Enterococcus faecolis* host) [M45]
Bacteriolytic activity	
Resolution of peptidoglycan	N-acetylmuramoyl-L-alanine amidase (not peptidase) [M15]
Resolution of peptidoglycan (*Staphylococcus aureas*)	β-lytic metalloendopeptidase (*Lysobacter enzymogenes*) [M23], staphylolysin [M23], lysostaphin [M37]
Biosynthesis	
Biosynthesis of bacterial cell walls	Zinc D-Ala-D-Ala carboxypeptidase [M15]
Sporulation (*Bacillus*)	γ-D-glutamyl-meso-(L)-diaminopimelate peptidase [M14]
Development	
Cell-cell fusion	ADAMs [M12]
Cell migration	MMPs [M12]
Morphogenesis	ADAMs [M12], bone morphogenetic protein 1 (BMP-1) [M12], MMPs [M10], tolkin (*Drosophila*) [M12], tolloid [M12]
Release of cytokines and growth factors	ADAMs [M12], MMPs [M10]
Effects on immune systems	
Disruption of insect immune system	Immune inhibitor A [M6]
IgA, IgG degradation	IgA specific metalloendopeptidase [M26], mirabilysin [M10]
Infection	
Diarrhea	Fragilysin (*Bacteriodes fragilis*) [M10]
Opportunistic bacterial infection	Coccolysin (*Enterococcus faecalis*) [M4], pseudolysin (*Pseudomonas aeruginosa*) [M4], aeruginolysin (*Pseudomonae aeruginosa*) [M10]
Protozoan infection	Leishmanolysin (*Leishmania*) [M8]
Viral polyprotein processing	Hepatitis C virus endopeptidase 2 [M44], vaccinia virus proteinase [M44]
Virulence factor activation of toxins of *Vibrio cholerae*	Hemagglutinin/protease 9 (*Vibrio cholerae*) [M4]
Nutrition	
Intestinal absorption of folic acid	Glutamate carboxypeptidase II [M28]
Peptide and protein processing	
Alzheimer's precursor protein processing(α-secretase activity)	ADAM 17 (TACE) [M12]
Cell signaling/release of a transcription factor	S2P protease [M50], SpoIVFB (*Bacillus subtilis*) [M51], ADAM-10 [M12]

Metallopeptidases contain a divalent metal ion at the active site. The catalytic metal ion is usually coordinated by three amino acid side-chain ligands. A water molecule that is essential for hydrolysis of the peptide bond also coordinates with the metal ion as a fourth ligand in the active form of metallopeptidase. In most cases, the metal ion is zinc, but in some cases, it is cobalt, manganese, or nickel (Figure 35).[88]

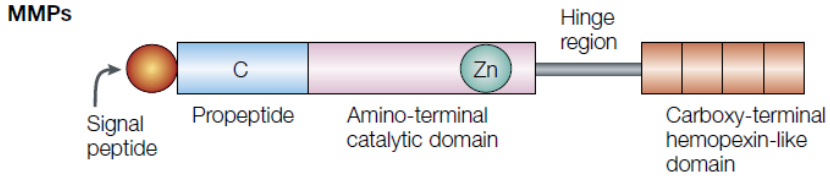

Figure 35. The generic structure of matrix metalloproteinases (MMPs). 'C' at the propeptide region denotes the cysteine residue that ligates the zinc in the catalytic domain to keep the enzyme inactive.[88]

Recently, many scientists have sought to extend the technology of the natural metalloproteases to develop reagents that cleave polypeptide chains at sites determined by proximity to a metal chelate.[89] Artificial metalloproteases have proven to be a powerful tool in the modulation/degradation of Aβ aggregation. However, their design and development is demanding, and only a few groups are currently working on this topic.

Kroll in 1951 discovered for the first time that Cu^{2+}, and to a lesser extend Co^{2+} and Ni^{2+}, hydrolyzed amino acid esters.[90] Years after that, in 1987, Collman and Sutton proposed that octahedral Co^{3+} complexes could chelate the N-terminus of a peptide leading to hydrolyze.[91] Later in 1996, Junghun Suh started deeply investigating artificial metalloproteases cleaving several biological systems hydrolytically.[92] In 1998, Suh *et al.* introduced the tetracyclic tetramine 1,4,7,10-tetraazacyclododecane or usually called cyclen. The goal of his study was to introduce Cu^{2+} into cyclen attached to a backbone of artificial proteases called PCD (poly- (cholоromethylstyrene-*co*-divinylbenzene)) precharged with guanidinium groups to recognize carboxylate and phosphate ester anions in γ-globulin (Gbn) as a target. It was found that the first immobile artificial proteinase was able to hydrolyze Gbn with 10^8-fold acceleration. This research marked the most dramatic turning point of using cyclen complexed with Co(III) as artificial metalloproteinase.[93]

[88] Yong V.W et al., *Nature Reviews*, **2001**, *2*, 502-511.
[89] Rana T.M., Meares C.F., *Proc. Natl. Acad. Sci. USA*, **1991**, *88*, 10578-10582.
[90] Koll H., *J.Am.Chem.Soc.*, **1952**, *74*, 2036.
[91] Sutton P. and Buckingham D., *Acc. Chem. Res.*, **1987**, *20*(10), 357-364.
[92] Suh J., Oh S., *Bioorg. Med. Chem. Lett.*, **1996**, *6*(10), 1067-1070.
[93] Jang B. *et al.*, *J.Am.Chem.Soc.*, **1998**, *120*(46), 12008-12016.

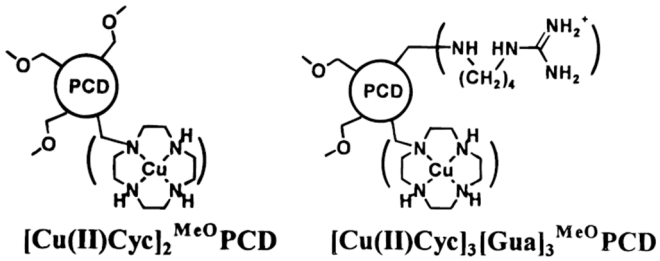

Figure 36. PCD derivatives synthesized by Suh *et al.*[93]

After that, different Co(III)/Cu(II)-cyclen derivatives were synthesized using different targets such as myoglobin[94] or peptide deformylase.[95] In 2007, a combinatorial library of 888 candidates utilizing Co(III)-cyclen as a core and $A\beta_{40}$ and $A\beta_{42}$ as focused targets was performed by Suh *et al.*. Thanks to an exhaustive MALDI-TOF-MS experiment, it was found that only four artificial metalloproteases were able to cleave $A\beta_{40}$ and $A\beta_{42}$ peptides, which translates into a reduction of Aβ oligomers and therefore slows down the formation of fibrils. These results were relevant in the study of artificial metalloproteinases, as standards for building molecules against Aβ aggregation were established. For example, it was probed that introducing several aromatic moieties into the molecules since they have an affinity for Aβ plaques or triazine as a core because of its easy manipulation and the wide range of biological activities due to similarities to purine or pyrimidine.[96] A mechanism by which cyclen can hydrolyze peptide bonds was also proposed. The mechanism is showed in Scheme 1.[97]

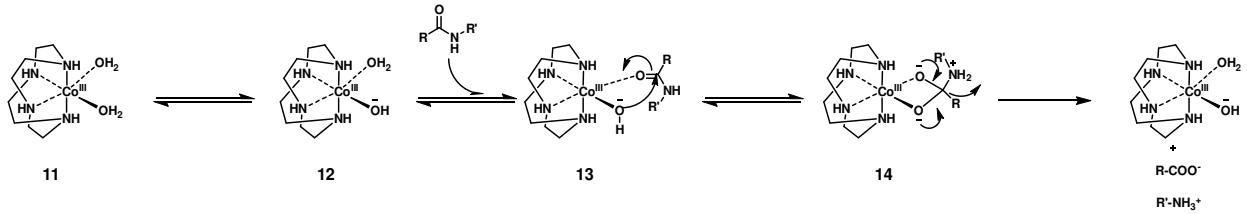

Scheme 1. The mechanism proposed by Suh to hydrolyze a peptide bond with Co(III)-cyclen.[98]

The Co(III)-cyclen catalyst **11** in the effective concentration acts as a Lewis acid which is able to cleave the amide bond of a peptide. The Co(III)-cyclen hydroxide ion form **12** nucleophilically attacks the carbonyl carbon atom of the peptide bond, carrying out the formation of a tetrahedral complex **14**, which affects the catalytic rate, breaking the peptide bond.[98,99] Understanding the mechanism of the simplest Co(III)-cyclen molecule, several

[94] Suh J., *Acc.Chem.Res.*, **2003**, *36*, 562-570.
[95] Suh J. *et al.*, *J.Am.Chem.Soc.*, **2005**, *127*, 2396-2397.
[96] Suh J. *et al.*, *Angew. Chem. Int. Ed.*., **2007**, *46*, 7064-7067.
[97] Suh J., Chei W., *Curr.Opin.Chem.Biol.*., **2008**, *12*, 207-213.
[98] Suh J., Chei W., Ju H., *J.Biol.Inorg.Chem.*, **2011**, *16*, 511-519.
[99] Suh J. *et al.*, *J. Biol. Inorg. Chem.*, **2009**, *14*, 151-157.

Co(III)-cyclen derivatives using triazine as a core were synthesized and evaluated against protein aggregation utilizing MALDI-TOF to evaluate the cleavage of Aβ peptide, h-IAPP or α-synuclein.[96, 100, 101]

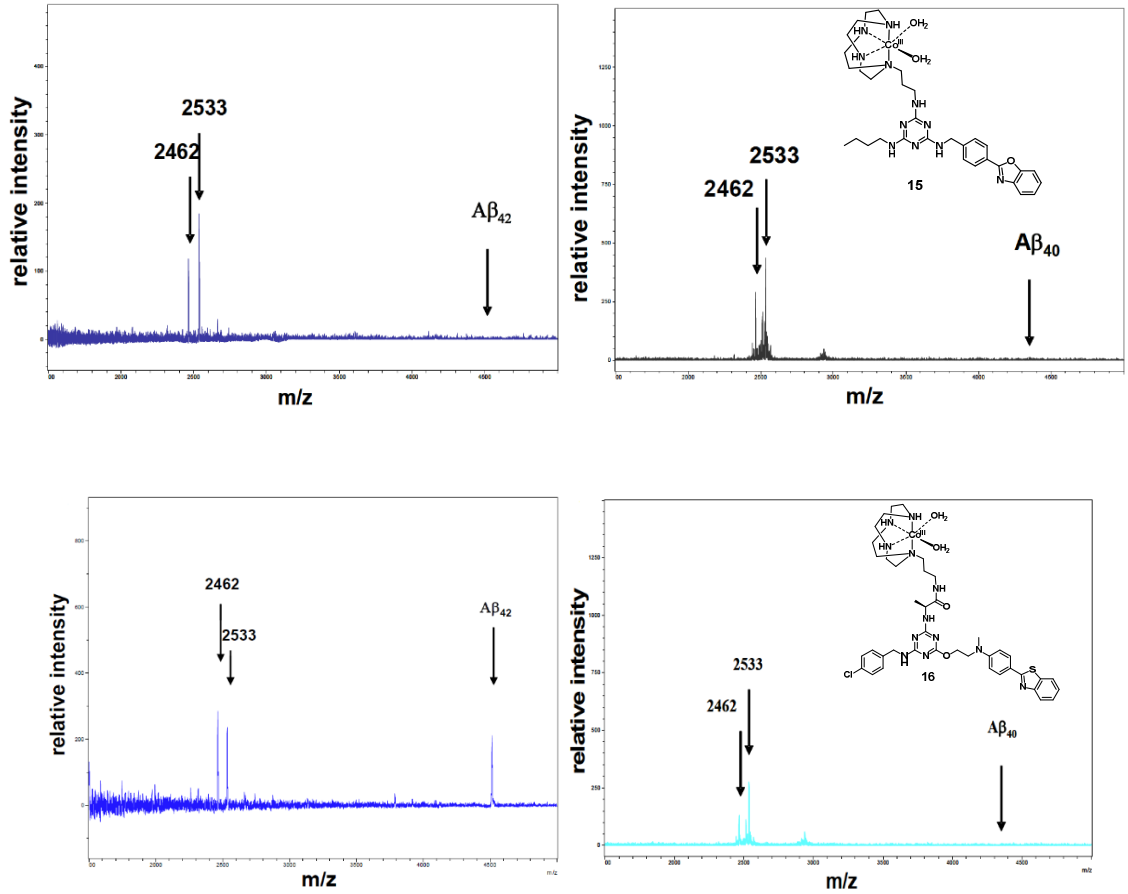

Figure 37. MALDI-TOF mass spectrum of Co(III)-cyclen derivatives obtained by incubation of 4 μM of $A\beta_{40}$ or $A\beta_{42}$ and 3 μM of Co(III)-ligand **15** and **16** at pH 7.5 (0.050 M phosphate buffer) at 37 °C. The peaks with *m/z* of 2462 and 2533 correspond to Aβ (1-20) and Aβ (1-21), respectively. [96, 100, 101]

Suh and his co-workers were able to cut and visualize, thanks to the triazine derivative molecules, different aggregate proteins. With all this information and the scientific progress in artificial metalloproteases, a rational design was carried out in this thesis to achieve the goal that will be discussed in section 2.

[100] Suh J., *Asian J.Org.Chem.*, **2014**, *3*, 18-32.
[101] Lee T.Y. *et al.*, *Bioorg. Med.Chem. Lett.*, **2012**, *22*, 5689-5693.

2. Aim of this work

AD is the most predominant form of dementia, with 60-70% of the cases.[40] AD is a neurodegenerative disease based on misfolding and aggregation of certain proteins in the brain. The peptide $A\beta_{42}$ is considerably abundant in patients with AD. When this peptide reaches abnormal levels in the brain, it leads to cytotoxic effects and disrupts cell function, guiding to a cognitive decline and personality disorders in the patient who suffers AD. Numerous researchers have tried to address the trouble of Aβ aggregation, reasoning a good strategy based on the well-known processes where abnormal levels of Aβ are involved. The most obvious procedure is to interrupt the first stage of the ACH where Aβ is cleaved from APP and leads to Aβ aggregation.

Multivalent interactions play a decisive role in biological systems for recognition, adhesion, and signal processes, and offer the advantage of a multiple and thus dramatically enhanced binding on a molecular scale with high affinity and specificity on different interfaces or molecules. The binding partners form cooperative, multiple receptor–ligand interactions that are based on individually weak, noncovalent bonds and are thus generally reversible.[102] Recently, the application of multivalence principles have been observed in nanotechnology with the attachment of multiple identical or different ligands to the surface of a NP, since the binding affinity to biological processes may be improved thanks to cooperative effects of the ligands.

As mentioned in section 1.3.3, peptides, aminopyrazoles and artificial metalloproteases seem to be the best options to address Aβ aggregation. For this reason, an innovative tool including these three therapeutic approaches to interrupt Aβ aggregation absorbed on the surface of an AuNP was designed. A new term that refers to the disaggregation machine was created by Prof. Thomas Schrader and Prof. Stephan Barcikowski: TRINADES, which means TRIfunctional NAnoparticle DESign to rescue neuro system failure caused by protein aggregation (Figure 38).

[102] Haag R. *et al.*, *Angew. Chem. Int. Ed. Engl.*, **2012**, *51*, 2-29.

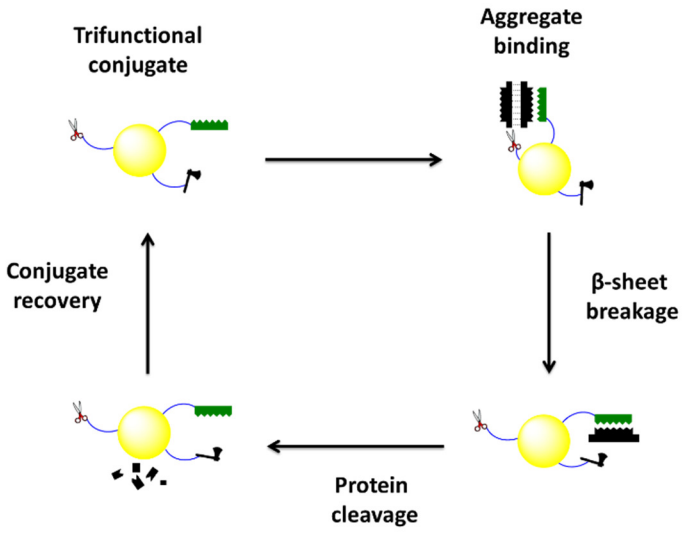

Figure 38. Schematic model of TRINADES against protein aggregation. β-sheet selector in green, β-sheet breaker in red (scissors) and artificial protease in black (axe).

A nanoparticle is equipped with three units: an Aβ-selector, an Aβ-breaker and an artificial metalloprotease. The Aβ selector is specifically designed to target the toxic Aβ oligomers. The Aβ breaker prevents longer peptides from forming β-sheet structures and aggregating. The artificial protease binds non-covalently to the absorbed protein molecules and cuts them into smaller fragments, which lack any significant aggregation propensity and dissociates them from the nanoparticle surface, regenerating the free nanoparticle and closing the catalytic cycle.

In previous attempts, the Aβ-selector and the Aβ-breaker were successfully synthesized. The Aβ-selector reduces Aβ cell toxicity, but it was not suitable as an aggregation inhibitor.[54] As mentioned in section 1.3.3.1, D3 (Aβ-selector) was specifically designed to target the Aβ oligomers and transform them into non-toxic aggregates.[60,61] Due to the non-inhibitory effect of the Aβ-selector, in recent studies, D3 conjugates (D3_5+, D3_8+ and D3_10+) were immobilized in the surface of AuNPs and investigated against Aβ aggregation. D3 derivatives supported on an AuNP were demonstrated to have a strong inhibitory effect on Aβ aggregation, converting Aβ into non-toxic aggregates. Furthermore, several Aβ-breakers (aminopyrazole hybrids), which reduce Aβ cell toxicity and are able to inhibit protein aggregation, were synthesized, immobilized on a gold nanoparticle surface and evaluated to probe them as aggregation inhibitors. It was found that Trimer_5+ showed the most substantial inhibitory effect even to lower concentrations. Both ligands (D3_5+ and Trimer_5+) were supported on an AuNP in different ratios, and a strong interaction with Aβ was shown in different biophysical assays. A multivalent effect with different ligands was

demonstrated, implying that the ligands supported on NPs are better inhibitors of the protein aggregation than free ligand, and therefore supporting the TRINADES approach.[85]

This thesis is aimed at the design, synthesis and evaluation of artificial metalloproteases against Aβ aggregation. For this purpose, various artificial proteases were synthesized with a cysteine moiety to support them on the surface of the AuNP and build a multivalent NP with the three units conforming the TRINADES. Due to the small size of the AuNPs (7 nm), they can interact with cells or proteins and penetrate the blood-brain barrier (BBB) into the brain, which is a must for the success of this approach.[103] Furthermore, the effectiveness of the cobalt complexes was evaluated with biophysical assays against protein aggregation.

Additionally, the final chapter of this thesis shows a new variety of Aβ breakers to control fibril formation. It was demonstrated by Prof. Michael Ehrmann and his co-workers that the serine protease HTRA1 is able to degrade aggregated and fibrillary tau and potentially cleave β-strands.[104] The aminopyrazoles (β-sheet breakers) were designed containing a sequence of hydrogen bonds following a DAD pattern, which proved to bind more strongly to β-sheet structures, preventing the formation of longer peptides.[74] A synergistic effect between HtrA1 and aminopyrazoles will be studied by performing a disaggregation machine.

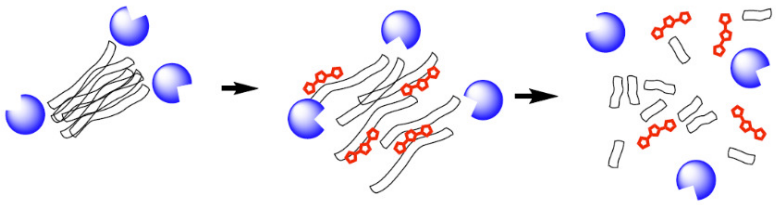

Figure 39. Novel disaggregation machine. β-sheet breaker in red (aminopyrazoles) and HtrA1 protease in blue.[104]

HTRA1 seems to be able to destabilize fibril formation, generating space for the aminopyrazoles to disrupt the hydrogen bonds, leaving single strands. In the last instance, HTRA1 is ready to proteolytically cleave the single chains. The best β-sheet breakers were evaluated alone and consequently in the presence of HTRA1 to obtain the highest collaborative effect.[105]

[103] Dykman L., Khlebtsov N., *Acta Naturae*, **2011**, *3*(2), 34-55.
[104] Tenntaedt A. *et al.*, *J. Biol. Chem.*, **2012**, *287*(25), 20931-20941.
[105] Proposal of the Collaborative Research Centre 1093.

3. Results

3.1 Artificial metalloproteases against protein aggregation

As commented in section 1.3.3.4, Suh found that cyclen was the most remarkable organic molecule to use as the catalytic center for artificial proteases to aim for the hydrolysis of peptide bonds. After an intense investigation of Suh's seminal work about artificial metalloproteases, different molecules containing a cyclen moiety that is capable of hosting Co^{3+} were developed.[96,100,101]

3.1.1 Artificial metalloproteases design

Out of several trials to find the perfect molecule, Suh found that the triazine-core molecules were able to cut Aβ peptide, h-IAPP or α-synuclein. In addition, he studied cobalt complexes containing 2-phenylbenzothizole or 2-phenylbenzooxazole moieties, finding a high affinity to the insoluble polymeric aggregates.[96,100,101] For this reason a model molecule with these three parts with a cysteine residue in one of the three available positions of a cyanuric chloride was synthesized, based on Suh's studies.

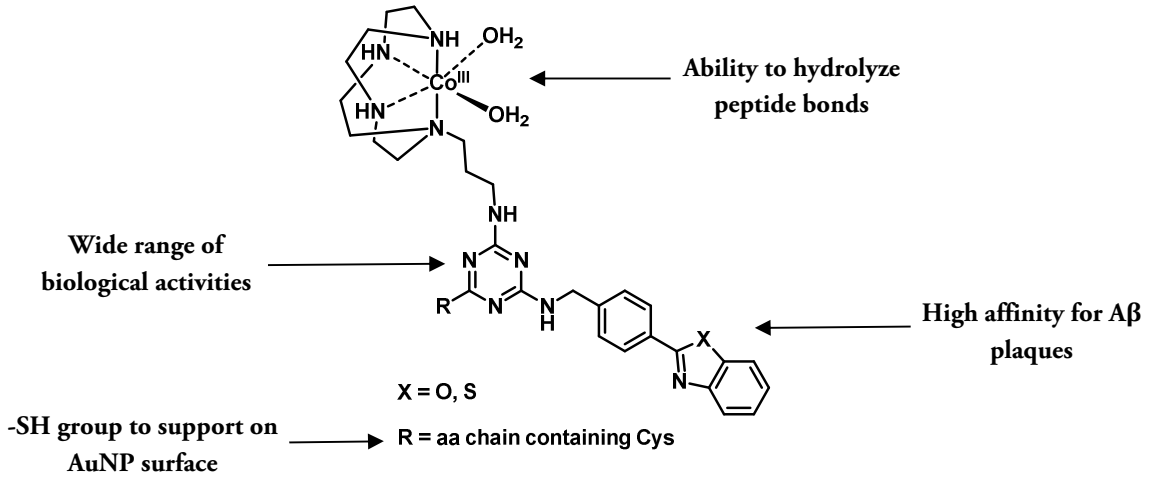

Figure 40. Schematic structure of the model molecule based on Suh's studies.[110]

The first approach of this synthesis was to obtain a cyclen derivative to be attached in the first position of the cyanuric chloride. For that purpose, three of the four available NH positions of the aza-crown ether 1,4,7,10-tetraazacyclododecane (cyclen) were blocked with a Boc protecting group, leaving a free position that was functionalized with a short alkyl chain containing a terminal amino group (Scheme 2).

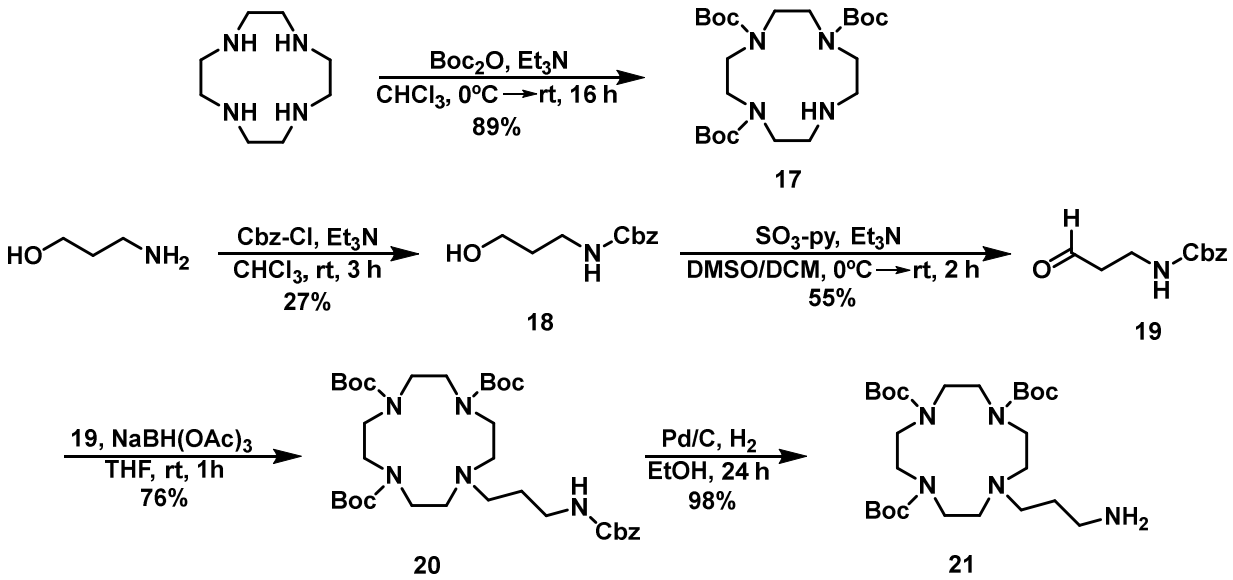

Scheme 2. Synthesis of the cyclen derivative **21**.

To control the selectivity and introduce only three Boc groups into cyclen, three equivalents of di-*tert*-butyl dicarbonate (Boc_2O) and triethylamine were used, obtaining **17**.[106] In the present case, the secondary amine of the cyclen attacks a carbonyl position of Boc_2O, creating *tert*-butyl carbonate and subsequently producing carbon dioxide gas, evidencing the importance of avoiding a closed reaction system. Then, the triethylamine extracts the proton from the positively charged amine.

To yield the final molecule, the alkyl chain, 3-amino-1-propanol was first protected with benzyl chloroformate (Cbz) to avoid any interaction of the amine group in the following reaction steps. Then, a Parikh-Doering oxidation[107] was carried out using a sulfur trioxide-pyridine complex to obtain the corresponding aldehyde **19** (Scheme 3).

Firstly, the DMSO is activated using sulfur trioxide. The activated DMSO is attacked nucleophilically by the alcohol. The intermediate product formed is now deprotonated by pyridine. In addition, sulfate is split off by a rearrangement, which is separated off in a complex with the pyridinium. Et_3N then protonates the alkoxy sulfonium ion to form the sulfonium yield. The subsequent β-elimination via a cyclic transition state leads to the cleavage of dimethyl sulfide so that the end product, the aldehyde, is formed.[108]

[106] Green K.N., Lincoln K.M., Gonzalez P., Texas Christian University, US 2014/0206862 A1, **2014**.
[107] Parikh J., Doering W., *J. Am. Chem. Soc.*, **1967**, *89*(21), 5505-5507.
[108] Tojo G., Fernández M., Oxidation of alcohols to aldehydes and ketones, Springer, **2006**.

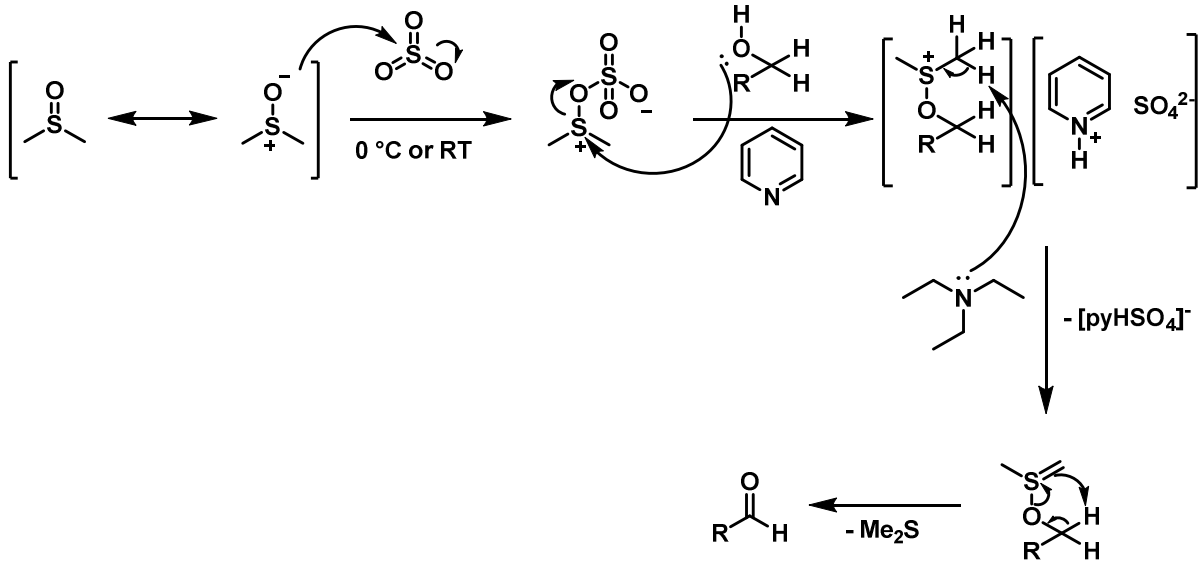

Scheme 3. Mechanism of Parikh-Doering oxidation.[107]

In the last step, a reductive amination was performed to achieve **20**. The strategy of using an aldehyde alkyl chain and the protected cyclen in the presence of sodium triacetoxyhydroborate (STAB), a powerful reducing agent, can avoid the problem of overalkylation that accompanies direct alkylation of amines with alkyl halides.[109] The compound **20** was subjected to hydrogenation to remove the Cbz protecting group, leaving a free amine in the cyclen-protected derivative **21**.[110]

An oxazole derivative was synthesized to be introduced in the second available position of the 1,3,5-triazine core. For that purpose, the 2-phenylbenzoxazole derivative **22** was synthesized utilizing polyphosphoric acid (PPA), which activates the carbonyl group of the 4-aminomethylbenzoic, picks up the water of the condensation and catalyzes the benzoxazole ring enclosure (Scheme 4).[111]

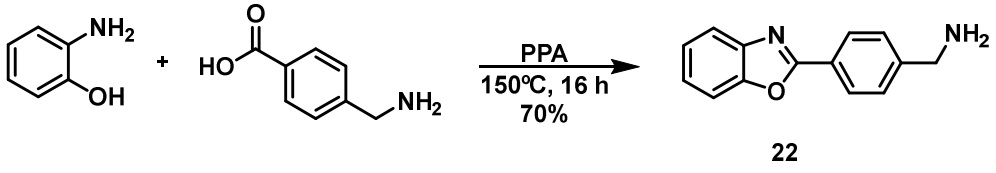

Scheme 4. Synthesis of the 2-phenylbenzoxazole derivative **22**.[111]

A dipeptide explicitly designed to achieve the goal of building TRINADES was prepared to substitute the third available position of the 1,3,5-triazine core. It is composed of a cysteine

[109] Abdel-Magid A.F. *et al.*, *J. Org. Chem.*, **1996**, *61*(11), 3849-3862.
[110] Jeong K. *et al.*, *J. Ind. Eng. Chem.*, **2009**, *15*, 342-347.
[111] So Y-H., Heeschen J., *J. Org. Chem.*, **1977**, *62*, 3552-3561.

bearing a thiol residue, which can be used to attach the whole construct to the AuNP surface, and a valine, which acts as a spacer between cysteine and the triazine core to prevent any interactions during cobalt introduction in the cyclen macrocycle.

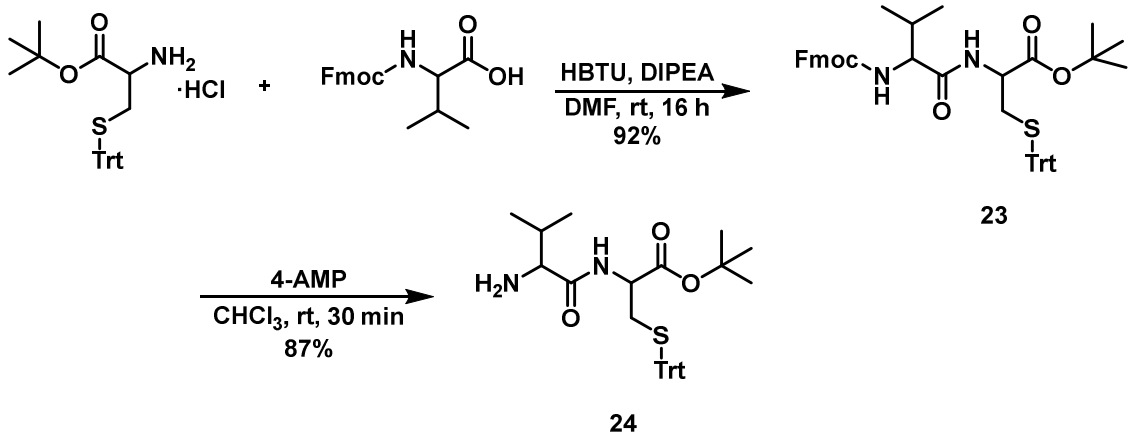

Scheme 5. Strategy for the synthesis of H_2N-Val-Cys(Trt)-OH **24**.

Solution-phase peptide synthesis was carried out between a protected cysteine with a free amine, and a Fmoc-protected valine, obtaining the intermediate **23**. After the coupling, the Fmoc group was removed using 4-aminomethylpiperidine (4-AMP) to afford the dipeptide **24**. 4-AMP was used due to the solubility of the produced adduct in phosphate buffer (pH 5.5), making its removal by usual extraction possible (Scheme 5 and 6).[112,113]

[112] Carpino *et al.*, *Org. Proc. Res. Dev.*, **2003**, *7*(1), 28-37.
[113] Carpino *et al., J. Org. Chem.*, **1990**, *55*(2), 721-728.

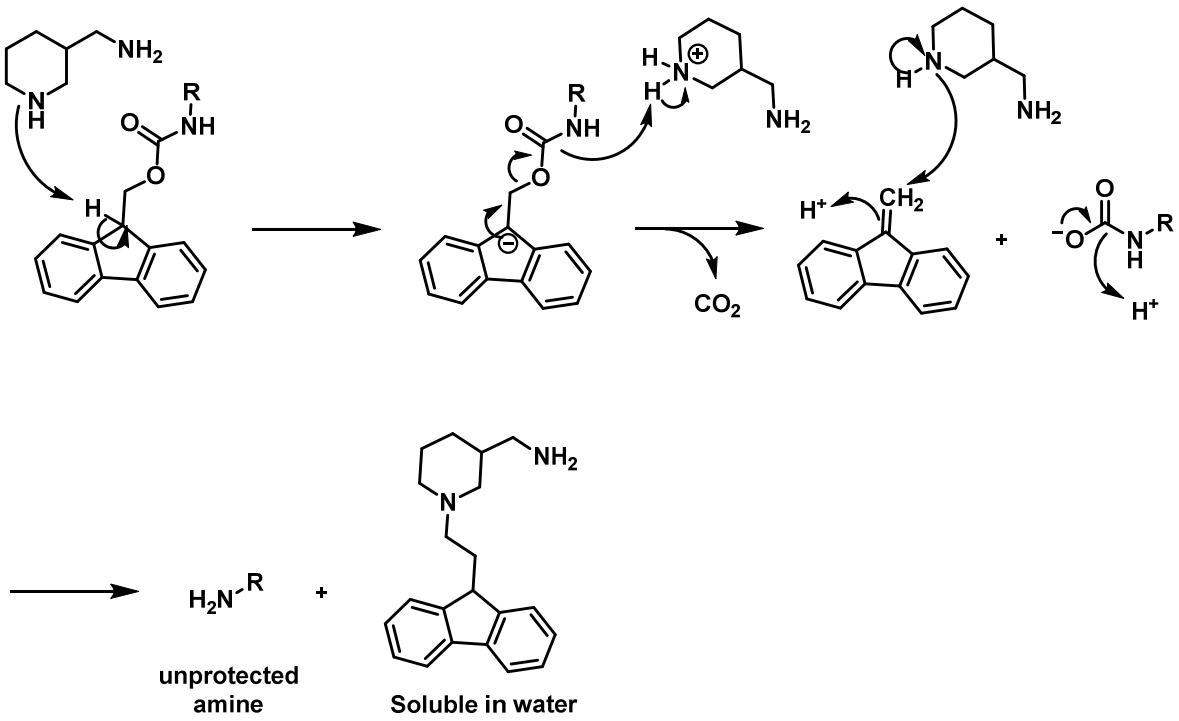

Scheme 6. Mechanism of Fmoc deprotection of an amino acid using 4-AMP.

Once the structures **21**, **22**, **24** were obtained, the three positions of the cyanuric chloride had to be substituted. Cyanuric chloride has temperature-dependent differential reactivity for the displacement of chlorides with nucleophiles during nucleophilic aromatic substitution (S_NAr). Each addition of electron-donating groups increases the electron density of the ring, lowering its reactivity and therefore making successive substitutions a challenge. The first substitution is generally performed at low temperatures around 0 °C, while the second one takes place at room temperature. The third replacement, the most demanding one, requires elevated temperatures of 70-100 °C (Scheme 7).[114]

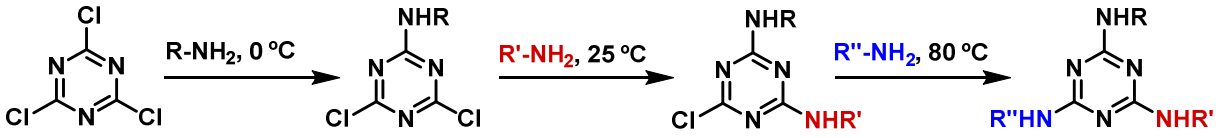

Scheme 7. Differential temperature dependence of the reactivity of cyanuric chloride.[114]

2-phenylbenzoxazole derivative **22** was firstly introduced to cyanuric chloride. For this purpose, a S_NAr was performed at 0 °C with DIPEA as an auxiliary base. The second position of the triazine core was substituted with the dipeptide **24**. In this case, trials at

[114] Hatfield S., "Aplications of triazine chemistry: education, remediation, and drug delivery", Texas, **2007**.

room temperature were unsuccessful, due to the poor reactivity of **25**, and the temperature had to be increased to 80 °C to achieve full conversion of the starting material (Scheme 8).

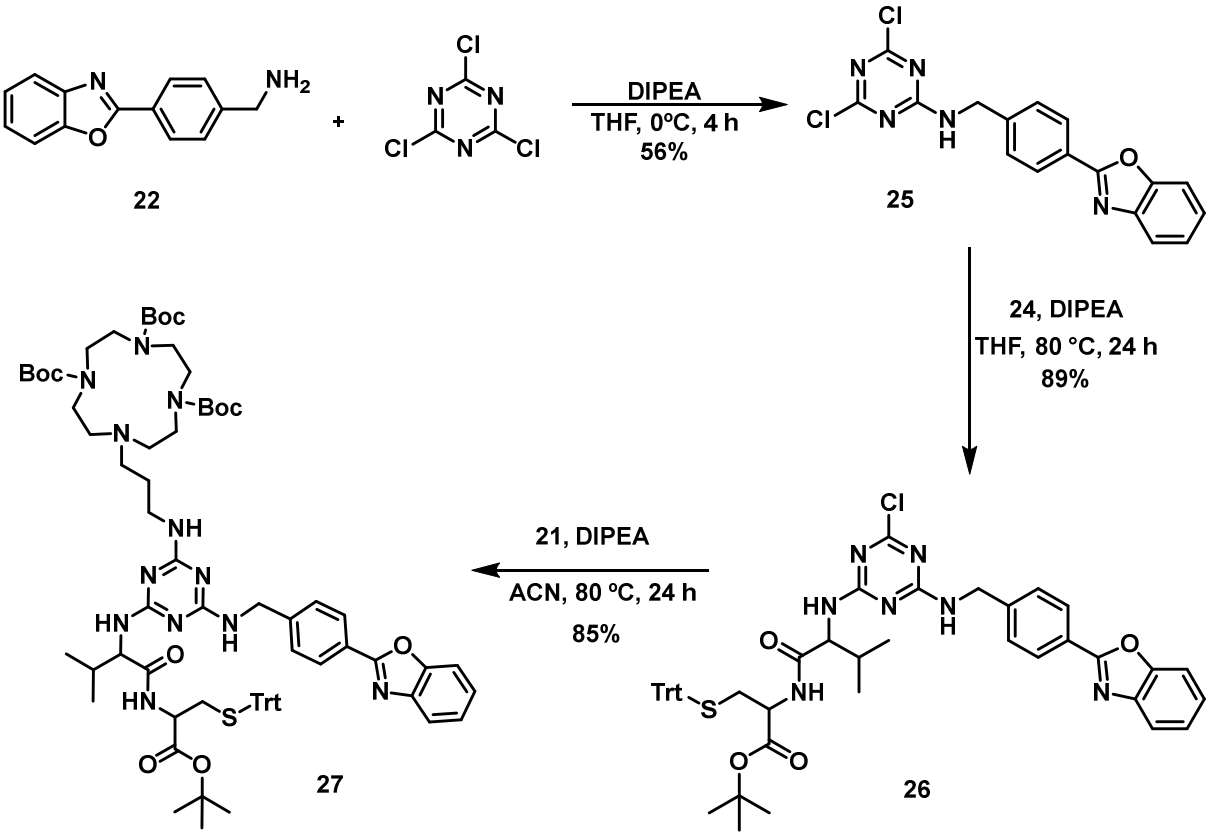

Scheme 8. Synthetic sequence to obtain the tri-substituted triazine derivative **27**.

To complete the synthesis, **21** was introduced in the third position of the triazine derivative **26**. It was found that the success of this last substitution was highly dependent on the reaction conditions. Preliminary trials with THF failed to afford the desired product, even over a temperature range of 80-120 °C. Attempts with absolute acetonitrile at 80 °C were also ineffective, indicating that this transformation required inert conditions. When anhydrous acetonitrile was used at 80 °C under an argon atmosphere, **27** was obtained with an 85% yield (Scheme 8).

Then, all the protecting groups of **27** were removed using mild acidic conditions. To achieve this aim, a TFA/DCM (95%) and TIPS (5%) mixture was used to remove the Boc, *tert*-butyl and Trt groups, leaving **28** in TFA salt form (Scheme 9).

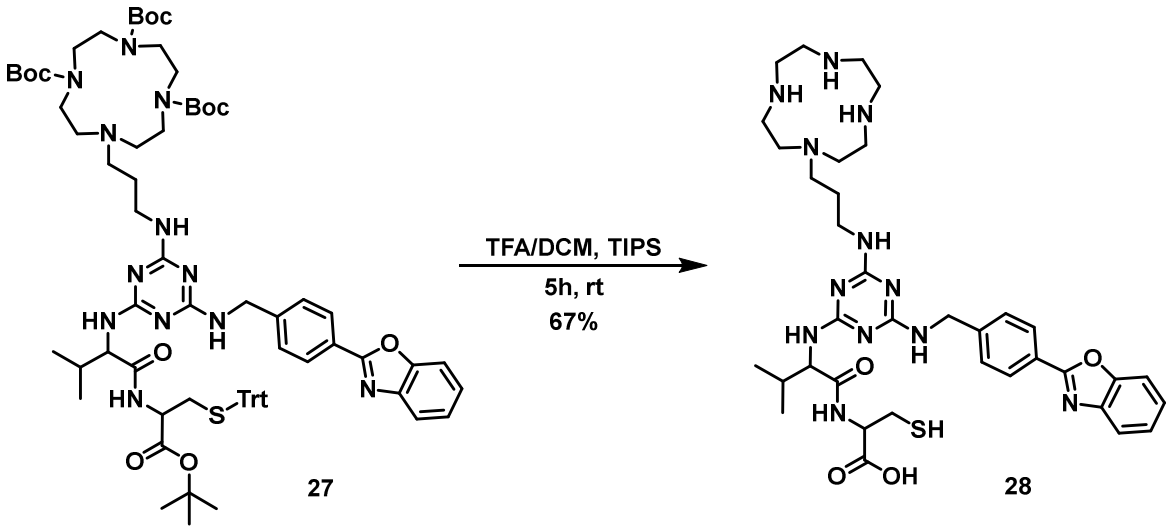

Scheme 9. Deprotection of **27**.

Finally, the product **28** was complexed with Co(III). It was essential to remove the TFA salt of the cyclen to achieve a successful complexation of the Co(III) inside the macrocycle. The salt-free **28** was obtained by basification (LiOH) by stirring the reaction for 90 minutes. After basification, a Co(II) salt was oxidized to Co(III) under an oxygen atmosphere, which coordinated to the cyclen macrocycle to afford **29** (Scheme 10). The reaction can be monitored by the color change of the reaction mixture, which shifts from a wine-red tone to deep purple when the chelation is complete. **29** was characterized by NMR, HPLC and MS techniques. Due to its paramagnetic character**,** the relaxation times during NMR analysis were drastically reduced and therefore the peaks became exceedingly broad and hard to resolve. An HPLC method to identify artificial metalloproteases was developed at λ= 545 nm, where Co(III) is observed.

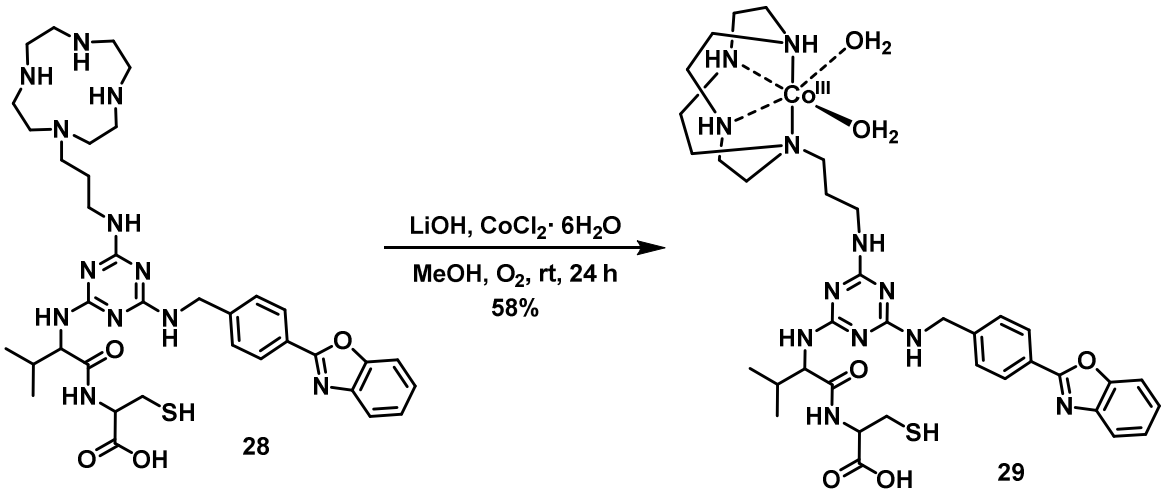

Scheme 10. Synthesis of the artificial metalloprotease **29**.

After successfully obtaining the cobalt-complexed triazine derivative **29**, another pathway to obtain new artificial metalloproteases was explored, featuring a 1,3,5-benzoate core. In this case, the coupling of the different substituents to the central core unit is achieved via amide couplings, which is likely to prevent the reactivity issues faced with aromatic substitutions on the cyanuric chloride core.

For this purpose, the commercially available trimethyl benzene-1,3,5-tricarboxylate was mono-hydrolyzed using NaOH, achieving **30** and leaving a carboxylic acid prepared for the subsequent coupling (Scheme 11).[115] This reaction is a crucial point of this synthesis design, since each of the esters has to be addressed individually to allow a stepwise introduction of the 2-phenylbenzoxazole derivative **22**, the dipeptide **24** and the cyclen derivative **21**. A precise control of the addition rate of the base is essential to avoid multiple hydrolyses.

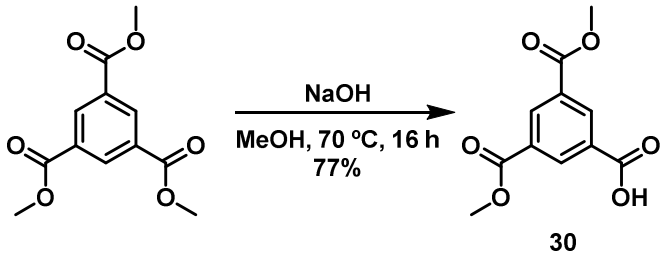

Scheme 11. Hydrolysis of the trimethyl benzene-1,3,5-tricarboxylate.

In the first instance, the oxazole derivative **22** was introduced to the mono-deprotected core **30** using PyCloP as a coupling reagent, obtaining **31**. Following this reaction, one equivalent of LiOH was used to hydrolyze another methyl ester, getting **32** (Scheme 12).

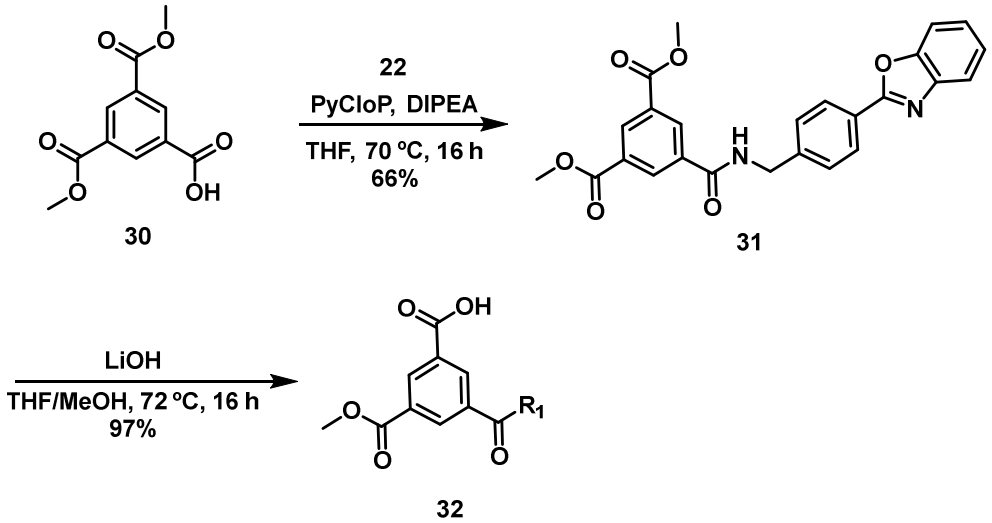

Scheme 12. First coupling reaction of the benzoate core.

[115] Zhou Y. *et al.*, *Cryst. Growth Des.*, **2017**, *17*, 6653-6659.

Next, the dipeptide **22** was introduced to **32** obtaining the di-substituted benzoate **33**, followed by the hydrolysis of the last methyl ester. Unfortunately, the reaction did not proceed as expected, and the formation of multiple side-products was observed. Presumably, the *tert*-butyl group was also removed under these harsh reaction conditions, leaving another free carboxylic acid that could interfere with the formation of the desired product **34** (Scheme 13).[116]

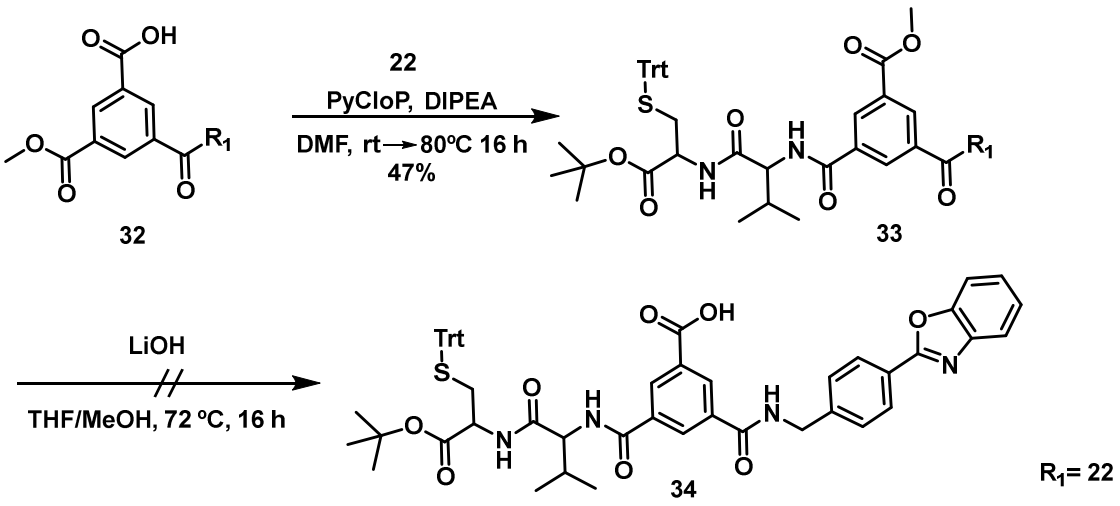

Scheme 13. First attempt to synthesize compound **34**.

After these disappointing findings, the synthetic strategy was modified to avoid any side-reactions with the dipeptide residue.

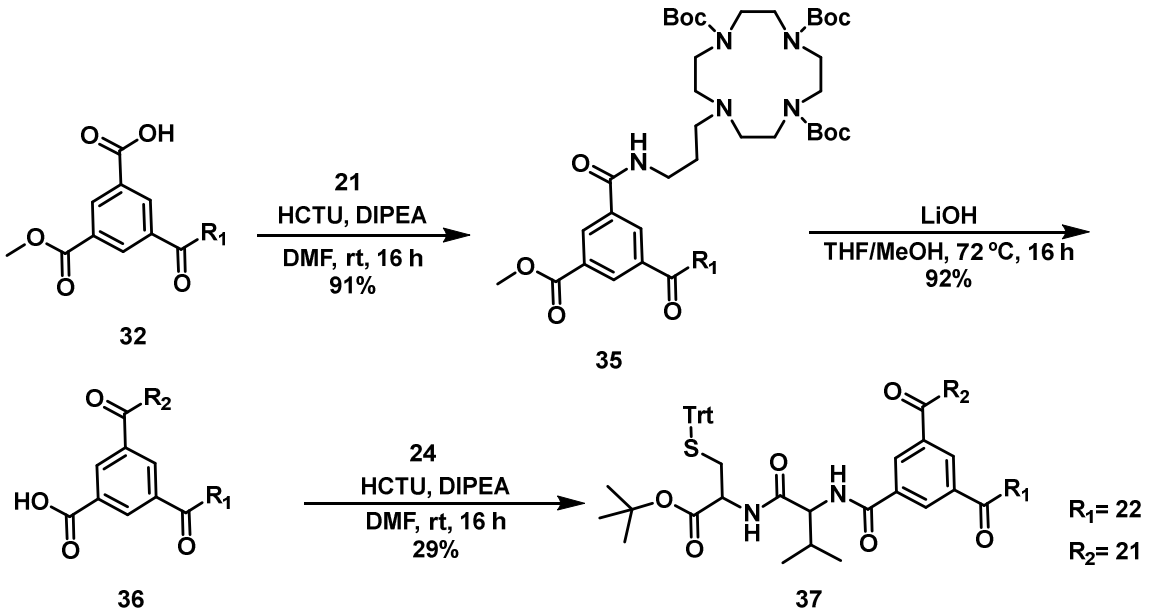

Scheme 14. Synthetic sequence to obtain the tri-substituted benzoate derivative **35**.

[116] Filali E. *et al.*, *Synlett.*, **2009**, *2*, 205-208.

To this end, the cyclen derivative **21** was first coupled with **32**. In this case, HCTU was used as a coupling reagent since trials with PyCloP were unsuccessful. Then, the last methyl ester was hydrolyzed, and a subsequent coupling with the dipeptide **22** afforded the target tri-substituted benzoate derivative **37** (Scheme 14).

Finally, all the protecting groups of **37** were removed using mild acidic conditions, and the product **38** was complexed with cobalt(III) under an oxygen atmosphere to afford the novel artificial metalloprotease **39** (Scheme 15), which was characterized by NMR, HPLC and MS techniques. As with the previously synthesized cobalt complex **29**, the characterization of **39** by NMR spectroscopy was also challenging, due to its paramagnetic nature.

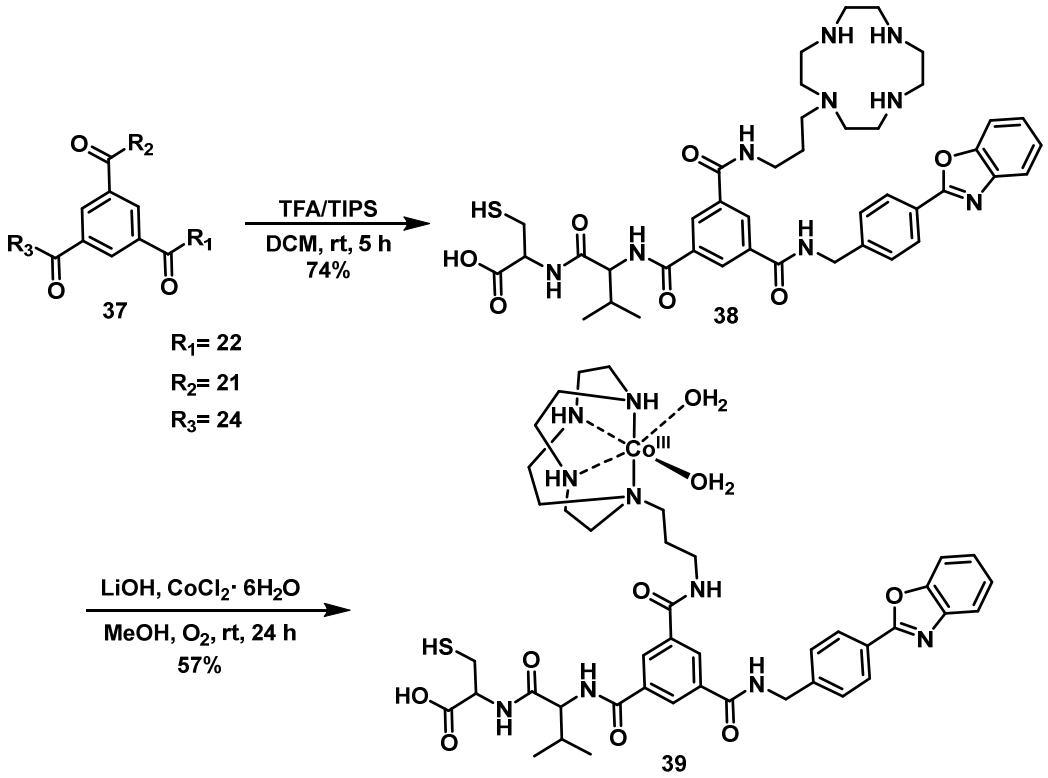

Scheme 15. Deprotection and complexation to achieve **39**.

To determine the contribution of the heterocyclic substituent to the cleaving activity of this family of artificial proteases, a new structure containing a thiazole ring was envisioned. Cleavage agents containing 2-phenylbenzothiazole have previously been exploited as the core unit for imaging agents of $A\beta_{42}$ amyloids in PET scanning of AD patients.[117] As mentioned before, 2-phenylbenzothiazole and 2-phenylbenzoxazole have a high affinity for insoluble polymeric aggregates.[101] For that reason, the 2-phenylbenzothiazole derivative **40** was synthesized utilizing PPA, following the exact mechanism of the 2-phenylbenzoxazole **22** (Scheme 16).

[117] Matthis C. *et al.*, *J. Med. Chem.*, **2003**, *46*, 2740-2754.

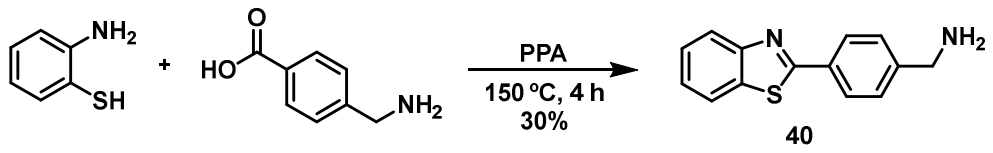

Scheme 16. Synthesis of the 2-phenylbenzothiazole derivative **40**.[111]

Using the synthetic sequence to obtain the tri-substituted derivative 37 as a model, a similar synthesis was carried out in order to obtain the novel 1,3,5-benzoate derivative **45**. Firstly, the 2-phenylbenzothiazole **40** was coupled with the free carboxylic acid product **30**, getting **41**. Subsequently, a hydrolysis of the methyl ester was carried out controlling the amount of LiOH, since only one of the two methyl esters should be cleaved, followed by the introduction of **21** to the mono-deprotected product **42** to afford **43**. Then, the remaining methyl protecting group was removed, leading to **44**. Finally, the last coupling with the dipeptide **24** was performed, achieving the new benzoate derivative **45** (Scheme 17).

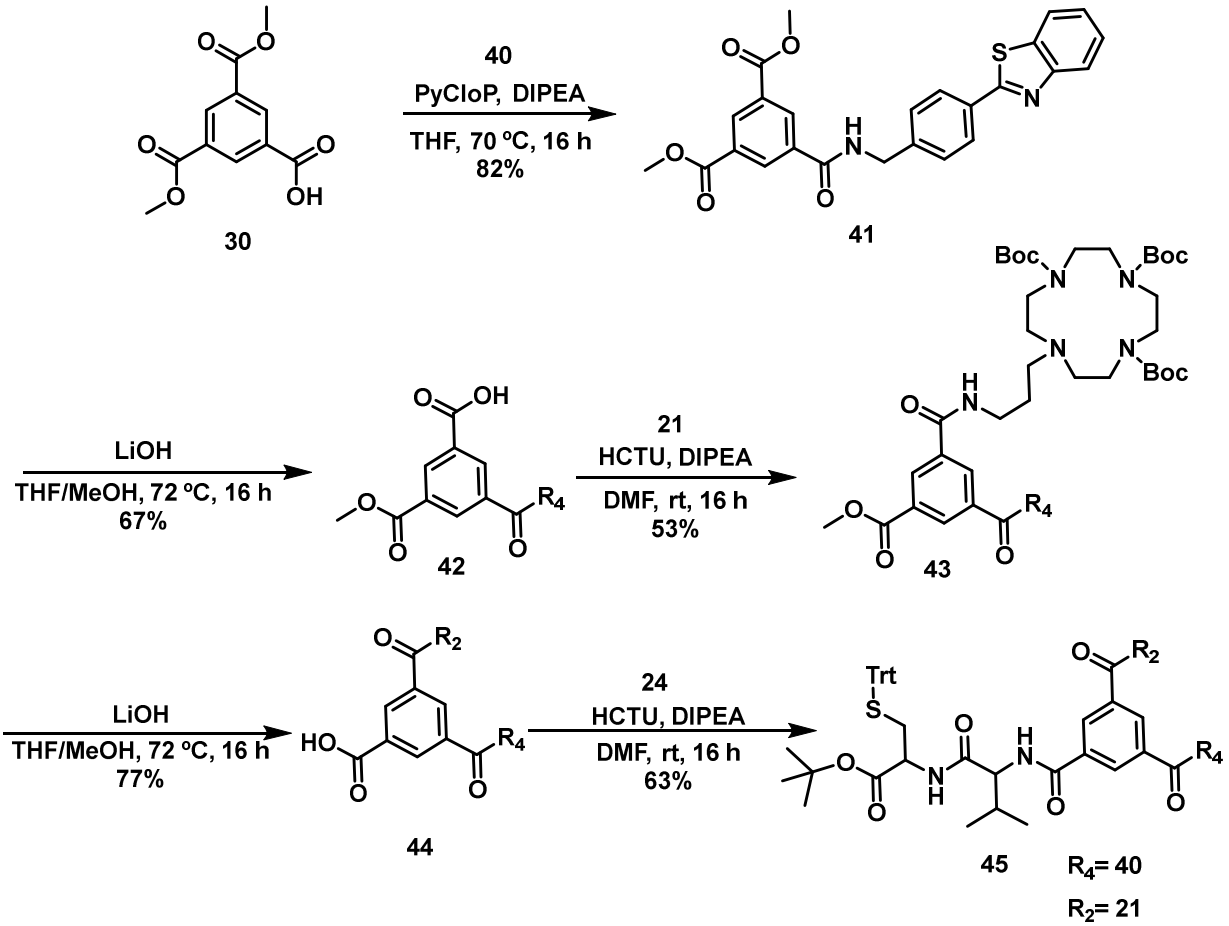

Scheme 17. Synthetic route to obtain the tri-substituted benzoate derivative **45**.

To effect the cobalt introduction inside the macrocyclic cyclen, all the protecting groups of **45** were first removed using mild acidic conditions, and then the product **46** was complexed with cobalt(III) under an oxygen atmosphere to afford the novel artificial metalloprotease **47**

(Scheme 18), which was characterized by NMR, HPLC and MS techniques. Peak broadening made the characterization of **47** by NMR spectroscopy a challenge.

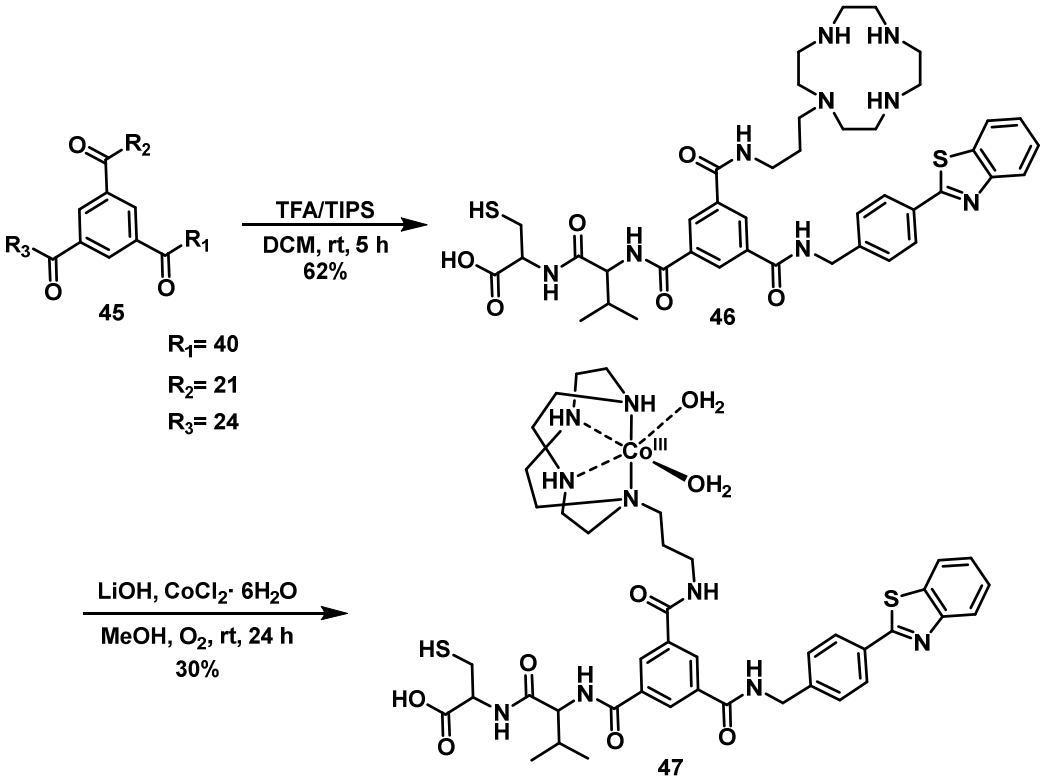

Scheme 18. Synthetic route to obtain the tri-substituted benzoate derivative **47**.

To test the cleavage strength of the artificial proteases **29**, **39** and **47**, a control protease was designed to be used in the forthcoming experiments to compare the active power of cleavage of the proteases. For this purpose, a Parikh-Doering oxidation[107] was performed to introduce a short alkyl chain to the cyclen derivative **17**, obtaining **48**. Deprotection of the Boc protecting groups was carried out under mild acidic conditions at room temperature. The deprotected product **49** was complexed with Co(III), achieving the objective molecule **50**, which was characterized by NMR, HPLC, IR and MS techniques (Scheme 19). Thanks to the HPLC method that was developed to observe Co(III) complexes at λ = 545 nm, the pure product could be isolated by preparative-HPLC, obtaining **50** with a 97% purity.

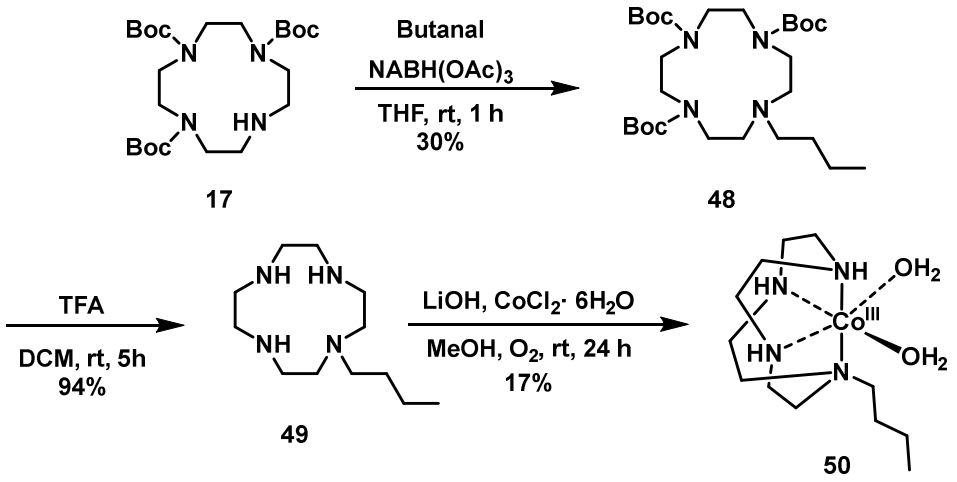

Scheme 18. Synthetic pathway to obtain the control artificial metalloprotease **50**.

3.1.2 Thioflavin T experiment

Thioflavin T (ThT) is a cationic benzothiazole dye that exhibits enhanced fluorescence upon binding to amyloid fibrils. It is widely used to diagnose amyloid fibrils, both ex vivo and in vitro. The structure of thioflavin T (Figure 41) has a hydrophobic end with a dimethylamino group attached to a phenyl group, linked to a more polar benzothiazole group containing N and S.[118]

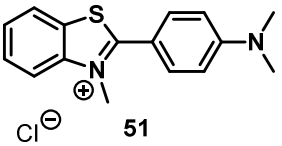

Figure 41. Structure of ThT 51.

ThT binds specifically to amyloid fibrils and is commonly used for the identification and quantification of amyloid fibrils in vitro, which has become the premier technique used to monitor fibrillation kinetics in real-time. The free ThT in aqueous conditions shows weak fluorescence with λ_{em}= 440 nm and λ_{ex}= 350 nm, but when ThT is added to samples containing β-sheet-rich deposits, also in a low micromolar range, it fluoresces intensely with λ_{em}= 490 nm and λ_{ex}=440 nm.[119] The interaction mechanism between ThT and amyloid fibrils involves the intercalation of ThT molecules within grooves between solvent-exposed side chains of the amyloid fibrils that run parallel to the fibril axis.[120] The interaction

[118] Khurana R. *et al.*, *J. Struct. Biol.*, **2005**, *151*, 229-238.
[119] Hudson S.A. *et al.*, *FEBS journal*, **2009**, 5960-5972.
[120] Noormägi A. *et al.*, *J. Pept. Sci.*, **2012**, *18*, 59-64.

between fibrils and ThT prevents rotational motion from occurring within the molecule, releasing energy in the form of fluorescence emission and allowing increased fluorescence to be measured.[121] As shown in figure 41, when ThT is complexed with monomers, small oligomers or amorphous aggregates of the Aβ peptide, no significant fluorescence occurs, but it fluoresces when binds to larger oligomers, protofibrils and fibrils due to the predominant β-sheet conformation.[122]

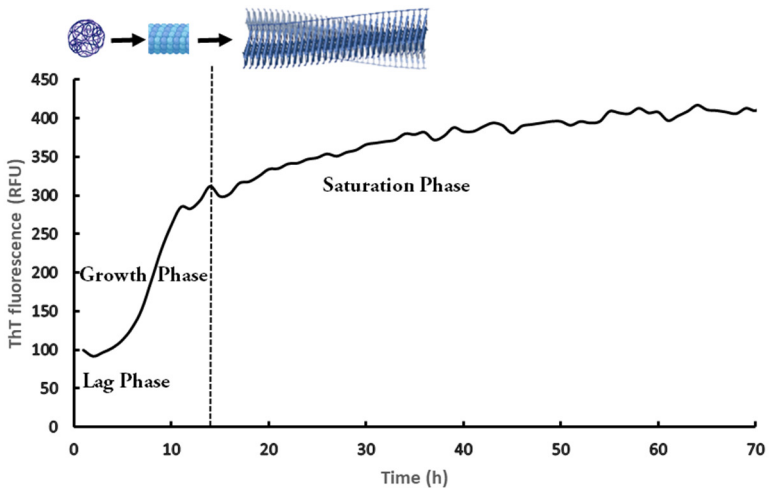

Figure 42. Aggregation kinetics of 10 μM $A\beta_{42}$ at 37 °C measured over three days of incubation.[123]

Fibril formation is a nucleation-dependent polymerization process which can be simply described by a sigmoid curve, indicative of a three-stage process consisting of protein misfolding, nucleation, and fibril elongation. In the first phase called *lag phase*, between 0 to 5 hours, soluble monomers associate to form nuclei and the transition to oligomer species with β-sheet conformation occurs. In the *growth phase*, larger ordered structures (protofibrils) are formed. After 20 hours, fibrils are completely formed during the *saturation phase*.[123]

Subsequently, the different artificial proteases **29**, **39**, **47** and **50** were tested to determine the inhibition of $A\beta_{42}$ aggregation. To exclude self-interaction or an interaction of the ligands with ThT, the samples were measured individually without Aβ-peptide. For this reason, the proteases were measured with and without ThT dye. As shown in figure 43, the free artificial metalloproteases showed no intrinsic fluorescence or interactions with ThT, and consequently all the compounds could be tested using this method.

[121] Hackl E.V *et al.*, *Eur. Biophys. J.*, **2015**, *44*, 249-261.
[122] Krebs M.R.H. *et al.*, *J. Struct. Biol.*, **2005**, *149*, 30-37.
[123] Iannuzzi C. *et al.*, *Int. J. Mol. Sci.*, **2013**, *14*, 14287-14300.

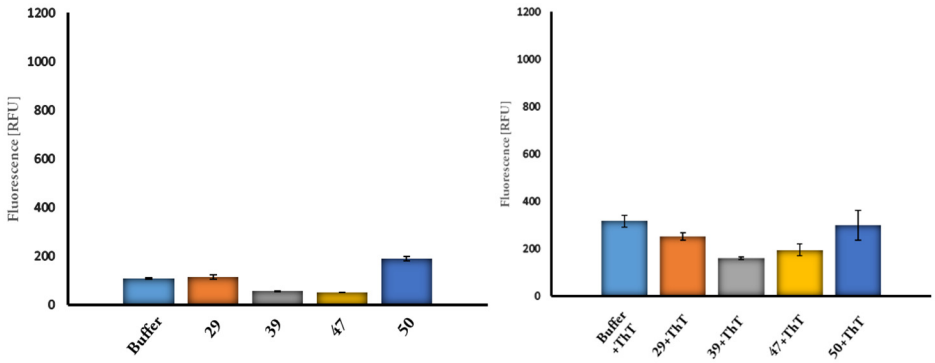

Figure 43. Self-fluorescence investigations of ligands 29, 39, 47 and 50 without (left) and with ThT (right), using 60 µM Ligand and 3.03 µM ThT.

To carry out the ThT experiments in presence of $A\beta_{42}$, the purchased Aβ-peptide first has to be monomerized with hexafluoroisopropanol (HFIP) and dissolved in DMSO to prepare the stock solution. The effect of the artificial proteases on the inhibition of Aβ aggregation was investigated with different concentrations of the ligands. For this purpose, the artificial metalloproteases **29**, **39**, **47** and **50** were incubated with $A\beta_{42}$ for 24 hours and 5 days. The values are expressed as a percentage, having the $A\beta_{42}$ control the highest possible value (100%).

By the addition of a 6 times excess of the respective artificial metalloprotease, the ThT signal was drastically reduced by 99% in **29**, 95% in **39**, 96% in **47** and 16% in **50** after incubation with $A\beta_{42}$ for 24 hours. A very strong inhibitory effect was observed for the artificial metalloprotease derivatives, but no significant reduction of the fluorescence signal was perceived in the case of the control protease **50** after 24 hours of incubation. Similar results were obtained after 5 days of incubation. Moreover, the strong reduction of the ThT signal may mean that a single cleavage of the peptide by the protease in enough to inhibit protein aggregation (Figure 44).

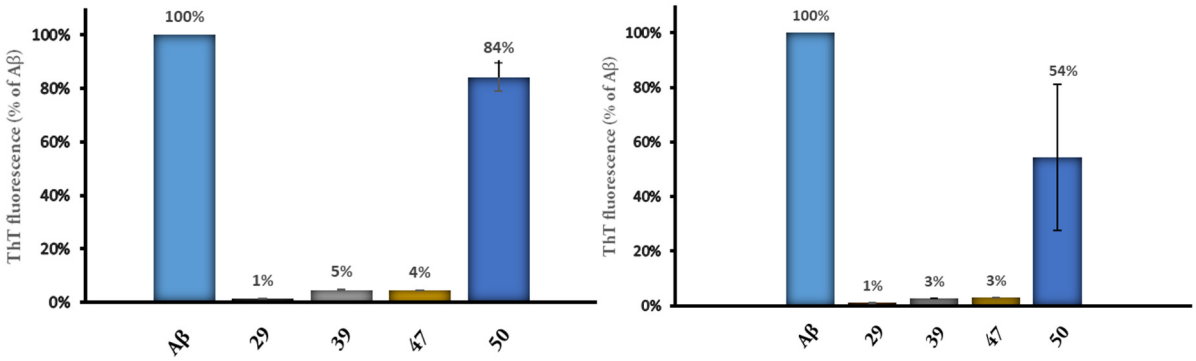

Figure 44. Inhibition of 10 µM $A\beta_{42}$ with 60 µM artificial metalloproteases at pH 7.0 and 37 °C after 24 hour (left) and 5 days (right) of incubation.

For that reason, the artificial metalloproteases were investigated in more detail, using different concentrations. In figure 45, the results with equimolar concentrations of peptide and proteases are shown. In these concentration ratios, all the artificial metalloproteases still show inhibition activity, with the exception of **50,** which does not reduce protein aggregation.

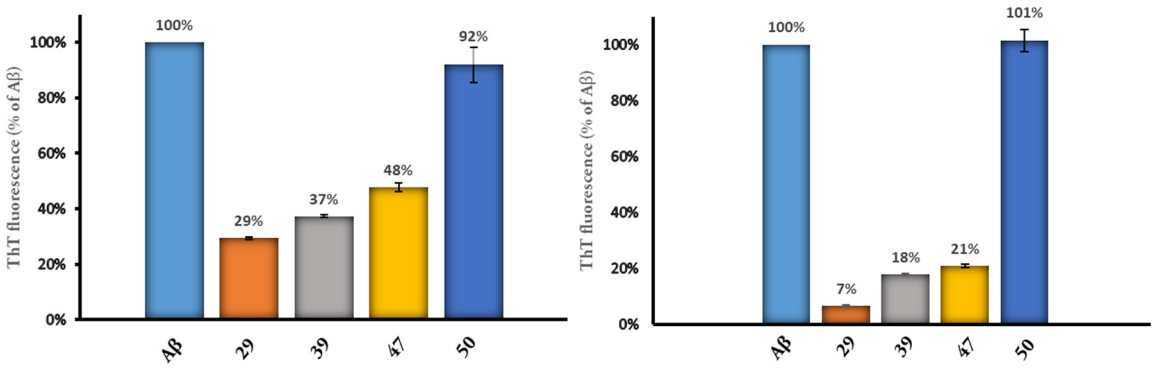

Figure 45. Inhibition of 10 µM $A\beta_{42}$ with 10 µM artificial metalloproteases at pH 7.0 and 37 °C after 24 hour (left) and 5 days (right) of incubation.

Another experiment was performed, with 10 times less concentration of artificial proteases than $A\beta_{42}$ to verify the inhibition influence of the artificial metalloproteases in low concentrations. The experiment was carried out after 1 day and 5 days of incubation of $A\beta_{42}$, obtaining similar results of the inhibition of Aβ aggregation in both measurements. In this low concentration range, the activity limit is reached for artificial metalloproteases **29**, **39** and **47**, with a reduction of aggregation of just 50% (Figure 46).

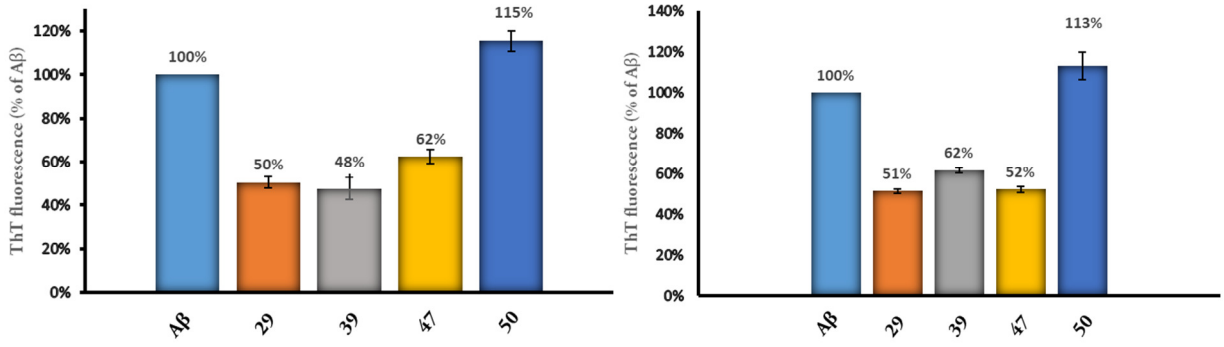

Figure 46. Inhibition of 10 µM $A\beta_{42}$ with 1 µM artificial metalloproteases at pH 7.0 and 37 °C after 24 hour (left) and 5 days (right) of incubation.

With 100 times less concentration, the artificial metalloproteases had no influence on fibril formation and did not exhibit an inhibitory effect (Figure 47). With all the results, it can be concluded that the concentration of the artificial proteases is important to achieve a strong inhibition of Aβ aggregation.

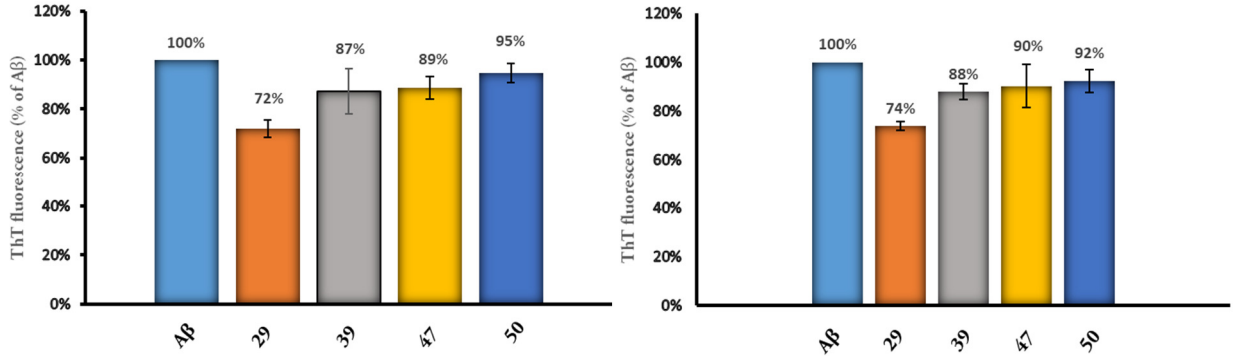

Figure 47. Inhibition of 10 μM $A\beta_{42}$ with 0.1 μM artificial metalloproteases at pH 7.0 and 37 °C after 24 hour (left) and 5 days (right) of incubation.

A disaggregation ThT experiment was carried out to know if the artificial metalloproteases have an influence on pre-existing Aβ aggregates. For this purpose, $A\beta_{42}$ was incubated for 24 hours to reach the saturation phase where fibrils are formed. Then, a 6 times excess of the artificial proteases was added, and the disaggregation effect was followed over a period of 5 days. The different artificial metalloproteases showed a drastic reduction of fluorescence, indicating that the ligands **29**, **39** and **47** were also able to disaggregate fibrils (Figure 48).

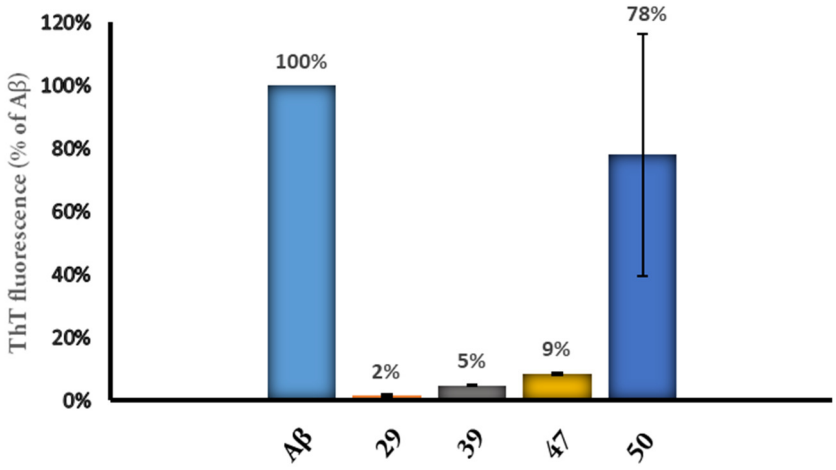

Figure 48. Disaggregation of 10 μM $A\beta_{42}$ with 60 μM artificial metalloproteases at pH 7.0 and 37 °C after 5 days of incubation.

However, these studies showed a poor reproducibility and the values differed between repetitions, presumably due to solubility issues of the fluorophore and the hydrophobic parts of the molecules. For that reason, in the next section, conformational changes of Aβ with the different artificial metalloproteases are investigated by CD spectroscopy. [117,124]

[124] Foderà V. *et al., J. Phys. Chem. B.*, **2008**, *112*, 15174-15181.

3.1.3 Circular Dichroism

Circular Dichroism (CD) spectroscopy is a valuable biophysical tool for studying the structure of biomolecules such as proteins or DNA, in solution.[125] It's a convenient method that measures the interaction of polarized light with optically active substances (asymmetric molecules) in solution.[126] CD provides a very advantageous experimental method for the determination of the secondary structure and environmentally induced structural changes in proteins, since the different forms of the primary secondary structural elements found in proteins (e.g., α-helix, β-sheet, and random loop) exhibit distinctly different CD spectrum (Figure 49).[127]

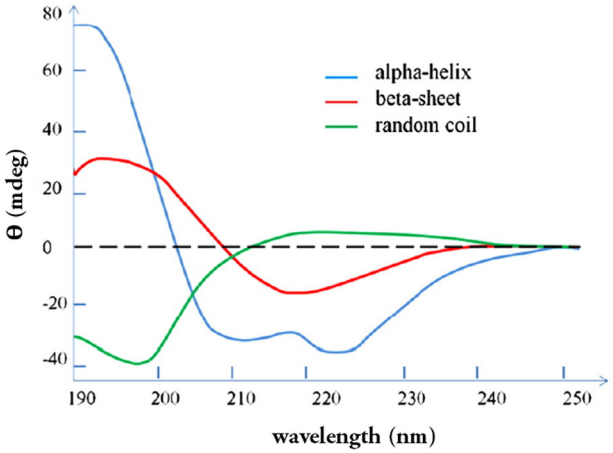

Figure 49. CD spectra of the secondary structures of a protein.[127]

The CD spectrum can be used to distinguish between two areas:

- Far UV (< 250 nm): peptide bond absorption (n → n*, n → n*) 220 nm, 190 nm.
- Near UV (250-300 nm): aromatic amino acids (n → n*) 260 to 320 nm.
  disulfide bridges: (n → σ*) approx. 260 nm.[128]

To study the influence of the artificial metalloproteases on the secondary structure of $A\beta_{42}$, the CD spectrum of a 10 µM solution of $A\beta_{42}$ was recorded as a reference sample. Thereby, a previously monomerized Aβ peptide was incubated in potassium phosphate buffer (pH = 7.3) at 650 rpm and 25 °C. The CD measurements were taken after 0 hours, 1 hour and after 1 day incubation period (Figure 50).

[125] Dodero V. *et al.*, *Front. Biosci.*, **2011**, *16*, 61-73.
[126] Greenfield N., *Nature Protocol*, **2005**, *1*, 2876-2890.
[127] Wei Y. *et al.*, *Biochim. Biophys. Acta Proteins Proteom.*, **2014**, *12*, 2331-2337.
[128] Kelly S.M., Price N.C., *Curr. Protein Pept. Sci.*, **2000**, *1*, 349-384.

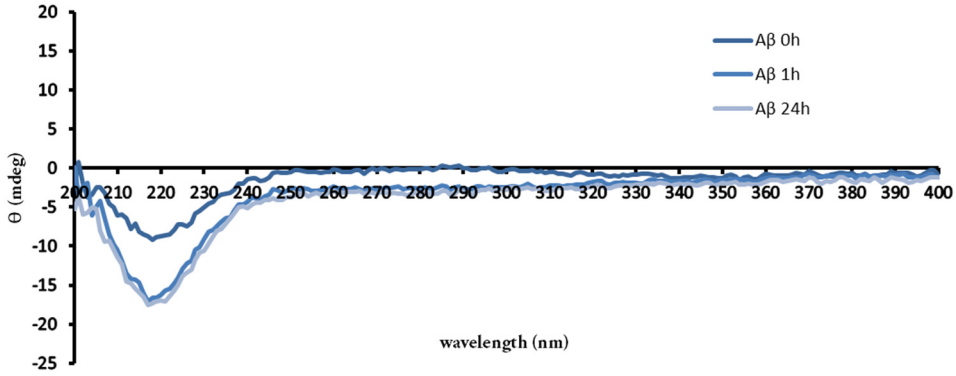

Figure 50. CD measurements of 10 μM $A\beta_{42}$ after 0 h, 1 h and 1 day incubation period (25 °C, 650 rpm).

When $A\beta_{42}$ was added to the buffer aqueous solution, the β-sheet structure was confirmed by the appearance of a negative band at 218 nm, which increased its intensity after 24 hours of incubation. This band is characteristic of the β-sheet secondary structure of Aβ.[129] CD measurements of the artificial metalloproteases without the presence of $A\beta_{42}$ also were carried out to consider their specific band in the following experiments (Figure 51).

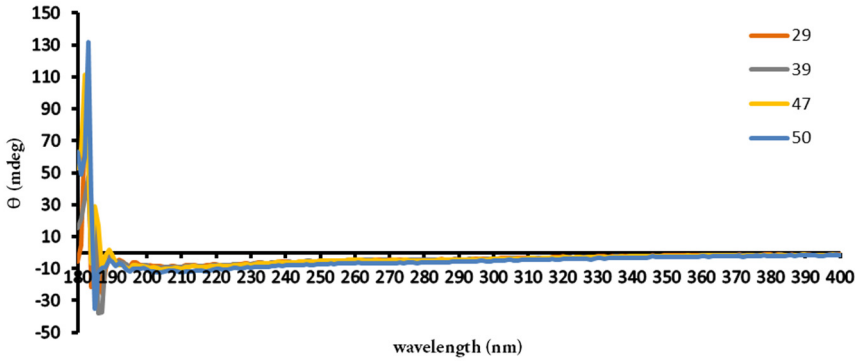

Figure 51. CD spectra of 10 μM artificial metalloproteases **29**, **39**, **47** and **50** in potassium phosphate buffer without $A\beta_{42}$ (25 °C).

The artificial metalloproteases did not show any particularly pronounced band in CD spectra (figure 50). For that reason, CD measurements were made with $A\beta_{42}$ to investigate the influence of the cobalt complexes on the Aβ secondary structure. The CD measurements were carried out in water since the artificial metalloproteases are water soluble. Stock solutions of the artificial metalloproteases in water (500 μM) were prepared. A CD spectrum of $A\beta_{42}$ without ligand after 24 h of aggregation time was included in the artificial metalloproteases spectra to be used as a reference (black continuous line in Figure 52).

[129] Rangachari V. *et al.*, *Biochemistry*, **2007**, *46*, 12451-12462.

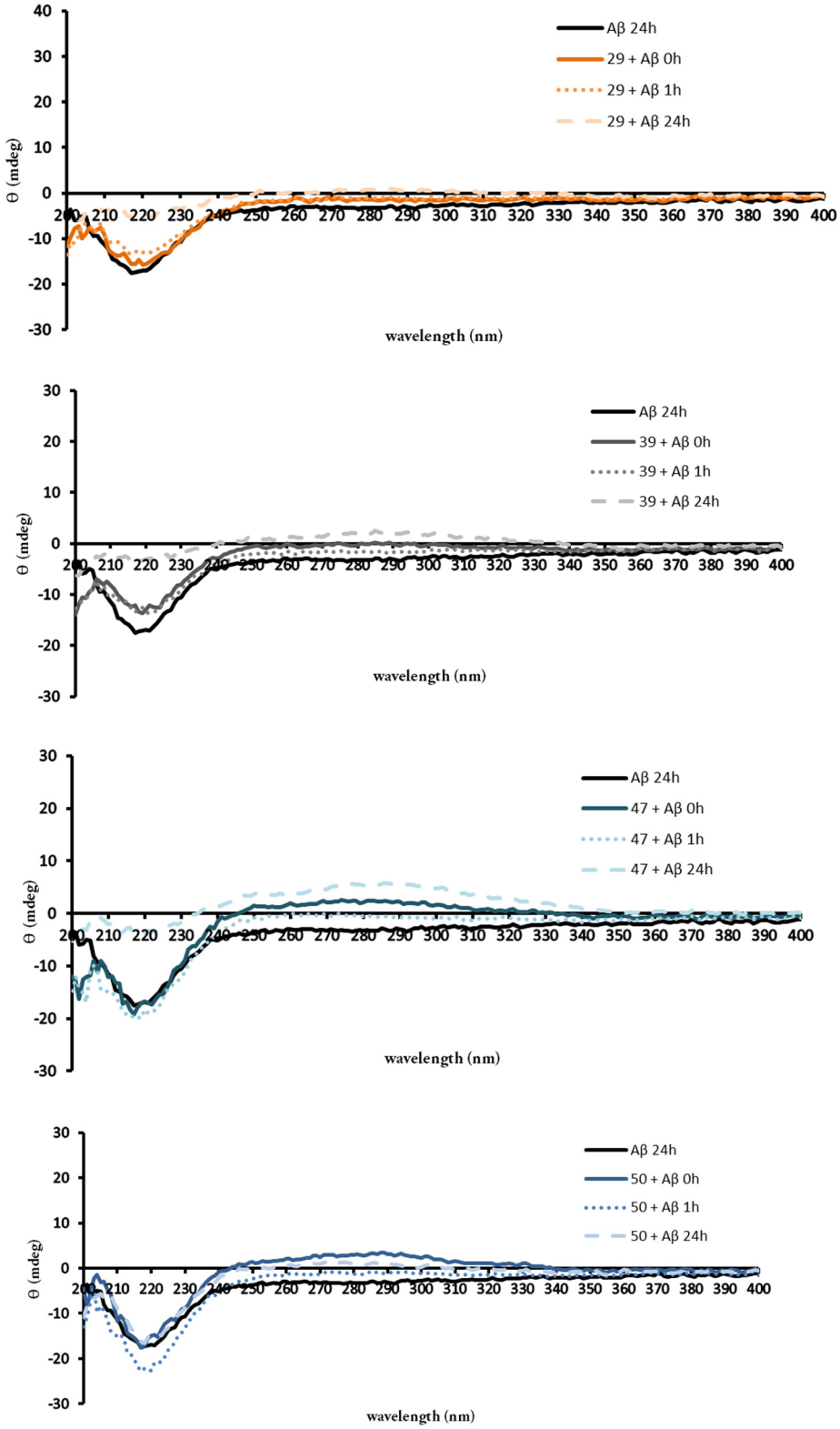

Figure 52. CD spectra of 10 μM artificial metalloproteases **29**, **39**, **47** and **50** in potassium phosphate buffer with 10 μM $A\beta_{42}$ after 0 h, 1 h and 1 day incubation period (25 °C, 650 rpm).

In general, the negative band at 218 nm under the influence of the artificial metalloproteases **29**, **39** and **47** was not as pronounced as the $A\beta_{42}$ reference ($A\beta_{42}$ incubated for 24 hours),

even after 24 hours of incubation at 25 °C, which means that the artificial proteases alter the secondary structure of $A\beta_{42}$. In the case of the artificial metalloprotease **50**, there was no major influence on the secondary structure of $A\beta_{42}$ since the spectrum was not altered, even after 24 hours of incubation, where fibril formation occurs and the β-sheet conformation is predominant. Besides, a slight positive Cotton effect in the range 250-300 nm appeared in all the CD spectra (particularly pronounced in **47**), which provides information about an interaction with the postulated binding site (KLVFF) of $A\beta_{42}$ (Figure 52).

3.1.4 Proteomics-MS

A proteomic assay was stablished in order to understand the cleavage mechanism of the artificial proteases in protein aggregation. A new collaboration was created with the "Analytics Core Facility Essen (ACE)" of the University of Duisburg-Essen, directed by Dr. Farnusch Kaschani.

A sensitive assay was needed to detect cleavage of $A\beta_{42}$. For that reason, a proteomic approach was selected since the technique allow us to analyze the peptide cleavage from the original full length of Aβ.

To perform a first experiment, $A\beta_{42}$ was previously monomerized, lyophilized and a stock solution in HPLC-LC/MS-grade water was prepared. Stock solutions of the artificial metalloproteases **29**, **39**, **47** and **50** were also dissolved in HPLC-LC/MS-grade water. The final samples were added in 1.5 mL polypropylene Eppendorf™ microtubes, with a final total volume of 1 mL.

A sample of $A\beta_{42}$ (4 µM) as a reference to compare the cleavage and the intensity of the fragment of the peptide was prepared. In addition, different control references (1 µM) with the artificial proteases were prepared. Then, $A\beta_{42}$ (4 µM) was incubated for 24 hours with an artificial metalloprotease (1µM) in phosphate buffer at pH 7.5 and 37 °C. All the samples were vortexed for 5 seconds, sonicated for 30 seconds, precipitated with 4 volumes of acetone and frozen with liquid nitrogen, except the control of $A\beta_{42}$ and the reference of the artificial proteases. All the frozen samples were given to Dr. Kaschani to be processed.

After thawing, the samples were centrifuged for 20 min at 18000 rpm. Then, approximately 500 µL of supernatant were transferred to a 96-well plate and the samples were dried in a speedvac at 60°C for 3 hours. The volume reduction was approximately of 85% (final volume of 70 µL). The samples were taken up in 25 µL 0.1% FA and loaded onto EvoTips as described in manufacturers rapid protocol. When loading was done the samples were overlayed with 100 µL 0.1% FA. Finally, the samples were analyzed by LC-MS/MS. Protein quantification and analysis of the large MS data sets were interpreted with the free software

Perseus, developed by the Max-Planck-Institute of Biochemistry. A database with the $A\beta_{42}$ sequence was used as a standard to recognize the generated peptides fragments.

For visual inspection, the probability score (negative log P-value) can be plotted against the size of the effect (the confidence of the assay) using a Volcano Plot. The upper left part (green) of the plot shows the values that appear significantly less often compares to the reference of the assay. In the upper right corner (orange), the values that appear more often are exhibited, indicating a certain selectivity (more confident values). Results at the bottom of the plot (pink) are less abundant and appear with the same intensity as the control of the experiment (Figure 53).[130]

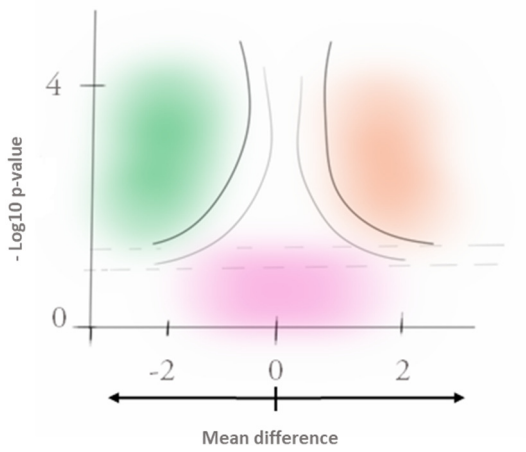

Figure 53. Volcano plot to visualize selectivity profiles.

Using the Perseus software, 103 peptides of interest from $A\beta_{42}$ were identified in this search, and after filtering all the data according to valid values, only 80 peptides remained. Although, the intensities of the peptides were very low (low concentration of the samples) the experiment worked and different cleavages of $A\beta_{42}$ were identified, but only in the samples containing artificial proteases. As shown in figure 54, there are numerous peptides only in the complex-treated samples and not in the FA controls. Also, some peptides were found in the FA control, probably due to the carry-over of the experiment. Additionally, it is noticed that the most frequently appearing peptide fragments vary depending on the protease used.

[130] Rudolph J., Cox J., *J. Proteome Res.*, **2019**, *18*, 2052-2064.

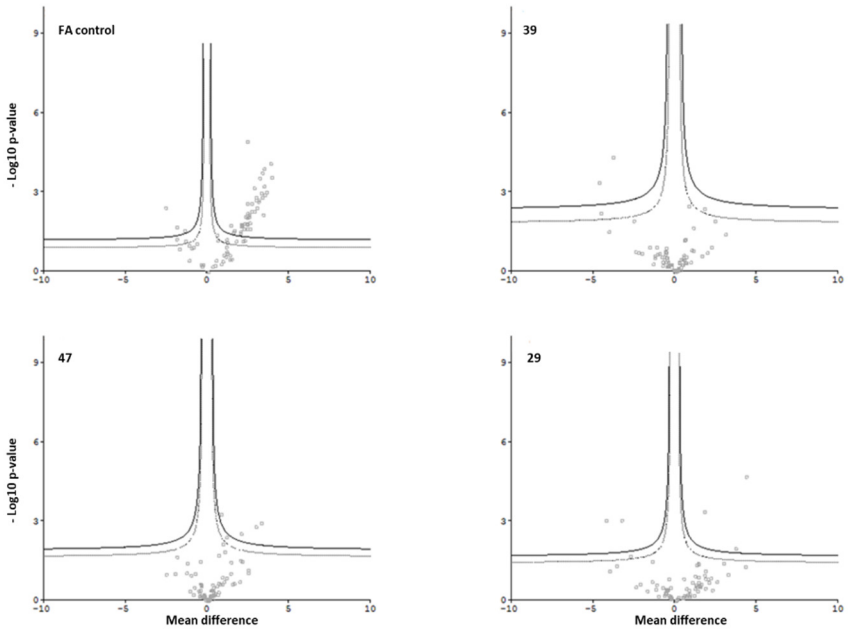

Figure 54. Hawaii plot of the entire data set of the first experiment.

The Perseus software also provides the possibility to identify where the cleavages in the $A\beta_{42}$ sequence occurred. In figure 55, the different cleavages on the volcano plots of the artificial proteases are shown.

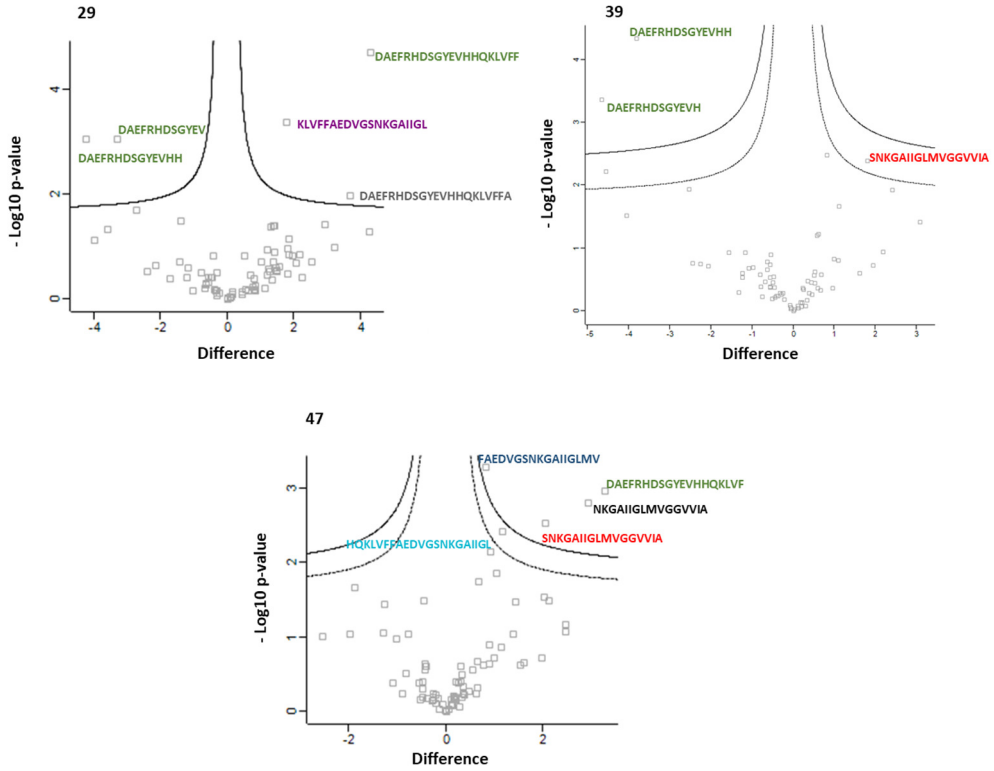

Figure 55. Hawaii plot of the entire data set of the treatment of $A\beta_{42}$ with different artificial metalloproteases. The most relevant detected peptide fragments are indicated.

In Table 3, all the cleavages with a higher intensity and more abundant probability to appear that were found upon treatment with the different artificial proteases are summarized. All the artificial proteases presented cuts in a peptide level, evidencing the success of the experiment. As commented in section 1.3.3.4, Suh and his co-workers performed MS experiments and two main cuts of $A\beta_{42}$ were found by the action of their artificial metalloproteases in $A\beta_{(1-20)}$ and $A\beta_{(1-21)}$, which corresponds with the DAEFRHDSGYEVHHQKLVFF and DAEFRHDSGYEVHHQKLVFFA sequences, respectively. Our artificial metalloprotease **29**, which was based on Suh's molecule with a slight modification of the structure, was able to cut $A\beta_{42}$ in three parts: $A\beta_{(1-20)}$, $A\beta_{(1-21)}$ and $A\beta_{(16-34)}$. **39** only cut $A\beta_{(26-42)}$, but **47** was able to cut in 5 different positions ($A\beta_{(1-19)}$, $A\beta_{(20-39)}$ $A\beta_{(25-42)}$ $A\beta_{(26-42)}$ and $A\beta_{(14-34)}$) of $A\beta_{42}$, being the most powerful artificial protease synthesized in this thesis.

Table 3. Summary of all the $A\beta_{42}$ cleavages made by the artificial proteases.

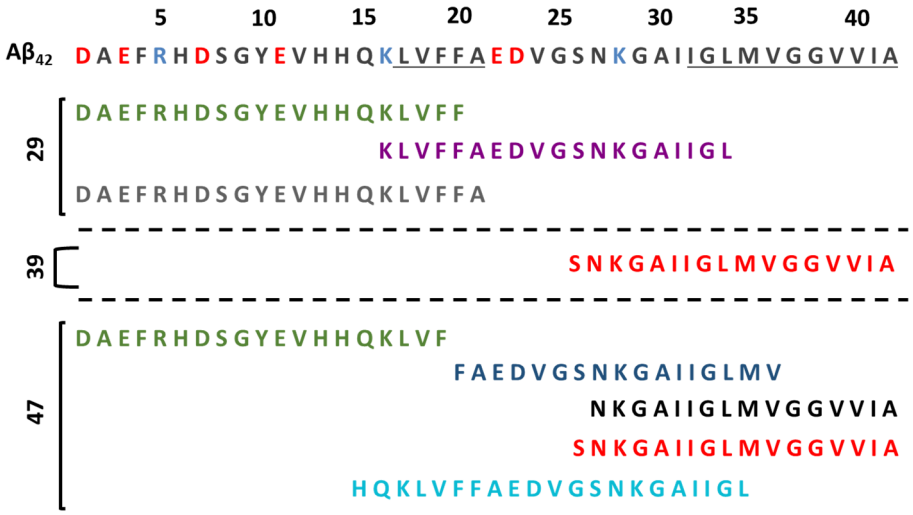

However, the results were a bit unpredictable since the peptide intensities fluctuated significantly. In addition, the missing controls without artificial proteases ($A\beta_{42}$ reference) made it hard to decide if the found cleavages corresponded to the artificial proteases treatment or to the treatments during sample preparation, since $A\beta_{42}$ was not treated like the other samples and could not be used for the experiment. Therefore, another experiment was performed, optimizing the conditions and sample preparation.

To perform the second experiment, the final samples were added in 1.5 mL polypropylene Eppendorf™ microtubes, with a final total volume of 50 µL. Three different samples of $A\beta_{42}$ (16 µM) as reference to compare the cleavage and the intensity of the fragment of the peptide were prepared: 1) in water without incubation 2) in phosphate buffer without incubation 3) in phosphate buffer after 24 hours of incubation at 37 °C. All the samples

were vortexed for 5 seconds, sonicated for 30 seconds, precipitated with 4 volumes of acetone and frozen with liquid nitrogen. Then, 8 µM and 16 µM of $A\beta_{42}$ was incubated for 24 hours with 2 µM and 8 µM artificial metalloprotease in phosphate buffer at pH 7.5 and 37 °C, respectively. All the samples were vortexed for 5 seconds, sonicated for 30 seconds, precipitated with 4 volumes of acetone and frozen with liquid nitrogen. All the frozen samples were also given to Dr. Kaschani to be processed.

After thawing, the samples were centrifuged for 20 min at 18000 rpm. Then, approximately 200 µL of supernatant were transferred to a 96-well plate and the samples were dried in a speedvac at 60°C for 90 min. The samples were taken up in 25 µL 0.1% FA and loaded onto EvoTips as described in manufacturers rapid protocol. When loading was done the samples were overlayed with 100 µL 0.1% FA. Finally, the samples were analyzed by LC-MS/MS. The MS data sets were interpreted with the free software Perseus.

The results were deeply checked, and the intensities of the peptides were too low to identify all the cleavages correctly. In the assay, 100 peptides of interest from $A\beta_{42}$ were identified by comparison with the reference database. After filtering all the data according to valid values, only 78 peptides remained (three less than the previous experiment). In figure 56, the volcano plots of the average of the peptide intensities, using $A\beta_{42}$ in water without incubation as a reference, are shown. Unfortunately, all the peptides that appeared in the samples containing artificial metalloproteases were also present in the volcano plot of the $A\beta_{42}$ reference in water, meaning that the appearance of those peptides cannot be attributed to the cleavage activity of the artificial metalloproteases.

The problem in this experiment was found to be in the treatment of the $A\beta_{42}$ reference previous to the incubation. To monomerize $A\beta_{42}$, HFIP was used and removed via lyophilization. In this step a new lyophilization equipment was used. The high vacuum of the lyophilizer ($8 \cdot 10^{-6}$ bar), added to the acidic pH of the HFIP (2-3) might have led to an unwanted cleavage to $A\beta_{42}$, which has been previously reported in the literature.[131,132] Besides, ThT and CD experiments carried out with the same monomerized $A\beta_{42}$ showed unusual results, since the protein could not aggregate over 24 hours of incubation.

[131] Roy I., Gupta M.N, *Biotechnol. Appl. Biochem.*, **2004**, *39*, 165-177.
[132] Schmid R.D., *Adv. Biochem. Eng.*, **1979**, *12*, 41-117.

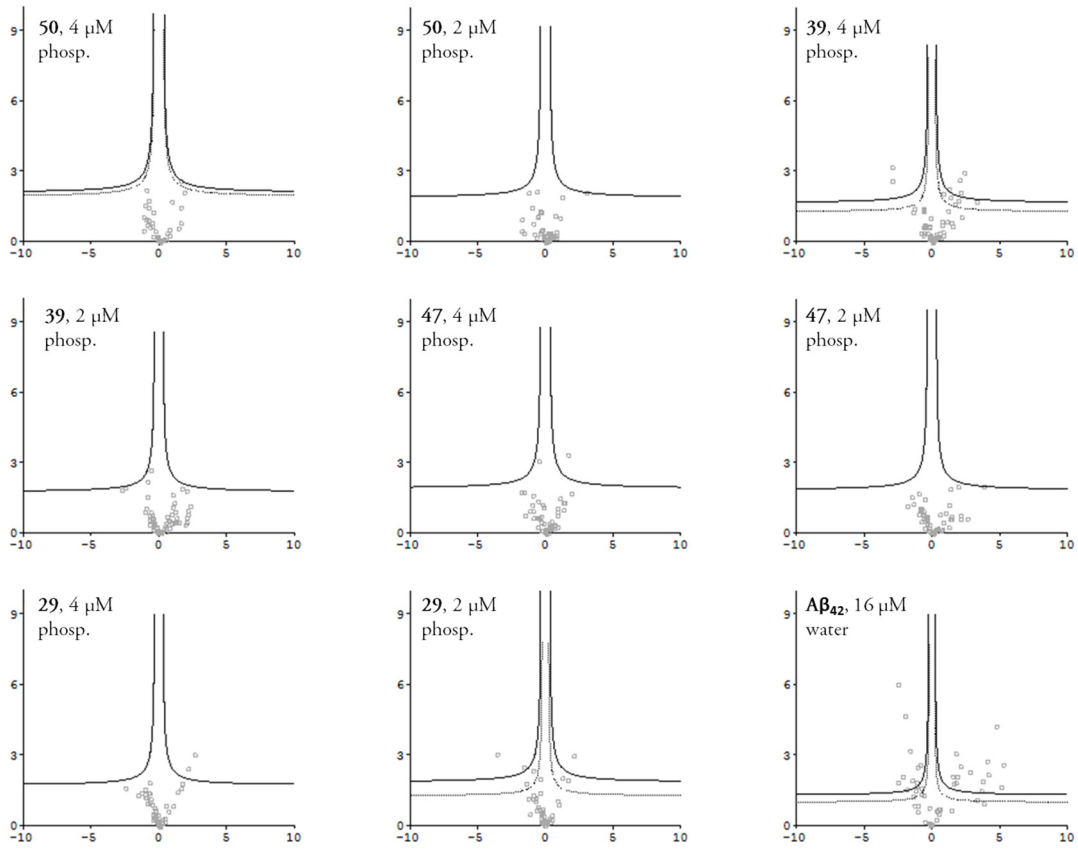

Figure 56. Hawaii plot of the entire data set of the experiment.

In conclusion, the obtained results are erratic and do not provide enough evidence to affirm that the proteases act at the peptide level and produce additional cleavage events. This last experiment contradicts the first one, so further modifications to optimize the sample preparation have to be made in order to confirm the active influence of the artificial metalloproteases on the Aβ protein.

3.1.5 Discussion

Within the scope of this work, new artificial metalloproteases were designed and developed after an intense investigation of Suh's seminal work. The artificial metalloproteases **29**, **39**, **47** and **50** were successfully synthesized and tested for their interaction with the Aβ by biophysical methods such as CD spectroscopy or thioflavin T experiments.

In ThT studies, the Aβ aggregation was strongly inhibited by the artificial metalloproteases **29**, **39** and **47**. After 5 days of incubation with $A\beta_{42}$, the artificial metalloproteases were able to reduce the fluorescence by 99%, 97% and 97%, respectively. Different concentrations of the artificial metalloproteases were tried to find their limit where do not affect the Aβ aggregation. When the artificial metalloproteases were stoichiometrically added to $A\beta_{42}$, a moderate inhibition of up to 93%, 82% and 79% was shown after 5 days of incubation,

respectively. With 10 times less concentration of artificial proteases than $A\beta_{42}$, the inhibition could only be reduced by half, even after 5 days of incubation. No inhibition was shown when the concentration of the artificial metalloproteases was 100 times less than $A\beta_{42}$. Since the experiments showed reproducibility problems, further biophysical assays were performed to determine the influence of the artificial metalloproteases in Aβ aggregation.

The investigations of the destabilization of the β-sheet conformation were performed by CD measurements. The artificial proteases **29**, **39** and **47** could destabilize the secondary structure of $A\beta_{42}$ reducing the negative band by half after 24 hours of incubation. A new positive band with a maximum in 270 nm appeared, indicating an interaction with the aromatic amino acids of the binding site of the $A\beta_{42}$ (KLVFF), evidencing that the artificial metalloproteases can interfere on the secondary structure of $A\beta_{42}$.

The first experiment of the proteomics showed a substancial cleavage of $A\beta_{42}$ from the artificial proteases. **47** was able to cut $A\beta_{42}$ in 5 different fragments, revealing the powerful action of this artificial metalloprotease. However, a second proteomic assay was carried out, since the $A\beta_{42}$ reference was not include in the first experiment because no treatment of the sample was made. The second experiment was not as successful as the first one. The artificial metalloproteases showed only a few cleavages, but these fragments were also present in the $A\beta_{42}$ reference sample. The proteomic assays did not show consistent results and further optimizations have to be made.

3.2 β-sheet breakers against protein aggregation

Amyloidosis is a collective term for a diverse group of diseases characterized by misfolding of soluble precursor proteins, eventually forming highly ordered amyloid cross β-fibrils which deposit in various tissues.[133] The most common systemic amyloidosis is amyloid light-chain (AL) amyloidosis caused by an abnormality in plasma cells. The abnormal plasma cells produce an abnormal form of light chain proteins (LCs) that become misfolded and deposited in and around the tissues, mainly in the heart and kidneys, producing organ damage. There is no cure for this or another type of amyloidosis since amyloid deposits cannot be directly removed. However, different treatments are applied to patients who suffer AL amyloidosis, such as chemotherapy or stem cell transplantation.[134]

Ehrmann and his co-workers, in previous studies, demonstrated that the serine protease HTRA1 is able to degrade aggregated and fibrillary tau and potentially cleave β-strands. In recent studies, Pedroza demonstrated that HTRA1 is able to target amyloid LC fibrils in AL amyloidosis.[135]

As it is well-known, aminopyrazoles (β-sheet breakers) were proved to prevent protein aggregation into amyloid fibrils by interacting with non-aggregated soluble forms. Already formed amyloid fibrils can be dissociated by chaperones and proteases such as HTRA1, which can occur in two steps. First, the chaperone loosens the amyloid structure, after which isolated peptides of these fibrils can bind to the protease's active site, where they are degraded into small peptides that do not aggregate. It was thought that our β-sheet breakers could be helpful in the disaggregation step where, after HTRA1 pulls on individual polypeptides, the aminopyrazoles could move in and prevent re-association of the loosened and extracted polypeptides back into the amyloid fibrils. Therefore, the aminopyrazole derivatives developed and synthesized in our group were tested against protein aggregation by Prof. Dr. Michael Ehrmann and his co-workers.

3.2.1 Aminopyrazoles design

As mentioned in chapter 1.3.3.3, aminopyrazoles were designed to bind strongly β-sheet structures due to a large number of hydrogen bonds (DAD) preventing longer peptides. In this chapter, a new synthesis pathway with a view of optimizing times and reagents is presented.

[133] Fotiou D. *et al.*, *HemaSphere*, **2020**, *4*.
[134] Palladini G., *Blood*, **2020**, *136*(23), 2620-2627.
[135] Pedroza. L, "The implication of the human serine protease HTRA1 in immunoglobulin light chain amyloidosis", Essen, **2020**.

The present synthesis features a sequence of amide couplings, where an amino group is reacted with a carboxylic group to form a strong amide bond. It is important to note that, since each monomer bears both functionalities, they needed to be orthogonally protected to avoid self-coupling reactions and to deprotect each group selectively.

Firstly, 5-nitro-3-pyrazole carboxylic acid was protected with a methyl group, which can easily be removed in further steps with LiOH. For this purpose, thionyl chloride was used in presence of methanol to mask the carboxylic acid as a methyl ester, to give **52**. This method was used for convenience instead of the traditional conditions employing HCl gas, since it eliminates side reactions, long reaction times, and column purification. After that, the NH of the pyrazole had to be protected to avoid any undesired interactions. PMB group was chosen due to its stability and facile cleavage conditions, affording **54**. The PMB derivative **53** was synthesized following a S_N2 pathway between 4-methoxybenzyl alcohol in presence of HBr.[76]

To be able to form a dimeric pyrazole unit, two different monomers were prepared: one possessing a free amino group and another one with a free carboxylic acid (Scheme 19). To achieve this, the PMB-protected pyrazole **54** was treated with tin chloride to obtain **55**, following a sequence of single-electron transfers (SET).[136] On the other hand, a hydrolysis of the methyl ester **54** was carried out to obtain **56**.[76]

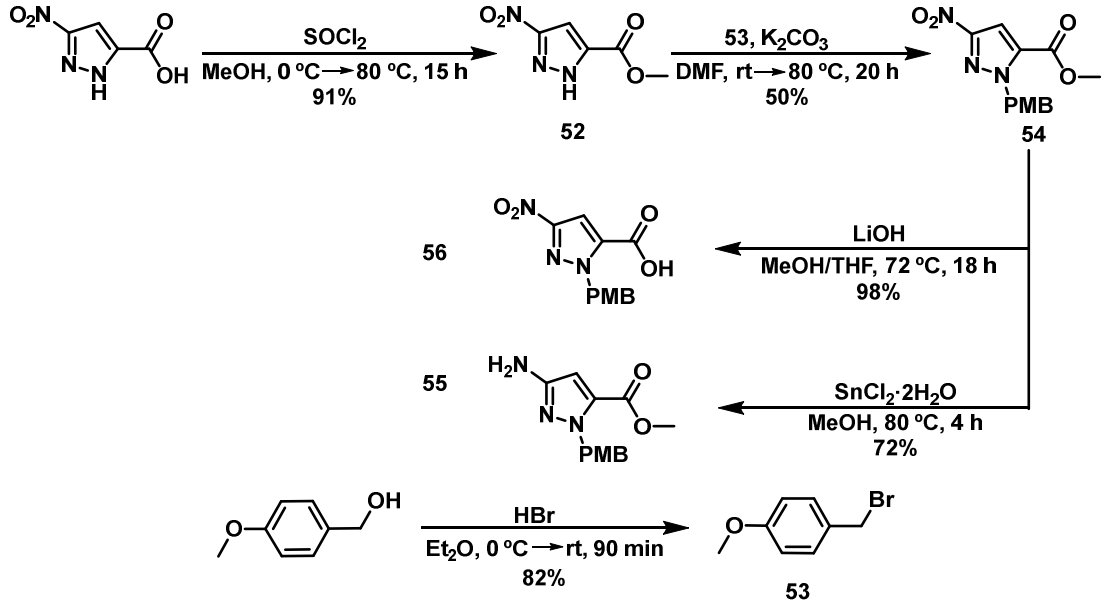

Scheme 19. Synthetic route to obtain the monomeric pyrazole derivatives **55** and **56**.

After that, the monomer aminopyrazole **55** was coupled with the monomer acid **56** to yield **57**. In order to achieve the trimeric unit of pyrazoles, a similar reaction-sequence as before

[136] Li B. *et al.*, *J. Org. Chem.*, **2015**, *80*, 5444-5456.

was followed, first reducing the nitro group of the dimeric pyrazole unit **57** employing tin chloride, to give **58**, and subsequently coupling it with another monomeric acid unit **56** to obtain the protected trimer derivative **59**. Then, the methyl ester was hydrolyzed to yield the PMB-protected **60**, which will be coupled to different peptide-sequences to create hybrid molecules designed to disaggregate amyloid fibrils (Scheme 20).[76]

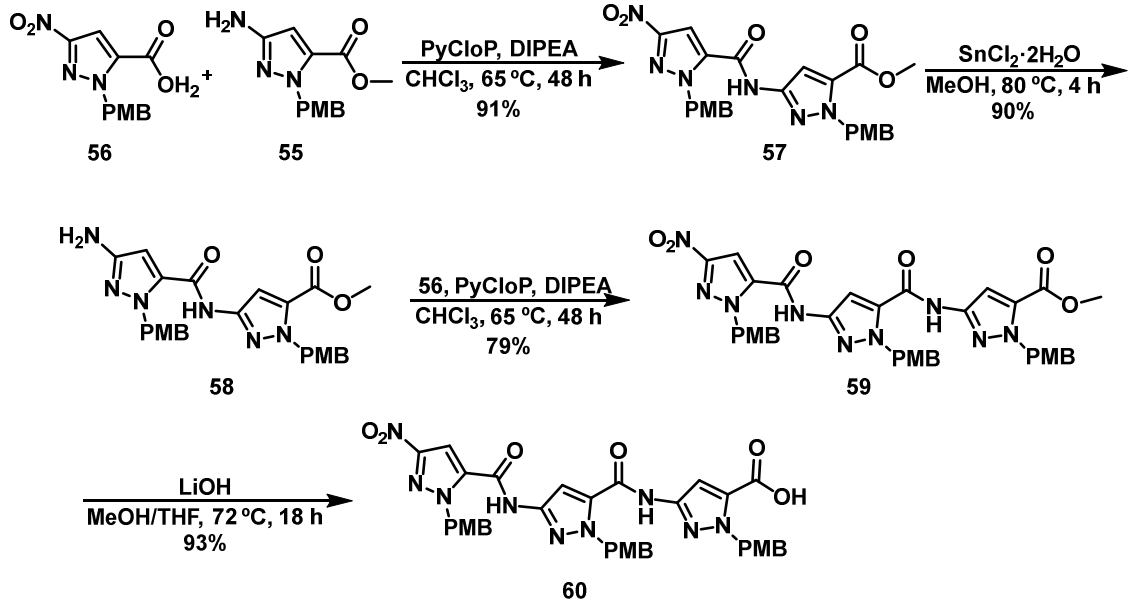

Scheme 20. Synthetic pathway of the protected trimeric pyrazole **60**.

To provide some of the final hybrid molecules with more water solubility, the introduction of a triethyleneglycol (TEG) spacer was envisioned. For that purpose, the TEG spacer was synthesized according to the literature[77,137,138] (Scheme 21).

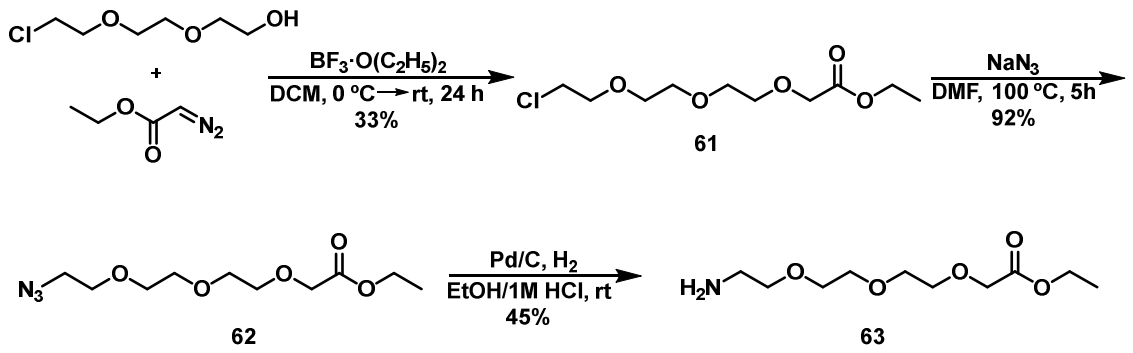

Scheme 21. Synthesis of the spacer **63**.

[137] Boumrah *et al.*, *Tetrahedron Letters*, **1991**, *32*, 7735.
[138] Boumrah *et al.*, *Tetrahedron*, **1997**, *53*, 6977-6992.

The spacer TEG **63** was coupled to the trimer **60**, to yield **64**. Then, the methyl ester **64** was hydrolyzed, affording **65**.[77] The PMB protected **65** was also coupled with different peptides to obtain the aminopyrazoles hybrids, which were tested against LC aggregation (Scheme 22).

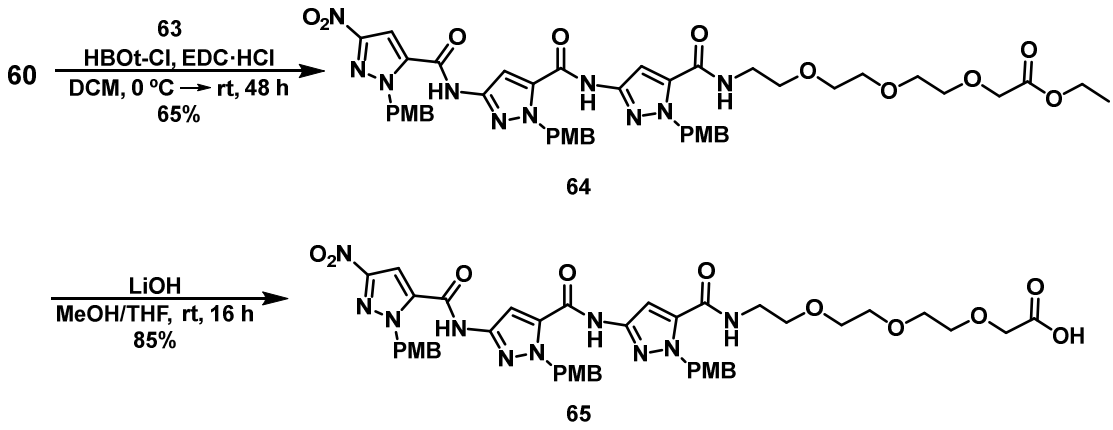

Scheme 22. Synthetic pathway of the protected trimeric pyrazole derivative **63**.

The peptides with different amino acid sequences were prepared following the General Method I described in the chapter 4 of this thesis, and the various β-sheet breakers were synthesized following the General Method III (Tables 4 and 5). All the compounds were tested by ThT fluorescence, CD, AFM and sedimentation assays to confirm the inhibition of fibril formation in AL amyloidosis.

The peptide fragments to be coupled to the hybrid molecules consist of short amino acid chains selected from the sequence of proteins involved in amyloidosis diseases. Soto *et al.* found that the LPPFD peptide is able to significantly reduce Aβ plaques in AD model mice,[58] since the two aromatic phenylalanine residues stabilize the complex in which the β-sheet breaker is bond to the Aβ peptide backbone via hydrogen bonds. E. M. Mandelkow, E. Mandelkow and their co-workers demonstrated that the hexapeptide motifs VQIVYK and VQIINK were essential to initiate tau aggregation.[139] Therefore, these peptides were selected to be coupled to the trimer acid **60** and trimer-TEG acid **65** to form hybrid molecules.

-SFDSSSNSASLSISGLKTEDEAD-

Figure 56. SAI-VL sequence from LCs.

The water soluble NKKLDLSN peptide was also chosen from the tau sequence due to its potential contribution to the solubility of the aminopyrazole derivative. Finally, the

[139] von Bergen M. et al., *PNAS*, **2000**, *97*(10), 5129-5134.

amyloidogenic core from the LC sequence was explored and the peptides SGLKTEDE and DSSSNS were selected to examine their effectiveness against LC aggregation (figure 56).[140] These three last compounds were only coupled to **65** since the presence of the TEG spacer proved to be essential to make these hybrid molecules water-soluble.

Table 4. First β-sheet breakers evaluated against LC and Aβ aggregation.

Structure	Name	Mw (g/mol)
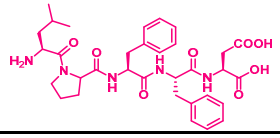	LPFFD **68**	637.73
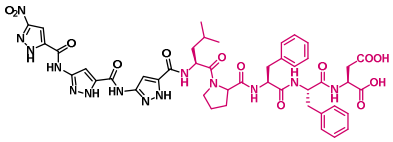	Trimer-LPFFD **69**	994.98
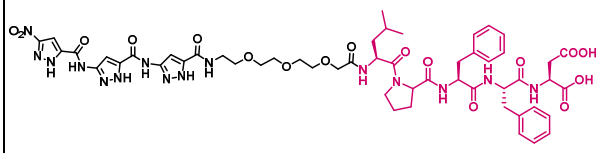	Trimer-TEG-LPFFD **7**	1184.19
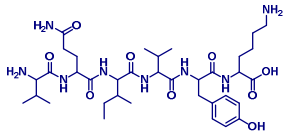	VQIVYK **70**	748.92
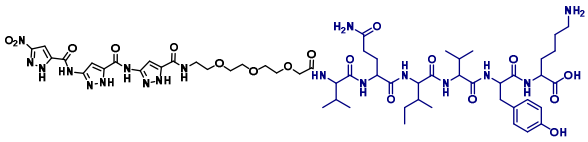	Trimer-TEG-VQIVYK **71**	1295.38
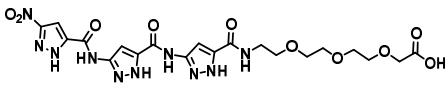	Trimer-TEG acid **67**	564.47
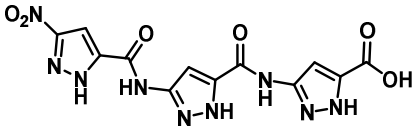	Trimer acid **66**	375.26

[140] Pradham T. *et al.*, *BioRxiv,* **2020**.

Table 5. β-sheet breakers that are currently being evaluated against LC and Aβ aggregation.

Structure	Name	Mw (g/mol)
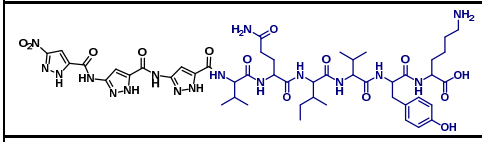	Trimer-VQIVYK **72**	1106.17
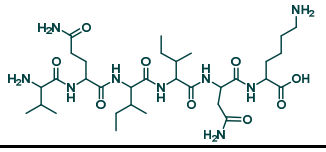	VQIINK **73**	713.88
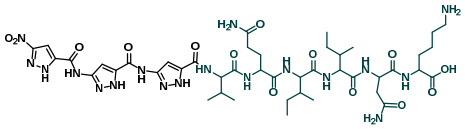	Trimer- VQIINK **74**	1071.12
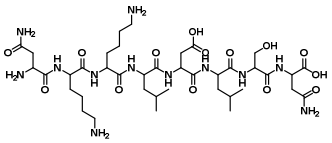	NKKLDLSN **75**	931.06
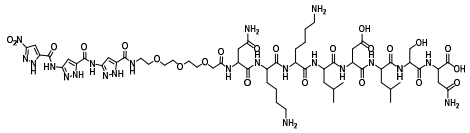	Trimer-TEG-NKKLDLSN **76**	1477.42
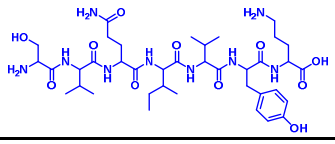	SVQIVYK **77**	821.97
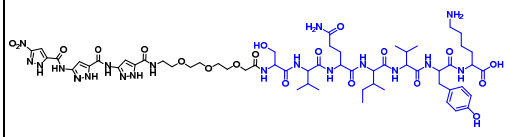	Trimer-TEG-SVQIVYK **78**	1382.46
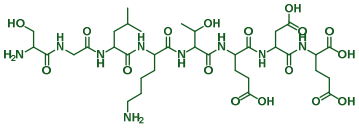	SGLKTEDE **79**	877.90
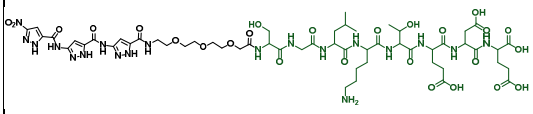	Trimer-TEG-SGLKTEDE **80**	1424.36
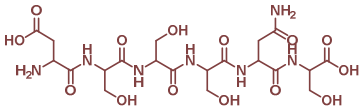	DSSSNS **81**	595.52
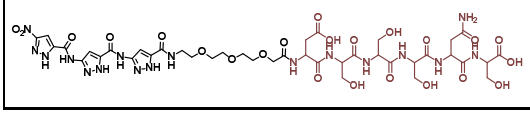	Trimer-TEG-DSSSNS **82**	1141.98

Additionally, some of **60** and **65** were subjected to harsh acidic conditions to remove the PMB group, affording **66** and **67,** respectively. Their potential against amyloid fibril aggregation were also evaluated, serving as a control molecule to determine whether the peptide residues present in their hybrid molecule counterparts have a positive influence in their disaggregation capability.

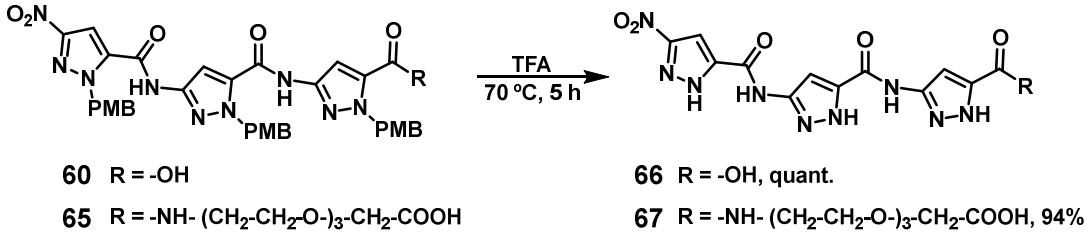

Scheme 23. Synthetic route towards the unprotected trimeric pyrazole derivatives **66** and **67**.

3.2.2 Thioflavin T experiment

A thioflavin T fluorescence assay was performed in order to monitor fibril formation by the lack of ThT fluorescence signal compared to the control. Only preliminary results for the hybrid compounds (β-sheet breakers) of table 4 are shown in this section, since several experiments are currently being carried out with the aminopyrazoles of the table 5. All the ThT experiments with LCs were performed by Dr. Laura Pedroza.

The ThT experiment was carried out in the presence of SAI-VL (from LC sequence). For this reason, the molecules **7**, **66**, **67**, **68**, **69**, **70** and **71**(concentration: 120 µM) were incubated with 16.5 µM SAI-VL at 37 °C in 10 mM Hepes, 100 mM NaCl, at pH 7.6 containing 0.4 µg/µl heparin sodium salt. The data was recorded after 0, 1, 2, 4 and 7 days of incubation (figure 57).

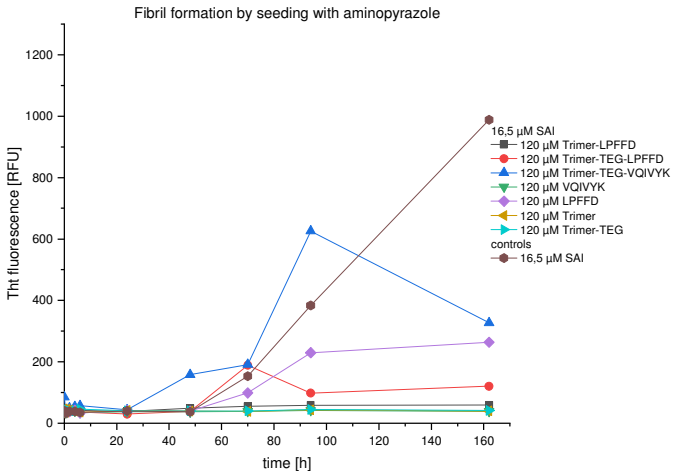

Figure 57. Fluorescence studies of SAI-VL fibril formation in presence of β-sheet breakers.

After 2 days of incubation, the reference sample SAI-VL increased its signal, indicating fibril formation that reached elevated levels after 4 days. In the case of the aminopyrazole hybrids incubated with SAI-VL, only **7**, **70**, **66** and **67** showed inhibition of fibril formation of SAI-VL, and after 4 days no change in the ThT fluorescence signal was observed. The LC proteins are β-sheet-rich both in its aggregated and native forms, so it was hypothesized that the aminopyrazoles hybrids prevented longer peptides from forming β-sheet structures and aggregates. Complementary techniques were carried out to confirm the inhibition of fibril formation.

Since ThT fluorescence experiment can also be used as a quantitative technique, the potential of **7** to inhibit fibril formation**,** which was the most promising among all the evaluated molecules, was quantified. For this experiment, 16.5 µM of SAI-VL was incubated 37 °C with or without **7** (120 µM) in 10 mM Hepes, 100 mM NaCl, at pH 7.6 with additional 0.4 µg/µl heparin sodium salt. 5 µl aliquots were taken after 1 day, 2 days and 4 days, and were incubated in 12 µM ThT/Gylcine and measured at λ= 480 nm. As mentioned before, after 2 days the ThT fluorescence signal of SAI-VL rose up due to fibril formation. In presence of **7**, the fluorescence signal did not changed (even after 4 days of incubation) indicating that **7** could inhibit fibril formation of SAI-VL (Figure 58).

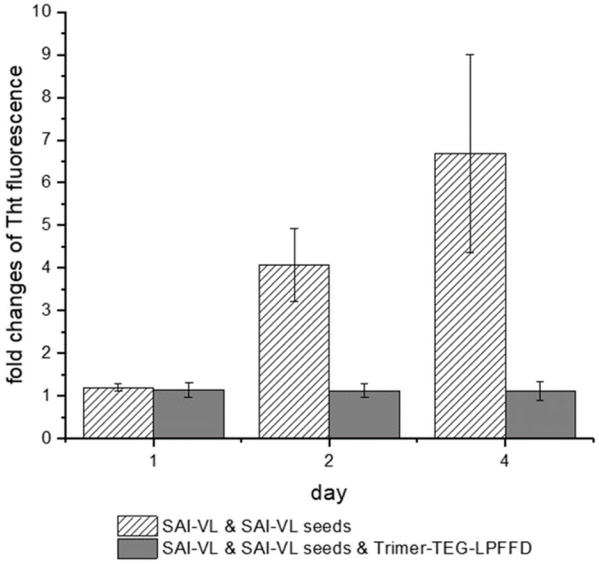

Figure 58. Quantification of SAI-VL fibril formation with the aminopyrazole derivative **7**.

Simultaneously, an additional experiment was carried out in our working group to evaluate the inhibition potential of the hybrid molecules against the aggregation of $A\beta_{42}$, since this protein is involved in other amyloidosis diseases such as AD. The compounds **7**, **66**, **67**, **68**, **69**, **70** and **71** (60 µM) were incubated in the presence of 10 µM $A\beta_{42}$ at pH 7.0 and 37 °C

for 5 days. The values are expressed as a percentage, having the $A\beta_{42}$ control the highest possible value (100%) (Figure 59).

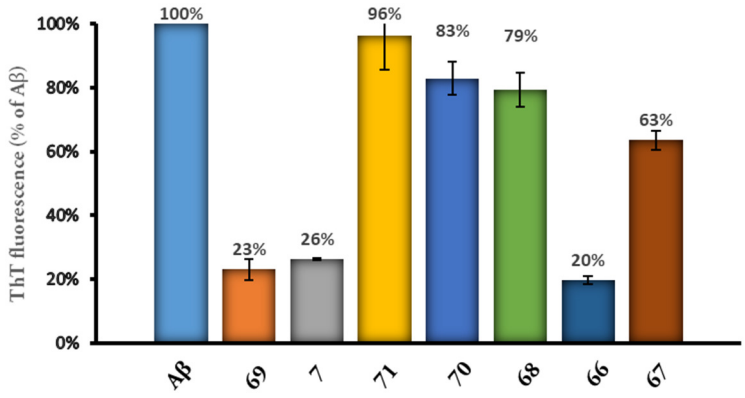

Figure 59. Inhibition of 10 µM $A\beta_{42}$ with 60 µM aminopyrazoles derivatives at pH 7.0 and 37 °C after 5 days of incubation.

The aminopyrazoles **7**, **66** and **69** were able to inhibit fibril formation of $A\beta_{42}$ drastically, showing a decrease in aggregation of around 80%. **67** exhibited a moderate inhibition of 37%. Hybrid aminopyrazole **71** was not able to inhibit fibril formation. The obtained results with $A\beta_{42}$ are in accordance with those obtained with LC, evidencing the potential of these molecules against the aggregation of various proteins involved in amyloidosis diseases. However, these studies showed a poor reproducibility and the values differed between repetitions, presumably due to solubility issues of the fluorophore and the hydrophobic parts of the molecules. Therefore, additional techniques were carried out, such as CD or AFM.

3.2.3 Circular Dichroism

CD measurements were carried out in our working group for the aminopyrazoles **7**, **66**, **67**, **69** and **71** against $A\beta_{42}$ to investigate conformational changes. Only substances that were soluble in pure water, pure HFIP or water/HFIP mixtures were suitable to be tested with CD spectroscopy, since DMSO absorbs in our range of interest and therefore cannot be used for this experiment. Stock solutions of **7**, **69**, **71**, **67** in pure HFIP (250 µM) and **66** in water/5%HFIP (250 µM) were prepared. The samples were prepared in potassium phosphate buffer (pH = 7.3) at room temperature, and measurements were taken after 0 hours, 1 hour and 1 day incubation period.

CD measurements of the hybrid aminopyrazoles without the presence of $A\beta_{42}$ were also carried out to consider their specific band in the following experiments (Figure 60).

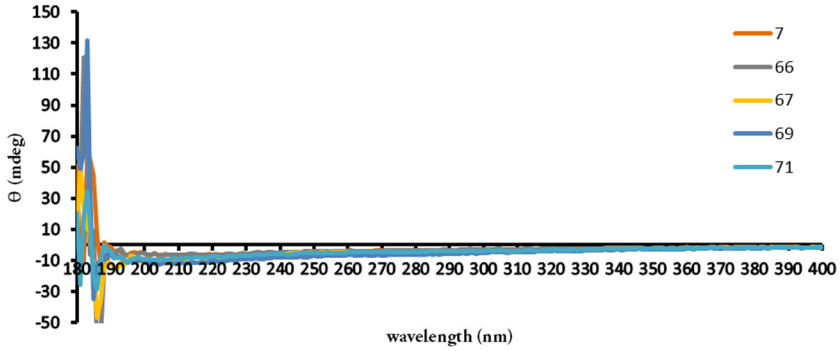

Figure 60. CD spectra of 10 µM aminopyrazoles derivatives **7**, **66**, **67**, **69** and **71** in potassium phosphate buffer without $A\beta_{42}$ (25 °C).

The hybrid aminopyrazoles did not show any particularly pronounced band in CD spectra around the characteristic negative band at 218 nm that could interfere with the CD experiment (figure 61).

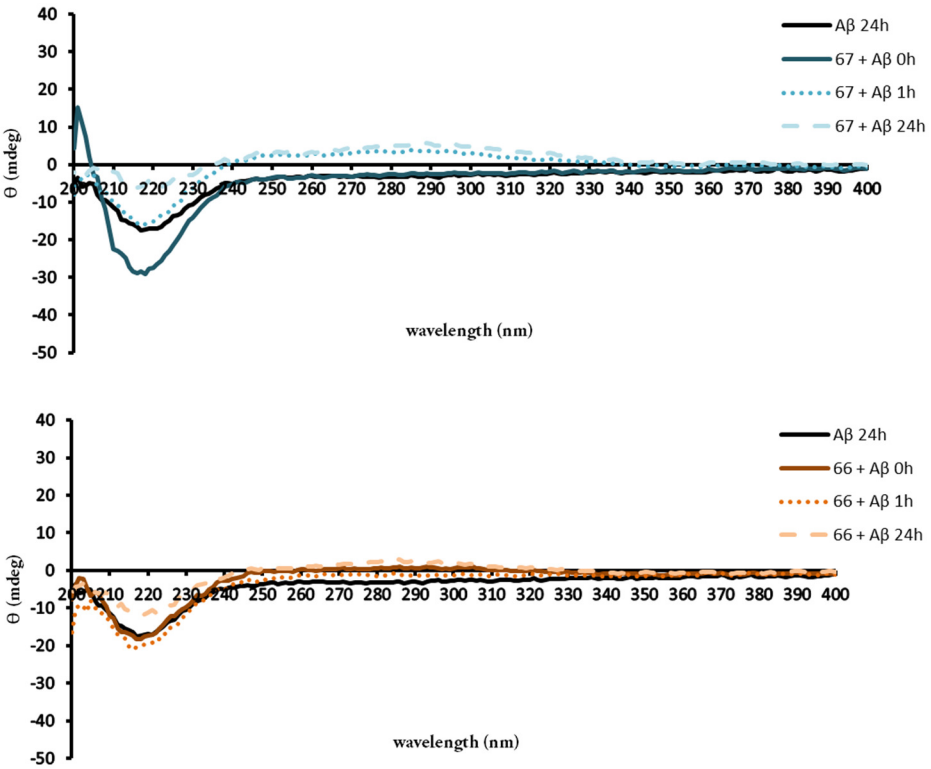

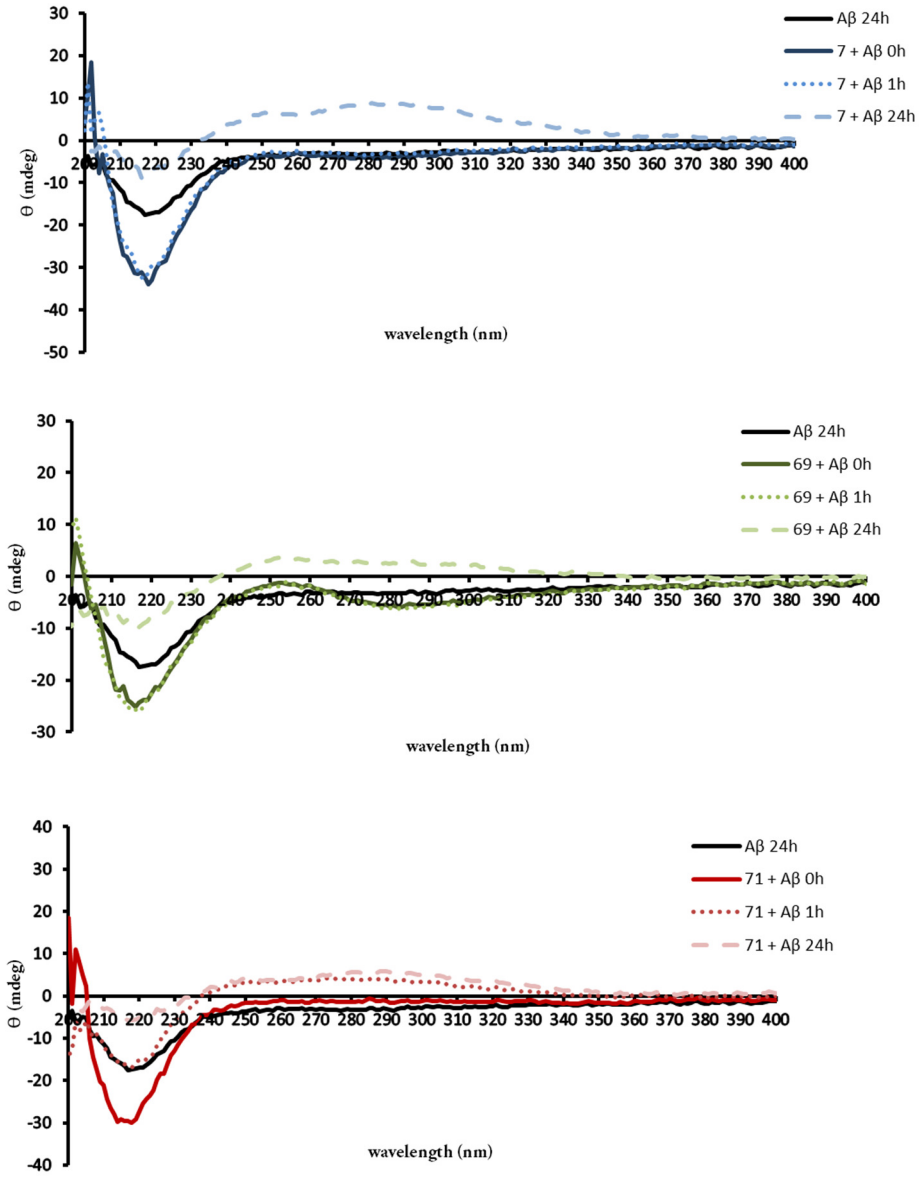

Figure 61. CD spectra of 10 µM aminopyrazoles derivatives **7**, **66**, **67**, **69** and **71** in potassium phosphate buffer with 10 µM $A\beta_{42}$ after 0 h, 1 h and 1 day incubation period (25 °C, 650 rpm).

All the hybrid compounds had no major influence after 1 hour on the secondary structure of $A\beta_{42}$ since the band spectrum at 218 nm was not altered. After 24 hours, the spectrum of the aminopyrazole **66** showed a minor variation, but the conformation of $A\beta_{42}$ did not seem to be altered. The hybrid aminopyrazoles **67**, **69** and **71**were able to reasonably destabilize the β-sheet structure and showed a slight positive cotton effect around 270 nm. Besides, the β-sheet breaker **7** had a strong influence on $A\beta_{42}$ after 24 hours of incubation, destabilizing β-sheet structure of $A\beta_{42}$. It showed a new strongly positive Cotton effect between 260 nm and 320 nm, which is the absorption range for aromatic amino acids, correlating with a possible complexation of the ligand with the phenylalanines (λ= 255-277 nm in CD) 19 and 20 of the binding site of $A\beta_{42}$ (KLVFF). Although **7** showed a strong destabilization and

interaction with the secondary conformation of $A\beta_{42}$, further experiments were carried out to confirm these observations.

3.2.4 Sedimentation assay

Sodium dodecyl sulfate–polyacrylamide gel electrophoresis (SDS-PAGE) experiments were carried out to additionally investigate if the aminopyrazoles derivatives interfere in fibril formation. All the experiments were performed by Dr. Laura Pedroza.

SDS-PAGE is a technique to analyze protein samples that can provide information of purity, subunit composition, molecular weight, and relative abundance. In our case, the SDS-PAGE provided us with the separation and analysis of the SAI-VL protein according to the molecular weight.[141] A control of fibril formation by sedimentation assays of formed fibrils in the absence and presence of aminopyrazoles derivatives was carried out. Therefore, after fibril formation, the solutions were ultra-centrifuged and the supernatant and pellet fractions were separated. The samples were prepared and charged to the polyacrylamide gel following the Laemmli protocol.[142] After applying a voltage, the proteins moved through to the polyacrylamide matrix according to their molecular weight. The proteins were visualized by Coomassie staining, and by comparing them with the control protein, the molecular weight of the remaining protein could be estimated.

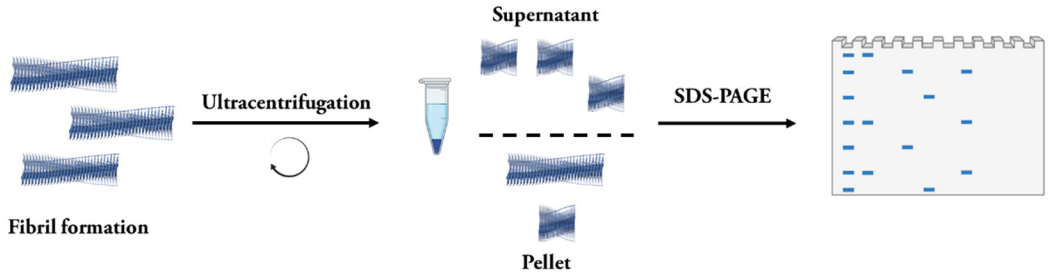

Figure 62. Schematic representation of the techniques used to analyze fibril formation.

This technique also allows us to distinguish which hybrid molecules interfere with fibril formation, since ultracentrifugation separates the components of a solution based on their size and density, and viscosity of the solvent. If most of the protein is found in the supernatant fraction, that implies that the aminopyrazole derivatives interfere with SAI-VL fibril formation and causes that SAI protein is in the supernatant, where there is no presence of fibrils.

[141] Berkelman T., Sun C., *Bio-rad laboratories Inc.*, **2009**, 5911.
[142] Laemmli U.K., *Nature*, **1970**, *227*, 680-685.

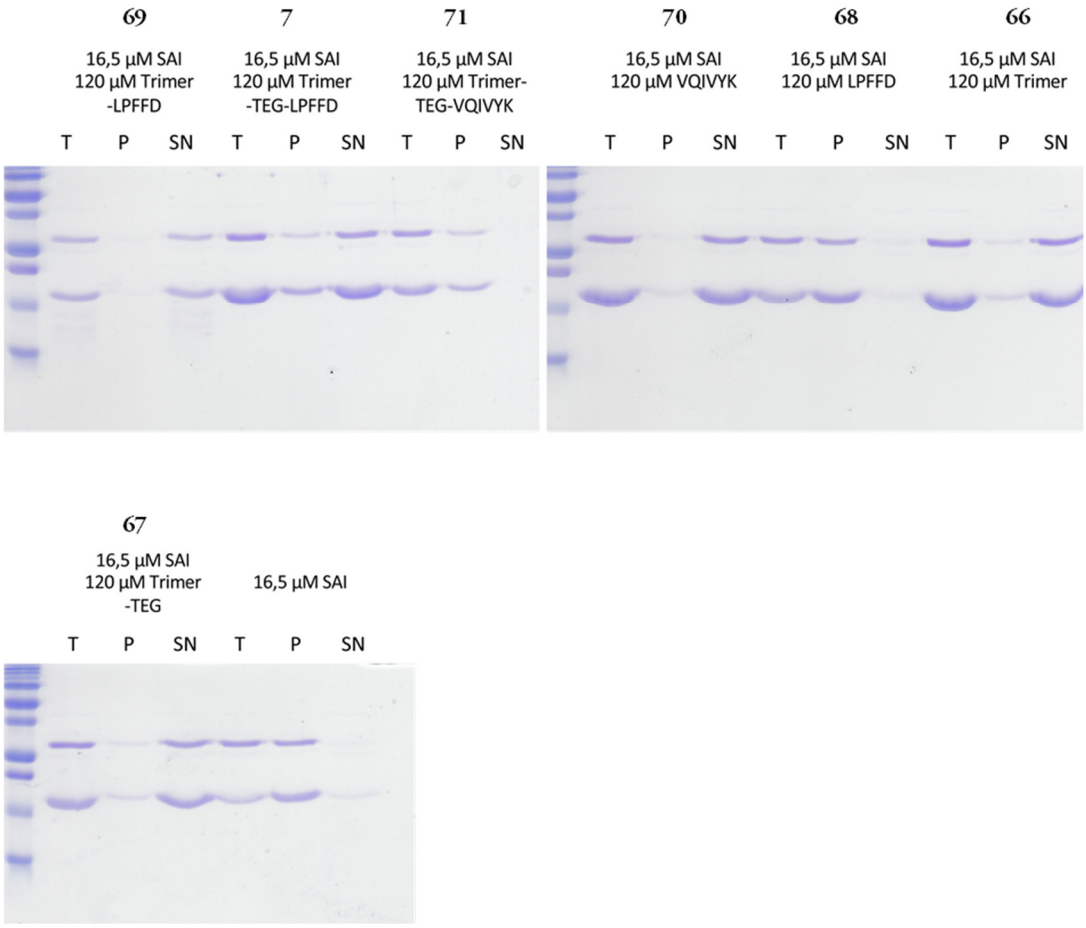

Figure 63. SDS-PAGE showing the interference of the aminopyrazole derivatives with SAI-VL fibril formation (T= total, P=pellet, SN= supernatant).

As shown in figure 63, the compounds **68** and **71**, and certainly the control SAI-VL protein, presented an intense band in the pellet fraction, indicating the existence of fibrils. Intense bands were present in the SDS-PAGE of the molecules **67**, **69**, **7**, **70** and **66**, referring to an interference of the aminopyrazoles with the SAI protein. These results coincide with the fluorescence experiments and CD spectroscopy, additional assays were carried out to demonstrate the absence or presence the fibrils when the aminopyrazoles were added to fibrillary SAI.

3.2.5 Atomic Force Microscopy (AFM)

Atomic force microscopy (AFM) is a high resolution method to examine surfaces in in a scale of 10 nm - 100 µm with an unprecedented accuracy. AFM provides a 3D profile of the surface on a nanoscale, by measuring forces (attractive, such as van der Waals forces, and

repulsive, such as Coulomb repulsions) between a sharp probe (<10 nm) and surface at an extremely short distance (0.2-10 nm probe-sample separation).[143]

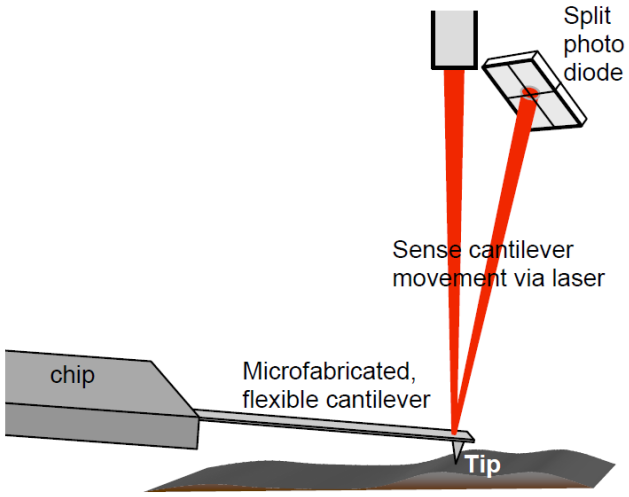

Figure 64. Diagram of an atomic force microscope (AFM).[143]

The probe is supported on the end of a flexible cantilever to which the measuring tip is attached. The AFM tip softly touches the surface of the sample, and a laser tracks the movement of the cantilever caused by the small forces between the probe and the surface. Therefore, an image of the surface structure can be generated from the collected data (figure 65).[144]

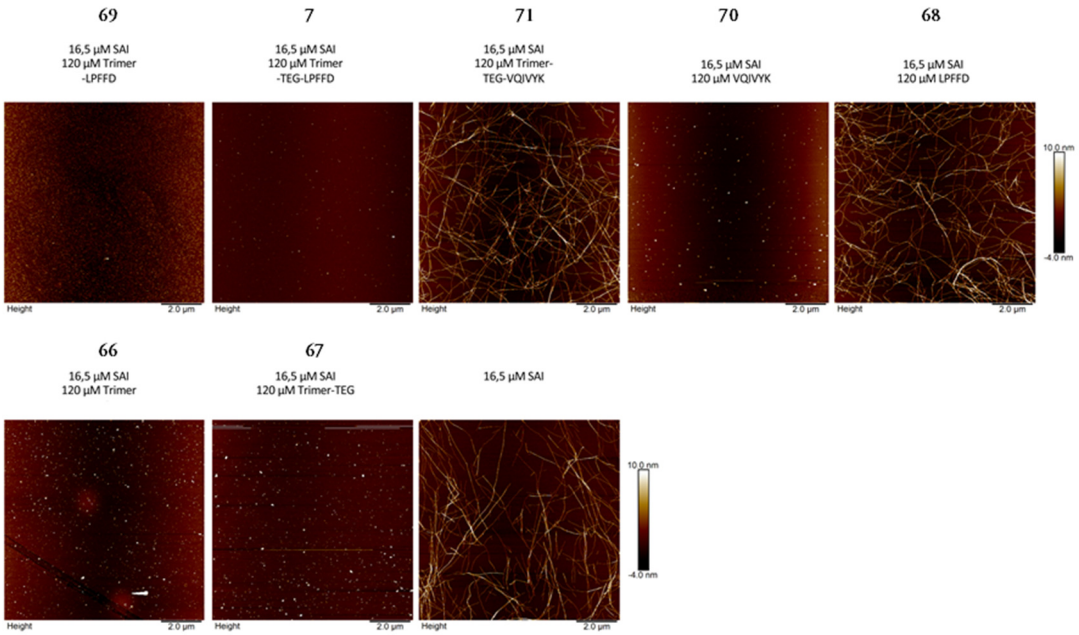

Figure 65. AFM images of the aminopyrazoles derivatives **7**, **66**, **67**, **68**, **69**, **70** and **71** in presence of SAI-VL.

[143] Wilson R., Bullen H., "Basic theory: atomic force microscopy", Northen Kentuchy.
[144] Haugstad G., "Atomic force microscopy: understanding basic modes and advanced applications", Wiley online libray, **2012**.

All the AFM experiments were carried out by Dr. Laura Pedroza. All the acquired AFM images are shown in figure 63. SAI-VL (16.5 µM) was incubated at 37 °C with β-sheet breakers (120 µM) in 10 mM Hepes, 100 mM NaCl, at pH 7.6 with additional 0.4 µg/µl heparin sodium salt and the images were recorded after 4 days. Fibrillary structures were only present in the aminopyrazole **71** and the peptide **68**, and as expected in the control of SAI-VL.

In view of the excellent results obtained with the hybrid molecule **7** in ThT experiments, SDS-PAGE and CD spectroscopy, it was selected to quantify the fibril formation by AFM analysis. **7** did not exhibit fibril formation, but amorphous aggregates (black arrow) and small delicate fibrils (blue arrow) appeared on the surface when the image is zoomed in. The software recognizes the fibrils automatically and then thanks to the Ridge Detection tool in ImageJ, it was possible to count the total length of the fibril structures for SAI-VL alone and for SAI-VL in presence of the aminopyrazole **7** (Figure 66). The software counted the total length for SAI-VL fibrils and it varied between 100 and 400 µm. In contrast, any fibril structure in the case of the SAI-VL in presence of 7 were counted.

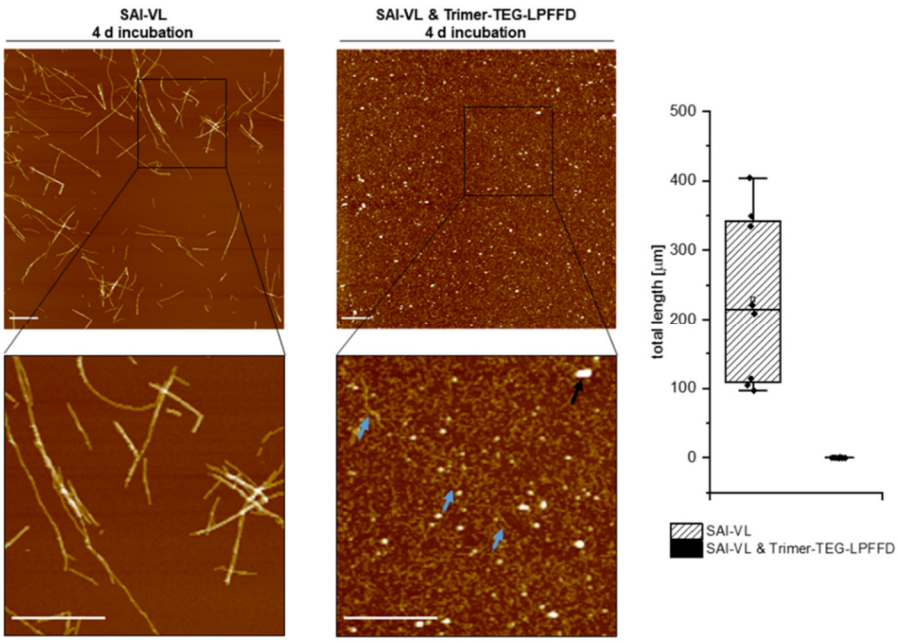

Figure 66. SAI-VL fibril morphology in presence of **7**.

After obtaining closer images of the inhibition of fibril formation of SAI-VL with **7**, we could conclude that the aminopyrazole **7** alters fibril formation but does not completely inhibit it. This is contrary to the ThT results that suggested a strong fibril formation. This phenomena was observed before with aminopyrazoles in previous attempts in our working group[76] but it is still unknown if these small fibrils can aggregate to form larger fibrils. Since

CD results indicate a destabilization of the β-sheet structure of $A\beta_{42}$ in presence of **7**, we can assume that it disrupts fibril formation by binding to the β-sheet conformation, which has also been confirmed by AFM studies with LC.

3.2.6 Discussion

In this chapter, preliminary results of new β-sheet breakers were summarized. The new β-sheet breakers were synthesized following the General Methods I and III. Some of this new β-sheet breakers were tested against amyloid proteins that aggregate overtime (SAI-VL and $A\beta_{42}$).

In ThT studies, the hybrid molecule **7** showed significant inhibitory effects, both with SAI-VL and $A\beta_{42}$ fibril formation. When SAI-VL aggregates normally, the ThT fluorescence shows a seven-fold increase. However, when molecule **7** was present, the ThT fluorescence did not increase over 4 days, meaning that the aggregation of SAI-VL was drastically reduced. In the presence of $A\beta_{42}$, the β-sheet breakers **7**, **66** and **69** presented a crucial inhibitory effect on fibril formation after 5 days of incubation, reducing the fluorescence to a 26%, 20% and 23% of the value for aggregated $A\beta_{42}$ alone, respectively.

In CD experiments, the compounds **68**, **69**, **7**, **70**, **71**, **67** and **66** had no major influence on the β-sheet structure of $A\beta_{42}$ after incubating for 1 hour. The compounds **67**, **69**, **7** and **71** influenced the secondary conformation of $A\beta_{42}$ after 24 hours of incubation, reducing the negative band by half. This time-dependence can be explained with the development of protofibrils after 15 hours of incubation, followed by the formation of fibrils where the β-sheet conformation is predominant. So it can be assumed that these molecules can destabilize β-sheet structures and thus, prevent fibril formation.

In sedimentation assays using ultracentrifugation and subsequently SDS-PAGE, the compounds **67**, **69**, **7**, **70** and **66** exhibited a band in the supernatant, indicating that these β-sheet breakers interfere with the fibril formation. In the case of the β-sheet breakers **71** and **68**, most of the fibrils were found in the pellet, denoting that these compounds are not suitable to control protein aggregation.

Finally, in the analysis of the AFM images, the compounds **71** and **68** showed no reduction in LC fibrils after 4 days of incubation, while the tested molecules **69**, **7**, **70**, **67** and **66** did. Taking the hybrid aminopyrazole **7** as the best potential inhibitor of fibril formation based on the above results, closer AFM images were taken. It was possible to conclude that **7** altered fibril formation but did not inhibit it since amorphous aggregates and small delicate fibrils were detected.

3.3 Outlook

In the present work, several artificial metalloproteases were synthesized and evaluated to be one step closer to reaching the goal of this study: to prepare a nanomachine which is able to disaggregate Aβ protein. Further experiments should be carried out in order to optimize the structure and the cleavage strength of the artificial metalloproteases. For that reason, new structural cores and transition metals, such as Cu(II), should be studied. It is known that Cu(II) is a biological metal ion predestined to bind Aβ peptide, since this ion participate in neutransmission in glutamatergic synapses.[145] AFM studies to obtain images of the artificial metalloproteases acting against protein aggregation should also be performed, with the purpose of understanding the mechanism of action of an artificial metalloprotease.

It is still unknown why the artificial proteases have the power to inhibit, disaggregate and destabilize the Aβ peptide in the ThT and CD experiments, while the second proteomic assays showed no evidence of the artificial metalloproteases having any influence on the distribution of the peptide fragments. For this reason, additional proteomic assays should be performed with optimized conditions for the sample preparation, varying the concentration or the buffer conditions. $A\beta_{42}$ should also be employed without any treatment to avoid any interference. It would be useful to use new short proteins involved in amyloidosis disease such as α-synuclein or h-IAPP to consider the specificity and applicability of the artificial metalloproteases. It would also be interesting to use a faster MS technique such as MALDI-TOF-MS, to compare the results with the proteomic assays.

After optimizing the artificial metalloproteases, their effectiveness will be proved supporting them on the surface of an AuNP. Selecting the most powerful artificial protease, a disaggregating nanomachine will be constructed to fight against protein aggregation. For that purpose, a β-sheet selector, a β-sheet breaker and an artificial metalloprotease will be supported on the same AuNP and their strength will be evaluated with different biophysical assays.

Additionally in this thesis, some promising results of new β-sheet breakers were shown, finding that the hybrid aminopyrazole **7** was able to alter the fibril formation of the amyloid proteins SAI and $A\beta_{42}$. AFM images showed amorphous aggregates and small fibrils instead of a complete inhibition or degradation of fibrils. In order to underpin these results and to obtain further information of the effect of the aminopyrazoles on LCs, further experiments will be carried out to prove the consequence of the amorphous aggregates and small fibrils that remains after incubating the aminopyrazole with LCs. Perhaps, these small fibrils could

[145] Stefaniak E. *et al.*, *Chem. Eur. J.*, **2021**, 27, 2798-2809.

act as nuclei, aggregate and form fibrils. Furthermore, the rest of the aminopyrazoles are currently being tested using ThT fluorescence experiments, CD spectroscopy, sedimentation assays and AFM. Special attention should be paid to the results of the aminopyrazoles containing LCs fragments (molecules **80** and **82**), which can potentially show an increased disruption of protein aggregation, considering that the new β-sheet breakers are mainly tested on LCs.

4. Experimental Details

4.1 Materials and Methods

Chemicals and solvents

The chemicals and solvents used in this work were obtained from the companies Acros Organics, Alfa Aesar, Baechchem, Carbolution Chemicals, Fluka, Fluorochem, Iris Biotech GMBH, Sigma Aldrich, TCI chemicals and Thermo Fisher Scientific. Amino acids, coupling reagents and polymer resins for peptide synthesis were purchased from Iris Biotech GMBH, Merck and Novabiochem. Solvents were distilled as required, and the solvents were stored over molecular sieves. Experiments involving moisture sensitive compounds were carried out under an argon atmosphere using anhydrous solvents. Room temperature refers to 25 °C. The compounds were characterized by a combination of nuclear magnetic resonance spectroscopy (NMR), high-performance liquid chromatography (HPLC), high-resolution mass spectrometry (HRMS) and melting point (mp).

Thin Layer Chromatography and column chromatography

The monitoring of the reactions was carried out by thin layer chromatography using silica gel sheets type F254 (Macherey-Nagel), with a layer thickness of 0.2 mm. Compounds were detected with UV light at 254 nm and 365 nm. Products were purified using flash column chromatography (Merck Silica gel 60, 230-400 mesh).

Ninhydrin test

Colour test to monitor completeness of amino acid coupling in Solid Phase Peptide Synthesis (SPPS). A sample of the peptide resin (resin beads) was taken thanks to a spatula after an amino acid coupling and transfer to a small Eppendorf. 75 µl phenol (80% phenol in ethanol), 100 µl KCN solution (2 mL a 1 mM aqueous KCN solution in 98 mL pyridine) and 75 µl ninhydrin solution (5% ninhydrin in ethanol (w / v)) were mixed with the sample at 90°C for 5 minutes.[146] If the resin beads and the solution stays yellow the coupling is successful, if not (blue color) another coupling step is necessary.

Nuclear Magnetic Resonance spectroscopy (NMR)

Nuclear resonance spectra (^{1}H and ^{13}C NMR) were recorded at room temperature using Bruker Advance DMX300 (300 MHz), AV NEO 400 (400 MHz), Bruker Advance DRX500 (500 MHz) and Bruker Advance DRX600 (600 MHz) from Bruker. Samples were prepared as solutions in deuterated solvent and referenced to the internal non-deuterated

[146] Kaiser test kit, Sigma Aldrich.

solvent peak. Chemical shifts were expressed in ppm (δ) downfield of tetramethylsilane. Coupling constants are given in Hertz (Hz). The spectra were evaluated using the MESTRENOVA program from MESTRELAB RESEARCH.

High-performance liquid chromatography (HPLC) and preparative HPLC

HPLC measurements were performed on a Jasco with a UV / Vis detector (UV-975, DG-2080-53 solvent degasser, LG-980-02S 3-channel solvent mixer). A column from Phenomenex (model Luna® 5µM C18 (2) 100, Å 100/10 mm) was used for 60 min. The separation took place with a gradient of water / acetonitrile with 0.1% TFA.

Preparative HPLC was carried out on a Jasco with UV/Vis detector (MD-4010, Teflon AF solvent degasser, variable speed dynamic solvent mixer). A column from Phenomenex (model Luna® 5µM C18 (2) 100 Å, 150/21.2 mm) was used for 60 min. The separation took place with a gradient of water / acetonitrile with 0.1% TFA.

Mass spectrometry

The LC-MS spectra were recorded with an LC-MS system equipped with a liquid chromatograph from Agilent Technologies (1260 Infinity) and a high resolution time-of-flight mass spectrometer from Bruker Daltonics (Maxis 4G). A YMC Triart C18 (50x1 mm I.D. with 3 µm particle size) was used as analytical column. The mobile phase contained water with 0.1% formic acid (A) and methanol with 0.1% formic acid (B) at a flow rate of 100 µL/min. The gradient was established as follows: 0 min, 10% B, 30 min 100% B and was maintained for 30 min.

Mass spectrometry was performed on a Bruker Maxis 4G using electrospray as ionization source (ESI) in positive mode. The eluent was introduced into the ion course of the mass spectrometer. Nitrogen was used as nebulizing gas and dry gas. The nebulizer gas pressure was set to 29.0 psi and the dry gas was set to 5.0 L/min at 250 °C. The capillary voltage was set to - 4500 V. The end plate offset was set to -500 V. The acquisition was performed in scan mode in the m/z range 100 – 2900. The MS system was controlled by the software Hystar version 3.2. The data was analysed using compass data analysis version 4.1.

Melting points

Melting points were measured on a B-540 Büchi apparatus.

Buffers

A PBS buffer was used for fluorescence spectroscopy, consisted of 137 mM NaCl, 2.7 mM KCl, 1.4 mM KH_2PO_4, 4.3 mM Na_2HPO_4 (pH= 7.3) for $A\beta_{42}$ and 10 mM Hepes, 100 mM NaCl, pH 7.6 with additional 0.4 µg/µl heparin sodium salt for LC.

A KaPi buffer was used for circular dichroism, consisted of 100 mM K_2HPO_4/ KH_2PO_4 (pH=7.0).

A PBS buffer was used for proteomics, consisted of 50 mM Na_2HPO_4/ NaH_2PO_4 (pH=7.5).

A 10xSDS running buffer was used for SDS-PAGE, consisted of 1.92 M Glycine, 333 mM tris/HCL (pH= 8.3) and 1% SDS.

A 5xSDS loading dye was used for SDS-PAGE, consisted of 0.3 M tris/HCL (pH= 8.3), 10% SDS, 40% glycerol, 0.01% bromophenol blue and 30 mM DTT.

For AFM measurements a buffer consisted of 10 mM Hepes, 100 mM NaCl, pH 7.6 with additional 0.4 µg/µl heparin sodium sal, was used.

Circular dichroism spectroscopy

All the samples were measured in a quartz cuvette (d= 0.1 cm) using a Jasco J-815 CD spectrometer at 25°C to obtain the spectra.

Fluorescence spectroscopy

The measurements of the proteases were carried out on a Spark spectrometer from Tecan. All the thioflavin T measurements were performed at 37 °C using a Corning™ Low-Volume 384-Well Black Flat Bottom Polystyrene microplate.

The measurements of the β-sheet breakers were carried out on a SpectraMax M5e spectrometer. All the thioflavin T meausurements were performed at 37 °C using black, half area, and clear bottom 96 well plate.

Atomic Force Microscopy (AFM)

A MultiMode 8 microscope with ScanAsyst-Air from Bruker was used to capture AFM images on Mica (Plano GmbH). Silicone measuring tips with a nitride cantilever (0.4 N/m, Bruker) and a rotated geometry were utilized. The samples were evaluated using the NanoScope Analysis (version 1.5, Bruker) and ImageJ (National Institute of Health) programs.

Proteomics-MS

Experiments were performed by Dr. Farnusch Kaschani (University of Duisburg-Essen) on an Orbitrap Elite instrument (Thermo) coupled to an Evosep One gradient off-set focusing UHPLC (ultra high pressure liquid chromatography) system (Evosep). The analytical column was a commercially available EV-1106 (15 & 30 samples/day; 150 µm ID × 15 cm,

packed with Dr Maisch GmbH C-18 AQ) coupled to an EV-1086 Stainless steel emitter (Evosep). The analytical column/emitter assembly was attached to a nanospray flex ion source (Thermo) and operated at room temperature. The LC was equipped with 2 mobile phases: solvent A (0.1% FA, in water) and solvent B (0.1% FA in ACN). The Evosep One is controlled by the Chronos software (Axel Semrau). All solvents were of UHPLC grade (Sigma).

Mechanics calculations

Images and force field calculations were performed with Maestro 11 by Schrödinger.

4.2 General Methods

4.2.1 General Method I

A wang resin pre-installed with a Fmoc-protected amino acid were used to prepare the peptides by manual Fmoc solid-phase peptide synthesis. In order to ensure complete conversion or deprotection, the resin had to be swollen in DMF for 120 minutes before the actual solid phase synthesis started. The coupling of the commercially available Fmoc amino acids was carried out with the coupling reagent HBTU in the presence of DIPEA. 8.00 eq. Fmoc-amino acid, 7.62 eq. HBTU and 16.0 eq. DIPEA were used per coupling step. A 20% piperidine solution in DMF was used to cleave the Fmoc protecting group. The completeness of the individual coupling steps was checked with the Kaiser test. For this purpose, some resin balls were removed, washed thoroughly with DMF and mixed with the Kaiser test solution. The test solution was heated for 5 minutes at 90 ° C in a thermomixer. If the reaction was incomplete, the respective coupling step was repeated and checked again. Steps 2 and 3 (Table 6) were repeated until the complete synthesis of the desired peptide and after the synthesis, the resin was dried (step 4).

Table 6. Steps in a manual solid phase peptide synthesis.

Reaction step	Reagents	Time
1. Resin swelling	3 mL DMF	120 Minutes
2. Fmoc cleavage	1. 20% Piperidine in DMF 2. 20% Piperidine in DMF 3. Wash with 5x 500 µL DMF	1. 3 Minutes 2. 10 Minutes
3. Coupling	8.00 eq. Fmoc-aa-OH in 7.62 eq. HBTU solution (0.5 M in DMF) 16.00 eq. DIPEA	30 min to 24 h
4. Dehydration	1. 5x 500 µL DMF 2. 5x 500 µL DCM 3. 5x 500 µL Diethylether	

A test cleavage was carried out for each peptide in order to check the completeness of the synthesis. For that purpose, a cleavage cocktail containing trifluoroacetic acid (93%), triisopropylsilane (5%) and distilled water (2%) was added to the resin and stirred for 5 h at room temperature. The peptide was precipitated from cold diethyl ether and washed three times with cold diethyl ether. The peptide was then dissolved in 0.1% aqueous TFA and

freeze-dried. The purity of the peptides was checked by HPLC, NMR and mass spectroscopy.

4.2.2 General Method II

The automated solid-phase peptide synthesis was carried out by Heike Wöll from the Schrader working group (Organic Chemistry, University of Duisburg-Essen) on a microwave peptide synthesizer (Liberty, CEM GmbH). The synthesis was carried out in a 0.10 mmol scale, whereby the resin used was initially swollen in 5 ml DMF for 5 hours with shaking.

The solution concentrations used were as follows:

Fmoc-amino acid 0.20 M in DMF

Activator (HCTU) 0.50 M in DMF

Base (DIPEA) 2.00 M in NMP

Deprotection agent (piperidine) 20% in DMF

After completion of the synthesis, the peptide was washed with the dichloromethane and dried in high vacuum. A test cleavage was carried out for each peptide prepared in order to check the completeness of the synthesis (by mass spectrometry) and its purity (by HPLC). The resin was mixed with 93% TFA, 5% TIPS and 2% distilled water and shaken for 5 h at room temperature. The solution was then filtered, and the peptide was precipitated from the clear solution with cooled diethyl ether. The solution was centrifuged, the supernatant was decanted off and the peptide was washed three times with cold diethyl ether. After drying the solid, this was dissolved in 0.1% aqueous TFA and freeze-dried. The purity of the peptides was checked by HPLC, NMR and mass spectroscopy.

4.2.3 General Method III

Resin-immobilized peptides synthesized following the general method I or II were further reacted by a manual solid phase method with PMB protected trimer derivatives containing a free carboxylic acid. First, the Fmoc group of the peptides immobilized on the resin were deprotected and then the PMB-protected trimer acid was coupled to the N-terminus of the peptide. After cleavage from the resin, the PMB protective groups had to be additionally removed. For this purpose, the crude product was dissolved in trifluoroacetic acid (4 ml) under argon atmosphere and stirred at 70 °C for 5 h. After the completion of the reaction, the solution was slowly cooled to 0 °C and the product was fractionally precipitated from diethyl ether. The individual fractions were washed three times with diethyl ether, dissolved in 0.1% aqueous TFA and freeze-dried. The purity was checked by HPLC, NMR and mass spectroscopy.

4.3 Synthetic Procedures

Tri-tert-butyl 1,4,7,10-tetraazacyclododecane-1,4,7-tricarboxylate (17)[101]

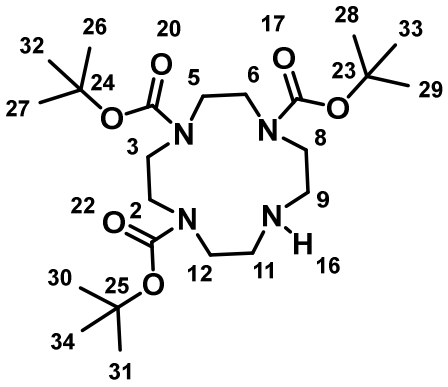

A solution of Boc_2O (8.79 mmol, 3.03 eq.) in 10 mL $CHCl_3$ was added dropwise to a solution of cyclen (2.90 mmol, 1.00 eq.) and triethylamine (8.79 mmol, 3.03 eq.) in 15 mL $CHCl_3$ while cooled in an ice bath (2 hours). The solution was warmed to room temperature and stirred overnight. The reaction mixture was washed with water, the organic layer was dried over Na_2SO_4, filtered and solvent removed under reduced pressure. Silica column chromatography DCM/MeOH 10:1 provided pure compound **17** (1.2254 g, 2.59 mmol, 89%). **R_f**: 0.30. **Mp**: 85.4 °C. **^{1}H-NMR** (600 MHz, $CDCl_3$)**:** δ [ppm] = 3.61 (s, 3H,11-H and 9´-H), 3.33 (d, *J* = 61.9 Hz, 10H,8-H, 6-H, 5-H, 3-H and 2-H), 2.85 (s, 3H, 12-H and 9´-H), 1.45 (d, *J* = 10.3 Hz, 27H, $C(CH_3)_3$). **^{13}C-NMR** (151 MHz, $CDCl_3$)**:** δ [ppm] = 155.83 (22-C, 20-C and 17-C), 80.08 (25-C), 79.58 (24-C and 23-C), 51.12 (12-C and 8-C), 50.68 (6-C, 5-C, 3-C and 2-C), 49.66 (11-C and 9-C), 28.82 (CH_3), 28.67 (CH_3), 28.63 (CH_3). **HRMS**: (ESI, m/z) calcd for $C_{23}H_{44}N_4O_6$ $[M+H]^+$ 473.3334; found 473.3354.

Benzyl (3-hydroxypropyl)carbamate (18)[92]

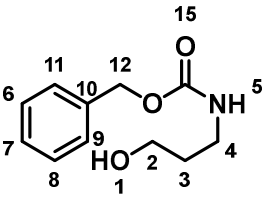

To the solution of 5.07 mL of 3-amino-1-propanol (66.57 mmol, 1.00 eq.) in 100 mL of chloroform was added 9.28 mL of triethylamine (66.57 mmol, 1.00 eq.). To the stirred solution, 9.38 mL of benzyl chloroformate (66.57 mmol, 1.00 eq.) was added dropwise. The reaction mixture was stirred for 3 hours, the washed with 5% of aqueous citric acid, brine and dried over Na_2SO_4. The solvent was removed, and the column chromatography afforded the compound as a colorless solid with 27% yield (3.75 g, 17.92 mmol). **R_f**: 0.26. **Mp**: 53.8 °C. **^{1}H-NMR** (300 MHz, $CDCl_3$)**:** δ [ppm] = 7.42 – 7.25 (m, 5H, 11-H, 9-H, 8-H, 7-H and 6-H), 5.10 (s, 2H, 12-H), 3.67 (t, *J* = 5.8 Hz, 2H, 2-H), 3.35 (q, *J* = 6.1 Hz, 2H, 4-H), 2.44 (s, 1H, 1-H), 1.70 (p, *J* = 6.0 Hz, 2H, 3-H). **^{13}C-NMR** (75 MHz, $CDCl_3$)**:** δ [ppm] = 157.45 (15-C), 136.59 (10-C), 128.66 (11-C and 9-C), 128.29 (6-C), 128.23 (8-C and 7-C), 67.00 (12-C), 59.73 (2-C), 37.90 (4-C), 32.72 (3-C). **HRMS**: (ESI, m/z) calcd for $C_{11}H_{15}N_1O_3$ $[M+H]^+$ 232.0944; found 232.0969.

Benzyl (3-oxopropyl)carbamate (19)[92]

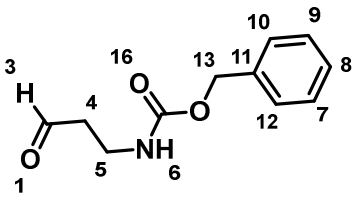

To the solution of 0.504 g of **18** (2.39 mmol, 1.00 eq.) in DMSO/DCM (5mL/5mL) cooled to 0°C were added 1.69 mL of triethylamine (12.14 mmol, 5.08 eq.). To the stirred solution, 1.156 g of sulfur trioxide-pyridine complex (7.26 mmol, 3.04 eq.) were added. The reaction mixture was stirred for 1 hour in an ice bath. After 1 hour, the reaction was stirred for 1 hour at room temperature. After addition of 50 mL DCM, the reaction mixture was washed with 10% aqueous $CuSO_4$, 5% aqueous citric acid and brine. The solvent was evaporated and the product was purified by column chromatography obtaining a white solid (0.27 g, 1.32 mmol, 55%). **R_f**: 0.1. **Mp**: 64.3 °C. **^{1}H-NMR** (300 MHz, $CDCl_3$)**:** δ [ppm] = 9.80 (s, 1H), 3-H), 7.39-7.31 (m, 5H, 12-H, 10-H, 9-H, 8-H and 7-H), 5.15 (br s, 1H, 6-H), 5.09 (s, 2H,13-H), 3.49 (q, *J* = 6.0 Hz, 2H, 5-H), 2.74 (t, *J* = 5.8 Hz, 2H, 4-H). **^{13}C-NMR** (75 MHz, $CDCl_3$)**:** δ [ppm] = 201.22 (1-C), 156.43 (16-C), 136.53 (11-C), 128.66 (12-C and 10-C), 128.28 (9-C and 7-C), 128.21 (8-C), 66.90 (13-C), 44.24 (4-C), 34.64 (5-C). **HRMS**: (ESI, m/z) calcd for $C_{11}H_{13}NO_3$ $[M+Na]^+$ 230.0788; found 230.0795.

Tri-tert-butyl-10-(3-(((benzyloxy)carbonyl)amino)propyl)-1,4,7,10-tetraazacyclododecane-1,4,7-tricarboxylate (20)[92]

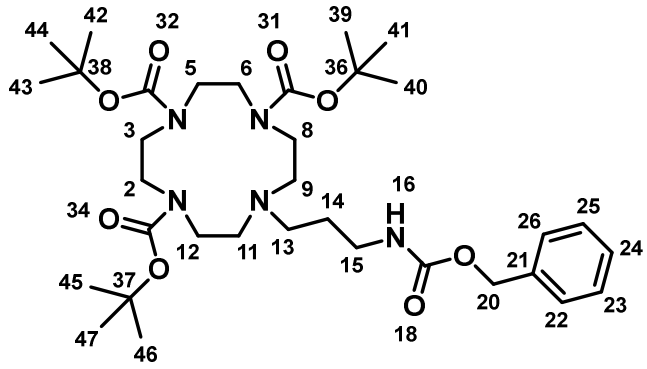

To the solution of 0.2524 g of **17** (0.53 mmol, 1.00 eq.) in 3.5 mL of THF were added the solution of 0.11 g of **19** (0.53 mmol, 1.00 eq.) in 3 mL of THF and 0.33 g of $NaBH(OAc)_3$ (1.54 mmol, 2.92 eq.) and the reaction was stirred for 1 hour. The solvent was evaporated and the reaction mixture was washed with 50 mL of saturated $NaHCO_3$ and extracted with ethyl acetate. The collected organic phase was washed with brine, dried over sodium sulfate and concentrated. The product was purified by column chromatography obtaining a white solid (0.26 g, 0.40 mmol, 76%). **R_f**: 0.4. **Mp**: 61.6 °C. **^{1}H-NMR** (300 MHz, $CDCl_3$)**:** δ [ppm] = 7.38 – 7.26 (m, 5H, 26-H, 25-H, 24-H, 23-H and 22-H), 5.61 (s, 1H, 16-H), 5.10 (s, 2H, 20-H), 3.57 – 3.28 (m, 13H, 12-H, 8-H, 6-H, 5-H, 3-H, 2-H and 13′-H), 3.17 (t, *J* = 6.3 Hz, 1H, 13′′-H), 2.60 (d, *J* = 37.6 Hz, 6H, 15-H, 11-H and 9-H), 1.66 (q, *J* = 7.0 Hz, 2H, 14-H), 1.46 (d, *J* = 1.7 Hz, 16H, $C(CH_3)_3$), 1.43 (s, 11H, $C(CH_3)_3$). **^{13}C-NMR** (151 MHz, $CDCl_3$)**:** δ [ppm] = 155.69 (34-C, 32-C and 31-C), 136.78 (21-C), 128.34 (26-C and 22-C), 127.96 (25-C and 23-C),

127.86 (24-C), 79.89 (36-C), 79.66 (38-C), 79.34 (37-C), 66.36 (20-C), 55.08 (5-C and 3-C), 54.45 (6-C and 2-C), 50.39 (12-C and 8-C), 49.86 (9-C), 48.26 (11-C), 47.52 (13-C), 38.74 (15-C), 28.60 (CH_3), 28.47 (CH_3), 28.42 (CH_3), 25.59 (14-C). **HRMS**: (ESI, m/z) calcd for $C_{34}H_{57}N_5O_8$ $[M+H]^+$ 664.4280; found 664.4280.

Tri-tert-butyl-10-(3-aminopropyl)-1,4,7,10-tetraazacyclododecane-1,4,7-tricarboxylate (21)[92]

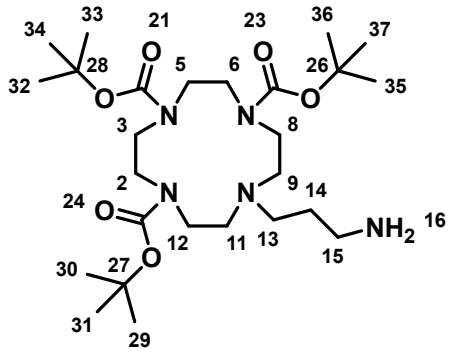

A suspension of 0.6 g of **20** and 10% mol Pd/C in 10 mL of ethanol were stirred under hydrogen for 24 hours at room temperature. The catalyst was filtered off on celite 545 and the solvent was evaporated to afford the amine compound as a yellowish solid (0.47 g, 0.90 mmol, 98%). **R_f**: 0.1. **Mp**: 56.5°C. **^{1}H-NMR** (300 MHz, $CDCl_3$)**:** δ [ppm] = 3.53-3.26 (m, 11H,8-H, 6-H, 5-H, 3-H and 2"-H), 2.96-2.78 (m, 3H, 15-H and 2'-H), 3.61 (s, 6H, 13-H, 11-H and 9-H), 1.95-1.68 (m, 2H, 14-H), 1.44 (d, J= 6.8 Hz, 27H, $C(CH_3)_3$). **^{13}C-NMR** (101 MHz, $CDCl_3$)**:** δ [ppm] = 156.39 (21-C), 155.93 (24-C), 155.54 (23-C), 80.07 (28-C), 79.85 (26-C), 79.55 (27-C), 54.83 (13-C), 53.85 (5-C and 3-C), 50.57 (6-C and 2-C), 50.03 (11-C), 49.48 (16-C), 48.11 (12-C and 8-C), 39.53 (15-C), 28.78 (CH_3), 28.64 (CH_3), 28.55 (CH_3), 26.02 (14-C). **HRMS**: (ESI, m/z) calcd for $C_{26}H_{51}N_5O_6$ $[M+H]^+$ 530.3912; found 530.3911.

(4-(benzo[*d*]oxazol-2-yl)phenyl)methanamine (22)[111]

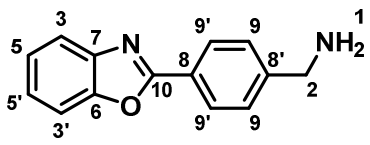

2.00 g of 4-aminomethyl benzoic (13.19 mmol, 1.00 eq.) and 1.44 g of 2-aminophenol (13.19 mmol, 1.00 eq.) were mixed together with 30 g of polyphosphoric acid and heated to 150°C under argon atmosphere overnight. The reaction mixture was cooled to room temperature with ice and poured into 33% ammonium hydroxide solution. The precipitate was filtered under reduced pressure. The precipitate was suspended in $NaHCO_3$ solution and it was washed with DCM. The combined organic phases were washed with brine and dried over Na_2SO_4, filtered and the solvent was removed under reduced pressure. It was obtained an orange solid (2.07 g, 9.26 mmol, 70%). **R_f**: 0.5. **Mp**: 118.2 °C. **^{1}H-NMR** (600 MHz, DMSO)**:** δ [ppm] = 8.14 (d, *J* = 8.1 Hz, 2H, 9-H and 9'-H), 7.82 – 7.75 (m, 2H, 5-H and 5'-H), 7.57 (d, *J* = 8.1 Hz, 2H, 9''-H), 7.44 – 7.38 (m, 2H, 3-H and 3'-H), 3.82 (s, 2H, 2-H), 1.93 (s, 2H, 1-H). **^{13}C-NMR** (151 MHz, DMSO)**:** δ [ppm] = 162.44 (10-C), 150.13 (6-C), 148.76 (7-C), 141.54 (8-C), 127.81 (9-C), 127.11 (8'-C), 125.33 (5-C),

124.81 (5'-C), 124.29 (8-C), 119.67 (3-C), 110.84 (3'-C), 45.39 (2-C). **HRMS**: (ESI, m/z) calcd for $C_{14}H_{12}N_2O$ $[M+H]^+$ 225.1022; found 225.1050.

tert-Butil *N*-((((9H-fluoren-9-yl)methoxy)carbonyl)valyl)-*S*-tritylcysteine (23)

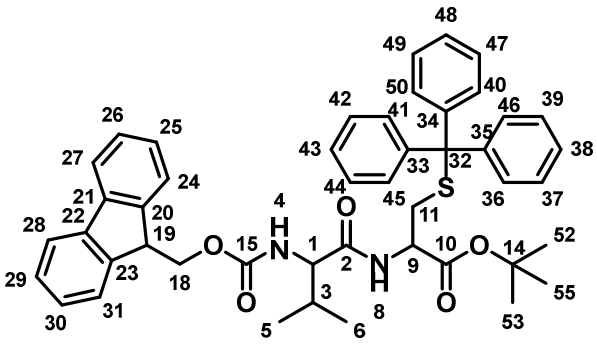

The H-*L*-Cys(Trt)-O^{t}Bu·HCl was dissolved in ethyl acetate and washed with a saturated solution $NaHCO_3$. The water phase was extracted with ethyl acetate. The combined organic phases were washed with brine, dried over sodium sulfate, filtered and the solvent was removed and the yellowish oil was used for the reaction. 0.185 g of Fmoc- L-Val-OH (0.545 mmol, 2.00 eq.) and 0.206 g of HBTU (0.545 mmol, 2.00 eq.) were dissolved in 3 mL of DMF. To this solution was added 188 µL of DIPEA (1.08 mmol, 4.00 eq.). The solution was stirred for 10 min. 0.115 g of H-*L*-Cys(Trt)-O^{t}Bu (0.27 mmol, 1.00 eq.) were dissolved in 4 mL of DMF. The reaction mixture was stirred overnight. The product was purified by column chromatography obtaining a white solid (0.24 g, 0.33 mmol, 92%). **R_f**: 0.64. **Mp**: 90.3 °C. **^{1}H-NMR** (400 MHz, DMSO): δ [ppm] = 8.34 (d, *J* = 7.5 Hz, 1H, 4-H), 7.89 (d, *J* = 7.5 Hz, 2H, 28-H and 27-H), 7.74 (dd, *J* = 10.4, 7.6 Hz, 2H, 31-H and 24-H), 7.44 – 7.38 (m, 3H, 48-H, 43-H and 28-H), 7.36 – 7.27 (m, 13H, CH belonging to Trt and Fmoc protenting groups), 7.22 (ddd, *J* = 8.3, 5.4, 2.1 Hz, 4H, 9-H and CH belonging to Trt protecting group), 4.29 – 4.18 (m, 3H,18-H and 6-H), 4.02 (q, *J* = 7.8 Hz, 1H, 19-H), 3.92 (dd, *J* = 9.1, 7.2 Hz, 1H, 1-H), 2.45 (dd, *J* = 12.2, 8.2 Hz, 1H, 11''-H), 2.35 – 2.22 (m, 1H, 11'-H), 1.99 – 1.91 (m, 1H, 3-H), 1.29 (s, 9H, 55-H, 53-H and 52-H), 0.86 (t, *J* = 7.0 Hz, 6H, 6-H and 5-H). **^{13}C-NMR** (101 MHz, DMSO): δ [ppm] = 171.12 (2-C), 169.11 (10-C), 156.08 (15-C), 144.10 (34-C, 33-C and 32-C), 143.90 (23-C), 143.75 (20-C), 140.69 22-C and 21-C), 129.02 (49-C, 47-C, 44.C, 42-C, 39-C and 37-C), 128.08 (50-C, 46-C, 45-C, 41-C, 40-C and 36-C), 127.64 (48-C, 43-C and 38-C), 127.05 (30-C and 25-C), 126.79 (29-C and 26-C), 125.41 (24-C), 125.37 (31-C), 120.09 (28-C and 27-C), 80.99 (14-C), 66.22 (32-C), 65.75 (18-C), 59.78 (1-C), 52.14 (9-C), 46.66 (19-C), 32.87 (11-C), 30.47 (3-C), 27.47 (55-C and 53-C), 26.44 (52-C), 19.20 (5-C), 18.17 (6-C). **HRMS**: (ESI, m/z) calcd for $C_{46}H_{48}N_2O_5S$ $[M+H]^+$ 763.3176; found 763.3177.

tert-Butyl *S*-trityl-*N*-valylcysteinate (24)

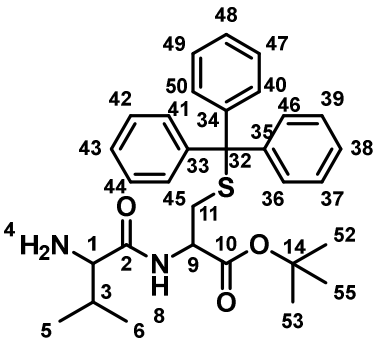

The starting material **23** was suspended in 5 mL of chloroform and treated with 5 mL of 4-AMP. After 30 minutes (end point determined by TLC analysis) 40 mL of chloroform were added, and the organic phase was washed with two 25 mL portions of brine to remove excess 4-AMP. Then, the organic phase was washed with five 25 mL portions of phosphate buffer of pH 5.5 and dried with Na_2SO_4. The solvent was removed to obtain yellowish oil (0.15 g, 0.29 mmol, 87%). **R_f**: 0.15. **^{1}H-NMR** (300 MHz, DMSO): δ [ppm] = 8.29 (d, *J* = 8.5 Hz, 1H, 8-H), 7.37 – 7.23 (m, 15H, CH $_{Trt}$), 4.18 – 4.09 (m, 1H, 9-H), 3.05 (d, *J* = 4.7 Hz, 1H, 2-H), 2.34 (m3-H, 1H, 11-H), 1.97 – 1.86 (m, 1H,), 1.32 (s, 9H, 55-H, 53-H and 52-H), 0.89 (d, *J* = 6.9 Hz, 3H, 6-H), 0.79 (d, *J* = 6.8 Hz, 3H, 5-H).**^{13}C-NMR** (75 MHz, DMSO): δ [ppm] = 173.53 (2-C), 169.12 (10-C), 144.03 (35-C, 34-C and 33-C), 128.96 ($CH_{aromatic}$), 128.0396 ($CH_{aromatic}$), 126.78 (48-C, 43-C and 38-C), 81.14 14-C), 66.08 (32-C), 59.18 (1-C), 51.62 (9-C), 33.14 (11-C), 31.19 (3-C), 27.45 (55-C, 53-C and 52-C), 19.29 (5-C), 16.80 (6-C). **HRMS**: (ESI, m/z) calcd for $C_{31}H_{38}N_2O_3S$ $[M+Na]^+$ 541.2495; found 541.2483.

N-(4-(benzo[*d*]oxazol-2-yl)benzyl)-4,6-dichloro-1,3,5-triazin-2-amine (25)[92]

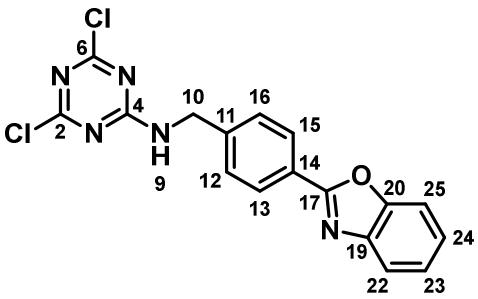

0.2 g of cyanuric chloride (1.11 mmol, 1.22 eq.) and 0.2056 g of **22** (0.92 mmol, 0.92 eq.) and 0.46 mL of DIPEA (2.76 mmol, 3.00 eq.) were mixed together in 50 mL of THF and the mixture was stirred for 4 hours in an ice bath. The residue obtained by evaporation of the mixture was purified by column chromatography to obtain a yellowish solid (0.1926 g, 0.52 mmol, 56%). **R_f**: 0.57. **Mp**: 223.4 °C. **^{1}H-NMR** (300 MHz, $CDCl_3$): δ [ppm] = 9.67 (t, 1H, 9-H), 8.17 (d, 2H, 15-H and 13-H), 7.79 (dd, 2H, 24-H and 23-H), 7.54 (d, 2H, 16-H and 12-H), 7.46-7.36 (m, 2H, 25-H and 22-H), 4.64 (d, 2H, 10-H). **^{13}C-NMR** (75 MHz, $CDCl_3$): δ [ppm] = 169.53 (6-C), 168.67 (2-C), 165.61 (4-C), 162.04 (17-C), 150.14 (20-C), 141.64 (11-C), 141.43 (19-C), 128.04 (16-C), 127.92 (12-C), 127.40 (14-C), 127.36 (15-C), 125.46 (13-C), 125.32 (24-C), 124.84 (23-C), 119.73 (22-C), 110.87 (25-C), 43.76 (10-C). **HRMS**: (ESI, m/z) calcd for $C_{17}H_{11}Cl_2N_5O$ $[M+H]^+$ 372.0413; found 372.0415.

***tert*-Butyl *N*-((4-((4-(benzo[*d*]oxazol-2-yl)benzyl)amino)-6-chloro-1,3,5-triazin-2-yl)valyl)-*S*-tritylcysteinate (26)**

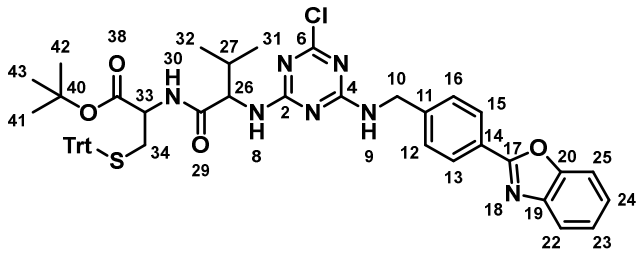

46.8 mg of **25** (0.126 mmol, 1.22 eq.) and 53.46 mg of **24** (0.103 mmol, 1.00 eq.) and 107.7 µL of DIPEA (0.628 mmol, 6.00 eq.) were mixed together in 10 mL of dry THF and 24 hours at 80 °C. The residue obtained by evaporation of the mixture was purified by column chromatography (5:1, Cy/EtOAc) to obtain a white solid (78.38 mg, 0.09 mmol, 89%). **Rf**: 0.34. **^{1}H-NMR** and **^{13}C-NMR** could not be fully processed because multiple isomers in solution were obtained. **HRMS**: (ESI, m/z) calcd for $C_{48}H_{48}ClN_7O_4S$ $[M+Na]^+$ 876.3069; found 876.3060.

tri-*tert*-Butyl 10-(3-((4-((4-(benzo[*d*]oxazol-2-yl)benzyl)amino)-6-((1-((1-(*tert*-butoxy)-1-oxo-3-(tritylthio)propan-2-yl)amino)-3-methyl-1-oxobutan-2-yl)amino)-1,3,5-triazin-2-yl)amino)propyl)-1,4,7,10-tetraazacyclododecane-1,4,7-tricarboxylate (27)

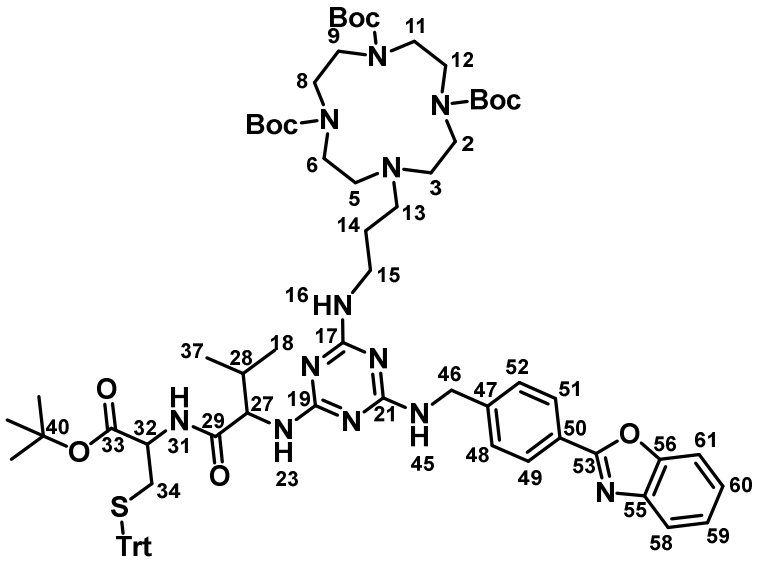

20 mg of **26** (0.023 mmol, 1.00 eq.) and 15.14 mg of **21** (0.028 mmol, 1.22 eq.) and 12.02 µL of DIPEA (0.07 mmol, 6.00 eq.) were mixed together in 3 mL of dry ACN and the mixture was stirred for 30 min in an ice bath. After this, the ice bath was removed, and the reaction was stirred under argon atmosphere at 80 °C for 1 day. The crude product was purified by column chromatography using 20:1 DCM/MeOH as eluent. A transparent oil was obtained (26.81 mg, 0.02 mmol, 85%). **Rf**: 0.80. **Mp**: 104.5 °C. **^{1}H-NMR** (400 MHz,

DMSO): δ [ppm] = 8.10 (d, *J* = 7.8 Hz, 2H, 51-H and 49-H), 7.81 – 7.69 (m, 2H, 61-H and 58-H), 7.49 (d, *J* = 8.3 Hz, 2H, 52-H and 48-H), 7.39 (td, *J* = 7.3, 6.5, 3.7 Hz, 2H, 60-H and 59-H), 7.29 (d, *J* = 4.2 Hz, 11H, CH_{Trt}), 7.21 (q, *J* = 4.3 Hz, 3H, CH_{Trt}), 4.70 – 4.45 (m, 2H, 46-H), 4.37 – 4.25 (m, 1H, 27-H), 4.08 (q, *J* = 8.0 Hz, 1H, 32-H), 3.36 (s, 11H, $CH_{2\ cyclen}$), 3.20 (s, 6H, $CH_{2\ cyclen}$), 2.59 (s, 3H, $CH_{2\ cyclen}$), 2.44 (s, 1H, 34"), 2.36 – 2.24 (m, 1H, 34'), 2.14 – 1.95 (m, 1H, 28-H), 1.55 (dd, *J* = 24.1, 13.7 Hz, 2H, 14-H), 1.36 (q, *J* = 13.4, 11.5 Hz, 27H, $CH_{3\ Boc}$), 1.27 (s, 9H, $CH_{3\ tBu}$), 0.92 – 0.76 (m, 6H, 37-H and 17-H). **^{13}C-NMR** (101 MHz, DMSO): δ [ppm] = 169.18 (29-C), 165.71 (33-C), 162.34 (53-C, 21-C, 19-C and 17-C), 154.99 (56-C), 154.73 ($C{=}O_{Boc}$), 154.46 ($CH_{3\ Boc}$), 150.15 (C_{Trt}), 144.13 (55-C), 141.57 (47-C), 129.02 (CH_{Trt}), 128.03 (CH_{Trt}), 127.65 (52-C, 50-C and 48-C), 127.12 (50-C and 49-C), 126.72 (CH_{Trt}), 125.34 (CH_{Trt}), 124.80 (59-C), 124.58 (60-C), 119.69 (58-C), 110.80 (61-C), 81.03 (40-C), 79.09 (C_{Boc}), 78.43 (C_{Boc}), 66.17 (C_{Trt}), 58.92 (27-C), 54.24 ($CH_{2\ cyclen}$), 53.75 ($CH_{2\ cyclen}$), 51.96 (32-C), 48.89 ($CH_{2\ cyclen}$), 48.15 ($CH_{2\ cyclen}$), 47.19 ($CH_{2\ cyclen}$), 46.70 ($CH_{2\ cyclen}$), 42.90 (46-C), 38.50 ($CH_{2\ cyclen}$), 33.06 (34-C), 28.27 (28-C), 28.04 ($CH_{3\ Boc}$), 27.99 ($CH_{3\ Boc}$), 27.42 ($CH_{3\ tBu}$), 22.10 (14-C), 19.32 (18-C), 18.27 (37-C). **HRMS**: (ESI, m/z) calcd for $C_{74}H_{98}N_{12}O_{10}S$ $[M+H]^+$ 1347.7322; found 1347.7310.

(3-((3-(1,4,7,10-tetraazacyclododecan-1-yl)propyl)carbamoyl)-5-((4-(benzo[*d*]thiazol-2-yl)benzyl)carbamoyl)benzoyl)valylcysteine (28)

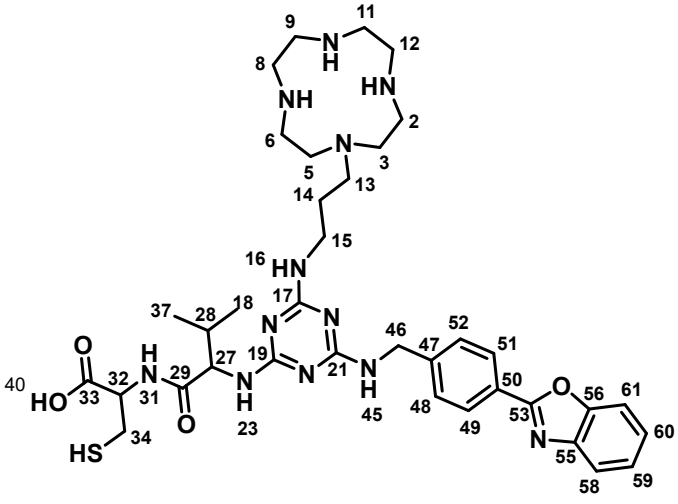

27 was treated with 95% of a solution of 50% trifluoroacetic acid in dichloromethane and 5% of triisopropylsilane for 5 hours and cold diethyl ether was added to the TFA solution. The precipitate was separated by centrifugation, washed with diethyl ether several times, and dried under argon to obtain the TFA salt. A white solid was obtained with 94.38 % purity (9.98 mg, 0.01 mmol, 67%). **^{1}H-NMR** (400 MHz, MeOD): δ [ppm] = 8.23 (d, *J* = 7.9 Hz, 2H, 51-H and 49-H), 7.77 – 7.71 (m, 1H, 58-H), 7.68 (dd, *J* = 6.2, 2.9 Hz, 1H, 51-H), 7.57 (q, *J* = 7.9 Hz, 2H, 52-H and 48-H), 7.42 (dt, *J* = 5.8, 2.4 Hz, 2H, 60-H and 59-H), 4.80 – 4.67 (m, 2H, 46-H), 4.54 (q, *J* = 6.3, 5.6 Hz, 1H, 27-H), 4.44 (td, *J* = 14.6, 14.1, 7.6 Hz, 1H, 32-H), 3.45 (ddd, *J* = 21.3, 10.5, 5.9 Hz, 2H, 15-H), 3.16 (d, *J* = 18.6 Hz, 6H, $CH_{2\ cyclen}$), 3.11 – 3.06 (m, 2H, CH_2

$_{cyclen}$), 2.99 – 2.85 (m, 8H, $CH_{2\ cyclen}$), 2.77 (d, *J* = 7.2 Hz, 3H, $CH_{2\ cyclen}$ and 34"-H), 2.72 – 2.66 (m, 1H, 34'-H), 2.29 – 2.13 (m, 1H, 28-H), 1.93 – 1.68 (m, 2H, 14-H), 1.30 – 1.24 (m, 1H, SH), 1.03 (dt, *J* = 27.8, 6.5 Hz, 6H, 37-H and 18-H). **^{13}C-NMR** (101 MHz, MeOD)**:** δ [ppm] = 173.05 (29-C), 172.90 (33-C), 164.47 (21-C), 163.18 (19-C), 162.94 (17-C), 162.70 (53-C), 152.18 (56-C), 143.60 (55-C), 142.92 (47-C), 129.42 (48-C), 129.24 (52-C), 129.06 (50-C), 126.96 (51-C), 126.29 (49-C), 120.74 (59-C), 119.02 (60-C), 117.09 (58-C), 111.96 (61-C), 61.52 (27-C), 56.30 (32-C), 51.51 ($CH_{2\ cyclen}$), 49.72 ($CH_{2\ cyclen}$), 45.83 ($CH_{2\ cyclen}$), 44.67 ($CH_{2\ cyclen}$), 43.59 ($CH_{2\ cyclen}$), 43.56 ($CH_{2\ cyclen}$), 43.50 ($CH_{2\ cyclen}$), 43.47 ($CH_{2\ cyclen}$), 43.44 ($CH_{2\ cyclen}$), 43.40 (46-C), 39.91 (15-C), 32.27 (28-C), 31.94 (34-C), 26.70 (14-C), 19.94 (18-C), 19.76 (37-C). **HPLC**: [A, 95→40], t_R= 2.683 min, (94.38%). **HRMS**: (ESI, m/z) calcd for $C_{36}H_{52}N_{12}O_4S$ $[M+H]^+$ 749.4028; found 749.4024.

Diaquacobaltate(III)-(3-((3-(1,4,7,10-tetraazacyclododecan-1-yl)propyl)carbamoyl)-5-((4-(benzo[*d*]thiazol-2-yl)benzyl)carbamoyl)benzoyl)valylcysteine (29)

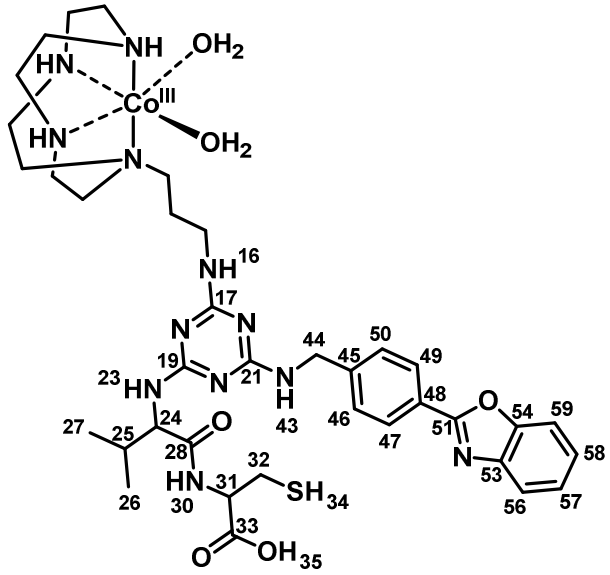

47.1 mg of **28** (0.06 mmol, 1.00 eq.) were dissolved in 2 mL of methanol under argon atmosphere. 1.29 mg of lithium hydroxide (0.05 mmol, 0.86 eq.) were added to this solution and the reaction mixture was stirred for 90 minutes at room temperature. 14.27 mg of $CoCl_2{\cdot}6H_2O$ (0.06 mmol, 1.00 eq.) were added and the reaction mixture was stirred under O_2 atmosphere at room temperature for 24 hours. The colour of the reaction changed from green to purple. The solvent was removed and the residue was purified by filtering with a filter of 0.20 µm. It was obtained a purple solid (29.33mg, 0.04 mmol, 58%). **^{1}H-NMR** (600 MHz, MeOD)**:** δ [ppm] = 8.11 – 7.99 (m, 2H, 49-H and 47-H), 7.57 (d, *J* = 30.9 Hz, 2H, 58-H and 57-H), 7.42 (d, *J* = 31.9 Hz, 2H, 50-H and 46-H), 7.27 (d, *J* =

15.2 Hz, 2H, 59-H and 56-H), 0.99 – 0.80 (m, 6H, 27-H and 26-H). **^{13}C-NMR** (151 MHz, MeOD): δ [ppm] = 164.19 (51-C), 151.85 (54-C), 142.64 (53-C), 128.77 (50-C and 46-C), 126.89 (48-C), 126.65 (49-C and 47-C), 125.98 (58-C and 57-C), 120.46 (56-C), 111.69 (59-C), 55.84 (31-C), 44.64 (44-C), 30.60 (32-C), 30.28 (25-C), 19.74 (27-C), 18.40 (26-C). **HPLC**: [A, 95→40, UV= 545 nm], t_R= 31.633 min, (96.32%). **HRMS**: (ESI, m/z) calcd for $C_{36}H_{53}CoN_{12}O_6S$ $[M+K]^+$ 879.2895; found 879.2881.

3,5-bis(Methoxycarbonyl)benzoic acid (30)[115]

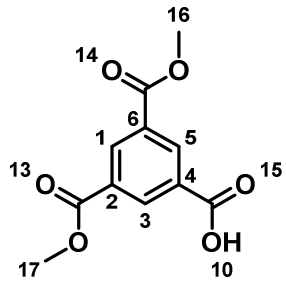

3.329 g of trimethyl benzene-1,3,5-tricarboxylate (13.2 mmol, 1.11 eq.) were dissolved in 140 mL of MeOH, aqueous NaOH (6mL, 12 mmol) was slowly added to the solution and the mixture was stirred for 16 hours under reflux. The solution was removed under reduced pressure, and the residue was added to the saturated $NaHCO_3$ solution (24 mmol, 2.00 eq.) with stirring for 1 hour at 50 °C. The suspension was filtered to remove the unreacted stating material and the filtrate was acidified with HCl concentrated. The formed precipitate was filtered and washed with water to give 2.2 g of compound as a white powder (2.20 g, 9.24 mmol, 77%). **R_f**: 0.63. **Mp**: 153.2 °C **^{1}H-NMR** (300 MHz, DMSO): δ [ppm] = 13.64 (s, 1H, 10-H), 8.57 (d, *J* = 1.7 Hz, 2H, 5-H and 1-H), 8.53 (t, *J* = 1.7 Hz, 1H, 3-H), 3.90 (s, 6H, 17-H and 16-H). **^{13}C-NMR** (75 MHz, DMSO): δ [ppm] = 165.59 (15-C), 165.43 (14-C), 164.57 (13-C), 133.53 (1-C), 133.23 (5-C), 132.97 (3-C), 132.09 (6-C), 131.95 (2-C), 130.70 (4-C), 52.64 (17-C and 16-C). **HRMS**: (ESI, m/z) calcd for $C_{11}H_{10}O_6$ $[M+H]^+$ 239.0550; found 239.0551.

Dimethyl 5-((4-(benzo[*d*]oxazol-2-yl)benzyl)carbamoyl)isophthalate (31)

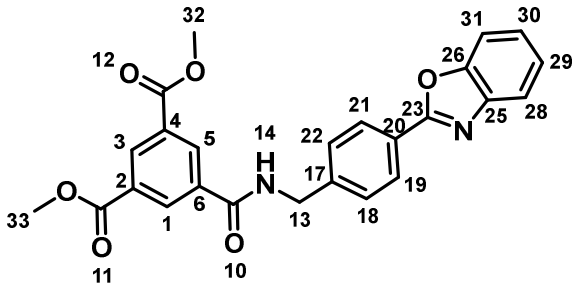

0.353 g of **30** (1.48 mmol, 1.10 eq.) and 0.3 g of **22** (1.33 mmol, 1.00 eq.) were dissolved in 80 mL of THF. To this solution, 1.46 g of PyCloP (3.46 mmol, 2.60 eq.) and 1.86 mL of DIPEA (10.64 mmol, 8.00 eq.) were added. The reaction mixture was refluxed for 1 day. After removal the solvent, the product was purified by column chromatography using DCM/MeOH 60:1 as eluent. The product was crystallized in MeOH obtaining yellow solid was obtained (0.29 g, 0.88 mmol, 66%). **R_f**: 0.24. **Mp**: 221.4 °C. **^{1}H-NMR** (300 MHz, DMSO): δ [ppm] = 9.60 (t, *J* = 5.9 Hz, 1H, 14-H), 8.74 (d, *J* = 1.5 Hz, 2H, 5-H and 1-H), 8.59 (t, *J* = 1.3 Hz, 1H, 3-H), 8.17 (d, *J* = 8.1 Hz, 2H, 21-H and 19-H), 7.78 (dd, *J* = 9.2, 4.7 Hz, 2H, 31-H and 31-H), 7.57 (d, *J* = 8.2 Hz, 2H, 22-H and 18-H), 7.44 – 7.37

(m, 2H, 30-H and 29-H), 4.62 (d, *J* = 5.7 Hz, 2H, 13-H), 3.92 (d, *J* = 0.7 Hz, 6H, 33-H and 32-H). **^{13}C-NMR** (75 MHz, DMSO): δ [ppm] = 164.90 (10-C), 164.27 (12-C and 11-C), 162.14 (23-C), 150.11 (26-C), 143.41 (17-C), 141.45 (25-C), 135.18 (6-C), 132.12 (2-C), 131.91 (4-C), 130.56 (3-C), 128.13 (22-C and 18-C), 127.34 (20-C), 125.39 (21-C, 19-C, 5-C and 1-C), 124.99 (29-C), 124.80 (30-C), 119.69 (28-C), 110.83 31-C), 52.63 (33-C and 32-C), 42.73 (13-C). **HRMS**: (ESI, m/z) calcd for $C_{25}H_{20}N_2O_6$ $[M+H]^+$ 445.1394; found 445.1401.

3-((4-(benzo[*d*]oxazol-2-yl)benzyl)carbamoyl)-5-(methoxycarbonyl)benzoic acid (32)

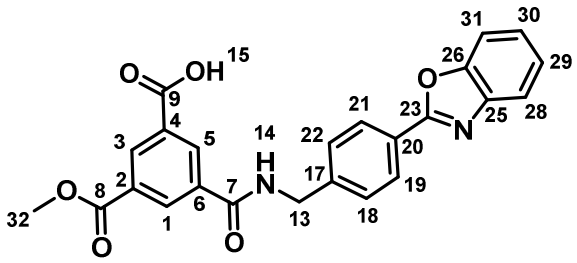

100 mg of **31** (0.22 mmol, 1.00 eq.) ere dissolved in 7 mL of THF and 3 mL of MeOH. 6.46 mg of LiOH (0.27 mmol, 1.20 eq.) were added to this solution and the mixture was refluxed overnight. The product was purified by column chromatography using DCM/MeOH/AcOH 20:1:0.1 as eluent obtaining a white solid (93.9 mg, 0.22 mmol, 97%). **R_f**: 0.37. **Mp**: 283.2 °C. **^{1}H-NMR** (600 MHz, DMSO): δ [ppm] = 9.50 (t, *J* = 5.8 Hz, 1H, 14-H), 8.73 (s, 1H, 3-H), 8.64 (s, 1H, 5-H), 8.53 (s, 1H, 1-H), 8.18 (d, *J* = 8.3 Hz, 2H, 21-H and 19-H), 7.81 – 7.77 (m, 2H, 31-H and 28-H), 7.57 (d, *J* = 8.3 Hz, 2H, 22-H and 18-H), 7.44 – 7.39 (m, 2H, 30-H and 29-H), 4.60 (d, *J* = 5.8 Hz, 2H, 13-H), 3.90 (s, 3H, 32-H). **^{13}C-NMR** (151 MHz, DMSO): δ [ppm] = 165.89 (9-C and 7-C), 165.48 (8-C), 162.24 (23-C), 150.16 (26-C), 143.86 (25-C), 141.50 (17-C), 134.20 (6-C and 2-C), 132.41 (4-C), 132.34 (3-C), 129.34 (5-C), 128.10 (22-C and 18-C), 127.36 (1-C), 125.44 (21-C, 20-C and 19-C), 124.92 (30-C), 124.86 (29-C), 119.74 (28-C), 110.90 (31-C), 52.32 (32-C), 42.67 (13-C). **HRMS**: (ESI, m/z) calcd for $C_{24}H_{18}N_2O_6$ $[M+H]^+$ 431.1238; found 431.1239.

Methyl 3-((4-(benzo[*d*]oxazol-2-yl)benzyl)carbamoyl)-5-((1-((1-(*tert*-butoxy)-1-oxo-3-(tritylthio)propan-2-yl)amino)-3-methyl-1-oxobutan-2-yl)carbamoyl)benzoate (33)

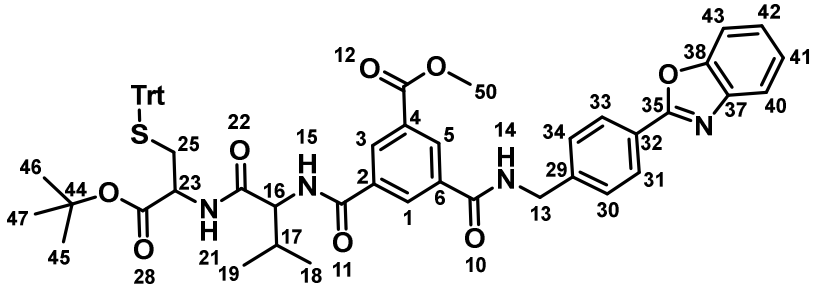

50.5 mg of **32** (0.12 mmol, 1.00 eq.) and 131.4 mg of **24** (0.25 mmol, 2.00 eq.) were added to 3 mL of DMF. To this solution, 110.17 mg of PyCloP (0.25 mmol, 2.2 eq.) and 60.9 µL of DIPEA (0.35 mmol, 3.00 eq.) were added. The reaction mixture was stirred at RT overnight and 4h at 80 °C. After removal the solvent, the residue was taken up in DCM and washed with water. The product was purified by column chromatography using Cy/EtOAc 3:1 as eluent, obtaining a white solid (51.4 mg, 0.06 mmol, 47%). **R_f**: 0.2. **^{1}H-NMR** (600 MHz, DMSO): δ [ppm] =9.51 (t, *J* = 5.9 Hz, 1H, 14-H), 8.75 (d, *J* = 8.9 Hz, 1H, 15-H), 8.67 (t, *J* = 1.6 Hz, 1H, 1-H), 8.64 (t, *J* = 1.6 Hz, 1H, 3-H), 8.60 (t, *J* = 1.6 Hz, 1H, 5-H), 8.50 (d, *J* = 7.5 Hz, 1H, 21-H), 8.18 (d, *J* = 8.3 Hz, 2H, 33-H and 31-H), 7.81 – 7.77 (m, 2H, 43-H and 40-H), 7.58 (d, *J* = 8.4 Hz, 2H, 34-H and 30-H), 7.45 – 7.39 (m, 2H, 42-H and 41-H), 7.33 – 7.27 (m, 12H, CH_{Trt}), 7.22 (tt, *J* = 6.2, 1.7 Hz, 3H, CH_{Trt}), 4.63 (d, *J* = 5.8 Hz, 2H, 13-H), 4.43 (t, *J* = 8.5 Hz, 1H, 16-H), 4.04 – 4.02 (m, 1H, 23-H), 3.92 (s, 3H, 50-H), 2.48 – 2.45 (m, 1H, 25''-H), 2.34 (dd, *J* = 12.2, 5.5 Hz, 1H, 25'-H), 2.13 – 2.10 (m, 1H, 17-H), 1.28 (s, 9H, $CH_{3\ tBu}$), 0.93 (dd, *J* = 11.9, 6.7 Hz, 6H, 19-H and 18-H). **^{13}C-NMR** (151 MHz, DMSO): δ [ppm] = 170.75 (C=O), 169.01 (C=O), 165.38 (C=O), 165.09 (C=O), 164.97 (C=O), 162.20 (35-C), 150.16 (38-C), 144.08 (CH_{Trt}), 143.60 (29-C), 141.50 (37-C), 134.77 (6-C and 2-C), 131.12 (4-C), 130.85 (1-C), 129.97 (34-C and 30-C), 129.00 (CH_{Trt}), 128.15 (CH_{Trt}), 128.05(33-C and 31-C), 127.39 (3-C), 126.76 (5-C), 125.46 (CH_{Trt}), 125.01 (41-C), 124.87 (42-C), 119.75 (40-C), 110.90 (43-C), 80.98 (44-C), 66.19 (C-$_{Trt}$), 59.74 (16-C), 58.76 (23-C), 52.55 (50-C), 42.71 (13-C), 32.85 (25-C), 30.26 (17-C), 27.45 ($CH_{3\ tBu}$), 26.33 ($CH_{3\ tBu}$), 20.76 ($CH_{3\ tBu}$), 19.27 (19-C), 18.84 (18-C). **HRMS**: (ESI, m/z) calcd for $C_{55}H_{54}N_4O_8$ $[M+Na]^+$ 953.3557; found 953.3555.

tri-*tert*-Butyl 10-(3-(3-((4-(benzo[*d*]oxazol-2-yl)benzyl)carbamoyl)-5-(methoxycarbonyl)benzamido)propyl)-1,4,7,10-tetraazacyclododecane-1,4,7-tricarboxylate (35)

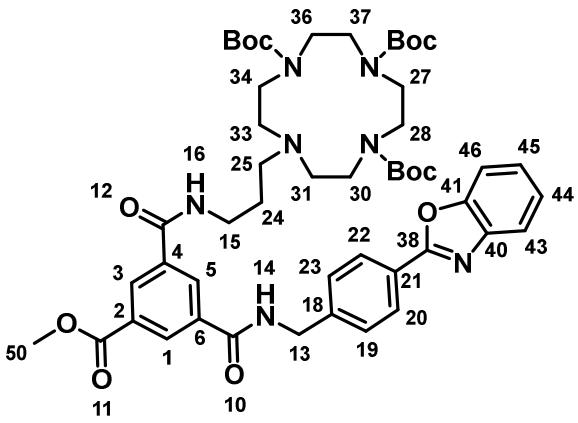

77.9mg of **32** (0.18 mmol, 1.00 eq.) were added to 6 mL of DMF. 191.7 mg of **21** (0.36 mmol, 2.00 eq.), 163.2 mg of HCTU (0.39 mmol, 2.2 eq.) and 94.06 µL of DIPEA (0.54 mmol, 3.00 eq.) were added to this solution. The reaction mixture was stirred overnight at room temperature. After removal the solvent, the residue was taken up in DCM and was washed with water. The product was purified by column chromatography using DCM/MeOH 20:1 as eluent obtaining a yellow solid (71. 94 mg, 0.08 mmol, 91%). **R_f**: 0.43. **Mp**: 246.9 °C. **^{1}H-NMR** (600 MHz, $CDCl_3$)**:** δ [ppm] = 8.72 (d, *J* = 12.5 Hz, 2H, 3-H and 1-H), 8.58 (s, 1H, 5-H), 8.20 (d, *J* = 8.0 Hz, 2H, 22-H and 20-H), 7.83 (s, 1H, 14-H), 7.78 – 7.73 (m, 1H, 44-H), 7.61 – 7.55 (m, 1H, 45-H), 7.47 (d, *J* = 7.8 Hz, 2H, 23-H and 19-H), 7.38 – 7.32 (m, 2H, 46-H and 43-H), 7.30 (s, 1H, 16-H), 4.70 (d, *J* = 5.0 Hz, 2H, 13-H), 3.91 (s, 3H, 50-H), 3.63 – 3.18 (m, 16H, $CH_{2\ cyclen}$), 2.63 (s, 4H, 31-H and 25-H), 1.75 (s, 2H, 24-H), 1.44 (d, *J* = 20.7 Hz, 15H, $CH_{3\ Boc}$), 1.34 (s, 12H, $CH_{3\ Boc}$). **^{13}C-NMR** (151 MHz, $CDCl_3$)**:** δ [ppm] = 166.02 (12-C), 165.90 (10-C), 165.86 (11-C), 162.66 (38-C), 156.69 (C=O $_{Boc}$), 156.22 (C=O $_{Boc}$), 155.28 (C=O $_{Boc}$), 150.84 (41-C), 142.14 (18-C), 141.83 (40-C), 135.52 (4-C), 134.59 (6-C), 131.71 (2-C), 131.47 (5-C), 129.34 (23-C and 19-C), 128.59 (21-C), 128.47 (22-C), 128.14 (20-C), 128.04 (1-C), 126.61 (3-C), 125.37 (44-C), 124.80 (45-C), 120.14 (43-C), 110.76 (46-C), 80.23 (C- $_{Boc}$), 80.11 (C- $_{Boc}$), 79.73 (C- $_{Boc}$), 56.23 (50-C), 52.57 (25-C), 50.94 ($CH_{2\ cyclen}$), 50.12 ($CH_{2\ cyclen}$), 48.66 ($CH_{2\ cyclen}$), 47.60 ($CH_{2\ cyclen}$), 47.19 ($CH_{2\ cyclen}$), 44.02 (13-C), 38.72 (15-C), 28.71 ($CH_{3\ Boc}$), 28.60 ($CH_{3\ Boc}$), 28.55 ($CH_{3\ Boc}$), 26.51 (24-C). **HRMS**: (ESI, m/z) calcd for $C_{50}H_{67}N_7O_{11}$ $[M+H]^+$ 942.4971; found 942.4987.

3-((4-(benzo[*d*]oxazol-2-yl)benzyl)carbamoyl)-5-((3-(4,7,10-tris(*tert*-butoxycarbonyl)-1,4,7,10-tetraazacyclododecan-1-yl)propyl)carbamoyl)benzoic acid (36)

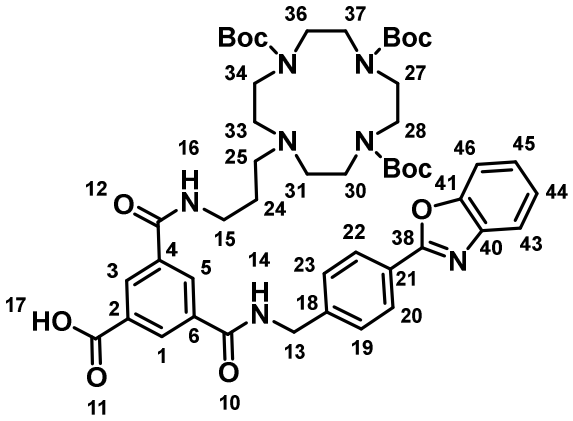

155.8 mg of **35** (0.16 mmol, 1.00 eq.) were dissolved in 7 mL of THF and 1 mL of MeOH. 4.3 mg of LiOH (0.18 mmol, 1.11 eq.) were added to this solution, the mixture was refluxed overnight. The product was purified by column chromatography using DCM/MeOH/AcOH 20:1:0.1 as eluent. A yellowish oil was obtained (0.14 g, 0.15 mmol, 92%). **R_f**: 0.42. **Mp**: 227.1 °C. **^{1}H-NMR** (600 MHz, DMSO): δ [ppm] = 13.45 (s, 1H, 17-H), 9.57 (t, *J* = 5.9 Hz, 1H, 14-H), 9.01 (t, *J* = 5.5 Hz, 1H, 16-H), 8.72 (s, 1H, 3-H), 8.63 (s, 1H, 5-H), 8.57 (s, 1H, 1-H), 8.18 (d, *J* = 8.3 Hz, 2H, 22-H and 20-H), 7.79 (td, *J* = 8.7, 7.9, 2.0 Hz, 2H, 46-H and 43-H), 7.58 (d, *J* = 8.2 Hz, 2H, 23-H and 19-H), 7.42 (pd, *J* = 7.3, 1.3 Hz, 2H, 45-H amd 44-H), 4.61 (d, *J* = 5.5 Hz, 2H, 13-H), 3.68 – 3.54 (m, 9H, $CH_{2\ cyclen}$), 3.39 (q, *J* = 5.8 Hz, 2H, $CH_{2\ cyclen}$), 3.28 (dd, *J* = 20.7, 11.0 Hz, 6H, $CH_{2\ cyclen}$), 3.22 – 3.15 (m, 3H, $CH_{2\ cyclen}$), 2.02 – 1.96 (m, 2H, 24-H), 1.44 – 1.32 (m, 27H, $CH_{3\ Boc}$). **^{13}C-NMR** (151 MHz, DMSO): δ [ppm] = 166.39 (12-C), 165.15 (10-C), 165.04 (8-C), 162.20 (38-C), 155.63 (C=O $_{Boc}$), 150.16 (41-C), 143.67 (18-C), 141.49 (40-C), 134.93 (46-C), 134.73 (2-C), 131.32 (5-C), 130.59 (23-C and 19-C), 130.40 (21-C), 128.20 (22-C and 20-C), 127.36 (1-C), 125.47 (3-C), 124.99 (44-C), 124.88 (45-C), 119.75 (43-C), 110.89 (46-C), 80.22 (C- $_{Boc}$), 79.56 (C- $_{Boc}$), 54.91 (25-C), 51.61 ($CH_{2\ cyclen}$), 49.23 ($CH_{2\ cyclen}$), 49.16 ($CH_{2\ cyclen}$), 49.14 ($CH_{2\ cyclen}$), 47.86 ($CH_{2\ cyclen}$), 42.70 (13-C), 34.38 (15-C), 30.41 ($CH_{3\ Boc}$), 27.99 ($CH_{3\ Boc}$), 27.91 ($CH_{3\ Boc}$), 24.13 (24-C). **HRMS**: (ESI, m/z) calcd for $C_{49}H_{65}N_7O_{11}$ $[M+H]^+$ 928.4815; found 928.4824.

tri-*tert*-Butyl 10-(3-(3-((4-(benzo[*d*]oxazol-2-yl)benzyl)carbamoyl)-5-((1-((1-(*tert*-butoxy)-1-oxo-3-(tritylthio)propan-2-yl)amino)-3-methyl-1-oxobutan-2-yl)carbamoyl) benzamido)propyl)-1,4,7,10-tetraazacyclododecane-1,4,7-tricarboxylate (37)

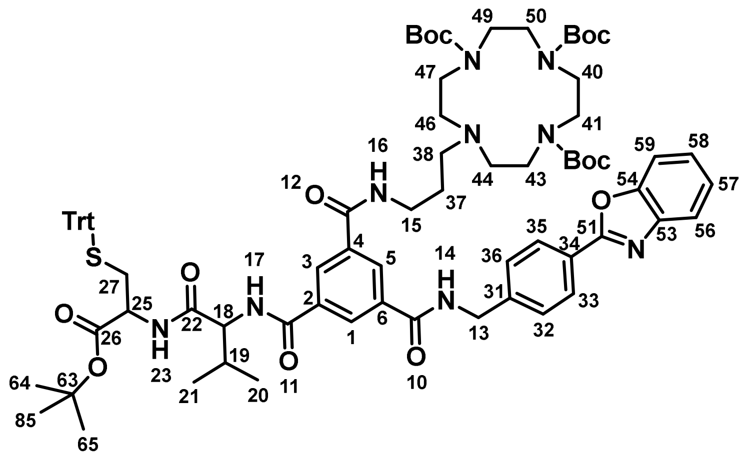

40 mg of **36** (0.04 mmol, 1.00 eq.) were added to 6 mL of DMF. 44.7 mg of **24** (0.08 mmol, 2.00 eq.), 39.1 mg of HCTU (0.09 mmol, 2.2 eq.) and 22.5 µL of DIPEA (0.13 mmol, 3.00 eq.) were added to this solution. The reaction mixture was stirred overnight at room temperature. After removal the solvent, the residue was taken up in DCM and was washed with water. The product was purified by column chromatography using DCM/MeOH 10:1 as eluent obtaining yellow oil (17.9 mg, 0.01 mmol, 29%). **R_f**: 0.55. **Mp**: 130.5 °C. **^{1}H-NMR** (600 MHz, DMSO): δ [ppm] = 9.38 (t, *J* = 5.8 Hz, 1H, 14-H), 8.72 (s, 1H, 17-H), 8.50 (q, *J* = 8.7, 7.6 Hz, 4H, 23-H, 5-H, 3-H and 1-H), 8.45 (s, 1H, 16-H), 8.18 (d, *J* = 8.3 Hz, 2H, 35-H and 33-H), 7.81 – 7.77 (m, 2H, 59-H and 56-H), 7.59 (s, 1H, 36-H), 7.57 (s, 1H, 32-H), 7.44 – 7.39 (m, 2H, 58-H and 57-H), 7.34 – 7.27 (m, 12H, CH $_{\text{Trt}}$), 7.24 – 7.20 (m, 3H, CH $_{\text{Trt}}$), 4.63 (d, *J* = 5.8 Hz, 2H, 13-H), 4.46 (t, *J* = 8.4 Hz, 1H, 18-H), 4.04 (q, *J* = 7.7 Hz, 1H, 25-H), 3.51 – 3.35 (m, 5H, $CH_{2\ \text{cyclen}}$), 3.31 – 3.27 (m, 4H, 15-H and $CH_{2\ \text{cyclen}}$), 3.24 (d, *J* = 8.1 Hz, 5H, $CH_{2\ \text{cyclen}}$), 2.65 (s, 2H, 38-H), 2.56 (d, *J* = 19.0 Hz, 4H, $CH_{2\ \text{cyclen}}$), 2.48 – 2.44 (m, 1H, 27''-H), 2.34 (dd, *J* = 12.2, 5.5 Hz, 1H, 27'-H), 2.13 – 2.07 (m, 1H, 19-H), 1.73 – 1.66 (m, 2H, 37-H), 1.37 (s, 10H, $CH_{3\ \text{Boc}}$), 1.34 (d, *J* = 5.7 Hz, 16H, $CH_{3\ \text{Boc}}$), 1.29 (s, 8H, $CH_{3\ \text{Boc}}$ and $CH_{3\ \text{tBu}}$), 1.23 (s, 2H, $CH_{3\ \text{tBu}}$), 0.93 (dd, *J* = 13.2, 6.7 Hz, 6H, 21-H and 20-H). **^{13}C-NMR** (151 MHz, DMSO): δ [ppm] = 170.78 (22-C), 169.01 (26-C), 165.56 (10-C), 165.50 (12-C), 165.40 (11-C), 162.20 (51-C), 154.99 (C=O $_{\text{Boc}}$), 154.73 (C=O $_{\text{Boc}}$), 154.44 (C=O $_{\text{Boc}}$), 150.16 (54-C), 144.07 (C- $_{\text{Trt}}$), 143.69 (31-C), 141.50 (53-C), 135.12 (2-C), 134.66 (4-C), 134.44 (6-C), 129.01 (CH $_{\text{Trt}}$), 128.81 (5-C, 3-C and 1-C), 128.14 (36-C and 32-C), 128.06 (CH $_{\text{Trt}}$), 127.75 (CH $_{\text{Trt}}$), 127.36 (35-C and 33-C), 126.77 (34-C), 125.46 (CH $_{\text{Trt}}$), 125.00 (57-C), 124.87 (58-C), 119.75 (56-C), 110.88 (59-C), 80.98 (C- $_{\text{Boc}}$), 78.46 (C- $_{\text{Boc}}$), 66.23 (C-

$_{Trt}$), 58.48 (18-C), 52.24 (25-C), 42.67 ($CH_{2\ cyclen}$), 40.05 (13-C) 37.90 (15-C), 32.85 (27-C), 30.57 (19-C), 28.27 ($CH_{3\ Boc}$), 28.04 ($CH_{3\ Boc}$), 27.99 ($CH_{3\ tBu}$), 27.46 ($CH_{3\ tBu}$), 19.27 (21-C), 18.72 (20-C). **HRMS**: (ESI, m/z) calcd for $C_{80}H_{101}N_9O_{13}S$ $[M+H]^+$ 1428.7312; found 1428.7300.

(3-((3-(1,4,7,10-tetraazacyclododecan-1-yl)propyl)carbamoyl)-5-((4-(benzo[*d*]oxazol-2-yl)benzyl)carbamoyl)benzoyl)valylcysteine (38)

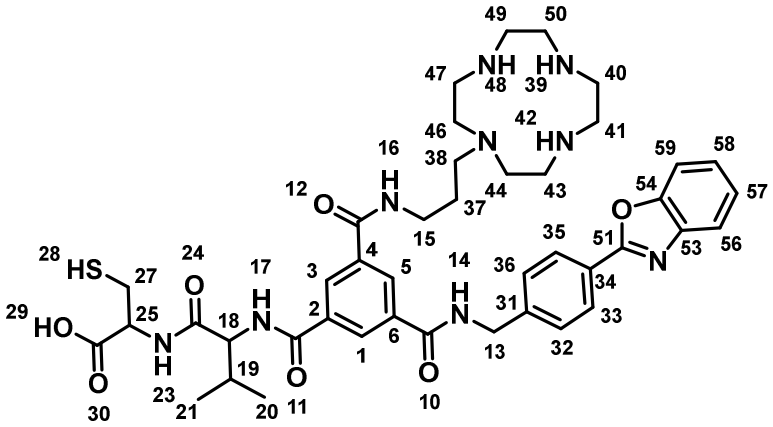

The starting material **37** was treated with 95% of a solution of 50% TFA in DCM and 5% of TIPS for 5 hours and diethyl ether was added to the TFA solution. The precipitate was separated by centrifugation, washed with diethyl ether several times, and dried under argon to obtain the TFA salt. The product was purified with a semipreprative-HPLC obtaining a white solid with 98% purity (7.69 g, 9 µmol, 74%). **^{1}H-NMR** (600 MHz, MeOD): δ [ppm] = 8.50 (t, *J* = 1.7 Hz, 1H, 1-H), 8.48 (t, *J* = 1.6 Hz, 1H, 5-H), 8.44 (t, *J* = 1.7 Hz, 1H, 3-H), 8.19 (d, *J* = 8.3 Hz, 2H, 35-H and 33-H), 7.71 – 7.68 (m, 1H, 56-H), 7.65 – 7.63 (m, 1H, 59-H), 7.57 (d, *J* = 8.3 Hz, 2H, 36-H and 32-H), 7.38 (ddd, *J* = 7.0, 4.9, 1.6 Hz, 2H, 58-H and 57-H), 4.68 (s, 2H, 13-H), 4.61 (dd, *J* = 7.0, 4.4 Hz, 1H, 25-H), 4.44 (d, *J* = 8.1 Hz, 1H, 18-H), 3.47 – 3.39 (m, 2H, 15-H), 3.15 (br s, 8H, $CH_{2\ cyclen}$), 2.95 (dd, *J* = 14.0, 4.4 Hz, 5H, 38"-H and $CH_{2\ cyclen}$), 2.92 – 2.84 (m, 5H, 38'-H and $CH_{2\ cyclen}$), 2.70 (t, *J* = 6.8 Hz, 2H, 48-H and 42-H), 2.19 (dq, *J* = 14.0, 6.9 Hz, 2H, 27-H), 1.82 (t, *J* = 6.9 Hz, 2H, 37-H), 1.24 (s, 1H, 39-H), 1.07 – 1.01 (m, 6H, 21-H and 20-H). **^{13}C-NMR** (151 MHz, MeOD): δ [ppm] = 173.85 (30-C), 172.76 (24-C), 168.79 (10-C), 168.65 (12-C), 168.57 (11-C), 164.39 (51-C), 152.01 (54-C), 144.44 (31-C), 142.77 (53-C), 136.52 (2-C), 136.45 (4-C), 136.37 (6-C), 130.61 (1-C), 130.44 (5-C), 129.97 (3-C), 129.37 (36-C and 32-C), 128.86 (34-C), 126.95 (35-C and 33-C), 126.76 (57-C), 126.11 (58-C), 120.56 (56-C), 111.79 (59-C), 61.27 (18-C), 56.17 (25-C), 54.79 ($CH_{2\ cyclen}$), 49.85 (38-C), 45.53 ($CH_{2\ cyclen}$), 44.48 (13-C), 43.51 ($CH_{2\ cyclen}$), 43.30 ($CH_{2\ cyclen}$), 38.59 (15-C), 32.04 (19-C), 31.22 (27-C), 26.63 (37-C), 19.77 (21-C), 19.32 (20-C). **HPLC**: [A, 90→40], t_R= 2.975 min, (98%). **HRMS**: (ESI, m/z) calcd for $C_{42}H_{55}N_9O_7S$ $[M+H]^+$ 830.4018; found 830.4012.

Diaquacobaltate(III)-(3-((3-(1,4,7,10-tetraazacyclododecan-1-yl)propyl)carbamoyl)-5-((4-(benzo[*d*]oxazol-2-yl)benzyl)carbamoyl)benzoyl)valylcysteine (39)

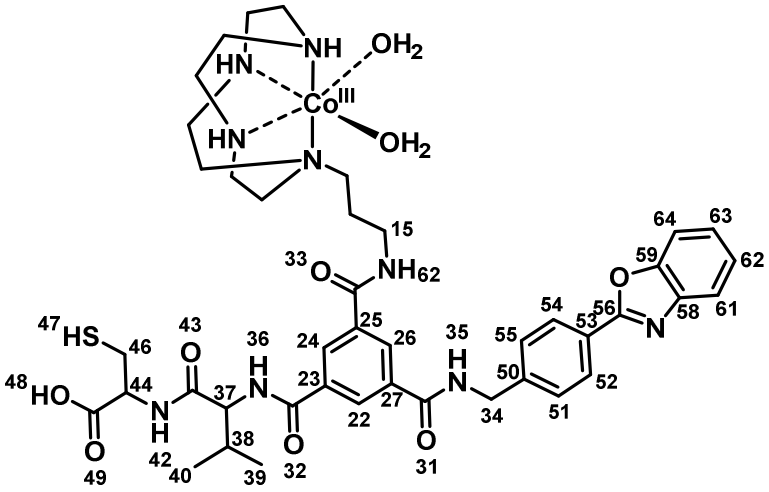

15.4 mg of **38** (0.002 mmol, 1.00 eq.) were dissolved in 2 mL of methanol under argon atmosphere. 0.37 mg of lithium hydroxide (0.001 mmol, 0.86 eq.) were added to this solution and the reaction mixture was stirred for 90 minutes at room temperature. 4.28 mg of $CoCl_2 \cdot 6H_2O$ (0.002 mmol, 1.00 eq.) were added and the reaction mixture was stirred under O_2 atmosphere at room temperature for 24 hours. The colour of the reaction changed from brown to purple. The solvent was removed and the residue was purified by filtering with a filter of 0.20 µm. It was obtained a purple solid (9.36 mg, 0.01 mmol, 57%). **^{1}H-NMR** (600 MHz, MeOD)**:** δ [ppm] = 8.22 (d, *J* = 7.9 Hz, 2H, 26-H and 22-H), 8.08 (s, 1H, 24-H), 7.72 (d, *J* = 7.1 Hz, 1H, 61-H), 7.66 (d, *J* = 7.7 Hz, 1H, 64-H), 7.61 – 7.58 (m, 2H, 55-H and 51-H), 7.46 – 7.37 (m, 4H, 63-H, 62-H, 54-H and 52-H). **HPLC**: [A, 95→40, UV= 545 nm], t_R= 26.975-33.308 min. **HRMS**: (ESI, m/z) calcd for $C_{42}H_{52}CoN_9O_7S$ $[M+H]^+$ 886.3115; found 886.3040.

(4-(Benzo[*d*]thiazol-2-yl)phenyl)methanamine (40)[111]

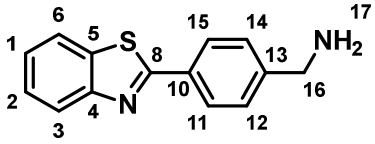

A mixture of 0.71 mL of 2-aminotiophenol (6.74 mmol, 1.00 eq.) and 1.02 g of 4-(aminomethyl)benzoic acid (6.74 mmol, 1.00 eq.) were dissolved in polyphosphoric acid and the reaction was left under reflux for 4 hours. After cooling with ice, the reaction mixture was dissolved in 5% NaOH aqueous solution and extracted with CH_2Cl_2. The organic phase was the extracted with 0.1 N HCl aq. solution and washed with CH_2Cl_2. The aqueous phase was basified to pH aprox. 10-12 with a 5M NaOH aqueous solution and extracted with CH_2Cl_2. The organic phase was dried over NA_2SO_4 and the solvent was evaporated obtaining a pale blue solid (0.49 g, 2.02 mmol, 30%). **R_f**: 0.77. **Mp**: 113.8 °C. **^{1}H-NMR** (400 MHz, MeOD)**:** δ [ppm] = 8.04 – 7.94 (m, 4H, 15-H, 11-H, 6-H

and 3-H), 7.54 – 7.46 (m, 3H, 14-H, 12-H, 2-H), 7.41 (ddd, *J* = 8.3, 7.2, 1.2 Hz, 1H, 1-H), 3.84 (s, 2H, 16-H). **^{13}C-NMR** (101 MHz, MeOD)**:** δ [ppm] = 169.95 (8-C), 155.19 (5-C), 147.65 (13-C), 136.15 (4-C), 133.27 (10-C), 129.33 (15-C and 11-C), 128.79 (14-C and 12-C), 127.83 (1-C), 126.75 (2-C), 123.83 (3-C), 123.08 (6-C), 46.53 (16-C). **HRMS**: (ESI, m/z) calcd for $C_{14}H_{12}N_2S$ $[M+H]^+$ 241.0794; found 241.0794.

Dimethyl 5-((4-(benzo[*d*]thiazol-2-yl)benzyl)carbamoyl)isophthalate (41)

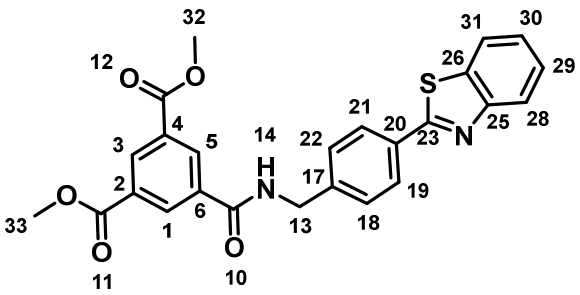

141.73 mg of **40** (0.59 mmol, 1.10 eq.) and 130.7 mg of **32** (0.54 mmol, 1.00 eq.) were dissolved in 40 mL of distilled THF. To this solution was added 592.1 mg of PyCloP (1.40 mmol, 2.60 eq.) and 0.75 mL of DIPEA (4.32 mmol, 8.00 eq.). The reaction mixture was refluxed overnight. After removal the solvent, the product was purified by column chromatography using DCM/MeOH 60:1 as eluent. It was obtained a pale purple solid (0.11 g, 0.25 mmol, 82%). **R_f**: 0.4. **Mp**: 205.8 °C. **^{1}H-NMR** (400 MHz, $CDCl_3$)**:** δ [ppm] = 8.79 (t, *J* = 1.6 Hz, 1H, 3-H), 8.66 (d, *J* = 1.6 Hz, 2H, 5-H and 1-H), 8.09 – 8.04 (m, 3H, 31-H, 28-H and 21-H), 7.90 (d, *J* = 8.0 Hz, 1H, 19-H), 7.52 – 7.46 (m, 3H, 29-H, 22-H and 18-H), 7.39 (td, *J* = 7.7, 7.3, 1.1 Hz, 1H, 30-H), 6.84 (t, *J* = 5.7 Hz, 1H, 14-h), 4.74 (d, *J* = 5.8 Hz, 2H, 13-H), 3.95 (s, 6H, 33-H and 32-H). **^{13}C-NMR** (101 MHz, $CDCl_3$)**:** δ [ppm] =168.02 (10-C), 165.65 (12-C and 11-C), 165.61 (23-C), 153.22 (25-C), 141.49 (17-C), 135.11 (26-C), 134.68 (6-C), 133.54 (4-C and 2-C), 132.51 (3-C), 132.32 (20-C), 131.40 (5-C and 1-C), 128.77 (21-C and 19-C), 128.24 (22-C and 18-C), 126.83 (29-C), 125.71 (30-C), 123.07 (21-C), 121.85 (28-C), 52.79 (33-C and 32-C), 44.08 (13-C). **HRMS**: (ESI, m/z) calcd for $C_{25}H_{20}N_2O_5S$ $[M+H]^+$ 461.1166; found 461.1181.

3-((4-(Benzo[*d*]thiazol-2-yl)benzyl)carbamoyl)-5-(methoxycarbonyl)benzoic acid (42)

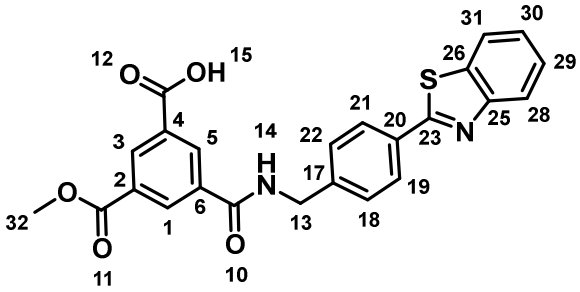

103.5 mg of **41** (0.23 mmol, 1.00 eq.) were dissolved in 7 mL of THF and 3 mL of MeOH. 5.38 mg of LiOH (0.23 mmol, 1.00 eq.) were added to this solution, the mixture was refluxed overnight. The product was purified by column chromatography using DCM/MeOH/AcOH 20:1:0.1 as eluent obtaining a pale grey solid (67.23 mg, 0.15 mmol, 67%). **R_f**: 0.34. **Mp**: 267.8 °C. **^{1}H-NMR** (400 MHz, DMSO): δ [ppm] = 13.59 (br s, 1H, 15-H) 9.59 (t, *J* = 5.9 Hz, 1H, 14-H), 8.74 (dt, *J* = 11.6, 1.7 Hz, 2H, 3-H and 1-H), 8.61 (t, *J* = 1.6 Hz, 1H, 5-H), 8.17 – 8.11 (m, 1H, 19-H), 8.06 (td, *J* = 8.2, 1.4 Hz, 3H, 31-H, 28-H and 21-H), 7.58 – 7.50 (m, 3H, 19-H, 22-H and 18-H), 7.46 (ddd, *J* = 8.3, 7.2, 1.2 Hz, 1H, 30-H), 4.60 (d, *J* = 5.8 Hz, 2H, 13-H), 3.93 (s, 3H, 32-H). **^{13}C-NMR** (101 MHz, DMSO): δ [ppm] = 167.13 (10-C), 166.04 (12-C), 165.14 (11-C), 164.51 (23-C), 153.58 (25-C), 142.95 (17-C), 135.15 (4-C), 134.41 (26-C), 132.35 (6-C), 132.19 (2-C), 131.98 (3-C), 131.84 (20-C), 131.57 (1-C), 130.46 (21-C and 19-C), 128.31 (5-C), 127.31 (22-C and 18-C), 126.66 (29-C), 125.50 (30-C), 122.81 (31-C), 122.35 (28-C), 52.65 (32-C), 42.72 (13-C). **HRMS**: (ESI, m/z) calcd for $C_{24}H_{18}N_2O_5S$ $[M+H]^+$ 447.1009; found 447.1016.

tri-*tert*-Butyl 10-(3-(3-((4-(benzo[*d*]thiazol-2-yl)benzyl)carbamoyl)-5-(methoxycarbonyl)benzamido)propyl)-1,4,7,10-tetraazacyclododecane-1,4,7-tricarboxylate (43)

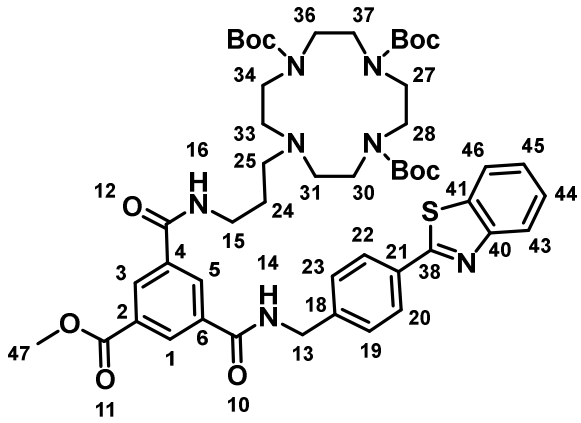

56.3 mg of **42** (0.13 mmol, 1.10 eq.) were added to 6 mL of DMF. 60.07 mg of **21** (0.11 mmol, 1.00 eq.), 122 mg of HCTU (0.30 mmol, 2.60 eq.) and 158 µL of DIPEA (0.91 mmol, 3.00 eq.) were added to this solution. The reaction mixture was stirred overnight at room temperature. After removal the solvent, the residue was taken up in DCM and was washed with water. The product was purified by column chromatography using DCM/MeOH 20:1 as eluent obtaining an orange solid (68.32 mg, 0.07mmol, 53%). **R_f**: 0.32. **Mp:** 111.3 °C. **^{1}H-NMR** (400 MHz, DMSO): δ [ppm] = 9.49 (t, *J* = 6.0 Hz, 1H, 14-H), 8.83 (s, 1H, 16-H), 8.63 (dt, *J* = 7.6, 1.7 Hz, 2H, 5-H and 3-H), 8.56 (t, *J* = 1.7

Hz, 1H, 1-H), 8.17 – 8.12 (m, 1H, 20-H), 8.11 – 8.03 (m, 3H, 31-H, 28-H and 21-H), 7.57 – 7.51 (m, 3H, 29-H, 22-H and 18-H), 7.46 (ddd, *J* = 8.3, 7.2, 1.2 Hz, 1H, 30-H), 4.60 (d, *J* = 5.8 Hz, 2H, 13-H), 3.93 (s, 3H, 47-H), 3.41 (d, *J* = 21.1 Hz, 4H, $CH_{2\ cyclen}$), 3.31 – 3.19 (m, 10H, 15-H and $CH_{2\ cyclen}$), 2.60 (dt, *J* = 32.3, 9.1 Hz, 6H, 25-H and $CH_{2\ cyclen}$), 1.69 (t, *J* = 7.8 Hz, 2H, 24-H), 1.38 – 1.32 (m, 27H, $CH_{3\ Boc}$). **^{13}C-NMR** (101 MHz, DMSO): δ [ppm] = 167.11 (10-C), 165.40 (12-C), 164.94 (11-C), 164.78 (38-C), 155.00 (C=O $_{Boc}$), 154.75 (C=O $_{Boc}$), 154.46 (C=O $_{Boc}$), 153.58 (40-C), 142.99 (18-C), 135.56 (4-C), 134.94 (6-C), 134.40 (41-C), 131.57 (2-C), 130.88 (5-C), 130.29 (22-C and 20-C), 130.08 (23-C and 19-C), 128.32 (1-C), 127.28 (3-C), 126.66 (44-C), 125.51 (45-C), 122.81 (46-C), 122.35 (43-C), 78.48 (C- $_{Boc}$), 54.24 ($CH_{2\ cyclen}$), 53.78 ($CH_{2\ cyclen}$), 52.56 (47-C), 42.69 (13-C), 37.94 (15-C), 28.27($CH_{3\ Boc}$), 28.04 ($CH_{3\ Boc}$), 28.00 ($CH_{3\ Boc}$). **HRMS**: (ESI, m/z) calcd for $C_{50}H_{67}N_7O_{10}S$ $[M+H]^+$ 958.4743; found 958.4735.

3-((4-(Benzo[*d*]thiazol-2-yl)benzyl)carbamoyl)-5-((3-(4,7,10-tris(*tert*-butoxycarbonyl)-1,4,7,10-tetraazacyclododecan-1-yl)propyl)carbamoyl)benzoic acid (44)

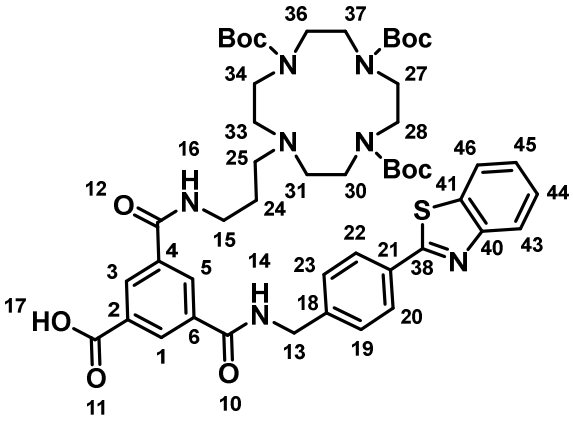

45.2 mg of **43** (0.047 mmol, 1.00 eq.) were dissolved in 7 mL of THF and 3 mL of MeOH. 1.36 mg of LiOH (0.056 mmol, 1.2 eq.) were added to this solution, the mixture was refluxed overnight. The product was purified by column chromatography using DCM/MeOH/AcOH 20:1:0.1 as eluent, affording **44** as a white solid (34.29 mg, 0.04 mmol, 77%). **R_f**: 0.37. **Mp**: 110.3 °C. **^{1}H-NMR** (400 MHz, DMSO): δ [ppm] = 12.80 (br s, 1H, 17-H), 9.45 (t, *J* = 5.6 Hz, 1H, 14-H), 8.80 (s, 1H, 16-H), 8.61 (s, 1H, 5-H), 8.55 (s, 2H, 3-H and 1-H), 8.14 (dd, *J* = 8.0, 1.1 Hz, 1H, 20-H), 8.10 – 8.02 (m, 3H, 46-H, 43-H and 22-H), 7.58 – 7.49 (m, 3H, 44-H, 23-H and 19-H), 7.49 – 7.38 (m, 1H, 45-H), 4.59 (d, *J* = 5.7 Hz, 2H, 13-H), 3.36 – 3.19 (m, 14H, 15-H and $CH_{2\ cyclen}$), 2.64 (t, *J* = 7.5 Hz, 2H, 25-H), 2.61 – 2.51 (m, 4H, $CH_{2\ cyclen}$), 1.69 (t, *J* = 7.9 Hz, 2H, 24-H), 1.35 (d, *J* = 3.7 Hz, 27H, $CH_{3\ Boc}$). **^{13}C-NMR** (101 MHz, DMSO): δ [ppm] = 172.06 (11-C and 10-C), 167.13 (12-C), 165.46 (38-C), 155.01 (C=O $_{Boc}$), 154.47 (C=O $_{Boc}$), 153.58 (40-C), 143.18 (18-C), 135.08 (4-C), 134.40 (6-C), 131.51 (41-C), 130.48 (2-C), 130.30 (5-C), 128.28 (23-C and 19-C), 127.26 (22-c and 20-C), 126.65 (1-C), 125.49 (3-C), 122.81 (45-C and 44-C), 122.34 (46-C and 43-C), 78.48 (C- $_{Boc}$), 53.83 ($CH_{2\ cyclen}$),

42.65 (13-C), 37.92 (15-C), 28.28 ($CH_{3\ Boc}$), 28.04 ($CH_{3\ Boc}$), 28.01 ($CH_{3\ Boc}$), 21.10 (24-C). **HRMS**: (ESI, m/z) calcd for $C_{49}H_{65}N_7O_{10}S$ $[M+H]^+$ 944.4586; found 944.4586.

tri-*tert*-Butyl 10-(3-(3-((4-(benzo[*d*]thiazol-2-yl)benzyl)carbamoyl)-5-((1-((1-(*tert*-butoxy)-1-oxo-3-(tritylthio)propan-2-yl)amino)-3-methyl-1-oxobutan-2-yl)carbamoyl)benzamido)propyl)-1,4,7,10-tetraazacyclododecane-1,4,7-tricarboxylate (45)

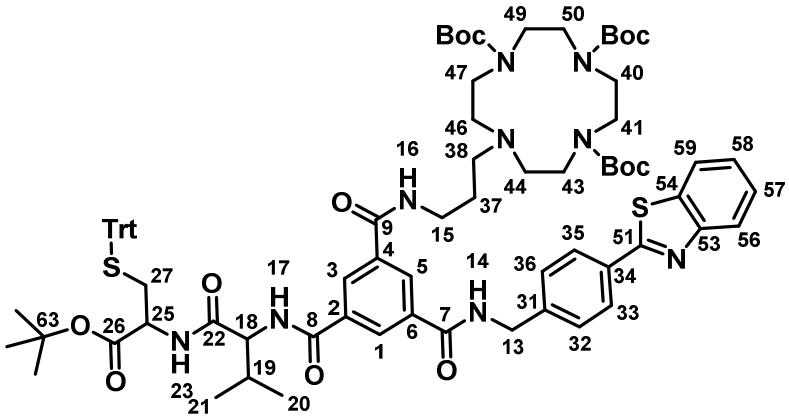

52.4 mg of **44** (0.06 mmol, 1.00 eq.) were added to 6 mL of DMF. 57.6 mg of **24** (0.11 mmol, 2.00 eq.), 45.5 mg of HCTU (0.11 mmol, 2.2 eq.) and 31.35 µL of DIPEA (0.18 mmol, 3.00 eq.). The reaction mixture was stirred overnight at room temperature. After removal the solvent, the residue was taken up in dichloromethane and was washed with water. The product was purified by column chromatography using DCM/MeOH 10:1 as eluent. It was obtained a yellow oil (50.50 mg, 0.03 mmol, 63%). **R_f**: 0.73. **Mp**: 76.3 °C. **^{1}H-NMR** (600 MHz, DMSO): δ [ppm] = 9.18 (t, *J* = 6.0 Hz, 1H, 14-H), 8.53 (s, 1H, 17-H), 8.34 – 8.29 (m, 2H, 5-H and 1-H), 8.27 (d, *J* = 1.6 Hz, 1H, 3-H), 8.15 (d, *J* = 7.6 Hz, 1H, 23-H), 7.97 – 7.93 (m, 1H, 59-H), 7.91 – 7.84 (m, 2H, 35-H and 33-H), 7.77 (s, 1H, 16-H), 7.71 – 7.64 (m, 1H, 58-H), 7.49 (dd, *J* = 8.2, 4.0 Hz, 1H, 57-H), 7.38 – 7.32 (m, 2H, 36-H and 32-H), 7.30 – 7.25 (m, 1H, 56-H), 7.18 – 6.99 (m, 15H, CH_{Trt}), 4.42 (d, *J* = 5.8 Hz, 1H, 13"-H), 4.27 (t, *J* = 8.3 Hz, 1H, 13'-H), 4.06 – 4.02 (m, 1H, 25-H), 3.84 (dtd, *J* = 25.9, 7.8, 5.6 Hz, 1H, 18-H), 3.33 – 3.18 (m, 3H, $CH_{2\ cyclen}$), 3.09 – 2.98 (m, 4H, $CH_{2\ cyclen}$), 2.70 (s, 2H, $CH_{2\ cyclen}$ and 27"-H), 2.54 (s, 2H, $CH_{2\ cyclen}$ and 27'-H), 2.50 (s, 4H, $CH_{2\ cyclen}$), 2.47 (t, *J* = 8.1 Hz, 1H, , $CH_{2\ cyclen}$), 2.37 (d, *J* = 16.8 Hz, 2H, $CH_{2\ cyclen}$), 2.28 (ddd, *J* = 12.2, 8.2, 6.6 Hz, 1H, , $CH_{2\ cyclen}$), 2.15 (ddd, *J* = 12.1, 10.6, 5.4 Hz, 1H, $CH_{2\ cyclen}$), 1.91 (dt, *J* = 14.0, 7.0 Hz, 1H, 19-H), 1.83 – 1.70 (m, 1H, $CH_{2\ cyclen}$), 1.68 (s, 1H, 37"-H), 1.51 (s, 1H, 37'-H), 1.16 (dd, *J* = 16.6, 9.9 Hz, 16H, $CH_{3\ Boc}$), 1.11 (d, *J* = 7.3 Hz, 9H, $CH_{3\ tBu}$), 1.05 (d, *J* = 15.5 Hz, 3H, $CH_{3\ Boc}$), 0.74 (dd, *J* = 13.0, 6.7 Hz, 3H, 21-H), 0.67 – 0.61 (m, 3H, 20-H). **^{13}C-NMR** (151 MHz, DMSO): δ [ppm] = 169.03 (9-C) , 167.09 (7-C), 165.41 (26-C), 164.58 (22-C), 162.29 (8-C), 155.00 ($C{=}O_{Boc}$), 154.74 ($C{=}O_{Boc}$), 154.45 ($C{=}O_{Boc}$), 153.58 (51-C), 144.08 (CH_{Trt}), 143.09 (31-C), 134.40 (34-C), 131.54 (57-C), 129.04 (6-C, 4-C and 2-C), 129.01 (3-C), 128.80 (5-C and 1-C), 128.27 (32-C), 128.09 (CH_{Trt}), 128.07 (54-C and 53-C), 127.26 (36-C), 126.82 (CH_{Trt}),

126.78 (CH $_{Trt}$), 126.64 (35-C), 125.49 (58-C and 56-C), 122.80 (33-C), 122.32 (59-C), 80.99 (63-C), 78.47 (C- $_{Boc}$), 66.24 (C- $_{Trt}$), 57.06 (18-C), 52.24 (25-C), 40.95 (13-C), 38.24 (15-C), 35.77 (27-C), 30.76 (19-C), 30.56 (38-C), 28.27 ($CH_{3\ Boc}$), 28.03 ($CH_{3\ Boc}$), 27.99 ($CH_{3\ tBu}$), 27.46 ($CH_{3\ tBu}$), 22.47 (37-C), 19.18 (21-C), 18.71 (20-C). Since Cyclen has inefficient electronic relaxation, there is a broadening effect and signal loss in NMR. **HRMS**: (ESI, m/z) calcd for $C_{80}H_{101}N_9O_{12}S_s$ $[M+H]^+$ 1445.7115; found 1445.7115.

(3-((3-(1,4,7,10-Tetraazacyclododecan-1-yl)propyl)carbamoyl)-5-((4-(benzo[*d*]thiazol-2-yl)benzyl)carbamoyl)benzoyl)valylcysteine (46)

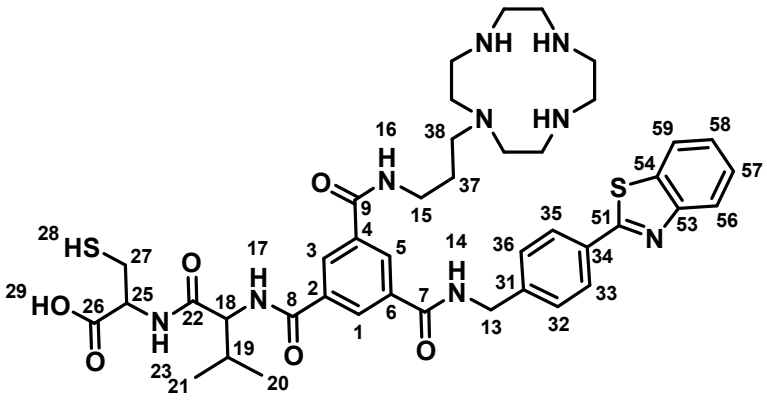

The starting material **45** was treated with 95% of a solution of 50% TFA in DCM and 5% of TIPS for 5 hours and diethyl ether was added to the TFA solution. The precipitate was separated by centrifugation, washed with diethyl ether several times, and dried under argon to obtain the TFA salt. A white solid with 87 % purity was obtained (18.30 mg, 0.02 mmol, 62%). **Mp**: 161.3 °C. **^{1}H-NMR** (600 MHz, MeOD): δ [ppm] = 12.85 (s, 1H, 29-H), 9.39 (t, *J* = 6.1 Hz, 1H, 14-H), 8.83 (t, *J* = 5.7 Hz, 1H, 17-H), 8.54 – 8.47 (m, 3H, 5-H, 3-H and 1-H), 8.47 – 8.41 (m, 2H, 23-H and 16-H), 8.15 (dd, *J* = 8.0, 1.1 Hz, 1H, 56-H), 8.10 – 8.07 (m, 2H, 35-H and 33-H), 8.05 (d, *J* = 8.0 Hz, 1H, 59-H), 7.55 (dd, *J* = 7.7, 6.1 Hz, 3H, 58-H, 36-H and 32-H), 7.49 – 7.45 (m, 1H, 57-H), 4.62 (d, *J* = 6.1 Hz, 2H, 13-H), 4.49 – 4.36 (m, 2H, 25-H and 18-H), 3.09 – 2.99 (m, 9H, $CH_{2\ cyclen}$), 2.89 (ddd, *J* = 13.3, 8.7, 4.5 Hz, 1H, 27"-H), 2.84 – 2.77 (m, 5H, $CH_{2\ cyclen}$), 2.74 (d, *J* = 6.0 Hz, 4H, $CH_{2\ cyclen}$), 2.58 (t, *J* = 7.7 Hz, 2H, 15-H and $CH_{2\ cyclen}$), 2.15 (dq, *J* = 13.7, 6.7 Hz, 1H, 27'-H), 1.72 (t, *J* = 7.6 Hz, 2H, 37-H), 1.25 (s, 1H, 28-H), 0.98 (dd, *J* = 12.8, 6.7 Hz, 6H, 21-H and 20-H). **^{13}C-NMR** (151 MHz, MeOD): δ [ppm] = 171.43 (26-C), 167.10 (22-C), 165.72 (7-C), 165.59 (9-C), 165.54 (8-C), 158.10 (51-C), 153.56 (53-C), 143.08 (31-C), 134.94 (54-C), 134.76 (2-C), 134.39 (6-C and 4-C), 131.58 (34-C), 129.03 (3-C and 1-C), 128.65 (5-C), 128.30 (36-C and 32-C), 127.30 (35-C and 33-C), 126.72 (57-C), 125.56 (58-C), 122.81 (59-C), 122.38 (56-C), 58.85 (18-C), 54.92 (25-C), 54.56 (46-C and 44-C), 49.59 (38-C), 47.59 ($CH_{2\ cyclen}$), 44.27 ($CH_{2\ cyclen}$), 42.65 ($CH_{2\ cyclen}$), 41.93 ($CH_{2\ cyclen}$), 40.20 (13-C), 37.44 (15-C), 30.70 (19-C), 30.49 (27-C), 25.43 (37-C), 19.25

(21-C), 18.90 (20-C). **HPLC**: [A, 60→80], t_R= 3.683 min, (87%). **HRMS**: (ESI, m/z) calcd for $C_{42}H_{55}N_9O_6S_2$ $[M+H]^+$ 846.3789; found 846.3792.

Diaquacobaltate(III(3-((3-(1,4,7,10-tetraazacyclododecan-1-yl)propyl)carbamoyl)-5-((4-(benzo[*d*]thiazol-2-yl)benzyl)carbamoyl)benzoyl)valylcysteine (47)

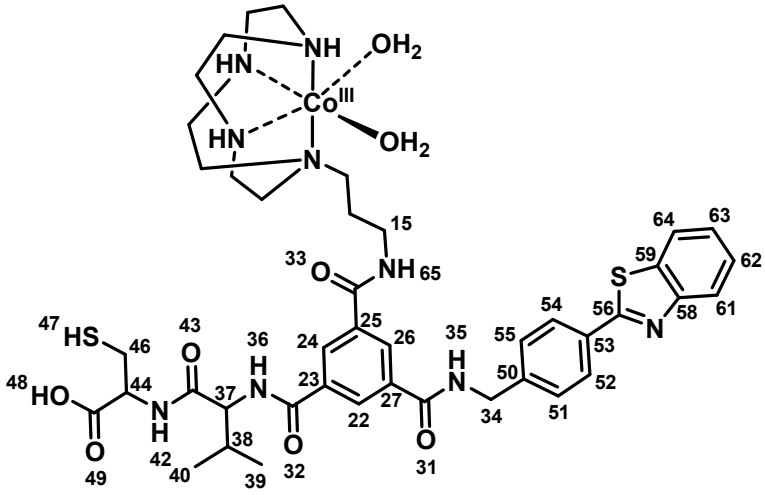

9.6 mg of **46** (0.01 mmol, 1.00 eq.) were dissolved in 2 mL of methanol under argon atmosphere. 0.23 mg of lithium hydroxide (0.009 mmol, 0.86 eq.) were added to this solution and the reaction mixture was stirred for 90 minutes at room temperature. 2.68 mg of $CoCl_2 \cdot 6H_2O$ (0.01 mmol, 1.00 eq.) were added and the reaction mixture was stirred under O_2 atmosphere at room temperature for 24 hours. The colour of the reaction changed from brown to purple. The solvent was removed and the residue was purified by filtering with a filter of 0.20 µm. It was obtained a purple solid with 30% yield (3.07 mg, 3.4 µmol). **^{1}H-NMR** (400 MHz, MeOD)**:** δ [ppm] = 8.64 – 8.23 (m, 3H, 26-H, 24-H and 22-H), 8.06 (d, *J* = 8.1 Hz, 1H, 61-H), 8.00 – 7.96 (m, 1H, 64-H), 7.96 – 7.82 (m, 2H, 55-H and 51-H), 7.57 – 7.32 (m, 4H, 63-h, 62-H, 54-H and 52-H). **HPLC**: [A, 95→40, UV= 545 nm], t_R= 28.050-34.158 min. **HRMS**: (ESI, m/z) calcd for $C_{42}H_{52}CoN_9O_7S_2$ $[M+H]^+$ 902.2887; found 902.0994.

tri-*tert*-Butyl 10-butyl-1,4,7,10-tetraazacyclododecane-1,4,7-tricarboxylate (48)[92]

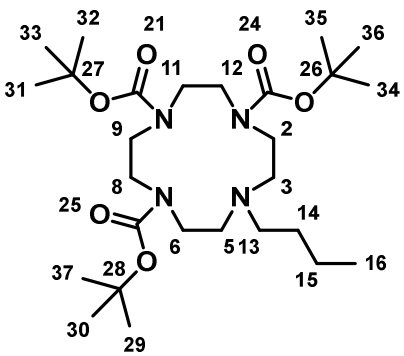

To the solution of 0.1018 g of **17** (0.21 mmol, 1.00 eq.) in 3.5 mL of THF were added the solution of 0.015 g of butanal (0.21 mmol, 1.00 eq.) in 3 mL of THF and 0.13 g of $NaBH(OAc)_3$ (0.61 mmol, 2.92 eq.). The reaction was stirred for 1 hour. The solvent was evaporated and the reaction mixture was mixed with 50 mL of saturated Na_2CO3 and extracted with ethyl acetate. The collected organic phase was washed with brine, dried over sodium

sulfate and concentrated. The product was purified by column chromatography obtaining a colorless solid with 30% yield. **R_f**: 0.55. **Mp**: 59.0 °C. **^{1}H-NMR** (300 MHz, $CDCl_3$): δ [ppm] = 3.61 – 3.16 (m, 12H, 6-H, 8-H, 9-H, 11-H, 12-H and 2-H), 2.70 – 2.42 (m, 6H, 13-H, 5-H and 3-H), 1.44 (s, 8H, $C(CH_3)_3$), 1.42 (s, 13H, $C(CH_3)_3$), 1.40 (s, 6H, $C(CH_3)_3$), 1.32 – 1.18 (m, 4H, 15-H and 14-H), 0.90 (t, *J* = 7.2 Hz, 3H, 16-H). **^{13}C-NMR** (75 MHz, $CDCl_3$): δ [ppm] = 156.21 (21-C), 155.80 (24-C), 155.55 (25-C), 79.53 (27-C), 79.31 (28-C and 26-C), 55.21 (13-C), 53.96 11-C and 9-C), 52.76 (12-C and 8-C), 49.99 (6-C and 2-C), 48.11 (5-C and 2-C), 28.80 (CH_3), 28.63 (CH_3), 27.02 (CH_3), 26.47 (14-C), 21.11 (15-C), 14.18 (16-C). **HRMS**: (ESI, m/z) calcd for $C_{27}H_{52}N_2O_6$ $[M+H]^+$ 529.3960; found 529.3964.

1-Butyl-1,4,7,10-tetraazacyclododecane (49)

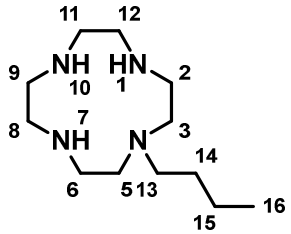

48 was treated with 50% TFA in DCM for 5 hours and diethyl ether was added to the TFA solution. The precipitate was separated by centrifugation, washed with diethyl ether several times, and dried under argon to obtain the TFA salt as a yellowish oil with 94% yield. **^{1}H-NMR** (600 MHz, DMSO): δ [ppm] = 3.03 (dd, 8H, 12-H, 11-H, 9-H and 8-H), 2.82 (s, 4H, 6-H and 2-H), 2.74 (s, 4H, 5-H and 3-H), 2.52 (s, 2H, 13-H), 1.44-1.37 (m, 2H, 14-H), 1.23 (h, *J* = 7.4 Hz, 2H, 15-H), 0.89 (t, *J* = 7.3 Hz, 3H, 16-H).**^{13}C-NMR** (151 MHz, DMSO): δ [ppm] = 158.65 (CO, TFA salt), 158.43 (CO, TFA salt), 157.21(CO, TFA salt), 157.99 (CO, TFA salt), 119.46 (C-F, TFA salt), 117.49 (C-F, TFA salt), 115.53 (C-F, TFA salt), 113.57 (C-F, TFA salt), 51.91 (13-C), 47.75 (5-C and 3-C), 44.20 (11-C and 9-C), 43.29 (6-C and 2-C), 41.96 (12-C and 8-C), 25.65 (14-C), 20.13 (15-C), 13.90 (16-C). **HRMS**: (ESI, m/z) calcd for $C_{12}H_{28}N_4$ $[M+H]^+$ 229.2387; found 229.2413.

Diaquacobaltate (III)-1-butyl-1,4,7,10-tetraazacyclododecane (50)

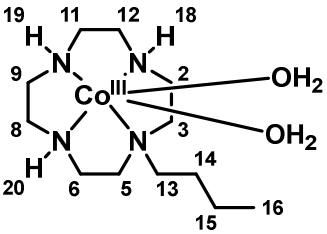

22.9 mg of 4**9** (0.069 mmol, 1.00 eq.) were dissolved in 6 mL of methanol under argon atmosphere. 1.44 mg of lithium hydroxide (0.06 mmol, 0.86 eq.) were added to this solution and was stirred for 90 minutes at room temperature. 16.59 mg of $CoCl_2{\cdot}6H_2O$ (0.069 mmol, 1.00 eq.) were added and the reaction mixture was stirred under O_2 atmosphere at room temperature for 24 hours. The colour of the reaction changed from red wine to purple. The solvent was removed and the residue was purified by semi-preparative HPLC. It was obtained a pink solid with 17% yield. **^{1}H-NMR** (400 MHz, MeOD): δ [ppm] = 8.49 (s, 1H, NH), 6.86 (s, 1H, NH), 6.50 (s, 1H, NH), 3.84 – 3.72 (m, 1H, , $CH_{2\ cyclen}$), 3.61 – 3.46 (m, 2H, , $CH_{2\ cyclen}$), 3.25 – 3.13 (m, 4H, , $CH_{2\ cyclen}$),

3.13 – 2.82 (m, 6H, , $CH_{2\ cyclen}$ and 13-H), 2.65 – 2.43 (m, 5H, , $CH_{2\ cyclen}$), 1.91 – 1.70 (m, 2H, 14-H), 1.49 – 1.32 (m, 2H, 15-H), 1.00 (t, *J* = 7.4 Hz, 3H, 16-H). **^{13}C-NMR** (151 MHz, MeOD)**:** δ [ppm] = 166.50 (C=O, TFA salt), 114.18 (C-F, TFA salt), 63.49 (13-C), 59.15, ($CH_{2\ cyclen}$), 59.00 ($CH_{2\ cyclen}$), 57.87 ($CH_{2\ cyclen}$), 56.29 ($CH_{2\ cyclen}$), 51.60 ($CH_{2\ cyclen}$), 50.71 ($CH_{2\ cyclen}$), 24.55 (14-C), 21.82 (15-C), 13.89 (16-C). **HPLC**: [A, 95→40, UV= 545 nm], t_R= 29.958 min, (97%). **HRMS**: (ESI, m/z) calcd for $C_{12}H_{25}CoN_4$ $[M+H]^+$ 285.1484; found 285.1487; calcd for $C_{12}H_{32}CoN_4O_2$ $[M+Na]^+$ 346.1749; found 347.**1491.**

Methyl 3-nitro-1*H*-pyrazole-5-carboxylate (52)

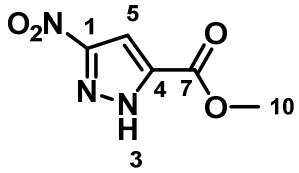

6.79 g of 5-nitro-3-pyrazole carboxylic acid (43.22 mmol, 1.00 eq.) were dissolved in 80 mL of MeOH anhydrous. The solution was cooled to 0 °C and 4.70 mL of $SOCl_2$ were added to this solution. The resulting yellow solution was heated to 80 °C for 15 hours. The solvent was removed and the solid was taken up in $CHCl_3$ and filtered with pore 4. The solid was dried in a high vacuum, and the compound **52** could be obtained as a yellowish solid (6.72 g , 39.27 mmol, 91%). **R_f:** 0.64. **^{1}H-NMR** (300 MHz, $CDCl_3$)**:** δ [ppm] = 7.41 (s, 1H, 3-H), 4.01 (s, 3H, 10-H). **^{13}C-NMR** (75 MHz, $CDCl_3$)**:** δ [ppm] = 158.59 (7-C), 156.91 (1-C), 135.94 (4-C), 104.98 (5-C), 53.36 (10-C).

4-Methoxybenzyl bromide (53)[76]

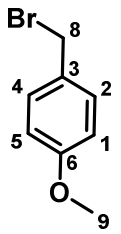

12.3 ml of 4-methoxybenzyl alcohol (anisyl alcohol) X (99.15 mmol, 1.00 eq.) were dissolved in 150 mL of diethyl ether. This solution was cooled to 0 °C and 40 mL of hydrogen bromide (48% in water) were added dropwise. The reaction mixture was stirred at room temperature for 90 minutes. Subsequently, 100 mL of saturated sodium bromide solution were added. After separation of the phases, the organic phase was first dried over potassium carbonate and then over sodium sulfate. After filtration of the drying agent, the solvent was removed in a membrane pump vacuum to leave 16.33 g (81.66 mmol, 82%) of yellowish compound. The resulting product had to be stored cold. **R_f:** 0.83. **^{1}H-NMR** (300 MHz, $CDCl_3$)**:** δ [ppm] = 7.35 (d, J = 8.8Hz, 2H, 4-H and 2-H), 6.89 (d, J = 8.8Hz, 2H, 5-H and 1-H), 4.51 (s, 2H, 8-H), 3.81 (s, 3H, 9-H). **^{13}C-NMR** (75 MHz, $CDCl_3$)**:** δ [ppm] =159.50 (6-C), 130.80 (4-C), 119.70 (2-C), 114.60 (5-C and 1-C), 55.46 (9-C), 33.96 (8-C).

Methyl *N*-*p*-methoxybenzyl-3-nitro-1*H*-pyrazole-5-carboxylate (54)[76]

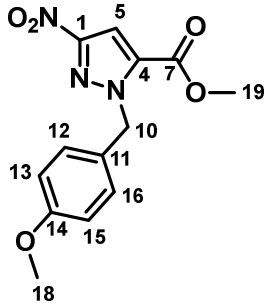

1.004 g of **52** (5.84 mmol, 1.00 eq.) were dissolved in absolute DMF (40 mL). After addition of 1.76 g of **53** (8.77 mmol, 1.50 eq.) and 1.61 g of potassium carbonate (11.68 mmol, 2.00 eq.), the suspension was stirred at room temperature for 30 minutes and at 50 °C for 20 hours. After completion of the reaction, the mixture was acidified to pH = 1 with 1 M HCl and extracted four times with 35 mL of diethyl ether. The combined organic phases were washed with water, dried over sodium sulfate, filtered and the solvent was concentrated under reduced pressure in the membrane vacuum. The product crystallized as a colorless substance overnight at - 28 °C (2.90 mmol, 50%). **R_f:** 0.47. **^{1}H-NMR** (300 MHz, $CDCl_3$)**:** δ [ppm] = 7.39 (s, 1H, 5-H), 7.39-7.33 (m, 2H, 16-H and 12-H), 6.86- 6.83 (m, 2H, 15-H and 13-H), 5.76 (s, 2H, 10-H), 3.92 (s, 3H, 18-H), 3.78 (s, 3H, 19-H). **^{13}C-NMR** (75 MHz, $CDCl_3$)**:** δ [ppm] = 160.12 (7-C), 158.72 (14-C), 154.15 (1-C), 133.96 (4-C), 130.05 (16-C and 12-C), 126.90 (11-C), 114.52 (15-C and 13-C), 107.49 (5-C), 56.15 (10-C), 55.42 (18-C), 52.87 (19-C).

Methyl 3-amino-1-(4-methoxybenzyl)-1*H*-pyrazole-5-carboxylate (55)[136]

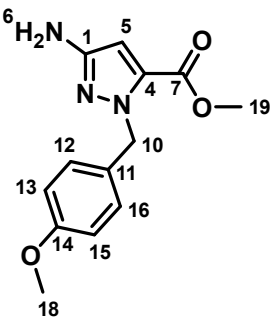

4 mL of MeOH and 0.93g of $SnCl_2{\cdot}2H_2O$ (4.12 mmol, 6.00 eq.) were added to **54**. The suspension was heated at 80 °C for 4 hours. The reaction flask was allowed under cool to RT. After most of MeOH was removed, water and ethyl acetate were added to the residue. Solid K_2CO_3 was carefully added to the resulting mixture until pH was above 10. The ethyl acetate layer was separated from the heterogeneous mixture, and the aqueous phase was extracted with ethyl acetate. The combined organic layers were washed with brine and dried over sodium sulfate. The solvent was evaporated under vacuum. The crude product was purified by column chromatography. As a light yellow solid, the product was obtained with a 72 % yield (0.1312 g, 0.50 mmol). **R_f:** 0.37. **^{1}H-NMR** (300 MHz, DMSO)**:** δ [ppm] = 7.10 (d, *J* = 8.5 Hz, 2H, 16-H and 12-H), 6.86 (d, *J* = 8.4 Hz, 2H, 15-H and 13-H), 6.00 (s, 1H, 5-H), 5.36 (s, 2H, 10-H), 4.90 (s, 2H, 6-H), 3.77 (s, 3H, 18-H), 3.71 (s, 3H, 19-H).**^{13}C-NMR** (75 MHz, DMSO)**:** δ [ppm] = 159.70 (7-C), 158.50 (14-C), 154.60 (1-C), 131.09

(4-C), 130.02 (16-C and 12-C), 128.54 (11-C), 113.71 (15-C and 13-C), 96.93 (5-C), 55.02 (10-C), 52.44 (18-C), 51.78 (19-C).

1-(4-Methoxybenzyl)-3-nitro-1*H*-pyrazole-5-carboxylic acid (56)[76]

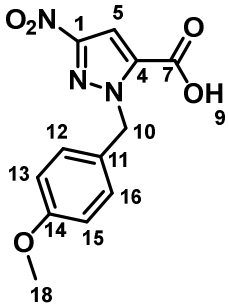

0.1932 g of **54** (0.687 mmol, 1.00 eq.) were dissolved in 5 mL of methanol and 5 mL of tetrahydrofuran. After addition of 2 mL of water and 18 mg of lithium hydroxide (0.756 mmol, 1.11 eq.), the reaction mixture was heated under reflux for 18 hours. The solvent was removed under reduced pressure and the yellowish oil residue was taken up in water. With stirring, the solution was acidified to pH=1. The precipitate was filtered off, washed wit 1M hydrochloric acid and dried in a high vacuum. 179.4 mg (0.64 mmol, 98%) of colorless solid could be isolated. **R_f:** 0.3. **^{1}H-NMR** (300 MHz, DMSO)**:** δ [ppm] =7.50 (s, 1H, 5-H), 7.23 (d, *J* = 8.7 Hz, 2H, 16-H and 12-H), 6.91 (d, *J* = 8.7 Hz, 2H, 15-H and 13-H), 5.75 (s, 2H, 10-H), 3.73 (s, 3H, 18-H). **^{13}C-NMR** (75 MHz, DMSO)**:** δ [ppm] = 159.17 (7-C), 159.06 (14-C), 153.62 (1-C), 135.72 (4-C), 129.24 (16-C and 12-C), 127.67 (11-C), 114.02 (15-C and 13-C), 107.07 (5-C), 55.07 (10-C), 54.87 (18-C).

Methyl 1- (4-methoxybenzyl)- 3 –(1- (4-methoxybenzyl)- 3- nitro- 1*H*- pyrazole -5-carboxamido)- 1*H*-pyrazole-5- carboxylate (57)[76]

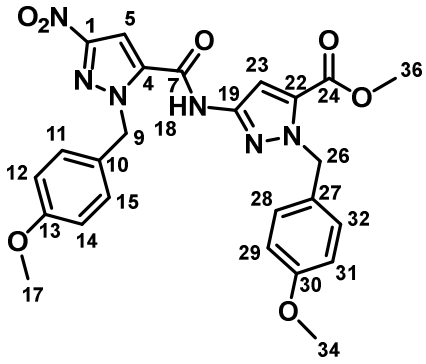

Under argon atmosphere 0.876 g of **55** (3.35 mmol, 1.00 eq.) and 1.022 g of **56** (3.68 mmol, 1.10 eq.) were dissolved in 130 mL of absolute chloroform. To this solution was added 3.67 g of Pyclop (8.71 mmol, 2.60 eq.) and 4.60 mL of DIPEA (26.8 mmol, 8.00 eq.), dropwise. The reaction solution was refluxed for 2 days. After removal of the solvent in the membrane pump vacuum, the product was purified by column chromatography on silica gel (cyclohexane: ethyl acetate 3:1). As a colorless solid the compound 6 was obtained with a 91% yield (1.5962 g, 3.06 mmol). **R_f:** 0.31. **^{1}H-NMR** (300 MHz, $CDCl_3$)**:** δ [ppm] = 8.44 (s, 1H, 18-H), 7.38-7.35 (m, 2H, 15-H and 11-H), 7.34 (s, 1 H, 23-H), 7.21 (s, 1H, 5-H), 7.19-7.16 (m, 2H, 28-H and 32-H), 6.83-6.79 (m, 4H, 31-H, 29-H, 14-H and 12-H), 5.79 (s, 2H, 26-H), 5.58 (s, 2H, 9-H), 3.90 (s, 3H, 36-H), 3.76 (s, 3H,17-H), 3.75 (s, 3H, 34-H). **^{13}C-NMR** (75 MHz, $CDCl_3$)**:** δ [ppm] = 159.93 (7-C), 159.87 (24-C), 159.52 (13-C), 155.07 (30-C), 154.27 (1-C), 144.48 (19-C),

136.42 (22-C), 132.56 (4-C), 130.13 (15-C and 11-C), 129.39 (32-C and 28-C), 128.64 (10-C), 127.25 (27-C), 114.29 (14-C and 12-C), 114.13 (31-C and 29-C), 103.38 (5-C), 102.95 (23-C), 56.00 (26-C), 55.38 (9-C), 54.23 (34-C and 17-C), 52.32 (36-C).

Methyl 3- (3-amino- (1- (4-methoxybenzyl) - 1*H* -pyrazole-5- carboxamido) - 1-(4-methoxybenzyl) - 1*H*-pyrazole-5-carboxylate (58)[136]

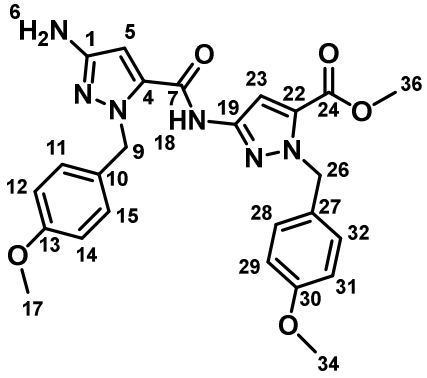

30 mL of MeOH and 1.65 g of $SnCl_2 \cdot 2H_2O$ (7.32, 6.00 eq.) were added to **57** (1.22 mmol, 1.00 eq.). The suspension was heated at 80 °C for 3 hours. The reaction flask was allowed under cool to RT. After most of MeOH was removed, water and ethyl acetate were added to the residue. Solid K_2CO_3 was carefully added to the resulting mixture until pH was above 10. The ethyl acetate layer was separated from the heterogeneous mixture, and the aqueous phase was extracted with ethyl acetate. The combined organic layers were washed with brine and dried over sodium sulfate. The solvent was evaporated under vacuum. The crude product was purified by column chromatography obtaining a yellow solid (0.5434 g, 90%). **R_f:** 0.15. **^{1}H-NMR** (300 MHz, $CDCl_3$)**:** δ [ppm] = 8.21 (s, 1H, 18-H), 7.35 (s, 1H, 23-H), 7.26-7.20 (m, 4H, 32-H, 28-H, 15-H and 11-H), 7.26 (s, 1H, 5-H)6.84-6.79 (m, 4H, 31-H, 29-H, 14-H and 12-H), 5.94 (br s, 1H, 6-H), 5.60 (s, 2H, 26-H), 5.53 (s, 2H, 9-H), 3.87 (s, 3H, 36-H), 3.77 (s, 3H, 17-H), 3.75 (s, 3H, 34-H). **^{13}C-NMR** (75 MHz, $CDCl_3$)**:** δ [ppm] = 160.06 (7-C), 159.45 (24-C), 159.20 (30-C and 13-C), 153.05 (1-C), 145.27 (19-C), 135.11 (22-C), 132.37 (15-C and 11-C), 129.84 (32-C and 28-C), 129.27 (4-C), 129.23 (10-C), 128.95 (27-C), 114.16 (14-C and 12-C), 114.03 (31-C and 29-C), 102.85 (23-C), 94.11 (5-C), 55.39 (26-C), 55.36 (9-C), 54.09 (34-C), 53.48 (17-C), 52.20 (36-C).

Methyl 1-(4-methoxybenzyl)-3-(1-(4-methoxybenzyl)-3-(1-(4-methoxybenzyl)-3-nitro-1*H*-pyrazole-5-carboxamido)-1*H*-pyrazole-5-carboxamido)-1*H*-pyrazole-5-carboxylate (59)[76]

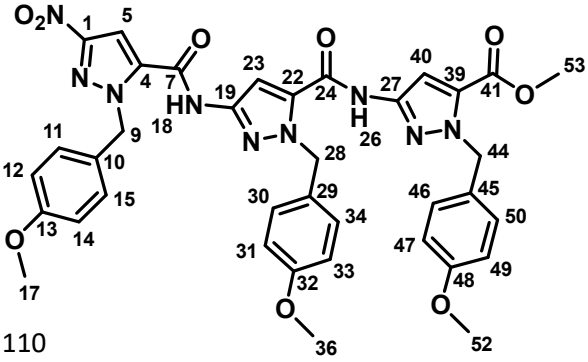

0.90 g of **58** (1.83 mmol, 1.00 eq.) and 0.59 g of **56** (2.14 mmol, 1.17 eq.) were added in 120 mL of absolute chloroform. After addition of 2.00 g of PyClop (4.76 mmol, 2.60 eq.) and 2.57 mL of DIPEA (14.64 mmol, 8.00 eq.), the solution was heated

under reflux for two days. After removal the solvent, the product was purified by column chromatography on silica gel (cyclohexane: ethyl acetate 3:1). As a colorless solid compound was obtained with a 79 % yield(1.043 g, 1.39 mmol). **R_f:** 0.27. **^{1}H-NMR** (300 MHz, DMSO)**:** δ [ppm] = 11.52 (s, 1H, 18-H), 11.44 (s, 1H, 26-H), 7.99 (s, 1H, 5-H), 7.73 (s, 1H, 23-H), 7.28 (d, *J* = 8.7 Hz, 2H, 15-H and 11-H), 7.23 (s, 1H, 40-H), 7.19 (dd, *J* = 8.6, 1.7 Hz, 4H, 50-H, 46-H, 34-H and 30-H), 6.89 (ddd, *J* = 7.9, 5.0, 2.1 Hz, 6H, 49-H, 47-H, 33-H, 31-H, 14-H and 12-H), 5.81 (s, 2H, 9-H), 5.66 (s, 2H, 28-H), 5.59 (s, 2H, 44-H), 3.85 (s, 3H, 53-H), 3.72 (s, 3H, 17-H), 3.71 (s, 3H, 36-H), 3.70 (s, 3H, 52-H). **^{13}C- NMR** (75 MHz, DMSO)**:** δ [ppm] = 159.29 (41-C), 159.02(13-C), 158.74 (32-C), 158.66 (48-C), 157.06 (7-C), 155.41 (24-C), 153.52 (1-C), 145.61 (19-C), 144.85 (27-C), 136.72 (4-C), 134.11 (39-C), 131.22 (9-C), 129.48 (28-C), 129.28 (44-C), 129.02 (15-C and 11-C), 128.85 (34-c and 30-C), 128.75 (50-C and 46-C), 127.90 (22-C), 113.99 (14-C and 12-C), 113.87 (33-C and 31-C), 113.80 (49-C and 48-C), 105.02 (5-C), 102.94 (23-C), 100.96 40-C), 55.04 (44-C, 28-C and 9-C), 53.29 (52-C, 36-C and 17-C), 52.16 (53-C).

Methyl 1-(4-methoxybenzyl)-3-(1-(4-methoxybenzyl)-3-(1-(4-methoxybenzyl)-3-nitro-1*H*-pyrazole-5-carboxamido)-1*H*-pyrazole-5-carboxamido)-1*H*-pyrazole-5-carboxylic acid (60)[76]

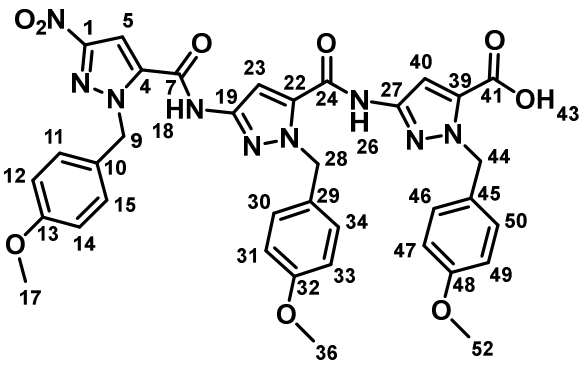

1.0904 g of the **59** (1.45 mmol 1.00 eq.) were dissolved in 40mL of THF and 20 mL of MeOH. After addition of 2 mL of water and 88 mg of lithium hydroxide (3.69 mmol, 2.54 eq.), the reaction mixture was heated under reflux for 18 hours. The solution was acidified to pH=1 with dilute hydrochloric acid with vigorous stirring. The precipitate was filtered off, washed with 1M HCl and dried in high vacuum. 1.004 g (1.36 mmol, 93%) of the colorless solid could be isolated. **R_f:** 0.63. **^{1}H-NMR** (300 MHz, DMSO)**:** δ [ppm] = 13.51 (br s, 1H, 43-H), 11.50 (s, 1H, 26-H), 11.36 (s, 1H, 18-H), 7.97 (s, 1H, 5-H), 7.70 (s, 1H, 23-H), 7.28-7.25 (m, 2H, 15-H and 11-H), 7.15 (s, 1H, 40-H), 7.19-7.14 (m, 4H, 50-H, 46-H, 34-H and 30-H), 6.90-6.85 (m, 6H, 49-H, 47-H, 33-H, 31-H, 14-H and 12-H), 5.80 (s, 2H, 9-H), 5.65 (s, 2H, 28-H), 5.59 (s, 2H, 44-H), 3.71 (s, 3H, 17-H), 3.70 (s, 3H, 36-H), 3.69 (s, 3H, 52-H). **^{13}C-NMR** (75 MHz, DMSO)**:** δ [ppm] = 160.32 (41-C), 159.02 (24-C), 158.65 (7-C), 157.01 (48-C), 155.41 (32-C), 153.52 (13-C), 145.39 (1-C), 144.82 (27-C and 19-C), 136.73 (4-C), 134.20 (39-C), 132.53 (10-C), 129.49 (29-C),

129.34 (45-C), 129.29 (15-C and 11-C), 128.84 (34-C and 30-C), 128.68 (50-C and 46-C), 127.89 (22-C), 113.99 (14-C and 12-C), 113.85 (33-C and 31-C), 113.80 (49-C and 47-C), 105.02 (5-C), 102.99 (40-C and 23-C), 55.05 (28-C and 9-C), 55.04 (44-C), 55.01 (52-C, 36-C and 17-C).

Ethyl (2-(2-(2-chloroethoxy)-ethoxy)-ethoxy)-acetate (61)[77]

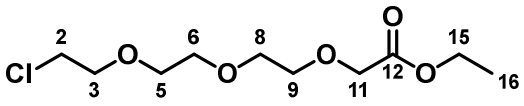

Under argon, 4.31 mL of 2-(2-chloroethoxy)-ethoxy-ethanol (30.0 mml, 1.00 eq.) were dissolved in 90 mL of DCM. To the cooled solution, at 0°C, was added 3.15 mL of ethyl diazoacetate (30.0 mmol, 1.00 eq.) and 4-5 drops of boron trifluoride diethyl etherate (gas evolution). The reaction was stirred at 0 °C for 30 minutes and at room temperature for further 24 hours. To check the completeness of the reaction, an additional 2-3 drops of boron trifluoride diethyl etherate were added. Since no more gas evolution was observed, the reaction mixture was mixed with 15 mL of 10 % NaOH solution and stirred 10 minutes. The organic phase was washed 3 times with 50 mL of water and dried over Na_2SO_4. After removal of the solvent, the crude product was purified by column chromatography using 5:1 Cy/EtOAc as eluent with 33% yield. **R_f:** 0.3.**^{1}H-NMR** (300 MHz, $CDCl_3$)**:** δ [ppm] = 4.21 – 4.12 (m, 2H, 15-H), 4.10 (d, *J* = 1.1 Hz, 2H, 11-H), 3.76 – 3.53 (m, 12H, 9-H, 8-H, 6-H, 5-H, 3-H and 2-H), 1.24 (td, *J* = 7.2, 1.1 Hz, 3H, 16-H). **^{13}C-NMR** (75 MHz, $CDCl_3$)**:** δ [ppm] = 170.43 (12-C), 71.93 (3-C), 70.91 (6-C), 70.73 (5-C), 70.67 (8-C), 70.62 (9-C), 68.75 (11-C), 60.79 (15-C), 42.73 (2-C), 14.23 (16-C).

Ethyl 2-(2-(2-(2-azidoethoxy)ethoxy)ethoxy)acetate (62)[77]

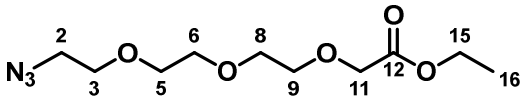

Under argon, 1.27 g of **61** (4.98 mmol, 1.00 eq.) and 0.49 g of sodium azide (7.48 mmol, 1.50 eq.) were added in 15 mL of absolute DMF and heated for 5 hours at 100 °C. After cooling, the DMF was removed. The residue was taken up in 50 mL of DCM and washed 3 times with water. The organic phase was dried over sodium sulfate, filtered and the solvent was removed. It was obtain yellowish oil (0.698 g, 92 %). **R_f:** 0.31. **^{1}H-NMR** (300 MHz, $CDCl_3$)**:** δ [ppm] = 4.15-4.07 (m, 2H, 15-H), 4.05 (s, 2H, 11-H) 3.68-3.58 (m, 10H, 9-H, 8-H, 6-H, 5-H and 3-H), 3.29 (t, J=5.0 Hz, 2H, 2-H), 1.19 (t, J=7.1 Hz, 3H, 16-H). **^{13}C-NMR** (75 MHz, $CDCl_3$)**:** δ 170.30 (12-C), 70.89 (6-C), 70.64 (5-C), 70.57 (8-C), 69.97 (3-C), 69.74 (9-C), 68.69 (11-C), 60.70 (15-C), 50.61 (2-C), 14.11 (16-C). **IR:** 2099 cm^{-1} = - N_3.

Ethyl 2-(2-(2-(2-aminoethoxy)ethoxy)ethoxy)acetate (63)[77]

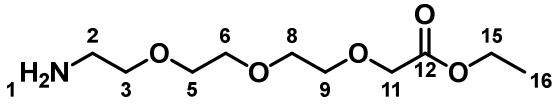

0.698 g of **62** (2.67 mmol, 1.00 eq.) were dissolved in 16 mL of ethanol, treated with 5.34 mL (5.34 mmol, 2.00 eq.) of 1M HCl and 70 mg of Pd/C (10 mol 5) and stored under hydrogen atmosphere at room temperature until complete conversion. The catalyst was filtered off through Celite 545 and the solvent was removed. The resulting hydrochloride compound can be stored at -18 °C for several months. Thus, the work-up to the amine was carried out. 1.03 g of hydrochloride compound were dissolved in 70 mL of chloroform and washed with 10 mL of a saturated solution of K_2CO_3 and finally with 7 mL of water. The organic phase was dried over Na_2SO_4 and the solvent was removed obtaining a yellow oil (0.2868 g, 45%). **^{1}H-NMR** (300 MHz, $CDCl_3$)**:** δ [ppm] = 4.18 (q, *J* = 7.1 Hz, 2H,15-H), 4.12 (d, *J* = 0.9 Hz, 2H, 11-H), 3.71 – 3.59 (m, 8H, 9-H, 8-H, 6-H and 5-H), 3.49 (td, *J* = 5.3, 1.5 Hz, 2H, 3-H), 2.85 (s, 2H, 2-H), 1.89 (s, 2H, 1-H), 1.25 (td, *J* = 7.1, 1.0 Hz, 3H, 16-H). **^{13}C-NMR** (75 MHz, $CDCl_3$)**:** δ [ppm] = 170.53 (12-C), 73.23 (3-C), 70.93 (6-C), 70.69 (8-C), 70.64 (9-C), 70.33 (5-C), 68.78 (11-C), 60.88 (15-C), 41.78 (2-C), 14.27 (16-C).

Methyl 1-(1-(4-methoxybenzyl)-3-(1-(4-methoxybenzyl)-3-(1-(4-methoxybenzyl)-3-nitro-1*H*- pyrazole-5-carboxamido)-1*H*- pyrazole-5-carboxamido)-1*H*- pyrazol-5-yl)-1-oxo-5,8,11-trioxa-2-azatridecan-13-oate (64)[77]

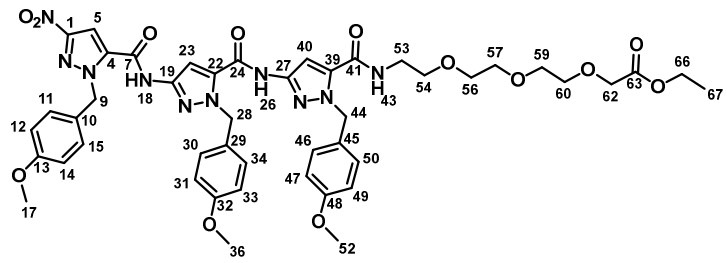

Under argon atmosphere, 0.500 g (0.67 mmol, 1.00 eq.) of **60** were dissolved in 50 mL of DCM. At intervals of 10 minutes, 0.356 g of HBOt-Cl (2.01 mmol, 3.00 eq.), 0.385 g of EDC·HCl (2.01 mmol, 3.00 eq.) and 0.287 g of **63** (1.21 mmol, 1.80 eq.) were added to the suspension at 0 °C. The solution was stirred for 48 hours at room temperature. The organic phase was washed with 50 mL each of 1M hydrochloric acid, saturated sodium bicarbonate solution and saturated sodium chloride solution and dried over Na_2SO_4. After removal of the solvent under reduced pressure, the residue was purified by column chromatography on silica gel with DCM / MeOH (50: 1) to give 0.420 g of the slightly yellowish solid (0.44 mmol, 65 %). **R_f:** 0.25. **^{1}H-NMR** (600 MHz, DMSO)**:** δ [ppm] = 11.50 (s, 1H, 18-H), 11.34 (s, 1H, 26-H), 8.69 (t, *J* = 5.6 Hz, 1H, 43-H), 7.98 (d, *J* = 4.7 Hz, 1H, 5-H), 7.71 (s, 1H, 23-H), 7.33 (s, 1H, 40-H), 7.27 (d, *J* = 8.8 Hz, 2H, 15-H and 11-H), 7.18 (dd, *J* = 8.6, 6.3 Hz, 4H, 50-H, 46-H, 34-H and 30-H), 6.91 – 6.85 (m, 6H, 49-H, 47-H, 33-H, 31-H, 14-H and 12-H), 5.81 (s, 2H, 44-H), 5.67

(s, 2H, 28-H), 5.61 (s, 2H, 9-H), 4.11 (s, 2H, 62-H), 4.10 – 4.07 (m, 2H, 66-H), 3.71 (d, *J* = 1.5 Hz, 6H, 17-H and 32-H), 3.70 (s, 3H, 52-H), 3.60 (dd, *J* = 6.1, 3.3 Hz, 2H, 56-H), 3.56 (dd, *J* = 6.1, 3.3 Hz, 2H, 57-H), 3.55 – 3.51 (m, 3H, 53-H and 52''-H), 3.51 – 3.48 (m, 1H, 52'-H), 3.44 (dd, *J* = 6.1, 3.8 Hz, 1H, 59''-H), 3.38 (dt, *J* = 7.0, 4.1 Hz, 3H, 60-H and 59'-H), 1.17 (t, *J* = 7.1 Hz, 3H, 67-H). **^{13}C-NMR** (151 MHz, DMSO)**:** δ [ppm] = 170.11 (63-C), 159.15 (41-C), 159.06 (7-C), 158.67 (24-C), 158.63 (13-C), 156.91 (32-C), 155.44 (48-C), 153.56 (1-C), 145.21 (19-C), 144.89 (27-C), 136.76 (4-C), 134.92 (39-C), 129.79 (10-C), 129.58 (29-C), 129.36 (45-C), 128.97 (15-C and 11-C), 128.76 (50-C, 46-C, 33-C and 30-C), 127.94 (22-C), 114.03 (5-C), 113.84 14-C and 12-C), 113.75 (49-C, 47-C, 33-C and 31-C), 105.07 (40-C), 100.92 (23-C), 69.95 (57-C), 69.83 (56-C), 69.58 (59-C), 69.47 (60-C), 68.57 (56-C), 67.71 (62-C), 60.07 (66-C), 55.09 (17-C), 55.07 (36-C), 55.06 (52-C), 55.01 (9-C), 54.91 (28-C), 53.16 (44-C), 52.75 (53-C), 14.04 (67-C).

1-(1-(4-methoxybenzyl)-3-(1-(4-methoxybenzyl)-3-(1-(4-methoxybenzyl)-3-nitro-1*H*-pyrazole-5-carboxamido)-1*H*-pyrazole-5-carboxamido)-1*H*-pyrazol-5-yl)-1-oxo-5,8,11-trioxa-2-azatridecan-13-oic acid (65)[77]

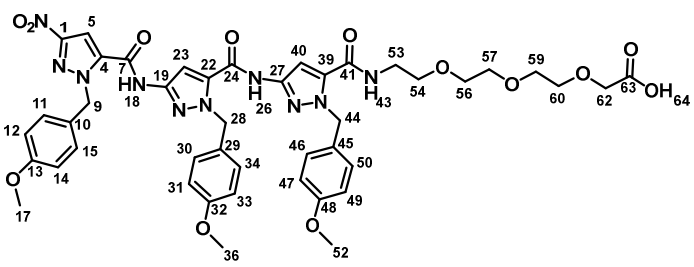

0.402 g of **64** (0.42 mmol, 1.00 eq.) were dissolved in 40 mL of THF/MeOH mixture (1:1) and mixed with 51 mg of LiOH (2.10 mmol, 5.00 eq.). The reaction mixture was stirred overnight at room temperature. The solvent was removed and the residue was taken up in 100 mL of water and the solution was acidified with 1M HCL. It was possible to obtain 0.3342 g of a white solid (0.35 mmol, 85 %). **R_f**: 0.89. **^{1}H-NMR** (300 MHz, DMSO)**:** δ [ppm] = 12.56 (s, 1H, 64-H), 11.50 (s, 1H, 18-H), 11.34 (s, 1H, 26-H), 8.72 (t, *J* = 5.4 Hz, 1H, 43-H), 7.99 (s, 1H, 5-H), 7.72 (s, 1H, 23-H), 7.34 (s, 1H, 40-H), 7.28 (d, *J* = 8.6 Hz, 2H, 50-H and 46-H), 7.18 (dd, *J* = 8.7, 2.6 Hz, 4H, 34-H, 30-H, 15-H and 11-H), 6.89 (t, *J* = 8.4 Hz, 6H, 49-H, 47-H, 33-H, 31-H, 14-H and 12-H), 5.82 (s, 2H, 44-H), 5.68 (s, 2H, 28-H), 5.62 (s, 2H, 9-H), 4.01 (s, 2H, 62-H), 3.71 (d, *J* = 2.6 Hz, 9H, 52-H, 36-H and 17-H), 3.54 (q, *J* = 5.9, 5.2 Hz, 10H, 60-H, 59-H, 57-H, 56-H and 54-H), 3.41 – 3.35 (m, 2H, 53-H). **^{13}C-NMR** (75 MHz, DMSO)**:** δ [ppm] = 171.54 (63-C), 159.11 (41-C), 159.02 (13-C), 158.64 (32-C), 158.59 (48-C), 156.88 (7-C), 155.40 (24-C), 153.52 (1-C), 145.16 (19-C), 144.84 (27-C), 136.73 (4-C), 134.91 (22-C), 134.32 (39-C), 129.75 (10-C), 129.54 (29-C), 129.30 (45-C), 128.92 (15-C and 11-C), 128.71 (34-C and 30-C), 127.89 (49-C and 47-C), 113.99 (5-C), 113.80 (14-C and 12-C), 113.71 (49-C, 47-C, 33-C and 31-C), 105.01 (40-C),

99.57 (23-C), 69.78 (57-C), 69.69 (54-C), 69.64 (59-C), 69.50 (60-C), 68.57 (56-C), 67.52 (62-C), 55.04 (36-C and 17-C), 55.01 (52-C), 53.15 (28-C and 9-C), 52.72 (44-C).

3-(3-(3-nitro-1*H*-pyrazole-5-carboxamido)-1*H*-pyrazole-5-carboxamido)-1*H*-pyrazole-5-carboxylic acid (66)

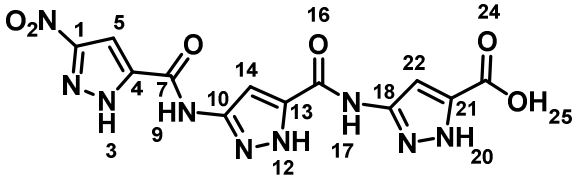

53.1 mg of **60** (72.17 µmol) were dissolved in 3 mL of TFA under argon atmosphere and stirred at 70 °C for 5 hours. The greenish solution was added to cold diethyl ether. The precipitate was filtered and was dried in an oil pump vacuum. A white solid was obtained with a quantitative yield. **^{1}H-NMR** (600 MHz, DMSO): δ [ppm] = 14.97 (br s, 1H, N-H pyrazole 3-H), 13.46 (br s, 2H, N-H pyrazole, 20-H and 12-H), 11.41 (s, 1H, N-H amide 17-H), 11.15 (brs, 1H, N-H amide 9-H), 7.94 (s, 1H, CH pyrazole 5-H), 7.54 (br s, 1H, CH pyrazole 14-H), 7.01 (s, 1H, CH pyrazole 22-H). **^{13}C-NMR** (151 MHz, DMSO): δ [ppm] = 160.54 (24-C), 156.64 (16-C), 155.90 (7-C), 155.07 (18-C, 10-C and 1-C), 138.70 (21-C, 13-C and 4-C), 102.31(22-C), 100.04 (14-C), 98.16 (5-C).

1-(3-(3-(3-nitro-1*H*-pyrazole-5-carboxamido)-1*H*-pyrazole-5-carboxamido)-1*H*-pyrazol-5-yl)-1-oxo-5,8,11-trioxa-2-azatridecan-13-oic acid (67)

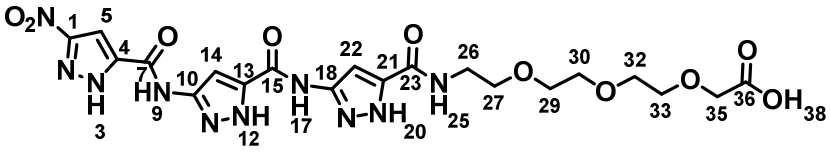

41.6 mg (44.75 µmol) of **65** were dissolved in trifluoroacetic acid (3mL) under argon atmosphere and heated to 70 °C with stirring for 5 hours. The brown solution was added to cold diethyl ether, was filtered and dried in an oil pump vacuum. A white solid was obtained with a 94% yield. **^{1}H-NMR** (600 MHz, DMSO): δ [ppm] = 14.97 (s,1H, N-H pyrazole 20-H), 13.46 (s, 1H, 38-H), 13.19 (s, 2H, 12-H and 3-H), 11.12 (s, 2H, 17-H and 9-H), 8.58 (s, 1H, 22-H), 7.82 (s, 1H, 14-H), 7.57 (s, 1H, 5-H), 7.20 (s, 1H, 25-H), 4.01 (s, 2H, 35-H), 3.60-3.51 (m, 10H, 33-H, 32-H, 30-H, 29-H and 27-H), 3.41-3.38 (m, 2H, 26-H). **^{13}C-NMR** (151 MHz, DMSO): δ [ppm] = 171.66 (C=O), 156.35 (6 x C pyrazole), 102.31 (3 x CH pyrazole), 69.80 (CH_2), 69.74 (CH_2), 69.68 (CH_2), 69.57 (CH_2), 68.82 (CH_2), 67.59 (CH_2), 38.55 (26-C).

(*S*)-Leucyl-(*S*)-prolyl-(*S*)-phenylalanyl-(*S*)-phenylalanyl-(*S*)- aspartic acid (LPFFD) (68)

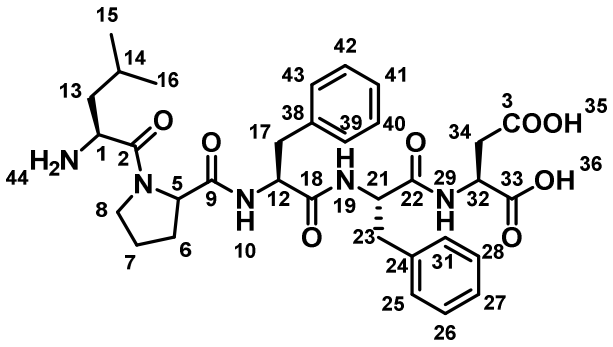

For the preparation of the peptide LPFFD, a preloaded Fmoc-Asp(O^{t}Bu)-wang resin was used. The resin had a loading number of 0.69 mmol / g. The synthesis was carried out according to general method I using,

Fmoc-Asp(O^{t}Bu)-wang resin	0.1078 g (0.074 mmol, 1.00 eq.)
Fmoc-Phe-OH	0.2306 g (0.595 mmol, 8.00 eq.)
Fmoc-Phe-OH	0.2306 g (0.595 mmol, 8.00 eq.)
Fmoc-Pro-OH	0.2008 g (0.595 mmol, 8.00 eq.)
Fmoc-Leu-OH	0.2103 g (0.595 mmol, 8.00 eq.)
HBTU	1.1377 g (0.566 mmol, 7.62 eq.)
DIPEA	0.828 mL (1.19 mmol, 16.00 eq.)

A small cleavage of 58.1 mg of resin was carried out, obtaining 20 mg of a pink solid (0.031 mmol, 78%). **^{1}H-NMR** (600 MHz, DMSO)**:** δ [ppm] = 12.73 (s, 1H, 35-H), 12.41 (s, 1H, 36-H), 8.36 (d, J = 8.1 Hz, 1H, 29-H), 8.03 (d, J = 8.3 Hz, 3H, 44-H and 19-H), 7.87 (d, J = 7.6 Hz, 1H, 10-H), 7.28 – 7.13 (m, 10H, CH $_{phenyl}$), 4.59 – 4.52 (m, 2H, 21-H and 12-H), 4.45 – 4.37 (m, 2H, 27-H and 5-H), 4.11 – 3.99 (m, 1H, 8‘‘-H), 3.71 – 3.61 (m, 1H, 8’-H), 3.03 (dd, J = 14.3, 4.7 Hz, 1H, 1-H), 2.95 (dd, J = 14.2, 4.7 Hz, 1H, 34’-H), 2.83 – 2.75 (m, 2H, 23’-H and 17’-H), 2.70 (dd, J = 16.7, 6.1 Hz, 1H, 34’’-H), 2.65 – 2.52 (m, 2H, 23’’-H and 17’’-H), 2.05 – 1.95 (m, 1H, 14-H), 1.91 – 1.70 (m, 4H, 13”-H, 7’-H and 6-H), 1.56 – 1.43 (m, 2H, 13’’-H and 7’’-H), 0.92 (dd, J = 8.3, 6.6 Hz, 6H, 16-H and 15-H). **^{13}C-NMR** (151 MHz, DMSO)**:** δ [ppm] = 172.22 (3-C), 171.67 (33-C), 170.74 (22-C), 170.55 (9-C), 170.46 (18-C), 167.58 (2-C), 137.54 (38-C), 137.52 (24-C), 129.30 (CH_{phenyl}), 128.86 (CH_{phenyl}), 128.10 (CH_{phenyl}), 127.99 (CH_{phenyl}), 127.96

(CH_{phenyl}), 126.23 (41-C), 126.14 (27-C), 59.30 (5-C), 53.70 (12-C), 53.46 (21-C), 49.46 (1-C), 48.63 (32-C), 46.70 (8-C), 40.06 (13-C), 37.66 (17-C), 37.35 (34-C), 36.13 (23-C), 28.98 (6“-C), 24.44 (6‘-C), 23.39 (14-C), 23.14 (7-C), 21.09 (16-C and 15-C). **HPLC**: [A, 95→40], t_R= 24.333 min, (97%). **HRMS**: (ESI, m/z) calcd for $C_{33}H_{43}N_5O_8$ $[M+H]^+$ 638.3184; found: 638.3189.

(*S*)-Valyl-(*S*)-glutaminyl-(*S*)-isoleucyl-(*S*)-valyl-(*S*)-tyrosyl-(*S*)-lysine (VQIVYK) (70)

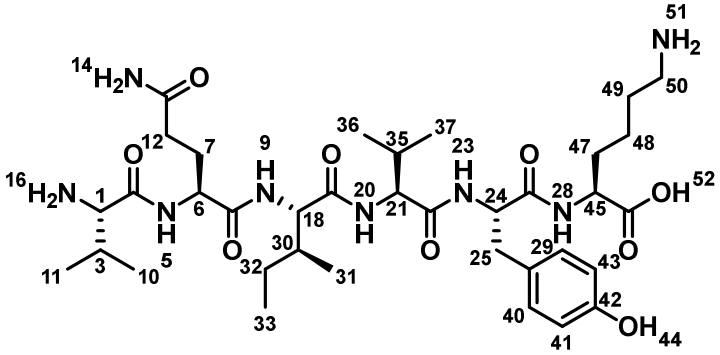

For the preparation of the peptide VQIVYK, a preloaded Fmoc-Lys(Boc)-wang resin was used. The resin had a loading number of 0.64 mmol / g. The synthesis was carried out according to general method I using,

Fmoc-Lys(Boc)-wang resin	0.1568 g (0.10 mmol, 1.00 eq.)
Fmoc-Tyr(*t*Bu)-OH	0.3676 g (0.80 mmol, 8.00 eq.)
Fmoc-Val-OH	0.2715 g (0.80 mmol, 8.00 eq.)
Fmoc-Ile-OH	0.2827 g (0.80 mmol, 8.00 eq.)
Fmoc-Gln-OH	0.4886 g (0.80 mmol, 8.00 eq.)
Fmoc-Val-OH	0.2715 g (0.80 mmol, 8.00 eq.)
HBTU	1.4220 g (0.762 mmol, 7.62 eq.)
DIPEA	1.393 mL (1.60 mmol, 16.00 eq.)

A small cleavage of 49.6 mg of resin was carried out, obtaining 7.6 mg of a white solid (0.01 mmol, 13%). **^{1}H-NMR** (600 MHz, DMSO): δ [ppm] = 12.65 (s, 1H, 52-H), 9.14 (s, 1H, 44-h), 8.46 (d, *J* = 7.7 Hz, 1H, 5-H), 8.07 (t, *J* = 8.2 Hz, 2H, 20-H and 9-H), 7.95 (d, *J* = 8.2 Hz, 1H, 23-H), 7.76 (d, *J* = 9.1 Hz, 1H, 28-H), 7.27 (d, *J* = 2.5 Hz, 1H, 14“-H), 7.00 (d, *J* = 8.5 Hz, 2H, 40-H and 29-H), 6.81 – 6.77 (m, 1H, 14‘-H), 6.60 (d, *J* = 8.6 Hz, 2H, 43-H and 41-H), 4.48 (td, *J* = 8.6, 4.6 Hz, 1H, 24-H), 4.36 (q, *J* = 7.2 Hz, 1H, 6-H), 4.19 (t, *J* = 8.3 Hz, 1H, 18-H), 4.12 (ddd, *J* = 19.4, 8.7, 6.2 Hz, 2H, 45-H and 21-H), 3.51 – 3.47 (m, 1H, 1-H), 2.88 (dd, *J* = 14.3, 4.5 Hz, 1H, 25“-H), 2.75 (t, *J* = 7.6 Hz, 2H, 50-

H), 2.67 (dd, *J* = 14.3, 9.2 Hz, 1H, 35‘-H), 2.17 – 1.96 (m, 3H, 12-H and 3-H), 1.93 – 1.78 (m, 2H, 47‘‘-H and 35-H), 1.78 – 1.66 (m, 3H, 49‘‘-H, 47‘-H and 30-H), 1.54 (ddt, *J* = 26.4, 11.3, 7.1 Hz, 3H, 49‘-H and 7-H), 1.43 – 1.36 (m, 1H, 32‘‘-H), 1.32 (h, *J* = 7.5 Hz, 2H, 48-H), 1.10 – 0.99 (m, 1H, 32‘-H), 0.89 (dd, *J* = 10.1, 6.9 Hz, 6H, 11-H and 10-H), 0.75 (h, *J* = 7.0 Hz, 12H, 37-H, 36-H, 33-H and 31-H). **^{13}C-NMR** (151 MHz, DMSO): δ [ppm] = 173.70 (C=O), 173.40 (C=O), 170.91 (C=O), 170.74 (C=O), 170.71 (C=O), 155.75 (42-C), 129.92 (40-C and 29-C), 127.54 (39-C), 114.80 (43-C and 41-C), 57.70 (1-C), 57.59 (21-C), 56.86 (18-C), 53.70 (24-C), 52.09 (6-C), 51.90 (45-C), 38.63 (50-C), 36.62 (25-C), 36.20 (30-C), 31.32 (12-C), 30.62 (49-C), 30.19 (35-C and 3-C), 28.11 (47-C), 26.55 (7-C), 24.25 (32-C), 22.23 (48-C), 19.14 (37-C), 18.46 (36-C), 18.09 (11-C), 17.53 (10-C), 15.24 (31-C), 10.81 (33-C). **HPLC-MS:** [A, 10%→100%], t_R= 8.3 min (100%), MS (ES+, m/z) 749.4556 $[M+H]^+$. **HRMS**: (ESI, m/z) calcd for $C_{36}H_{60}N_8O_9$ $[M+H]^+$ 749.4556; found 749.4567.

(*S*)-Valyl-(*S*)-glutaminyl-(*R*)-isoleucyl-(*S*)-isoleucyl-(*S*)-asparaginyl-(*S*)-lysine (VQIINK)(73)

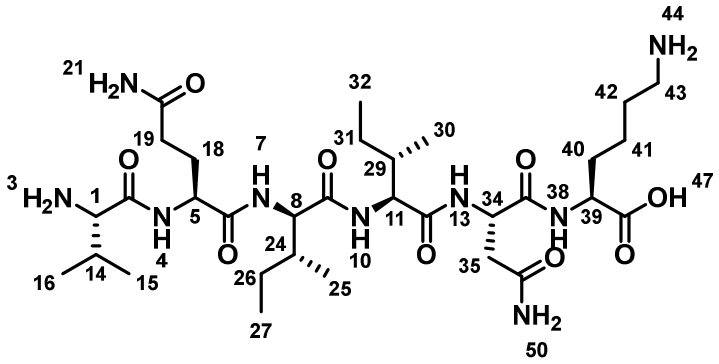

For the preparation of the peptide VQIINK, a preloaded Fmoc-Lys(Boc)-wang resin was used. The resin had a loading number of 0.64 mmol / g. The synthesis was carried out according to general method I using,

Fmoc- Lys(Boc)-wang resin	0.1128 g (0.072 mmol, 1.00 eq.)
Fmoc-Asn(Trt)-OH	0.3440 g (0.571 mmol, 8.00 eq.)
Fmoc-Ile-OH	0.2040 g (0.571 mmol, 8.00 eq.)
Fmoc Ile-OH	0.2040 g (0.571 mmol, 8.00 eq.)
Fmoc-Gln-OH	0.3520 g (0.571 mmol, 8.00 eq.)
Fmoc-Val-OH	0.1960 g (0.571 mmol, 8.00 eq.)
HBTU	1.4220 g (0.550 mmol, 7.62 eq.)

DIPEA	1.003 mL (1.152 mmol, 16.00 eq.)

A small cleavage of 62.9 mg of resin was carried out, obtaining 17.7 mg of a white solid (0.025 mmol, 62%). **^{1}H-NMR** (600 MHz, DMSO): δ [ppm] = 12.65 (s, 1H, 47-H), 8.54 (d, *J* = 7.8 Hz, 1H, 4-H), 8.14 (t, *J* = 8.8 Hz, 2H, 13-H and 7-H), 7.90 (s, 1H, 38-H), 7.80 (d, *J* = 8.8 Hz, 1H, 10-H), 7.33 (d, *J* = 2.5 Hz, 1H, 21''-H), 7.28 (d, *J* = 2.5 Hz, 1H, 50''-H), 6.91 (s, 1H, 21'-H), 6.81 – 6.77 (m, 1H, 50'-H), 4.55 (td, *J* = 7.6, 5.5 Hz, 1H, 34-H), 4.37 (q, *J* = 7.5 Hz, 1H, 5-H), 4.17 (dtd, *J* = 38.1, 8.2, 5.4 Hz, 3H, 39-H, 11-H and 8-H), 3.59 (d, *J* = 5.6 Hz, 1H, 1-H), 2.75 (t, *J* = 7.6 Hz, 2H, 35''-H and 24-H), 2.39 (dd, *J* = 15.8, 7.6 Hz, 1H, 35'-H), 2.09 (dddd, *J* = 49.3, 24.3, 14.5, 6.6 Hz, 3H, 19''-H, 18''-H and 14-H), 1.82 (ddq, *J* = 16.0, 10.4, 5.4, 4.3 Hz, 1H, 40''-H), 1.71 (ddq, *J* = 15.7, 7.7, 4.5, 3.2 Hz, 4H, 43''-H, 40'-H, 29-H and 19'-H), 1.60 – 1.49 (m, 3H, 43'-H, 42''-H and 18'-H), 1.44 – 1.37 (m, 2H, 31''-H and 26''-H), 1.33 (t, *J* = 7.9 Hz, 2H, 41''-H and 42'-H), 1.24 (d, *J* = 7.1 Hz, 1H, 41'-H), 1.12 – 1.02 (m, 2H, 31'-H and 26'-H), 0.91 (d, *J* = 6.9 Hz, 6H, 16-H and 15-H), 0.79 (ddt, *J* = 10.6, 7.4, 5.8 Hz, 12H, 32-H, 30-H, 27-H and 25-H). **^{13}C-NMR** (151 MHz, DMSO): δ [ppm] = 173.65 (C=O), 171.22 (C=O), 170.82 (C=O), 170.79 (C=O), 170.61 (C=O), 167.70 (C=O), 57.24 (1-C), 56.88 (8-C), 56.57 (11-C), 52.20 (5-C), 51.67 (39-C), 49.45 (34-C), 38.63 (24-C), 36.91 (35-C), 36.64 (29-C), 36.16 (19-C), 31.27 (42-C), 30.52 (43-C), 29.94 (14-C), 27.98 (40-C), 26.50 (18-C), 24.24 (26-C), 24.12 (31-C), 22.12 (41-C), 18.19 (15-C), 17.66 (16-C), 15.34 (25-C), 15.17 (30-C), 10.87 (27-C), 10.73 (32-C). **HPLC**: [A, 95→40], t_R= 6.400 min, (96%). **HRMS**: (ESI, m/z) calcd for $C_{32}H_{59}N_9O_9$ $[M+H]^+$ 714.4509; found 714.4506.

(*S*)-asparaginyl-(*S*)-lysyl-(*S*)-lysyl-(*S*)-leucyl-(*S*)-aspartyl-(*S*)-leucyl-(*S*)-seryl-(*S*)-aspartic acid (NKKLDLSN)(75)

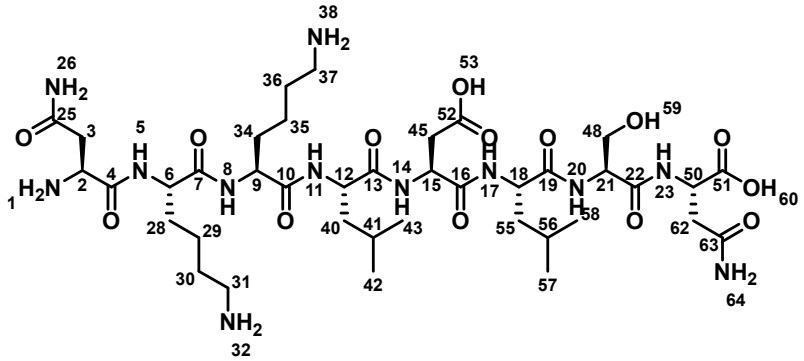

For the preparation of the peptide NKKLDLSN, a preloaded Fmoc- Asn(Trt)-wang resin was used. The resin had a loading number of 0.58 mmol / g. The synthesis was carried out according to general method II using,

Fmoc-Asn(Trt)-wang resin	0.172 g in 5.0 mL DMF

Fmoc-Asn(Trt)-OH	0.716 g in 6 mL DMF
Fmoc-Asp(O^{t}Bu)-OH	0.494 g in 6 mL DMF
Fmoc-Leu-OH	0.919 g in 13 mL DMF (twice)
Fmoc-Lys (Boc)-OH	0.656 g in 7 mL DMF
Fmoc-Ser (^{t}Bu)-OH	0.460 g in 6 mL DMF
HCTU	2.689 g in 13 mL DMF
DIPEA	3.5 mL in 10 mL DMF + 6.5 mL NMP
Piperidine	30 mL in 120 mL DMF
DMF	1.41 L
DCM	83 mL

A small cleavage of 50 mg of resin was carried out, obtaining 7.4 mg of a white solid (0.008 mmol, 27%). **^{1}H-NMR** (600 MHz, DMSO)**:** δ [ppm] = 12.47 (br s, 2H, 60-H and 53-H), 8.57 (d, *J* = 7.8 Hz, 1H, 17-H), 8.31 (d, *J* = 7.5 Hz, 1H, 5-H), 8.17 – 8.09 (m, 3H, 64‘‘-H, 11-H and 8-H), 8.05 – 7.98 (m, 2H, 1-H), 7.90 (d, *J* = 8.3 Hz, 1H, 14-H), 7.77 (d, *J* = 27.5 Hz, 4H, 38-H and 32-H), 7.71 – 7.68 (m, 1H, 20-H), 7.65 (d, *J* = 8.7 Hz, 1H, 23-H), 7.39 (dd, *J* = 12.4, 2.4 Hz, 1H, 26‘‘-H), 7.26 (s, 1H, 64‘-H), 6.91 (t, *J* = 3.9 Hz, 1H, 26‘-H), 4.86 (br s, 1H, 59-H), 4.58 – 4.46 (m, 2H, 50-H and 2-H), 4.38 – 4.25 (m, 4H, 21-H, 18-H, 15-H and 6-H), 4.20 (td, *J* = 8.2, 5.4 Hz, 1H, 9-H), 4.10 (dd, *J* = 8.7, 4.6 Hz, 1H, 12-H), 3.61 – 3.53 (m, 2H, 48-H), 2.76 (d, *J* = 11.1 Hz, 4H, 55-H and 40-H), 2.73 – 2.66 (m, 2H, 62‘‘-H and 45‘‘-H), 2.58 – 2.51 (m, 2H, 62‘-H and 45‘-H), 2.46 (d, *J* = 8.0 Hz, 1H, 3-H), 1.66 (ddt, *J* = 13.8, 10.3, 5.4 Hz, 2H, 34-H), 1.52 (m, 9H, 56-H, 41-H, 37‘‘-H, 36-H, 35-H and 28-H), 1.44 – 1.37 (m, 3H, 37‘-H and 31-H), 1.30 (ddd, *J* = 23.5, 12.2, 6.2 Hz, 4H, 30-H and 29-H), 0.91 – 0.77 (m, 12H, 58-H, 57-H, 43-H and 42-H). **^{13}C-NMR** (151 MHz, DMSO)**:** δ [ppm] = 172.59 (C=O), 172.53 (C=O), 172.21 (C=O), 171.83 (C=O), 171.74 (C=O), 171.36 (C=O), 171.31 (C=O), 171.20 (C=O), 170.90 (C=O), 170.69 (C=O), 170.11 (C=O), 169.52 (C=O), 169.41 (C=O), 168.07 (C=O), 61.65 (48-C), 55.02 (21-C), 52.48 (6-C), 52.44 (9-C), 50.78 (18-C), 50.56 (15-C), 49.21 (2-C), 49.00 (50-C), 48.70 (12-C), 41.33 (37-C and 31-C), 41.15 (3-C), 38.72 (55-C), 38.70 (40-C), 36.59 (62-C), 35.53 (45-C), 31.50 (34-C), 31.01 (28-C), 26.73 (30-C), 26.67 (41-C), 24.03 (36-C), 23.98 (56-C), 23.28 (35-C), 23.21 (57-C), 22.39 (58-C), 22.13 (29-C), 21.55 (43-C), 21.37 (42-C). **HPLC**: [A, 95→40], t_R=15.150 min, (99%). **HRMS**: (ESI, m/z) calcd for $C_{39}H_{69}N_{12}O_{14}$ $[M+2H]^{2+}$ 466.2640; found 466.2646.

(*S*)-seryl-(*S*)-valyl-(*S*)-glutaminyl-(*S*)-isoleucyl-(*S*)-valyl-(*S*)-tyrosyl-(*S*)-lysine (SVQIVYK)(77)

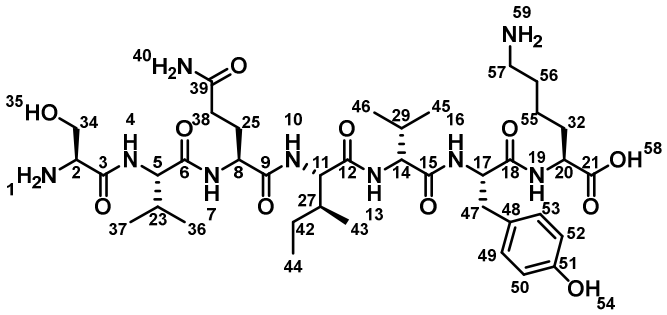

For the preparation of the peptide SVQIVYK, a preloaded Fmoc-Lys(Boc)-wang resin was used. The resin had a loading number of 0.64 mmol / g. The synthesis was carried out according to general method II using,

Fmoc- Lys(Boc)- wang resin	0.156 g in 5.0 mL DMF
Fmoc-Gln(Trt)-OH	0.6107 g in 5 mL DMF
Fmoc-Ile-OH	0.3534 g in 5 mL DMF
Fmoc-Ser (^{t}Bu)-OH	0.383 g in 5 mL DMF
Fmoc-Tyr (^{t}Bu)-OH	0.4595 g in 5 mL DMF
Fmoc-Val-OH	0.4073 g in 6 mL DMF (twice)
HCTU	1.4479 g in 7 mL DMF
DIPEA	1.38 mL in 4 mL DMF
Piperidine	83 mL in 332 mL DMF
DMF	1.14 L
DCM	83 mL

A small cleavage of 42.9 mg of resin was carried out, obtaining 12.5 mg of a white solid (0.02 mmol, 55%). **^{1}H-NMR** (600 MHz, DMSO)**:** δ [ppm] = 12.67 (s, 1H, 58-H), 9.15 (s, 1H, 54-H), 8.41 (d, *J* = 8.8 Hz, 1H, 13-H), 8.19 (d, *J* = 7.7 Hz, 1H, 7-H), 8.16 (d, *J* = 7.8 Hz, 1H, 19-H), 8.09 (s, 2H, 1-H), 7.92 (d, *J* = 8.1 Hz, 1H, 16-H), 7.88 (d, *J* = 8.8 Hz, 1H, 13-H), 7.76 (d, *J* = 9.0 Hz, 1H, 10-H), 7.72 (s, 2H, 59-H), 7.22 (d, *J* = 2.5 Hz, 1H, 40‘‘-H), 7.00 (d, *J* = 8.5 Hz, 2H, 53-H and 49-H), 6.78 – 6.75 (m, 1H, 40‘-H), 6.63 –

6.58 (m, 2H, 52-H and 50-H), 4.49 (td, *J* = 8.5, 4.5 Hz, 1H, 17-H), 4.31 – 4.22 (m, 2H, 20-H and 14-H), 4.20 (t, *J* = 8.3 Hz, 1H, 11-H), 4.17 – 4.09 (m, 2H, 8-H and 5-H), 3.94 (s, 1H, 2-H), 3.73 (dd, *J* = 11.3, 4.2 Hz, 1H, 34''-H), 3.61 (dd, *J* = 11.2, 6.7 Hz, 1H, 34'-H), 2.87 (dd, *J* = 14.3, 4.4 Hz, 1H, 47''-H), 2.75 (q, *J* = 6.4, 5.8 Hz, 2H, 57-H), 2.67 (dd, *J* = 14.3, 9.2 Hz, 1H, 47'-H), 2.13 – 2.02 (m, 2H, 38-H), 1.98 (dt, *J* = 13.5, 6.7 Hz, 1H, 29-H), 1.87 (h, *J* = 6.9 Hz, 1H,23-H), 1.81 (ddt, *J* = 11.6, 9.5, 5.9 Hz, 1H, 32''-H), 1.75 – 1.63 (m, 3H, 56''-H, 32'-H and 27-H), 1.55 (m, 3H, 56'-H and 25-H), 1.44 – 1.35 (m, 1H, 42''-H), 1.35 – 1.27 (m, 2H, 55-H), 1.05 – 1.03 (m, 1H, 42'-H), 0.86 (d, *J* = 6.8 Hz, 3H, 37-H), 0.83 (d, *J* = 6.8 Hz, 3H, 46-H), 0.79 – 0.71 (m, 12H, 45-H, 44-H, 43-H and 36-H). **^{13}C-NMR** (151 MHz, DMSO): δ [ppm] = 173.76 (C=O), 173.29(C=O), 171.11 (C=O), 170.90 (12-C), 170.73 (C=O), 170.66 (C=O), 170.25 (C=O), 166.67 (18-C), 155.76 (51-C), 129.91 (53-C and 49-C), 127.50 (48-C), 114.80 (52-C and 50-C), 60.55 (34-C), 57.57 (5-C), 57.52 (8-C), 56.73 (11-C), 54.08 (2-C), 53.62 (17-C), 52.25 (14-C), 51.60 (20-C), 38.63 (57-C), 36.65 (47-C), 36.39 (27-C), 31.43 (38-C), 30.87 (29-C), 30.60 (23-C), 30.49 (56-C), 27.81 (32-C), 26.54 (25-C), 24.20 (42-C), 22.29 (55-C), 19.18 (46-C), 19.12 (37-C), 18.11 (36-C), 17.87 (45-C), 15.22 (43-C), 10.88 (44-C). **HPLC**: [A, 95→40], t_R=16.950 min, (95%). **HRMS**: (ESI, m/z) calcd for $C_{39}H_{65}N_9O_{11}$ $[M+H]^+$ 836.4876; found 836.4881.

(*S*)-serylglycyl-(*S*)-leucyl-(*S*)-lysyl-(*S*)-threonyl-(*S*)-glutamyl-(*S*)-aspartyl-(*S*)-glutamic acid (SGLKTEDE)(79)

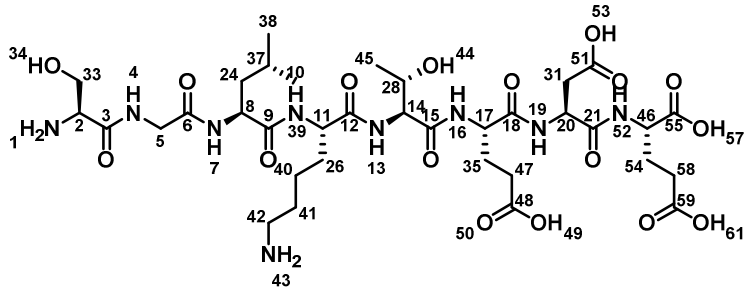

For the preparation of the peptide SGLKTEDE, a preloaded Fmoc- Glu(O^{t}Bu)-wang resin was used. The resin had a loading number of 0.77 mmol / g. The synthesis was carried out according to general method I using,

Fmoc- Glu(O^{t}Bu)-wang resin	0.1665 g (0.13 mmol, 1.00 eq.)
Fmoc-Asp(O^{t}Bu)-OH	0.4213 g (1.024 mmol, 8.00 eq.)
Fmoc-Glu(O^{t}Bu)-OH	0.4357 g (1.024 mmol, 8.00 eq.)
Fmoc-Thr(^{t}Bu)-OH	0.4071 g (1.024 mmol, 8.00 eq.)
Fmoc-Lys(Boc)-OH	0.4797 g (1.024 mmol, 8.00 eq.)
Fmoc-Leu-OH	0.3618 g (1.024 mmol, 8.00 eq.)

Fmoc-Gly-OH	0.3040 g (1.024 mmol, 8.00 eq.)
Fmoc-Ser (*t*Bu)-OH	0.3926 g (1.024 mmol, 8.00 eq.)
HBTU	1.991 g (0.975 mmol, 7.62 eq.)
DIPEA	2. 497 mL (2.048 mmol, 16.00 eq.)

A small cleavage of 55.7 mg of resin was carried out, obtaining 23 mg of a white solid (0.03 mmol, 62%). **^{1}H-NMR** (600 MHz, DMSO)**:** δ [ppm] = 12.32 (s, 3H, 61-H, 57-H and 53-H), 8.63 (t, *J* = 5.6 Hz, 1H, 4-H), 8.23 (d, *J* = 8.1 Hz, 1H, 7-H), 8.17 (d, *J* = 7.6 Hz, 1H, 19-H), 8.13 – 8.10 (m, 2H, 43-H), 8.08 (d, *J* = 8.4 Hz, 1H, 10-H), 8.00 (d, *J* = 7.8 Hz, 1H, 16-H), 7.86 (t, *J* = 8.0 Hz, 1H, 36-H), 7.73 – 7.65 (m, 3H, 13-H and 1-H), 4.54 (td, *J* = 8.2, 4.6 Hz, 1H, 20-H), 4.41 (q, *J* = 7.7 Hz, 1H, 11-H), 4.35 (td, *J* = 8.7, 5.1 Hz, 1H, 8-H), 4.27 (tt, *J* = 9.4, 4.9 Hz, 1H, 46-H), 4.17 (tt, *J* = 11.6, 6.7 Hz, 2H, 46-H and 17-H), 3.99 (p, *J* = 6.1 Hz, 1H, 14-H), 3.88 (q, *J* = 5.5 Hz, 1H, 2-H), 3.81 (td, *J* = 16.7, 5.5 Hz, 2H, 5-H), 3.72 (qt, *J* = 10.7, 4.5 Hz, 2H, 33-H), 2.76 (q, *J* = 6.9 Hz, 2H, 42-H), 2.68 (dd, *J* = 16.8, 4.6 Hz, 1H, 31‘‘-H), 2.26 (td, *J* = 12.5, 10.4, 6.9 Hz, 4H, 58-H and 43-H), 1.99 – 1.89 (m, 2H, 41‘‘-H and 35‘‘-H), 1.77 (dtd, *J* = 20.7, 10.4, 9.6, 4.0 Hz, 2H, 41‘-H and 35‘-H), 1.73 – 1.68 (m, 1H, 26-H), 1.59 – 1.48 (m, 5H, 54-H, 47-H and 37-H), 1.43 (q, *J* = 8.8, 8.0 Hz, 2H, 24-H), 1.28 (tt, *J* = 19.7, 10.1 Hz, 2H, 40-H), 1.02 (d, *J* = 6.2 Hz, 3H, 45-H), 0.86 (dd, *J* = 21.2, 6.5 Hz, 6H, 39-H and 38-H). **^{13}C-NMR** (151 MHz, DMSO)**:** δ [ppm] = 174.11 (55-C), 173.80 (C=O), 173.02 (C=O), 171.82 (C=O), 171.77 (C=O), 171.56 (C=O), 170.89 (C=O), 170.6 (C=O)1, 169.89 (C=O), 167.98 (C=O), 167.17 (6-C), 66.39 (28-C), 60.34 (33-C), 58.29 (14-C), 54.23 (2-C), 52.02 (8-C) , 51.75 (11-C), 51.36 (17-C), 50.97 (46-C), 49.43 (20-C), 41.95 (5-C), 41.43 (24-C), 38.71 (42-C), 36.02 (31-C), 30.98 (47-C), 29.97 (26-C), 29.93 (58-C), 27.55 (41-C), 26.50 (54-C), 26.27 (35-C), 24.22 (37-C), 22.94 (38-C), 22.13 (40-C), 21.75 (39-C), 19.69 (45-C). **HPLC**: [A, 95→40], t_R=13.625 min, (86%). **HRMS**: (ESI, m/z) calcd for $C_{35}H_{59}N_9O_{17}$ $[M+H]^+$ 878.4102; found 878.4104.

(*S*)-aspartyl-(*S*)-seryl-(*S*)-seryl-(*S*)-seryl-(*S*)-asparaginyl-(*S*)-serine (DSSSNS)(81)

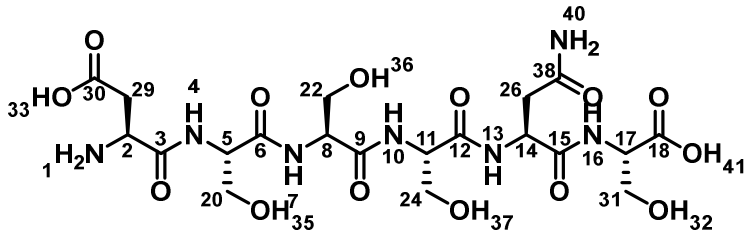

For the preparation of the peptide DSSSNS, a preloaded Fmoc-Ser-wang resin was used. The resin had a loading number of 0.64 mmol / g. The synthesis was carried out according to general method II using,

Fmoc- Ser- wang resin	0.156 g in 5.0 mL DMF
Fmoc-Ser (^{t}Bu)-OH	0.690 g in 9 mL DMF (three times)
Fmoc-Asn(Trt)-OH	0.5966 g in 5 mL DMF
Fmoc-Asp(O^{t}Bu)-OH	0.4114 g in 5 mL DMF
HCTU	1.241 g in 6 mL DMF
DIPEA	1.038 mL in 3 mL DMF
Piperidine	93 mL in 372 mL DMF
DMF	0.98 L
DCM	83 mL

A small cleavage of 47.3 mg of resin was carried out, obtaining 9.2 mg of a white solid (0.015 mmol, 52%). **^{1}H-NMR** (600 MHz, DMSO)**:** δ [ppm] = 8.62 (d, *J* = 7.8 Hz, 1H, 13-H), 8.12 (dd, *J* = 7.9, 3.9 Hz, 2H, 1-H), 8.01 (d, *J* = 7.4 Hz, 1H, 10-H), 7.83 (d, *J* = 7.8 Hz, 1H, 16-H), 7.37 (d, *J* = 2.4 Hz, 1H, 4-H), 6.95 – 6.92 (m, 1H, 7-H), 4.64 (td, *J* = 7.7, 5.4 Hz, 1H, 2-H), 4.45 – 4.39 (m, 1H, 11-H), 4.34 (dd, *J* = 9.2, 3.9 Hz, 1H, 5-H), 4.28 (dt, *J* = 7.9, 5.8 Hz, 1H, 8-H), 4.21 (dt, *J* = 7.8, 4.7 Hz, 1H, 17-H), 4.13 (dd, *J* = 8.5, 4.2 Hz, 1H, 14-H), 3.72 – 3.52 (m, 11H, $CH_{2\ serine}$), 2.84 (dd, *J* = 17.6, 4.2 Hz, 1H, 26''-H), 2.67 (dd, *J* = 17.6, 8.5 Hz, 1H, 26'-H), 2.58 (dd, *J* = 15.6, 5.4 Hz, 1H, 29''-H), 2.39 (dd, *J* = 15.5, 7.5 Hz, 1H, 29'-H). **^{13}C-NMR** (151 MHz, DMSO)**:** δ [ppm] = 171.70 (30-C), 171.67 (38-C), 171.29 (18-C), 170.86 (15-C), 170.15 (6-C), 169.71 (9-C), 169.55 (3-C), 168.12 (12-C), 61.63 ($CH_{2\ serine}$), 61.55 ($CH_{2\ serine}$), 61.27 ($CH_{2\ serine}$), 55.27 (8-C), 55.18 (11-C) and 5-C), 54.83 (17-C), 49.46 (2-C), 49.07 (14-C), 37.04 (29-C), 35.79 (26-C). **HPLC**: [A, 95→40], t_R=4.917min, (99%). **HRMS**: (ESI, m/z) calcd for $C_{20}H_{33}N_7O_{14}$ $[M+H]^+$ 596.2158; found 596.2187.

(3-(3-(3-Nitro-1*H*-pyrazole-5-carboxamido)-1*H*-pyrazole-5-carboxamido)-1*H*-pyrazole-5-carbonyl)-(*S*)-Leucyl-(*S*)-prolyl-(*S*)-phenylalanyl-(*S*)-phenylalanyl-(*S*)-aspartic acid (Trimer-LPFFD) (69)[77]

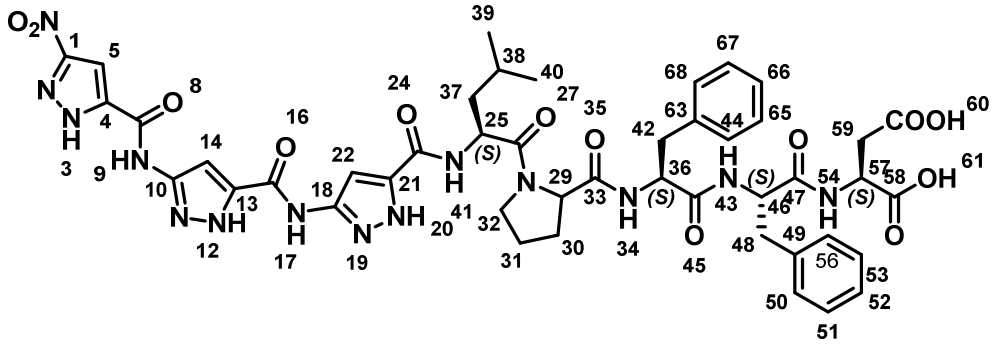

For the preparation of the hybrid molecule, the previously prepared H_2N-LPFFD-wang resin was used. The resin had a loading number of 0.69 mmol / g. The synthesis was carried out according to general method III using,

H_2N-LPFFD-wang resin	56.0 mg (0.039 mmol, 1.00 eq.)
Trimer-(PMB)-OH **60**	114.8 mg (0.156 mmol, 4.00 eq.)
HCTU	64.54 mg (0.156 mmol, 4.00 eq.)
Cl-HOBt	26.45 mg (0.156 mmol, 4.00 eq.)
DIPEA	54.35 µL (0.312 mmol, 8.00 eq.)

DMF/NMP: 5mL (80:20)

and obtaining 13.6 mg of a white solid (0.013 mmol, 35%). **^{1}H-NMR** (600 MHz, DMSO): δ [ppm] = 14.99 (s, 2H, 20-H and 12-H), 13.46 (s, 1H, 60-H), 13.20 (s, 1H, 61-H), 11.39 (s, 2H, 9-H and 3-H), 11.10 (s, 2H, 41-H and 17-H), 8.76 (s, 1H, 5-H), 8.07 (s, 1H, 54-H), 7.93 (s, 1H, 43-H), 7.78 (d, *J*= 10.3 Hz, 2H, 34-H), 7.58 (s, 1H, 14-H), 7.39 (s, 1H, 22-H), 7.31-7.11 (m, 10 H, CH phenyl), 4.74-4.68 (m, 1H, 46-H), 4.57-4.52 (m, 1H, 36-H), 4.50-4.44 (m, 1H, 57-H), 4.41 (dd, *J*= 13.0, 8.2 Hz, 1H, 25-H), 4.34 (dd, *J*= 10.8, 3.0 Hz, 1H, 29-H), 3.70 (d, *J*= 10.3 Hz, 2H, 59-H), 3.49 (s, 2H, 32-H), 3.05 (dd, *J*= 14.0, 4.6 Hz, 1H, 42'-H), 2.96 (dd, *J*= 13.9, 4.0 Hz, 1H, 42''-H), 2.84-2.76 (m, 2H, 48-H), 1.87-1.80 (m, 2H, 31-H), 1.71-1.64 (m, 2H, 30-H), 1.47-1.38 (m, 2H, 37-H), 1.23 (s, 1H, 38-H), 0.91 (d, *J*= 5.6 Hz, 6H, 40-H and 39-H). **^{13}C-NMR** (151 MHz, DMSO): δ [ppm] = 171.09 (C=O), 170.52 (C=O), 137.59 (1-C, 63-C, 49-C, 18-C, 10-C

and 4-C), 129.24 (CH phenyl), 129.22 (CH phenyl), 128.00 (CH phenyl), 127.94 (CH phenyl), 126.22 (13-C), 126.13 (21-C), 102.26 (CH pyrazole), 61.79 (29-C), 59.28 (36-C), 53.71 (25-C), 48.62 (57-C), 46.70 (31-C), 40.17 (37-C), 39.28 (48-C and 42-C), 28.72 (59-C), 24.36 (30-C), 24.21 (31-C),23.20 (38-C), 21.33 (40-C and 39-C). **HRMS**: (ESI, m/z) calcd for $C_{45}H_{50}N_{14}O_{13}$ $[M+H]^+$ 995.3755; found 995.3756.

(1-(3-(3-(3-Nitro-1*H*-pyrazole-5-carboxamido)-1*H*-pyrazole-5-carboxamido)-1*H*-pyrazol-5-yl)-1-oxo-5,8,11-trioxa-2-azatridecan-13-oyl)-(*S*)-Leucyl-(*S*)-prolyl-(*S*)-phenylalanyl-(*S*)-phenylalanyl-(*S*)- aspartic acid (Trimer-TEG- LPFFD) (7)[77]

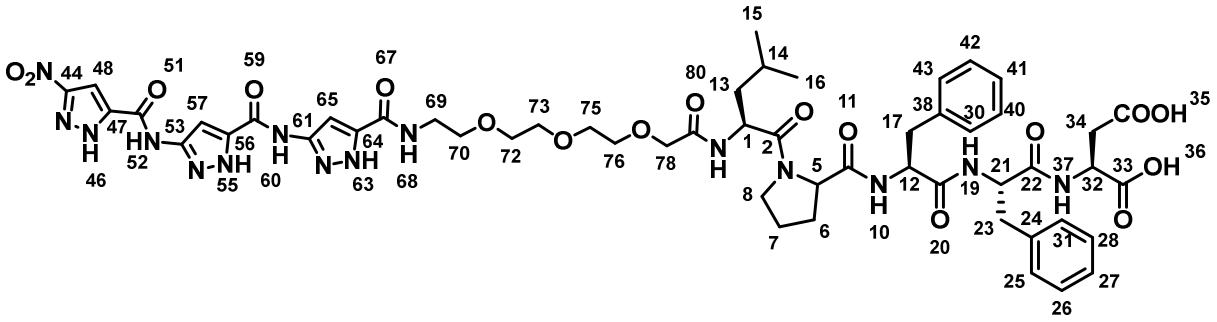

For the preparation of the hybrid molecule, the previously prepared H_2N-LPFFD-wang resin was used. The resin had a loading number of 0.69 mmol / g. The synthesis was carried out according to general method III using,

H_2N-LPFFD-wang resin	50.0 mg (0.035 mmol, 1.00 eq.)
Trimer-TEG-(PMB)-OH **65**	64.2 mg (0.069 mmol, 2.00 eq.)
HCTU	28.54 mg (0.069 mmol, 2.00 eq.)
DIPEA	24.03 µL (0.138 mmol, 4.00 eq.)

DMF/NMP: 5mL (80:20)

and obtaining 9.4 mg of a brown solid (0.007 mmol, 23%). **^{1}H-NMR** (600 MHz, DMSO): δ [ppm] = 14.97 (s, 1H, 63-H), 13.48 (s, 1H, 55-H), 13.14 (s, 2H,36-H and 35-H), 12.80 (s, 2H, 52-H and 46-H), 11.41 (s, 1H, 68-H), 11.08 (s, 1H, 60-H), 8.53 (s, 1H, 48-H), 8.01 (dd, *J*= 19.9 Hz, 1H, 37-H), 7.93 (s, 1H, 19-H), 7.79 (d, *J*= 8Hz, 1H, 10-H), 7.65 (d, *J*= 8.4 Hz, 1H, 57-H), 7.57 (d, *J*= 8.3 Hz, 1H, 65-H), 7.31-7.09 (m, 10 H, CH phenyl), 4.62-4.51 (m, 2H, 32-H and 12-H), 4.39 (dd, *J*= 9.7, 6.3 Hz, 1H, 21-H), 4.34-4.27 (m, 1H, 5-H), 3.90 (s, 2H, 78-H), 3.63-3.48 (m, 10H, 1-H, 76-H, 73-H, 72-H, 70-H and 8-H), 3.45-3.35 (m, 4H, 75-H and 23-H), 3.03 (dd, *J*= 13.9, 4.5 Hz, 1H, 69-H), 2.94 (dd, *J*= 14.1, 4.4 Hz, 1H, 37-H), 2.83-2.74 (m, 2H, 34-H), 2.72-2.64 (m, 1H, 17"-H), 2.63-2.60 (m, 1H, 17'-H), 1.95-1.89 (m, 1H, 7"-H), 1.80 (dd, *J*= 13.6, 7.1 Hz, 1H, 7'-H), 1.74 (d, *J*= 12.8 Hz, 1Hz, 6"-H), 1.58 (d, *J*= 11.3 Hz, 1H, 6'-H), 1.48-1.43 (m, 1H,

13“-H), 1.39-1.33 (m, 1H, 13‘-H), 1.09 (t, *J*= 7.0 Hz, 1H, 14-H), 0.86 (h, *J*= 6.6 Hz, 6H, 16-H and 15-H). **^{13}C-NMR** (151 MHz, DMSO)**:** δ [ppm] = 172.20 (C=O), 171.66 (C=O), 171.08 (C=O), 170.64 (C=O), 170.52 (C=O), 170.27 (C=O), 168.97 (C=O), 155.11 (61-H, 53-C and 44-C), 137.57 (38-C and 24-C), 137.53 (47-C), 129.23 (CH phenyl), 129.20 (CH phenyl), 129.09 (CH phenyl), 127.98 (CH phenyl), 127.93 (CH phenyl), 126.21 (56-C), 126.12 (64-C), 102.29 (65-C, 57-C and 48-C), 70.22 (78-C and 75-C), 69.72 (76-C), 69.57 (70-C), 68.79 (72-C), 64.91 (73-C), 59.20 (5-C), 53.80 (12-C), 53.46 (21-C), 48.62 (1-C), 48.00 (32-C), 46.64 (8-C), 40.30 (69-C and 13-C), 39.43 (23-C), 38.55 (34-C), 37.61 (17-C), 28.72 (6-C), 24.27 (14-C), 24.09 (7-C), 21.36 (15-C), 21.27 (16-C). **HRMS**: (ESI, m/z) calcd for $C_{53}H_{65}N_{15}O_{17}$ $[M+H]^+$ 1184.4755; found 1184.4758.

(1-(3-(3-(3-Nitro-1*H*-pyrazole-5-carboxamido)-1*H*-pyrazole-5-carboxamido)-1*H*-pyrazol-5-yl)-1-oxo-5,8,11-trioxa-2-azatridecan-13-oyl)-(*S*)-Valyl-(*S*)-glutaminyl-(*S*)-isoleucyl-(*S*)-valyl-(*S*)-tyrosyl-(*S*)-lysine (Trimer-TEG-VQIVYK)(71)

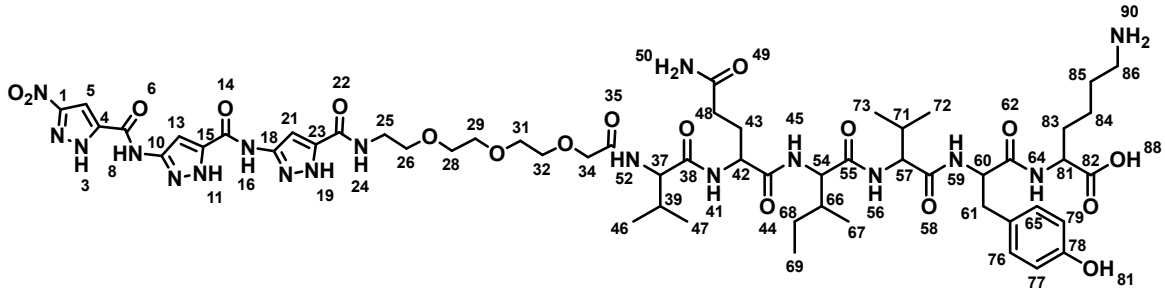

For the preparation of the hybrid molecule, the previously prepared H_2N-VQIVYK-wang resin was used. The resin had a loading number of 0.64 mmol / g. The synthesis was carried out according to general method III using,

H_2N-VQIVYK-wang resin	72.2 mg (0.046 mmol, 1.00 eq.)
Trimer-TEG-(PMB)-OH **65**	85.6 mg (0.092 mmol, 2.00 eq.)
HCTU	38.1 mg (0.092 mmol, 2.00 eq.)
DIPEA	32.1 µL (0.184 mmol, 4.00 eq.)

DMF/NMP: 5mL (80:20)

and obtaining 17.8 mg of a brown solid (0.014 mmol, 30%). **^{1}H-NMR** (600 MHz, DMSO)**:** δ [ppm] =14.97 (s, 1H, 3-H), 13.43 (s, 1H, 11-H), 13.20 (s, 1H, 19-H), 12.66 (s, 1H, 88-H), 11.43 (s, 1H, 8-H), 11.12 (s, 1H, 16-H), 8.57 (d, *J* = 48.1 Hz, 1H, 80-H), 8.25 (d, *J* = 7.8 Hz, 1H,13-H), 8.15 (d, *J* = 7.8 Hz, 1H, 24-H), 7.94 (s, 1H, 56-H), 7.90 (d, *J* = 8.0 Hz, 1H, 59-H), 7.86 (d, *J* = 8.6 Hz, 1H, 64-H), 7.74 (d, *J* = 9.0 Hz, 1H, 45-H), 7.62 (s, 3H, 52-H and 50-H), 7.46 (d, *J* = 8.9 Hz, 1H, 41-H), 7.24 (s, 1H, 21-H), 7.01 (d,

J = 8.4 Hz, 2H, 76-H and 65-H), 6.75 (s, 1H, 5-H), 6.61 (d, *J* = 8.4 Hz, 2H, 79-H and 77-H), 4.52 – 4.46 (m, 1H, 60-H), 4.27 (dt, *J* = 9.5, 4.7 Hz, 3H, 54-H, 42-H and 39-H), 4.17 (q, *J* = 7.2, 6.0 Hz, 2H, 81-H and 57-H), 4.14 – 4.08 (m, 1H, 37-H), 3.93 (s, 2H, 31"-H and 28'-H), 3.63 – 3.49 (m, 8H, 31'-H, 29-H, 28"-H, 26-H and 25-H), 2.88 (dd, *J* = 14.0, 3.9 Hz, 1H, 71-H), 2.75 (q, *J* = 6.3, 5.8 Hz, 2H, 86'-H and 61'-H), 2.14 – 2.02 (m, 2H, 48"-H and 32"-H), 1.96 (dq, *J* = 13.4, 6.7 Hz, 1H, 85'-H), 1.86 (dt, *J* = 14.3, 7.0 Hz, 2H, 86"-H and 61"-H), 1.81 (dt, *J* = 11.0, 5.6 Hz, 1H, 34-H), 1.70 (dt, *J* = 14.5, 7.0 Hz, 4H, 48'-H, 43"-H, 34"-H and 32'-H), 1.61 – 1.48 (m, 4H, 83"-H, 68"-H, 66-H and 43'-H), 1.40 (d, *J* = 4.3 Hz, 1H, 68'-H), 1.32 (dt, *J* = 16.2, 8.7 Hz, 2H, 84"-H and 83'-H), 1.23 (s, 1H, 85"-H), 1.04 (dt, *J* = 13.7, 7.9 Hz, 1H, 84-H), 0.84 (d, *J* = 6.7 Hz, 3H, 47-H), 0.80 (d, *J* = 6.7 Hz, 3H, 46-H), 0.77 – 0.72 (m, 12H, 73-H, 72-H, 69-H and 67-H). **^{13}C-NMR** (151 MHz, , DMSO-d_6): δ [ppm]= 173.71 (49-C), 173.29 (44-C), 171.11 (35-C), 170.96 (62-C), 170.73 (58-C), 170.66 (82-C), 170.47 (55-C), 168.94 (38-C), 157.80 (22-C), 155.89 (14-C, 6-C and 1-C), 155.74 (78-C, 18-C and 10-C), 129.90 (76-C, 65-C and4-C), 114.79 (79-C and 77-C), 102.29 (21-C, 13-C and 5-C), 70.31 (29-C and 26-C), 69.75 (34-C), 69.68 (31-C), 69.59 (32-C), 68.81 (28-C), 57.59 (37-C), 56.77 (57-C), 56.58 (54-C), 53.62 (60-C), 52.20 (42-C), 51.54 (81-C), 40.05 (25-C), 38.66 (86-C), 36.61 (68-C), 36.29 (61-C), 31.41 (48-C), 31.02 (85-C), 30.55 (71-C), 30.47 39-C), 27.71 (83-C), 26.51 (43-C), 24.23 (68-C), 22.27 (84-C), 19.16 (72-C), 19.11 (73-C), 18.10 (46-C), 17.89 (47-C), 15.20 (67-C), 10.85 (69-C). **HPLC**: [A, 95→40], t_R= 23.517 min, (91.6%). **HRMS**: (ESI, m/z) calcd for $C_{56}H_{82}N_{18}O_{18}$ $[M+H]^+$ 1295.6127; found 1295.6127.

(3-(3-(3-Nitro-1*H*-pyrazole-5-carboxamido)-1*H*-pyrazole-5-carboxamido)-1*H*-pyrazole-5-carbonyl)-(*S*)-Valyl-(*S*)-glutaminyl-(*S*)-isoleucyl-(*S*)-valyl-(*S*)-tyrosyl-(*S*)-lysine (Trimer- VQIVYK) (72)

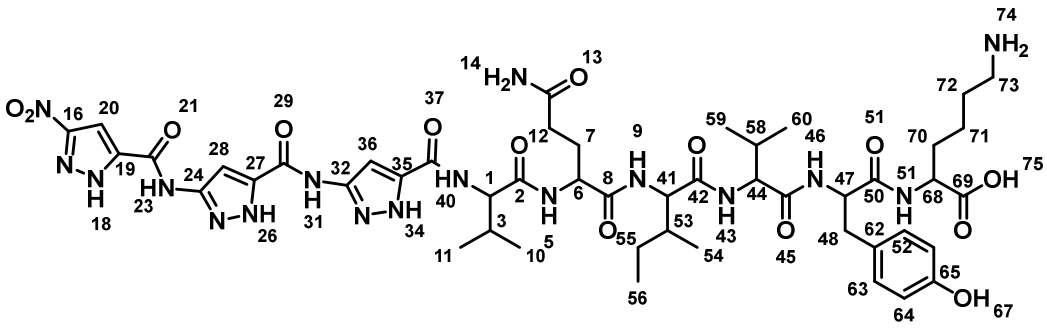

For the preparation of the hybrid molecule, the previously prepared H_2N-VQIVYK-wang resin was used. The resin had a loading number of 0.64 mmol / g. The synthesis was carried out according to general method III using,

H_2N-VQIVYK-wang resin	65.4 mg (0.042 mmol, 1.00 eq.)
Trimer-(PMB)-OH **60**	125.07 mg (0.17 mmol, 4.00 eq.)
HCTU	70.32 mg (0.17 mmol, 4.00 eq.)
Cl-HOBt	28.83 mg (0.17 mmol, 4.00 eq.)
DIPEA	58.53 µL (0.336 mmol, 8.00 eq.)

DMF/NMP: 5mL (80:20)

and obtaining 7.5 mg of a white solid (0.007 mmol, 16%). **^{1}H-NMR** (600 MHz, DMSO): δ [ppm] = 14.98 (s, 1H, 31-H), 13.52 (s, 1H, 75-H), 13.23 (s, 34-H) , 12.65 (s, 2H, 39-H and 23-H), 11.45 (s, 1H, 18-H), 11.11 (s, 1H, 26-H), 9.12 (s, 1H, 67-H), 8.26 (d, *J* = 7.1 Hz, 1H, 9-H), 8.15 (d, *J* = 7.8 Hz, 1H, 51-H), 7.94 (s, 1H, 20-H), 7.91 (d, *J* = 8.0 Hz, 1H, 43-H), 7.87 (d, *J* = 8.7 Hz, 1H, 5-H), 7.74 (d, *J* = 8.9 Hz, 1H, 46-H), 7.63 (s, 2H, 14-H), 7.23 (s, 1H, 28-H), 7.01 (d, *J* = 8.5 Hz, 2H, 63-H and 52-H), 6.74 (s, 1H, 36-H), 6.61 (d, *J* = 8.5 Hz, 2H, 66-H and 64-H), 4.49 (td, *J* = 8.5, 4.7 Hz, 1H, 44-H), 4.34 (dd, *J* = 13.5, 6.5 Hz, 1H, 41-H), 4.31 – 4.28 (m, 1H, 6-H), 4.21 – 4.15 (m, 2H, 68-H and 1-H), 4.15 – 4.10 (m, 1H, 47-H), 2.90 – 2.85 (m, 1H, 48"-H), 2.75 (dq, *J* = 12.4, 5.5, 5.1 Hz, 2H, 73-H), 2.67 (dd, *J* = 14.2, 9.1 Hz, 1H, 58-H), 2.09 (dt, *J* = 22.2, 7.8 Hz, 3H, 72"-H, 48'-H and 12"-H), 1.89 – 1.81 (m, 2H, 70"-H and 3-H), 1.71 (dd, *J* = 13.4, 7.2 Hz, 3H, 70'-H, 53-H and 12'-H), 1.61 – 1.55 (m, 1H, 72'-H), 1.52 (dd, *J* = 9.0, 6.0 Hz, 2H, 71"-H and 7"-H), 1.40 (dd, *J* = 9.1, 4.7 Hz, 1H, 55"-H), 1.36 – 1.29 (m, 2H, 71'-H and 7'-H), 1.23 (s, 1H, 74"-H), 1.04 (dt, *J* = 15.5, 7.9 Hz, 2H, 74'-H and 55'-H), 0.90 (d, *J* = 6.8 Hz, 6H, 56-H and 54-H), 0.75 (td, *J* = 12.6, 10.9, 7.1 Hz, 12H, 60-H, 59-H, 11-H and 10-H). **^{13}C-NMR** (151 MHz, DMSO): δ [ppm] =173.75 (13-C), 173.31 (8-C), 171.12 (2-C), 170.97 (49-C), 170.73 (45-C), 170.68 (69-C and 42-C), 158.10 (37-C), 157.87 (29-C and 21-C), 157.65 (65-C), 155.75 (16-C), 155.08 (32-C and 24-C-C), 129.91 (63-C, 62-C and 52-C), 127.51 (19-C), 118.08 (35-C and 27-C), 114.80 (66-C and 64-C), 102.33 (36-C, 28-C and 20-C), 57.61 (47-C), 56.79 (41-C), 54.16 (1-C), 53.64 (44-C), 52.23 (6-C), 51.56 (68-C), 38.67 (73-C), 36.61 (53-C), 36.34 (48-C), 31.46 (72-C and 12-C), 30.57 (3-C), 30.48 (58-C), 27.86 (70-C), 26.52 (7-C), 24.25 (55-C), 22.28 (71-C), 19.27 (59-C), 19.13 (60-C), 18.13 (11-C and 10-C), 15.22 (55-C), 10.90 (54-C). **HRMS**: (ESI, m/z) calcd for $C_{48}H_{67}N_{17}O_{14}$ $[M+H]^+$ 1106.5126; found 1106.5126.

(3-(3-(3-Nitro-1*H*-pyrazole-5-carboxamido)-1*H*-pyrazole-5-carboxamido)-1*H*-pyrazole-5-carbonyl)-(*S*)-Valyl-(*S*)-glutaminyl-(*R*)-isoleucyl-(*S*)-isoleucyl-(*S*)-asparaginyl-(*S*)-lysine (Trimer-VQIINK)(74)

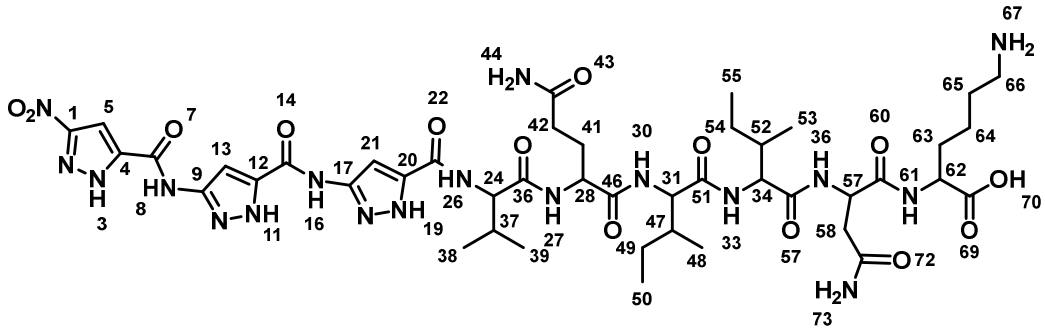

For the preparation of the hybrid molecule, the previously prepared H_2N-VQIINK-wang resin was used. The resin had a loading number of 0.64 mmol / g. The synthesis was carried out according to general method III using,

H_2N-VQIINK-wang resin	68.2 mg (0.043 mmol, 1.00 eq.)
Trimer-(PMB)-OH **60**	126.54 mg (0.17 mmol, 4.00 eq.)
HCTU	71.15 mg (0.17 mmol, 4.00 eq.)
Cl-HOBt	29.17 mg (0.17 mmol, 4.00 eq.)
DIPEA	59.92 µL (0.344 mmol, 8.00 eq.)

DMF/NMP: 5mL (80:20)

and obtaining 7.2 mg of a white solid (0.007 mmol, 16%). **^{1}H-NMR** (600 MHz , DMSO)**:** δ [ppm] = 14.98 (s, 1H, 16-H), 13.49 (s, 1H, 70-H), 13.20 (s, 1H, 19-H), 12.66 (s, 2H, 26-H and 8-H), 11.45 (s, 1H, 3-H), 11.14 (s, 1H, 11-H), 8.31 – 8.26 (m, 1H, 30-H), 8.13 (d, *J* = 7.3 Hz, 1H, 61-H), 7.94 (s, 1H, 5-H), 7.90 (dd, *J* = 7.9, 3.3 Hz, 1H, 27-H), 7.78 (d, *J* = 8.5 Hz, 1H, 33-H), 7.62 (s, 3H), 7.33 (s, 1H), 7.25 (s, 1H), 6.91 (s, 1H), 6.74 (s, 1H), 4.57 – 4.52 (m, 1H, 62-H), 4.33 (d, *J* = 11.1 Hz, 1H, 24-H), 4.32 – 4.28 (m, 1H, 31-H), 4.19 (q, *J* = 7.6, 6.7 Hz, 2H, 34-H and 28-H), 4.16 – 4.13 (m, 1H, 57-H), 2.78 – 2.73 (m, 2H), 2.41 (dd, *J* = 15.6, 7.6 Hz, 2H), 2.14 – 2.04 (m, 4H), 1.87 – 1.82 (m, 1H), 1.76 – 1.66 (m, 4H), 1.58 (dt, *J* = 14.0, 7.3 Hz, 1H), 1.54 – 1.48 (m, 2H), 1.44 – 1.38 (m, 2H), 1.33 (dt, *J* = 14.6, 7.4 Hz, 2H), 1.23 (s, 1H), 1.07 (dt, *J* = 14.0, 7.5 Hz, 2H), 0.90 (t, *J* = 7.0 Hz, 6H, 39-H and 38-H), 0.80 (dt, *J* = 14.0, 7.2 Hz, 12H, 55-H, 53-H, 50-H and 48-H).). With the information of mono- and bi-dimensional spectra that we have it was

not possible to assign all the signals. **^{13}C-NMR** (151 MHz, DMSO): δ [ppm] = 173.72 (43-C), 173.22 (72-C and 69-C), 171.21 (46-C), 170.99 (56-C), 170.82 (51-C), 170.80 (40-C), 170.78 (60-C and 22-C), 170.72 (14-C and 7-C), 155.89 (1-C), 155.06 (17-C and 9-C), 102.31 (21-C, 13-C and 5-C), 56.84 (24-C), 56.62 (34-C), 52.23 (31-C and 28-C), 51.56 (57-C), 49.47 (62-C), 40.05 (42-C), 38.66 (58-C), 38.56 (66-C), 36.82 (52-C), 36.60 (47-C), 36.32 (65-C), 31.43 (37-C), 30.46 (41-C), 27.80 (49-C), 26.47 (63-C), 24.24 (64-C), 24.17 (54-C), 22.11 (39-C), 19.24 (38-C), 15.33 (53-C), 15.17 (48-C), 10.92 (50-C), 10.85 (55-C). **HRMS**: (ESI, m/z) calcd for $C_{44}H_{66}N_{18}O_{14}$ $[M+H]^+$ 1071.5079; found 1071.5075.

(1-(3-(3-(3-Nitro-1*H*-pyrazole-5-carboxamido)-1*H*-pyrazole-5-carboxamido)-1*H*-pyrazol-5-yl)-1-oxo-5,8,11-trioxa-2-azatridecan-13-oyl)-(*S*)-asparaginyl-(*S*)-lysyl-(*S*)-lysyl-(*S*)-leucyl-(*S*)-aspartyl-(*S*)-leucyl-(*S*)-seryl-(*S*)-aspartic acid (Trimer-TEG-NKKLDLSN)(76)

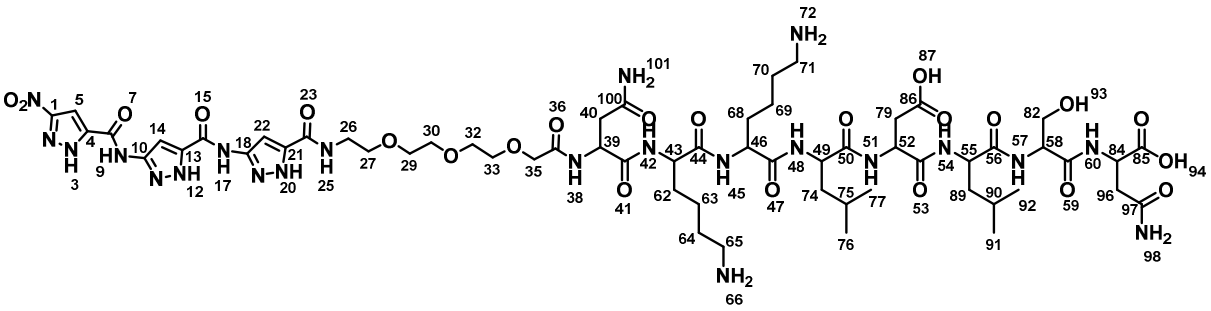

For the preparation of the hybrid molecule, the previously prepared H_2N-NKKLDLSN-wang resin was used. The resin had a loading number of 0.58 mmol / g. The synthesis was carried out according to general method III using,

H_2N-NKKLDLSN-wang resin	58.3 mg (0.03 mmol, 1.00 eq.)
Trimer-TEG-(PMB)-OH **65**	63.22 mg (0.07 mmol, 2.00 eq.)
HCTU	28.13 mg (0.07 mmol, 2.00 eq.)
DIPEA	23.53 µL (0.14 mmol, 4.00 eq.)

DMF/NMP: 5mL (80:20)

and obtaining 11.4 mg of a white solid (0.007 mmol, 26%). **^{1}H-NMR** (600 MHz, DMSO): δ [ppm] = 14.97 (s, 1H, 3-H), 13.49 (s, 1H, 12-H), 11.44 (s, 1H, 30-H), 11.11 (s, 1H, 9-H), 8.54 (d, *J* = 8.0 Hz, 1H, 17-H), 8.26 – 8.18 (m, 1H, 25-H), 8.04 (dt, *J* = 17.9, 8.0 Hz, 2H, NH), 7.96 – 7.90 (m, 2H, 60-H and 38-H), 7.84 – 7.79 (m, 1H, NH), 7.63 (s, 4H, 101-H and 98-H), 7.45 (d, *J* = 7.8 Hz, 1H, NH), 7.39 (s, 1H, CH $_{pyrazole}$), 7.23 – 7.16 (m, 1H, CH $_{pyrazole}$), 7.08 (d, *J* = 11.4 Hz, 1H, CH $_{pyrazole}$), 6.98 (s, 1H, NH), 4.53

(ddt, *J* = 26.2, 14.0, 6.5 Hz, 3H, 84-H, 49-H and 39-H), 4.31 – 4.24 (m, 2H, 58-H and 55-H), 4.21 (ddd, *J* = 13.4, 7.7, 3.4 Hz, 3H, 52-H, 46-H and 43-H), 3.97 – 3.87 (m, 3H, $CH_{2\ TEG}$), 3.55 (td, *J* = 13.1, 12.2, 6.3 Hz, 11H, $CH_{2\ TEG}$ and 82-H), 3.42 – 3.39 (m, 4H, $CH_{2\ TEG}$ and 74-H), 2.74 (dt, *J* = 15.8, 7.9 Hz, 6H, 89-H, 79-H and 40-H), 2.55 – 2.52 (m, 2H, 96-H), 1.67 (dd, *J* = 20.9, 8.4 Hz, 2H, 62-H), 1.58 – 1.46 (m, 9H, 90-H, 75-H, 70-H, 69-H and 68-H), 1.46 – 1.39 (m, 3H, 71H, 65-H and 63''-H), 1.34 – 1.25 (m, 3H, 64-H and 62'-H), 0.91 – 0.79 (m, 12H, CH_3). **^{13}C-NMR** (151 MHz, DMSO): δ [ppm] = 175.49 (C=O), 174.92 (C=O), 173.90 (C=O), 173.79 (C=O), 172.18 (C=O), 171.79 (C=O), 171.60 (C=O), 171.29 (C=O), 170.77 (C=O), 170.17 (C=O), 170.01 (C=O), 169.33 (C=O), 158.03 (C=O), 157.84 (C=O), 157.63 (C=O), 155.91 (C=O), 155.15 (C=O), 155.06 (18-C, 10-C and 1-C), 138.64 (21-C, 13-C and 4-C), 102.32 (22-C, 14-C and 5-C), 70.18 ($CH_{2\ TEG}$), 69.78 ($CH_{2\ TEG}$), 69.71 ($CH_{2\ TEG}$), 69.57 ($CH_{2\ TEG}$), 69.46 ($CH_{2\ TEG}$), 68.80 ($CH_{2\ TEG}$), 61.65 (82-C), 54.98 (58-C), 52.34 (46-C), 50.77 (43-C), 50.62 (55-C), 50.55 (52-C), 49.39 (39-C), 48.53 (84-C), 48.01 (49-C), 40.94 (71-C and 65-C), 38.74 (40-C), 38.60 (89-C), 38.51 (74-C), 36.93 (96-C), 35.51 (79-C), 31.00 (62-C), 30.84 (68-C), 26.92 (64-C), 26.57 (75-C), 24.03 (70-C), 23.38 (90-C), 23.28 (69-C), 23.18 (91-C), 22.90 (92-C), 22.32 (76-C), 22.06 (63-C), 21.44 (77-C). **HPLC**: [A, 95→40], t_R= 1.800 min, (100%). **HRMS**: (ESI, m/z) calcd for $C_{59}H_{92}N_{22}O_{23}$ $[M+2H]^{2+}$ 739.3426; found 739.3426.

(1-(3-(3-(3-Nitro-1*H*-pyrazole-5-carboxamido)-1*H*-pyrazole-5-carboxamido)-1*H*-pyrazol-5-yl)-1-oxo-5,8,11-trioxa-2-azatridecan-13-oyl)-(*S*)-seryl-(*S*)-valyl-(*S*)-glutaminyl-(*S*)-isoleucyl-(*S*)-valyl-(*S*)-tyrosyl-(*S*)-lysine (Trimer-TEG-SVQIVYK)(78)

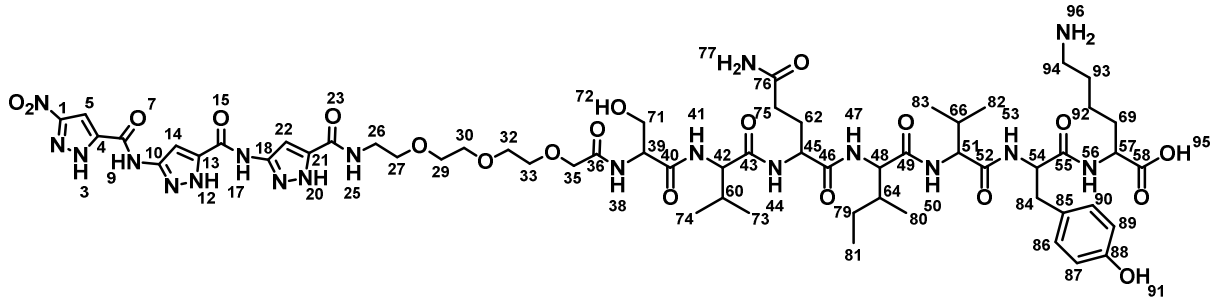

For the preparation of the hybrid molecule, the previously prepared H_2N-SVQIVYK-wang resin was used. The resin had a loading number of 0.64 mmol / g. The synthesis was carried out according to general method III using,

H_2N-SVQIVYK-wang resin	67.5 mg (0.04 mmol, 1.00 eq.)
Trimer-TEG-(PMB)-OH **65**	80.32 mg (0.09 mmol, 2.00 eq.)
HCTU	35.74 mg (0.09 mmol, 2.00 eq.)
DIPEA	29.90 µL (0.17 mmol, 4.00 eq.)

DMF/NMP: 5mL (80:20)

and obtaining 23.1 mg of a yellow solid (0.017 mmol, 42%). **^{1}H-NMR** (600 MHz, DMSO)**:** δ [ppm] = 14.98 (s, 1H, 3-H), 13.50 (s, 1H, 12-H), 13.21 (s, 1H, 20-H), 11.44 (s, 1H, 9-H), 11.12 (s, 1H, 17-H), 9.12 (s, 1H, 91-H), 8.57 (d, *J* = 8.5 Hz, 1H, 25-H), 8.14 (ddd, *J* = 19.2, 12.7, 7.7 Hz, 2H, 50-H and 44-H), 7.94 (s, 1H, 38-H), 7.91 – 7.82 (m, 2H, 53-H and 47-H), 7.73 (dd, *J* = 8.9, 6.2 Hz, 1H, 41-H), 7.62 (d, *J* = 6.8 Hz, 3H, 96-H and 56-H), 7.22 (d, *J* = 10.4 Hz, 1H, CH_{Tyr}), 7.00 (s, 1H, CH_{Tyr}), 6.76 (d, *J* = 11.8 Hz, 1H, CH_{Tyr}), 6.63 – 6.58 (m, 1H, CH_{Tyr}), 4.52 – 4.41 (m, 1H, 39-H), 4.30 – 4.08 (m, 6H, 57-H, 54-H, 51-H, 48-H, 45-H and 42-H), 3.96 – 3.91 (m, 2H, 35-H), 3.61 (q, *J* = 4.0 Hz, 3H, 71-H and CH_2 TEG), 3.58 (dd, *J* = 5.8, 3.0 Hz, 3H, CH_2 TEG), 3.53 (d, *J* = 5.8 Hz, 7H, CH_2 TEG), 3.40 (q, *J* = 5.9 Hz, 2H, CH_2 TEG), 2.88 (dd, *J* = 14.2, 4.4 Hz, 1H, 84''-H), 2.75 (p, *J* = 6.1, 5.7 Hz, 2H, 94-H), 2.67 (dd, *J* = 14.2, 9.1 Hz, 1H, 84'-H), 2.13 – 2.01 (m, 2H, 75-H), 1.96 (dq, *J* = 13.8, 6.6 Hz, 1H, 60-H), 1.87 (dd, *J* = 13.6, 6.8 Hz, 1H, 66-H), 1.84 – 1.79 (m, 1H, 69''-H), 1.69 (dd, *J* = 13.5, 7.6 Hz, 3H, 93''-H, 69'-H and 64-H), 1.58 (dt, *J* = 13.9, 7.2 Hz, 1H, 93'-H), 1.55 – 1.49 (m, 2H, 62-H), 1.43 – 1.37 (m, 1H, 79''-H), 1.36 – 1.29 (m, 2H, 92-H), 1.05 (tt, *J* = 14.4, 8.1 Hz, 1H, 79'-H), 0.87 – 0.72 (m, 18H, CH_3).**^{13}C-NMR** (151 MHz, DMSO)**:** δ [ppm] = 173.74 (C=O), 173.31 (C=O), 171.12 (C=O), 171.02 (C=O), 170.81 (C=O), 170.74 (C=O), 170.65 (C=O), 169.68 (C=O), 169.12 (C=O), 155.91 (C=O), 155.75 (C=O), 155.06 (88-C), 138.68 (4-C), 129.91 (CH_{Tyr}), 127.51 (85-C), 114.79 (CH_{Tyr}), 102.30 (22-C and 14-C), 70.20 (CH_2 TEG), 69.85 (35-C), 69.71 (CH_2 TEG), 69.67 (CH_2 TEG), 69.58 (CH_2 TEG), 68.81 (CH_2 TEG), 61.81 (71-C), 57.62 (42-C), 57.42 (45-C), 56.77 (48-C), 54.18 (39-C), 53.63 (54-C), 52.24 (51-C), 51.55 (57-C), 38.66 (94-C), 38.56 (84-C), 36.33 (64-C), 31.42 (75-C), 30.68 (60-C), 30.55 (66-C), 30.24 (93-C), 27.73 (69-C), 26.52 (62-C), 24.22 (79-C), 22.27 (92-C), 19.11 (83-C), 18.11 (73-C), 17.82 (74-C), 15.27 (82-C), 15.20 (80-C), 10.88 (81-C). **HPLC**: [A, 95→40], t_R= 2.025 min, (99%) **HRMS**: (ESI, m/z) calcd for $C_{59}H_{87}N_{19}O_{20}$ $[M+2H]^{2+}$ 691.8260; found 691.8272.

(1-(3-(3-(3-Nitro-1*H*-pyrazole-5-carboxamido)-*1H*-pyrazole-5-carboxamido)-1*H*-pyrazol-5-yl)-1-oxo-5,8,11-trioxa-2-azatridecan-13-oyl)-(*S*)-serylglycyl-(*S*)-leucyl-(*S*)-lysyl-(*S*)-threonyl-(*S*)-glutamyl-(*S*)-aspartyl-(*S*)-glutamic acid (Trimer-TEG-SGLKTEDE)(80)

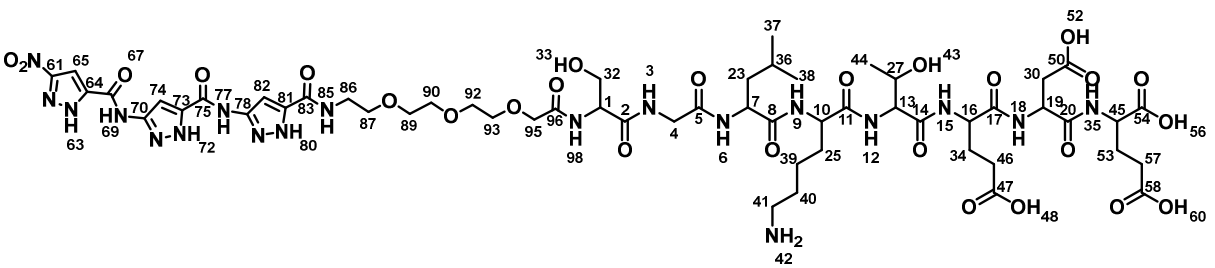

For the preparation of the hybrid molecule, the previously prepared H_2N-SGLKTEDE-wang resin was used. The resin had a loading number of 0.77 mmol / g. The synthesis was carried out according to general method III using,

H_2N-SGLKTEDE-wang resin	75.80 mg (0.058 mmol, 1.00 eq.)
Trimer-TEG-(PMB)-OH **65**	107.84 mg (0.116 mmol, 2.00 eq.)
HCTU	47.99 mg (0.116 mmol, 2.00 eq.)
DIPEA	40.41 µL (0.138 mmol, 4.00 eq.)

DMF/NMP: 5mL (80:20)

and obtaining 19.9 mg of a yellow solid (0.014 mmol, 24%). **^{1}H-NMR** (600 MHz, DMSO): δ [ppm] = 14.98 (s, 1H, 63-H), 13.51 (s, 2H, 80-H and 72-H), 12.51 (s, 2H, 56-H and 48-H), 11.44 (s, 2H,60-H and 52-H), 11.08 (s, 2H, 77-H and 69-H), 8.53 (s, 1H, 85-H), 8.37 – 8.31 (m, 2H, NH), 8.17 – 8.08 (m, 1H, NH), 7.99 (dd, *J* = 15.5, 7.8 Hz, 1H,), 7.94 (s, 1H, $CH_{pyrazole}$), 7.90 – 7.82 (m, 2H, NH), 7.68 (dd, *J* = 23.4, 7.3 Hz, 2H, NH and 42''-H), 7.61 (s, 1H, 42'-H), 7.52 (s, 1H, $CH_{pyrazole}$), 7.14 (s, 1H, $CH_{pyrazole}$), 4.54 (td, *J* = 8.1, 4.7 Hz, 1H, 19-H), 4.30 (ddt, *J* = 17.1, 8.1, 5.0 Hz, 4H, 16-H, 10-H, 7-H and 1-H), 4.20 – 4.15 (m, 2H, 45-H and 13-H), 3.99 (dt, *J* = 10.9, 6.4 Hz, 1H, CH_{TEG}), 3.95 (d, *J* = 4.9 Hz, 2H, 93-H), 3.75 – 3.66 (m, 3H, 32''-H and 4-H), 3.64 – 3.50 (m, 11H, 95''-H, 89-H, 32'-H and $CH_{2\ TEG}$), 3.39 (dt, *J* = 12.6, 6.3 Hz, 2H, 95'-H AND 41''-H), 2.76 (d, *J* = 8.9 Hz, 2H, 41'-H and 30''-H), 2.68 (dt, *J* = 16.3, 4.3 Hz, 1H, 30'-H), 2.26 (dtd, *J* = 24.3, 10.3, 9.8, 6.5 Hz, 4H, 40''-H, 34''-H and 25), 1.94 (dddt, *J* = 20.3, 14.8, 9.9, 5.2 Hz, 2H, 57''-H and 46''-H), 1.82 – 1.73 (m, 2H, 57'-H and 46'-H), 1.69 (s, 1H, 34'-H), 1.56 – 1.50 (m, 3H, 53-H and 36-H), 1.43 (dt, *J* = 14.2, 7.4 Hz, 2H, 23-H), 1.31 – 1.24 (m, 2H, 39-H), 1.23 (dd, *J* = 6.2, 2.2 Hz, 1H, 40'-H), 1.02 (dd, *J* = 6.3, 3.2 Hz, 3H, 44-H), 0.85 (ddd, *J* = 27.2, 8.2, 4.9 Hz, 6H, 38-H and 37-H). **^{13}C-NMR** (151 MHz, DMSO): δ [ppm] = 174.10 (C=O), 173.96 (C=O), 173.79 (C=O), 173.01 (C=O), 171.97 (C=O), 171.56 (C=O), 170.87 (C=O), 170.57 (C=O), 170.41 (C=O), 169.92 (C=O), 169.49 (C=O), 168.71 (67-C), 158.18 (83-C and 75-C), 157.95 (61-C), 155.89 (78-C), 155.07 (70-C), 138.67 (81-C, 73-C and 64-C), 102.31 (74-C), 98.09 (65-C), 96.80 (82-C), 70.24 (90-C), 70.07 (87-C), 69.81 (95-C), 69.70 (93-C), 69.57 (89-C), 68.81 (92-C), 66.39 (27-C), 61.66 (32-C), 58.24 (13-C), 54.56 (16-C), 52.03 (1-C), 51.77 (10-C and 7-C), 51.34 (45-C), 49.41 (19-C), 42.26 (4-C), 40.85 (23-C), 38.75 (86-C), 38.54 (41-C), 36.00 (30-C), 29.95 (25-C), 27.50 (46-C), 26.47 (57-C and 53-C), 26.25 (40-C), 24.15 (36-C), 22.91 (34-C), 22.10 (39-C), 21.58 (38-C), 21.47 (37-C), 19.67 (44-C). **HPLC**: [A, 95→40], t_R= 1.883 min, (98%) **HRMS**: (ESI, m/z) calcd for $C_{55}H_{81}N_{19}O_{26}$ $[M+H]^+$ 1424.5673; found 1424.5679.

(1-(3-(3-(3-Nitro-1*H*-pyrazole-5-carboxamido)-1*H*-pyrazole-5-carboxamido)-1*H*-pyrazol-5-yl)-1-oxo-5,8,11-trioxa-2-azatridecan-13-oyl)-(*S*)-aspartyl-(*S*)-seryl-(*S*)-seryl-(*S*)-seryl-(*S*)-asparaginyl-(*S*)-serine (Trimer-TEG-DSSSNS)(82)

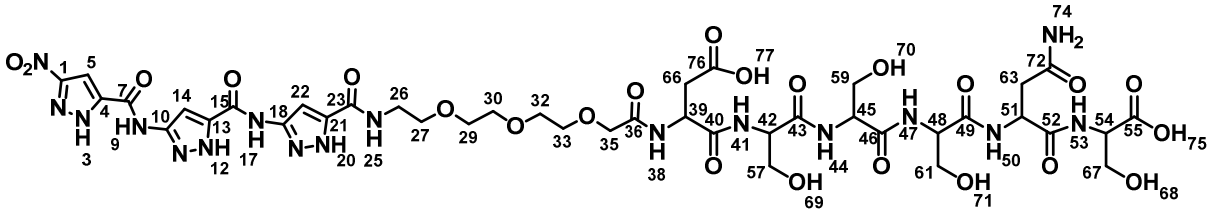

For the preparation of the hybrid molecule, the previously prepared H_2N-DSSSNS-wang resin was used. The resin had a loading number of 0.64 mmol / g. The synthesis was carried out according to general method III using,

H_2N-DSSSNS-wang resin	62.6 mg (0.04 mmol, 1.00 eq.)
Trimer-TEG-(PMB)-OH **65**	74.35 mg (0.08 mmol, 2.00 eq.)
HCTU	33.09 mg (0.08 mmol, 2.00 eq.)
DIPEA	27.88 µL (0.16 mmol, 4.00 eq.)

DMF/NMP: 5mL (80:20)

and obtaining 14.1 mg of a white solid (0.012 mmol, 31%). **^{1}H-NMR** (600 MHz, DMSO): δ [ppm] = 14.98 (s, 1H, 3-H), 11.43 (s, 1H, 12-H), 11.08 (s, 1H, 20-H), 8.53 (s, 1H, 25-H), 8.09 (t, *J* = 8.4 Hz, 1H, NH), 8.04 – 7.95 (m, 3H, 38-H, 41-H and 44-H), 7.94 (s, 1H, NH), 7.93 – 7.89 (m, 1H, 5-H), 7.82 (d, *J* = 7.8 Hz, 1H, NH), 7.52 (s, 1H, 14-H), 7.35 (d, *J* = 9.4 Hz, 1H, NH), 7.14 (s, 1H, 22-H), 6.95 (s, 1H, NH), 4.71 – 4.59 (m, 4H, $CH_{2\ TEG}$, 51-H and 39-H), 4.35 (dtt, *J* = 8.9, 5.8, 3.4 Hz, 2H, 45-H and 42-H), 4.28 (dt, *J* = 7.7, 5.7 Hz, 1H, 54-H), 4.22 (dtd, *J* = 7.7, 4.5, 2.5 Hz, 1H, 42-H), 3.94 – 3.90 (m, 2H, 35‘‘-H and $CH_{2\ Serine}$), 3.61 – 3.52 (m, 19H, $CH_{2\ Serine}$, 35‘-H, 33-H and 29-H), 3.40 (q, *J* = 5.9 Hz, 3H, $CH_{2\ TEG}$ and 26-H), 2.77 – 2.70 (m, 1H, 63‘‘-H), 2.63 – 2.55 (m, 2H, 66‘‘-H and 63‘-H), 2.39 (dt, *J* = 16.2, 8.1 Hz, 1H, 66‘-H). **^{13}C-NMR** (151 MHz, DMSO): δ [ppm] = 171.97 (C=O), 171.94 (C=O), 171.69 (C=O), 171.61 (C=O), 170.82 (C=O), 170.34 (C=O), 170.18 (C=O), 169.98 (C=O), 169.67 (C=O), 169.42 (C=O), 158.64 (23-C), 158.39 (7-C), 158.14 (15-C), 157.89 (18-C and 10-C), 155.08 (1-C), 138.70 (4-C), 116.36 (21-C), 114.43 (13-C), 102.31 (5-C), 98.10 (14-C), 96.83 (22-C),

70.21 (30-C), 70.18 (27-C), 69.77 (35-C), 69.72 (32-C), 69.58 (33-C), 68.81 (29-C), 61.71 ($CH_{2\ Serine}$), 61.60 ($CH_{2\ Serine}$), 61.50 ($CH_{2\ Serine}$), 61.24 ($CH_{2\ Serine}$), 55.27 (48-C and 45-C), 55.07 (54-C), 54.79 (42-C), 49.42 (39-C), 48.90 (51-C), 38.56 (26-C), 37.04 (66-C), 36.16 (63-C). **HPLC**: [A, 95→40], t_R= 1.867 min, (100%) **HRMS**: (ESI, m/z) calcd for $C_{40}H_{55}N_{17}O_{23}$ $[M+H]^+$ 1142.3729; found 1142.3740.

4.4 Monomerization of Aβ (1-42)

The peptide Aβ (1-42) from Bachem was incubated overnight at room temperature with the 1,1,1,3,3,3-hexafluoro-2-propanol (HFIP). Subsequently, the sample was lyophilized and stored at -20 °C until further use.

4.5 Thioflavin T fluoresecence

4.5.1 Kinetics of Aβ

For the kinetics of the Aβ aggregation, a solution (60 µL) of 10 µM previously monomerized Aβ was added in 10 mM PBS and 3.03 µM ThT and transferred into a 384-well plate. The ThT fluorescence intensity was measured every hour at 37 ° C (λ_{Ex}= 446 nm, λ_{Em}= 490 nm) over 72 hours. The microplate was shaken for 30 seconds before each measurement. Three measurements were carried out with a respective quadruple determination.

4.5.2 Disaggregation of Aβ by artificial metalloproteases

33 µM $Aβ_{42}$ in DMSO and 10 µM ThT in ddH_2O were incubated in 1xPBS at 37 °C for 24 hours. Only after incubation of $Aβ_{42}$, the ligands were incubated in a concentration of 198 µM. The disaggregation action of the ligand was followed over a period of 5 days.

4.5.3 Inhibition of Aβ by artificial metalloproteases

A stock solution of 300 µM in DMSO of $Aβ_{42}$, previously monomerized and lyophilized, a 62.7 µM stock solution of ThT in ddH_2O and 10xPBS buffer were used. The ligands were used in different concentrations: 60, 10, 1, 0.1 µM. To check the intrinsic fluorescence of the ligands or undesired interactions with the ligands, they were examined without Aβ both with and without ThT dye. Two measurements of the samples were carried out after 24 hours and 5 days incubated at 37 ° C and 650 rpm. The samples were measured in a 384-Well Black Flat Bottom. The control solutions without Aβ could be directly measured.The fluorescence intensity was measured at 37 ° C with λ_{Ex}= 446 nm and λ_{Em}= 490 nm). Each measurement cycle started with orbital shaking for 30 s to avoid larger Aβ aggregates. Each

measurement point was averaged over 40 light flashes. The manual gain was 100%. For the graphical representation, three measurements were carried out with a respective quadruple determination.

Table 7. Composition of the ThT inhibition mixtures.

	Aβ(1-42) 300 µM (µL)	Ligand 450 µM	DMSO	10x PBS	ThT Stock solution 62.7 µM
Only $Aβ_{42}$	10 µM	-	-	1x	3.03
$Aβ_{42}$+ Ligand	10 µM	variable	-	1x	3.03
Only Ligand	-	60 µM	7.33 %	1x	-
Ligand with ThT	-	60 µM	7.33 %	1x	3.03

4.5.4 Inbibition of SAI-VL fibril formation by aminopyrazoles

The inhibition of SAI-VL fibril formation by the aminopyrazole was investigated by Dr. Laura Pedroza from Ehrmann group. 16.5 µM SAI-VL was incubated at 37 °C with or without 120 µM aminopyrazole in 10 mM Hepes, 100 mM NaCl, pH 7.6 containing 0.4 µg/µl heparin sodium salt. Prior to the experiment, the aminopyrazole compound was dissolved in DMSO. Corresponding to the amount of DMSO added when incubating the LC protein with the compound, DMSO was added to the LC protein only samples. 5 µl aliquots were taken at the indicated time points, incubated with 12 µM ThT/Gylcine and measured at 480 nm .The ThT fluorescence was measured after 0, 1, 2 and 4 days. ThT fluorescence was excited at 440 nm and the emission measured at 480 nm with a set 455 nm cut off using the SpectraMax M5e.

4.6 Circular Dichroism

For CD spectra measurements, solutions of $Aβ_{42}$ alone, $Aβ_{42}$ with ligands and the ligands alone were prepared. $Aβ_{42}$ was previously monomerized, lyophilized and a 500 µM $Aβ_{42}$ stock solution was prepared in HFIP. The stock solutions of the artificial metalloproteases

were prepared in bidistilled water, **7**, **69**, **71**, **67** in pure HFIP (250 µM) and **66** in water/5%HFIP (250 µM). The samples were prepared in potassium phosphate buffer (pH = 7.3) at room temperature. The samples were incubated for a total of 4 d at 25 ° C and 650 rpm. The measurements were taken after 0 hours, 1 hour and 1 day incubation period (Table 8).

Table 8. Composition of the sample solutions investigated by CD measurements.

	Aβ (1-42) Stock Solution 500 µM [µL]	KaPi 10 mM[µL]	Ligand in HFIP/H_2O 250/500 µM [µL]	HFIP [µL]
Control solution	20	980	-	-
Ligand	-	960	20	20
Aβ + Ligand	20	960	20	-

4.7 Atomic force microscopy (AFM)

AFM images were taken by Dr. Laura Pedroza from Ehrmann group (University of Duisburg-Essen). SAI-VL (16.5 µM) was incubated at 37°C with or without the aminopyrazole (120 µM) in 10 mM Hepes, 100 mM NaCl, pH 7.6 with additional 0.4 µg/µl heparin sodium salt. 10 µl of a fibril sample in Hepes buffer was applied to a freshly cleaved mica surface (Plano GmbH). After an incubation period of 3 min at room temperature, the mica was cleaned with ddH_20 and dried under air flow. The sample were scanned using the PeakForce TappingTM mode on Air setting on the MultimodeTM 8 microscope (Bruker) carrying a Nanoscope V controller. A silicon nitride Scanasyst-Air (Bruker) tip with spring constant of 0.4 N/m and a rotated geometry was utilized. Recorded surfaces were third-order flattened using the Nanoscope Analysis 1.5 software. For length and height measurements, at least 3 randomly chosen regions (3x3 µm or 10x10 µm) were scanned and analysed by the Section tool and the Particle Analysis tool of the Nanoscope Analysis 1.5 software if not stated otherwise. The average height was measured with the Section tool by randomly placing 3 sections in each image and measuring the average height difference between the 5 highest and 5 lowest peaks. The Particle Analysis tool analyzes well isolated particles by defining a threshold height of pixel data. In this context, joint pixels above the threshold height are measured as particles. Alternatively, the length was measured

with the Ridge Detection tool in ImageJ (National Institute of Health). AFM images were acquired after 4 days of incubation.

4.8 Proteomics-MS

Experiments were performed by Dr. Farnusch Kaschani (University of Duisburg-Essen) on an Orbitrap Elite instrument (Thermo) coupled to an Evosep One gradient off-set focusing UHPLC (ultra high pressure liquid chromatography) system (Evosep).

To perform the experiment, $A\beta_{42}$ was previously monomerized, lyophilized and a stock solution in HPLC-LC/MS-grade water was prepared. Stock solutions of the artificial metalloproteases were also dissolved in HPLC-LC/MS-grade water. The final samples were added in 1.5 mL polypropylene Eppendorf™ microtubes, with a final total volume of 50 µL. 8 µM and 16 µM of $A\beta_{42}$ was incubated for 24 hours with 2 µM and 8 µM artificial metalloprotease in phosphate buffer at pH 7.5 and 37 °C, respectively. All the samples were vortexed for 5 seconds, sonicated for 30 seconds, precipitated with 4 volumes of acetone and frozen with liquid nitrogen. All the frozen samples were given to Dr. Kaschani to be processed.

After thawing, the samples were centrifuged for 20 min at 18000 rpm. Then, approximately 200 µL of supernatant were transferred to 96 well plate and the samples were dried in a speedvac at 60°C for 90 min. The samples were taken up in 25 µL 0.1% FA and loaded onto EvoTips as described in manufacturers rapid protocol. When loading was done the samples were overlayed with 100 µL 0.1% FA. Finally, the samples were analyzed by LC-MS/MS. Protein quantification and analysis of the large MS data sets were interpreted with the free software Perseus, developed by the Max-Planck-Institute of Biochemistry. A database with the $A\beta_{42}$ sequence was used as a standard to recognize the generated peptides fragments.

5. References

1. Towards a dementia plan: a WHO guide, *World Health Organization*, **2018**.

2. C. Patterson, World Alzheimer Report 2018: The state of the art of dementia research: New frontiers, *Alzheimer's disease Int*ernational, **2018**.

3. Global action plan on the public health response to dementia 2017-2025, *World Health Organization*, **2017**.

4. Avramopoulos D., *Genome Medicine*, **2009**, *1*(34).

5. Pallas, M.; Camis, A., *Current Pharmaceutical Design*, **2006**, *12*(33), 4389-4408.

6. Mucke, L. Alzheimer's disease. *Nature*, **2009**, *461*, 895–897.

7. Stelzmann, R.A.; Norman Schnitzlein; H. and Reed Murtagh, F., *Clinical Anatomy*, **1995**, *8*, 429-431.

8. Alzheimer, A; *Zeitschrift für die gesamte Neurologie und Psychiatrie*, **1911**, *1*, 356-385.

9. Bondi, M.W.; Edmonds, E.C.; Salmon, D.P., *Journal of the International Neuropsychological Society*, **2017**, *23*,818-831.

10. taken from: http://dementiasos.files.wordpress.com/2011/12/dem-plaque-tangle.jpg, (Accessed March 27, **2020**).

11. Wippold, F.J.; Cairns, N.; Vo, K.; Holtzman, D.M.; Morris, J.C., *American Journal of Neuroradiology*, **2007**.

12. Mot, R.T.; Hulette, M.C., *Neuroimaging Clinics*, **2005**, *15*(4), 755 – 765.

13. Nalivaeva N.; Turner A., *FEBS letters*, **2013**, *587*(13), 2046-2054.

14. Zheng H.; Koo E.H., *Molecular Neurodegeneration*, **2011**, *6*(27).

15. Wolfe M.S, *Journal of Medicinal Chemistry*, **2001**, *44*(13), 2039-2060.

16. a) Chiang P.K.; Lam M.A.; Luo Y.; *Current Molecular Medicine*, **2008**, *6*, 580-584. b) Teplow D.B., *Amyloid: The Journal of Protein Folding Disorders*, **1998**, *5*, 121-142. c) Ahmed M.; Davis J.; Aucoin D. *et al.*, *Nature Structural and Molecular Biology*, **2010**, *17*, 561-567.

17. a) Ritcher L.; Munter L. Ness J. *et al.*, *Proc. Natl. Acad.Sci. U.S.A,* **2010**, *107*(33), 14597-14602. b) Serpell L.C., *Biochimica et biophysica acta*, **2009**, *1502*(1), 16-30.

18. Goldsbury C.; Mocanu M.; Thies E. *et al.*, *Traffic*, **2006**, *7*(7), 873-888.

19. a) Moore et al., *Cell Reports*, **2015**, *11*, 689-696. b) Peters F.; Salihoglu H.; Pratsch K. et al., *The EMBO journal*, **2019**, *38*(23).

20. Hardy J.A.; Higgins G.A., *Science*, **1992**, *256*(5054), 184-185.

21. Scheuner D.; Eckman C.; Jensen M. *et al.*, *Nature Medicine*, **1996**, *2*, 864-870.

22. McLean C.A.; Robert A.; Cherny *et al.*, *Annals of Neurology*, **1999**, *46*(6), 860-866.

23. Cizas P.; Budvytyte R.; Morkuniene R. *et al.*, *Arch Biochem Biophys*, **2010,** *496*, 84-92.

24. DaSilva K.A.; Shaw J.E.; McLaurin J., *Experimental Neurology*, **2010**, *223*, 311-321.

25. Finder V.H.; Glockshuber R., *Neurodegenerative Diseases*, **2007**, *4*, 13-27.
26. Teplow D.B. *et al.*, *The Journal of Biological Chemistry*, **1999**, *274*(36), 25945-259952.
27. Streltsov V. *et al.*, *The Journal of Neuroscience*, **2011**, *31*, 1419-1426.
28. Lühr T.; Ritter C.; Adrian M. *et al.*, *Proc. Natl. Acad.Sci. U.S.A,* **2005**, *102*, 17342-17347.
29. Armstrong R.A., *Folia Neuropathologica*, **2014**, *52*, 211-225.
30. Wirths O.; Multhaup G.; Bayer T.A., *Journal of Neurochemistry*, **2004**, *91*, 513-520.
31. Wolfe M., *Scientifica*, **2012**,*4*.
32. Avila J. *et al.*, *Physiol. Rew.*, **2004**, *84*, 361-384.
33. Gendron T., Petrucelli L., *Mol. Neurodegeneration*, **2009**, *3*(13).
34. Zhang W. *et al.*, *Nature*, **2020**, 283-287.
35. Peterson D. *et al.*, *Biochemistry*, **2008**, *47*, 7393-7404.
36. Alzheimer's Association, *Azlheimer's & Dementia*, **2011**, *7*, 208-244.
37. Com es diagnostic l'Alzheimer?, *Fundació Pasqual Maragall*, **2017**.
38. Laforce R.; Rabinovici G.D, *Alzheimer's Research & Therapy*, **2011**, *3*(31).
39. Prakash P.; Hethava K.P.; Korte N.; Izquierdo P. *et al.*, *Biorxiv*, **2020**.
40. Alzheimer's Association, *Alzheimers Dement.*, **2020**.
41. Apostolova L.G., *Continuum*, **2016**, *22*, 419-434.
42. Sharma K., *Molecular Medicine Reports*, **2019**, *20*, 1479-1487.
43. Blennow K.; de Leon M.J; Zetterberg H., *The Lancet*, **2006**, *368*, 9533, 387-403.
44. Schenk D.; Barbour R.; Dunn W. *et al.*, *Nature*, **1999**, *400*, 173-177.
45. Vellas B.; Black R.; Rhal L.J. *et al.*, *Current Alzheimer Research*, **2009**, *6*, 144-151.
46. Marciani D.J, *Research*, **2019**.
47. Lemere C.A., *Molecular Neurodegeneration*, **2013**, *8*(36).
48. Schenk D.; Hagen M.; Seubert P., *Current Opinion in Immunology*, **2004**, *16*, 599-606.
49. Folch J.; Petro D. *et al.*, *Neural Plasticity*, **2016**, Article ID 8501693.
50. Egan M.F. *et al., Alzheimer's Research & Therapy*, **2019**, *11*(68).
51. Kennedy M.E *et al.*, *Science Translational Medicine*, **2016**, *8*(363).
52. Doody R.S *et al.*, *The New England Journal of Medicine*, **2013**, *369*(4).
53. Coric V.; Salloway S.; van Dyck C.H. *et al.*, *JAMA Neurology*, **2015**, *72*, 1324-1333.
54. Vlieghe P. *et al.*, *Drug Discovery Today*, **2010**, *15*(1/2), 40-56.
55. Tjernberg L.O. *et al.*, *The Journal of Biological Chemistry*, **1996**, *271*(15), 8545-8548.
56. Gordon D.J. *et al.*, *The Journal of Peptide Research*, **2002**, *60*, 37-55.
57. Estrada L.D; Lasagna C.; Soto C., *Pharmacological Mechanisms in Alzheimer's Therapeutics*, **2007**, *15*, 238-254.
58. Soto C. *et al.*, *Nature Medicine*, **1998**, *4*(7), 822-826.

59. a) Wiesehan K. *et al.*, *ChemBioChem*, **2003**, *4*, 748-753. b) Van Groen T. *et al.*, *ChemMedChem*, **2009**, *4*, 276-282. c) Funke A.S. *et al.*, *PLoS ONE*, **2012**, *7*(7).
60. Liu.H. *et al.*, *Rejuvenation Research*, **2010**, *13*(2-3), 210-213.
61. Funke S.A. *et al.*, *ACS Chemical Neuroscience*, **2010**, *1*, 1639-1648.
62. Schumacher N.M. *et al.*, *Science*, **1996**, *271*, 1854-1857.
63. Wiesehan K.; Willbold D., *ChemBioChem*, **2003**, *4*, 811-815.
64. *Muller-Schiffmann A. et al., Angewandte International Edition,* **2010,** *49, 8743-8746*.
65. Ladiwala *et al.*, *The Journal of Biological Chemistry*, **2011**, *286*(5), 3209-3218.
66. Ono K. *et al., Journal of Neurochemistry*, **2003**, *87*, 172-181.
67. DeToma A.S; Choi J.; Braymer J.; Lim M.H, *ChemBioChem*, **2011**, *12*(8), 1198-1201.
68. Blair L.J. *et al.*, *Alzheimer's research & Therapy*, **2013**, *5*(41).
69. Mokhtari Z. *et al.*, *Neurophysiology*, **2019**, *51*(4), 266-271.
70. Cisek K.; Cooper G.L.; Huseby C.J.; Kuret J., *Current Alzheimer Research*, **2014**, *11*, 918-927.
71. Ono K. *et al.*, *BBA*, **2004**, *1690*, 193-202.
72. Kirsten C.; Schrader T., *Chemical Communication*, **1996**, 2089-2090.
73. Kirsten C.; Schrader T., *Journal of the American Society*, **1997**, *119*(50), 12061-12068.
74. Rzepecki P., "Neue ß-Faltblattliganden zur Hemmung der Aggregation des Amyloid-ß-Peptids", Marburg, **2004**.
75. Rzepecki P. *et al.*, *The Journal of Biological Chemistry*, **2004**, *279*(46), 47497-47505.
76. Hochdörffer K., "Oligomere Aminopyrazole gegen die pathologische Aggregation des Alzheimer-Peptids", Essen, **2009.**
77. März-Berberich J., "Aminopyrazol-Hybridverbindungen gegen Aggregation und Neurotoxizität des Alzheimer-Peptids", Essen, **2010**.
78. Müller-Schiffmann A. *et al.*, *Brain*, **2016**, *139*(2), 509-525.
79. Hellmert M., "Hochentwickelte Aminopyrazol-Hybride gegen pathologische Prozesse der Alzheimer-Krankheit", Essen, **2014**.
80. Hellmert M. *et al.*, *Organic & Biomolecular Chemistry*, **2015**, *13*, 2974-2979.
81. Streich C.; Akkari L., *ACS Nano*, **2016**, *10*, 7582-7597.
82. Hu X. *et al.*, *Front.Bioeng. Biotechnol.*, **2020**, *8*(990).
83. Barcikowski S. *et al.*, *Appl. Phys. A.*, **2007**, *87*(1), 47-55.
84. taken from: https://www.uni-due.de/barcikowski/forschen.htm, (Accessed March 17, **2021**)
85. Akkari L.,"Neuartige peptidische Ligandenkonjugate zur Hemmung der pathologischen Aggregation von Amyloid-beta bei Morbus Alzheimer", Essen, **2017**.
86. Nagase H., *Current Protocols in Protein Sciencie*, **2001**, *21.4.1-21.4.13*.
87. Chang C., Werb Z., *Trends Cell Biol.*, **2001**, 11(11).

88. Yong V.W et al., *Nature Reviews*, **2001**, *2*, 502-511.
89. Rana T.M., Meares C.F., *Proc. Natl. Acad. Sci. USA*, **1991**, *88*, 10578-10582.
90. Koll H., *J.Am.Chem.Soc.*, **1952**, *74*, 2036.
91. Sutton P. and Buckingham D., *Acc. Chem. Res.*, **1987**, *20*(10), 357-364.
92. Suh J., Oh S., *Bioorg. Med. Chem. Lett.*, **1996**, *6*(10), 1067-1070.
93. Jang B. *et al.*, *J.Am.Chem.Soc.*, **1998**, *120*(46), 12008-12016.
94. Suh J., *Acc.Chem.Res.*, **2003**, *36*, 562-570.
95. Suh J. *et al.*, *J.Am.Chem.Soc.*, **2005**, *127*, 2396-2397.
96. Suh J. *et al.*, *Angew. Chem. Int. Ed.*., **2007**, *46*, 7064-7067.
97. Suh J., Chei W., *Curr.Opin.Chem.Biol.*., **2008**, *12*, 207-213.
98. Suh J., Chei W., Ju H., *J.Biol.Inorg.Chem.*, **2011**, *16*, 511-519.
99. Suh J. *et al.*, *J. Biol. Inorg. Chem.*, **2009**, *14*, 151-157.
100. Suh J., *Asian J.Org.Chem.*, **2014**, *3*, 18-32.
101. Lee T.Y. *et al.*, *Bioorg. Med.Chem. Lett.*, **2012**, *22*, 5689-5693.
102. Haag R. *et al.*, *Angew. Chem. Int. Ed. Engl.*, **2012**, *51*, 2-29.
103. Dykman L., Khlebtsov N., *Acta Naturae*, **2011**, *3*(2), 34-55.
104. Tenntaedt A. *et al.*, *J. Biol. Chem.*, **2012**, *287*(25), 20931-20941.
105. Proposal of the Collaborative Research Centre 1093.
106. Green K.N., Lincoln K.M., Gonzalez P., Texas Christian University, US 2014/0206862 A1, **2014**.
107. Parikh J., Doering W., *J. Am. Chem. Soc.*, **1967**, *89*(21), 5505-5507.
108. Tojo G., Fernández M., Oxidation of alcohols to aldehydes and ketones, Springer, **2006**.
109. Abdel-Magid A.F. *et al.*, *J. Org. Chem.*, **1996**, *61*(11), 3849-3862.
110. Jeong K. *et al.*, *J. Ind. Eng. Chem.*, **2009**, *15*, 342-347.
111. So Y-H., Heeschen J., *J. Org. Chem.*, **1977**, *62*, 3552-3561.
112. Carpino *et al.*, *Org. Proc. Res. Dev.*, **2003**, *7*(1), 28-37.
113. Carpino *et al., J. Org. Chem.*, **1990**, *55*(2), 721-728.
114. Hatfield S., "Aplications of triazine chemistry: education, remediation, and drug delivery", Texas, **2007**.
115. Zhou Y. *et al.*, *Cryst. Growth Des.*, **2017**, *17*, 6653-6659.
116. Filali E. *et al.*, *Synlett.*, **2009**, *2*, 205-208.
117. Matthis C. *et al.*, *J. Med. Chem.*, **2003**, *46*, 2740-2754.
118. Khurana R. *et al.*, *J. Struct. Biol.*, **2005**, *151*, 229-238.
119. Hudson S.A. *et al.*, *FEBS journal*, **2009**, 5960-5972.
120. Noormägi A. *et al.*, *J. Pept. Sci.*, **2012**, *18*, 59-64.
121. Hackl E.V *et al.*, *Eur. Biophys. J.*, **2015**, *44*, 249-261.
122. Krebs M.R.H. *et al.*, *J. Struct. Biol.*, **2005**, *149*, 30-37.
123. Iannuzzi C. *et al.*, *Int. J. Mol. Sci.*, **2013**, *14*, 14287-14300.

124. Foderà V. *et al., J. Phys. Chem. B.*, **2008**, *112*, 15174-15181.
125. Dodero V. *et al.*, *Front. Biosci.*, **2011**, *16*, 61-73.
126. Greenfield N., *Nature Protocol*, **2005**, *1*, 2876-2890.
127. Wei Y. *et al.*, *Biochim. Biophys. Acta Proteins Proteom.*, **2014**, *12*, 2331-2337.
128. Kelly S.M., Price N.C., *Curr. Protein Pept. Sci.*, **2000**, *1*, 349-384.
129. Rangachari V. *et al.*, *Biochemistry*, **2007**, *46*, 12451-12462.
130. Rudolph J., Cox J., *J. Proteome Res.*, **2019**, *18*, 2052-2064.
131. Roy I., Gupta M.N, *Biotechnol. Appl. Biochem.*, **2004**, *39*, 165-177.
132. Schmid R.D., *Adv. Biochem. Eng.*, **1979**, *12*, 41-117.
133. Fotiou D. *et al.*, *HemaSphere*, **2020**, *4*.
134. Palladini G., *Blood*, **2020**, *136*(23), 2620-2627.
135. Pedroza. L, "The implication of the human serine protease HTRA1 in immunoglobulin light chain amyloidosis", Essen, **2020**.
136. Li B. *et al.*, *J. Org. Chem.*, **2015**, *80*, 5444-5456.
137. Boumrah *et al.*, *Tetrahedron Letters*, **1991**, *32*, 7735.
138. Boumrah *et al.*, *Tetrahedron*, **1997**, *53*, 6977-6992.
139. von Bergen M. et al., *PNAS*, **2000**, *97*(10), 5129-5134.
140. Pradham T. *et al.*, *BioRxiv,* **2020**.
141. Berkelman T., Sun C., *Bio-rad laboratories Inc.*, **2009**, 5911.
142. Laemmli U.K., *Nature*, **1970**, *227*, 680-685.
143. Wilson R., Bullen H., "Basic theory: atomic force microscopy", Northen Kentuchy.
144. Haugstad G., "Atomic force microscopy: understanding basic modes and advanced applications", Wiley online libray, **2012**.
145. Stefaniak E. *et al.*, *Chem. Eur. J.*, **2021**, 27, 2798-2809.
146. Kaiser test kit, Sigma Aldrich.

6. Appendix

6.1 NMR spectra

^{1}H NMR (600 MHz, $CDCl_3$)

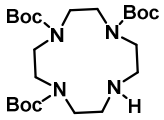

17

^{13}C NMR (151 MHz, $CDCl_3$)

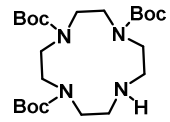

17

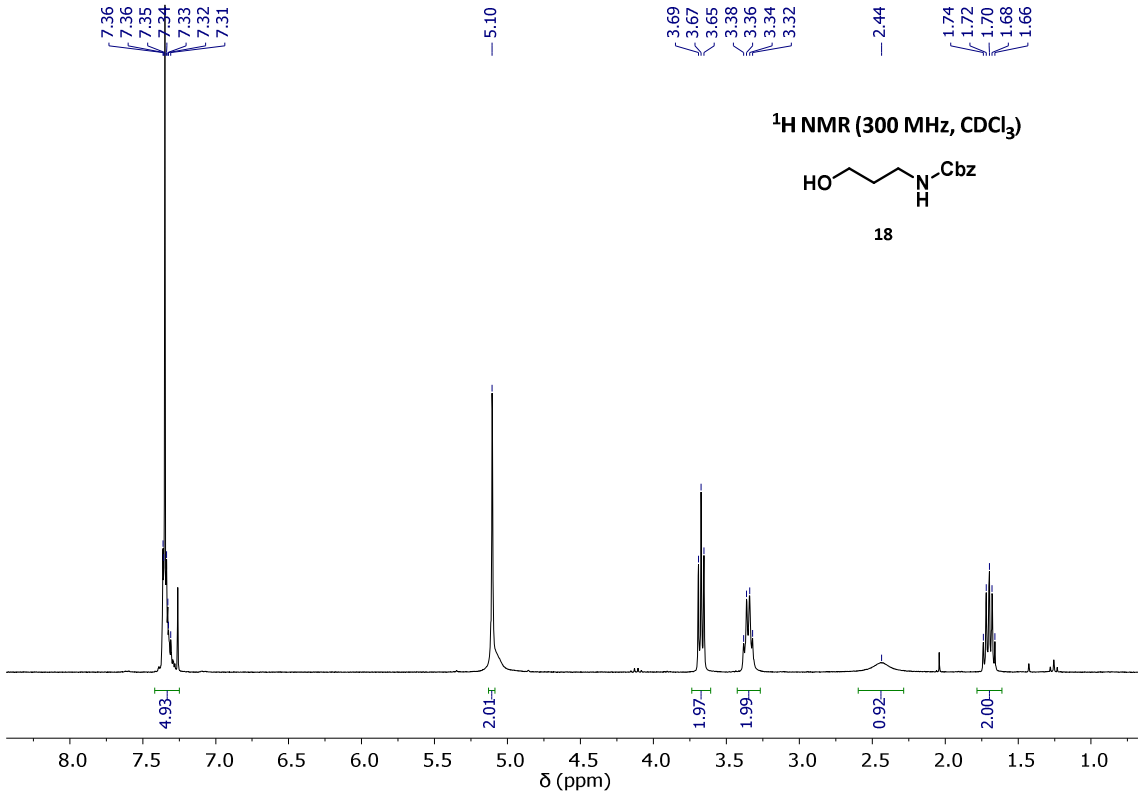

^{1}H NMR (300 MHz, $CDCl_3$)

18

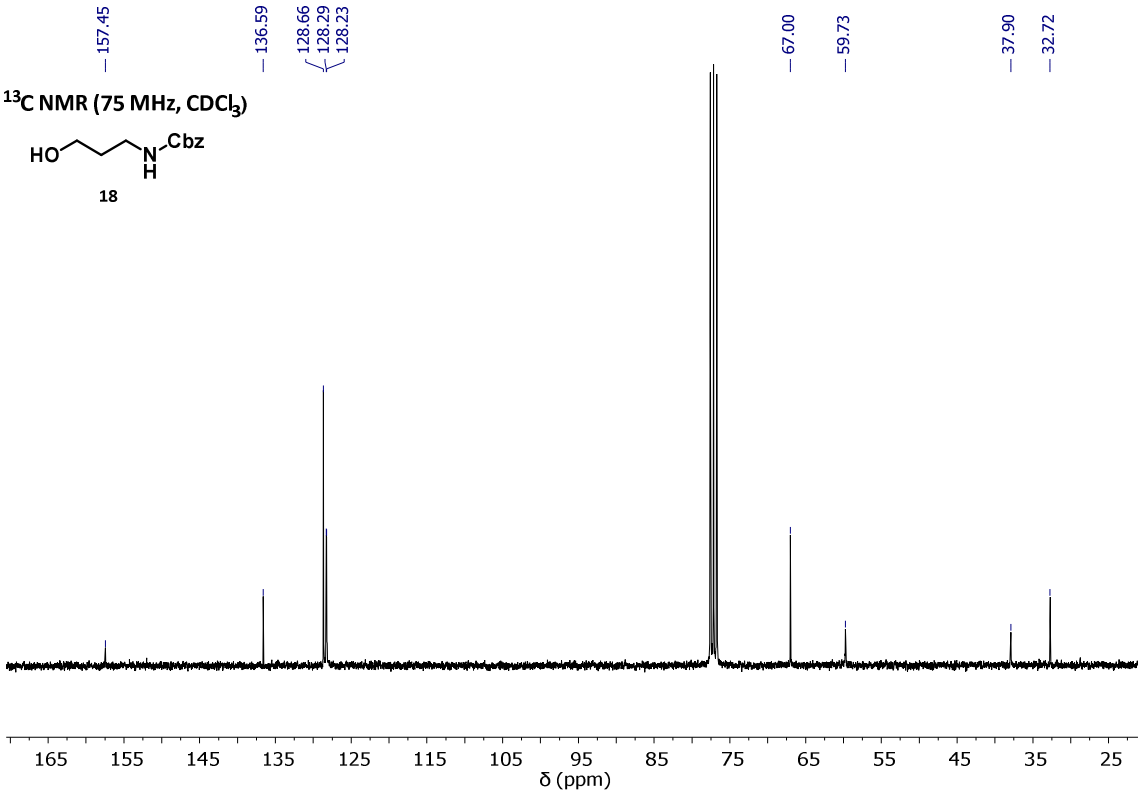

^{13}C NMR (75 MHz, $CDCl_3$)

18

^{1}H NMR (300 MHz, $CDCl_3$)

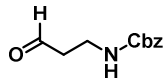

19

^{13}C NMR (75 MHz, $CDCl_3$)

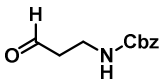

19

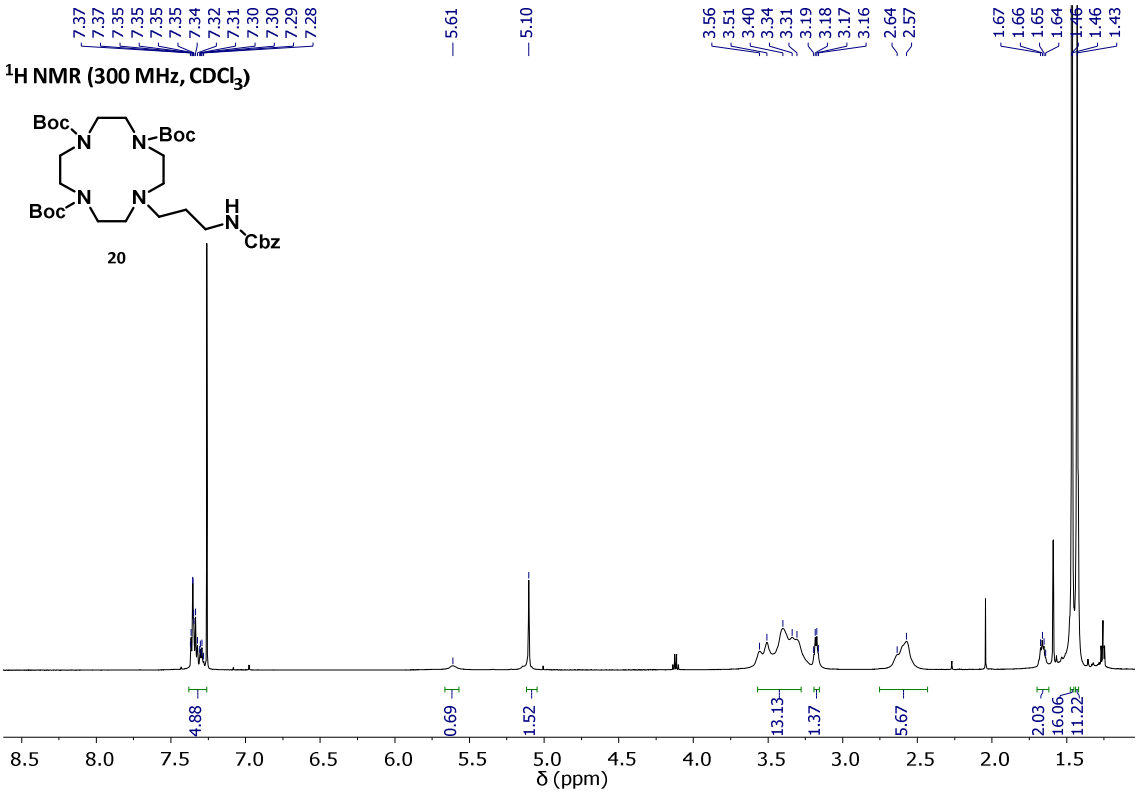
7.37
7.37
7.35
7.35
7.35
7.35
7.34
7.32
7.31
7.30
7.30
7.29
7.28
5.61
5.10
3.56
3.51
3.40
3.34
3.31
3.19
3.18
3.17
3.16
2.64
2.57
1.67
1.66
1.65
1.64
1.46
1.46
1.43
1H NMR (300 MHz, CDCl3)
Boc
N
N
Boc
Boc
N
N
H
N
Cbz
20
4.88
0.69
1.52
13.13
1.37
5.67
2.03
16.06
11.22
8.5
8.0
7.5
7.0
6.5
6.0
5.5
5.0
4.5
4.0
3.5
3.0
2.5
2.0
1.5
δ (ppm)

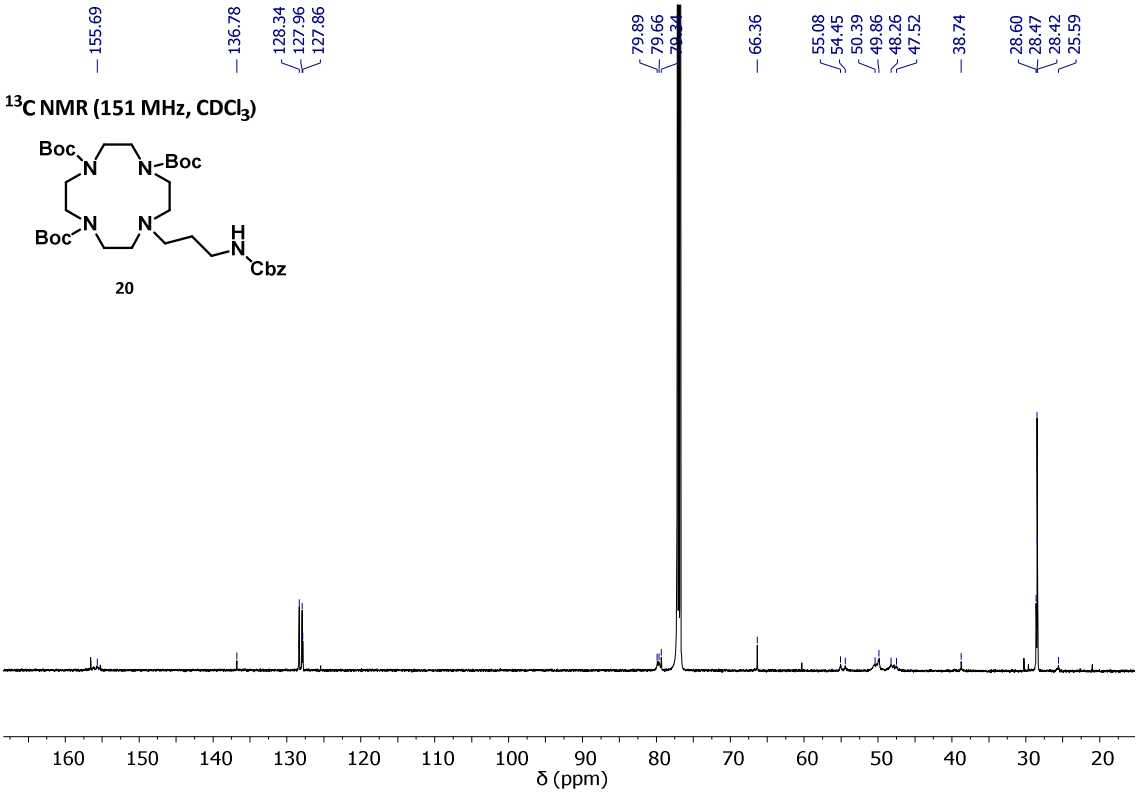
155.69
136.78
128.34
127.96
127.86
79.89
79.66
79.34
66.36
55.08
54.45
50.39
49.86
48.26
47.52
38.74
28.60
28.47
28.42
25.59
13C NMR (151 MHz, CDCl3)
Boc
N
N
Boc
Boc
N
N
H
N
Cbz
20
160
150
140
130
120
110
100
90
80
70
60
50
40
30
20
δ (ppm)

^{1}H NMR (300 MHz, $CDCl_3$)

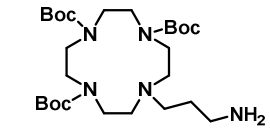

21

^{13}C NMR (101 MHz, $CDCl_3$)

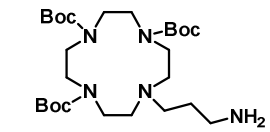

21

^{1}H NMR (600 MHz, DMSO)

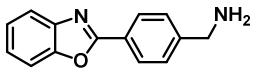

22

^{13}C NMR (151 MHz, DMSO)

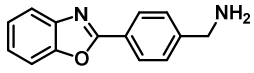

22

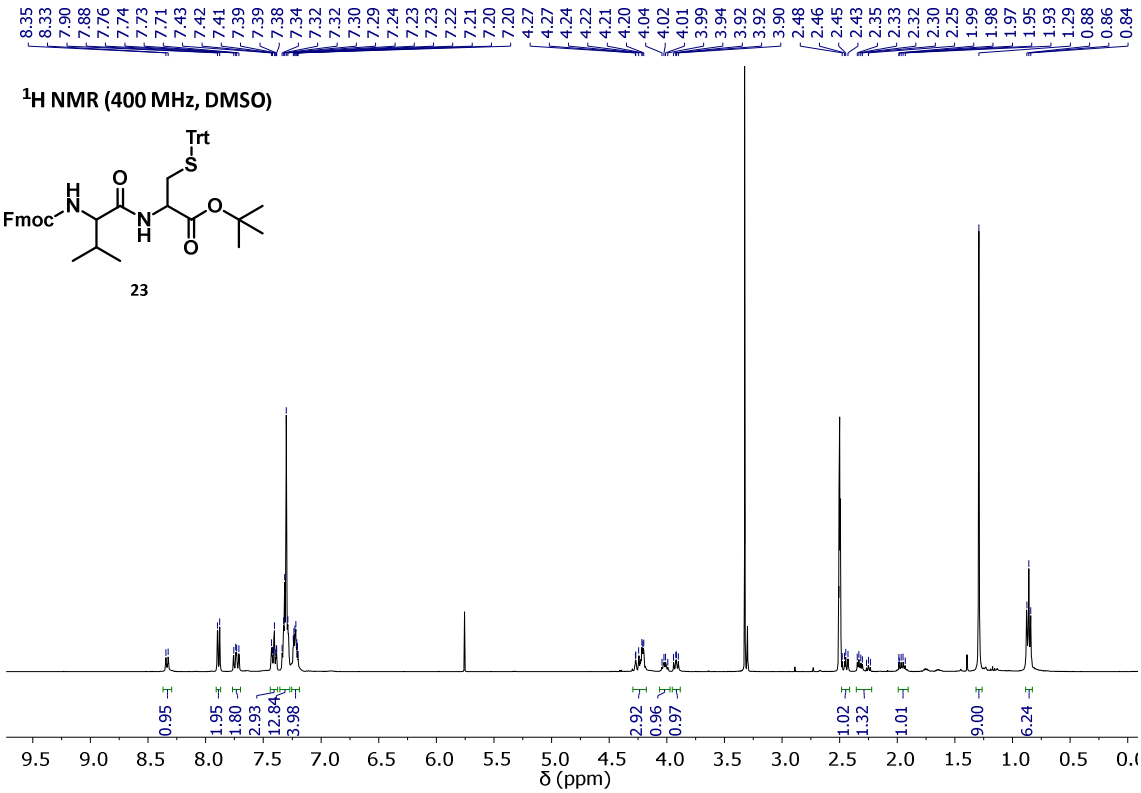
8.35 8.33 7.90 7.88 7.76 7.74 7.73 7.71 7.43 7.42 7.41 7.39 7.38 7.34 7.32 7.32 7.30 7.29 7.24 7.23 7.23 7.22 7.21 7.20 7.20 4.27 4.27 4.24 4.22 4.21 4.20 4.04 4.02 4.01 3.99 3.94 3.92 3.92 3.90 2.48 2.46 2.45 2.43 2.35 2.33 2.32 2.30 2.25 1.99 1.98 1.97 1.95 1.93 1.29 0.88 0.86 0.84
1H NMR (400 MHz, DMSO)
Trt
S
Fmoc
H
N
O
N
H
O
O
O
23
0.95 1.95 1.80 2.93 12.84 3.98 2.92 0.96 0.97 1.02 1.32 1.01 9.00 6.24
9.5 9.0 8.5 8.0 7.5 7.0 6.5 6.0 5.5 5.0 4.5 4.0 3.5 3.0 2.5 2.0 1.5 1.0 0.5
δ (ppm)

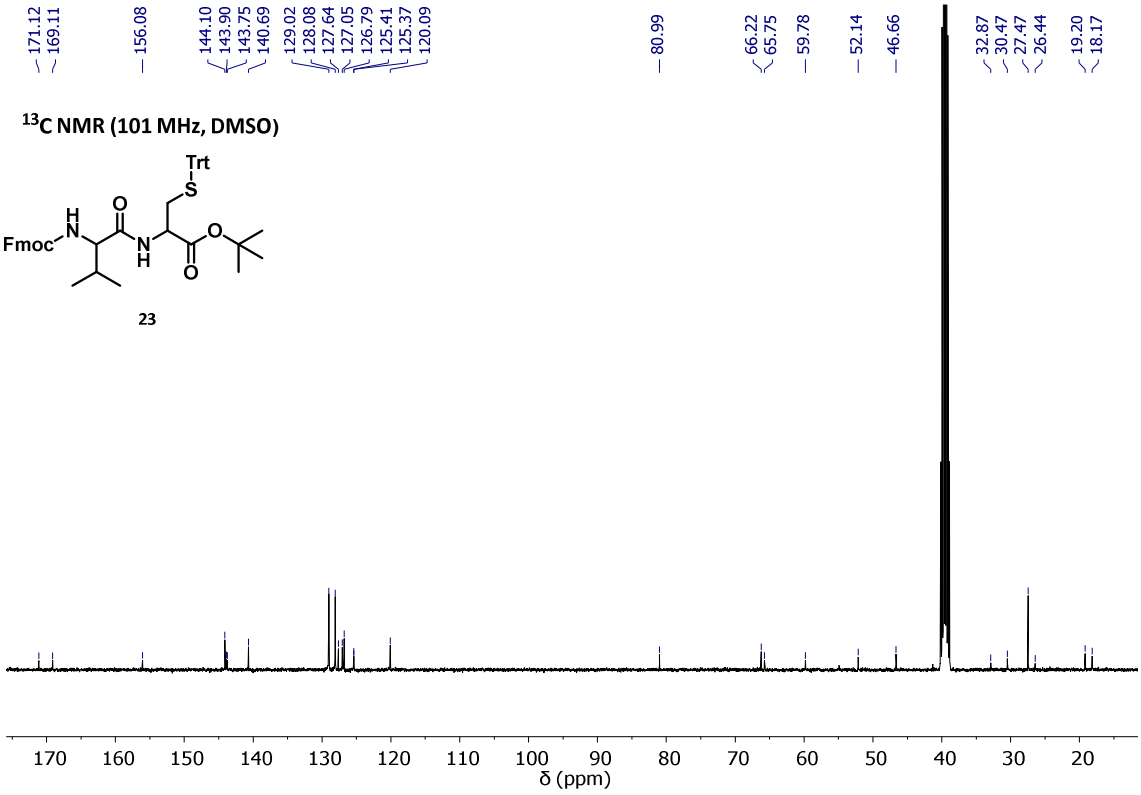
171.12 169.11 156.08 144.10 143.90 143.75 140.69 129.02 128.08 127.64 127.05 126.79 125.41 125.37 120.09 80.99 66.22 65.75 59.78 52.14 46.66 32.87 30.47 27.47 26.44 19.20 18.17
13C NMR (101 MHz, DMSO)
Trt
S
Fmoc
H
N
O
N
H
O
O
O
23
170 160 150 140 130 120 110 100 90 80 70 60 50 40 30 20
δ (ppm)

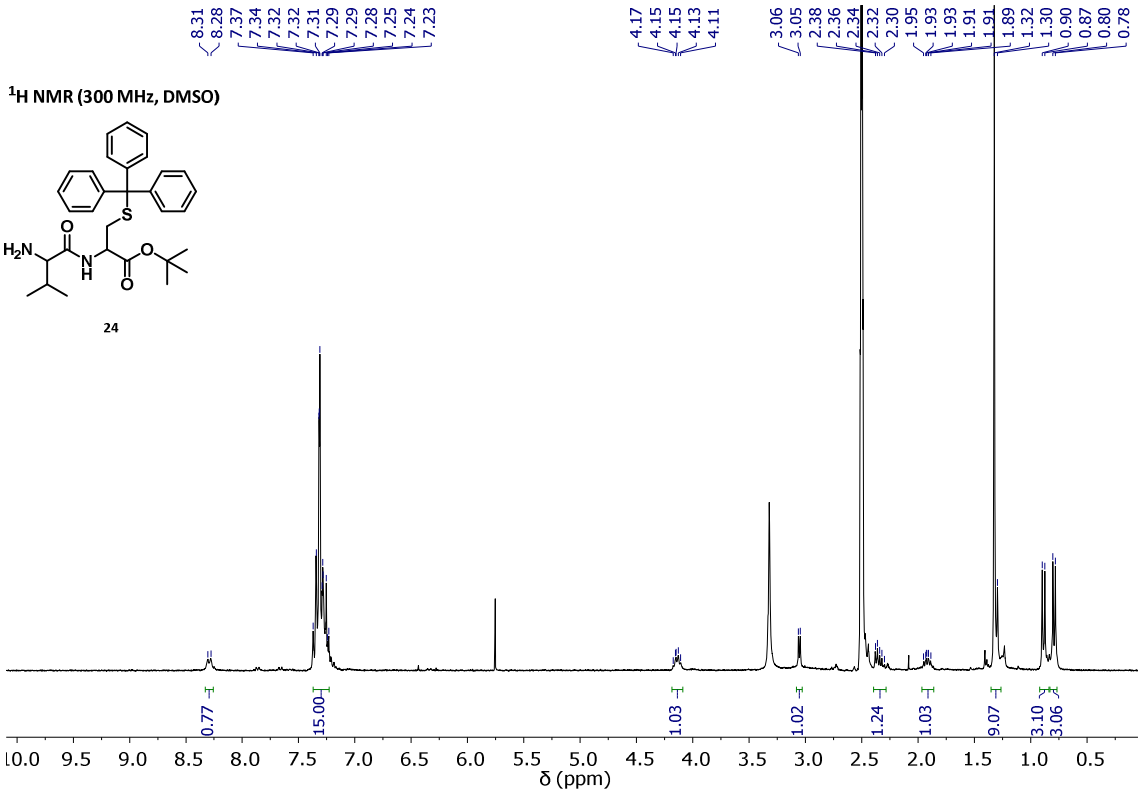

^{1}H NMR (300 MHz, DMSO)

24

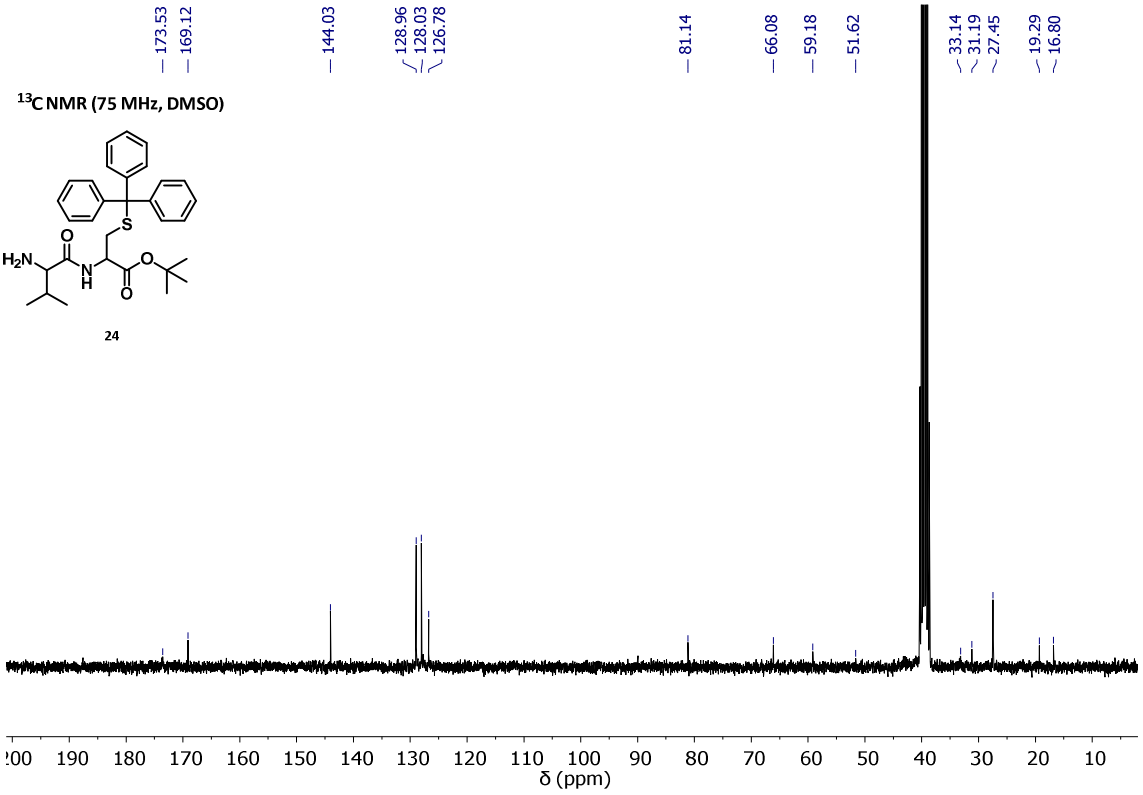

^{13}C NMR (75 MHz, DMSO)

24

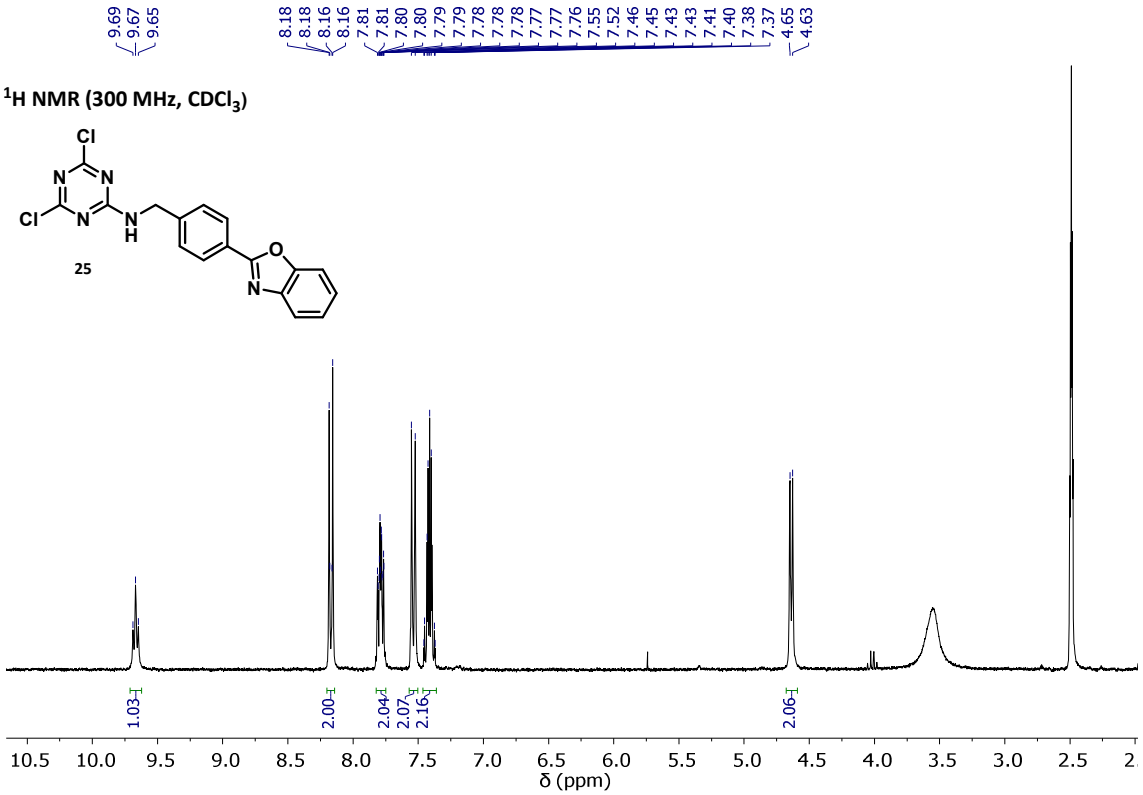
9.69
9.67
9.65
8.18
8.18
8.16
8.16
7.81
7.81
7.80
7.80
7.79
7.79
7.78
7.78
7.78
7.77
7.77
7.76
7.55
7.52
7.46
7.45
7.43
7.43
7.41
7.40
7.38
7.37
4.65
4.63
1H NMR (300 MHz, CDCl3)
Cl
N
N
Cl
N
N
H
O
N
25
1.03
2.00
2.04
2.07
2.16
2.06
10.5
10.0
9.5
9.0
8.5
8.0
7.5
7.0
6.5
6.0
5.5
5.0
4.5
4.0
3.5
3.0
2.5
δ (ppm)

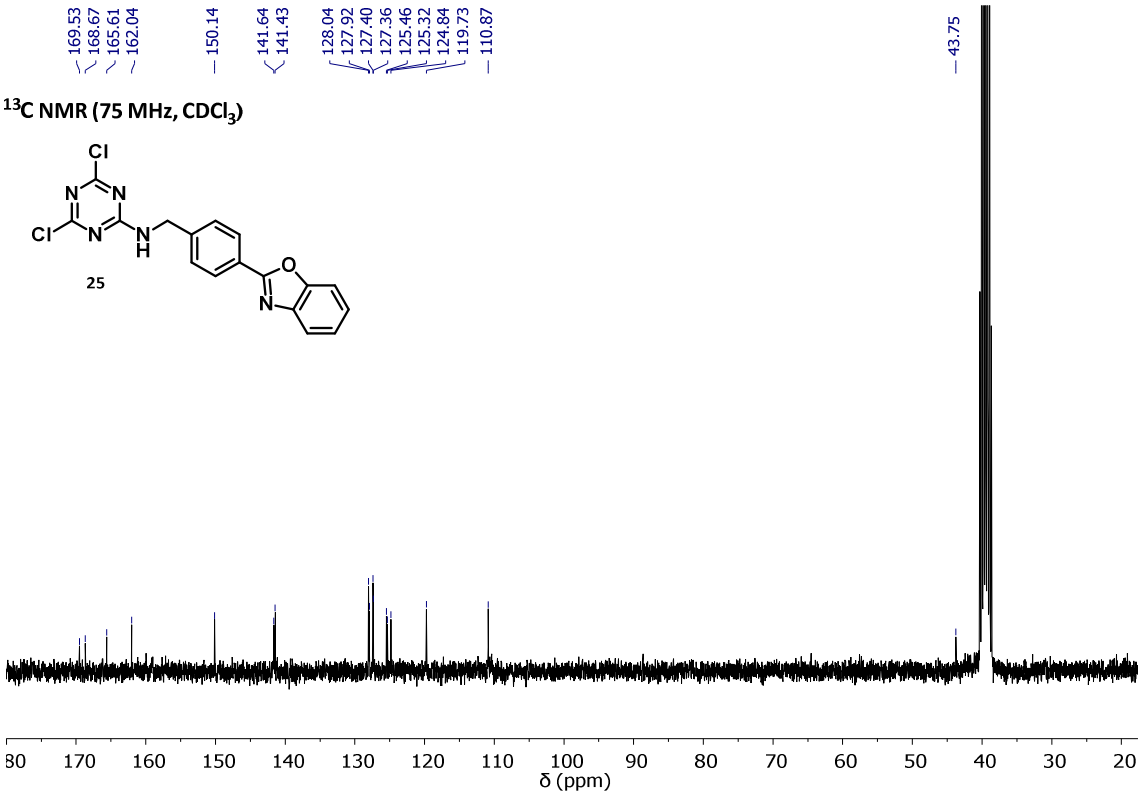
169.53
168.67
165.61
162.04
150.14
141.64
141.43
128.04
127.92
127.40
127.36
125.46
125.32
124.84
119.73
110.87
43.75
13C NMR (75 MHz, CDCl3)
Cl
N
N
Cl
N
N
H
O
N
25
80
170
160
150
140
130
120
110
100
90
80
70
60
50
40
30
20
δ (ppm)

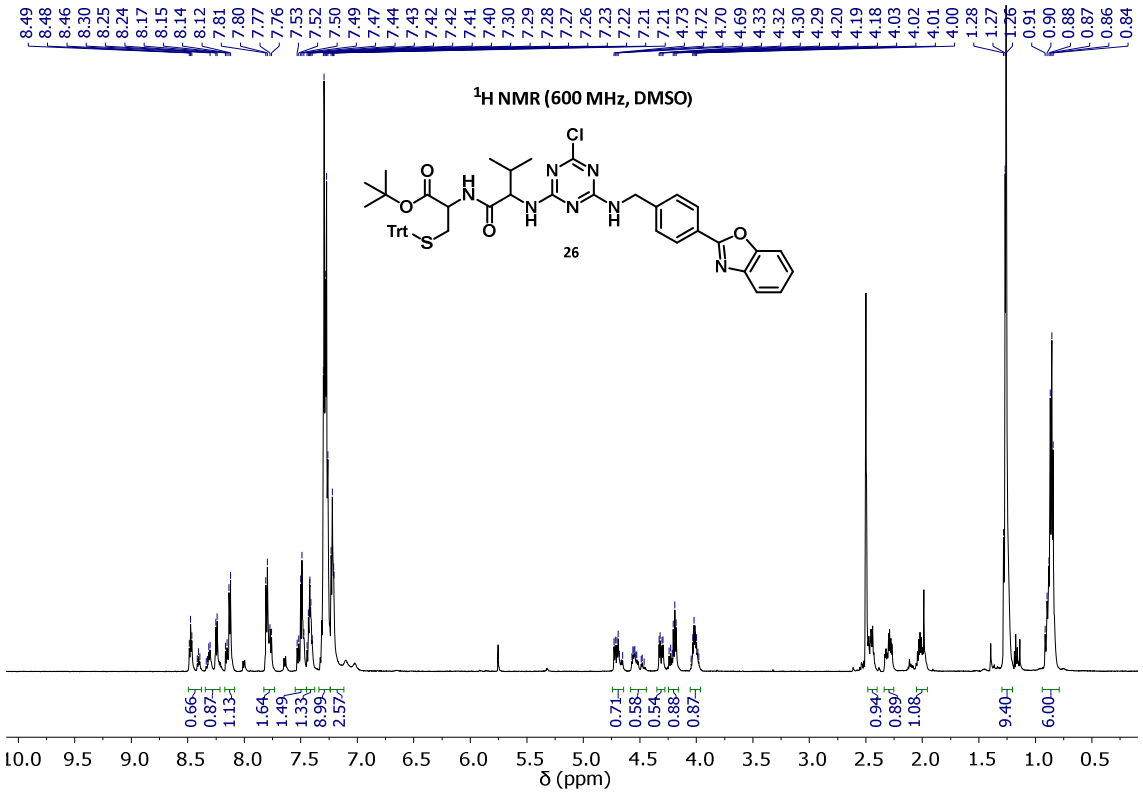
8.49 8.48 8.46 8.30 8.25 8.24 8.17 8.15 8.14 8.12 7.81 7.80 7.77 7.76 7.53 7.52 7.50 7.49 7.47 7.44 7.43 7.42 7.42 7.41 7.40 7.30 7.29 7.28 7.27 7.26 7.23 7.22 7.21 7.21 4.73 4.72 4.70 4.69 4.33 4.32 4.30 4.29 4.20 4.19 4.18 4.03 4.02 4.01 4.00 1.28 1.27 1.26 0.91 0.90 0.88 0.87 0.86 0.84
^{1}H NMR (600 MHz, DMSO)
Cl
Trt
S
26
0.66 0.87 1.13 1.64 1.49 1.33 8.99 2.57 0.71 0.58 0.54 0.88 0.87 0.94 0.89 1.08 9.40 6.00
10.0 9.5 9.0 8.5 8.0 7.5 7.0 6.5 6.0 5.5 5.0 4.5 4.0 3.5 3.0 2.5 2.0 1.5 1.0 0.5
δ (ppm)

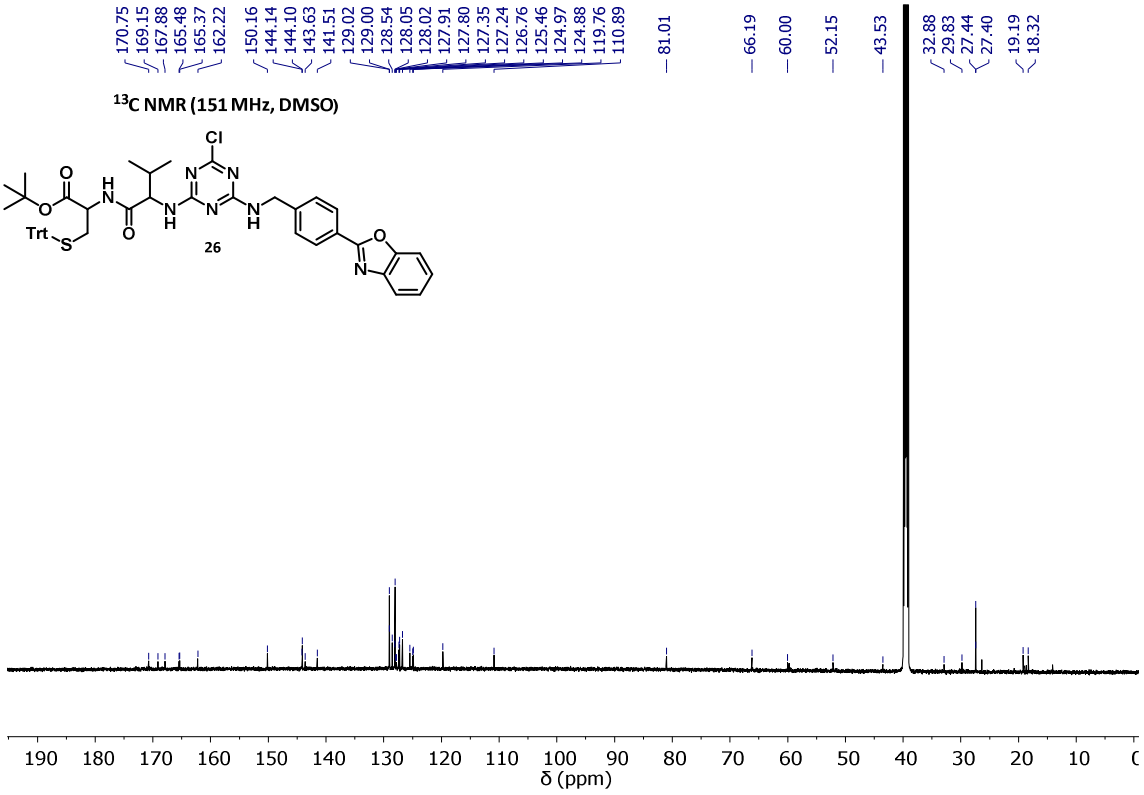
170.75 169.15 167.88 165.48 165.37 162.22 150.16 144.14 144.10 143.63 141.51 129.02 129.00 128.54 128.05 128.02 127.91 127.80 127.35 127.24 126.76 125.46 124.97 124.88 119.76 110.89 81.01 66.19 60.00 52.15 43.53 32.88 29.83 27.44 27.40 19.19 18.32
^{13}C NMR (151 MHz, DMSO)
Cl
Trt
S
26
190 180 170 160 150 140 130 120 110 100 90 80 70 60 50 40 30 20 10
δ (ppm)

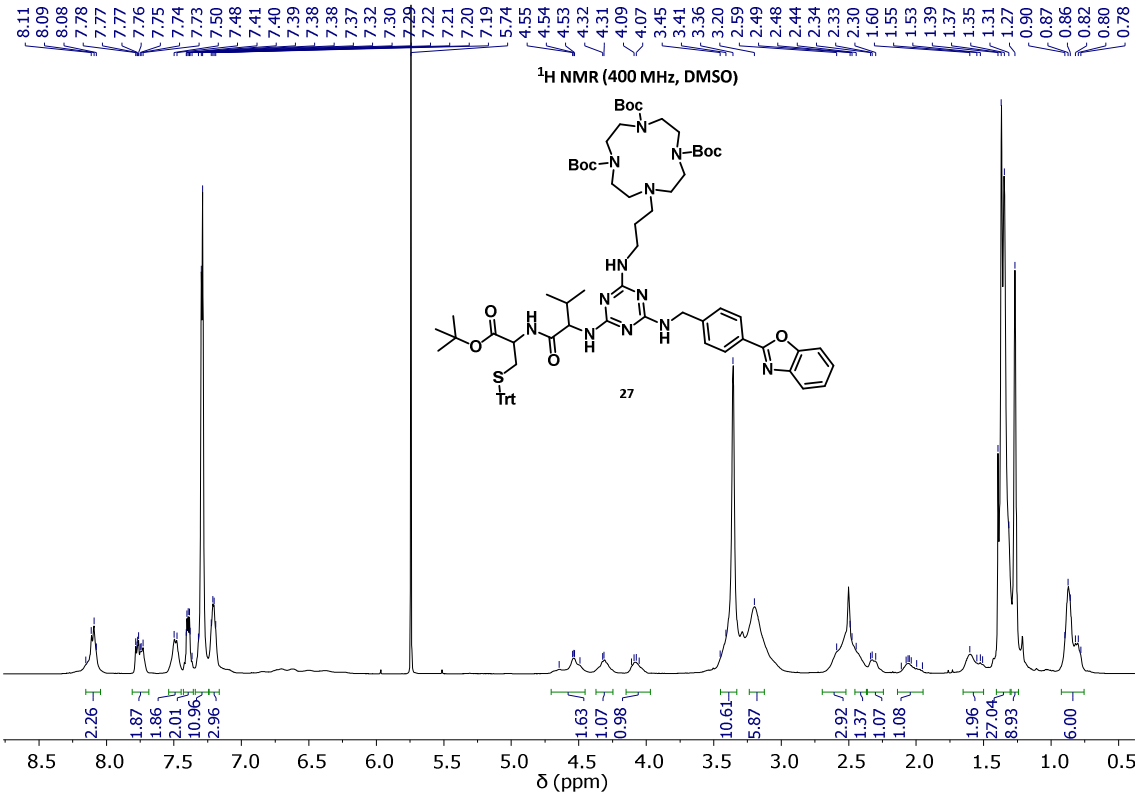
8.11 8.09 8.08 7.78 7.77 7.77 7.76 7.75 7.74 7.73 7.50 7.48 7.41 7.40 7.39 7.38 7.38 7.37 7.32 7.30 7.29 7.22 7.21 7.20 7.19 5.74 4.55 4.54 4.53 4.32 4.31 4.09 4.07 3.45 3.41 3.36 3.20 2.59 2.49 2.48 2.44 2.34 2.33 2.30 1.60 1.55 1.53 1.39 1.37 1.35 1.31 1.27 0.90 0.87 0.86 0.82 0.80 0.78
^{1}H NMR (400 MHz, DMSO)
Boc
Boc–N
N–Boc
HN
27
2.26 1.87 1.86 2.01 10.96 2.96 1.63 1.07 0.98 10.61 5.87 2.92 1.37 1.07 1.08 1.96 27.04 8.93 6.00
8.5 8.0 7.5 7.0 6.5 6.0 5.5 5.0 4.5 4.0 3.5 3.0 2.5 2.0 1.5 1.0 0.5
δ (ppm)

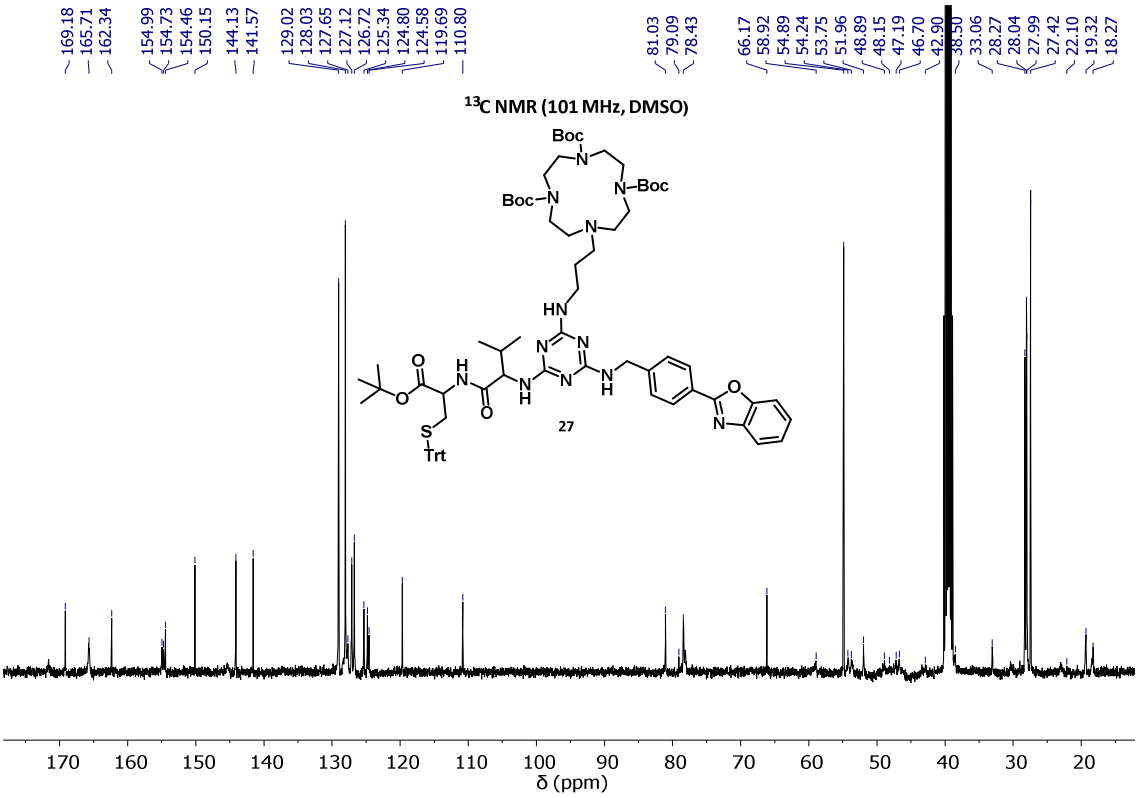
169.18 165.71 162.34 154.99 154.73 154.46 150.15 144.13 141.57 129.02 128.03 127.65 127.12 126.72 125.34 124.80 124.58 119.69 110.80 81.03 79.09 78.43 66.17 58.92 54.89 54.24 53.75 51.96 48.89 48.15 47.19 46.70 42.90 38.50 33.06 28.27 28.04 27.99 27.42 22.10 19.32 18.27
^{13}C NMR (101 MHz, DMSO)
Boc
Boc–N
N–Boc
HN
27
170 160 150 140 130 120 110 100 90 80 70 60 50 40 30 20
δ (ppm)

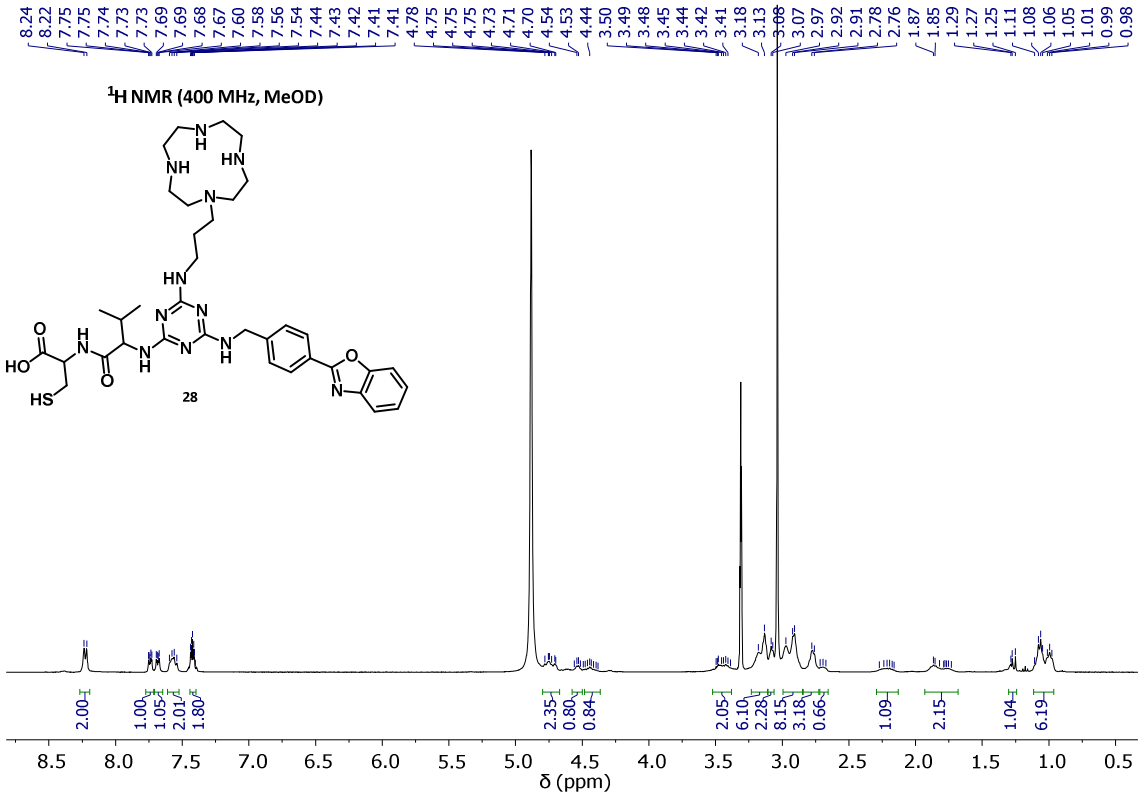
8.24 8.22 7.75 7.75 7.74 7.73 7.73 7.69 7.69 7.68 7.67 7.60 7.58 7.56 7.54 7.44 7.43 7.42 7.41 7.41 4.78 4.75 4.75 4.75 4.73 4.71 4.70 4.54 4.53 4.44 3.50 3.49 3.48 3.45 3.44 3.42 3.41 3.18 3.13 3.08 3.07 2.97 2.92 2.91 2.78 2.76 1.87 1.85 1.29 1.27 1.25 1.11 1.08 1.06 1.05 1.01 0.99 0.98
1H NMR (400 MHz, MeOD)
28
2.00 1.00 1.05 2.01 1.80 2.35 0.80 0.84 2.05 6.10 2.28 8.15 3.18 0.66 1.09 2.15 1.04 6.19
8.5 8.0 7.5 7.0 6.5 6.0 5.5 5.0 4.5 4.0 3.5 3.0 2.5 2.0 1.5 1.0 0.5
δ (ppm)

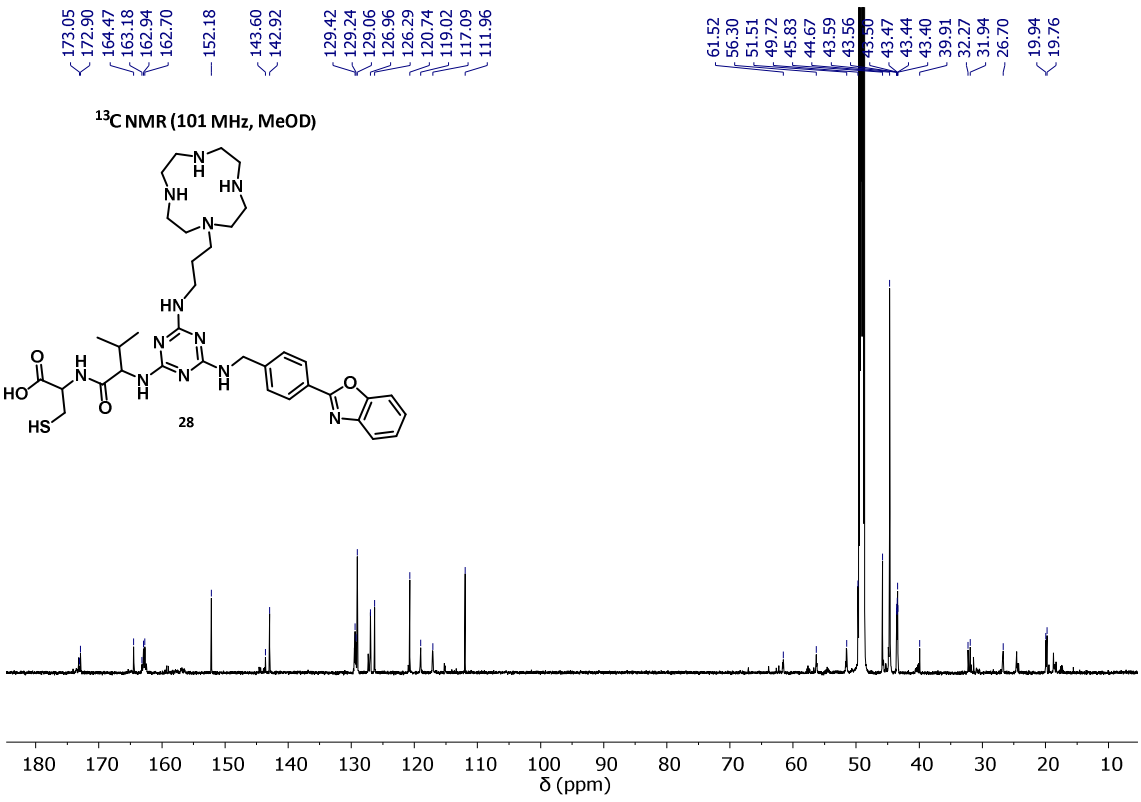
173.05 172.90 164.47 163.18 162.94 162.70 152.18 143.60 142.92 129.42 129.24 129.06 126.96 126.29 120.74 119.02 117.09 111.96
61.52 56.30 51.51 49.72 45.83 44.67 43.59 43.56 43.50 43.47 43.44 43.40 39.91 32.27 31.94 26.70 19.94 19.76
13C NMR (101 MHz, MeOD)
28
180 170 160 150 140 130 120 110 100 90 80 70 60 50 40 30 20 10
δ (ppm)

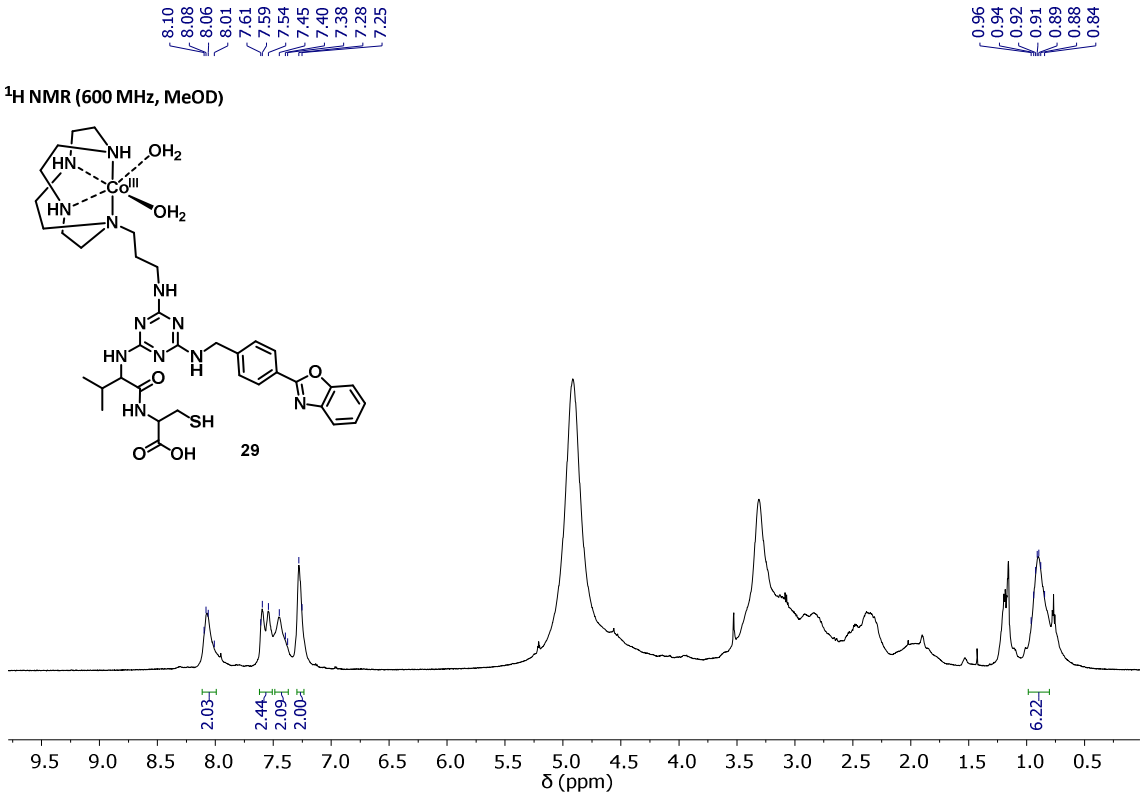
8.10
8.08
8.06
8.01
7.61
7.59
7.54
7.45
7.40
7.38
7.28
7.25
0.96
0.94
0.92
0.91
0.89
0.88
0.84
1H NMR (600 MHz, MeOD)
29
2.03
2.44
2.09
2.00
6.22
9.5 9.0 8.5 8.0 7.5 7.0 6.5 6.0 5.5 5.0 4.5 4.0 3.5 3.0 2.5 2.0 1.5 1.0 0.5
δ (ppm)

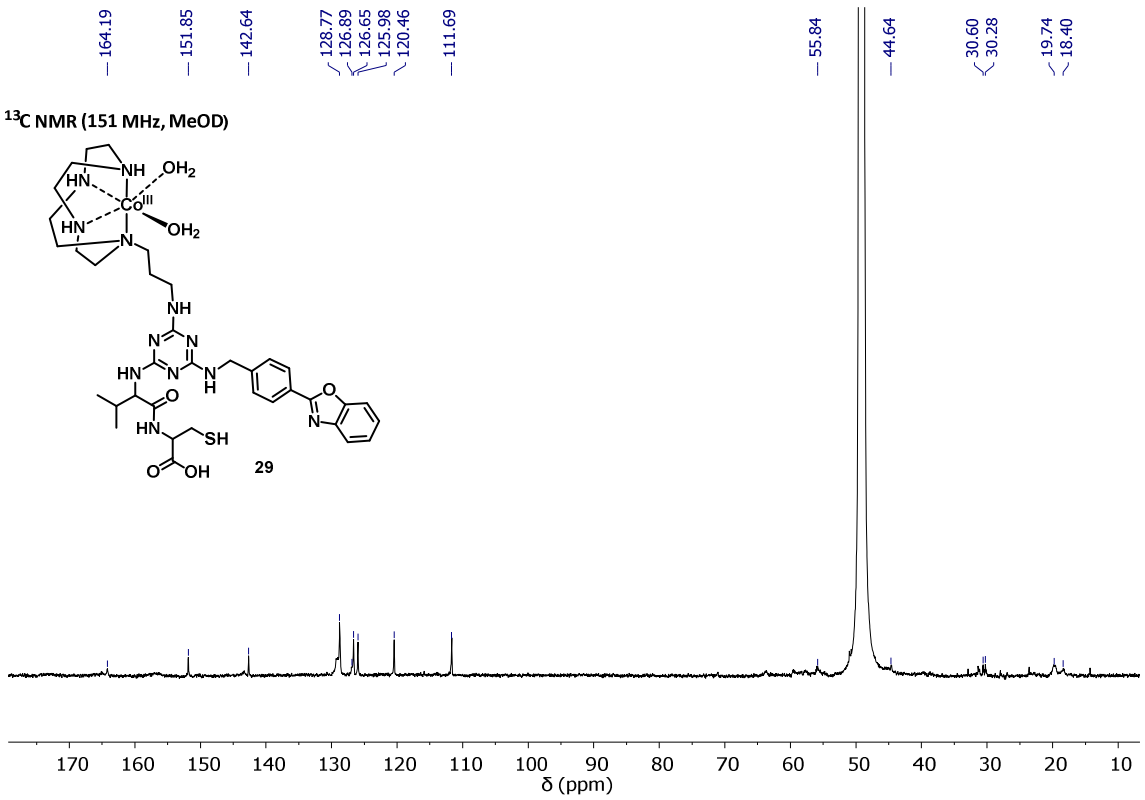
164.19
151.85
142.64
128.77
126.89
126.65
125.98
120.46
111.69
55.84
44.64
30.60
30.28
19.74
18.40
13C NMR (151 MHz, MeOD)
29
170 160 150 140 130 120 110 100 90 80 70 60 50 40 30 20 10
δ (ppm)

^{1}H NMR (300 MHz, DMSO)

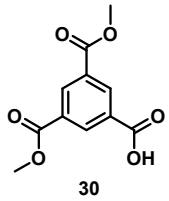

30

^{13}C NMR (75 MHz, DMSO)

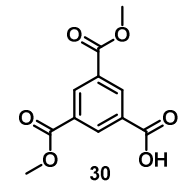

30

^{1}H NMR (300 MHz, DMSO)

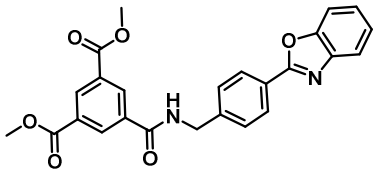

31

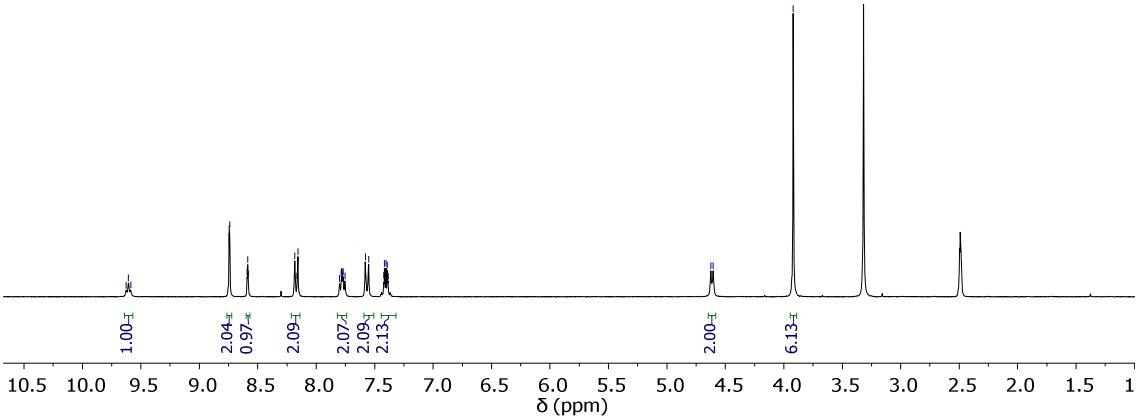

^{13}C NMR (75 MHz, DMSO)

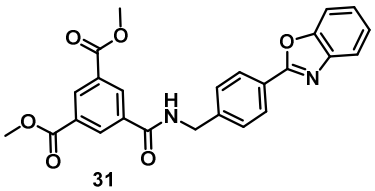

31

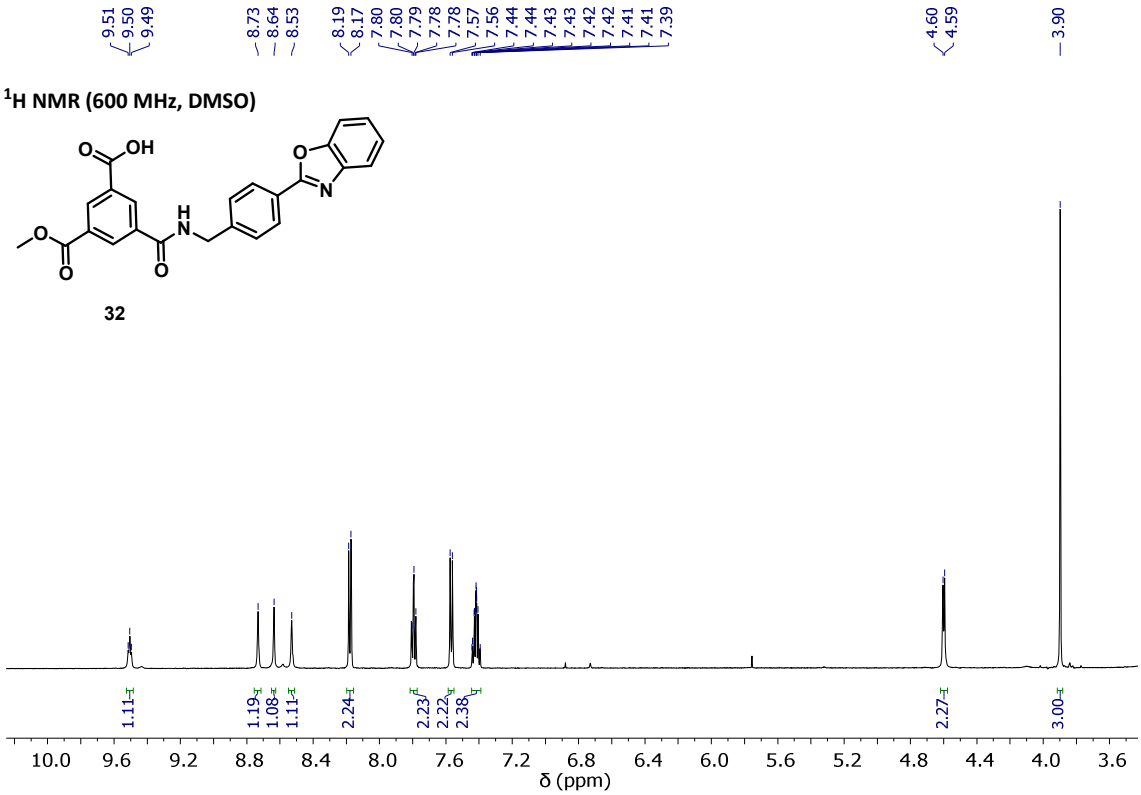

^{1}H NMR (600 MHz, DMSO)

32

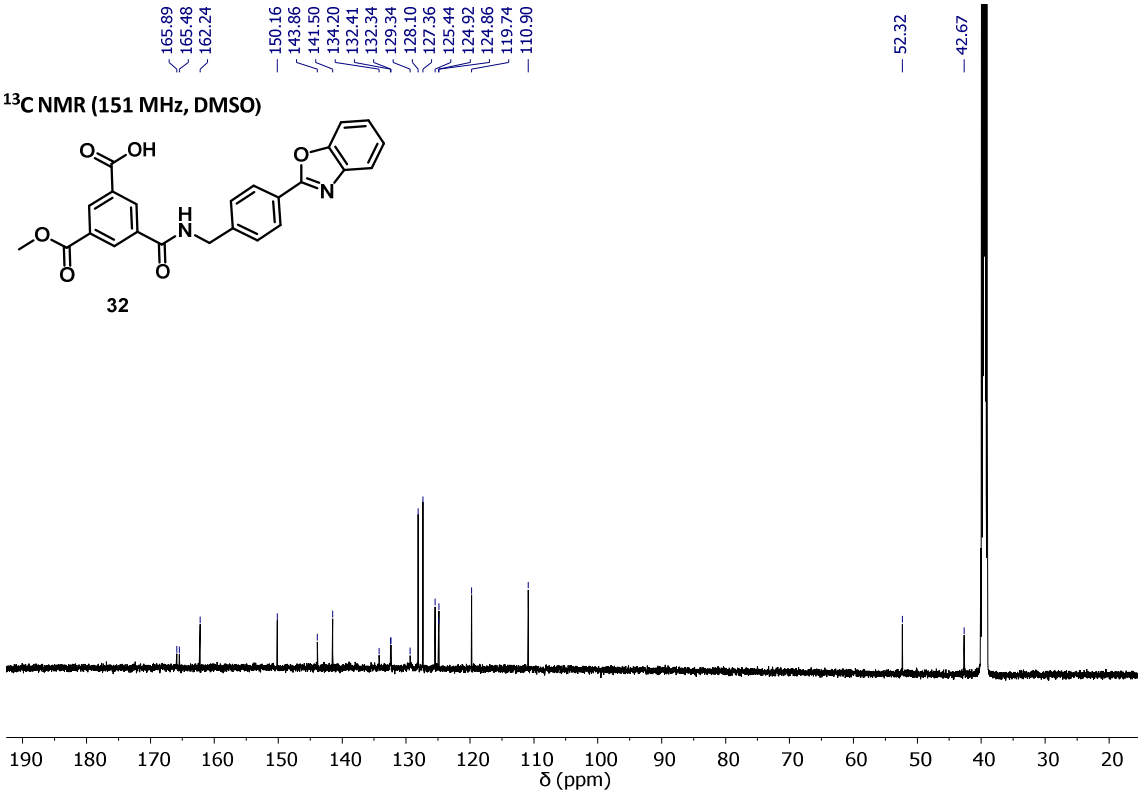

^{13}C NMR (151 MHz, DMSO)

32

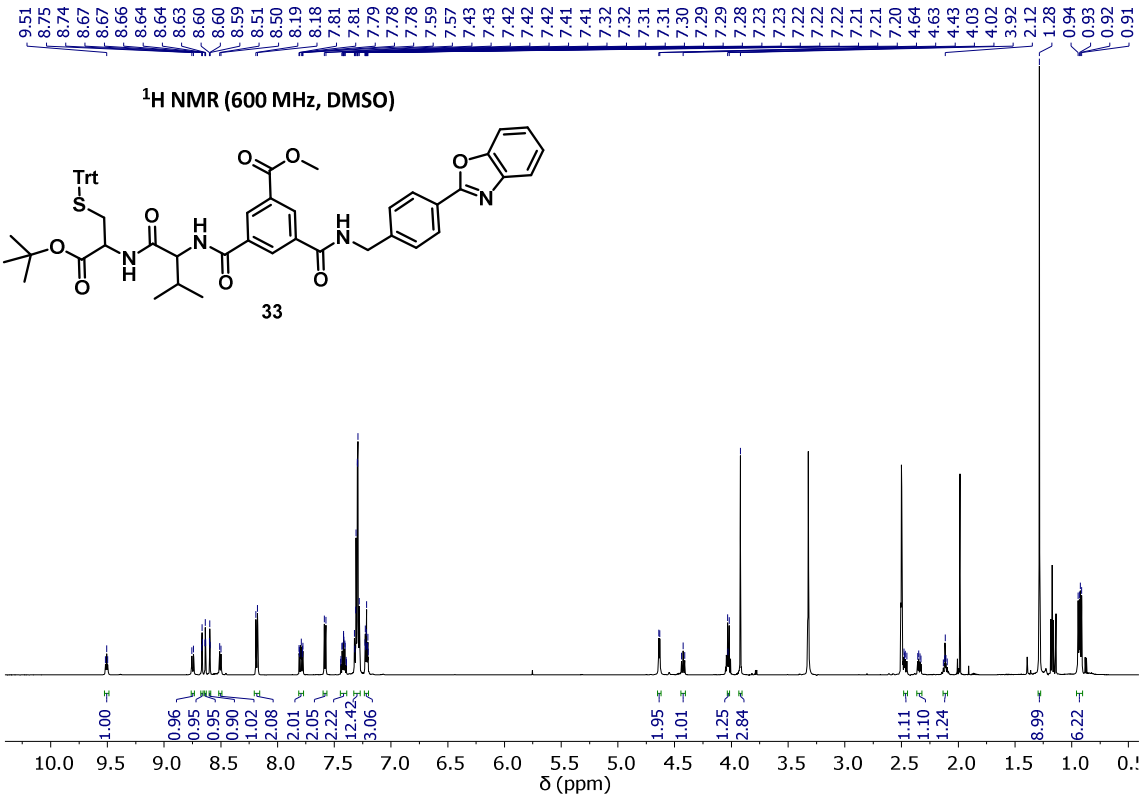
9.51 8.75 8.74 8.67 8.67 8.66 8.64 8.64 8.63 8.60 8.60 8.59 8.51 8.50 8.19 8.18 7.81 7.81 7.79 7.78 7.78 7.59 7.57 7.43 7.43 7.42 7.42 7.42 7.41 7.41 7.32 7.32 7.31 7.31 7.30 7.29 7.29 7.28 7.23 7.23 7.22 7.22 7.21 7.21 7.20 4.64 4.63 4.43 4.03 4.02 3.92 2.12 1.28 0.94 0.93 0.92 0.91
1H NMR (600 MHz, DMSO)
Trt
S
O
O
N
H
O
H
N
O
O
O
N
H
O
O
33
1.00 0.96 0.95 0.95 0.90 1.02 2.08 2.01 2.05 2.22 12.42 3.06 1.95 1.01 1.25 2.84 1.11 1.10 1.24 8.99 6.22
10.0 9.5 9.0 8.5 8.0 7.5 7.0 6.5 6.0 5.5 5.0 4.5 4.0 3.5 3.0 2.5 2.0 1.5 1.0
δ (ppm)

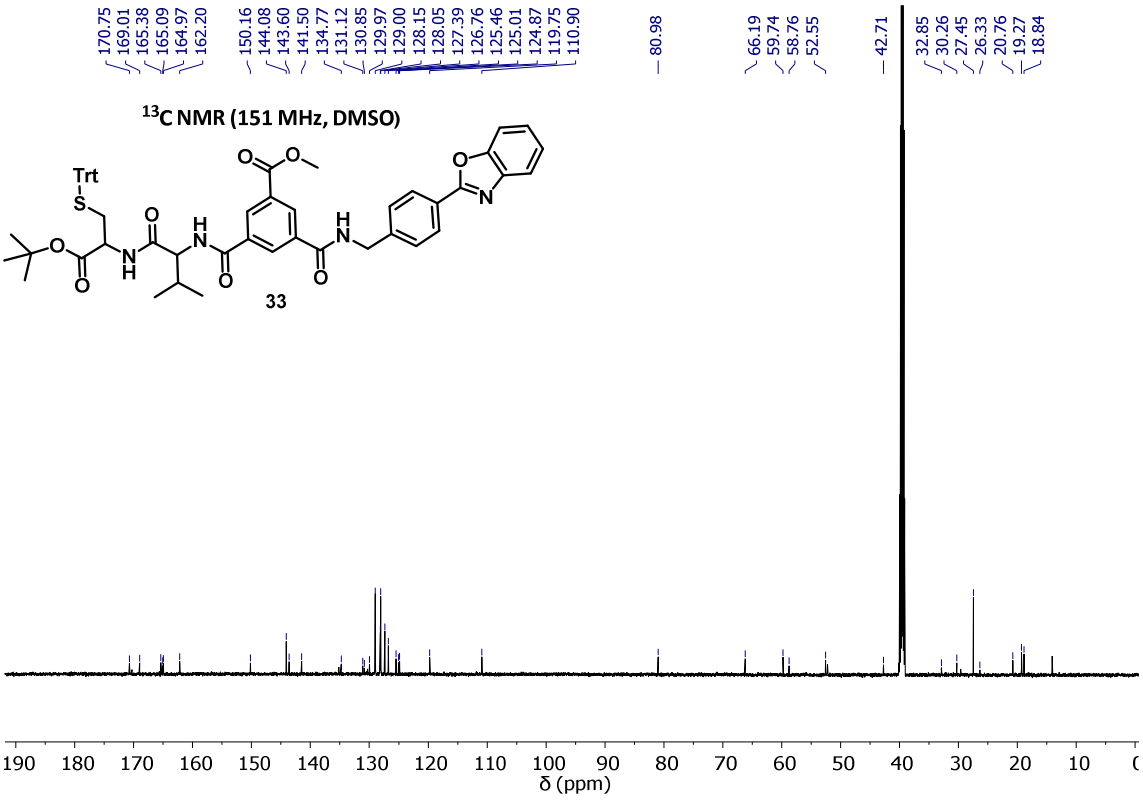
170.75 169.01 165.38 165.09 164.97 162.20 150.16 144.08 143.60 141.50 134.77 131.12 130.85 129.97 129.00 128.15 128.05 127.39 126.76 125.46 125.01 124.87 119.75 110.90 80.98 66.19 59.74 58.76 52.55 42.71 32.85 30.26 27.45 26.33 20.76 19.27 18.84
13C NMR (151 MHz, DMSO)
Trt
S
O
O
N
H
O
H
N
O
O
O
N
H
O
O
33
190 180 170 160 150 140 130 120 110 100 90 80 70 60 50 40 30 20 10
δ (ppm)

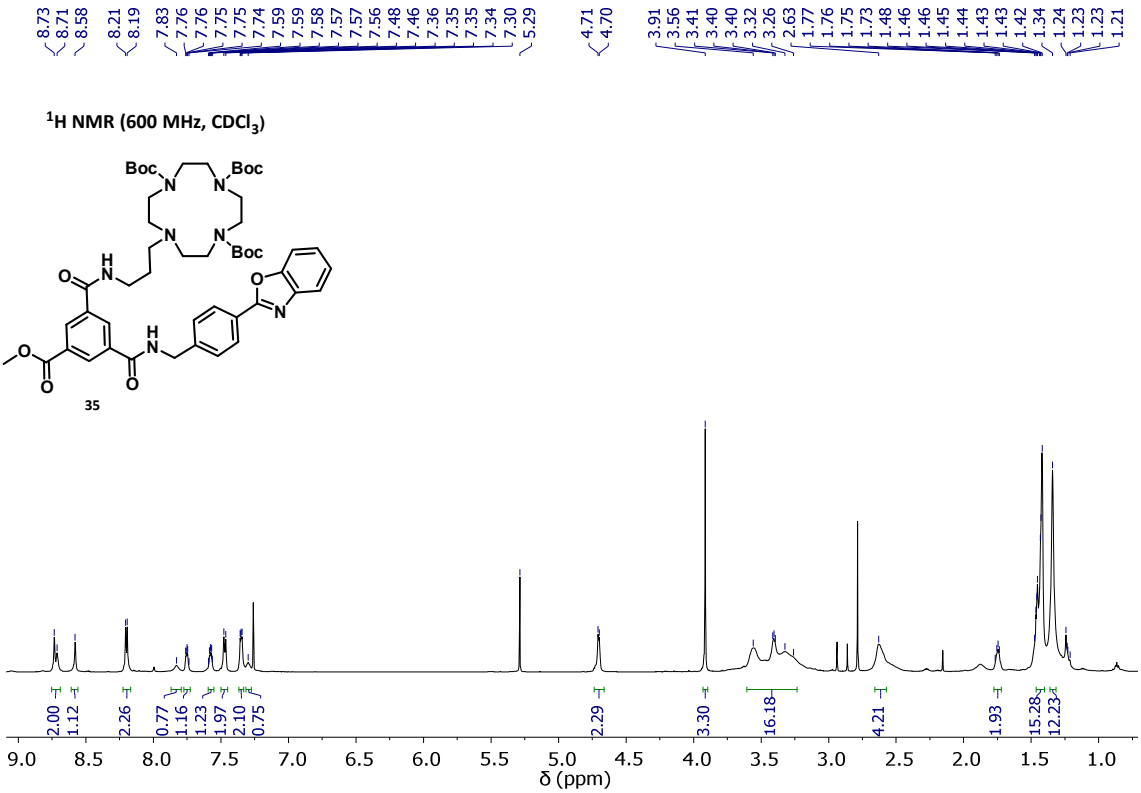
8.73 8.71 8.58 8.21 8.19 7.83 7.76 7.76 7.75 7.75 7.74 7.59 7.59 7.58 7.57 7.57 7.56 7.48 7.46 7.36 7.35 7.35 7.34 7.30 5.29 4.71 4.70 3.91 3.56 3.41 3.40 3.40 3.32 3.26 2.63 1.77 1.76 1.75 1.73 1.48 1.46 1.46 1.45 1.44 1.43 1.43 1.42 1.34 1.24 1.23 1.23 1.21
^{1}H NMR (600 MHz, CDCl$_3$)
Boc
Boc
Boc
35
2.00 1.12 2.26 0.77 1.16 1.23 1.97 2.10 0.75 2.29 3.30 16.18 4.21 1.93 15.28 12.23
9.0 8.5 8.0 7.5 7.0 6.5 6.0 5.5 5.0 4.5 4.0 3.5 3.0 2.5 2.0 1.5 1.0
δ (ppm)

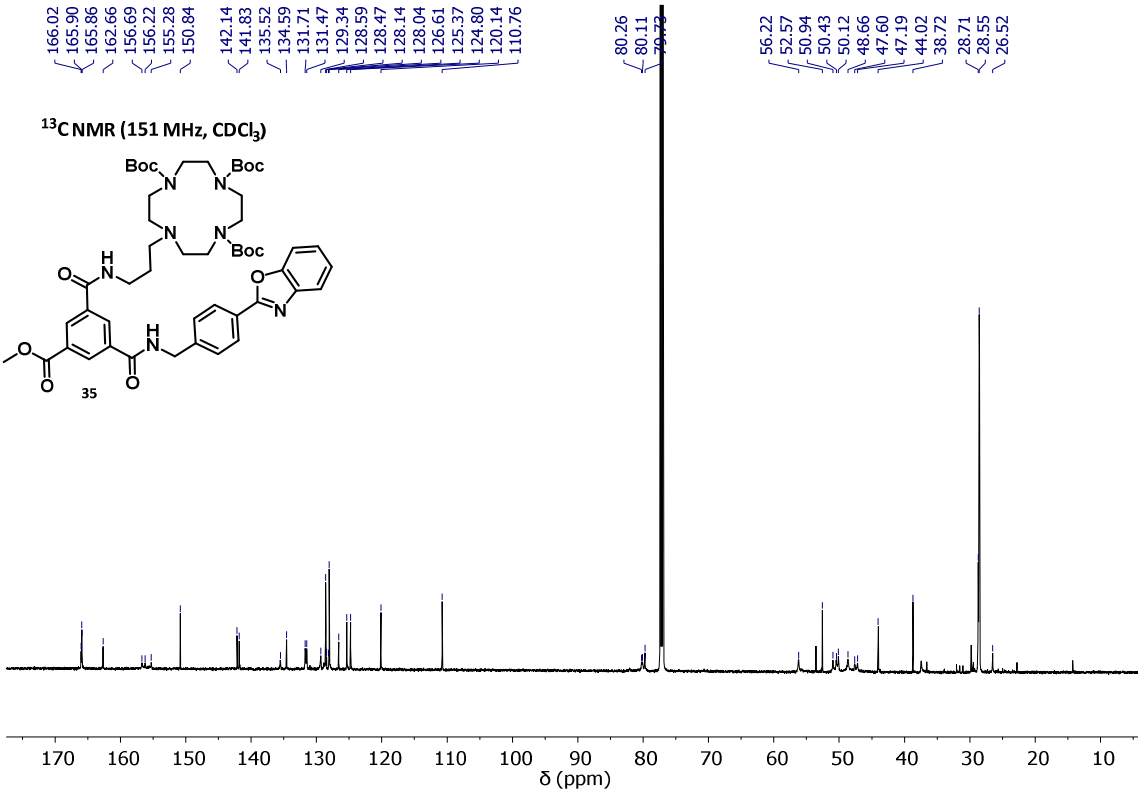
166.02 165.90 165.86 162.66 156.69 156.22 155.28 150.84 142.14 141.83 135.52 134.59 131.71 131.47 129.34 128.59 128.47 128.14 128.04 126.61 125.37 124.80 120.14 110.76 80.26 80.11 79.73 56.22 52.57 50.94 50.43 50.12 48.66 47.60 47.19 44.02 38.72 28.71 28.55 26.52
^{13}C NMR (151 MHz, CDCl$_3$)
Boc
Boc
Boc
35
170 160 150 140 130 120 110 100 90 80 70 60 50 40 30 20 10
δ (ppm)

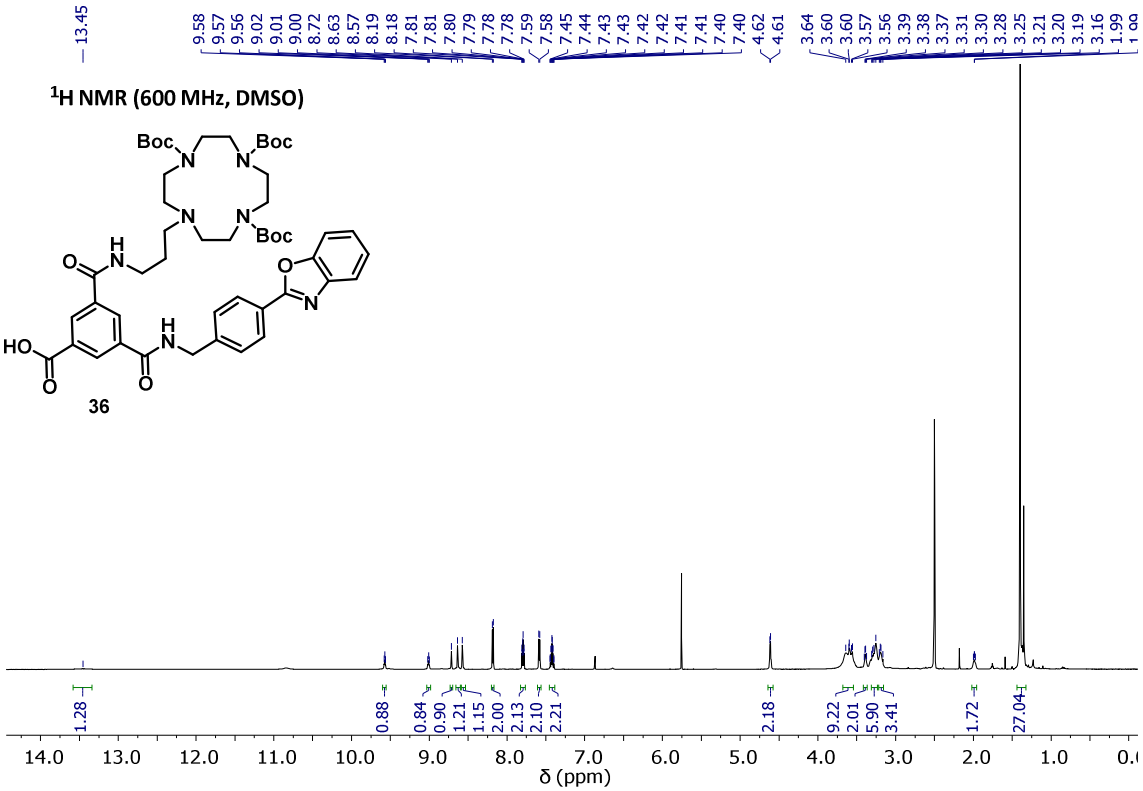
13.45
9.58 9.57 9.56 9.02 9.01 9.00 8.72 8.63 8.57 8.19 8.18 7.81 7.81 7.80 7.79 7.78 7.78 7.59 7.58 7.45 7.44 7.43 7.43 7.42 7.42 7.41 7.41 7.40 7.40 4.62 4.61 3.64 3.60 3.60 3.57 3.56 3.39 3.38 3.37 3.31 3.30 3.28 3.25 3.21 3.20 3.19 3.16 1.99
1H NMR (600 MHz, DMSO)
Boc
Boc
Boc
Boc
HO
36
1.28 0.88 0.84 0.90 1.21 1.15 2.00 2.13 2.10 2.21 2.18 9.22 2.01 5.90 3.41 1.72 27.04
14.0 13.0 12.0 11.0 10.0 9.0 8.0 7.0 6.0 5.0 4.0 3.0 2.0 1.0
δ (ppm)

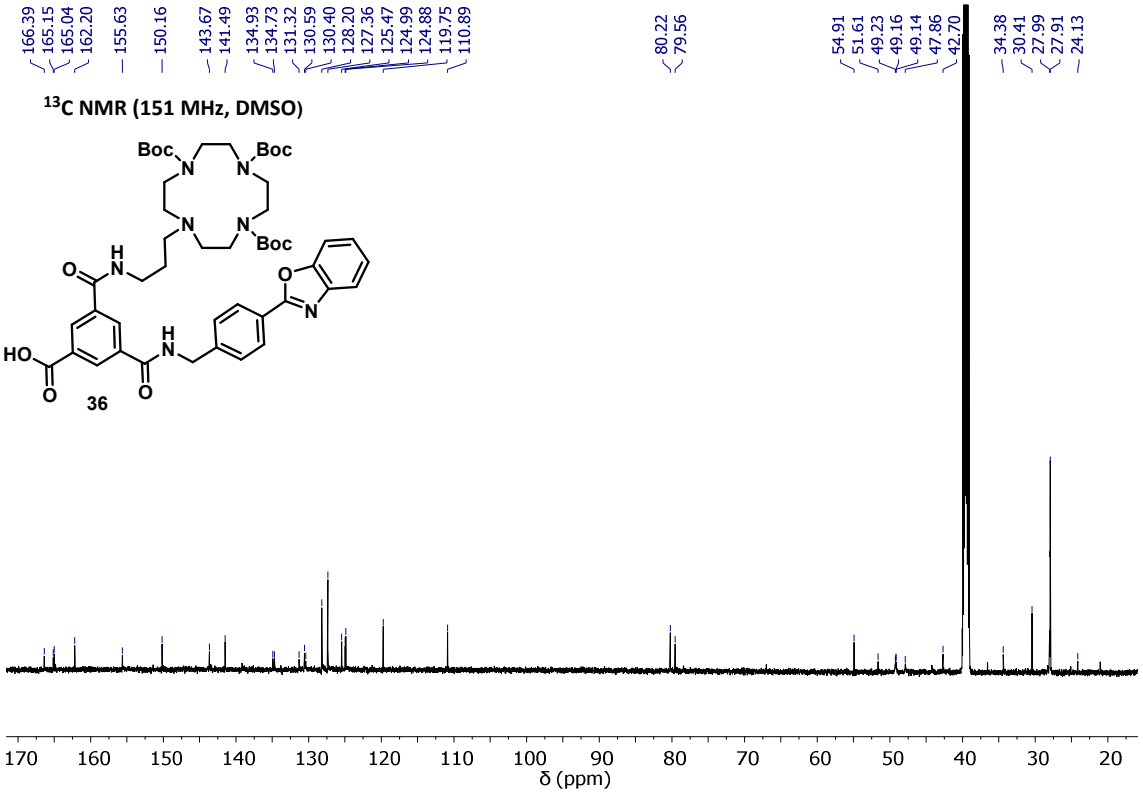
166.39 165.15 165.04 162.20 155.63 150.16 143.67 141.49 134.93 134.73 131.32 130.59 130.40 128.20 127.36 125.47 124.99 124.88 119.75 110.89
80.22 79.56
54.91 51.61 49.23 49.16 49.14 47.86 42.70
34.38 30.41 27.99 27.91 24.13
13C NMR (151 MHz, DMSO)
Boc
Boc
Boc
Boc
HO
36
170 160 150 140 130 120 110 100 90 80 70 60 50 40 30 20
δ (ppm)

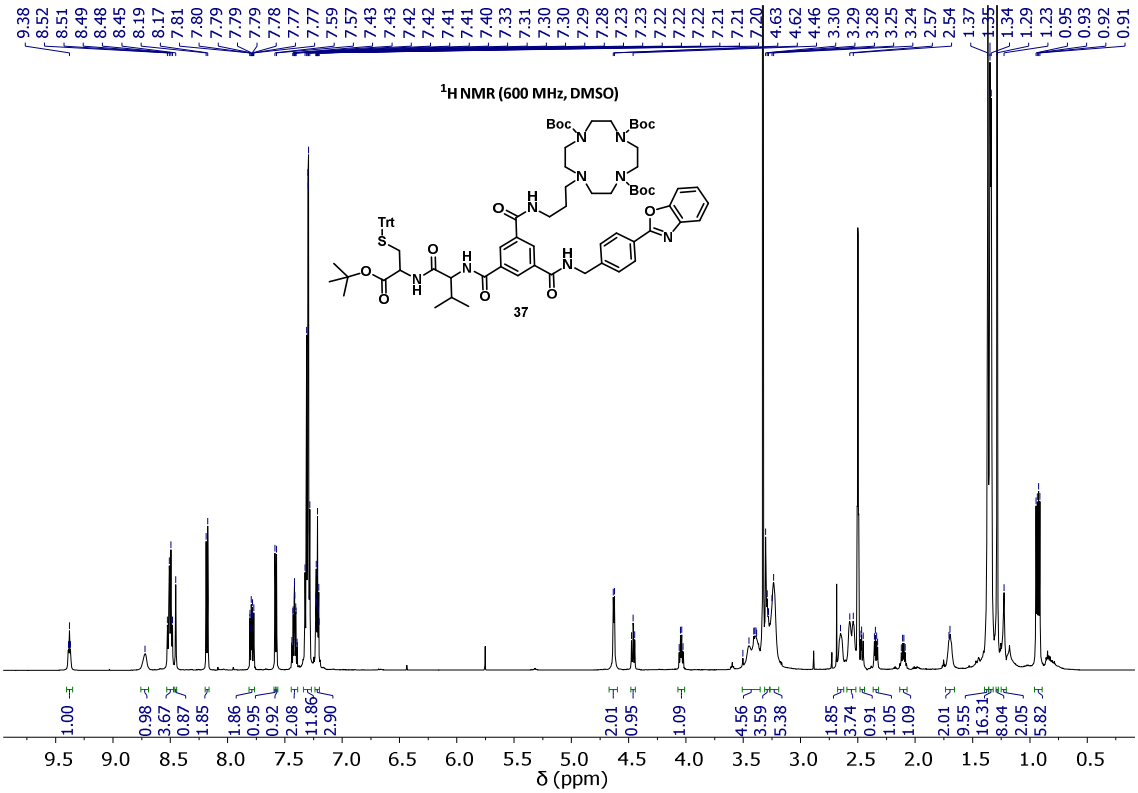
^{1}H NMR (600 MHz, DMSO)
37
δ (ppm)

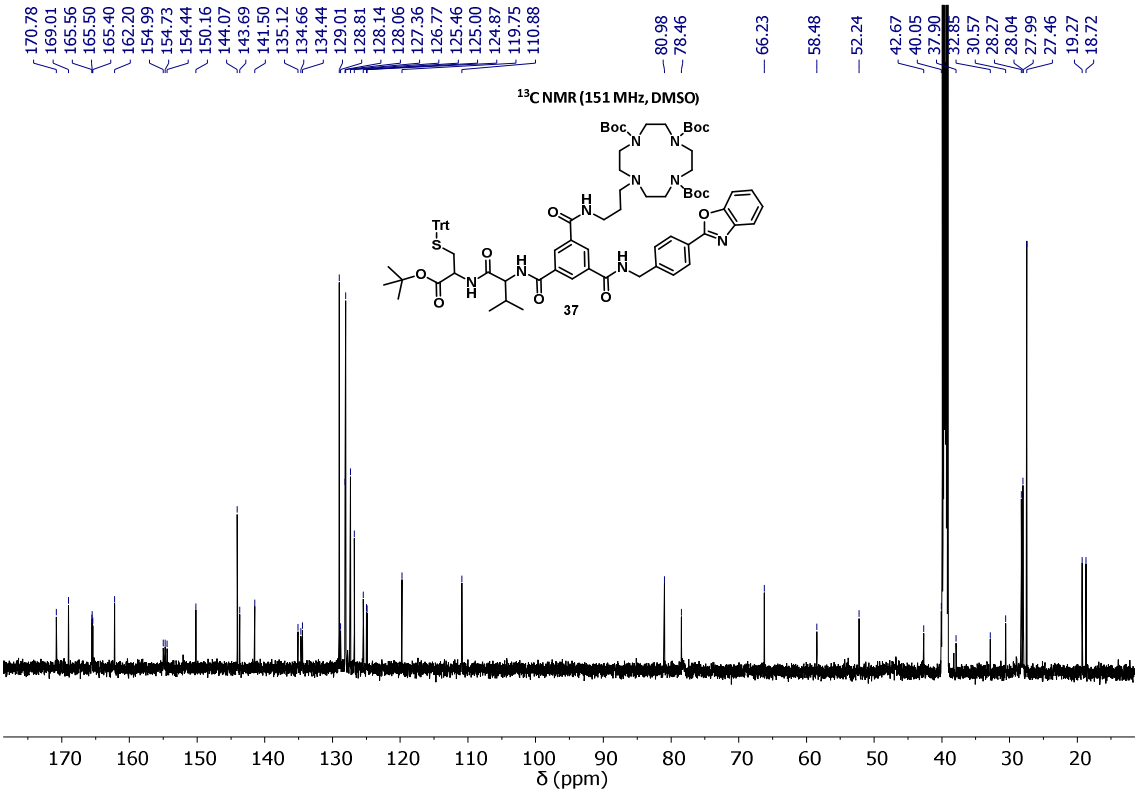
^{13}C NMR (151 MHz, DMSO)
37
δ (ppm)

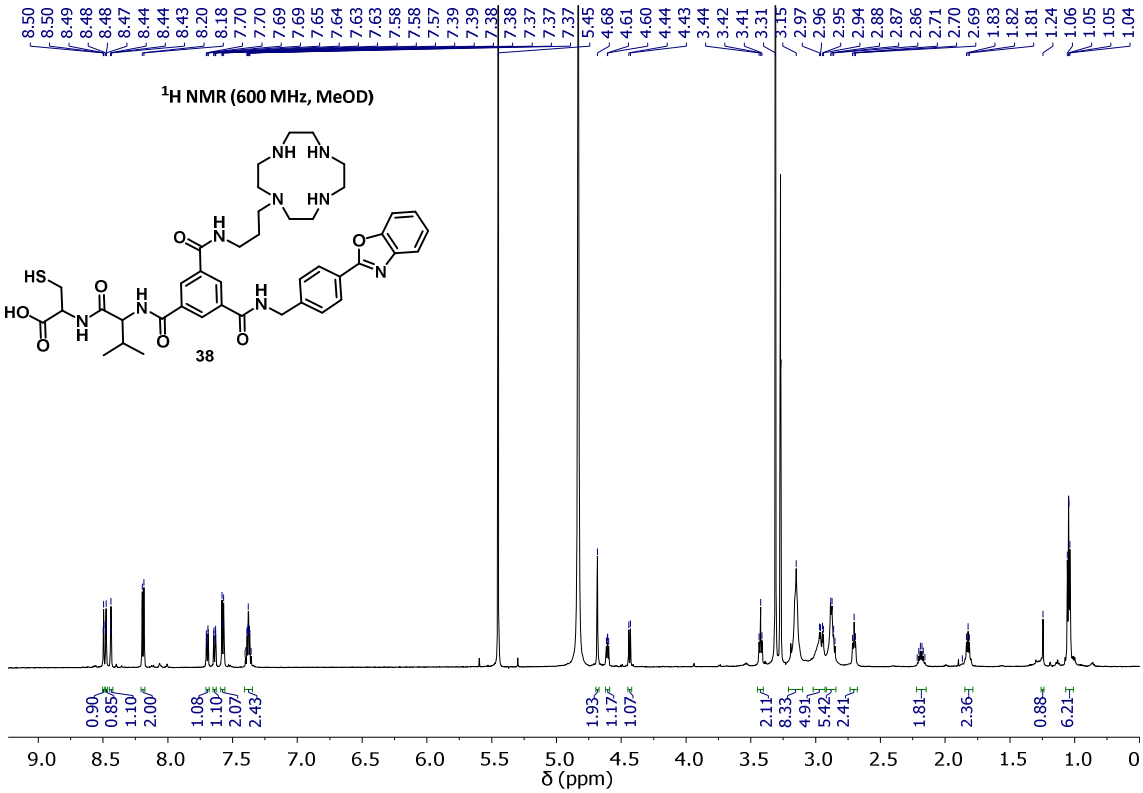
^{1}H NMR (600 MHz, MeOD)
38
δ (ppm)

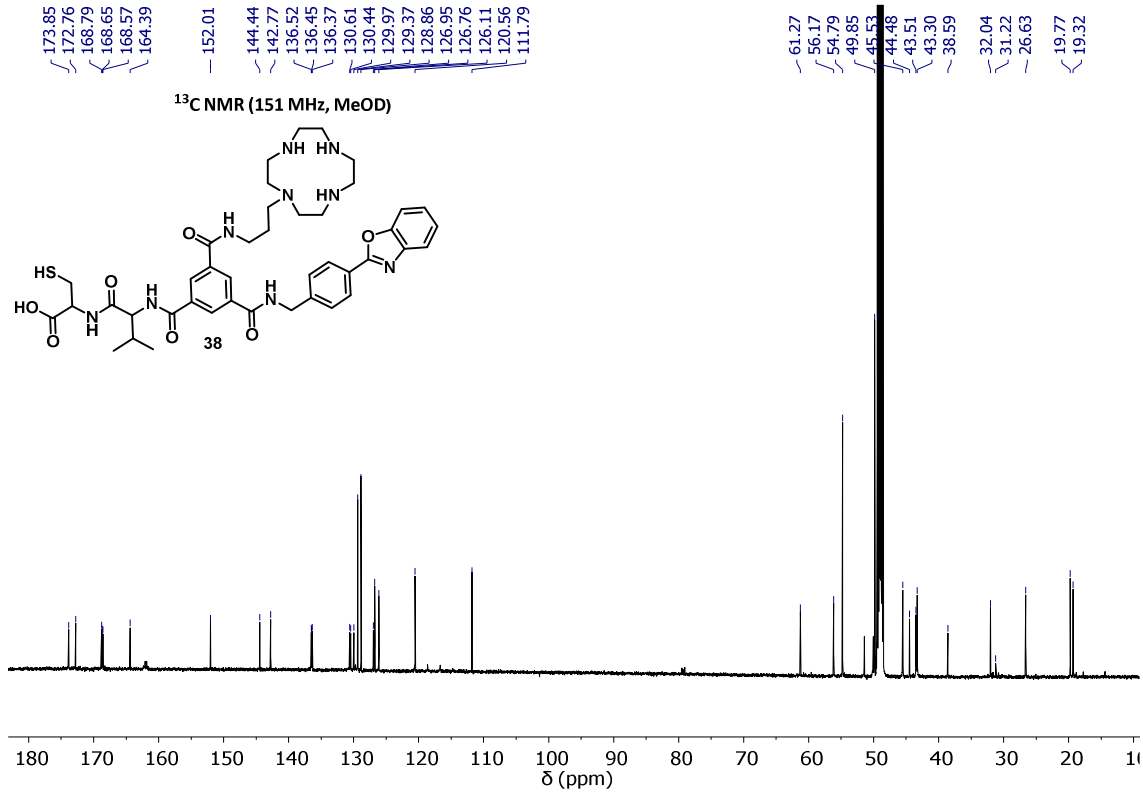
^{13}C NMR (151 MHz, MeOD)
38
δ (ppm)

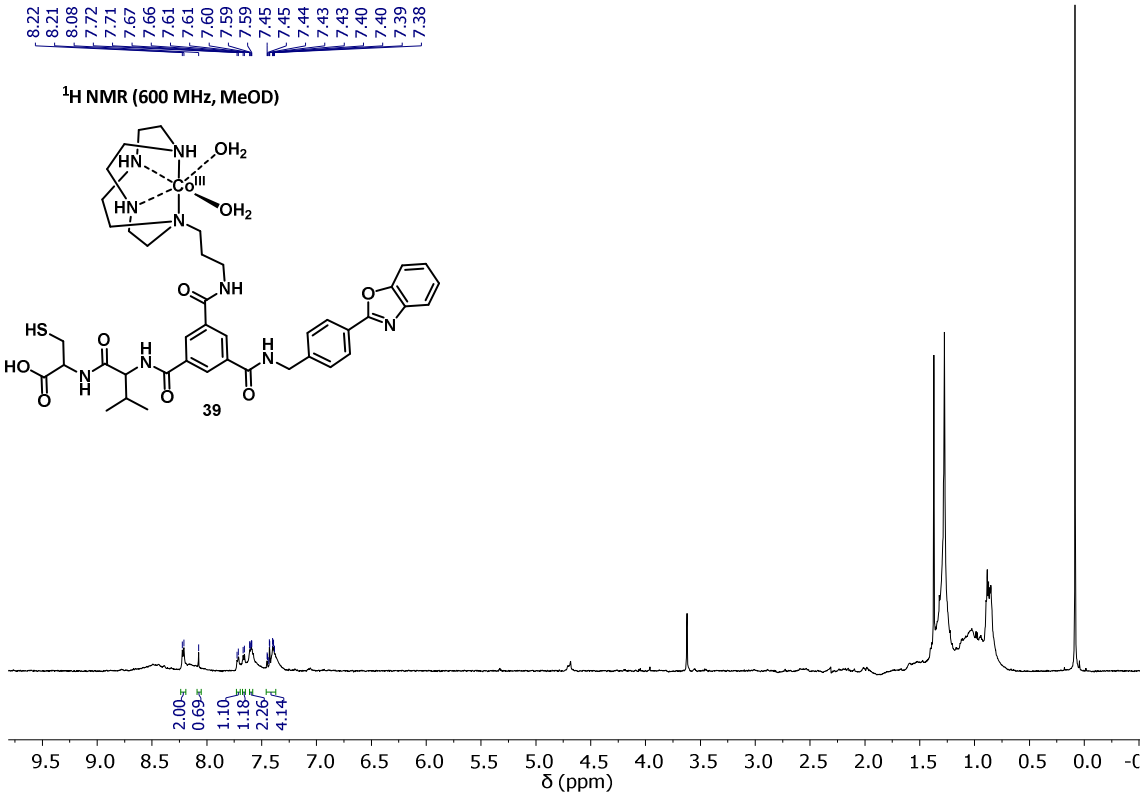

^{1}H NMR (600 MHz, MeOD)

39

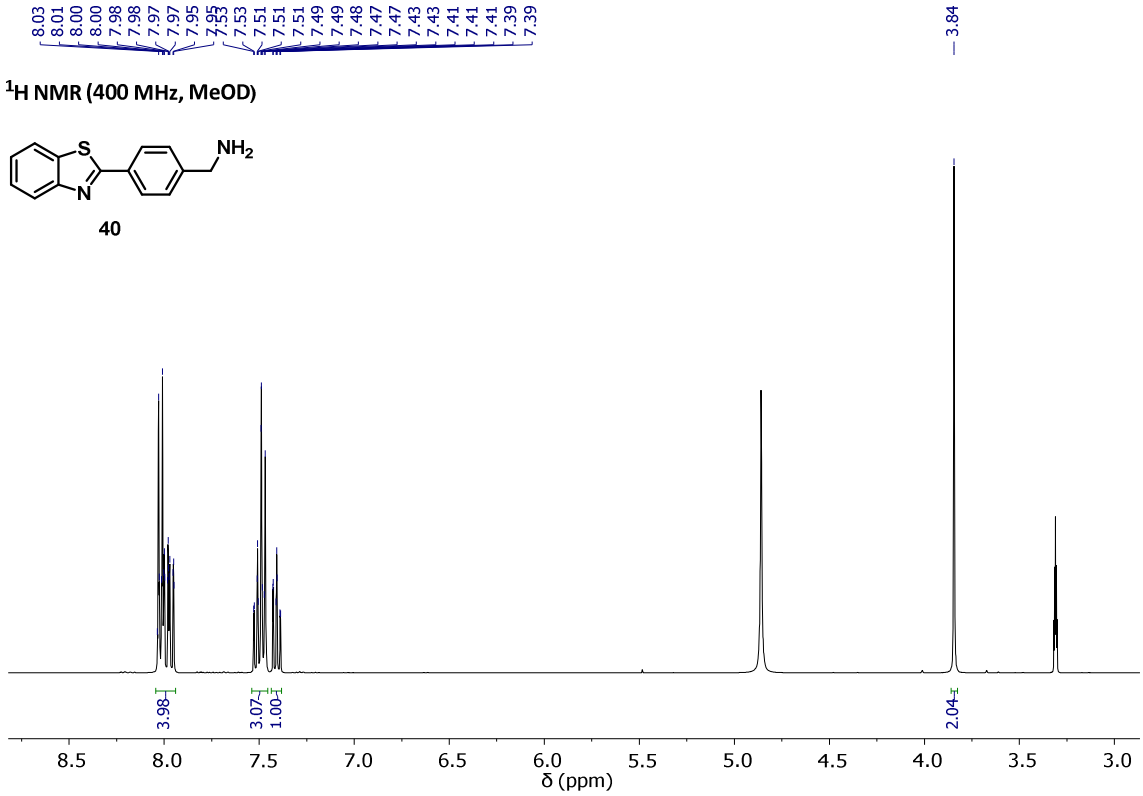

^{1}H NMR (400 MHz, MeOD)

40

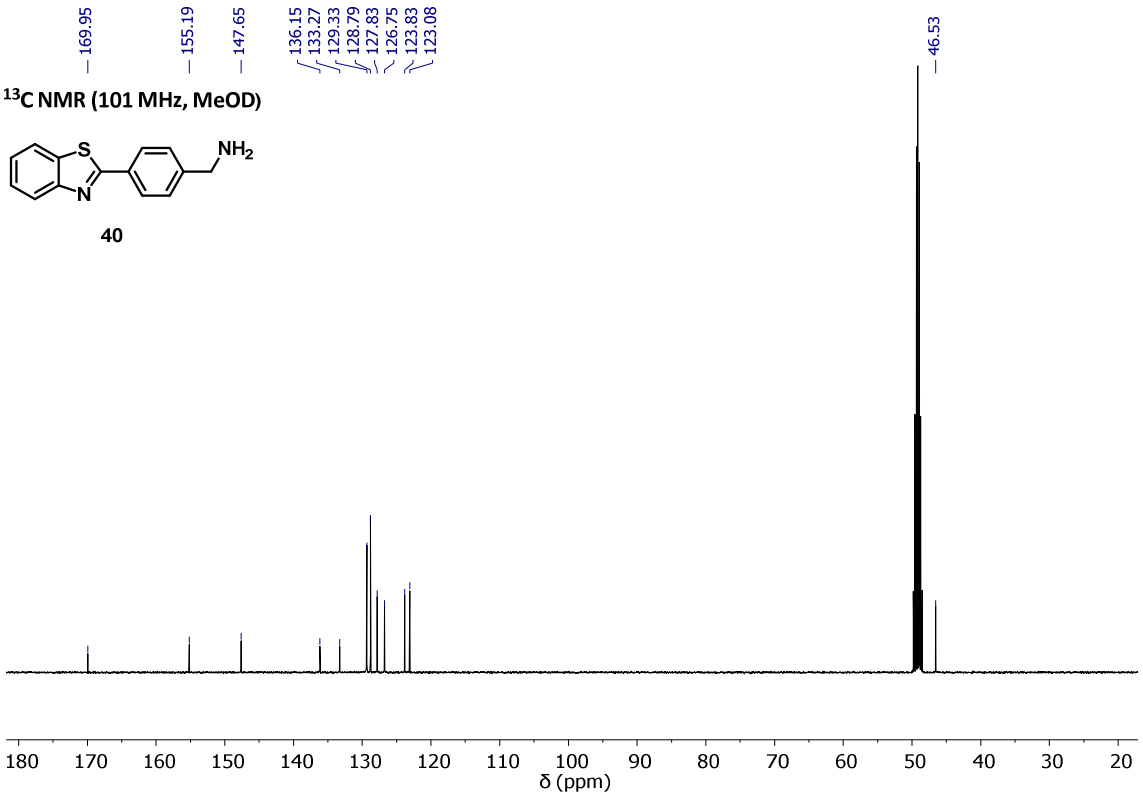

^{13}C NMR (101 MHz, MeOD)

40

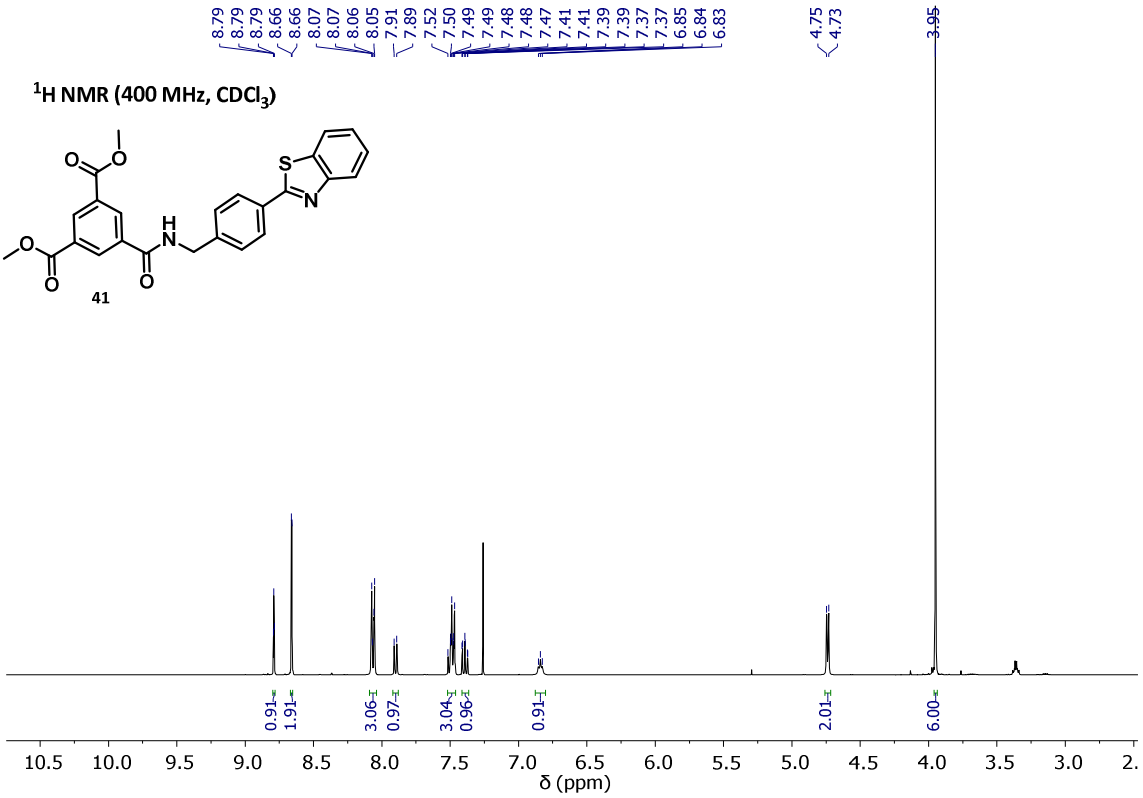

^{1}H NMR (400 MHz, $CDCl_3$)

41

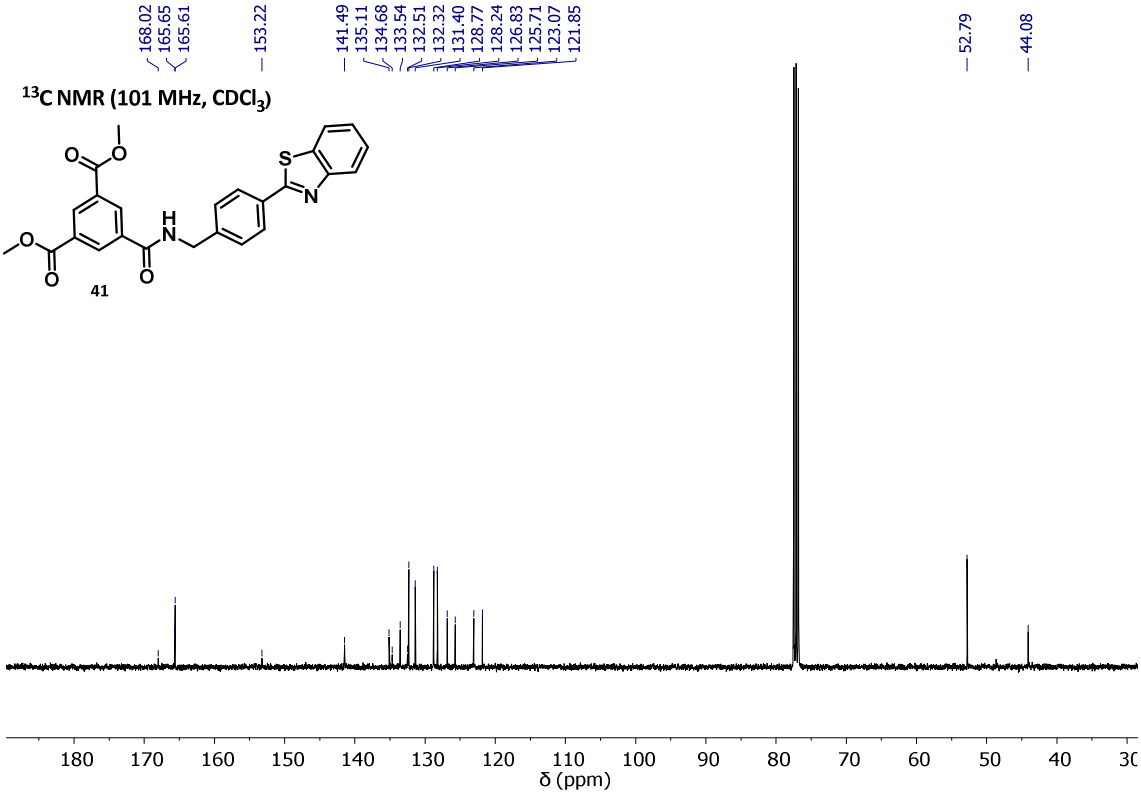
168.02
165.65
165.61
153.22
141.49
135.11
134.68
133.54
132.51
132.32
131.40
128.77
128.24
126.83
125.71
123.07
121.85
52.79
44.08
13C NMR (101 MHz, CDCl3)
41
δ (ppm)

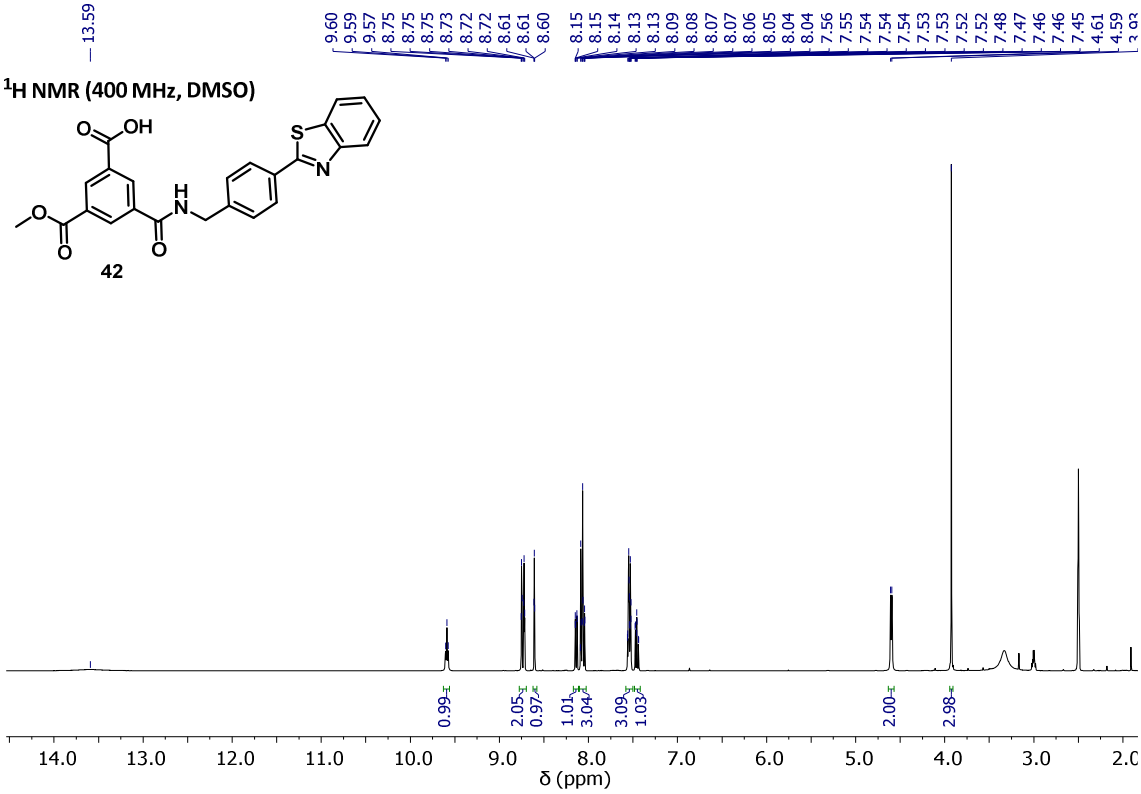
13.59
9.60
9.59
9.57
8.75
8.75
8.75
8.73
8.72
8.72
8.61
8.61
8.60
8.15
8.15
8.14
8.13
8.13
8.09
8.08
8.07
8.07
8.06
8.05
8.04
8.04
7.56
7.55
7.54
7.54
7.53
7.53
7.52
7.52
7.48
7.47
7.46
7.46
7.45
4.61
4.59
1H NMR (400 MHz, DMSO)
42
0.99
2.05
0.97
1.01
3.04
3.09
1.03
2.00
2.98
δ (ppm)

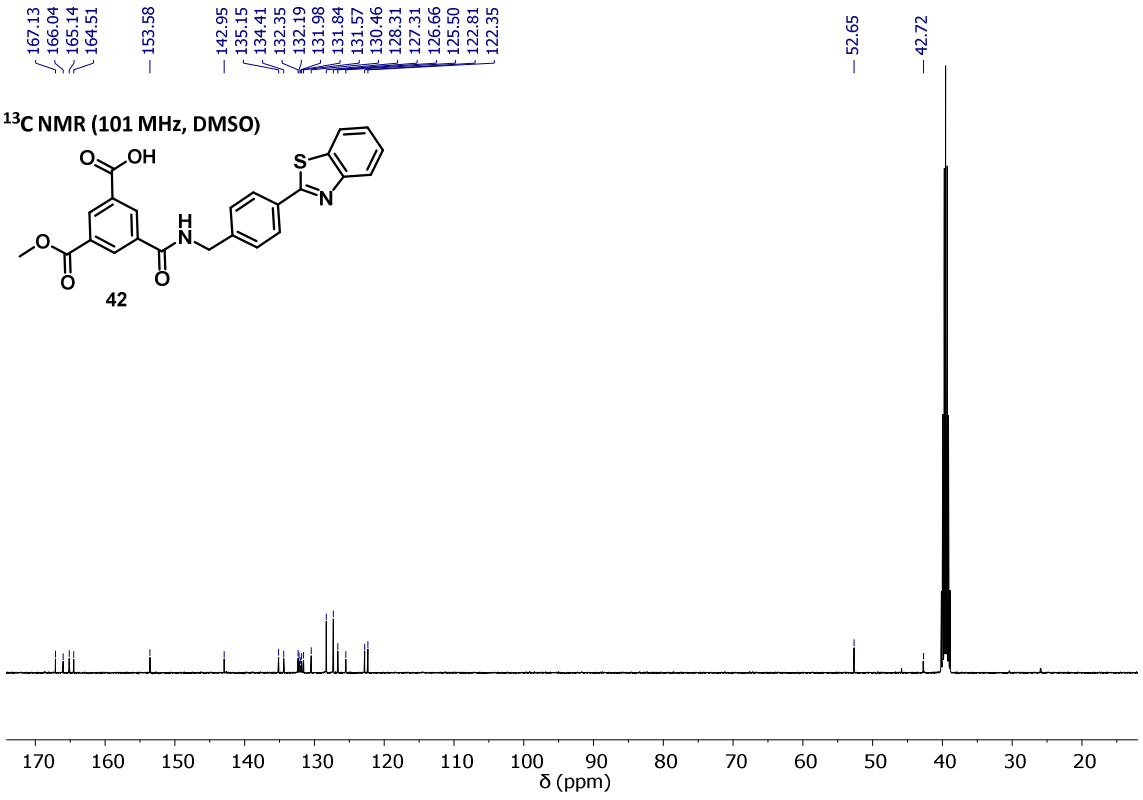
167.13
166.04
165.14
164.51
153.58
142.95
135.15
134.41
132.35
132.19
131.98
131.84
131.57
130.46
128.31
127.31
126.66
125.50
122.81
122.35
52.65
42.72
13C NMR (101 MHz, DMSO)
42
δ (ppm)

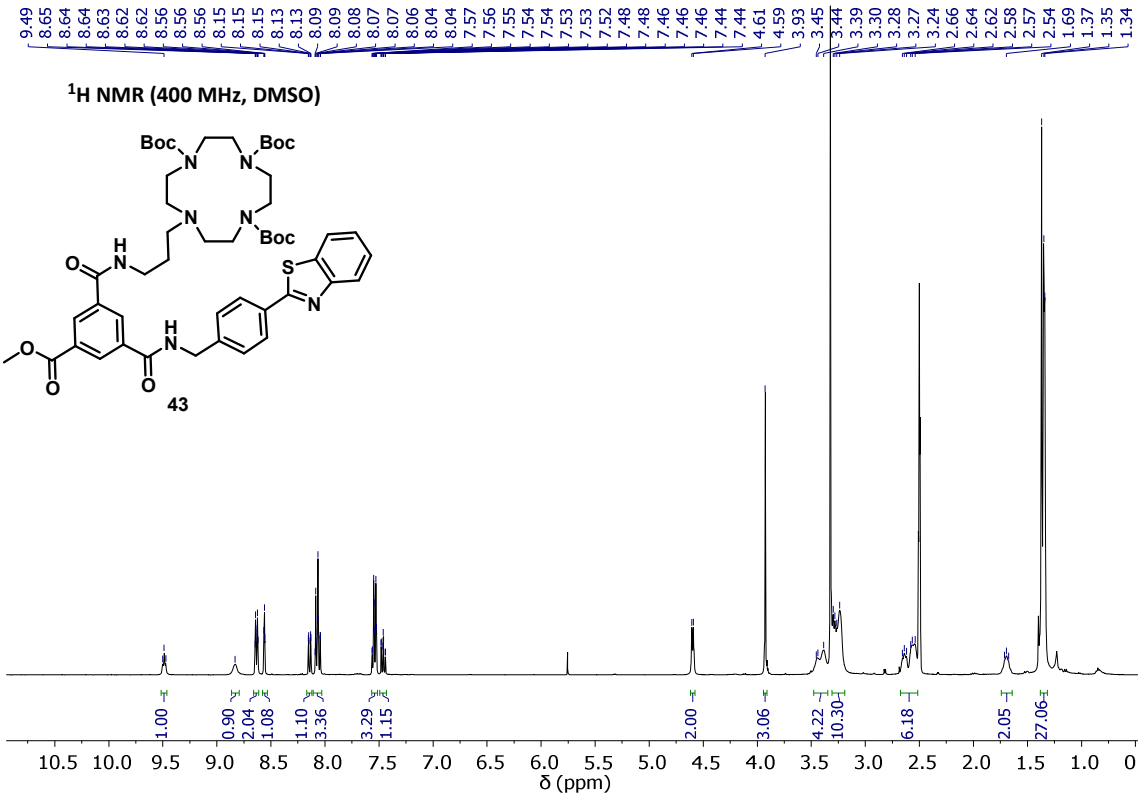
1H NMR (400 MHz, DMSO)
43
δ (ppm)

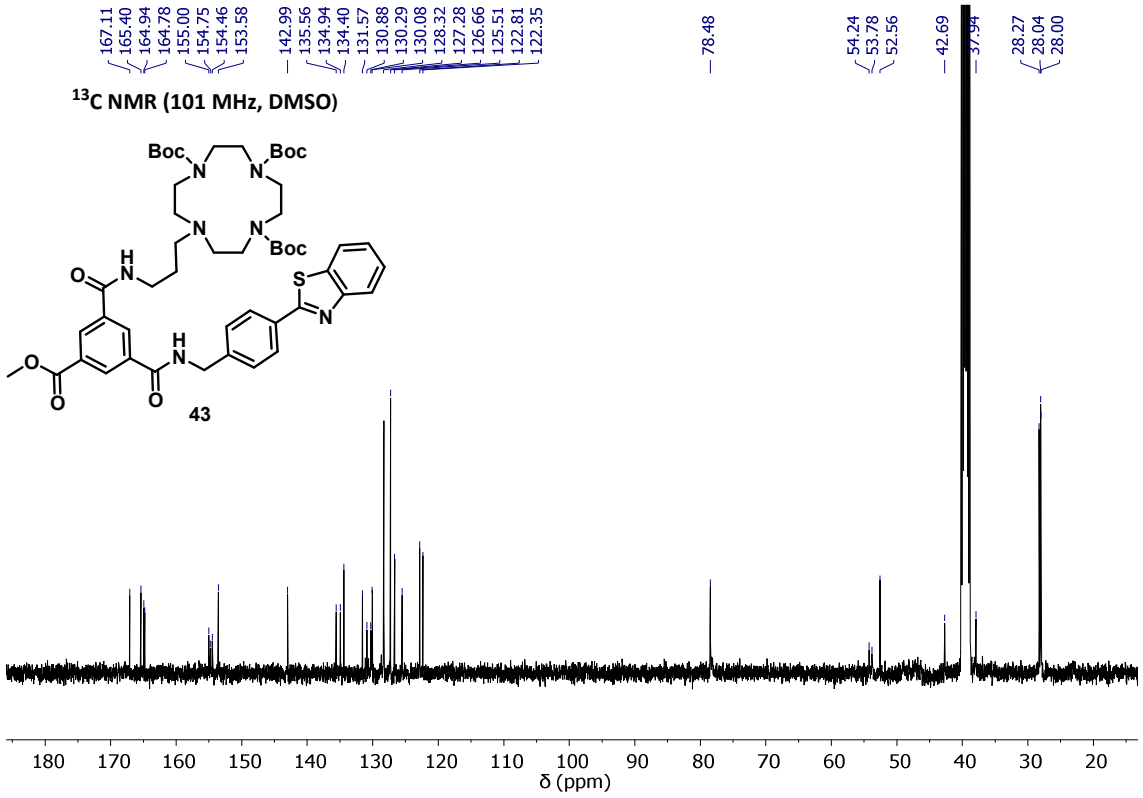
167.11
165.40
164.94
164.78
155.00
154.75
154.46
153.58
142.99
135.56
134.94
134.40
131.57
130.88
130.29
130.08
128.32
127.28
126.66
125.51
122.81
122.35
78.48
54.24
53.78
52.56
42.69
37.94
28.27
28.04
28.00
13C NMR (101 MHz, DMSO)
Boc
Boc
Boc
H
N
O
S
N
H
N
O
O
O
43
180
170
160
150
140
130
120
110
100
90
80
70
60
50
40
30
20
δ (ppm)

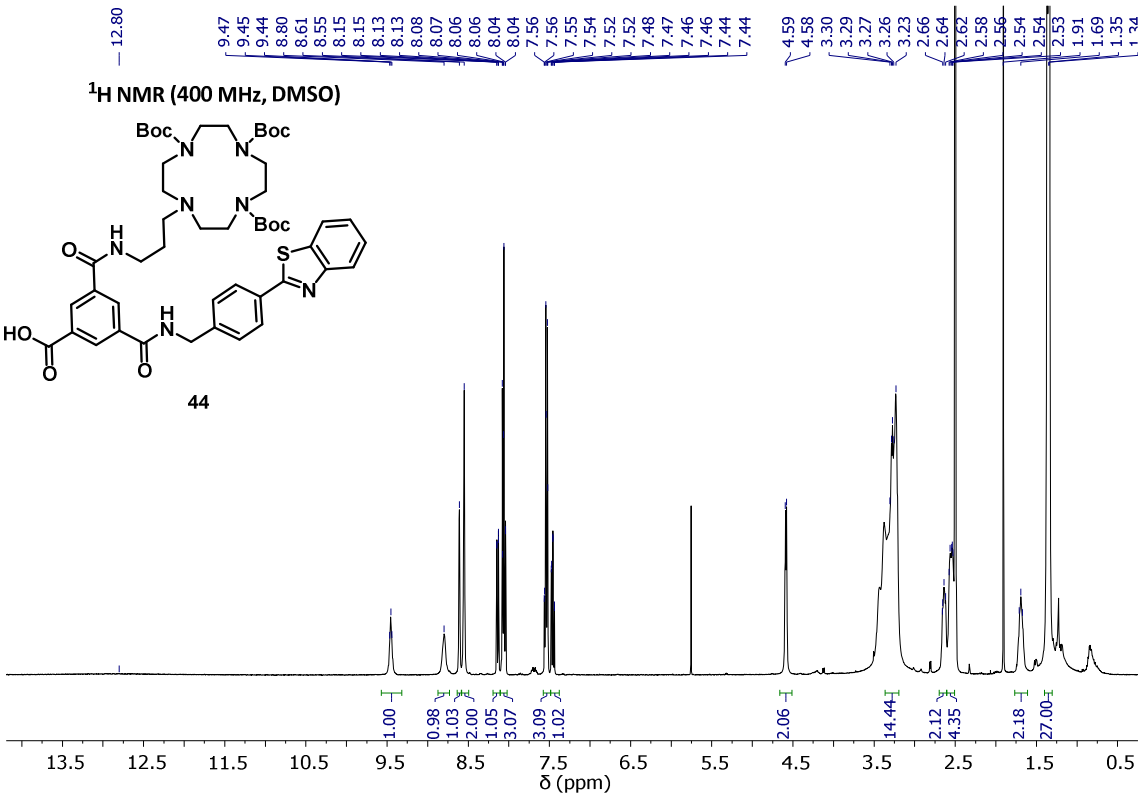
12.80
9.47
9.45
9.44
8.80
8.61
8.55
8.15
8.15
8.13
8.13
8.08
8.07
8.06
8.06
8.04
8.04
7.56
7.56
7.55
7.54
7.52
7.52
7.48
7.47
7.46
7.46
7.44
7.44
4.59
4.58
3.30
3.29
3.27
3.26
3.23
2.66
2.64
2.62
2.58
2.56
2.54
2.54
2.53
1.91
1.69
1.35
1H NMR (400 MHz, DMSO)
Boc
Boc
Boc
H
N
O
S
N
H
N
HO
O
O
44
1.00
0.98
1.03
2.00
1.05
3.07
3.09
1.02
2.06
14.44
2.12
4.35
2.18
27.00
13.5
12.5
11.5
10.5
9.5
8.5
7.5
6.5
5.5
4.5
3.5
2.5
1.5
0.5
δ (ppm)

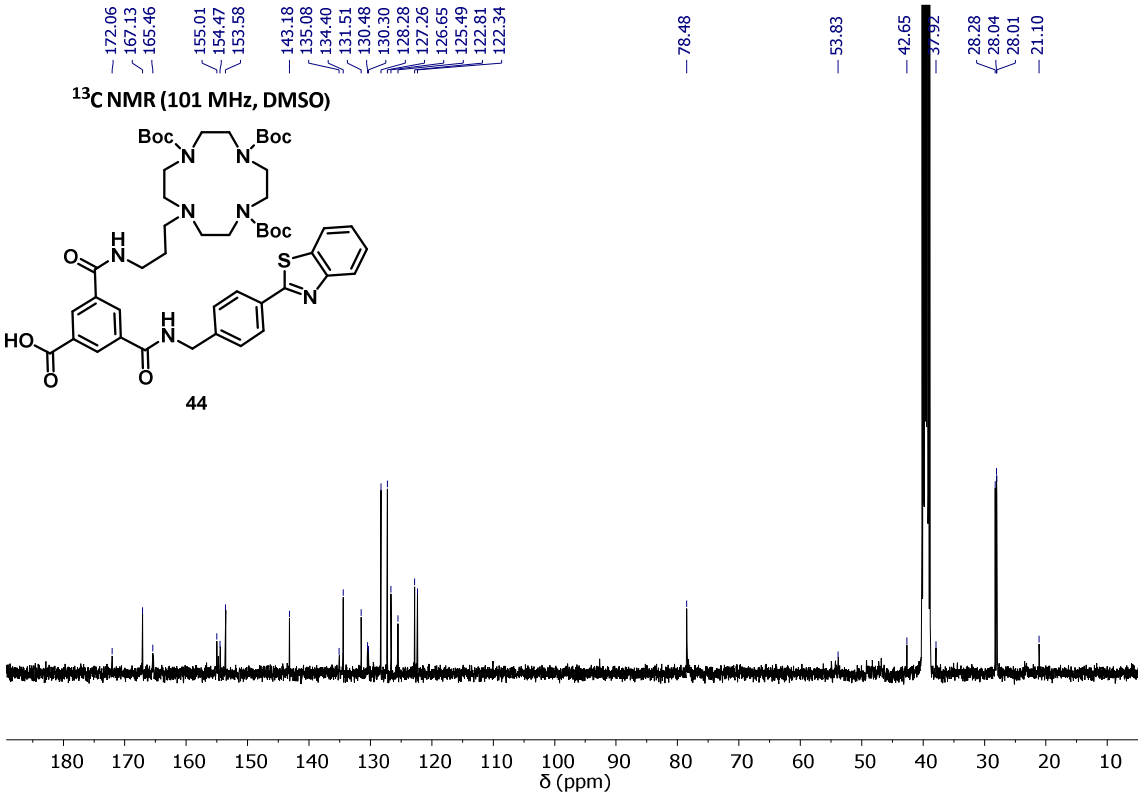
172.06
167.13
165.46
155.01
154.47
153.58
143.18
135.08
134.40
131.51
130.48
130.30
128.28
127.26
126.65
125.49
122.81
122.34
78.48
53.83
42.65
37.92
28.28
28.04
28.01
21.10
13C NMR (101 MHz, DMSO)
Boc
Boc
Boc
Boc
H
N
O
S
N
HO
O
H
N
O
O
44
180
170
160
150
140
130
120
110
100
90
80
70
60
50
40
30
20
10
δ (ppm)

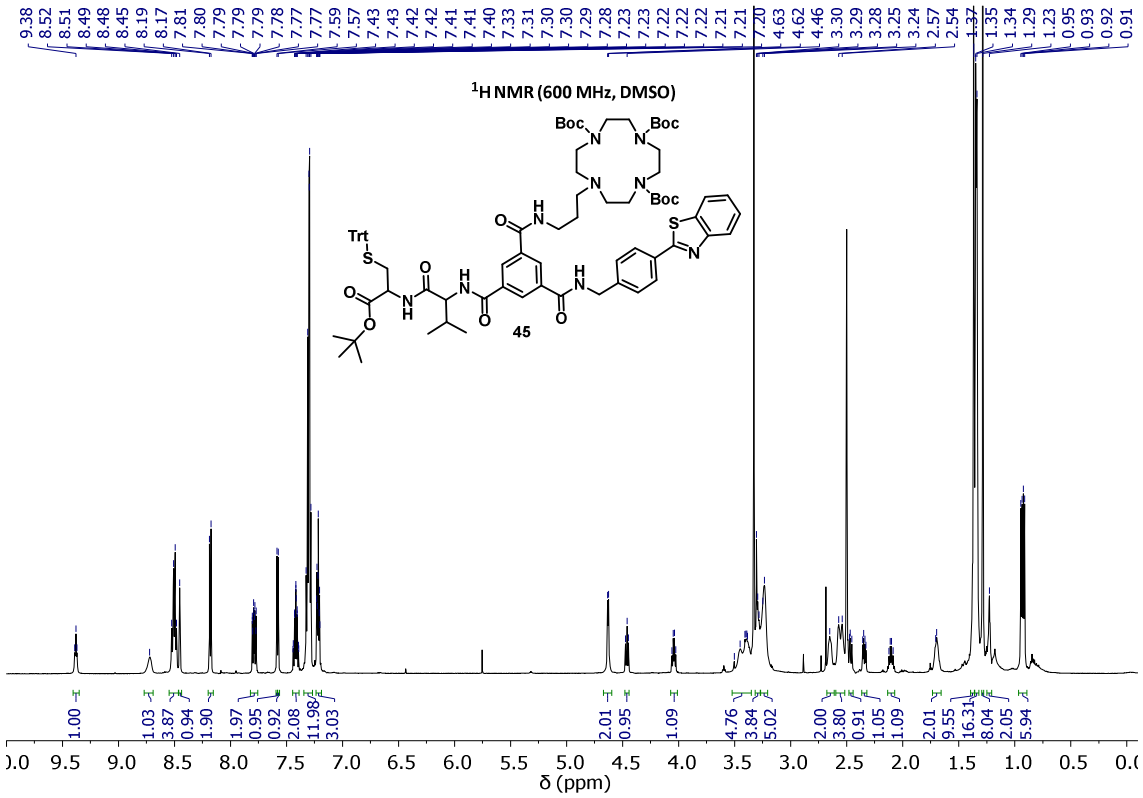
9.38
8.52
8.51
8.49
8.48
8.45
8.19
8.17
7.81
7.80
7.79
7.79
7.79
7.78
7.77
7.77
7.59
7.57
7.43
7.42
7.42
7.41
7.41
7.40
7.33
7.31
7.30
7.30
7.29
7.28
7.23
7.23
7.22
7.22
7.22
7.21
7.21
7.20
4.63
4.62
4.46
3.30
3.29
3.28
3.25
3.24
2.57
2.54
1.37
1.35
1.34
1.29
1.23
0.95
0.93
0.92
0.91
1H NMR (600 MHz, DMSO)
Boc
Boc
Boc
Boc
H
N
O
S
N
Trt
S
O
O
N
H
H
N
O
O
45
1.00
1.03
3.87
0.94
1.90
1.97
0.95
0.92
2.08
11.98
3.03
2.01
0.95
1.09
4.76
3.84
5.02
2.00
3.80
0.91
1.05
1.09
2.01
9.55
16.31
8.04
2.05
5.94
9.5
9.0
8.5
8.0
7.5
7.0
6.5
6.0
5.5
5.0
4.5
4.0
3.5
3.0
2.5
2.0
1.5
1.0
0.5
δ (ppm)

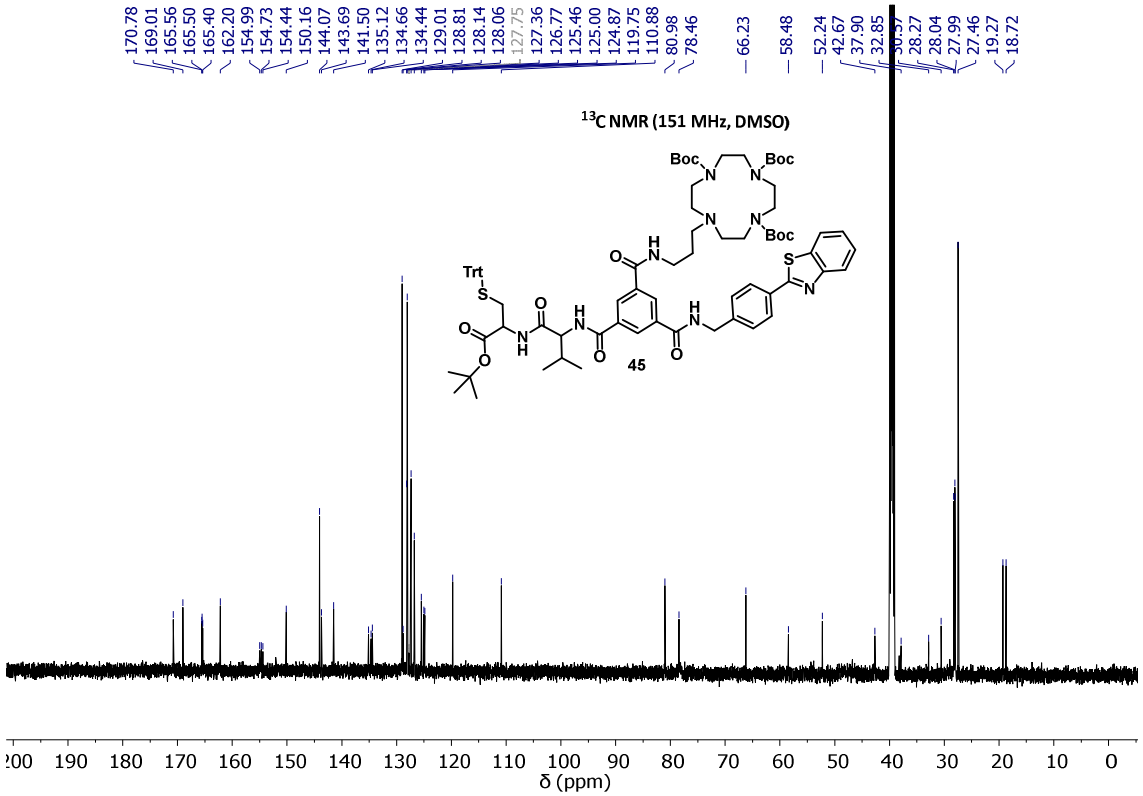
170.78
169.01
165.56
165.50
165.40
162.20
154.99
154.73
154.44
150.16
144.07
143.69
141.50
135.12
134.66
134.44
129.01
128.81
128.14
128.06
127.75
127.36
126.77
125.46
125.00
124.87
119.75
110.88
80.98
78.46
66.23
58.48
52.24
42.67
37.90
32.85
30.37
28.27
28.04
27.99
27.46
19.27
18.72
13C NMR (151 MHz, DMSO)
Boc
Boc
Boc
Trt
45
δ (ppm)

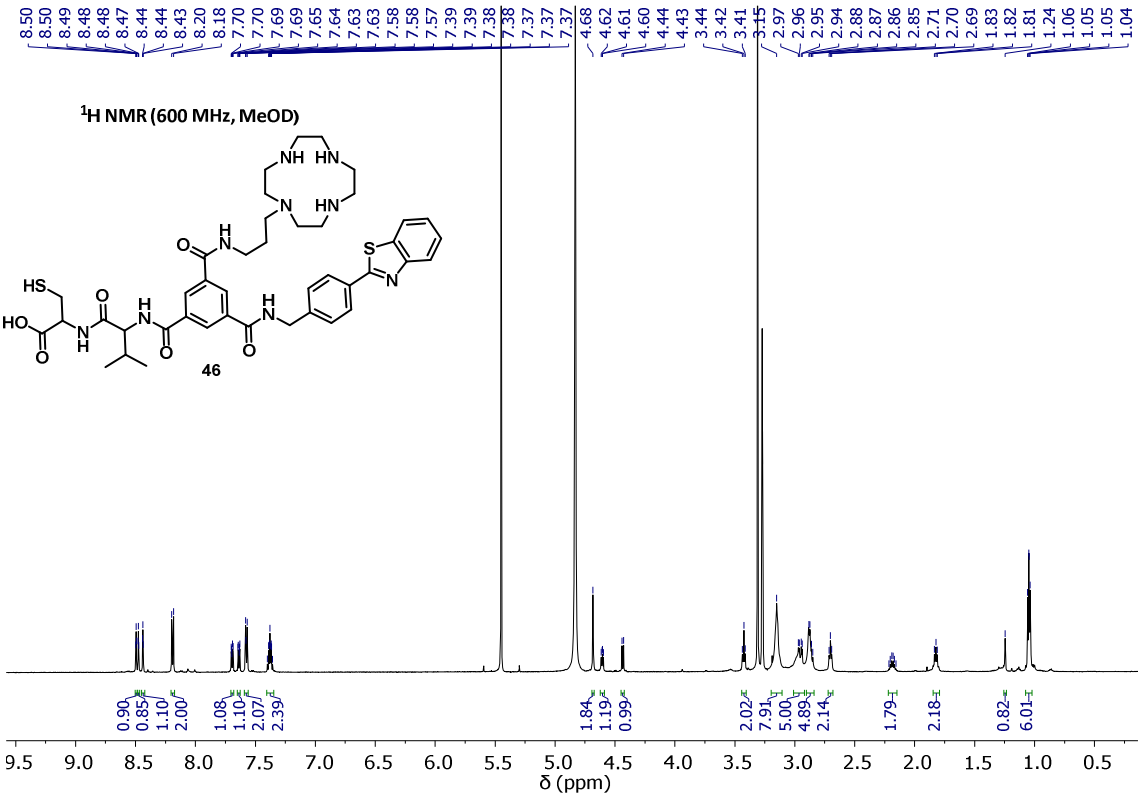
8.50
8.50
8.49
8.48
8.48
8.47
8.44
8.44
8.43
8.20
8.18
7.70
7.70
7.69
7.69
7.65
7.64
7.63
7.63
7.58
7.58
7.57
7.39
7.39
7.38
7.38
7.37
7.37
7.37
4.68
4.62
4.61
4.60
4.44
4.43
3.44
3.42
3.41
3.15
2.97
2.96
2.95
2.94
2.88
2.87
2.86
2.85
2.71
2.70
2.69
1.83
1.82
1.81
1.24
1.06
1.05
1.05
1.04
1H NMR (600 MHz, MeOD)
46
δ (ppm)

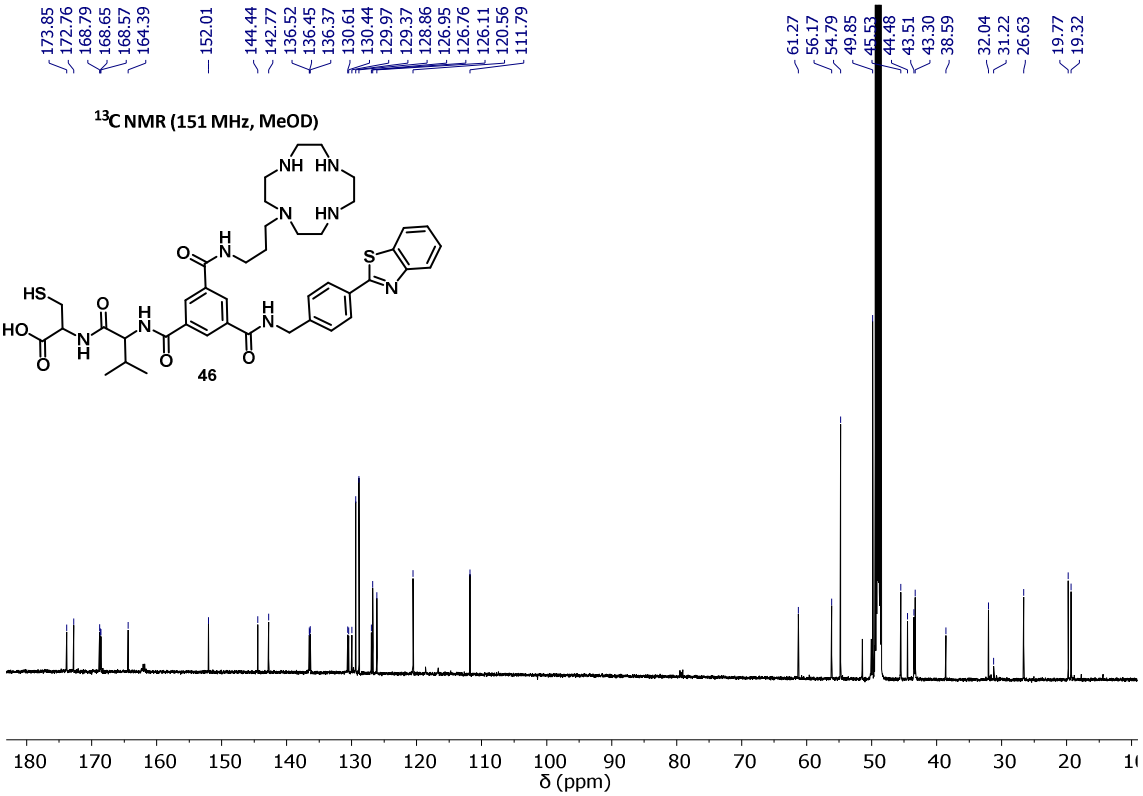
173.85
172.76
168.79
168.65
168.57
164.39
152.01
144.44
142.77
136.52
136.45
136.37
130.61
130.44
129.97
129.37
128.86
126.95
126.76
126.11
120.56
111.79
61.27
56.17
54.79
49.85
45.53
44.48
43.51
43.30
38.59
32.04
31.22
26.63
19.77
19.32
13C NMR (151 MHz, MeOD)
46
δ (ppm)

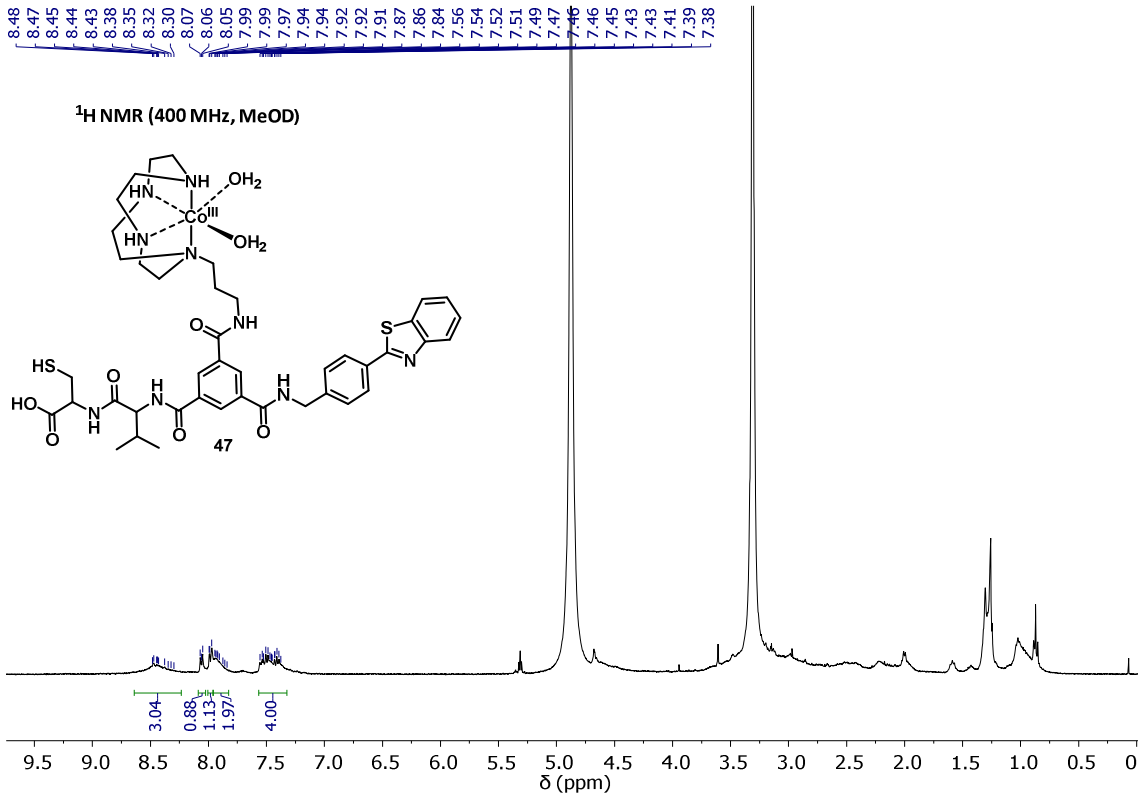
8.48
8.47
8.45
8.44
8.43
8.38
8.35
8.32
8.30
8.07
8.06
8.05
7.99
7.99
7.97
7.94
7.94
7.92
7.92
7.91
7.87
7.86
7.84
7.56
7.54
7.52
7.51
7.49
7.47
7.46
7.46
7.45
7.43
7.43
7.41
7.39
7.38
1H NMR (400 MHz, MeOD)
47
3.04
0.88
1.13
1.97
4.00
δ (ppm)

^{1}H NMR (300 MHz, $CDCl_3$)

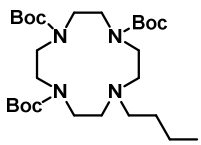

48

^{13}C NMR (75 MHz, $CDCl_3$)

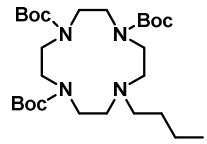

48

^{1}H NMR (600 MHz, DMSO)

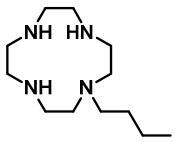

49

^{13}C NMR (151 MHz, DMSO)

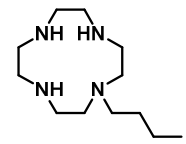

49

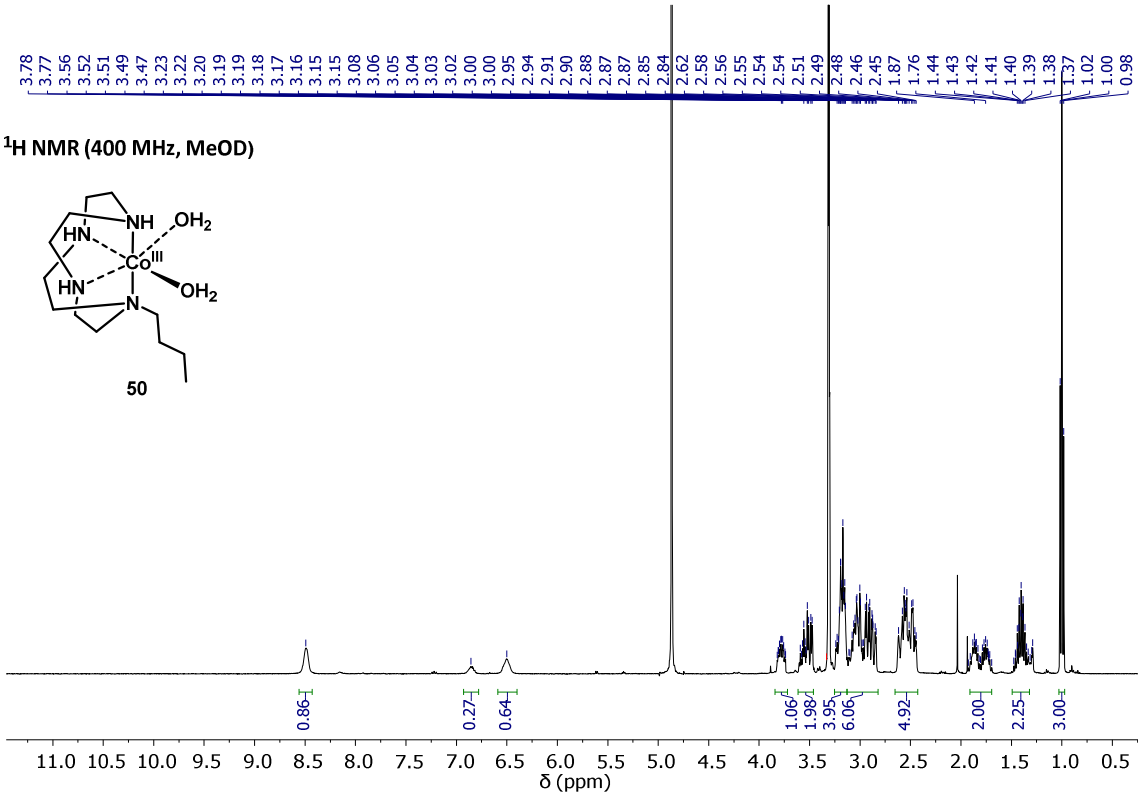

^{1}H NMR (400 MHz, MeOD)

50

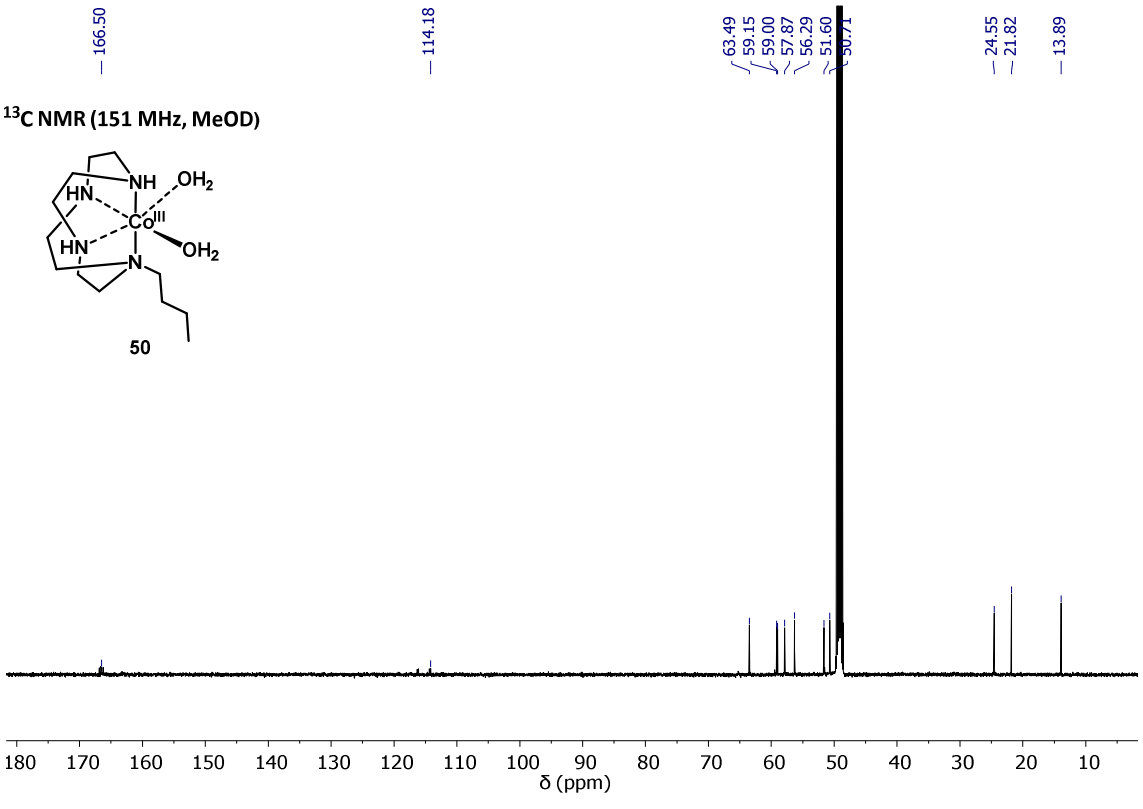

^{13}C NMR (151 MHz, MeOD)

50

^{1}H-NMR (300 MHz, $CDCl_3$)

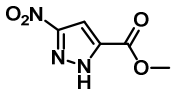

52

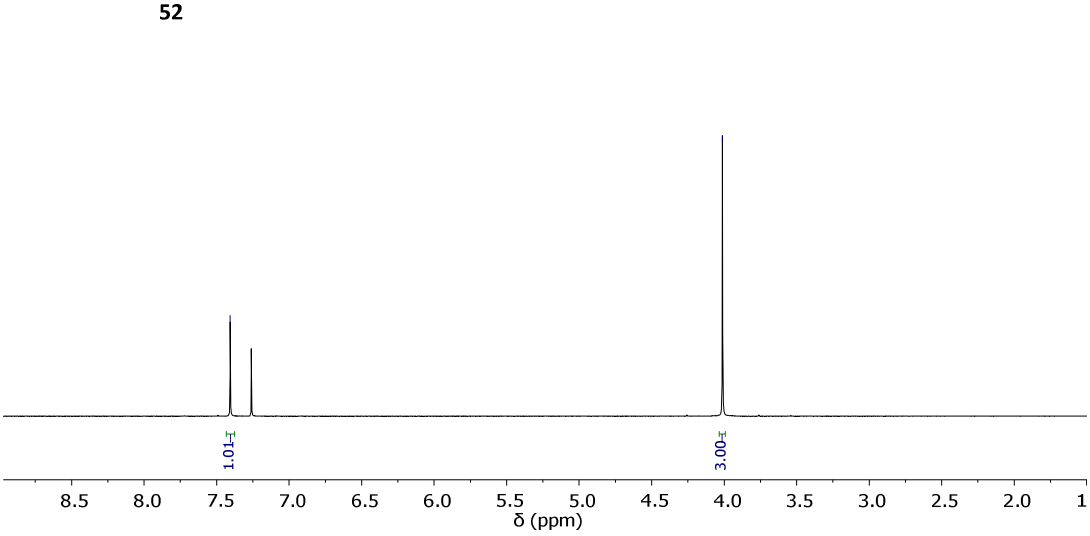

^{13}C NMR (75 MHz, $CDCl_3$)

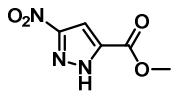

52

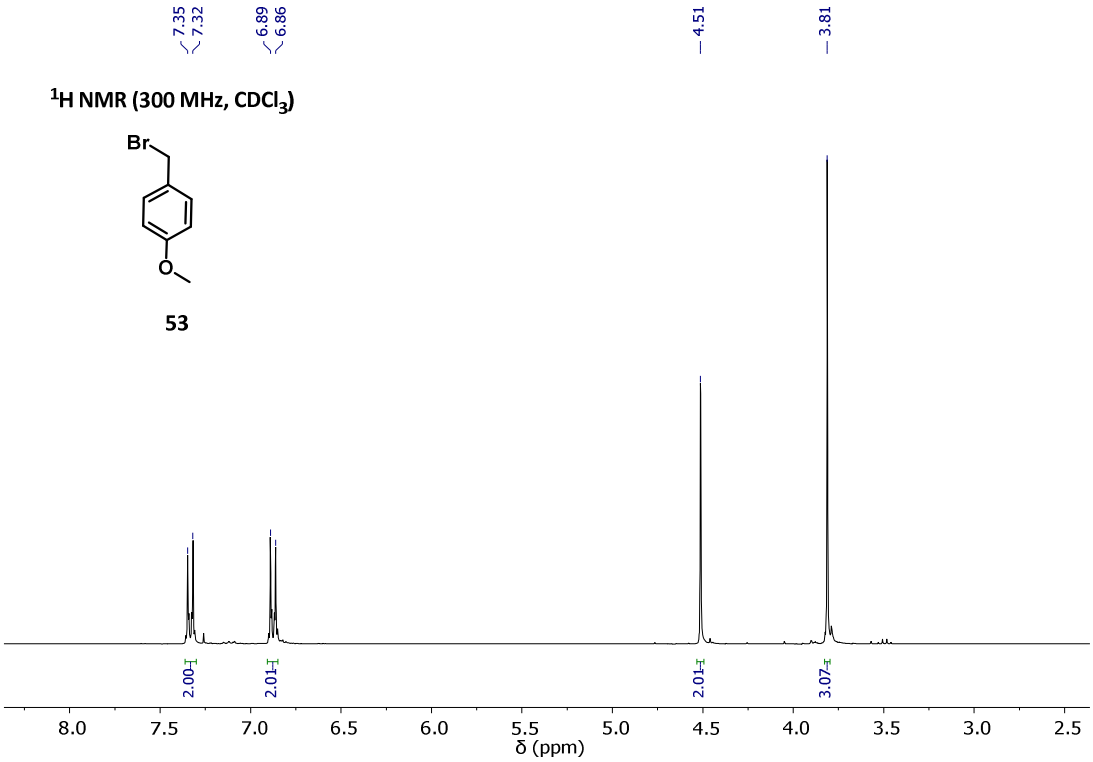

^{1}H NMR (300 MHz, $CDCl_3$)

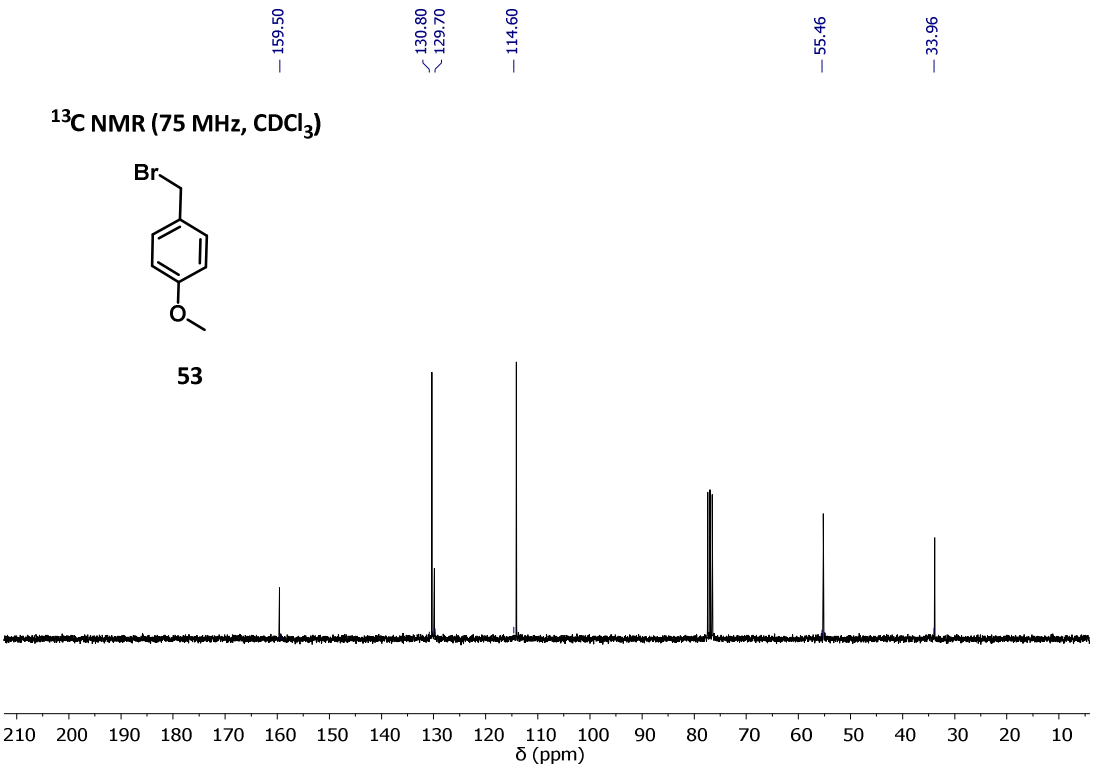

^{13}C NMR (75 MHz, $CDCl_3$)

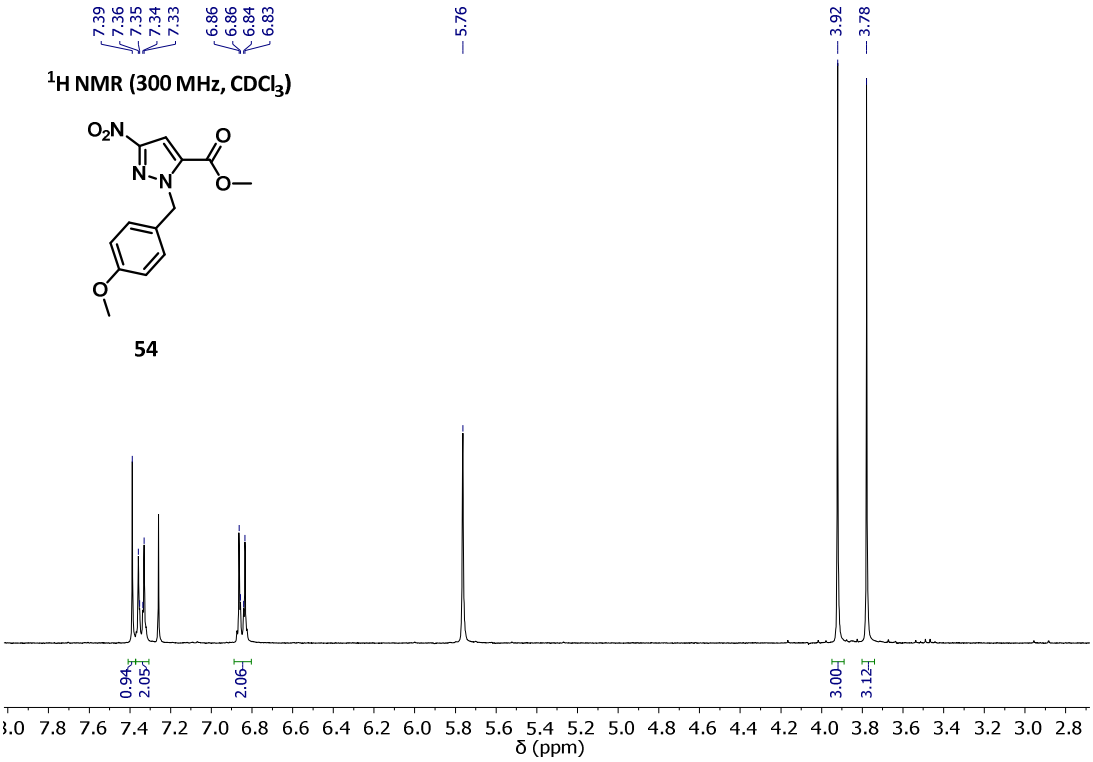
7.39
7.36
7.35
7.34
7.33
6.86
6.86
6.84
6.83
5.76
3.92
3.78
^{1}H NMR (300 MHz, CDCl$_3$)
O$_2$N
N
N
O
O
O
54
0.94
2.05
2.06
3.00
3.12
δ (ppm)

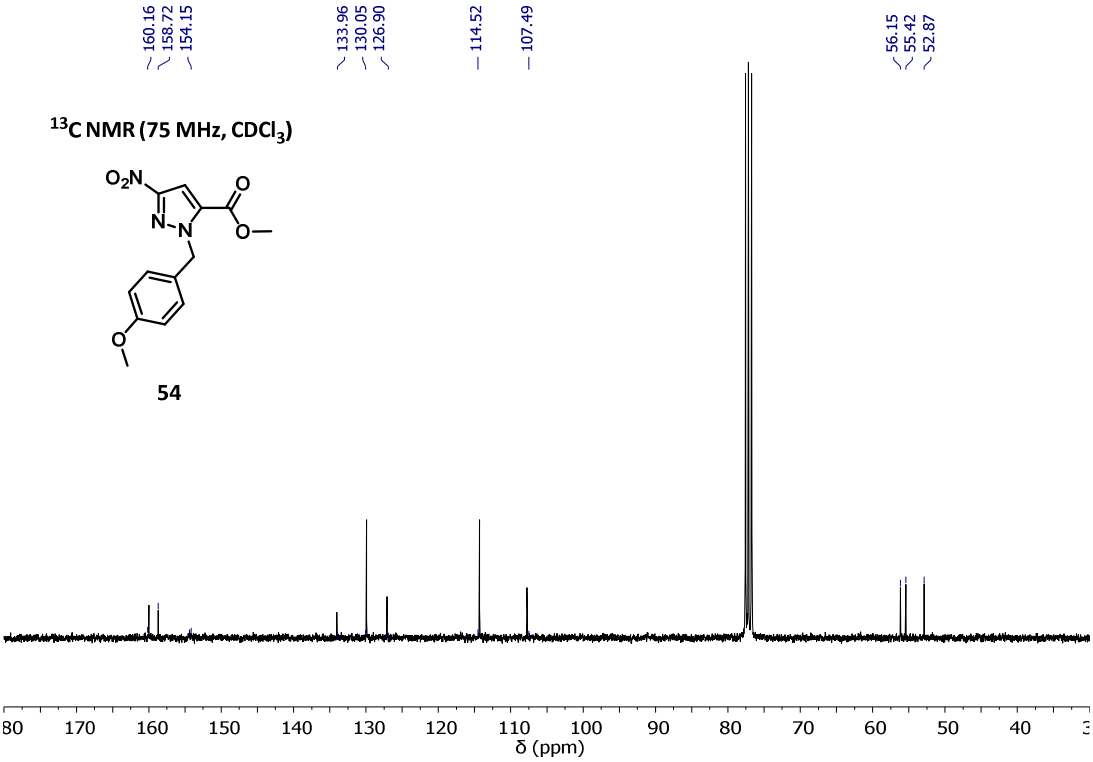
160.16
158.72
154.15
133.96
130.05
126.90
114.52
107.49
56.15
55.42
52.87
^{13}C NMR (75 MHz, CDCl$_3$)
O$_2$N
N
N
O
O
O
54
δ (ppm)

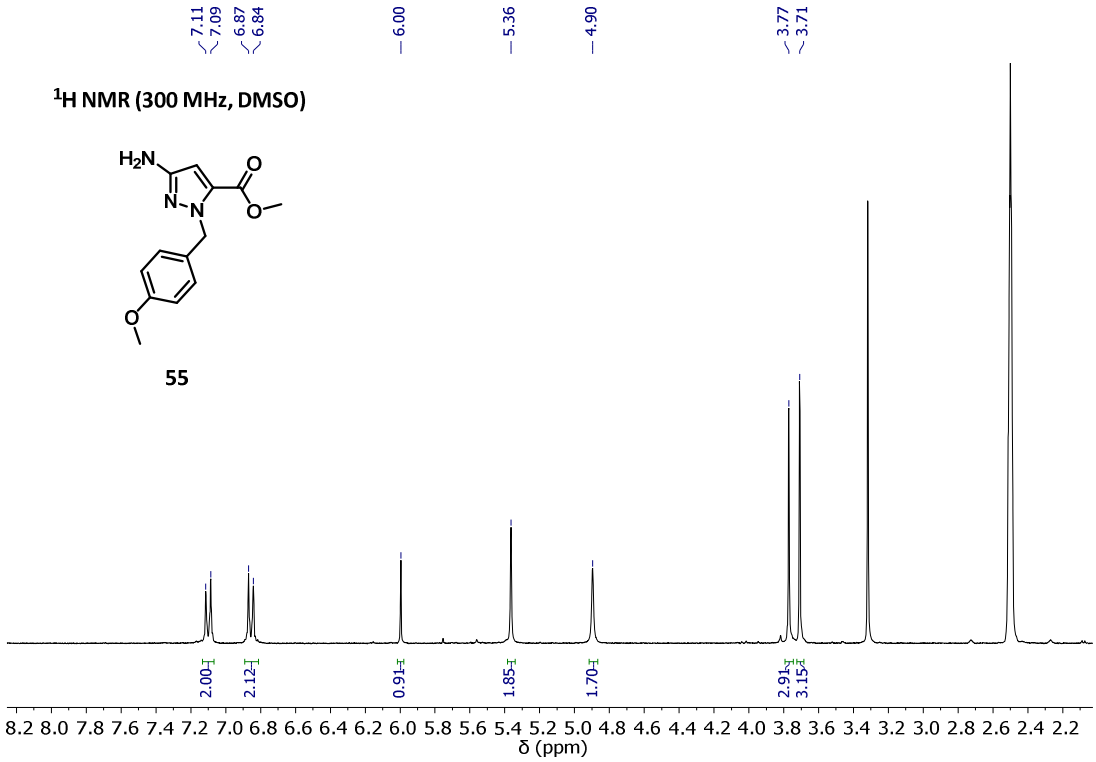
7.11
7.09
6.87
6.84
6.00
5.36
4.90
3.77
3.71
^{1}H NMR (300 MHz, DMSO)
H_2N
O
N
N
O
O
55
2.00
2.12
0.91
1.85
1.70
2.91
3.15
8.2 8.0 7.8 7.6 7.4 7.2 7.0 6.8 6.6 6.4 6.2 6.0 5.8 5.6 5.4 5.2 5.0 4.8 4.6 4.4 4.2 4.0 3.8 3.6 3.4 3.2 3.0 2.8 2.6 2.4 2.2
δ (ppm)

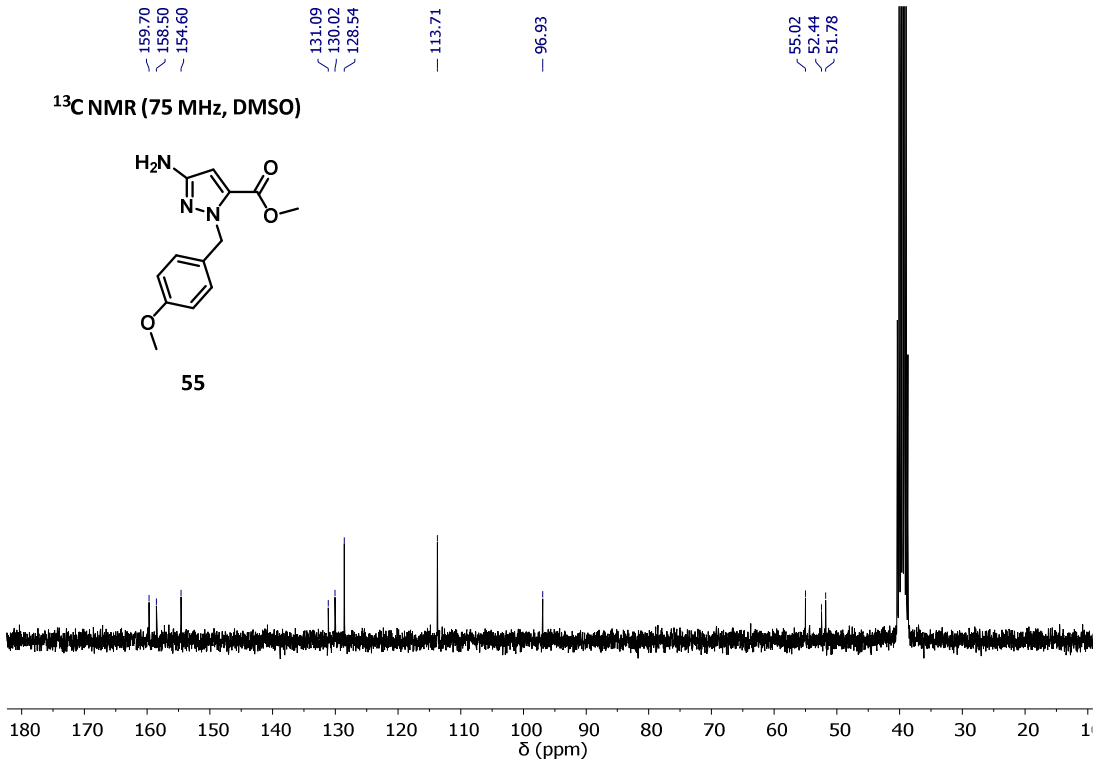
159.70
158.50
154.60
131.09
130.02
128.54
113.71
96.93
55.02
52.44
51.78
^{13}C NMR (75 MHz, DMSO)
H_2N
O
N
N
O
O
55
180 170 160 150 140 130 120 110 100 90 80 70 60 50 40 30 20
δ (ppm)

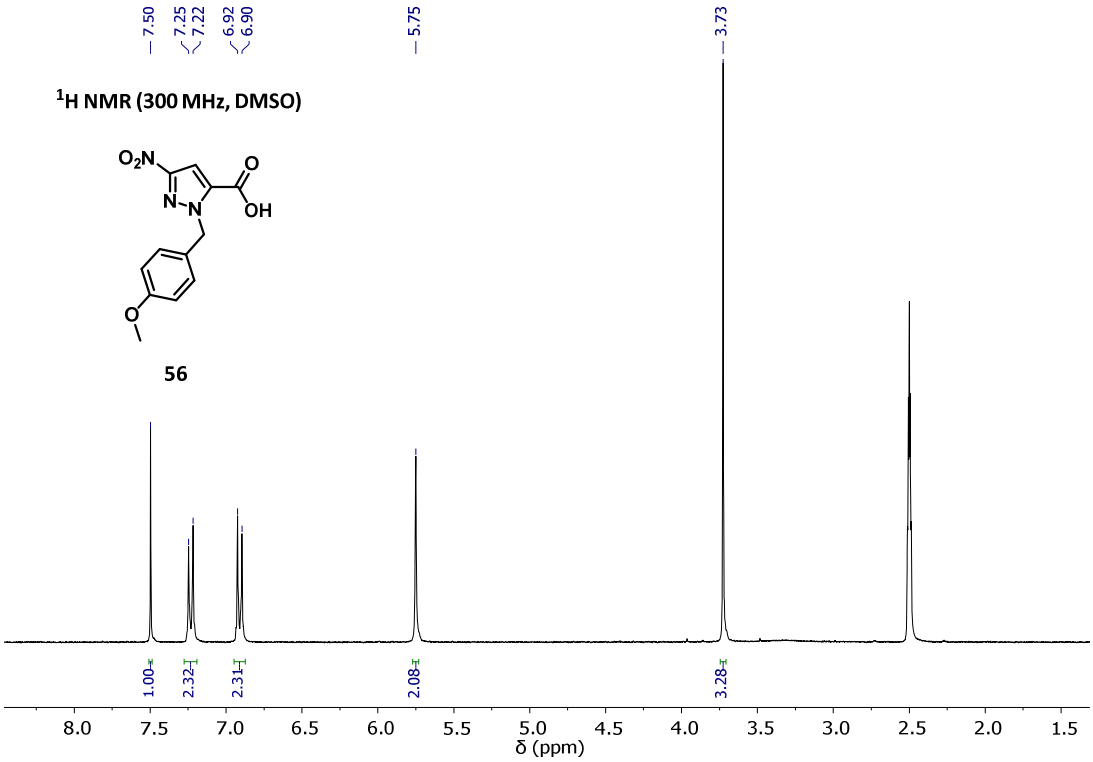
7.50
7.25
7.22
6.92
6.90
5.75
3.73
1H NMR (300 MHz, DMSO)
O2N
N
N
O
OH
O
56
1.00
2.32
2.31
2.08
3.28
8.0
7.5
7.0
6.5
6.0
5.5
5.0
4.5
4.0
3.5
3.0
2.5
2.0
1.5
δ (ppm)

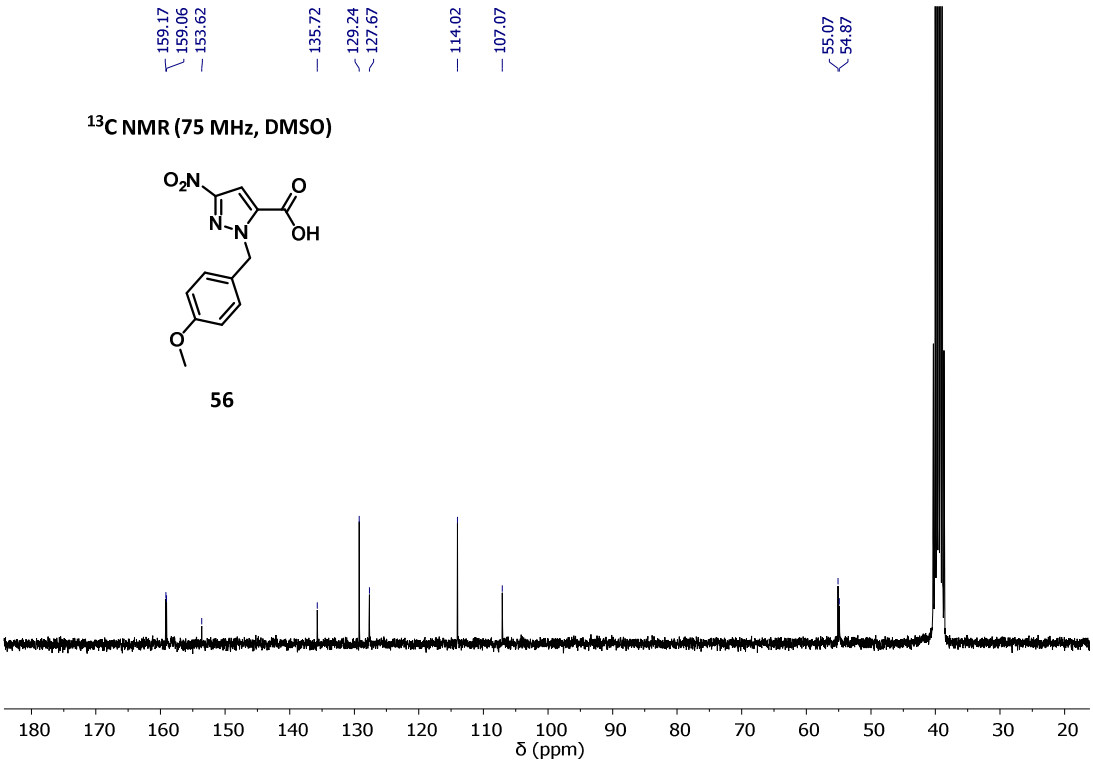
159.17
159.06
153.62
135.72
129.24
127.67
114.02
107.07
55.07
54.87
13C NMR (75 MHz, DMSO)
O2N
N
N
O
OH
O
56
180
170
160
150
140
130
120
110
100
90
80
70
60
50
40
30
20
δ (ppm)

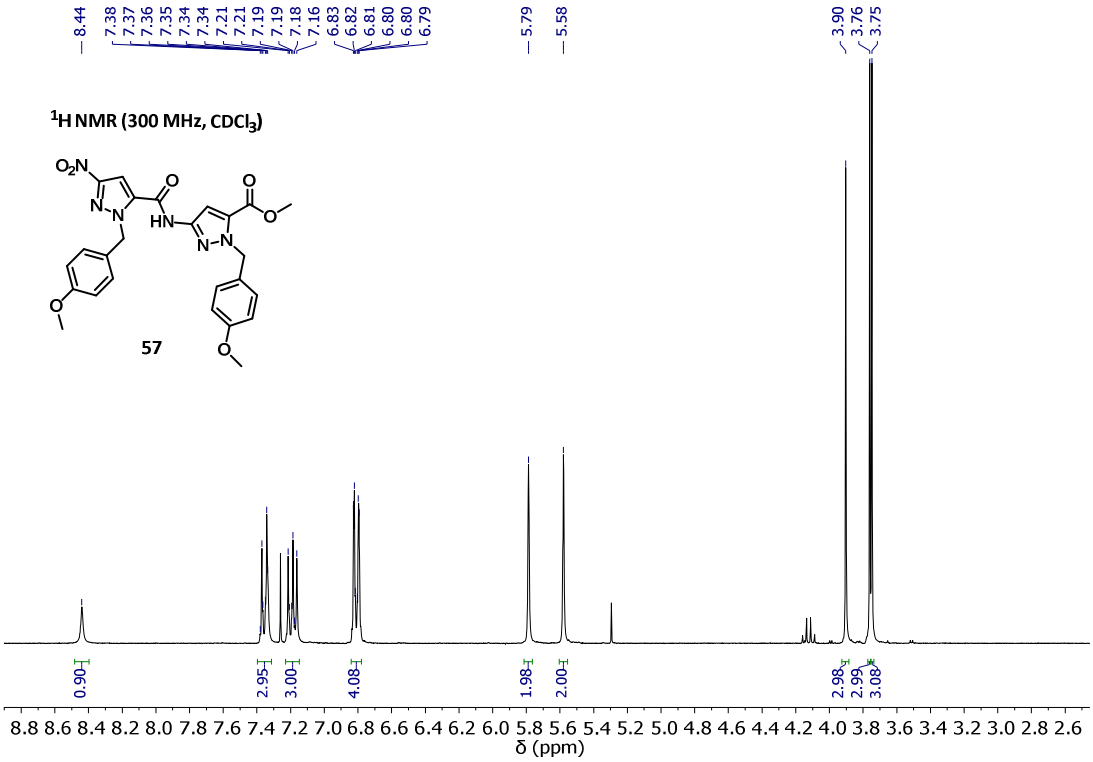

^{1}H NMR (300 MHz, $CDCl_3$)

57

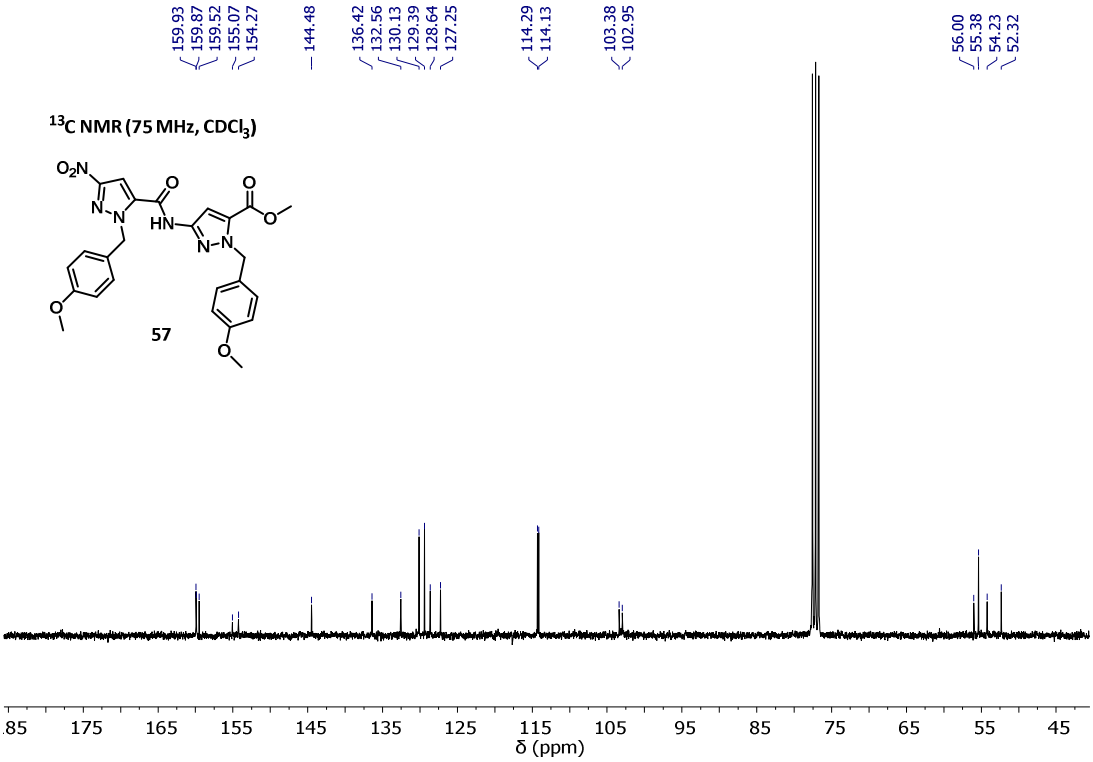

^{13}C NMR (75 MHz, $CDCl_3$)

57

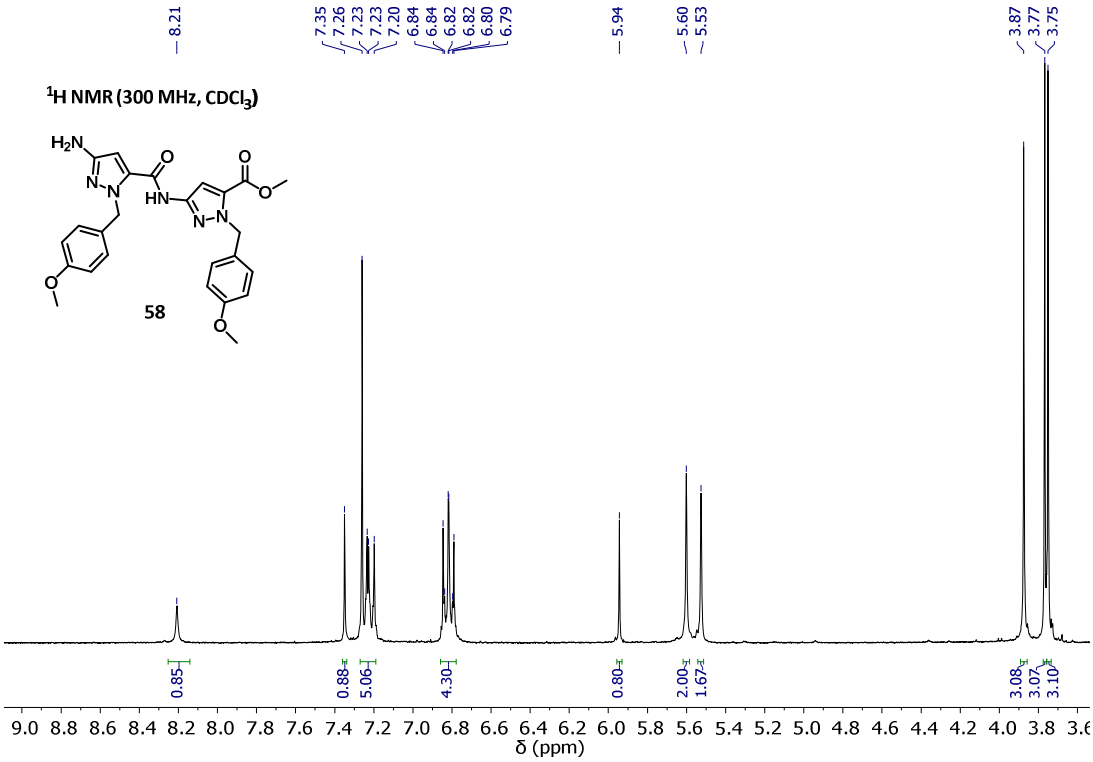

^{1}H NMR (300 MHz, $CDCl_3$)

58

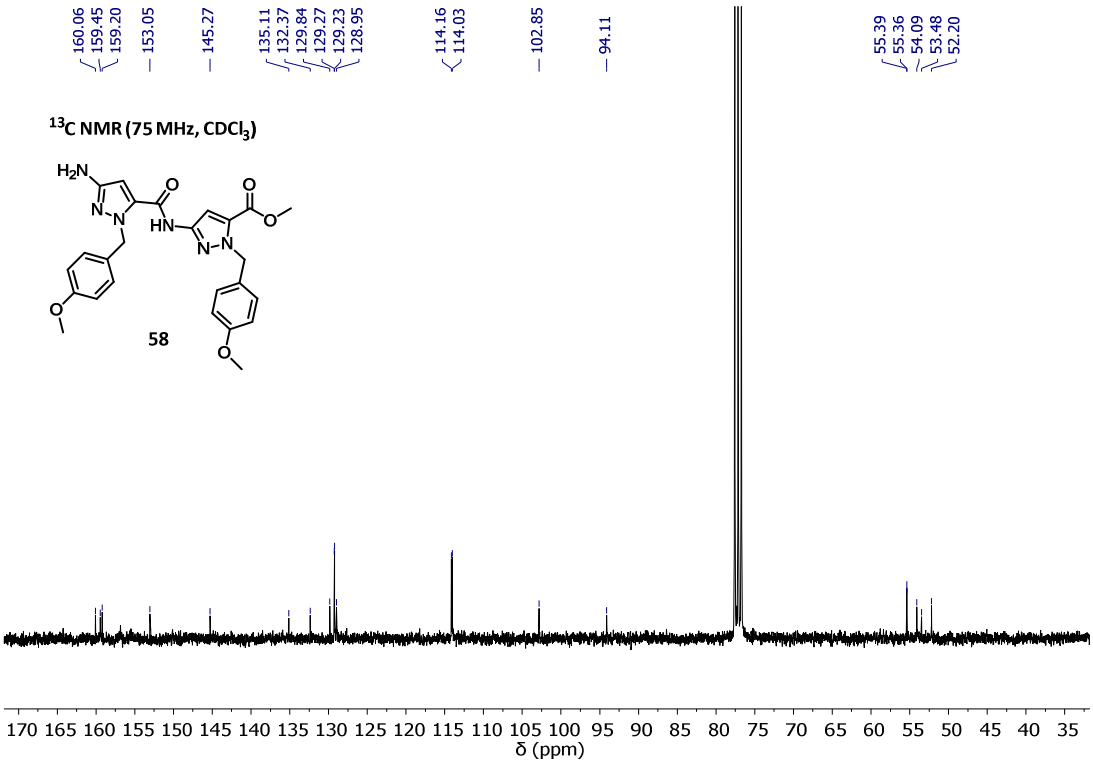

^{13}C NMR (75 MHz, $CDCl_3$)

58

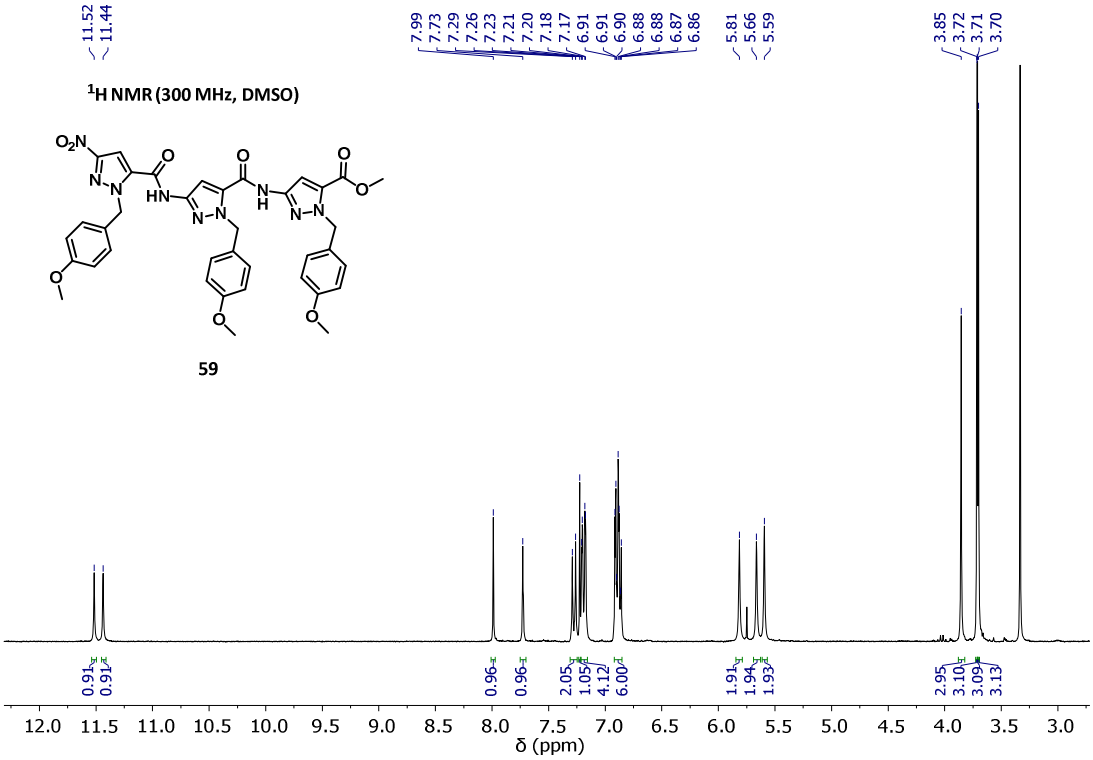

^{1}H NMR (300 MHz, DMSO)

59

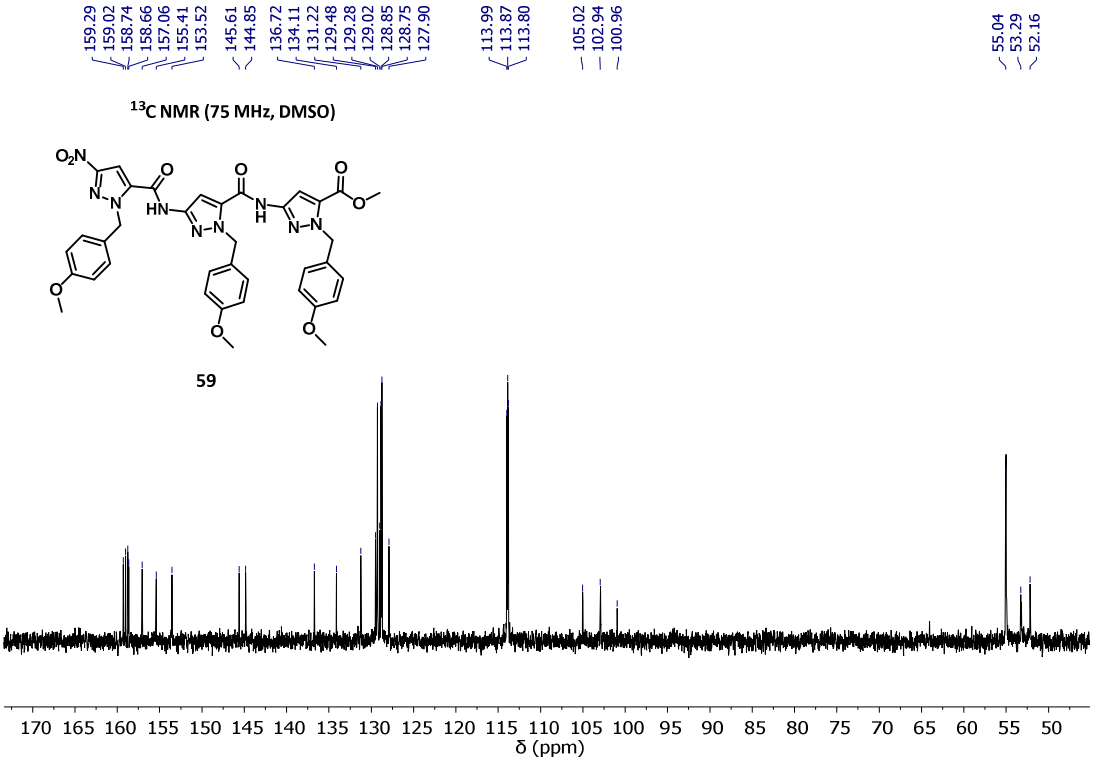

^{13}C NMR (75 MHz, DMSO)

59

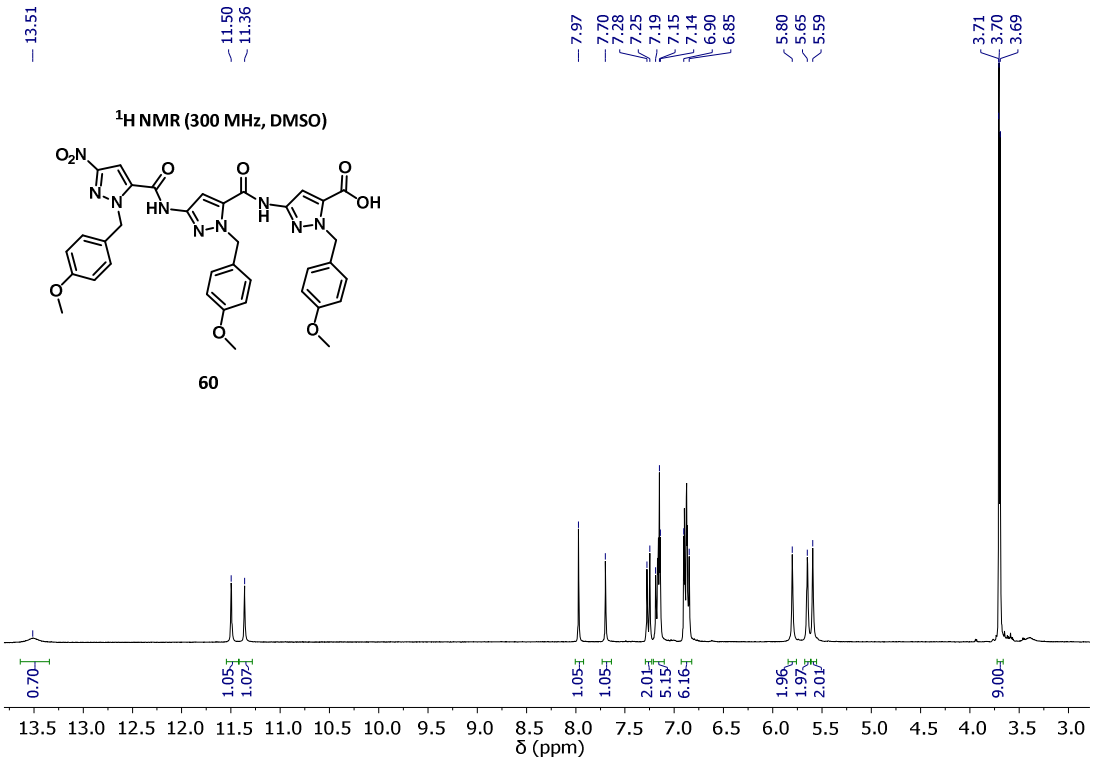

^{1}H NMR (300 MHz, DMSO)

60

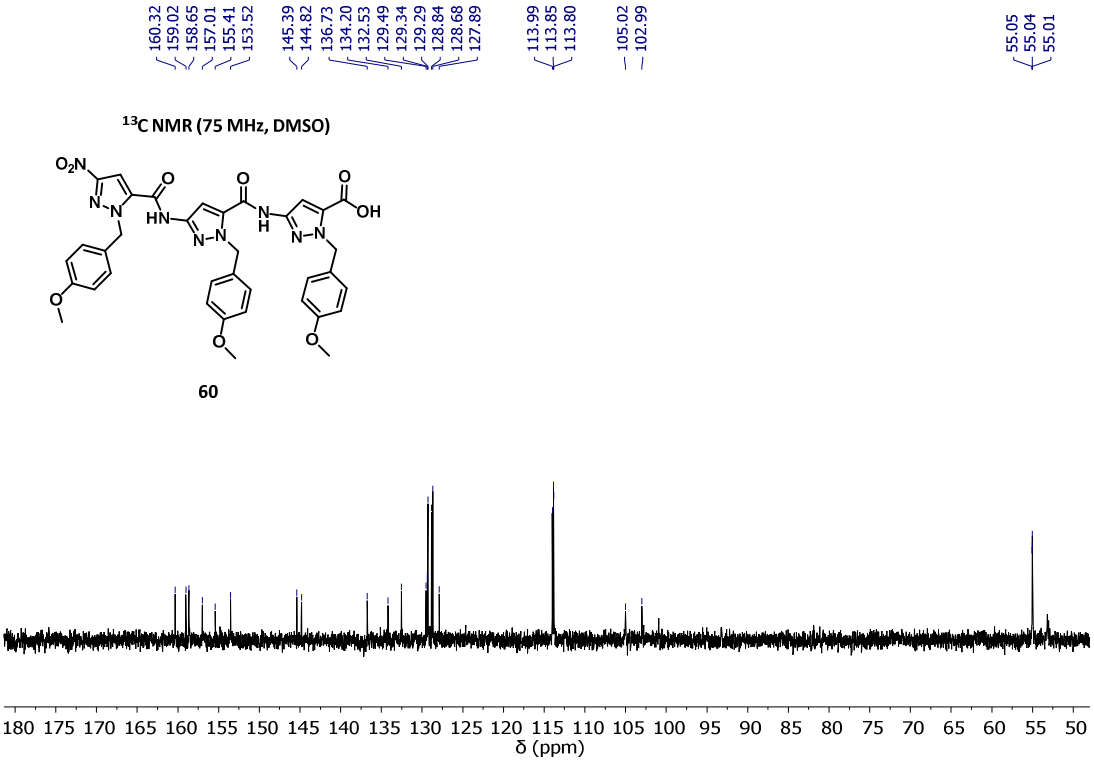

^{13}C NMR (75 MHz, DMSO)

60

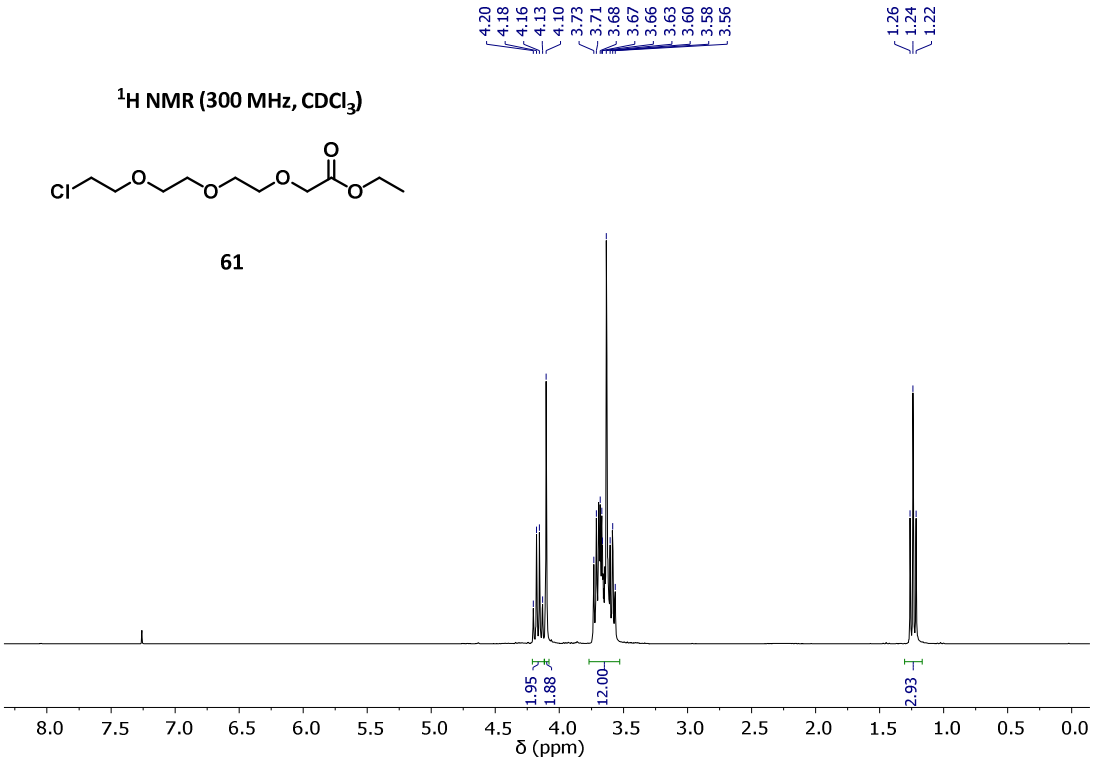
4.20
4.18
4.16
4.13
4.10
3.73
3.71
3.68
3.67
3.66
3.63
3.60
3.58
3.56
1.26
1.24
1.22
1H NMR (300 MHz, CDCl3)
Cl
O
O
O
O
O
61
1.95
1.88
12.00
2.93
8.0
7.5
7.0
6.5
6.0
5.5
5.0
4.5
4.0
3.5
3.0
2.5
2.0
1.5
1.0
0.5
0.0
δ (ppm)

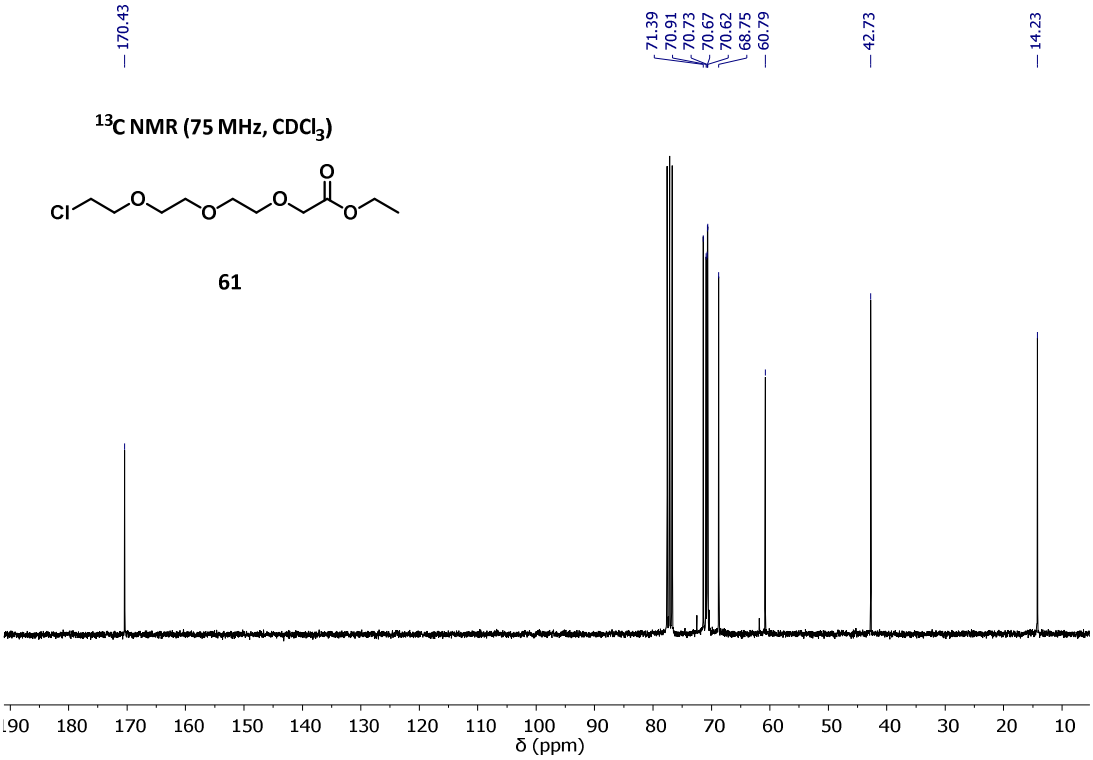
170.43
71.39
70.91
70.73
70.67
70.62
68.75
60.79
42.73
14.23
13C NMR (75 MHz, CDCl3)
Cl
O
O
O
O
O
61
190
180
170
160
150
140
130
120
110
100
90
80
70
60
50
40
30
20
10
δ (ppm)

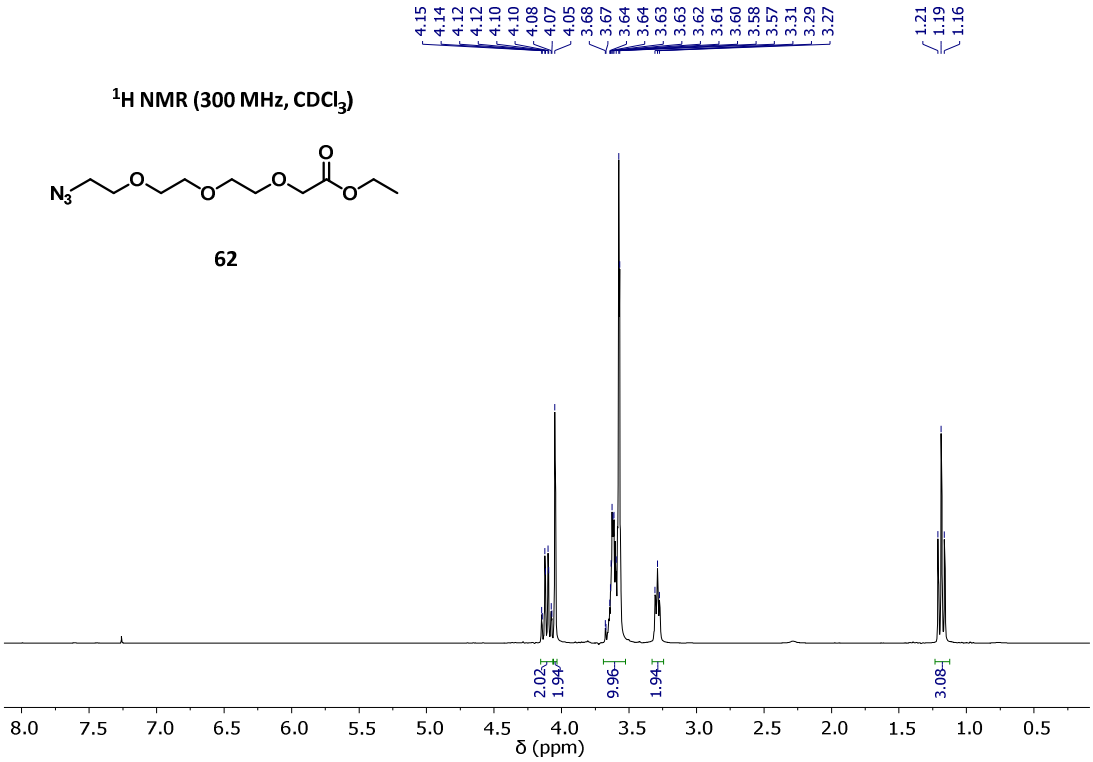

^{1}H NMR (300 MHz, $CDCl_3$)

62

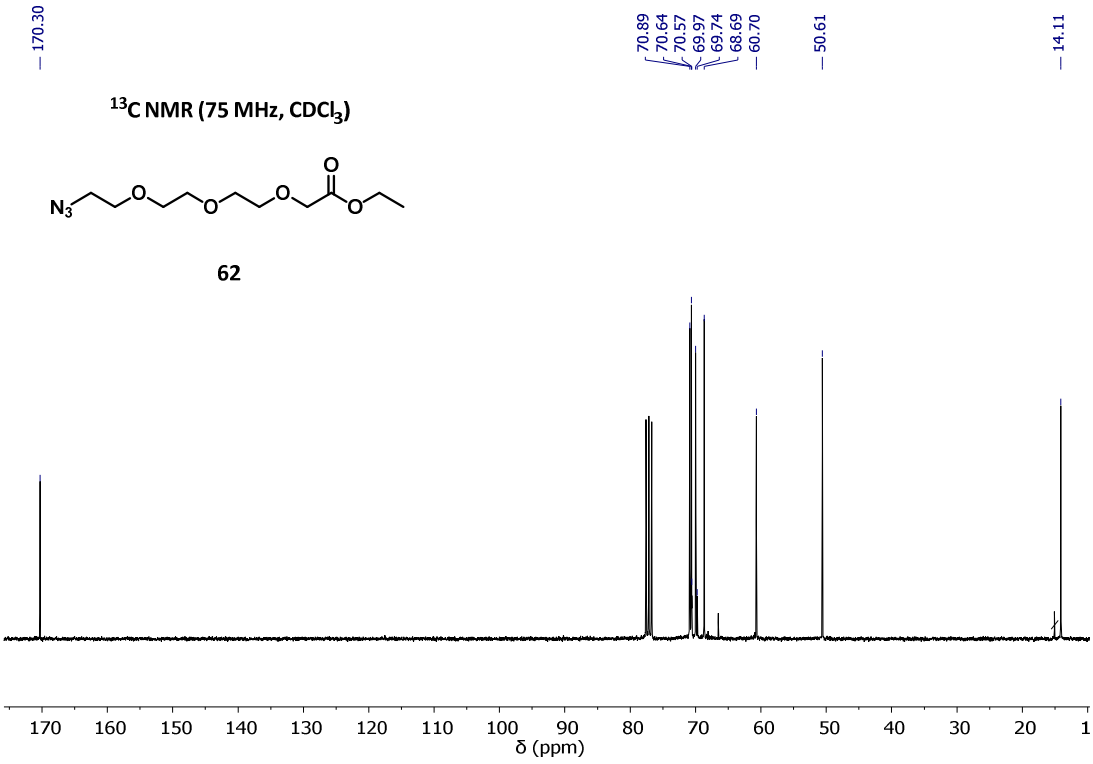

^{13}C NMR (75 MHz, $CDCl_3$)

62

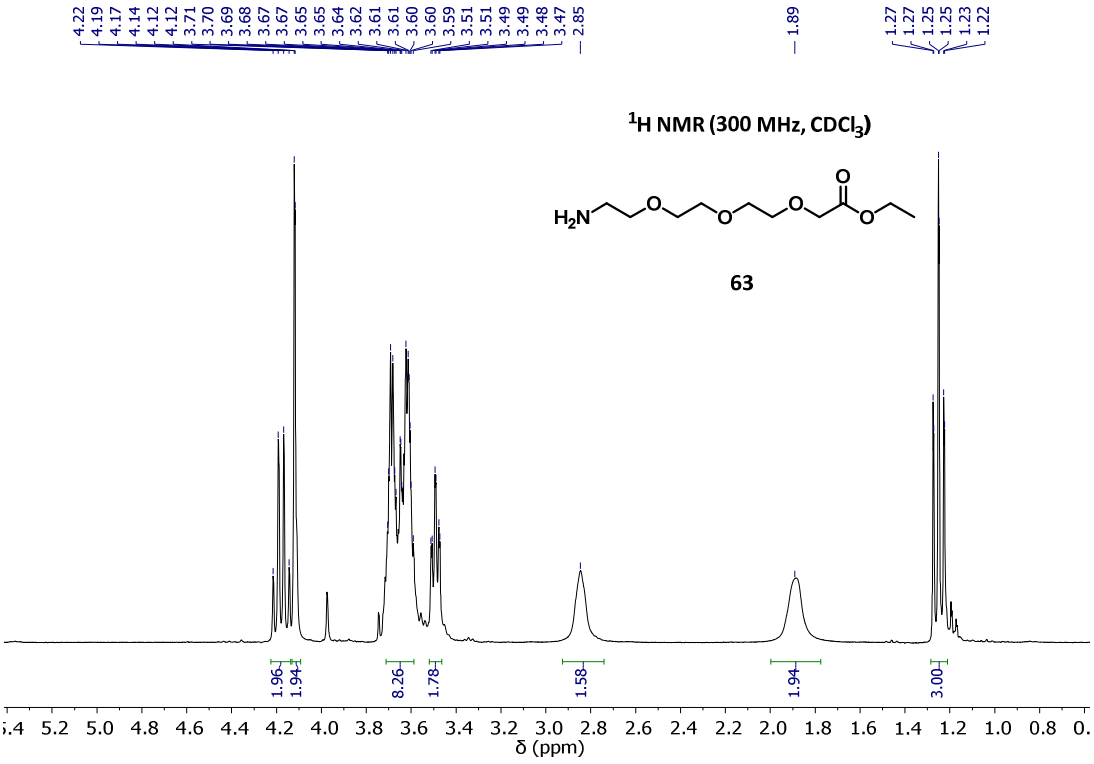
4.22 4.19 4.17 4.14 4.12 4.12 3.71 3.70 3.69 3.68 3.67 3.67 3.65 3.65 3.64 3.62 3.61 3.61 3.60 3.60 3.59 3.51 3.51 3.49 3.49 3.48 3.47 2.85
1.89
1.27 1.27 1.25 1.25 1.23 1.22
1H NMR (300 MHz, CDCl3)
H2N
O
63
1.96 1.94 8.26 1.78 1.58 1.94 3.00
δ (ppm)

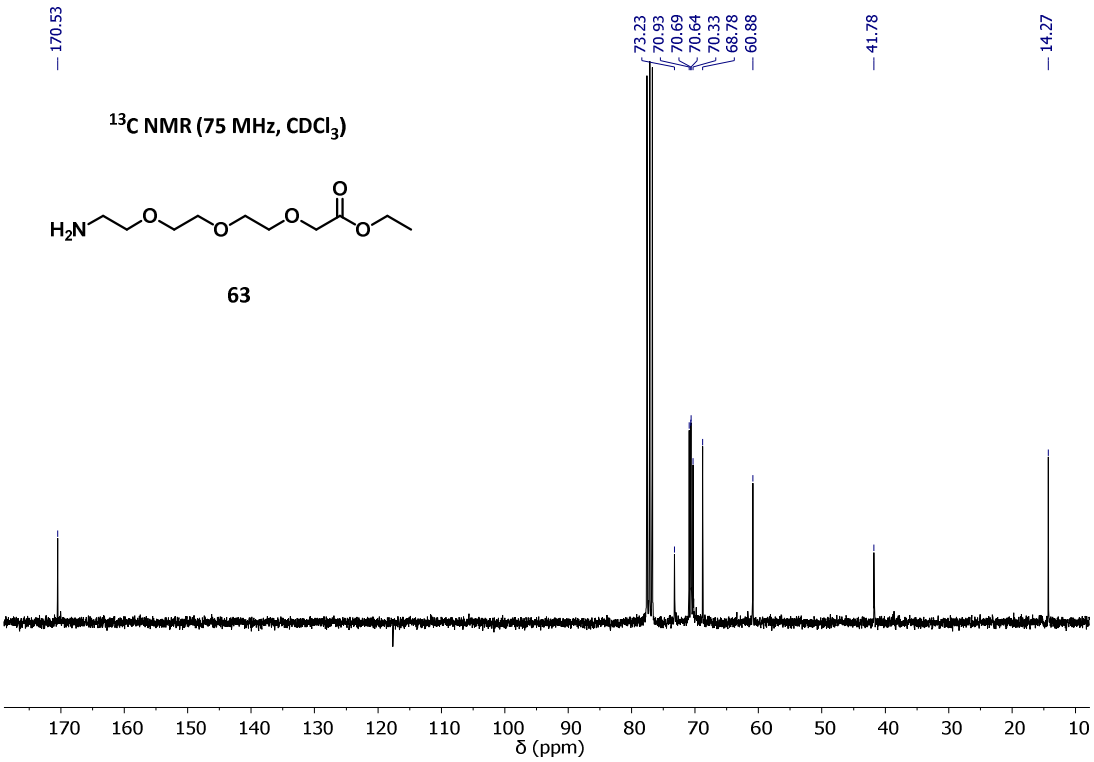
170.53
73.23 70.93 70.69 70.64 70.33 68.78 60.88
41.78
14.27
13C NMR (75 MHz, CDCl3)
H2N
O
63
δ (ppm)

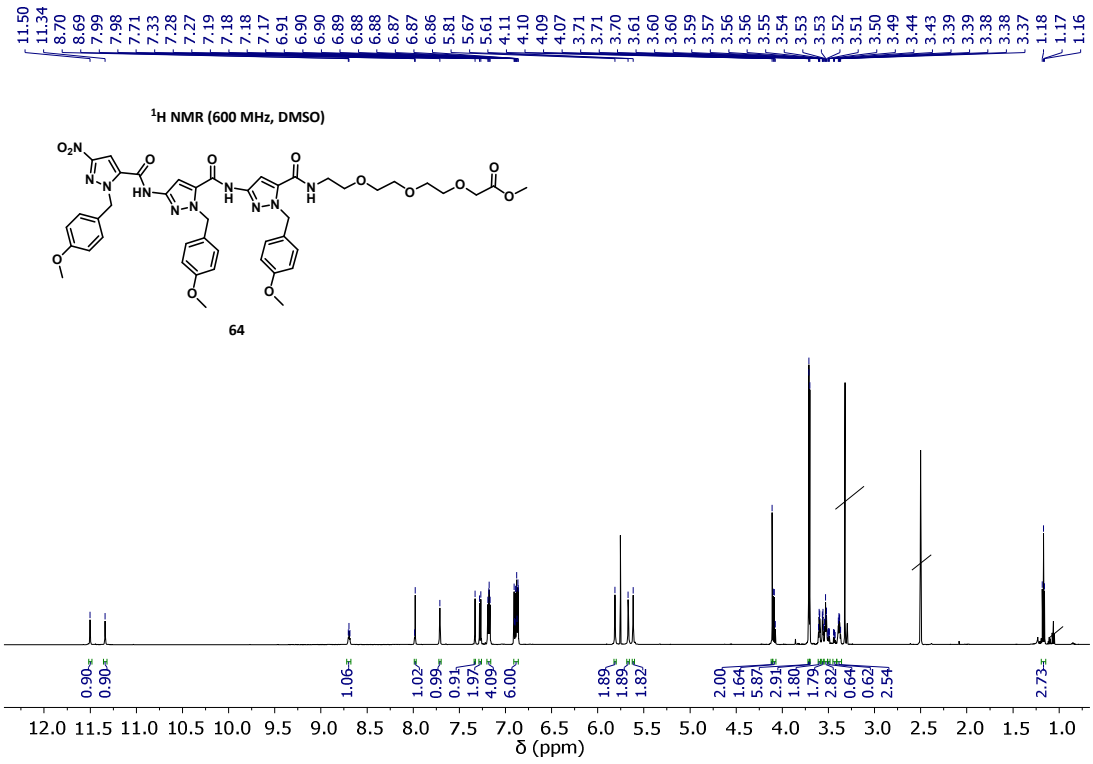
11.50
11.34
8.70
8.69
7.99
7.98
7.71
7.33
7.28
7.27
7.19
7.18
7.18
7.17
6.91
6.90
6.90
6.89
6.88
6.88
6.87
6.87
6.86
5.81
5.67
5.61
4.11
4.10
4.09
4.07
3.71
3.71
3.70
3.61
3.60
3.60
3.59
3.57
3.56
3.56
3.55
3.54
3.53
3.53
3.52
3.51
3.50
3.49
3.44
3.43
3.39
3.39
3.38
3.38
3.37
1.18
1.17
1.16
1H NMR (600 MHz, DMSO)
64
0.90
0.90
1.06
1.02
0.99
0.91
1.97
4.09
6.00
1.89
1.89
1.82
2.00
1.64
5.87
2.91
1.80
1.79
2.82
0.64
0.62
2.54
2.73
12.0 11.5 11.0 10.5 10.0 9.5 9.0 8.5 8.0 7.5 7.0 6.5 6.0 5.5 5.0 4.5 4.0 3.5 3.0 2.5 2.0 1.5 1.0
δ (ppm)

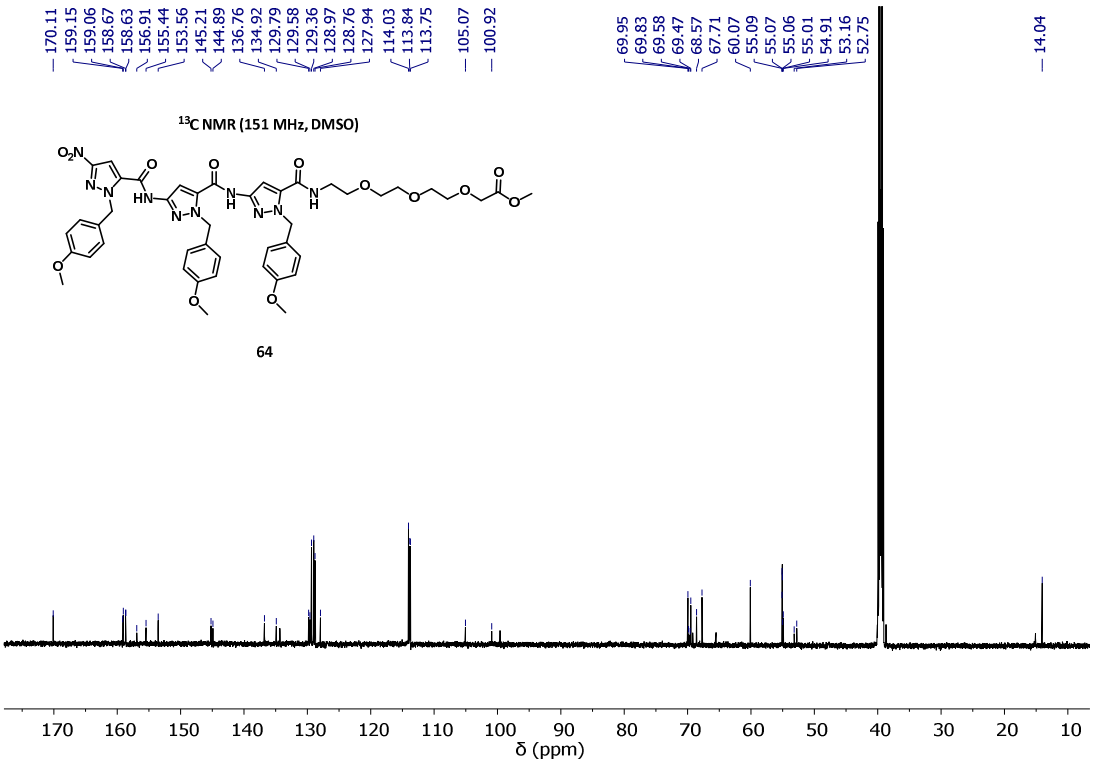
170.11
159.15
159.06
158.67
158.63
156.91
155.44
153.56
145.21
144.89
136.76
134.92
129.79
129.58
129.36
128.97
128.76
127.94
114.03
113.84
113.75
105.07
100.92
69.95
69.83
69.58
69.47
68.57
67.71
60.07
55.09
55.07
55.06
55.01
54.91
53.16
52.75
14.04
13C NMR (151 MHz, DMSO)
64
170 160 150 140 130 120 110 100 90 80 70 60 50 40 30 20 10
δ (ppm)

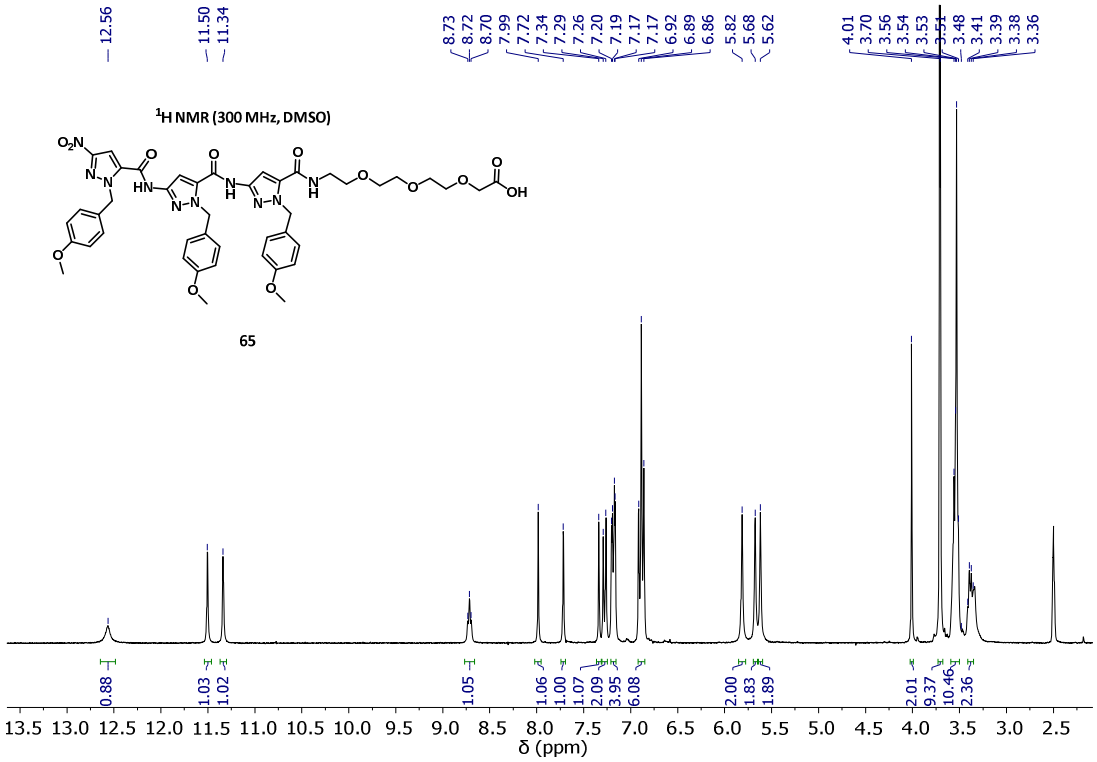

^{1}H NMR (300 MHz, DMSO)

65

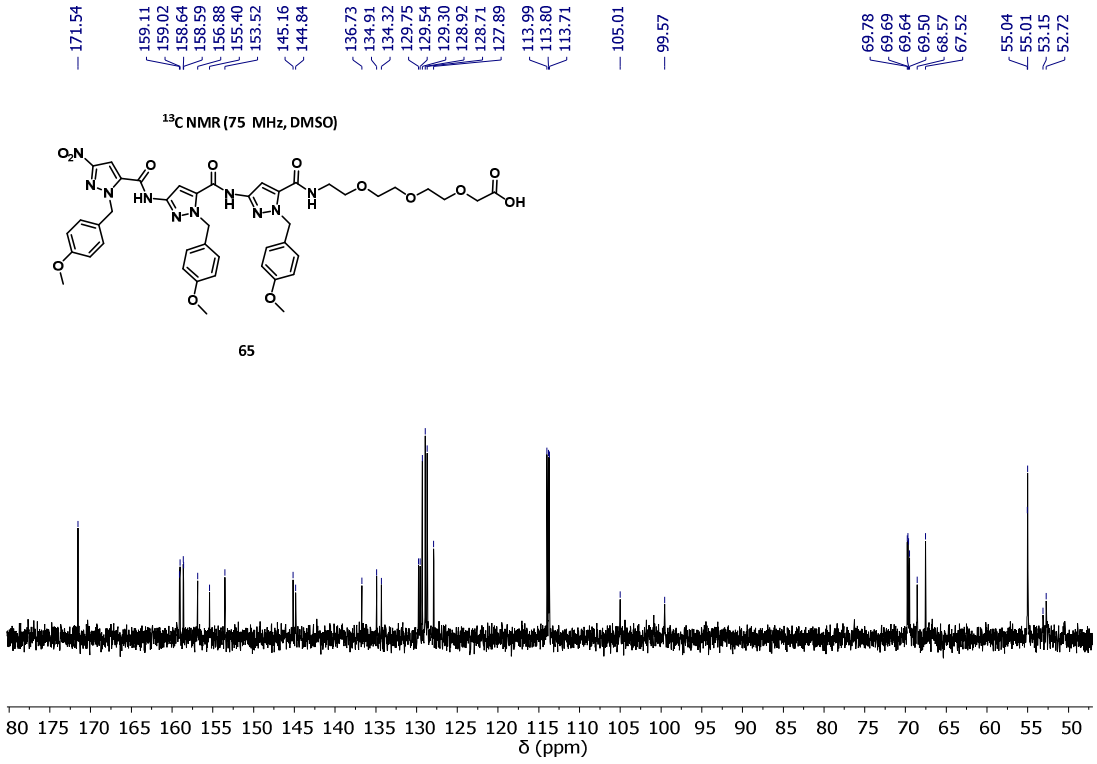

^{13}C NMR (75 MHz, DMSO)

65

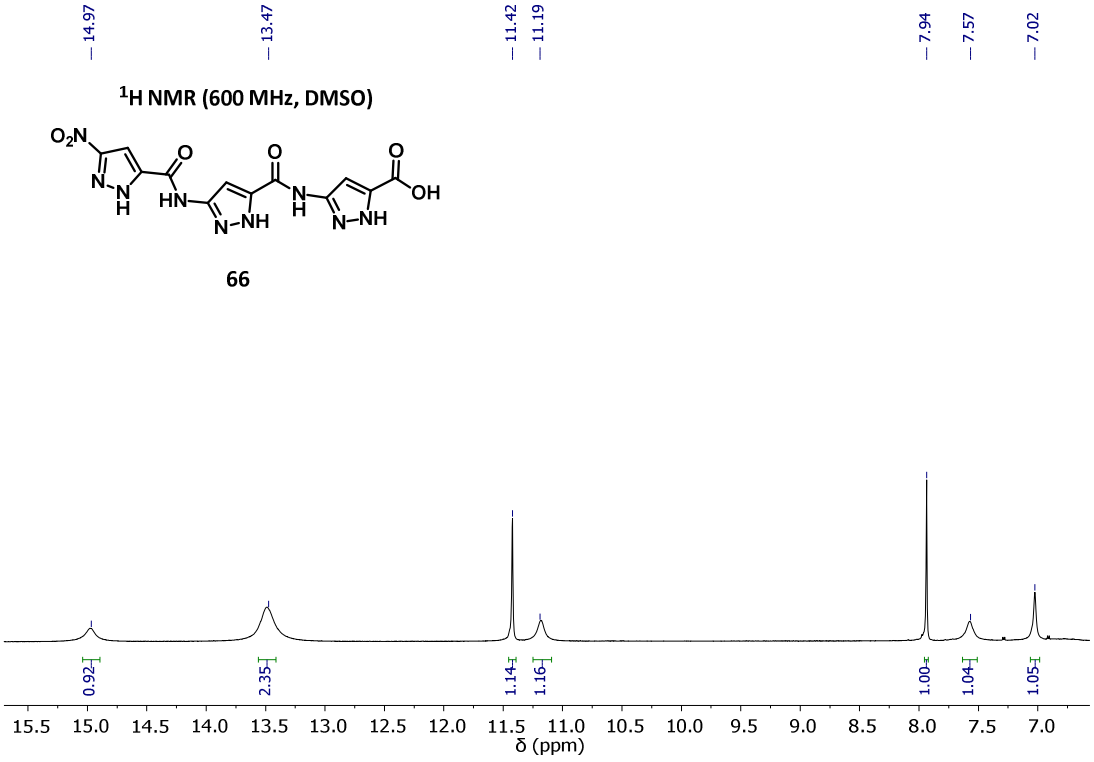

^{1}H NMR (600 MHz, DMSO)

66

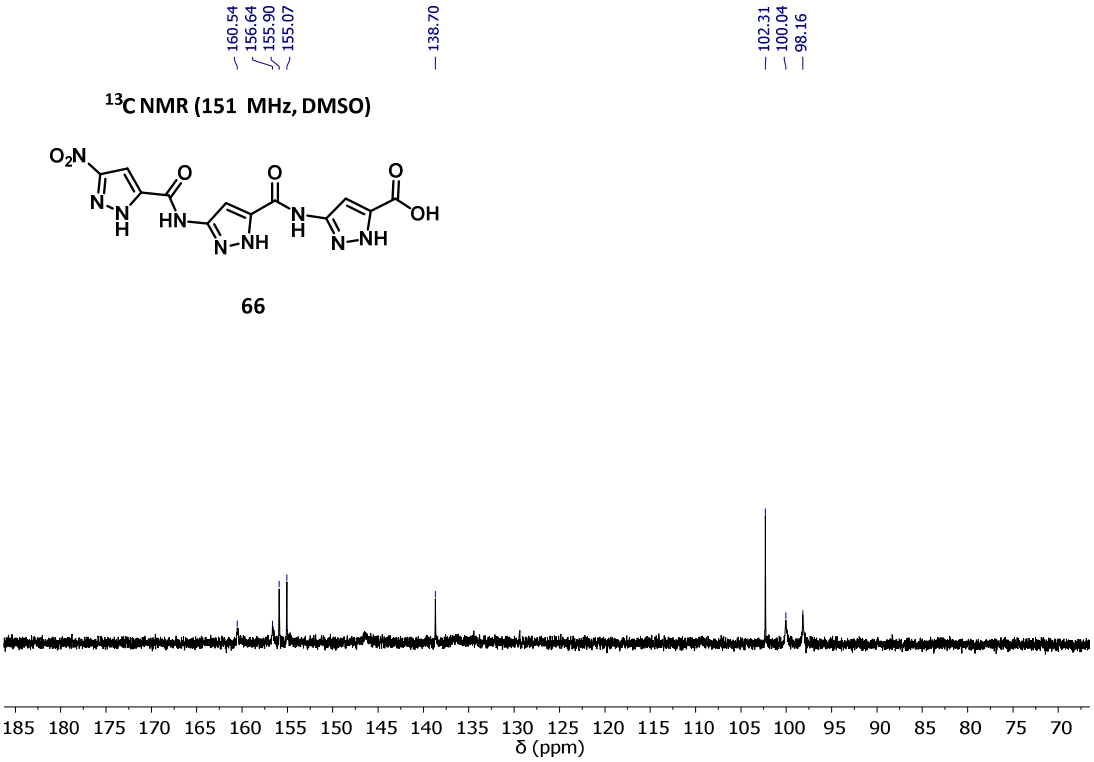

^{13}C NMR (151 MHz, DMSO)

66

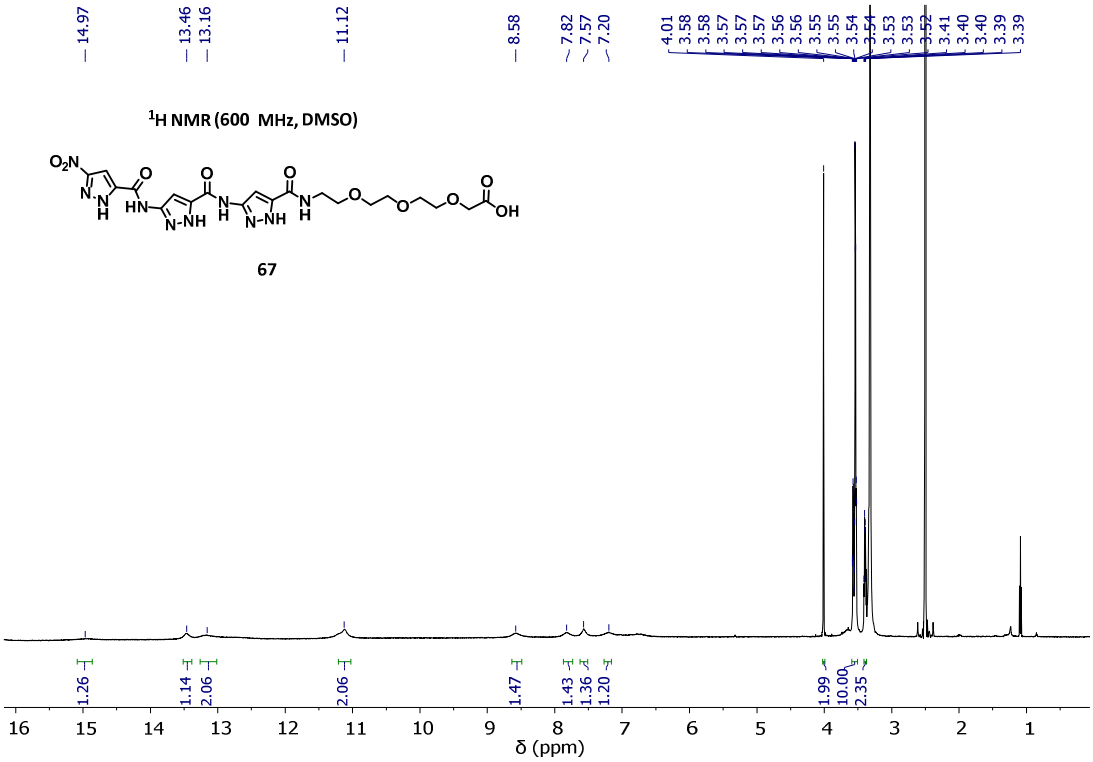
14.97
13.46
13.16
11.12
8.58
7.82
7.57
7.20
4.01
3.58
3.58
3.57
3.57
3.57
3.56
3.56
3.55
3.55
3.54
3.54
3.53
3.53
3.52
3.41
3.40
3.40
3.39
3.39
1H NMR (600 MHz, DMSO)
67
1.26
1.14
2.06
2.06
1.47
1.43
1.36
1.20
1.99
10.00
2.35
δ (ppm)

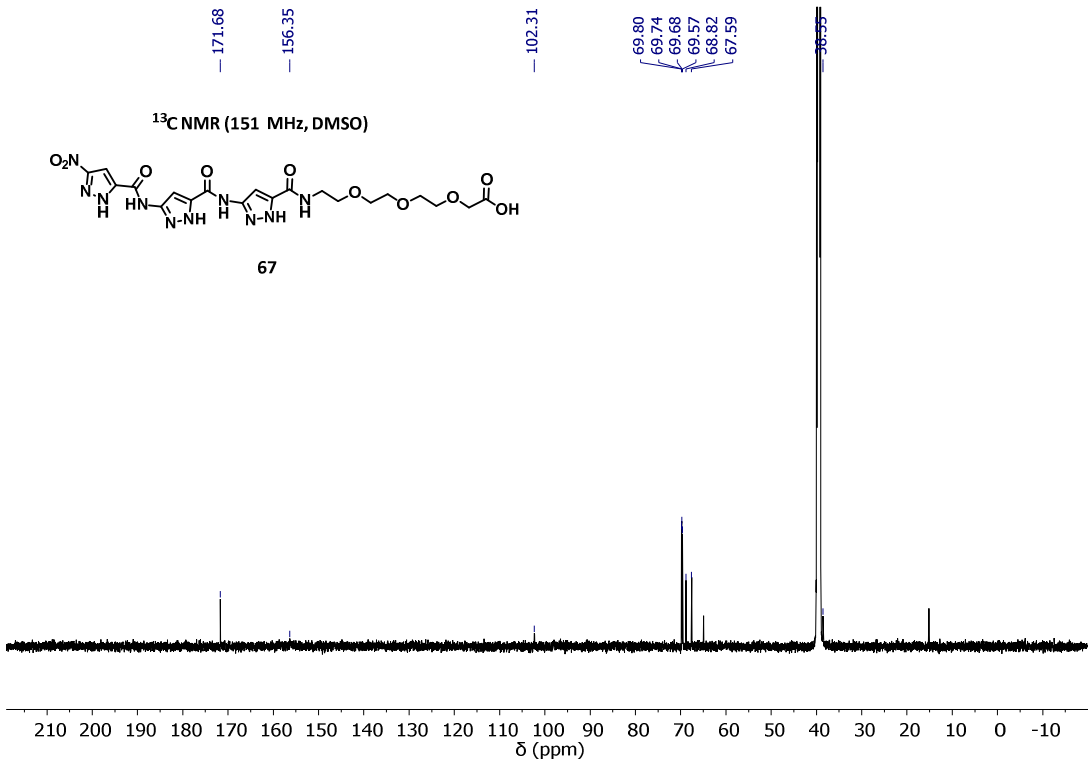
171.68
156.35
102.31
69.80
69.74
69.68
69.57
68.82
67.59
38.55
13C NMR (151 MHz, DMSO)
67
δ (ppm)

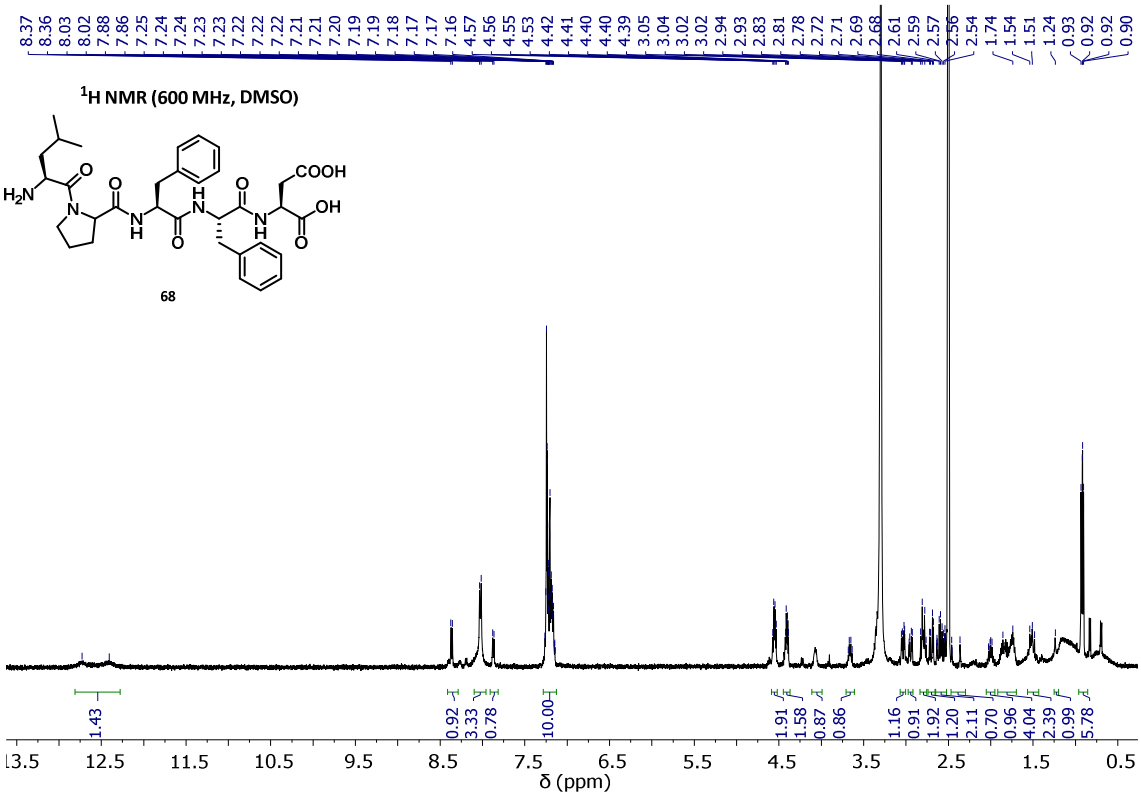
^{1}H NMR (600 MHz, DMSO)
68
δ (ppm)

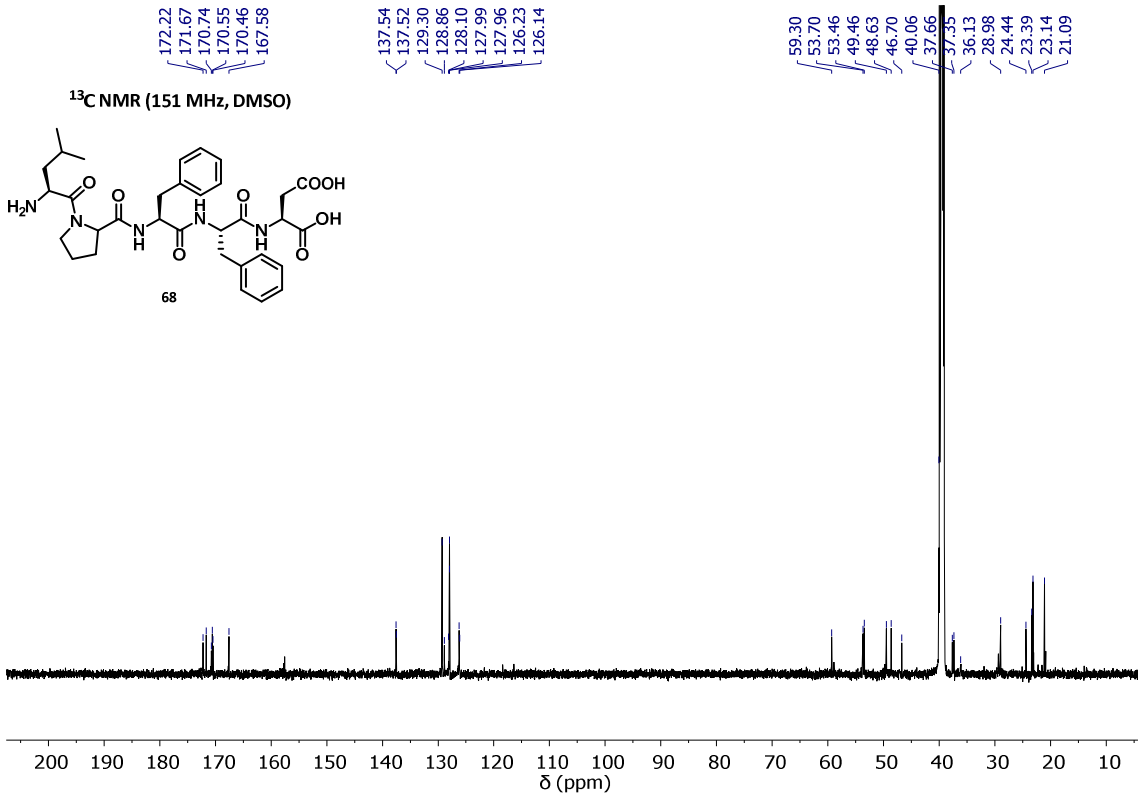
^{13}C NMR (151 MHz, DMSO)
68
δ (ppm)

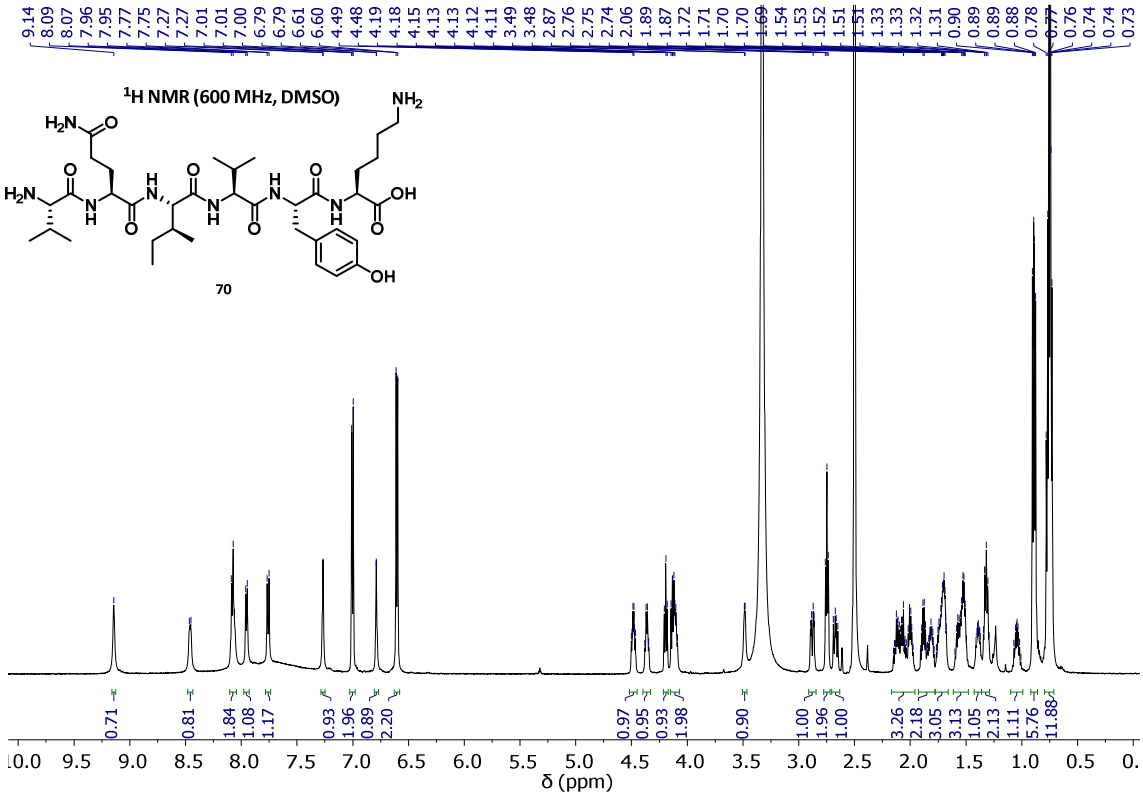
^{1}H NMR (600 MHz, DMSO)
70
δ (ppm)

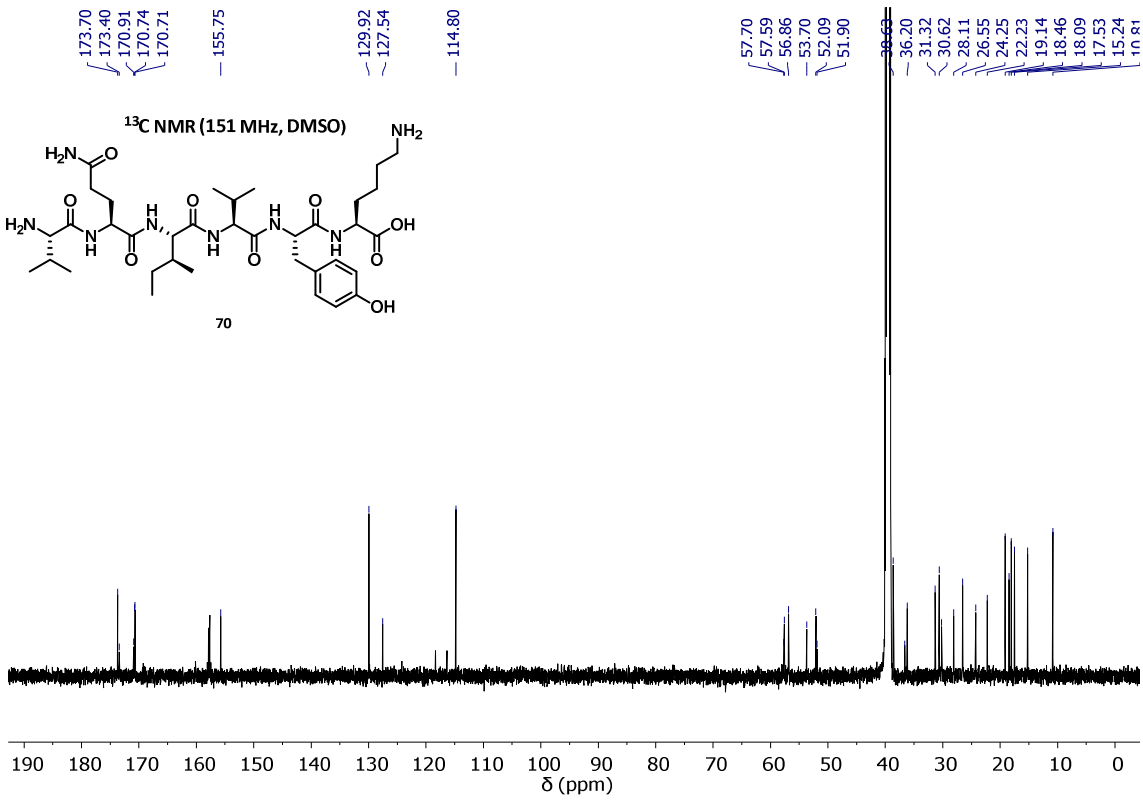
^{13}C NMR (151 MHz, DMSO)
70
δ (ppm)

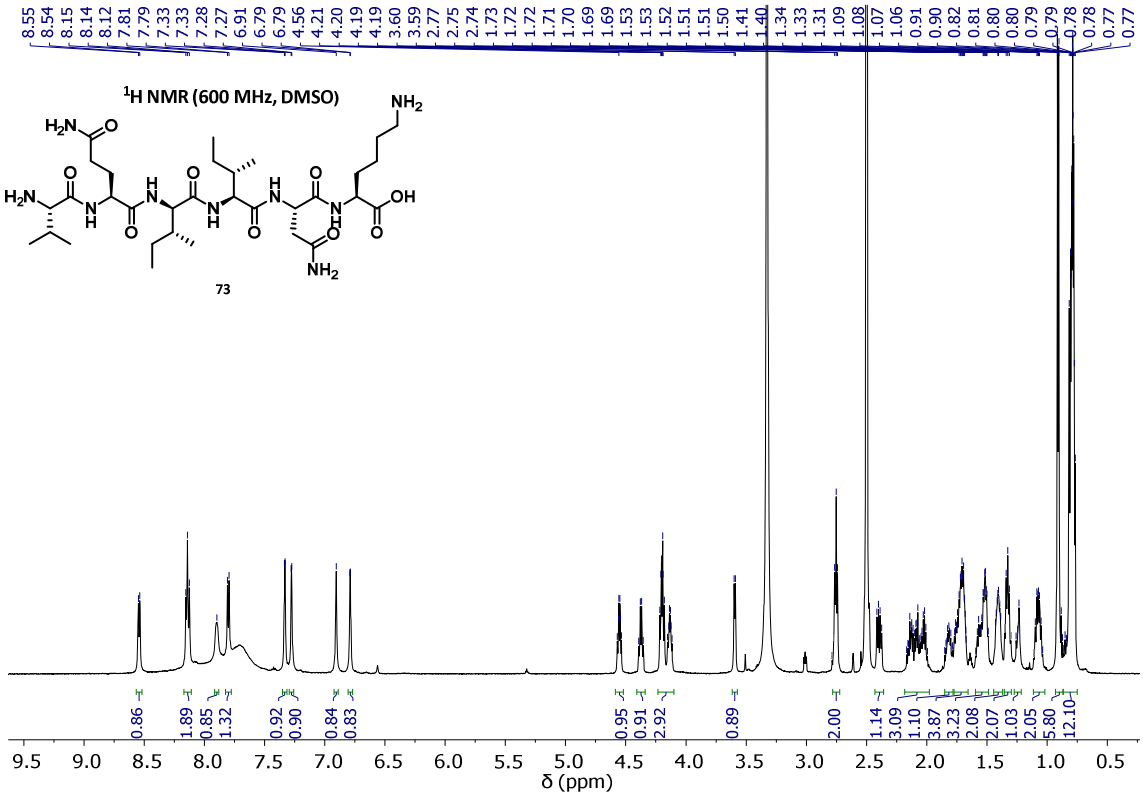
^{1}H NMR (600 MHz, DMSO)
73
δ (ppm)

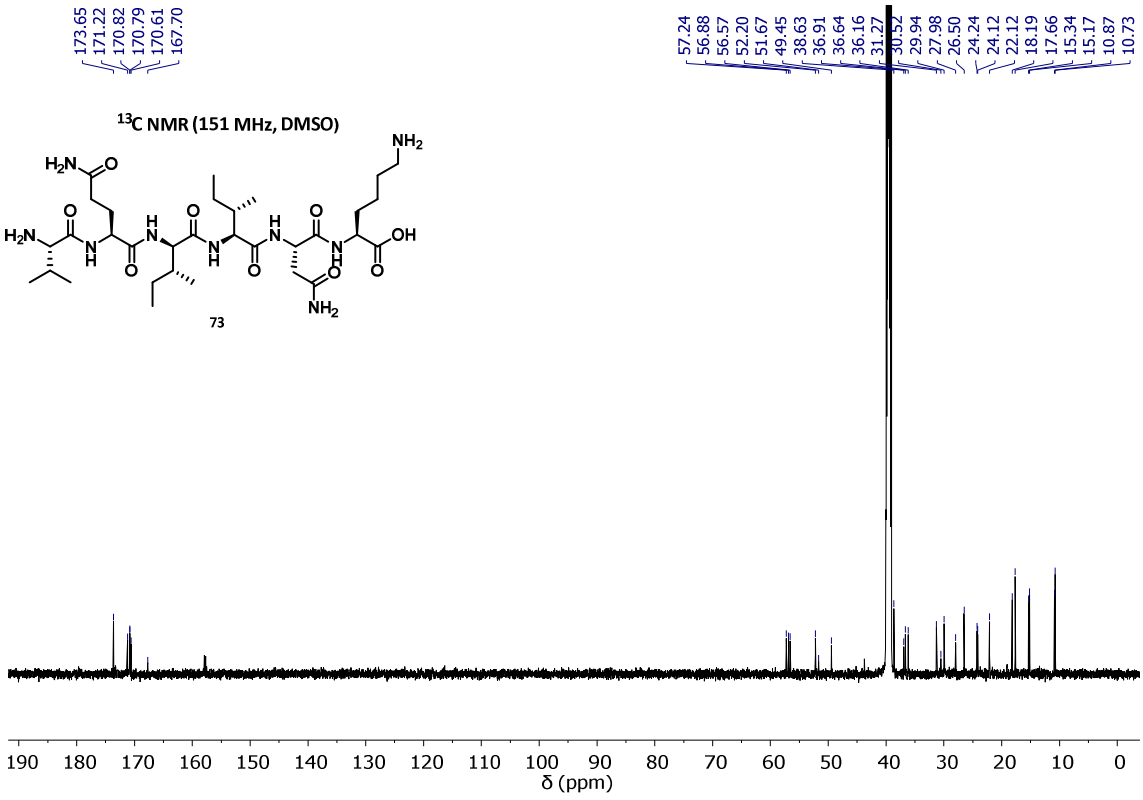
^{13}C NMR (151 MHz, DMSO)
73
δ (ppm)

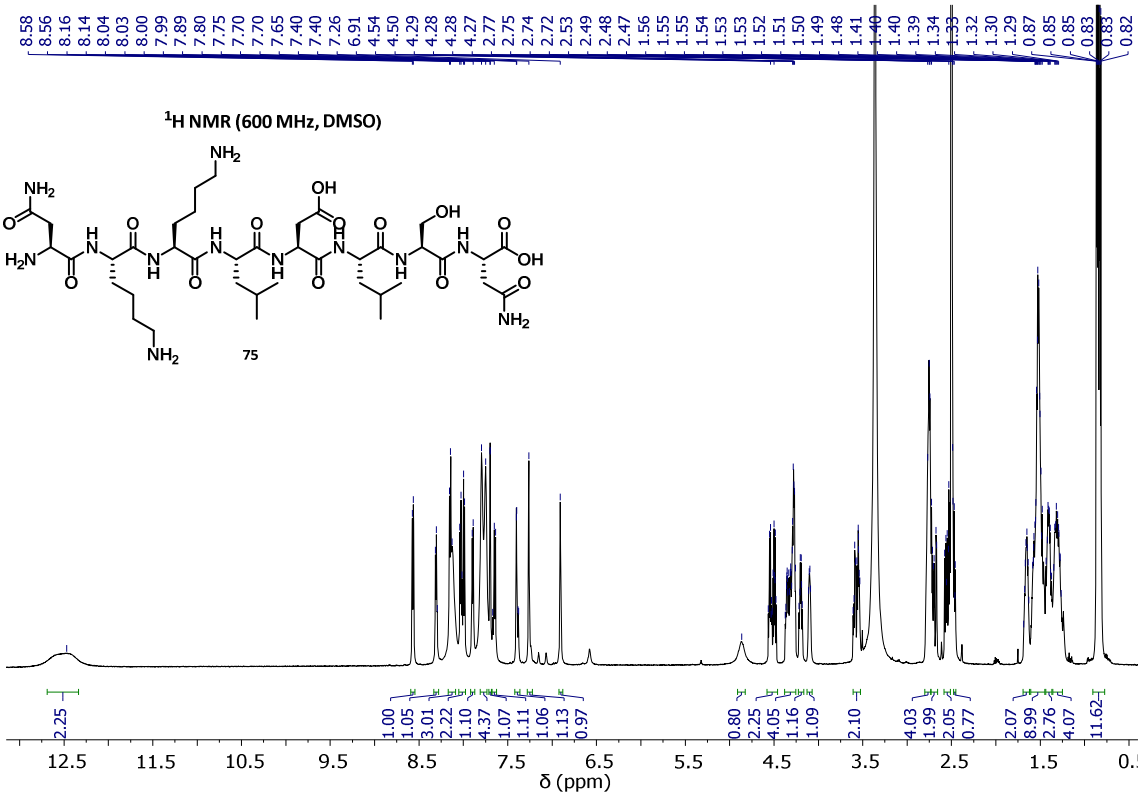
^{1}H NMR (600 MHz, DMSO)
75
δ (ppm)

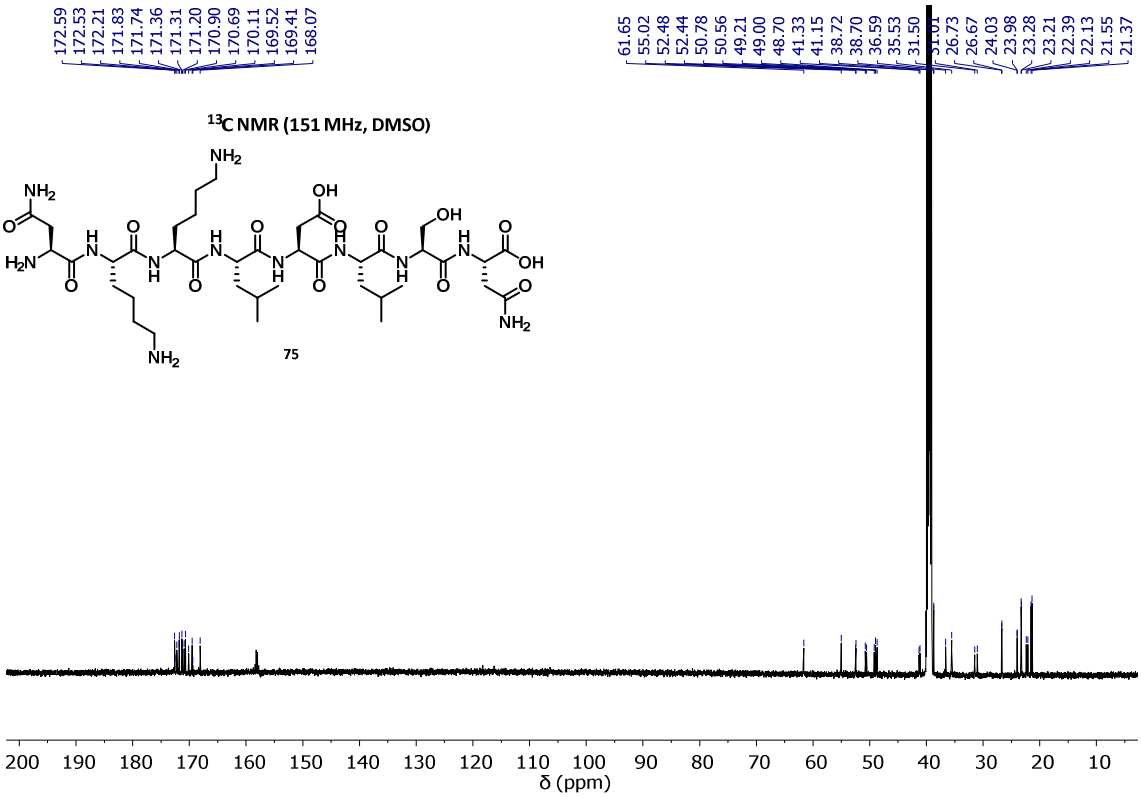
^{13}C NMR (151 MHz, DMSO)
75
δ (ppm)

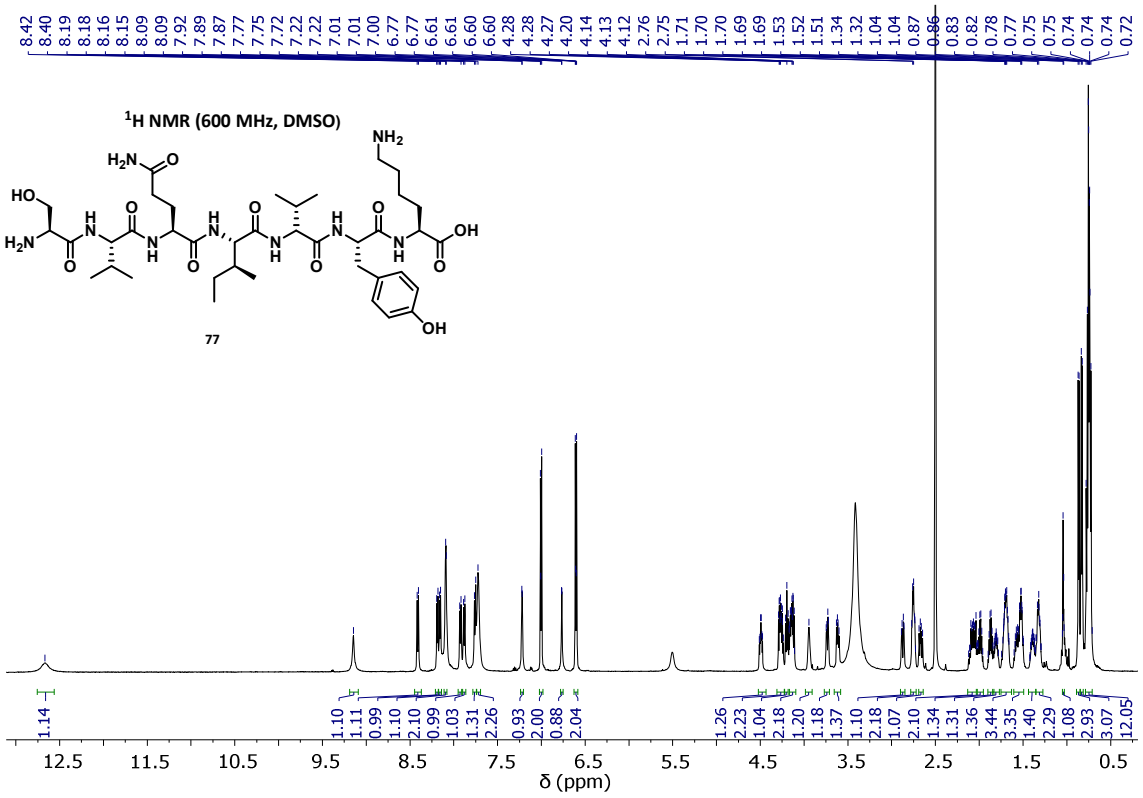

^{1}H NMR (600 MHz, DMSO)

77

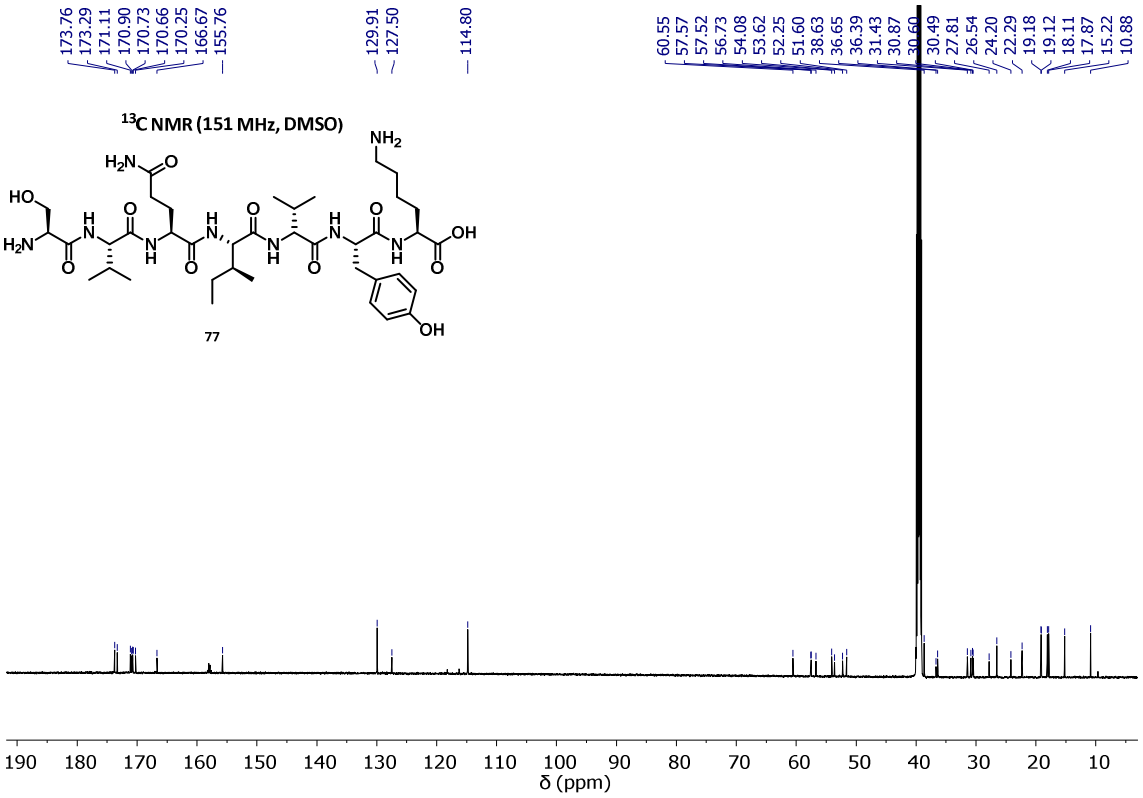

^{13}C NMR (151 MHz, DMSO)

77

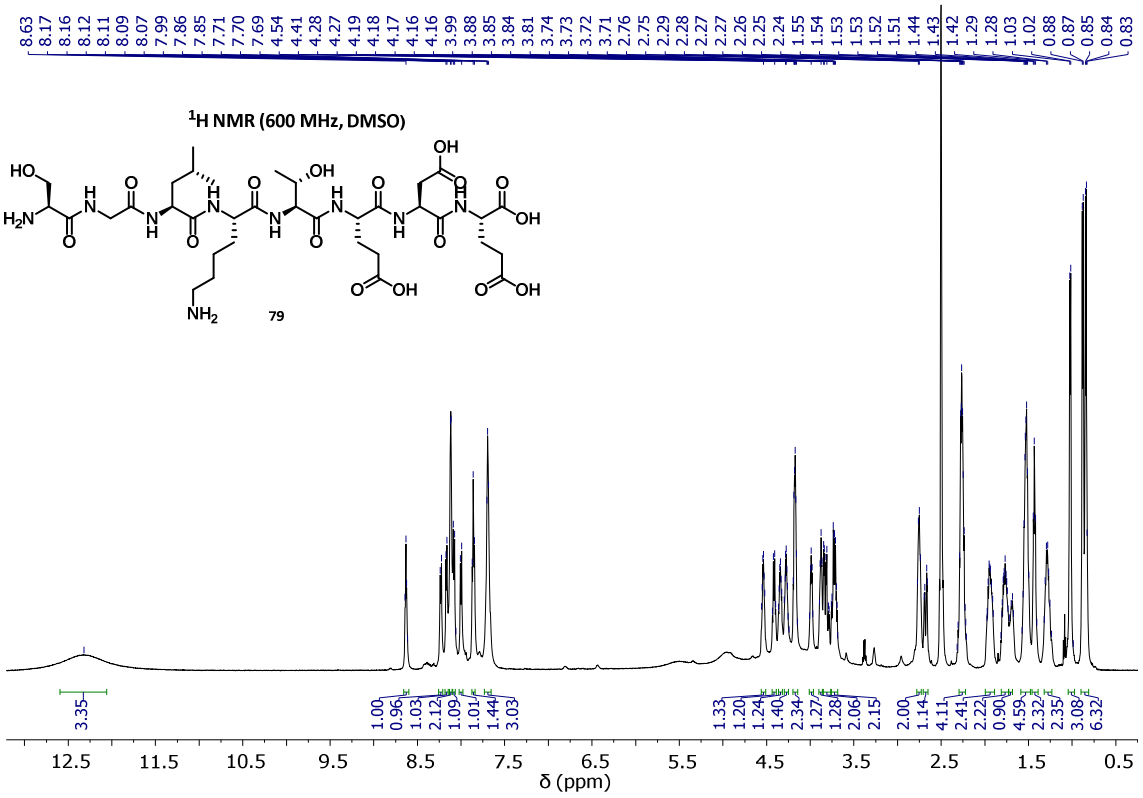
^{1}H NMR (600 MHz, DMSO)
79
δ (ppm)

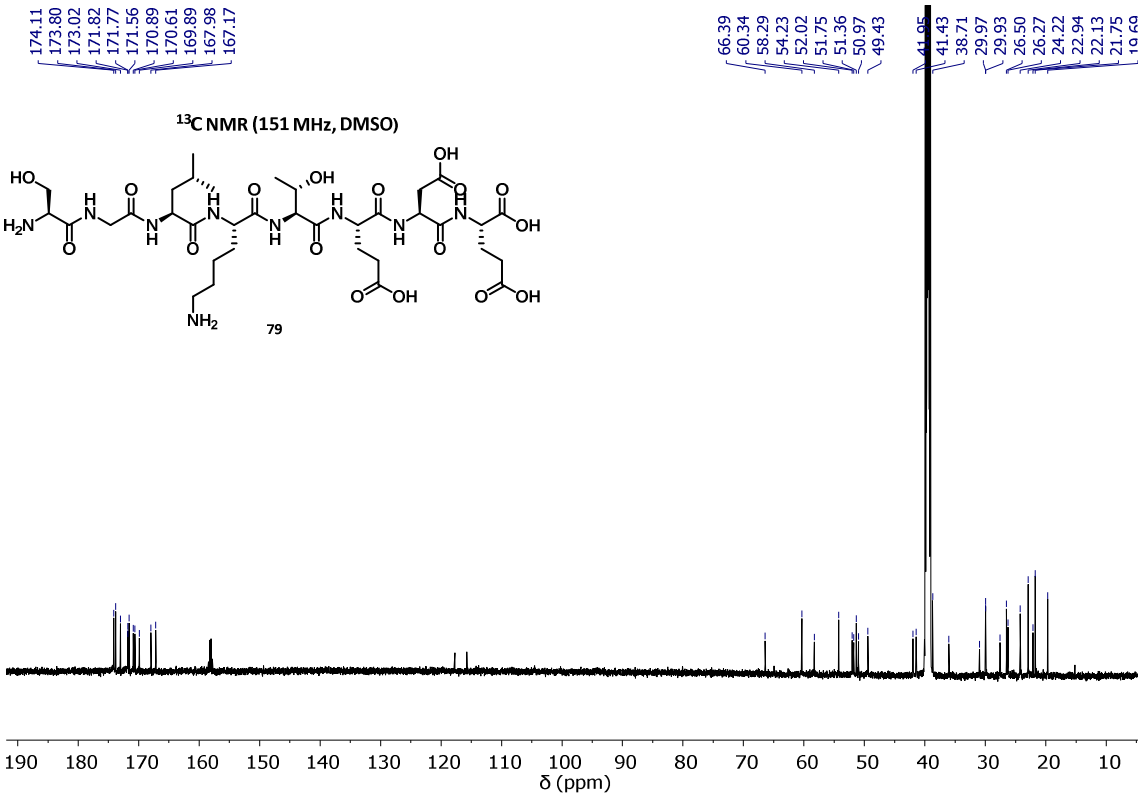
^{13}C NMR (151 MHz, DMSO)
79
δ (ppm)

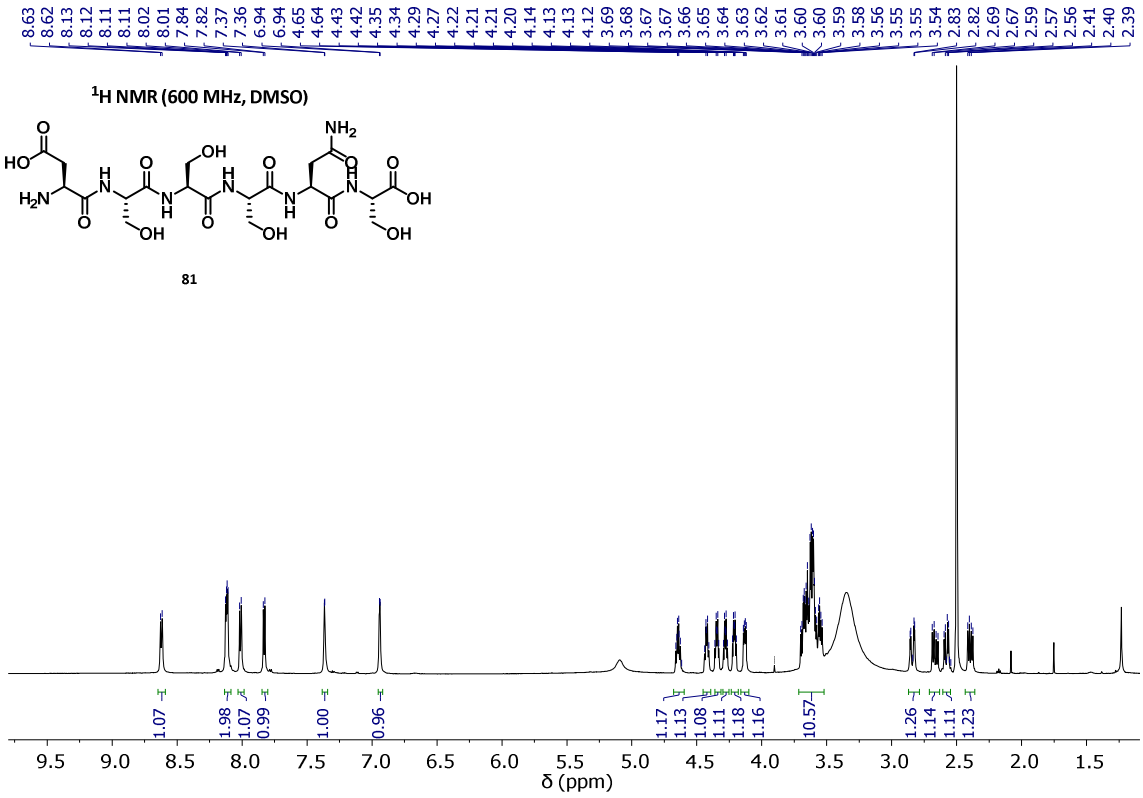
8.63 8.62 8.13 8.12 8.11 8.11 8.02 8.01 7.84 7.82 7.37 7.36 6.94 6.94 4.65 4.64 4.43 4.42 4.35 4.34 4.29 4.27 4.22 4.21 4.21 4.20 4.14 4.13 4.12 3.69 3.68 3.67 3.67 3.66 3.65 3.64 3.63 3.62 3.61 3.60 3.60 3.59 3.58 3.56 3.55 3.55 3.54 2.83 2.82 2.69 2.67 2.59 2.57 2.56 2.41 2.40 2.39
1H NMR (600 MHz, DMSO)
81
1.07 1.98 1.07 0.99 1.00 0.96 1.17 1.13 1.08 1.11 1.18 1.16 10.57 1.26 1.14 1.11 1.23
9.5 9.0 8.5 8.0 7.5 7.0 6.5 6.0 5.5 5.0 4.5 4.0 3.5 3.0 2.5 2.0 1.5
δ (ppm)

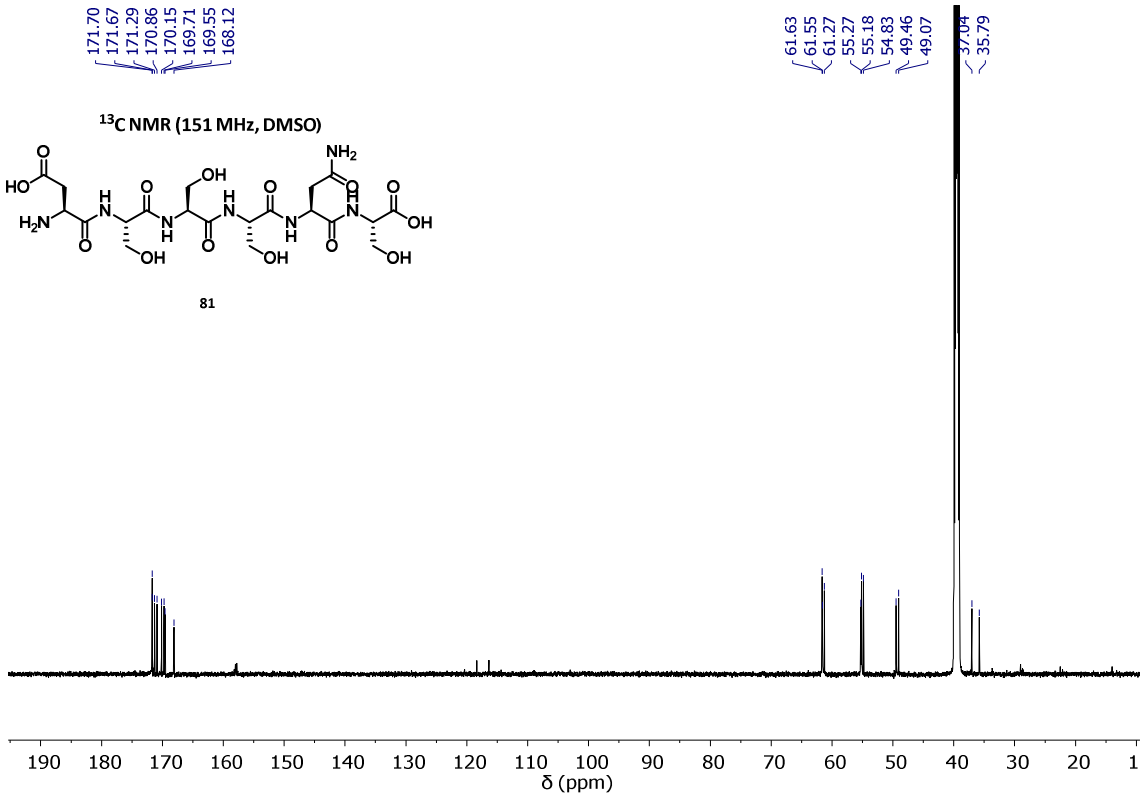
171.70 171.67 171.29 170.86 170.15 169.71 169.55 168.12
61.63 61.55 61.27 55.27 55.18 54.83 49.46 49.07 37.04 35.79
13C NMR (151 MHz, DMSO)
81
190 180 170 160 150 140 130 120 110 100 90 80 70 60 50 40 30 20 1
δ (ppm)

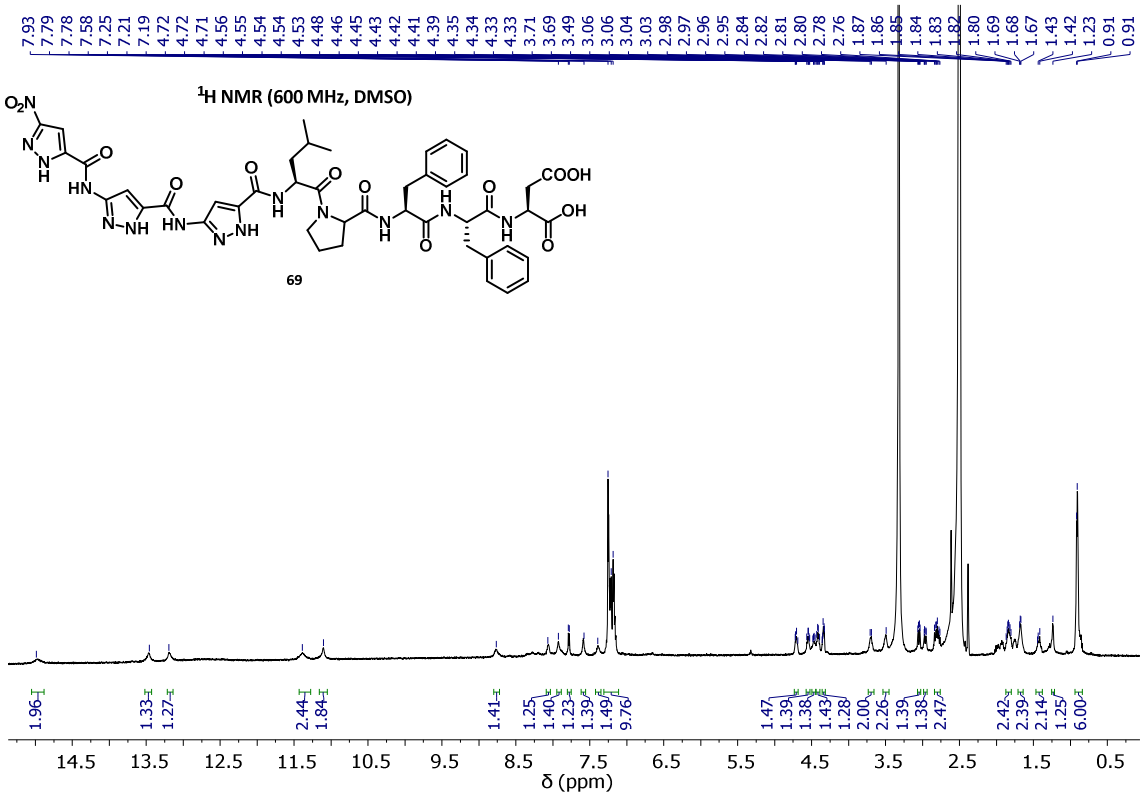
7.93 7.79 7.78 7.58 7.25 7.21 7.19 4.72 4.72 4.71 4.56 4.55 4.54 4.54 4.53 4.48 4.46 4.45 4.43 4.42 4.41 4.39 4.35 4.34 4.33 4.33 3.71 3.69 3.49 3.06 3.06 3.04 3.03 2.98 2.97 2.96 2.95 2.84 2.82 2.81 2.80 2.78 2.76 1.87 1.86 1.85 1.84 1.83 1.82 1.80 1.69 1.68 1.67 1.43 1.42 1.23 0.91 0.91
1H NMR (600 MHz, DMSO)
69
1.96 1.33 1.27 2.44 1.84 1.41 1.25 1.40 1.23 1.39 1.49 9.76 1.47 1.39 1.38 1.43 1.28 2.00 2.26 1.39 1.38 2.47 2.42 2.39 2.14 1.25 6.00
14.5 13.5 12.5 11.5 10.5 9.5 8.5 7.5 6.5 5.5 4.5 3.5 2.5 1.5 0.5
δ (ppm)

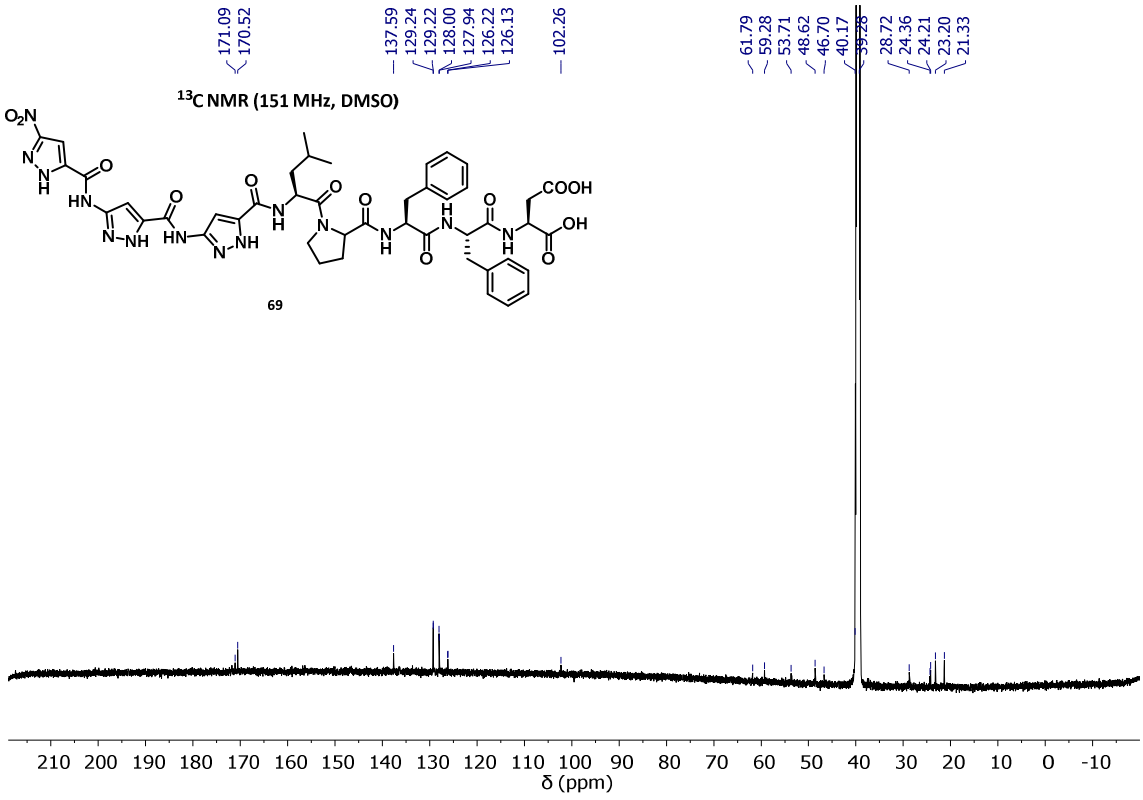
171.09 170.52 137.59 129.24 129.22 128.00 127.94 126.22 126.13 102.26 61.79 59.28 53.71 48.62 46.70 40.17 39.28 28.72 24.36 24.21 23.20 21.33
13C NMR (151 MHz, DMSO)
69
210 200 190 180 170 160 150 140 130 120 110 100 90 80 70 60 50 40 30 20 10 0 -10
δ (ppm)

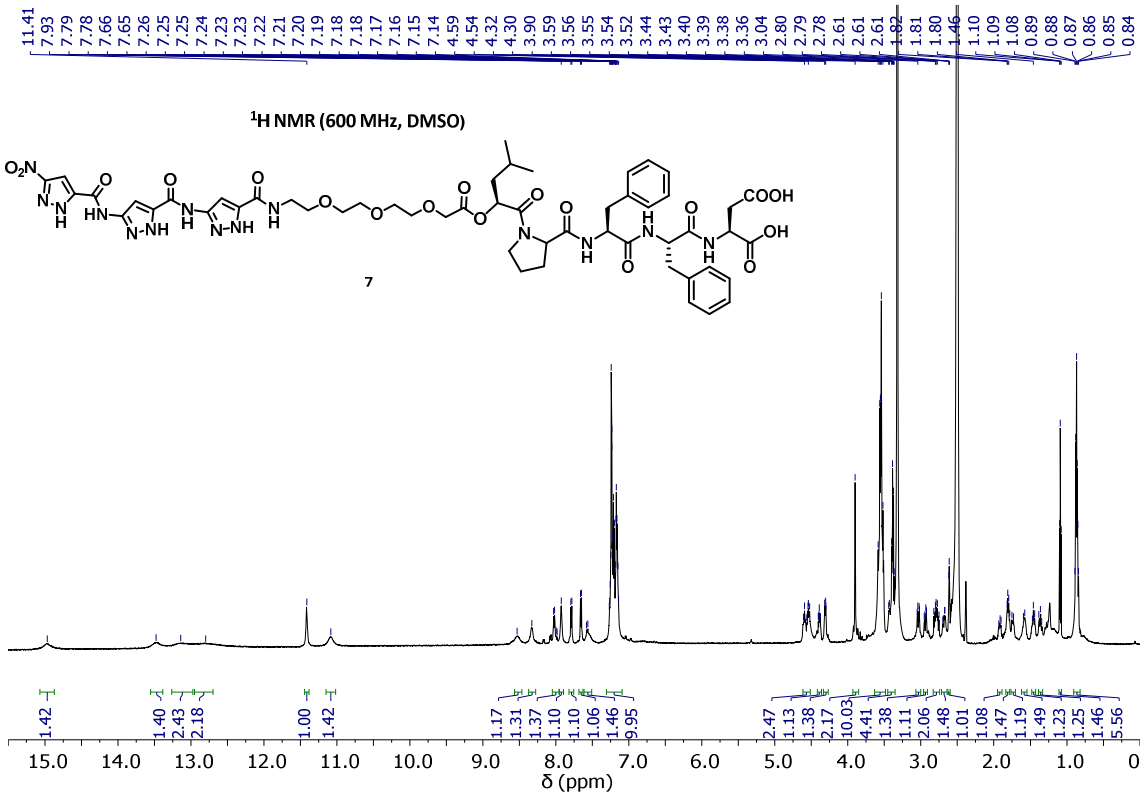
11.41
7.93
7.79
7.78
7.66
7.65
7.26
7.25
7.25
7.24
7.23
7.23
7.22
7.21
7.20
7.19
7.18
7.18
7.17
7.16
7.15
7.14
4.59
4.54
4.32
4.30
3.90
3.59
3.56
3.55
3.54
3.52
3.44
3.43
3.40
3.39
3.38
3.36
3.04
2.80
2.79
2.78
2.61
2.61
2.61
1.82
1.81
1.80
1.46
1.10
1.09
1.08
0.89
0.88
0.87
0.86
0.85
0.84
1H NMR (600 MHz, DMSO)
7
1.42
1.40
2.43
2.18
1.00
1.42
1.17
1.31
1.37
1.10
1.10
1.06
1.46
9.95
2.47
1.13
1.38
2.17
10.03
4.41
1.38
1.11
2.06
1.48
1.01
1.08
1.47
1.19
1.49
1.23
1.25
1.46
5.56
15.0
14.0
13.0
12.0
11.0
10.0
9.0
8.0
7.0
6.0
5.0
4.0
3.0
2.0
1.0
0
δ (ppm)

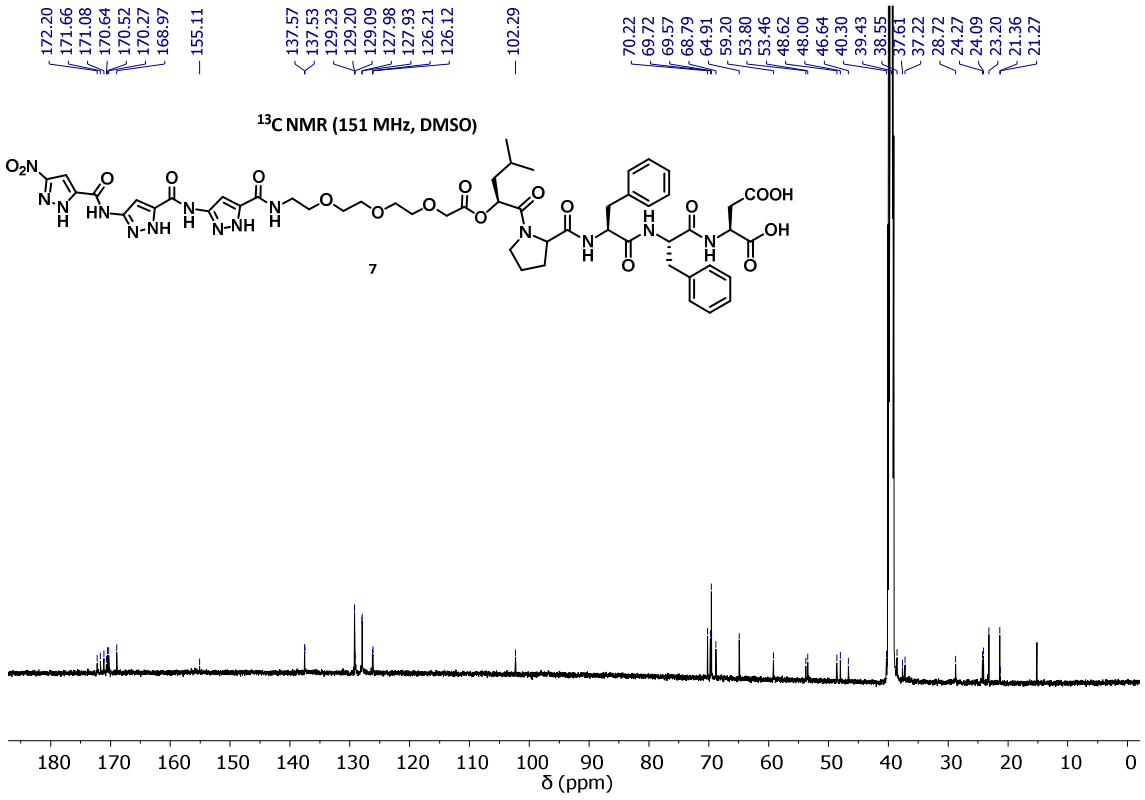
172.20
171.66
171.08
170.64
170.52
170.27
168.97
155.11
137.57
137.53
129.23
129.20
129.09
127.98
127.93
126.21
126.12
102.29
70.22
69.72
69.57
68.79
64.91
59.20
53.80
53.46
48.62
48.00
46.64
40.30
39.43
38.55
37.61
37.22
28.72
24.27
24.09
23.20
21.36
21.27
13C NMR (151 MHz, DMSO)
7
180
170
160
150
140
130
120
110
100
90
80
70
60
50
40
30
20
10
0
δ (ppm)

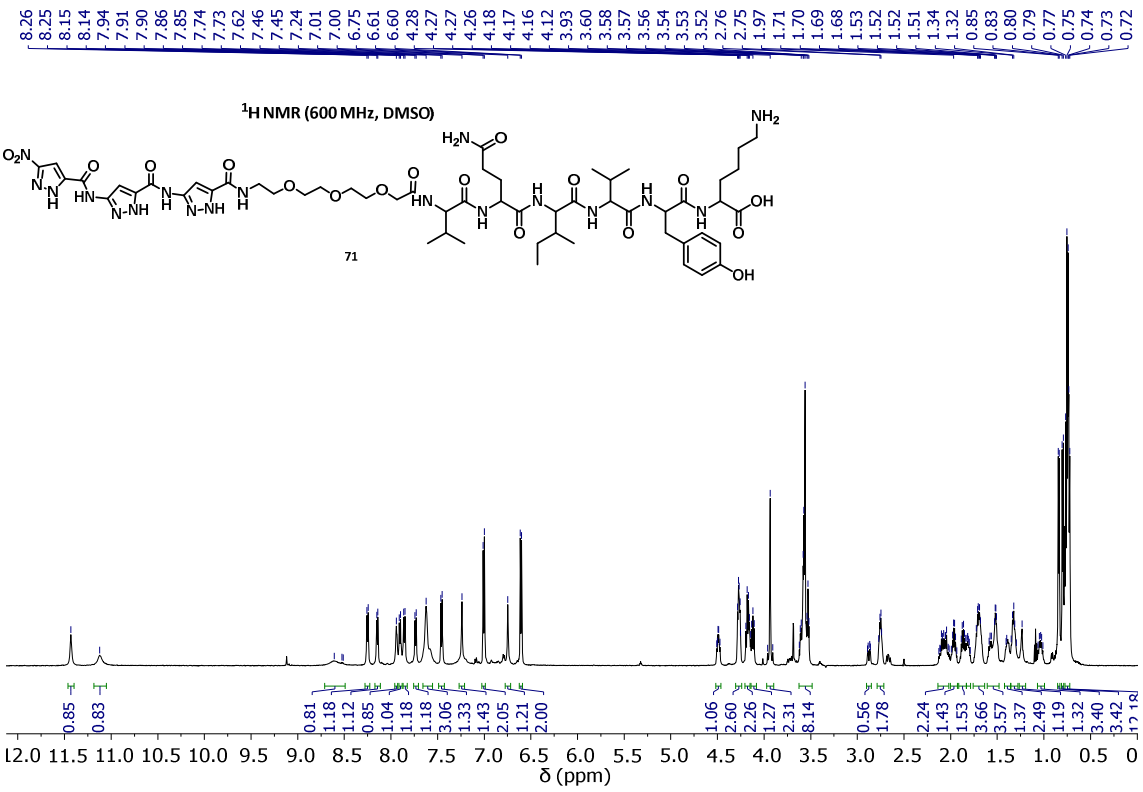
^{1}H NMR (600 MHz, DMSO)
71
δ (ppm)

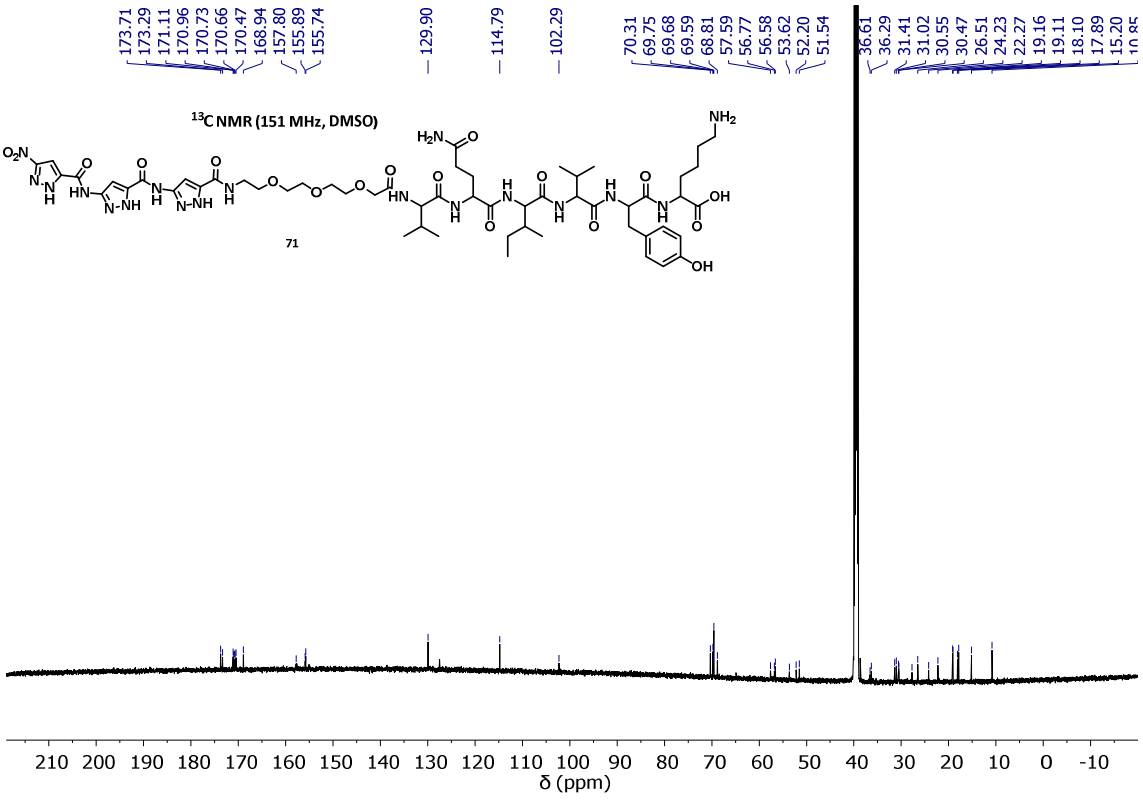
^{13}C NMR (151 MHz, DMSO)
71
δ (ppm)

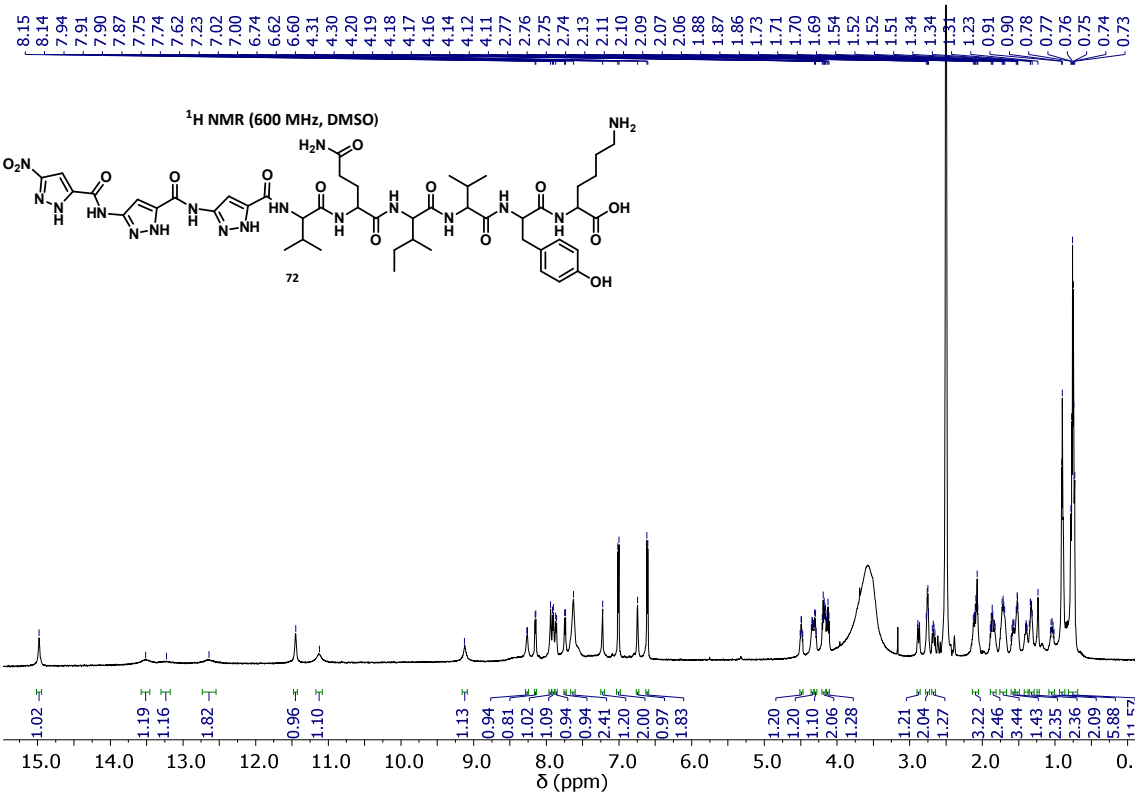
^{1}H NMR (600 MHz, DMSO)
72
δ (ppm)

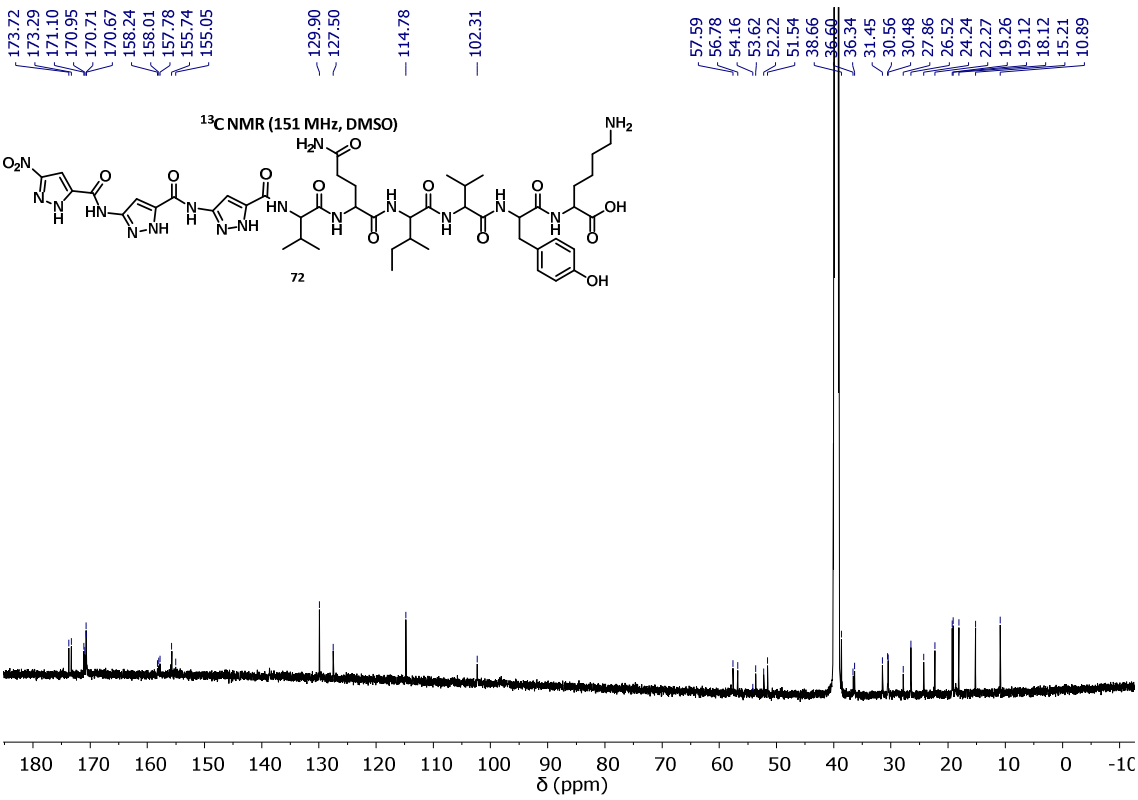
^{13}C NMR (151 MHz, DMSO)
72
δ (ppm)

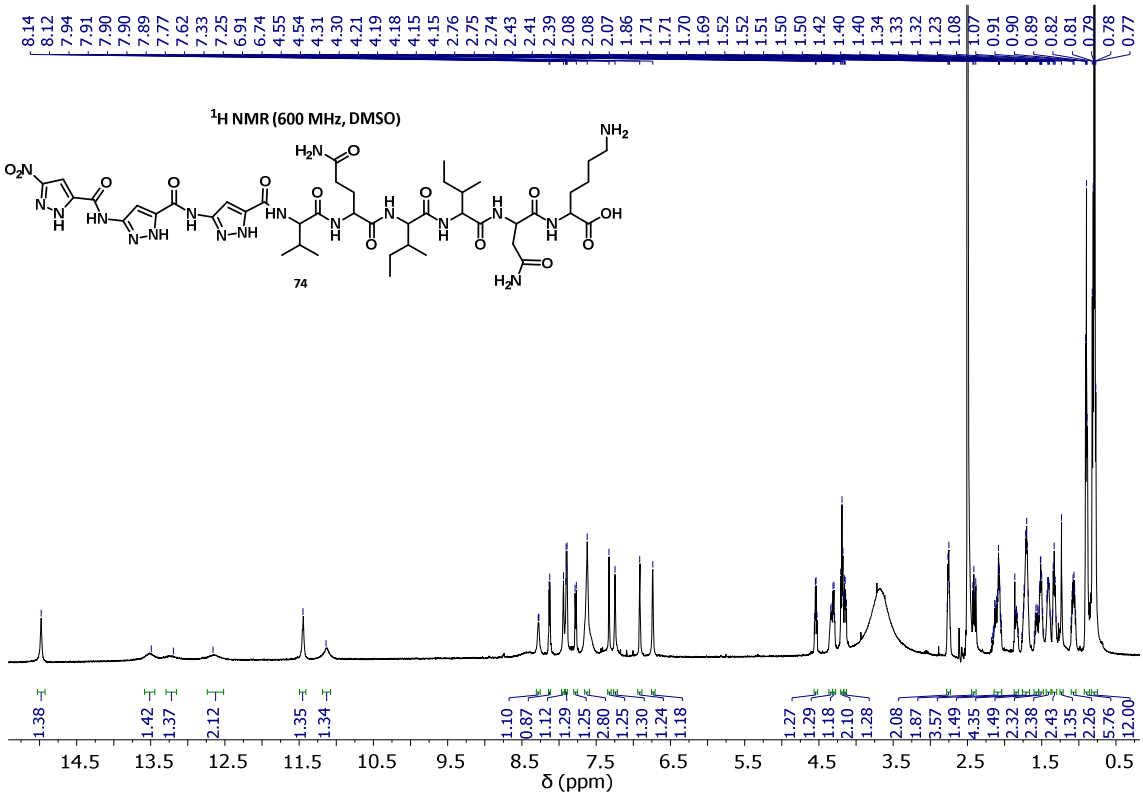
8.14 8.12 7.94 7.91 7.90 7.90 7.89 7.77 7.62 7.33 7.25 6.91 6.74 4.55 4.54 4.31 4.30 4.21 4.19 4.18 4.15 4.15 2.76 2.75 2.74 2.43 2.41 2.39 2.08 2.08 2.07 1.86 1.71 1.71 1.70 1.69 1.52 1.52 1.51 1.50 1.50 1.42 1.40 1.40 1.34 1.33 1.32 1.23 1.08 1.07 0.91 0.90 0.89 0.82 0.81 0.79 0.78 0.77
1H NMR (600 MHz, DMSO)
74
1.38 1.42 1.37 2.12 1.35 1.34 1.10 0.87 1.12 1.29 1.25 2.80 1.25 1.30 1.24 1.18 1.27 1.29 1.18 2.10 1.28 2.08 1.87 3.57 1.49 4.35 1.49 2.32 2.38 2.43 1.35 2.26 5.76 12.00
14.5 13.5 12.5 11.5 10.5 9.5 8.5 7.5 6.5 5.5 4.5 3.5 2.5 1.5 0.5
δ (ppm)

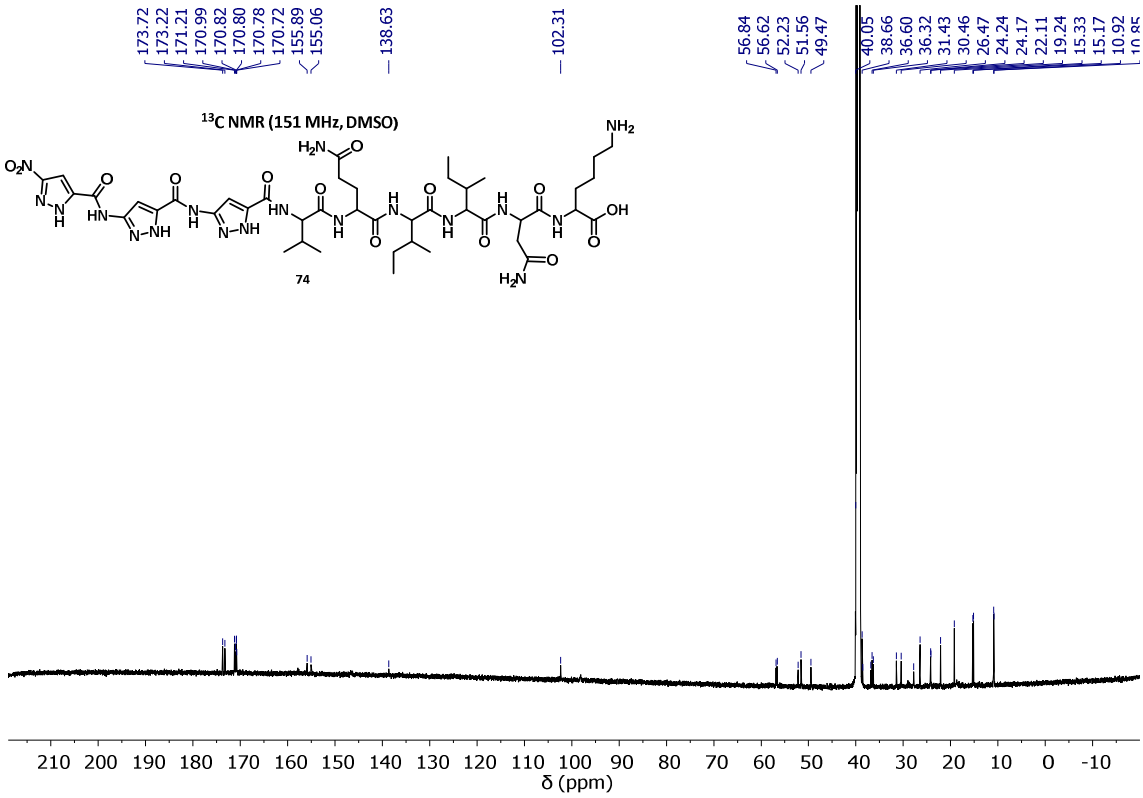
173.72 173.22 171.21 170.99 170.82 170.80 170.78 170.72 155.89 155.06 138.63 102.31 56.84 56.62 52.23 51.56 49.47 40.05 38.66 36.60 36.32 31.43 30.46 26.47 24.24 24.17 22.11 19.24 15.33 15.17 10.92
13C NMR (151 MHz, DMSO)
74
210 200 190 180 170 160 150 140 130 120 110 100 90 80 70 60 50 40 30 20 10 0 -10
δ (ppm)

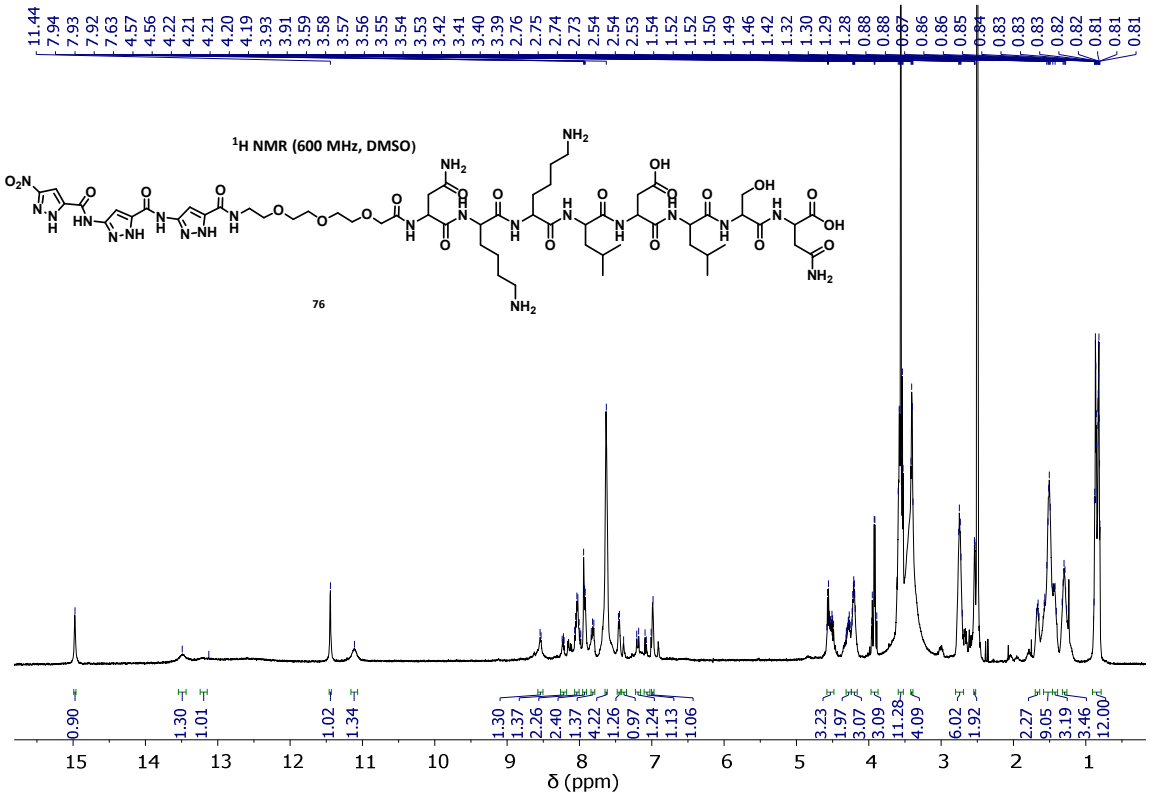
^{1}H NMR (600 MHz, DMSO)
76
δ (ppm)

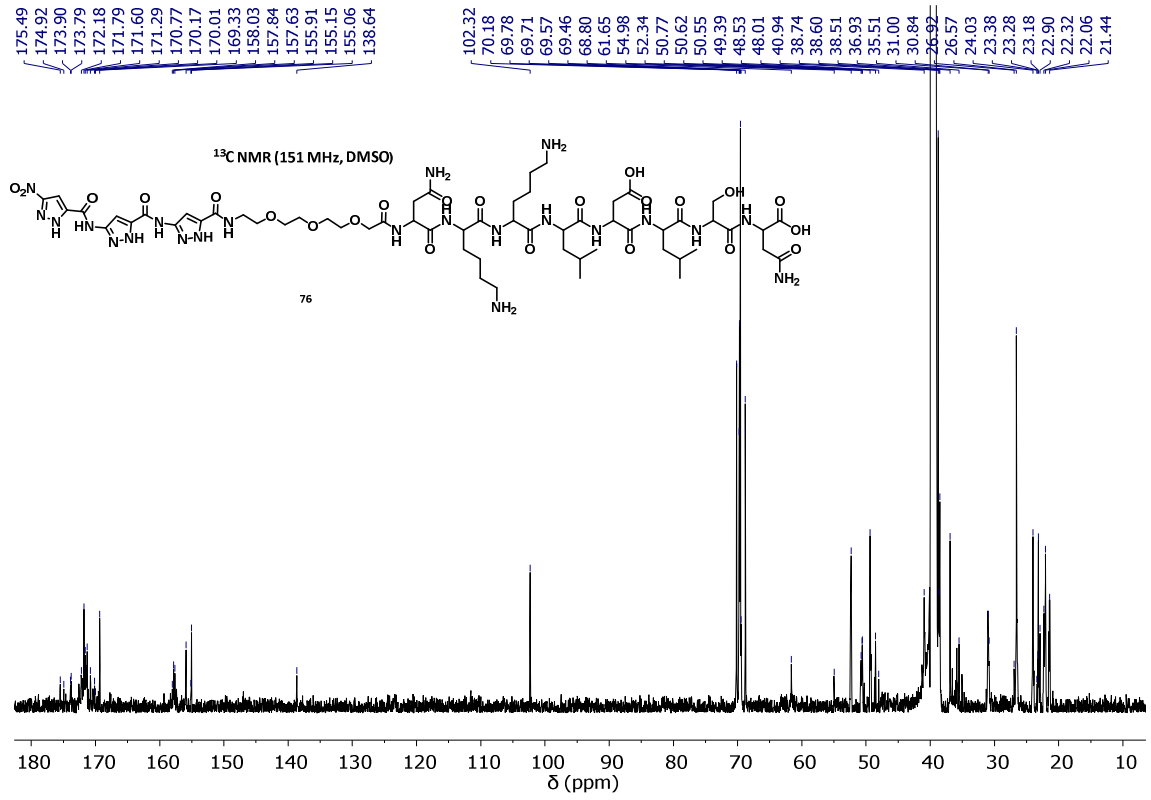
^{13}C NMR (151 MHz, DMSO)
76
δ (ppm)

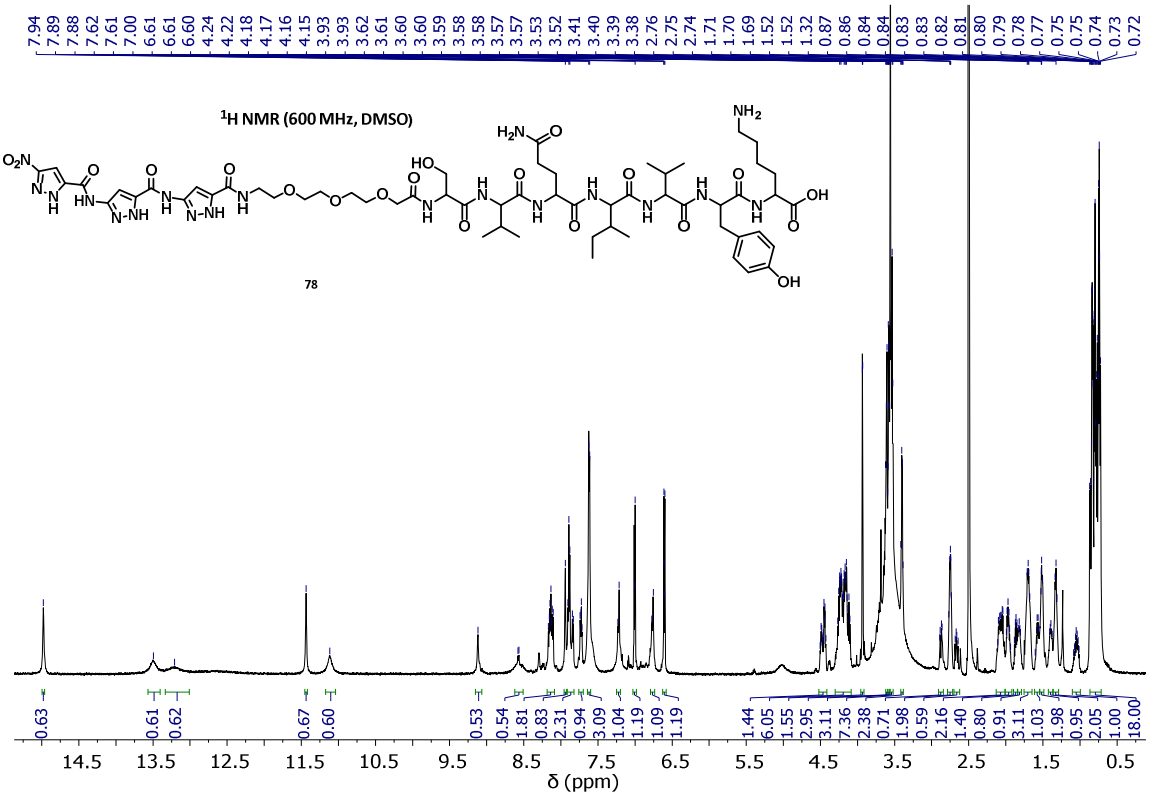
^{1}H NMR (600 MHz, DMSO)
78
δ (ppm)

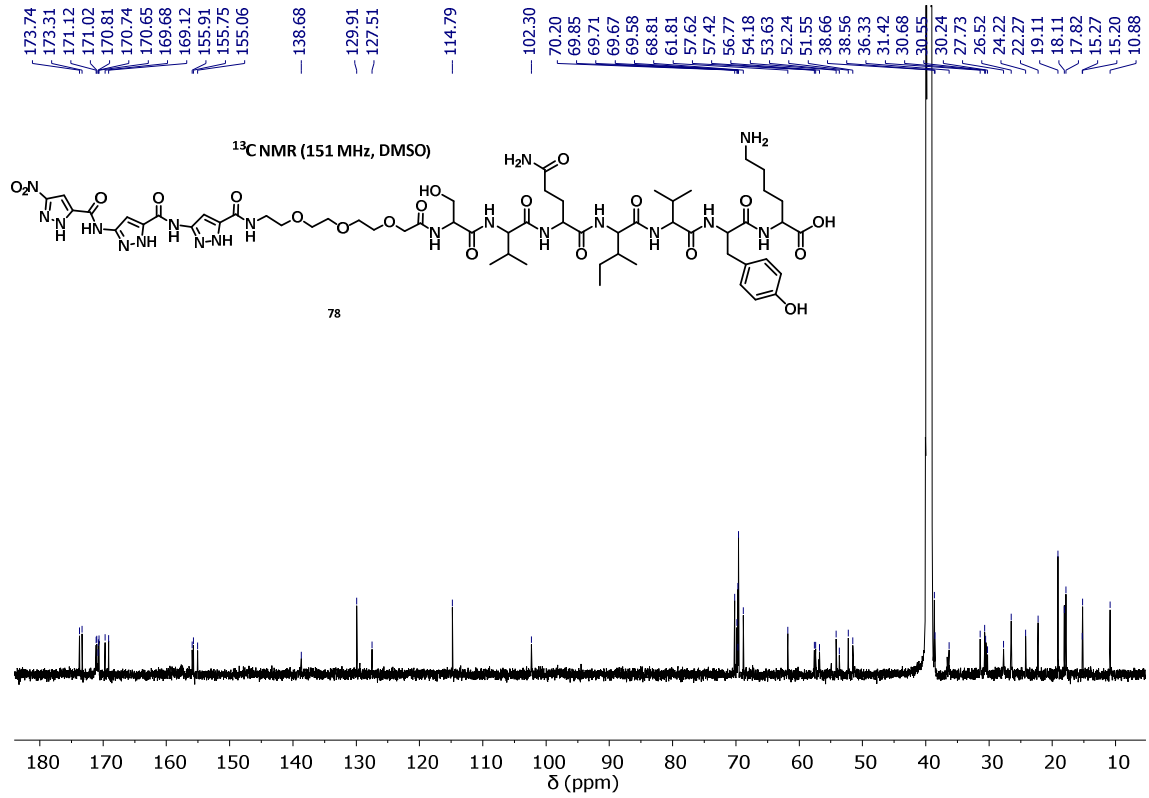
^{13}C NMR (151 MHz, DMSO)
78
δ (ppm)

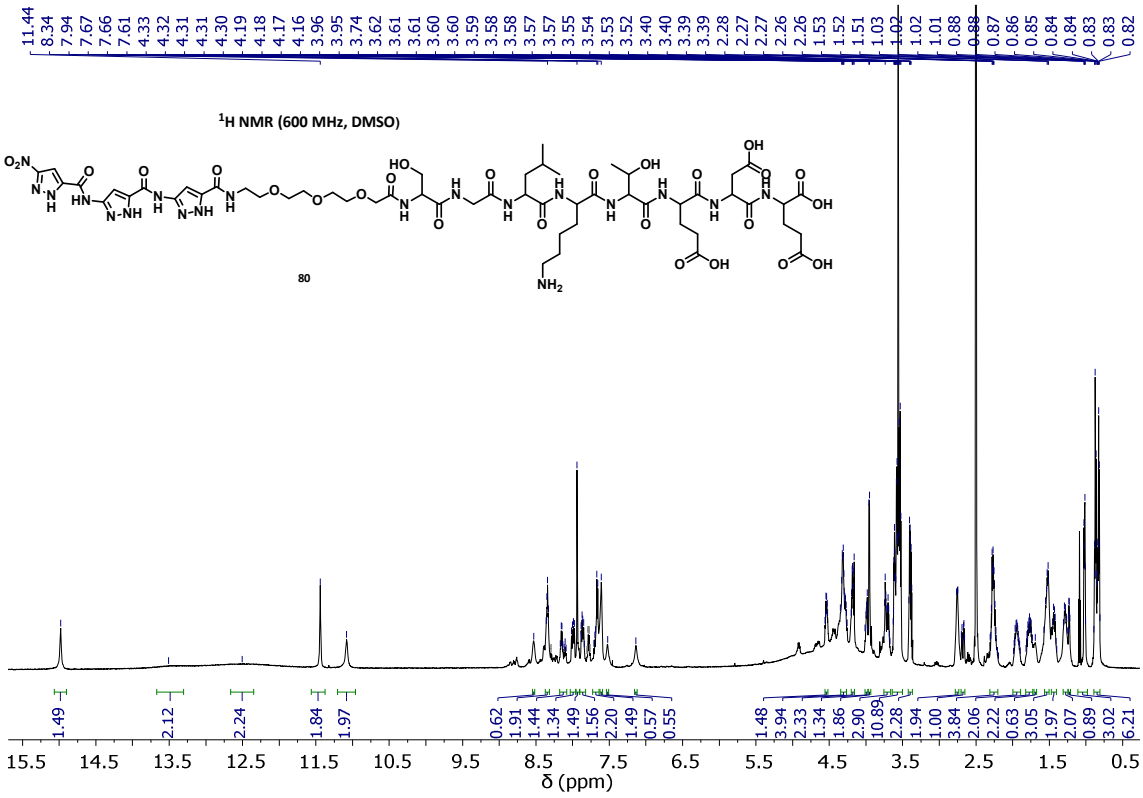
11.44
8.34
7.94
7.67
7.66
7.61
4.33
4.32
4.31
4.31
4.30
4.19
4.18
4.17
4.16
3.96
3.95
3.74
3.62
3.61
3.61
3.60
3.60
3.59
3.58
3.58
3.57
3.57
3.55
3.54
3.53
3.52
3.40
3.40
3.39
3.39
2.28
2.27
2.27
2.26
2.26
1.53
1.52
1.51
1.03
1.02
1.02
1.01
0.88
0.88
0.87
0.86
0.85
0.84
0.84
0.83
0.83
0.82
1H NMR (600 MHz, DMSO)
80
1.49
2.12
2.24
1.84
1.97
0.62
1.91
1.44
1.34
1.49
1.56
2.20
1.49
0.57
0.55
1.48
3.94
2.33
1.34
1.86
2.90
10.89
2.28
1.94
1.00
3.84
2.06
2.22
0.63
3.05
1.97
2.07
0.89
3.02
6.21
15.5
14.5
13.5
12.5
11.5
10.5
9.5
8.5
7.5
6.5
5.5
4.5
3.5
2.5
1.5
0.5
δ (ppm)

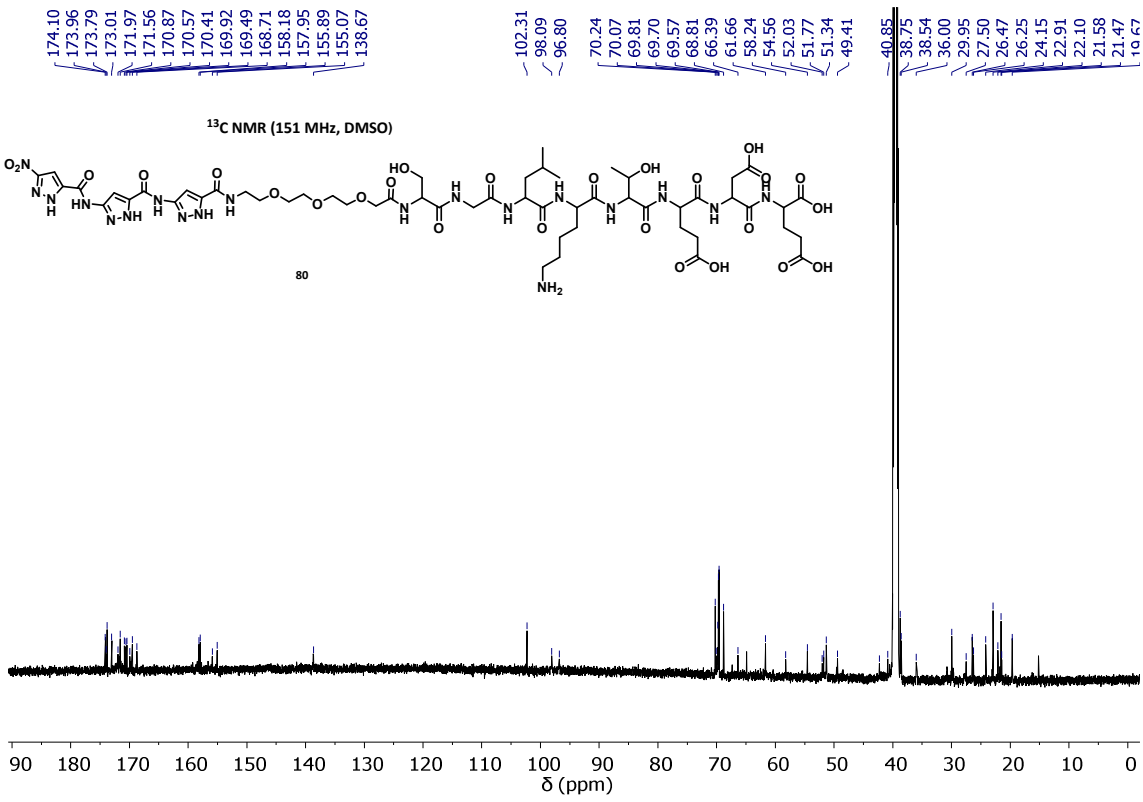
174.10
173.96
173.79
173.01
171.97
171.56
170.87
170.57
170.41
169.92
169.49
168.71
158.18
157.95
155.89
155.07
138.67
102.31
98.09
96.80
70.24
70.07
69.81
69.70
69.57
68.81
66.39
61.66
58.24
54.56
52.03
51.77
51.34
49.41
40.85
38.75
38.54
36.00
29.95
27.50
26.47
26.25
24.15
22.91
22.10
21.58
21.47
13C NMR (151 MHz, DMSO)
80
90
180
170
160
150
140
130
120
110
100
90
80
70
60
50
40
30
20
10
0
δ (ppm)

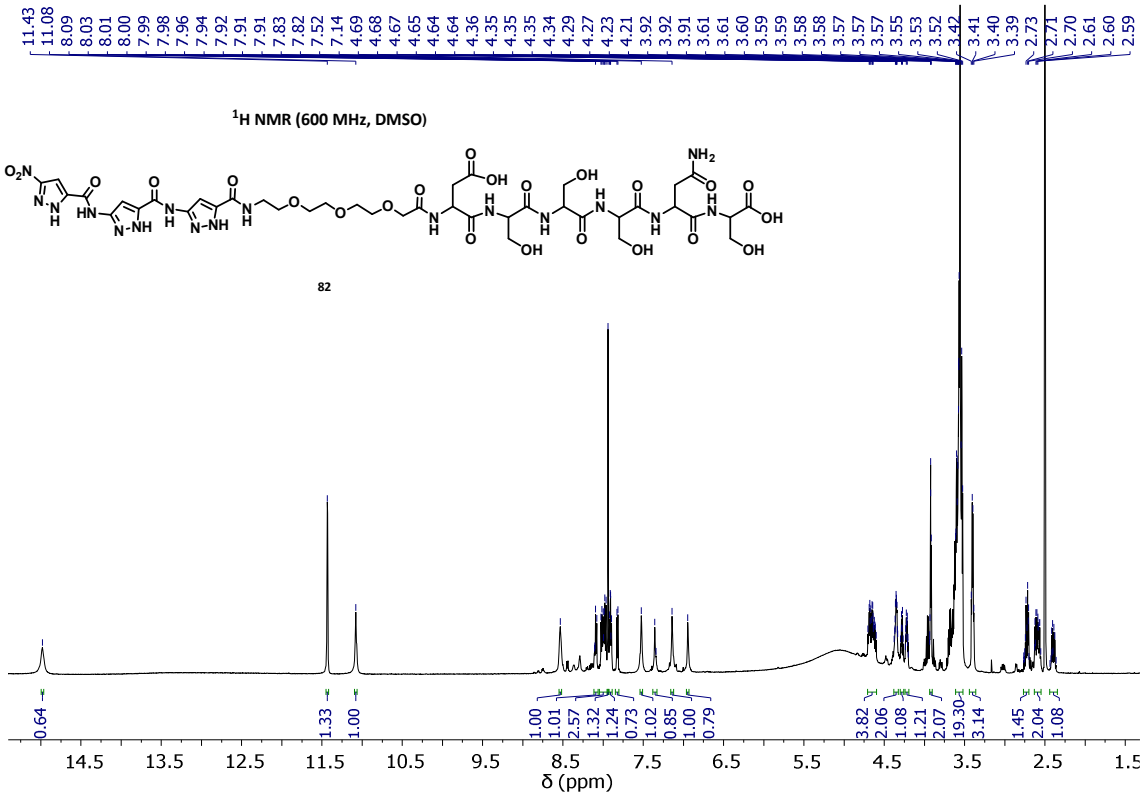
11.43
11.08
8.09
8.03
8.01
8.00
7.99
7.98
7.96
7.94
7.92
7.91
7.91
7.83
7.82
7.52
7.14
4.69
4.68
4.67
4.65
4.64
4.64
4.36
4.35
4.35
4.35
4.34
4.29
4.27
4.23
4.21
3.92
3.92
3.91
3.61
3.61
3.60
3.59
3.59
3.58
3.58
3.57
3.57
3.57
3.55
3.53
3.52
3.42
3.41
3.40
3.39
2.73
2.71
2.70
2.61
2.60
2.59
1H NMR (600 MHz, DMSO)
82
0.64
1.33
1.00
1.00
1.01
2.57
1.32
1.24
0.73
1.02
0.85
1.00
0.79
3.82
2.06
1.08
1.21
2.07
19.30
3.14
1.45
2.04
1.08
14.5
13.5
12.5
11.5
10.5
9.5
8.5
7.5
6.5
5.5
4.5
3.5
2.5
1.5
δ (ppm)

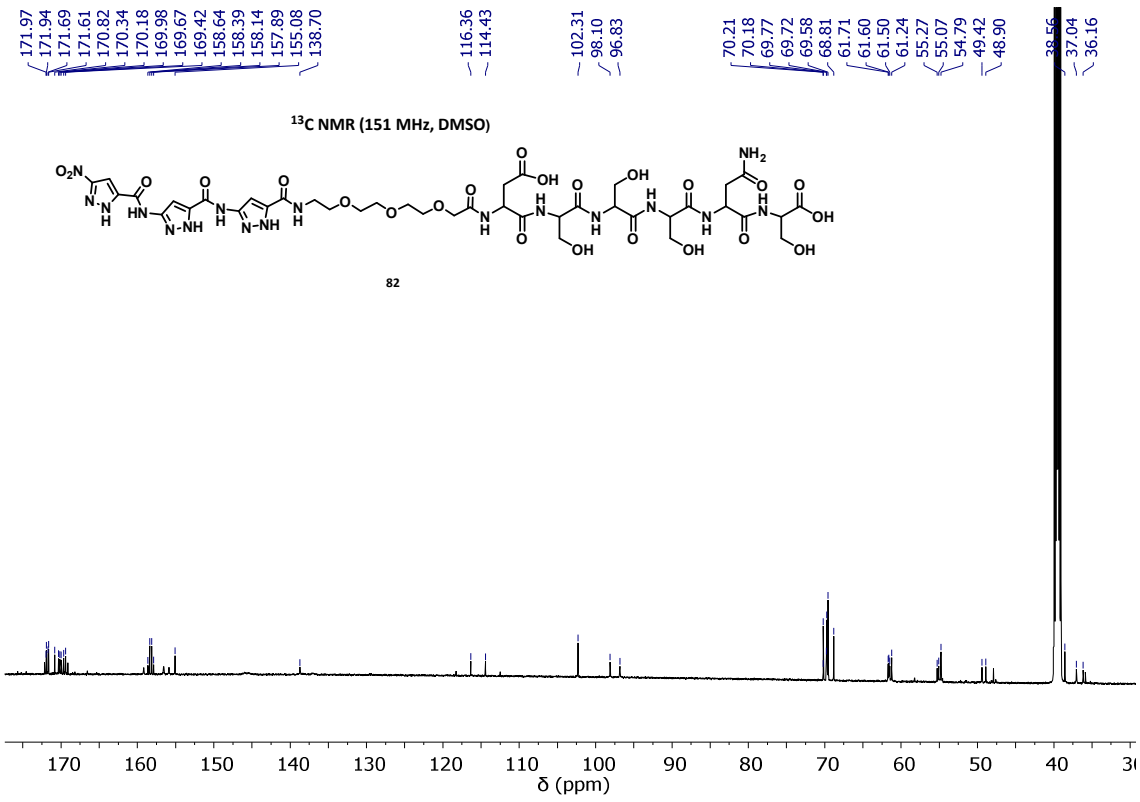
171.97
171.94
171.69
171.61
170.82
170.34
170.18
169.98
169.67
169.42
158.64
158.39
158.14
157.89
155.08
138.70
116.36
114.43
102.31
98.10
96.83
70.21
70.18
69.77
69.72
69.58
68.81
61.71
61.60
61.50
61.24
55.27
55.07
54.79
49.42
48.90
38.56
37.04
36.16
13C NMR (151 MHz, DMSO)
82
170
160
150
140
130
120
110
100
90
80
70
60
50
40
δ (ppm)

6.2 CURRICULUM VITAE

The curriculum vitae is not included in the online version for data protection reasons.

6.3 Acknowledgements/Agradecimientos

This doctoral thesis has been carried out at the University Duisburg-Essen under the direction of Dr. Prof. Thomas Schrader, whom I thank for the opportunity to do a doctorate on such a fascinating topic. I also thank for his dedication and support, which has made me grow both personally and professionally. Vielen Dank.

Also thanks to Dr. Prof. Michael Ehrmann for his understanding and support with the very interesting collaboration that has been made. To Dr. Laura Pedroza for the great work she has done with my compounds, without those wonderful results I could not have finished the thesis.

I want to make special mention of **Álvaro**, my partner and perfect co-worker, who has been my support both in the laboratory and emotionally. I think he would not have been able to finish the thesis if it were not for his insistence and his desire to live from day today. ESKERRIK ASKO ETA ASKO MAITE ZAITUT :3

Thank you to all my colleagues in the group Abbna, Philipp, Inesa, My-Hue, Nahid, Estelle, Antonio, Dennis and Don. But above all to Abbna Kirupakaran for her support in these years and for putting up with me both inside and outside the laboratory, really GRACIAS. To Sujenth Kirupakaran too, of course, AMIGO ;)

To Dr. Felix Niemeyer and Dr. Torsten Schaller for the good advice to solve all the problems that I have had during these years with the NMR.

To Heike Woll for all the headaches doing HPLC for my unsolvable molecules.

To Petra Schneider for putting out CDs of the infinite list of compounds I synthesized.

To Werner Karow, Gudrun Heinrich, and Dr. Florian Uteschil from the MS service of the University for insisting so much on my samples. I know there have been many samples, I hope it was not a bother.

To Alexandra Elbakyan, for making my thesis writing easier and faster.

To all the members of Justesa R&D department, Felix, Roberto, Álvaro, Mónica and Eugenia for teaching me so much during my stay there.

To Dr. Paula Morales and Dr. Nadine Jagerovic for their support over the years and for initiating me in the research career.

To Jose Luis González, thank you for the discussions about HPLC and "current news". See you very soon in Madrid.

To Louisa Waasmann and Suna Azhdari, thank you for your great friendship. I will miss you very much, but we will always have our Zoom meetings.

And finally to my biological family, my father, my mother, my grandmother and my brother for enduring all the phases of my doctorate thousands of kilometers away, as well as

the short stay of a month in Germany, lo sientiiii. And to my non-biological family but no less important, my mother-in-law, Charo, who supported us from day one in this adventure.
To Almudena, who unfortunately left us in 2020 due to the terrible disease discussed in this thesis.

La presente tesis doctoral ha sido realizada en la universidad Duisburg-Essen bajo la dirección del Dr. Prof. Thomas Schrader, a quien agradezco la oportunidad de realizar el doctorado en un tema tan fascinante. También le agradezco tanta dedicación y apoyo, la cual me ha hecho crecer tanto en lo personal como en lo profesional. Vielen Dank.

También dar las gracias al Dr. Prof. Michael Ehrmann por su comprensión y apoyo con la colaboración tan interesante que se ha realizado. A Laura Pedroza por el gran trabajo que ha hecho con mis compuestos, sin esos maravillosos resultados no podría haber terminado la tesis.

Quiero hacer mención especial a **Álvaro**, mi pareja y perfecto compañero de trabajo, que ha sido mi apoyo tanto en el laboratorio como emocionalmente. Creo que no hubiera sido capaz de terminar la tesis sino fuera por su insistencia y sus ganas de vivir el día a día. ESKERRIK ASKO ETA ASKO MAITE ZAITUT :3

Dar las gracias a todos mis compañeros del grupo Abbna, Philipp, Inesa, My-Hue, Nahid, Estelle, Antonio, Dennis y Don. Pero sobre todo a Abbna Kirupakaran por el apoyo en estos años y por aguantarme tanto dentro como fuera del laboratorio, de verdad GRACIAS. A Sujenth Kirupakaran también, por supuesto AMIGO ;)

A los Dr. Felix Niemeyer y Dr. Torsten Schaller por los buenos consejos para resolver todos los problemas que he tenido durante estos años con el RMN.

A Heike Woll por todos los quebraderos de cabeza haciendo HPLC para mis moléculas imposibles de resolver.

A Petra Schneider por llevar a cabo CD de la lista infinita de compuestos que sinteticé.

A Werner Karow, Gudrun Heinrich y al Dr. Florian Uteschil del servicio de MS de la universidad por insistir tanto con mis muestras. Sé que han sido muchas muestras, espero no haber sido una molestia.

A Alexandra Elbakyan, por hacerme la escritura de la tesis más fácil y rápida.

A todos los miembros del departamento de I+D de Justesa, Félix, Roberto, Álvaro, Mónica y Eugenia por enseñarme tanto durante mi estancia allí.

A la Dra. Paula Morales y la Dra. Nadine Jagerovic por el apoyo todos estos años e iniciarme en la investigación.

A Jose Luis González, gracias por las conversaciones sobre HPLC y noticias de actualidad. Nos vemos en Madrid muy pronto.
A Louisa Waasmann y Suna Azhdari, gracias por vuestra gran amistad. Os voy a echar mucho de menos, pero siempre nos quedarán nuestros Zoom meetings.
Y por último a mi familia biológica, mi padre, mi madre, mi abuela y mi hermano por aguantar a miles de kilómetros todas las fases de mi doctorado y la pequeña estancia de un mes en Alemania, lo sientiiii. Y a mi familia no biológica pero no por ello menos importante, mi suegra Charo que nos apoyó desde el día uno en esta aventura.
A la Almudena, que lamentablemente nos dejó en 2020 debido a la terrible enfermedad de la que se habla en esta tesis.